UNIVERSITAT DE BARCELONA

Novel potential determinants in endoplasmic reticulum stress, inflammation and insulin resistance: Apo CIII and sAPPβ

Gaia Botteri

UNIVERSITAT DE BARCELONA

PhD Thesis

NOVEL POTENTIAL DETERMINANTS IN ENDOPLASMIC RETICULUM STRESS, INFLAMMATION AND INSULIN RESISTANCE: Apo CIII and sAPPβ

Gaia Botteri

NOVEL POTENTIAL DETERMINANTS IN ENDOPLASMIC RETICULUM STRESS, INFLAMMATION AND INSULIN RESISTANCE: Apo CIII and sAPPβ

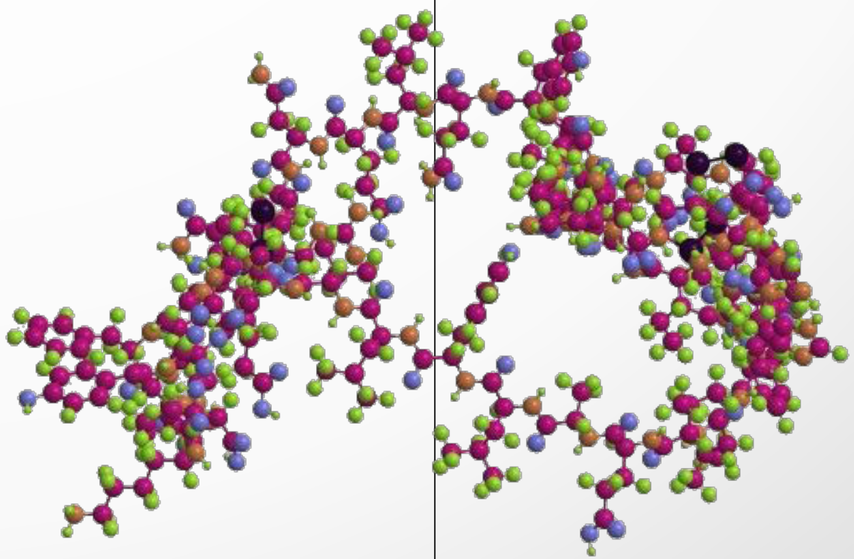

GAIA BOTTERI

2018

UNIVERSITAT DE BARCELONA

UNIVERSITY OF BARCELONA

FACULTY OF PHARMACY AND FOOD SCIENCES

DEPARTAMENT OF PHARMACOLOGY, TOXICOLOGY
AND THERAPEUTIC CHEMISTRY

Novel potential determinants in endoplasmic reticulum stress, inflammation and insulin resistance: Apo CIII and sAPPβ.

GAIA BOTTERI
2018

UNIVERSITY OF BARCELONA

FACULTY OF PHARMACY AND FOOD SCIENCES

DEPARTAMENT OF PHARMACOLOGY, TOXICOLOGY
AND THERAPEUTIC CHEMISTRY

PhD PROGRAM
DRUGS RESEARCH, DEVELOPMENT AND CONTROL

Novel potential determinants in endoplasmic reticulum stress, inflammation and insulin resistance: Apo CIII and sAPPβ.

Memory presented by Gaia Botteri to obtain the PhD title from the University of Barcelona

Director
Manuel Vázquez Carrera

PhD student
Gaia Botteri

GAIA BOTTERI
2018

The present work has been funded by:

Ministerio de Economía, Industria y Competividad

(SAF2012-30708)

(FPI BES-2013-062965)

Centro de Investigación Biomédica en Red de Diabetes y Enfermedades Metabólicas Asociadas

With the support of:

Institut de Recerca Sant Joan de Déu (IR-SJD). Esplugues de Llobregat, Barcelona, Spain.

Department of Biochemistry and Molecular Biology and Institut de Biomedicina de la Universidad de Barcelona (IBUB), University of Barcelona. Barcelona, Spain.

If the universe is the answer,
what is the question?

(L. Lederman, 1993)

Index

Abbreviations

Aβ	Amyloid β
AC	Adenylate cyclase
ACC	Acetyl-CoA carboxylase
ACOX	Acyl-coenzyme A oxidase
AD	Alzheimer's disease
ADAM	A disintegrin and metalloproteinase domain-containing protein
ADDLs	Amyloid derived diffusible ligands
ADP	Adenosine diphosphate
AGEs	Advanced glycation end-products
AMP	Adenosine monophosphate
AMPK	AMP-activated protein kinase
AP1	Activator protein 1
APLP	Amyloid precursor-like protein
Apo B	Apolipoprotein B
Apo CIII	Apolipoprotein CIII
Apo E	Apolipoprotein E
APP	Amyloid precursor protein
APRT	Adenine phosphoribosyltransferase
AS160	Akt substrate of 160 kDa
ATF3	Activating transcription factor 3
ATF4	Activating transcription factor 4
ATF6	Activating transcription factor 6
ATP	Adenosine triphosphate
BACE1	β-site amyloid precursor protein cleaving enzyme 1
BBB	Blood-brain barrier
BiP/GRP78	Binding immunoglobulin protein/78 kDa glucose-regulated protein
BMI	Body mass index
BSA	Bovine serum albumin
CACT	Carnitine-acylcarnitine translocase
CAMK IV	Calcium/calmodulin-dependent protein kinase IV
CAMKK	Calcium/calmodulin-dependent protein kinase kinase
cAMP	Cyclic-AMP
CE	Cholesterol esters
cGMP	Cyclic-guanosine monophosphate
CHOP	C/EBP homologous protein
CNS	Central nervous system
CoA	Coenzyme A
CPT1	Carnitine palmitoyltransferase 1
CRE	cAMP response element
CREB	cAMP response element binding protein
CREM	cAMP response element modulator
CSF	Cerebrospinal fluid
DAG	Diacylglycerol
DAMPs	Danger-associated molecular patterns
DGAT	Diglyceride acyltransferase
DMEM	Dulbecco's modified eagle's medium

DNA	Deoxyribonucleic acid
DNL	*De novo* lipogenesis
DR6	Death receptor 6
EDTA	Ethylendiaminetetraacetic acid
eIF2α	Eukaryotic initiation factor 2α
ELISA	Enzyme-Linked Immunosorbent assay
EMSA	Electrophoretic mobility shift assay
ER	Endoplasmic reticulum
ERK1/2	Extracellular signal–regulated kinases 1/2
ERSE	ER stress elements
FABPpm	Plasma membrane fatty acid-binding protein
FADH	Flavin adenine dinucleotide
FAO	Fatty acid oxidation
FAT/CD36	Fatty acid translocase/cluster of differentiation 36
FATP	Fatty acid transport protein
FBS	Fetal bovine serum
FOXO1	Forkhead box protein O1
GGA	Golgi-localized, γ-ear, ADP-ribosylation factor binding proteins
GLUT4	Glucose transporter 4
GPAT	Glycerol-3-phosphate acyltransferases
G6Pase	Gucose-6-phosphatase
Grb2	Growth factor receptor-bound protein 2
GS	Glycogen synthase
GSK3	Glycogen synthase kinase 3
GTP	Guanosine triphosphate
GTT	Glucose tolerance test
HDL	High-density lipoprotein
HEPES	Hydroxyethyl piperazineethanesulfonic acid
HFD	High fat diet
HL	Hepatic lipase
HSL	Hormone-sensitive lipase
IDE	Insulin degrading enzyme
IDL	Intermediate-density lipoproteins
IGF1R	Insulin-like growth factor 1 receptor
IKKβ	IκB kinase β
IκBα	Inhibitor of κB α
IL1	Interleukin 1
IL6	Interleukin 6
IRβ	β subunit of insulin receptor
IRE1	Inositol-requiring kinase 1
IRS	Insulin receptor substrates
ITT	Insulin tolerance test
JAK	Janus kinase
JNK	c-Jun N-terminal kinase
KO	Knock out
LCAT	Lecithin-cholesterol acyltransferase
LDL	Low-density lipoproteins

LDLR	Low-density lipoprotein receptor
LKB1	Liver kinase B1
LPL	Lipoprotein lipase
LRP	Lipoprotein receptor-related proteins
MAPK	Mitogen-activated protein kinase
MCAD	Medium-chain acyl-coenzyme A dehydrogenase
MCP1	Monocyte Chemoattractant Protein-1
MEK	MAPK-ERK kinase
M3	Merck 3
mTORC	Mammalian target of rapamycin complex 1
MTP	Microsomal triglyceride transfer protein
NADPH	Nicotinamide adenine dinucleotide phosphate
NEFA	Non-esterified fatty acids
NFκB	Nuclear factor κ-light-chain-enhancer of activated B cells
NQO1	NADPH dehydrogenase quinone 1
NRF	Nuclear respiratory factors
NRG1	Neuroregulin 1
NSAIDs	Non-steroidal anti-inflammatory drugs
Ntg	Non-transgenic
OXPHOS	Oxidative phosphorylation complexes
OvNa	Sodium orthovanadate
PAGE	Polyacrylamide gel electrophoresis
PAMPs	Pathogen-associated microbial patterns
PBA	4-phenylbutyrate
PBS	Phosphate buffer solution
PDK1	Phosphoinositide-dependent kinase 1
PDK4	Pyruvate dehydrogenase kinase 4
PEPCK	Phosphoenolpyruvate carboxykinase
PERK	Protein kinase RNA-like endoplasmic reticulum kinase
PET	Positron emission tomography
PFK2	Phosphofructo kinase 2
PGA1	Prostaglandin 1
PGC1α	Peroxisome proliferator-activated receptor gamma coactivator 1α
PGI2	Prostacyclin 1
PH	Pleckstrin homology domain
PI3K	Phosphoinositide 3-kinase
PIP2	Phosphatidylinositol 4,5-bisphosphate
PIP3	Phosphatidylinositol (3,4,5)-trisphosphate
PKA	Protein kinase A
PKB/Akt	Protein kinase B/Akt
PKC	Protein kinase C
PKG	Protein kinase G
p75NTR	Neurotrophin receptor p75
PP1A	Phosphatase protein 1A
PPARs	Peroxisome proliferator-activated receptors
PP2C	Phosphatase protein 2C
PPIA	Cyclophilin 1A

PMSF	Phenylmethylsulfonyl flouride
PPRE	PPAR response element
PSGL1	P-selectin glycoprotein ligand 1
PTB	Phosphotyrosine-binding domain
PUFA	Poly-unsaturated fatty acids
RCT	Reverse cholesterol transport
RNA	Ribonucleic acid
ROS	Reactive oxygen species
RT-PCR	Real time poly chain reaction
RXR	Retinoid X receptor
sAPPα	Soluble amyloid precursor protein α
sAPPβ	Soluble amyloid precursor protein β
SAT	Subcutaneous adipose tissue
SCD	Stearoyl-CoA desaturase
sdLDL	Small dense LDL
SDS	Sodium dodecyl sulphate
SH	Src homology domain
SiRNA	Small interference RNA
SIRT1	Sirtuin 1
SOCS	Suppressors of cytokine signalling
SOD1	Superoxide dismutase 1
SOS	Son of sevenless protein
SPT1	Serine c palmitoyltransferase
SREBP1	Sterol regulatory element-binding protein
STAT	Signal transducer and activator of transcription
sXBP1	Spliced x-box binding protein 1
TACE	Tumor necrosis factor α converting enzyme
TBS	Tris-buffered saline solution
T2D	Type 2 diabetes
Tfam	Mitochondrial transcription factor A
Tg	Transgenic
TG	Triglyceride
TGRLs	Triglyceride-rich lipoproteins
TIR	Toll/Interleukin 1 receptor
TLRs	Toll-like receptors
TNFα	Tumor necrosis factor α
TRB3	Tribbles 3
TZDs	Thiazolidindiones
UPR	Unfolding protein response
uXBP1	Unspliced x-box binding protein 1
VAT	Visceral adipose tissue
VLDL	Very low-density lipoproteins
VLDLR	VLDL receptor
WB	Western blot
WT	Wild type

Summary

Diabetes represents one of the biggest health challenges of the 21st century. Insulin resistance is the primary defect in the most common form of diabetes, type 2 diabetes mellitus (T2D), and is defined as a failure in the capacity of insulin to drive glucose into its target tissues. This condition both predicts and precedes the development of T2D.

Loss of insulin sensitivity in skeletal muscle is the major defect in T2D and is believed to be critical in the pathogenesis of this disease. Elucidating new molecular mechanisms involved in insulin resistance in skeletal muscle may lead to the development of new strategies for the prevention and treatment of T2D.

Insulin resistance develops as the result of the expansion of adipose tissue in obese individuals, which releases increased amounts of fatty acids, hormones, pro-inflammatory cytokines and other factors. Most of these molecules induce the activation of a chronic low-level inflammatory process that contributes to insulin resistance and T2D. The molecular mechanisms by which these molecules induce a low-grade and chronic inflammatory process in obese patients are not completely understood. However, some studies have shown that alterations in the endoplasmic reticulum (ER) might contribute to the development of an inflammatory status and consequently to insulin resistance.

Obesity and insulin resistance are also characterized by the presence of atherogenic dyslipidemia, which refers to elevated levels of triglycerides (TG) and the particles responsible for carrying these lipids in the plasma, the very low-density lipoproteins (VLDL), low levels of high-density lipoproteins (HDL), and increased levels of small, dense low-density lipoproteins (sdLDL). In addition to TG, VLDL also contain apolipoproteins, of which apolipoprotein CIII (Apo CIII) is one of the most abundant. Although plasma levels of VLDL and Apo CIII are increased in diabetic patients, little was known about whether the increase in the levels of these lipoproteins and apolipoproteins contributes to exacerbate insulin resistance and the mechanisms involved.

Recent evidence indicates that subjects suffering T2D are at higher risk of developing Alzheimer's Disease (AD). In addition, several evidences point out that the converse is also true, since cognitive impairment and Alzheimer's dementia can induce central and peripheral insulin resistance, thus increasing the risk of T2D.

The β-site Amyloid precursor protein Cleaving Enzyme 1 (BACE1) or β-secretase is a key enzyme involved in AD and is responsible for the cleavage of Amyloid Precursor Protein in the amyloidogenic pathway. It has been recently reported that BACE1 is also implicated in glucose metabolism. Thus, BACE1-deficient mice are protected against high fat diet (HFD)-induced glucose intolerance and inhibition of BACE1 activity increases insulin-independent glucose uptake. BACE1 is proteolytically active not only in the brain but also in skeletal muscle, suggesting that this enzyme might be involved in development of

systemic insulin resistance. However, little was known about whether BACE1 contributes to ER stress, inflammation and insulin resistance.

In this thesis, we report that the increase in the levels of VLDL can promote ER stress, inflammation, and insulin resistance in skeletal muscle through Apo CIII-mediated activation of the toll-like receptor 2.
Moreover, BACE1 inhibition in myotubes results in an improvement in lipid-induced ER stress, inflammation, and insulin resistance. Further, the product of BACE1 enzymatic activity, soluble amyloid precursor protein β (sAPPβ), mimics the effects of palmitate and induces ER stress, inflammation and insulin resistance.
Overall, these findings suggest that both VLDL-Apo CIII and sAPPβ are new determinants involved in ER stress, inflammation and insulin resistance in skeletal muscle.

I. Introduction

I. 1. The insulin signaling pathway and the regulation of glucose and lipid metabolism

Metabolism is the set of life-sustaining chemical transformations within the cells of the organism. It is characterized by a tight integration between the different organs, which allows the body to maintain the physiological energy balance and to properly execute its function.

All the metabolic processes are strictly regulated; however, if metabolic dysregulation occurs at some point, several pathologic status can develop (Engelgau *et al.*, 2000).

A large number of enzymes and hormones are involved in the control of metabolic functions. One of the most important is the hormone insulin. Insulin is an anabolic hormone that exerts several vital effects in the body, as summarized in Figure I.1. (Dimitriadis *et al.*, 2011).

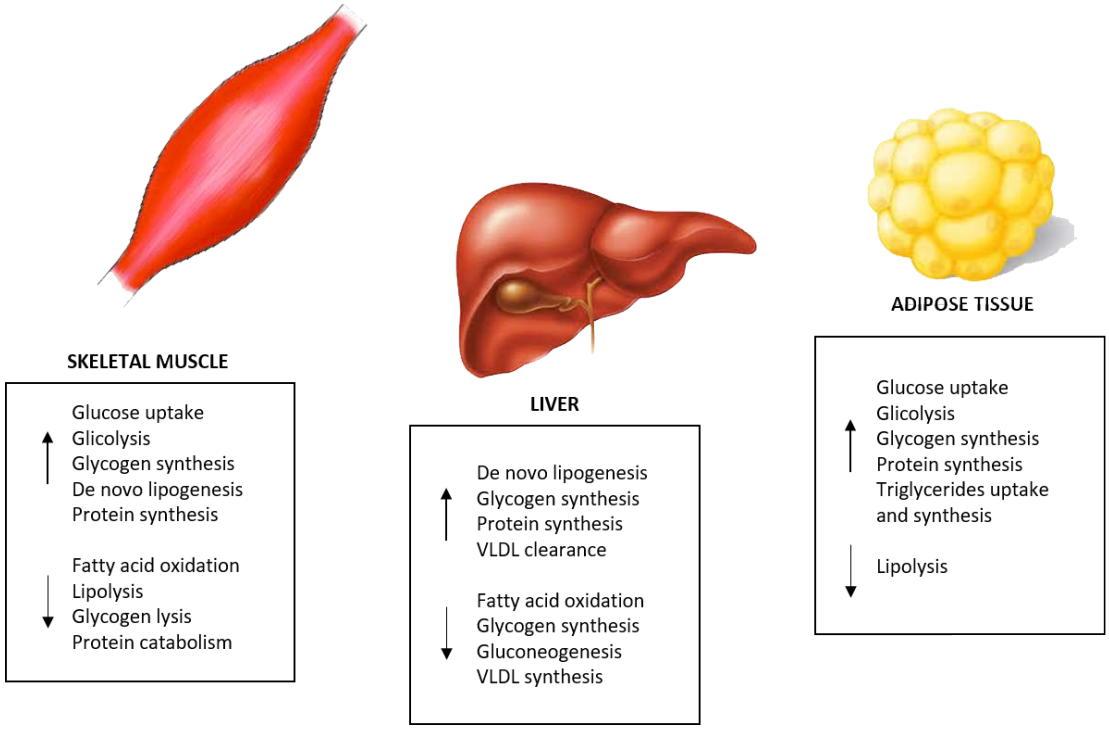

Figure I.1. Principal physiologic insulin effects in the organism (Dimitriadis *et al.*, 2011)

I. 1.1. Glucose metabolism

Glucose is a simple carbohydrate that represents the most important energetic substrate for many tissues, particularly those that play an essential role in maintaining the biological functions of the body and require using energy continuously. This is the case of the central nervous system (CNS), the hematic cells, such as red blood cells that carry the oxygen, and the cells of the immune system. The importance of glucose depends on its capacity to supply energy in a very short time, sometimes also in anaerobic conditions. This unicity

explain why glucose is the preferential substrate for many tissues, despite it is not the most efficient in terms of energy (Kcal) produced by its metabolism. For these reasons, an adequate glycemic control is of vital importance for body homeostasis (Engelgau *et al.*, 2000). Once glucose has passed from the bloodstream into the cells, it can be used for energy or for storage, depending on the tissue. Brain and adipose tissue usually use glucose for metabolic purposes, while liver and skeletal muscle keep it as energy reserve to use it in case of need (e.g. sudden and intense physical activity, lower glycemia, etc.).
If glucose is used for energy, it is rapidly converted into glucose-6-phosphate (G6P) by the enzyme hexokinase, which is ubiquitously expressed in all tissues, and enters the glycolytic pathway in order to produce adenosine triphosphate (ATP), the molecule that supplies energy to all the cells.
If glucose is used for storage, it is converted into glycogen through the glycogen synthesis pathway. Glycogen is a ramified polymer constituted by many residues of glucose. Skeletal muscle and liver accumulate big amounts of glycogen. In skeletal muscle, glycogen represents a stock of glucose easy to metabolize in case of physical activity. In liver, synthesis and degradation of glycogen are mutually regulated in order to maintain adequate concentrations of glucose in the blood. In fact, liver, in contrast to other tissues, expresses the glucose-6-phosphatase (G6Pase), a very important enzyme responsible for the conversion of G6P into free glucose. Only free glucose, but not G6P, can exit the cell and pass into the bloodstream. Liver also contributes to maintain euglycemia by synthetizing glucose from non-carbohydrate precursors through the gluconeogenic pathway, in which the phosphoenolpyruvate carboxykinase (PEPCK) represents the step-limiting enzyme.

Insulin is the most important endocrine hormone that controls glycemia and its secretion is strictly regulated by many factors. One of the most important is the change in blood glucose concentration: when glucose levels rise, insulin secretion is increased; when glucose levels are low, insulin secretion is inhibited. Insulin is responsible for maintaining the glucose levels in the blood within the physiological range (75-110 mg/dl). It activates glucose uptake and glycogen synthesis in skeletal muscle and other tissues, so this carbohydrate can be removed from the bloodstream and metabolized. Furthermore, insulin inhibits hepatic gluconeogenesis and activates hepatic glycogen synthesis (Dimitriadis *et al.*, 2011) by regulating many of the enzymes involved in these processes.
Insulin exerts its functions through several downstream biochemical cascades, that collectively constitute the insulin signaling pathway.

I. 1.1.1. The insulin signaling pathway

The insulin signaling pathway involves a very wide range of downstream cascades (Figure I.2.). Next, only the molecular pathways examined in the present thesis will be discussed.

I. 1.1.1.1. Insulin Receptor

The effects of insulin are initiated by its binding to a receptor present in the cell membrane. The insulin receptor is a transmembrane protein that contains α- and β subunits. The insulin receptor belongs to the subfamily of receptor tyrosine kinases (RTKs) (Aguirre *et al.*, 2000; Taniguchi *et al.*, 2006). Functionally, the insulin receptor behaves like a classic allosteric enzyme and functions as a dimer (Becker and Roth, 1990).

Insulin binds to the α-subunits of the homodimer, which faces the extracellular side of the cells. The β subunits are located on the cytosolic surface and are responsible for the tyrosine kinase enzyme activity which is triggered by the insulin binding. The activation by the ligand provokes the autophosphorylation of the β subunits on tyrosine residues in the positions 1146, 1150 and 1151 (White *et al.*, 1988). This triple autophosphorylation induces a conformational change in the structure of the molecule, which subsequently leads to the phosphorylation of other proteins inside the cell known as insulin receptor substrates (Mootha *et al.*, 2003).

I. 1.1.1.2. Insulin Receptor Substrates (IRS)

The IRS family includes six different isoforms. IRS1 and IRS2 are widely distributed, whereas IRS3 is largely limited to the adipocytes and the brain, and IRS4 is expressed primarily in embryonic tissue or cell lines. IRS5 and IRS6 seem to have limited tissue expression and function in signaling (Shaw, 2011). IRS proteins contain two different domains: the pleckstrin-homology domain (PH domain) and the phosphotyrosine-binding domain (PTB domain). Both these domains are located near the N-terminus, which accounts for the high affinity of these substrates for the insulin receptor. The center and the C-terminus of the IRS proteins contain up to 20 potential tyrosine-phosphorylation sites that, after phosphorylation by the insulin receptor β subunits, bind to intracellular molecules that contain the Src-homology-2 domains (SH2 domains). This union triggers the insulin downstream cascade and is responsible for the metabolic effects of the hormone (Shaw, 2011).

The C-terminus also contains several serine/threonine phosphorylation sites that are responsible for switching the downstream signaling off and play an important role in the development of insulin resistance, as it will be explained later.

The best studied SH2 proteins that bind to phosphorylated IRS proteins are adaptor molecules, such as the regulatory subunit of the phosphatidylinositol 3-kinase (PI3K) or the growth factor receptor-bound protein 2 (Grb2), which associates with son-of-sevenless (SOS) protein to activate the mitogen-activated protein kinases (MAPK) pathway (Taniguchi *et al.*, 2006).

I. 1.1.1.3. PI3K

PI3K plays a pivotal role in the insulin signaling pathway. In fact, PI3K inhibitors block almost all of insulin metabolic actions, including glucose transport, glycogen synthesis, lipid synthesis and adipocyte differentiation (Kurtz and Ray-Coquard, 2012).

The PI3K enzyme consists of a regulatory and a catalytic subunit, each of which exists in several isoforms. The best characterized isoform of the enzyme is the one containing the p85 regulatory subunit and the p110 catalytic subunit. The activation of the catalytic subunit depends on the interaction of the two SH2 domains in the regulatory subunit with the PTB domain in the IRS proteins. In fact, after the union of the SH2 domains with the phosphorylated IRS proteins the catalytic subunit moves closer to the membrane surface where it can phosphorylate its phospholipidic substrates. The PI3K catalyzes the formation of the lipid second messenger phosphatidylinositol 3 phosphate (PI3P), which can bind to the proteins that contain PH domains (Taniguchi *et al.*, 2006).

Among the proteins that bind PI3K, the AGC superfamily of serine/threonine kinase represents the most important substrate. This family contains more than fifteen kinases involved in many metabolic effects. The first proteins to be discovered, which give the name to the family, were protein kinase A [PKA, or cyclic adenosine monophosphate (cAMP)-dependent protein kinase], protein kinase G [PKG or cyclic guanosine monophosphate (cGMP)-dependent protein kinase] and protein kinase C (PKC), which are involved in lipid metabolism, cell survival and proliferation. However, the main AGC kinases involved in insulin signaling pathways are the 3-phosphoinositide-dependent protein kinase 1 (PDK1) and the protein kinase B (PKB), also called Akt. PDK1 is responsible for the phosphorylation and activation of Akt and other kinases (Alessi *et al.*, 1997).

I. 1.1.1.4. PDK1

PDK1 is a master kinase, which is crucial in the signaling pathways activated by several growth factors and hormones, including insulin. PDK1-deficient mice have a 40% decrease in body mass and a mild glucose intolerance (Bayascas *et al.*, 2008). The structure of PDK1 can be divided into two domains; the kinase or catalytic domain and the PH domain. The PH domain is responsible for the interaction of the kinase with phosphatidylinositols. The catalytic domain binds to the substrate molecules and phosphorylates them. PDK1 is activated when PI3P binds to the PH domain. This union triggers the phosphorylation of PDK1 substrates, such as Akt or PKCs (Mora *et al.*, 2004).

I. 1.1.1.5. PKB/Akt

Akt is a serine/threonine-specific protein kinase that plays a key role in multiple cellular processes such as glucose metabolism, apoptosis, cell proliferation, transcription and cell migration (Taniguchi *et al.*, 2006).

Three Akt isoforms have been identified. Akt1 is involved in cellular survival pathways, by inhibiting apoptotic processes. Akt1 is also able to induce protein synthesis pathways, and is therefore a key signaling protein in the cellular pathways that lead to skeletal muscle hypertrophy, and general tissue growth. Akt2 is an important signaling molecule in the insulin signaling pathway. It is required to induce glucose transport. Akt1-null mice, show no changes in glucose homeostasis, but the animals are smaller, consistent with a role for Akt1 in growth. In contrast, Akt2-deficient mice, have mild growth deficiency and display a diabetic phenotype (insulin resistance), again consistent with the idea that Akt2 is more specific for the insulin receptor signaling pathway (Garofalo *et al.*, 2003). The role of Akt3 is less clear, though it appears to be predominantly expressed in the brain. The three isoforms show a high homology at the structural level. They contain a PH domain, necessary for the binding to PI3P, and a catalytic domain, responsible for substrate phosphorylation. Once correctly positioned at the membrane via binding of PIP3 to PH domain, Akt can then be phosphorylated and activated by its activating kinases: the PDK1, that phosphorylates Akt oh threonine residues (Thr^{308} for Akt1, Thr^{309} for Akt2, Thr^{305} for Akt3), and the mammalian target of rapamycin complex 2 (mTORC2) kinase that phosphorylates Akt at serine residues (Ser^{473} for Akt1, Ser^{474} for Akt2, Ser^{472} for Akt3). Both phosphorylations on threonine and serine residues are required to a full activation of the Akt catalytic domain (Sarbassov *et al.*, 2005).

Once activated, Akt mediates most of the metabolic actions of insulin through the phosphorylation of several substrates, including other kinases, signaling proteins and transcription factors (see Figure I.2.).

Glycogen synthase kinase 3 (GSK3) was the first physiological Akt target to be identified and is one of the most important for the metabolic effects of insulin. Akt-mediated phosphorylation of GSK3 decreases its inhibitory activity toward the enzyme glycogen synthase. This leads to an increase in glycogen synthesis in liver and skeletal muscle (Ali *et al.*, 2001).

Another important target of Akt is the Akt substrate of 160 KDa protein (AS160). When AS160 is phosphorylated by Akt its activity is almost totally blocked. As a consequence, AS160 cannot carry out its inhibitory effect on its substrates anymore. The most important substrate of AS160 is the Rab-GTPase-activating protein which is involved in the cytoskeletal reorganization required for the translocation of the GLUT4 transporter to the plasma membrane (Kane *et al.*, 2002). Thus, when AS160 is inhibited by Akt, the Rab GTPase is activated and promotes the exocytosis of the vesicle containing GLUT4 on the

membrane surface, enhancing glucose uptake in skeletal muscle and adipose tissue (Miinea *et al.*, 2005).

GLUT4 is the glucose transporter responsible for insulin-regulated glucose storage. In contrast to other tissues, such as brain, where glucose demand is continuous, skeletal muscle needs a very accurate regulation of glucose uptake in response to metabolic stimuli (e.g. food intake, physical activity). This is the reason why GLUT4 isoform is usually stored inside the cell into vesicles, and it is translocated on the membrane surface only when the stimulus is present. This isoform has medium affinity for glucose (Km=5mM). Consequently, transport represents a limiting factor for glucose metabolism in myocytes. Interestingly, physical exercise upregulates the expression of GLUT4 on the membrane surface (Bryant *et al.*, 2002).

Due to its importance across numerous cellular functions, Akt activity is subjected to tight regulation. For example, it has been reported that tribbles-3 protein (TRB3) binds to unphosphorylated Akt and inhibits its phosphorylation and activation (Choi *et al.*, 2017; Zhang *et al.*, 2016). Other regulators, such as protein phosphatase 2A (PP2A) directly dephosphorylates and inactivates Akt (Liao and Hung, 2010).

There are additional effects of insulin: inhibition of gluconeogenesis through the forkhead box protein O1 (FOXO1) sequestration in the cytoplasm, inhibition of lipolysis, and increase in protein synthesis, as shown in Figure I.2.

I. 1.1.1.6. PKC family

As mentioned above, PKC kinases are member of the AGC kinase superfamily. PKC proteins regulate numerous cellular responses including gene expression, protein secretion, cell proliferation, glucose metabolism and the inflammatory response (Mellor and Parker, 1998).

The PKC family consists of fifteen isozymes in humans. They are divided into three subfamilies, based on their second messenger requirements: conventional (or classical), novel, and atypical. Conventional (c)PKCs contain the isoforms α, βI, βII, and γ. These require Ca^{2+}, diacylglycerol (DAG), and a phospholipid such as phosphatidylserine for activation. Novel (n)PKCs include the δ, ε, η, and θ isoforms, and require DAG, but do not require Ca^{2+} for activation. On the other hand, atypical (a)PKCs (including protein kinase Mζ and ι / λ isoforms) require neither Ca^{2+} nor DAG for activation, but they can be activated by phosphatidylinositols such as PI3P. Thus, the aPKCs are involved in insulin signaling pathway through the PI3K cascade. In fact, these isoforms contain a PH domain that can bind to PI3P. The binding allows the enzymes to move close to the membrane, where they can be phosphorylated and activated by PDK1. Many studies have reported that aPKCs play an important role in glucose uptake in myocytes and adipocytes (Farese, 2002). Indeed, once activated by PDK1, aPKCs can phosphorylate Rab-GTPase-activating

protein, enhancing its activity and promoting the exocytosis of GLUT4 containing vesicles (Imamura *et al.*, 2003).

I. 1.1.1.7. The MAPK pathway

The MAPK pathway is activated by insulin following the binding of the phosphorylated IRS protein to the SH2 domain on Grb2-SOS complex. This binding triggers the activation of the small GTPase Ras and subsequently leads to a kinase cascade that results in the phosphorylation and activation of the kinases called MEK1/2 (MAPK/ERK Kinase, isoform 1 and 2). Upon activation, MEK1/2 can in turn phosphorylate and activate the extracellular signal-regulated kinase 1 and 2 (ERK 1/2) and other MAPKs on threonine and tyrosine residues. Activated ERK1/2 phosphorylate various targets, therefore promoting cell growth and differentiation (Taniguchi *et al.*, 2006).

ERK1/2 have been shown to be necessary only for growth, survival, and differentiation aspects of insulin actions, but not for the other metabolic effects. Even so, it has been described that ERK1/2 are also involved in a negative feedback loop of insulin action by inhibiting the IRS proteins (Bouzakri *et al.*, 2003).

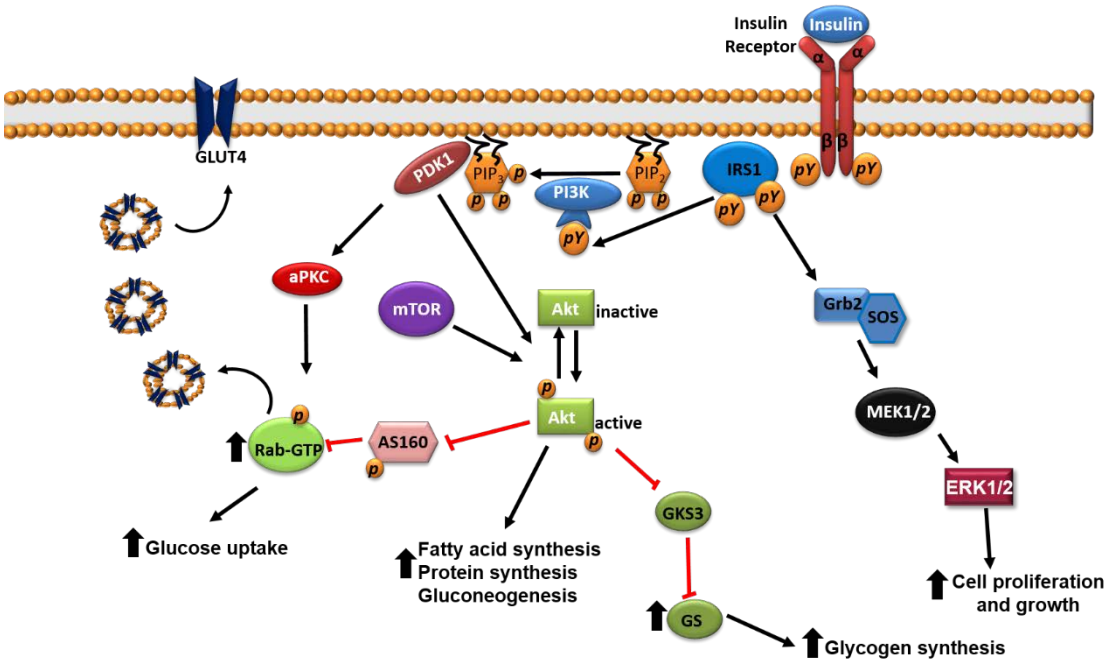

Figure I.2. Insulin signaling pathway: the binding of insulin to its receptor induces tyrosine (Y) phosphorylation of the β subunits of the receptor and its substrates (Mootha *et al.*, 2003). The downstream cascade involves many kinases, such as the Akt, which is responsible for the metabolic effects of the hormone, or the MEK1/2 that account for the effects of insulin as growth factor.

I. 1.2. Lipid metabolism

Although glucose is the preferential substrate used to obtain energy in many tissues, other substrates - such as lipids - can be metabolized to produce ATP. Actually, lipids can supply much more energy than carbohydrates in term of calories, even if the process is slower and cannot be used for immediate needs. When glucose levels raise after a meal, insulin not only stimulates glycolysis and glycogen synthesis, but also activates the synthesis of both fatty acids and TG in liver and adipose tissue. Insulin has a direct effect on many of the enzymes responsible for fatty acids and TG metabolism. For example, it activates acetyl-CoA carboxylase (ACC), responsible for fatty acid synthesis and inhibits hormone sensitive lipase (HSL), which is responsible for lipolysis in adipose tissue during fasting conditions (Cahill, 2006; Duncan *et al.*, 2007). Most of the lipids included in the diet are constituted by TG and have to be digested into fatty acids to be used by cells.

I. 1.2.1. Fatty acids

Fatty acids are carboxylic acids with a long unbranched aliphatic chain composed of a variable number of carbon atoms, from 4 to 28. The aliphatic chain can be either saturated or unsaturated, depending on the presence of carbon-carbon double bonds.

Saturated fatty acids have no double bonds. Thus, they are saturated with hydrogen and constitute a very important source of energy for cell metabolism, representing approximately 30% of the total of fatty acids in the body (Bennacer *et al.*, 2017).

Palmitic acid is the most abundant saturated fatty acid and is implicated in many metabolic functions. It is constituted by an unbranched chain with 16 atoms of carbon and represents the first fatty acid produced during fatty acid synthesis, being the precursor to longer fatty acids. Therefore, palmitic acid is a major body lipid component of animals. According to the World Health Organization, evidence is convincing that consumption of palmitic acid increases the risk of developing insulin resistance, T2D (Bergman and Ader, 2000) and cardiovascular disease (CVD) (Rioux and Legrand, 2007).

Unsaturated fatty acids contain one or more double bonds between carbon atoms in the aliphatic chain. They represent the major constituent of phospholipidic membrane in the cells. The most abundant unsaturated fatty acids are oleic acid, which is obtained from olive oil but is also produced in the body, linoleic acid, and α-linoleic acid. Linoleic and α-linoleic acids are designated essential acids since they cannot be synthetized in the cells and can only be supplied by the diet (Anez-Bustillos *et al.*, 2017).

Fatty acids in the organism can either come from the endogenous *de novo* lipogenesis (DNL) from carbohydrates, or they can derive from the diet. Various pieces of evidence indicate that the first option plays a minimal role *in vivo*. The exogenous origin therefore represents the preferred, major route of fatty acid supply to the body (Hellerstein, 2001).

Once absorbed at intestinal level and entered into the bloodstream, free fatty acids are transported by albumin to the target tissues. Here, they can pass through the cellular membranes by passive diffusion or, alternatively, by facilitated transport (Dourlen *et al.*, 2015). The mechanism of passive diffusion, also called flip-flop, is the preferential mechanism in a state of positive energy balance. It does not require waste of energy since is determined by the concentration gradient of fatty acids outside the cell. Otherwise, when the energy demand raises, passive diffusion is not quick enough to supply adequate amounts of fatty acids to the cell. As a consequence, transport of fatty acids into the cell is mediated by specific proteins such as the plasma membrane-associated fatty acid binding protein (FABPpm), particularly expressed in heart and skeletal muscle, and the transmembrane fatty acid transport proteins (FATPs), widely distributed in many tissues (Kawaguchi *et al.*, 2014). After fatty acids have finally entered into the tissue, they can either be metabolized to produce energy, or stored. The different destination depends on the type of tissue and on the body's energy demand. In liver and adipose tissue, fatty acids are usually re-esterified to form TG. In a physiological fed state, these molecules can be stored as a reserve of energy until necessary. In heart and skeletal muscle, fatty acids represent the preferential substrate for energy. Thus, once entered into these tissues, fatty acids are mainly metabolized through the β-oxidation process (Cahill, 2006).

I. 1.2.1.1. Fatty acid oxidation

The β-oxidation process is responsible for the degradation of fatty acids with short, medium and long aliphatic chain and contributes to production of many ATP molecules through the oxidative phosphorylation. For example, the oxidation of one molecule of palmitic acid leads to the production of 106 ATP molecules (Berg J, 2008).

The β-oxidation takes place into the mitochondrion, which is a double membrane-bound organelle. It contains outer and inner membranes composed of phospholipid bilayers and proteins separated by an intermembrane space. Fatty acids that have entered inside the cell, must be transported through the mitochondrial membrane to be oxidized. A previous activation is required, and fatty acids are esterified with a molecule of coenzyme A (Co-A) (Wang *et al.*, 2009) to form the acyl-CoA thioesters. This reaction is catalyzed by the enzyme fatty acyl-CoA synthetase. Once activated, fatty acyl-CoAs can pass the mitochondrial membrane through a mechanism of facilitated transport that involves the protein carnitine-palmitoyl transferase 1 (CPT1) (Rogers *et al.*, 2014).

I. 1.2.1.1.1. CPT1

The carnitine palmitoyltransferase system is an essential step in the β-oxidation of fatty acids. This transfer system is necessary because, while fatty acids are activated on the outer mitochondrial membrane, the activated fatty acids must be oxidized within the mitochondrial matrix. Long chain fatty acids such as palmitoyl-CoA, unlike short- and

medium-chain fatty acids, cannot freely diffuse through the mitochondrial membranes, and require a shuttle system to be transported to the mitochondrial matrix (Kerner and Hoppel, 2000) (Figure I.3.).

CPT1 is an integral membrane protein that associates with the mitochondrial outer membrane through transmembrane regions in the peptide chain. It is responsible for the formation of acyl-carnitines by catalyzing the transfer of the acyl group of an activated fatty acyl-CoA from CoA to L-carnitine. The product is often palmitoyl-carnitine (thus the name), but other fatty acids may also be substrates. This "preparation" allows for subsequent movement of the acyl-carnitine from the cytosol into the intermembrane space of mitochondria. Then, a translocase protein, called carnitine/acyl-carnitine translocase (CACT), transports the acyl-carnitine molecules from the intermembrane space into the mitochondrial matrix. Once in the mitochondria, the acyl-carnitine is re-converted into acyl-CoA by the enzyme CPT2 that catalyzes the inverse reaction of CPT1. CPT2 isoform is associated to the inner membrane of the mitochondria and, in contrast to the CPT1 isoform, does not represent a limiting step for the β-oxidation process (McGarry and Brown, 1997).

I. 1.2.1.1.2. The oxidation cascade

After re-conversion into acyl-CoA thioesters, fatty acids undergo reactions which include oxidation, hydration and thiolysis. Oxidation is catalyzed by the enzyme medium-chain acyl-CoA dehydrogenase (MCAD) in the mitochondria, or by the enzyme acyl-CoA oxidase (ACOX) in the peroxisomes (Thorpe and Kim, 1995; Varanasi *et al.*, 1994). For each cycle, a molecule of acetyl-CoA is released and the two cofactors nicotinamide adenine dinucleotide hydrate (NADH) and flavin adenine dinucleotide hydrate (FADH), in their reduced form, are produced.

The fatty acid chain is cut and shortened, since it loose two atoms of carbon during every cycle. This cascade proceeds until the last acetyl-CoA molecule is released.

In physiological conditions, the acetyl-CoA produced during fatty acid oxidation, enters the Krebs cycle to be oxidized to carbon dioxide and used to generate more molecules of NADH. On the other end, FADH and NADH cofactors formed during β-oxidation, undergo the oxidative phosphorylation process in order to produce ATP (Rogers *et al.*, 2014) (Figure I.3.).

I. 1.2.1.1.3. The oxidative phosphorylation

During oxidative phosphorylation, electrons are transferred from electron donors, such as NADH and FADH molecules, to electron acceptors, such as oxygen, in redox reactions. These redox reactions release energy, which is used to form ATP. The energy released by electrons flowing through this electron transport chain is used to transport protons across the inner mitochondrial membrane, in a process called electron transport. This generates

potential energy in the form of a pH gradient and an electrical potential across this membrane (Rogers *et al.*, 2014).

This store of energy is tapped when protons flow back across the membrane and down the potential energy gradient, through a large enzyme called ATP synthase. The ATP synthase uses the energy to transform adenosine diphosphate (ADP) into ATP, in a phosphorylation reaction (Figure I.3.).

The inner membrane of mitochondria accommodates many copies of the respiratory chain components, or OXPHOS complexes (I–IV). Together with ATP synthase (complex V) they form the machinery for ATP production. Complexes I–IV are multi-subunit enzymes that work in concert to create the electrochemical proton gradient across the mitochondrial inner membrane that is used by the ATP synthase to produce ATP via oxidative phosphorylation (Rogers *et al.*, 2014). During catalysis, the electron transfer between the complexes is mediated by two small components: lipid-soluble ubiquinone and water-soluble cytochrome c. They diffuse between the respiratory complexes I and III, and III and IV, respectively, and the latter takes them to form water from molecular oxygen. Many diseases and disorders, including insulin resistance, have been associated with a dysfunction in the activity of OXPHOS proteins (Chaban *et al.*, 2014).

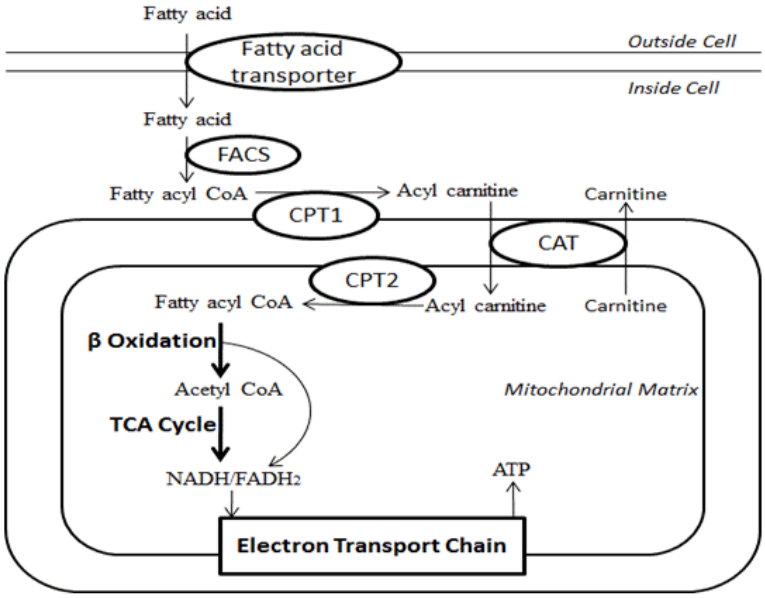

Figure I.3. Fatty acid transport and oxidation in the mitochondria: the enzymes CPT1 and 2 are responsible for the entrance of fatty acyl-CoAs into the mitochondria by exchanging them with carnitine. Once in the mitochondria matrix, the fatty acyl-CoA undergo the β-oxidation process that convert them into acetyl-CoA. Later, acetyl-CoA participates into the tricarboxylic acid (TCA) cycle where it is oxidized to CO_2. The TCA cycle provides reduced cofactors NADH and FADH, necessary for the electron transport chain to produce ATP (Fillmore *et al.*, 2014).

Next, some of the main molecular components involved in lipid metabolism and relevant to this thesis will be described.

I. 1.2.1.1.4. ACC

The ACC is the enzyme responsible for the first step of fatty acid synthesis. It catalyzes the irreversible carboxylation of acetyl-CoA to produce malonyl-CoA. This step requires a molecule of ATP.

The function of ACC is to regulate the metabolism of fatty acids. In fact, its product, malonyl-CoA, is a potent inhibitor of CPT1 activity (Brownsey *et al.*, 1997). When fatty acids synthesis is elevated, malonyl-CoA levels raise and inhibit CPT1, thus blocking the transfer of the fatty acyl group from acyl-CoA to L-carnitine. This step represents the limiting step for fatty acid oxidation in the mitochondria. Consequently, fatty acid degradation is blocked. This mechanism allows a precise balance between fatty acid synthesis and metabolism.

In mammals, two main isoforms of ACC are expressed, ACC1 and ACC2, which differ in both tissue distribution and function. ACC1 is found in the cytoplasm of all cells but is more abundant in lipogenic tissues, such as adipose tissue and lactating mammary glands, where fatty acid synthesis is important. In oxidative tissues, such as the skeletal muscle and the heart, the levels of ACC2 expressed are higher. ACC1 and ACC2 are both highly expressed in the liver where both fatty acid oxidation and synthesis are important. The differences in tissue distribution indicate that ACC1 maintains regulation of fatty acid synthesis whereas ACC2 mainly regulates fatty acid oxidation (Brownsey *et al.*, 1997).

The regulation of ACC is complex. It can be controlled transcriptionally by multiple promoters, or it can be regulated by direct phosphorylation.

ACC is inactive in the phosphorylated form while is activated through dephosphorylation. As mentioned above, insulin can activate ACC by inducing its dephosphorylation and promoting fatty acid synthesis (Witters *et al.*, 1988). On the contrary, protein phosphorylation and inactivation can result when glucagon or epinephrine bind to cell surface receptors. These receptors are coupled to protein G and their activation leads to the production of cAMP as secondary messenger. cAMP can in turn activate PKA that is responsible for the phosphorylation of ACC.

However, the main cause of ACC phosphorylation is the rise in AMP levels when the energy status of the cell is low, leading to the activation of AMP-activated protein kinase (AMPK). This is the main kinase regulator of ACC, able to phosphorylate a number of serine residues on both isoforms of ACC and thus convert the enzyme into its inactive form (Witters and Kemp, 1992).

I. 1.2.1.1.5. AMPK

AMPK is an enzyme that plays a critical role in cellular energy homeostasis. It belongs to a highly conserved eukaryotic protein family and it consists of three subunits (α, β and γ) that together make a functional enzyme. It is expressed in a number of tissues, including the liver, brain, and skeletal muscle (Day *et al.*, 2017).

The net effect of AMPK activation is stimulation of hepatic fatty acid oxidation, stimulation of skeletal muscle fatty acid oxidation and glucose uptake, inhibition of lipogenesis and TG synthesis and modulation of insulin secretion by pancreatic β-cells.

Functionally, AMPK is a serine/threonine kinase that becomes activated when phosphorylation takes place at threonine 172 in its catalytic domain (α subunit).

That residue is phosphorylated by at least two kinases: the liver kinase B1 (LKB1) and the calcium-/calmodulin-dependent kinase kinase 2 (CAMKK); and is dephosphorylated by many phosphatases such as the protein phosphatase 2A (PP2A) and the protein phosphatase 2C (PP2C) (Stapleton *et al.*, 1996).

AMPK is a sensor of ATP/AMP ratio and, thus, of cell energy level. In fact, AMPK is regulated allosterically mostly by competitive binding on its γ subunit between ATP (which allows phosphatase access to Threonine 172 and consequent dephosphorylation and inactivation of the enzyme) and AMP (which blocks the access on the Threonine 172 residue to phosphatases). During exercise or starvation, the ATP/AMP ratio in skeletal muscle decreases, leading to the activation of AMPK.

A part from the binding of ATP and AMP to the γ subunit, there are other mechanisms by which AMPK can be regulated; some of them involve multiple phosphorylation on other amino-acidic residues (Day *et al.*, 2017). For example, insulin inhibits AMPK by inducing its direct phosphorylation on the residues of Serine 48 in the α subunit, thus inducing a conformational change that prevents AMPK activation by the other upstream kinases (He *et al.*, 2016).

AMPK has numerous substrates and exerts different functions (Figure I.4.). As already explained, the principal substrate for AMPK is the ACC protein. When AMPK phosphorylates ACC, the enzyme is inactivated and the production of malonyl-CoA is blocked. The result is the inhibition of endogenous fatty acid synthesis and the increase in fatty acid oxidation (Jeon, 2016).

Another target for AMPK activity is HSL. AMPK activates the lipase, thus promoting lipolysis in the adipose tissue. Further, AMPK also phosphorylates and inactivates the AS160 protein, which exerts an inhibitory effect on the Rab-GTPase-activating protein. Consequently, the AMPK-mediated inhibition of AS160 increases the activity of Rab family GTPase proteins and induces fusion of GLUT4 vesicles with the plasma membrane. This cascade results in a promotion of glucose uptake in skeletal muscle (He *et al.*, 2016; Jeon, 2016). AMPK also stimulates glycolysis by activating phosphorylation of

phosphofructokinase 2 (PFK2) and inhibits glycogen synthesis through inhibitory phosphorylation of glycogen synthase (GS).

Moreover, AMPK is involved in mitochondrial biogenesis that is a crucial process for energy production and cellular response during nutrient deficiency. Genetic evidence indicates that AMPK controls mitochondrial biogenesis by regulating peroxisome proliferator-activated receptor (Price *et al.*) gamma coactivator 1α (PGC1α), a co-factor that promotes the transcription of nuclear-encoded mitochondrial genes (Minokoshi *et al.*, 2004; Price *et al.*, 2012).

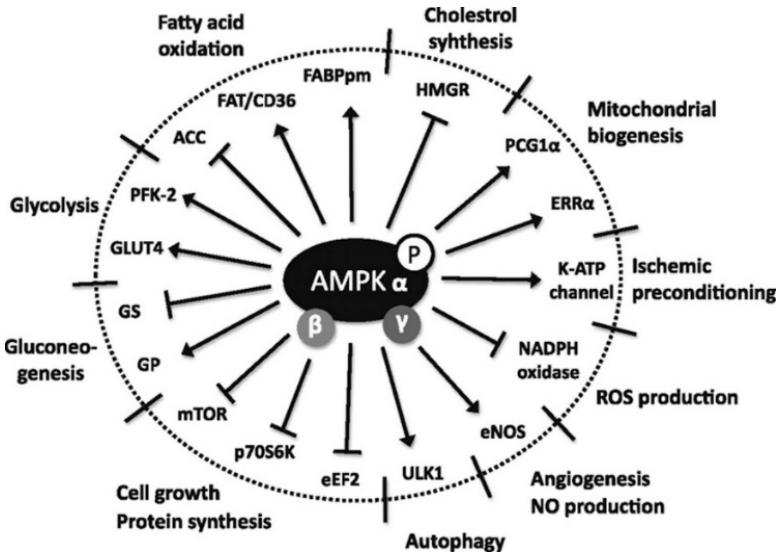

Figure I.4. AMPK substrates and functions. Under conditions of energy deficiency, the AMP/ADP ratio increases and AMPK is activated. Once phosphorylated, AMPK can activate several downstream pathways in order to maintain energy balance in the body (Harada *et al.*, 2012)

I. 1.2.1.1.6. <u>Peroxisome proliferator-activated receptors (PPARs)</u>

PPARs belong to the superfamily of nuclear receptors and work as transcriptional factors, regulating the expression of many genes. Three types of PPARs have been identified: α, γ, and β/δ. The α isoform is predominantly expressed in liver, kidney, heart, muscle and adipose tissue. The β/δ isoform is expressed in many tissues but markedly in brain, adipose tissue and skin. The γ isoform can be divided into four subtypes: γ1, virtually expressed in all tissues including heart, muscle, colon, kidney, pancreas, and spleen; γ2, expressed mainly in adipose tissue; γ3, expressed in macrophages, large intestine and white adipose tissue, and γ4, expressed in endothelial cells.

All PPARs isoforms share the same molecular structure. They contain an A/B domain that is located close to the N-terminus of the peptide chain and is responsible for the ligand-independent activation of the receptor; a C domain which is designate to the union with

specific regions of the target genes; a D domain involved in the interaction with many cofactors; and a E/F domain located close to the C-terminus, which contains the binding site for the ligands (Lee *et al.*, 2017).

To be functionally active, PPARs need to heterodimerize with the retinoid X receptor (RXR). The PPAR-RXR heterodimers bind to DNA sequences termed peroxisome proliferator response elements (PPREs) that are located in the promotor region of their target genes. In the absence of ligands, high affinity complexes are formed between PPAR-RXR heterodimers and nuclear co-repressor proteins that block gene transcription by sequestrating the heterodimer form the promoter region. Once the PPAR binds its ligand, a conformational change occurs resulting in dissociation of the co-repressor protein and binding to the PPRE sequences. Transcription of target genes is increased or decreased, depending on the gene (Clarke *et al.*, 1999; Tyagi *et al.*, 2011).

Endogenous ligands for PPARs include free fatty acids and eicosanoids. PPARs can regulate the expression of genes related with lipid metabolism, glucose homeostasis, cell differentiation and proliferation, inflammatory process and immune response.

PPAR ligands not only regulate the DNA-binding activity of PPARs, but also may control phosphorylation cascades, which in turn govern the phosphorylation status of PPARs. For instance, activation of the ERK1/2 protein kinase appears to increase the phosphorylation state of certain PPARs, which in turn alter their DNA-binding activity. Conversely, AMPK can improve PPARs activity and consequently increase mitochondrial biogenesis.

Regulation of gene transcription by PPARs extends beyond their ability to activate specific target gene in a ligand-dependent manner. In fact, it has been reported that the heterodimer itself, without binding to PPRE sequences, can downregulate the expression of other transcription factors. Among these, one of the most important is the signal transducer and activator of transcription (STAT), which is involved in the inflammatory response. Its inhibition can explain most of the anti-inflammatory effects of the PPARs (Tyagi *et al.*, 2011).

<u>PPARα</u>

The expression of the PPARα gene is highest in tissues with active fatty acid catabolism. These include liver, heart, brown adipose tissue, small and large intestine, and skeletal muscle. The role of PPARα in these tissues is to exert its effects on overall fatty acid catabolism. To exert its effects on lipid metabolism, PPARα must itself be targeted for transcriptional activation. Expression of the PPARα gene is regulated by numerous stimuli including stress and insulin release. In the liver, PPARα expression is activated in response to starvation, which allows for increased expression of PPARα target genes, leading to increased catabolism of fatty acids. PPARα is activated by several endogenous ligands such as arachidonic acid, linoleic acid, and many eicosanoids. Synthetic ligands for PPARα belong to the family of fibrates and are currently used as drugs against dyslipidemia.

PPARα also plays an important role in the inflammatory response, reducing the expression of many genes involved in the process (Lefebvre *et al.*, 2006).

PPARβ/δ

Activation of PPARβ/δ in adipose tissue, skeletal muscle, and cardiac muscle exerts a broad range of effects on cell growth, glucose homeostasis, lipid metabolism, and inflammatory responses. In adipose tissue, activation of PPARβ/δ results in increased expression of genes involved in fatty acid oxidation, such as ACOX, CPT1, and MCAD. PPARβ/δ also activates genes involved in TG metabolism such as HSL. In skeletal muscle, PPARβ/δ is involved in fatty acid transport and oxidation, mitochondrial respiration and thermogenesis, and oxidative metabolism. Expression of PPARβ/δ in skeletal muscle is 10- and 50-fold higher than PPARα and PPARγ, respectively. Activation of PPARβ/δ in skeletal muscle results in increased expression of some of the OXPHOS complexes involved in oxidative phosphorylation, such as the cytochrome oxidase II and the cytochrome oxidase IV. Fasting results in increased expression of PPARβ/δ, indicating that the receptor mediates the fasting-dependent rise in skeletal muscle fatty acid oxidation (Barish *et al.*, 2006).

Unlike PPARα and PPARγ, for which synthetic pharmacologically relevant ligands have been approved for clinical use, no PPARβ/δ agonists are currently available as drugs. However, several synthetic ligands have been identified and are being tested for treating dyslipidemias. Natural ligands for PPARβ/δ include 14– to 18–carbon fatty acids, 16– to 20-carbon polyunsaturated fatty acids (PUFAs), TG, prostacyclin I2 (PGI2), prostaglandin A1 (PGA1), and retinoic acid (Barish *et al.*, 2006).

PPARγ

PPARγ was originally identified as being expressed in differentiating adipocytes. It is now recognized as a master regulator of adipogenesis and is abundantly expressed in adipose tissue. PPARγ was identified as the target of the thiazolidinedione (TZD) class of insulin-sensitizing drugs. The mechanism of action of the TZDs is a function of the activation of PPARγ and the consequent induction of genes necessary for differentiation of adipocytes. This effect of PPARγ leads to increased secretion of insulin-sensitizing adipocytokines such as adiponectin from adipocytes. PPARγ is also involved in glucose homeostasis, since its activation enhances transcription of genes related with gluconeogenesis. In addition, PPARγ also plays a role in anti-inflammatory and anti-cancer pathways (Lehmann *et al.*, 1995).

I. 1.2.1.1.7. PGC1α

PGC1α is a transcriptional co-activator that regulates many genes involved in energy metabolism and mitochondrial biogenesis. This co-factor interacts with multiple transcription factors: among these, it activates the nuclear receptor PPARγ, the

mitochondrial transcription factor A (Tfam), the nuclear respiratory factors 1 and 2 (NRF1 and NRF2), thus inducing hundreds of nuclear encoded genes related with mitochondrial biogenesis (such as the OXPHOS complexes of the respiratory chain). Moreover, PGC1α increases the expression of antioxidant enzymes, such as superoxide dismutase 1 (SOD1) and sirtuins (Leick *et al.*, 2010), as well as genes related with glucose homeostasis, including PEPCK and G6Pase (Yoon *et al.*, 2001).

Consistent with its powerful role in cellular metabolism, PGC1α is heavily regulated both transcriptionally and post-transcriptionally, including direct phosphorylation by AMPK, PKA, GSK3 and Akt, and direct deacetylation by sirtuin1 (SIRT1) (Finck and Kelly, 2006) (Figure I.5.). PGC1α activity is also regulated by the NADH quinone oxidoreductase 1 (NQO1), a protein that is involved in oxidative phosphorylation and works as a sensor of the redox state of the cell (Adamovich *et al.*, 2013). It has been reported that the cAMP response element binding proteins (CREB) heavily increases PGC1α expression by binding to its promoter (Vercauteren *et al.*, 2006). On the contrary, the pro-inflammatory transcription factor nuclear factor-kappa B (NFκB) negatively downregulates PGC1α expression (Alvarez-Guardia *et al.*, 2010).

PGC1α is highly expressed in skeletal muscle, a tissue that has an important oxidative capacity. Endurance exercise has been shown to activate the PGC1α gene in human skeletal muscle (Holloszy, 1967). In fact, the increased calcium signaling during muscle contraction activates Ca^{2+}/calmodulin dependent protein kinase IV (CAMK IV), which in turn activates CREB transcription factor and leads to increased PGC1α expression (Baar *et al.*, 2002). The β-adrenergic stimulation also contributes significantly to PGC1α induction, by activating CREB transcription factor (Pilegaard *et al.*, 2003). In skeletal muscle, PGC1α not only regulates mitochondrial biogenesis, but also enhances expression of fatty acid transporter and induces angiogenesis. Thus, it plays a pivotal role in generating ATP and providing nutrients to the muscle (Tadaishi *et al.*, 2011). Moreover, increased expression of PGC1α in transgenic mice, has been shown to enhance glucose uptake, via increase in GLUT4 expression (Michael *et al.*, 2001). PGC1α can also increase fatty acid oxidation through the activation of PPARs receptors, and regulate lipid metabolism in skeletal muscle. Moreover, PGC1α was found to repress glucose oxidation in muscle cell lines by activating the expression of the gene encoding pyruvate dehydrogenase kinase 4 (PDK4). These latter results suggest that PGC1α controls muscle fuel selection by increasing fatty acid oxidation, while temporarily shutting down glucose oxidation. Inhibition of glucose oxidation combined with increased muscle glucose uptake could serve to replenish muscle glycogen stores to prepare for the next bout of exercise (Wende *et al.*, 2007).

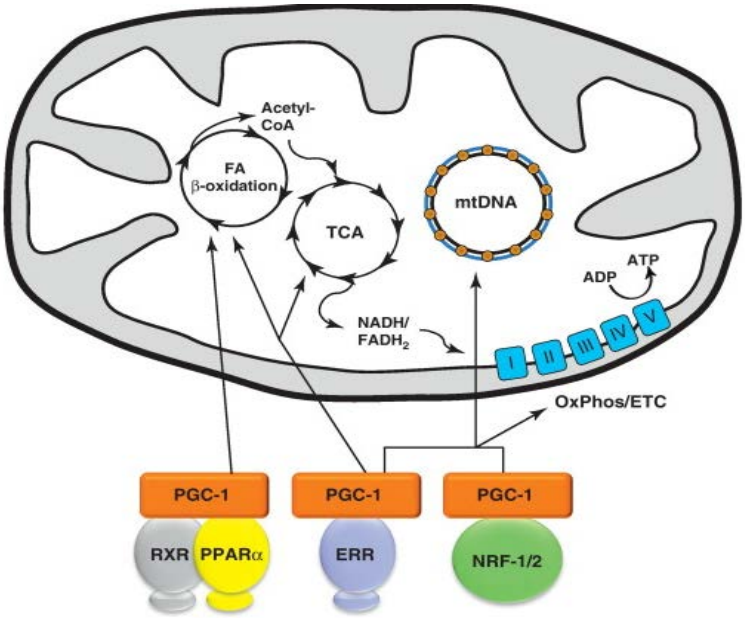

Figure I.5. PGC1α transcriptionally controls mitochondrial biogenesis and metabolism. PGC1α works as co-activator of several transcription factors, such as the nuclear respiratory factors 1 and 2 (NRF1 and 2) or the estrogen-related receptor (ERR) and the peroxisome proliferator-activated receptors (PPARs), which are involved in lipid metabolism, energy balance and mitochondrial biogenesis (Miura *et al.*, 2003).

I. 1.2.2. Plasma lipoproteins

During a situation of prolonged fasting when glucose levels are low, body starts to mobilize its TG stocks from the adipose tissue, through the lipolytic process.

Once the HSL has hydrolyzed TG molecules, they can enter into the bloodstream to reach other tissues. Since TG are apolar compounds, they need a carrier to be transported in the aqueous environment (polar) that is blood. Lipoproteins are responsible for this transportation. Once lipids have been released to the tissues, lipoprotein remnants deprived of their TG content can be re-uptaken by the liver. This cycle contributes to maintain an accurate lipid homeostasis in the blood (De Groot LJ, 2015) (Figure I.6.).

Lipoproteins are macromolecular structures formed by the association of proteins and lipids. They are constituted by two parts: an envelope and the core. The envelope is formed mainly by amphipathic lipids of the kind of phospholipids. These phospholipids have their polar part oriented to the aqueous surface, while the apolar part interacts with the hydrophobic core of the lipoprotein, formed mainly by cholesterol esters and TG.

The proteins that form these structures are called apolipoproteins. The hydrophilic amino acids of these apolipoproteins are oriented to the outside, while the hydrophobic amino acids interact with the apolar part of the lipoprotein structure (De Groot LJ, 2015). There are different kinds of lipoproteins, classified according to their density.

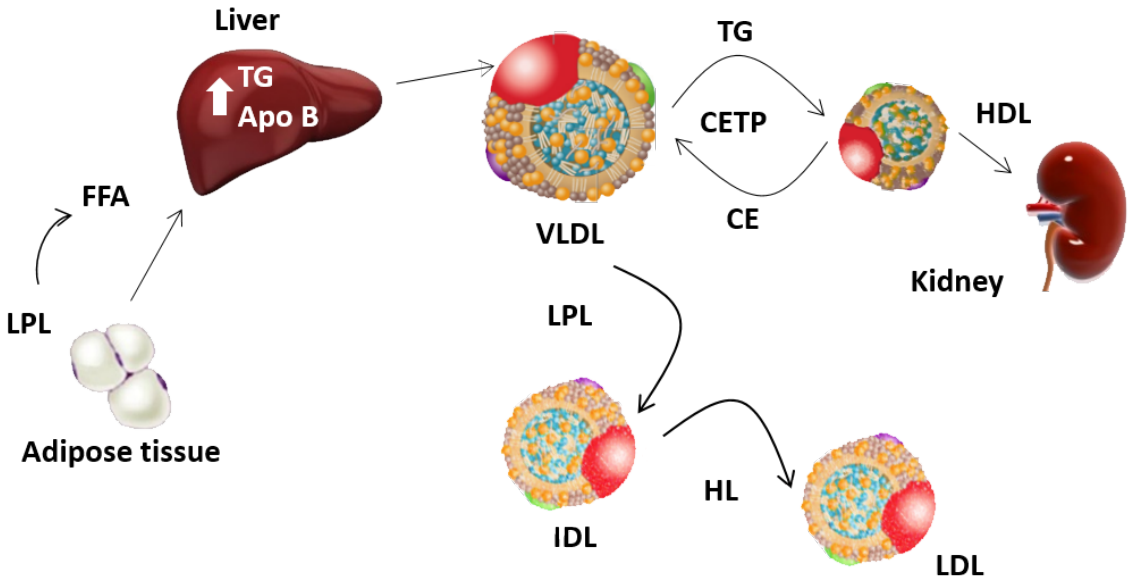

Figure I.6. Lipoprotein metabolism in physiological conditions. Lipolysis in adipose tissue supplies fatty acids necessary for VLDL assemblage in liver. VLDL contain TG (Ebtehaj *et al.*, 2017), cholesterol esters (CE), phospholipids and apolipoproteins. When VLDL release part of their TG through the action of lipoprotein lipase (LPL) they become IDL that are further metabolized by the hepatic lipase (HL) to LDL, that mainly contain cholesterol. VLDL also exchange cholesterol molecules with the HDL lipoproteins through the action of the cholesteryl ester transfer protein (CETP) (Fisher, 2012).

I. 1.2.2.1. Very low-density lipoproteins (VLDL)

VLDL are characterized by a diameter of 30-80 nm and a very low-density. They can be synthetized by the liver or the intestine, even though hepatic VLDLs are the most abundant (Gibbons *et al.*, 2004).

VLDL formation is highly dependent on the accumulation of TG in the cytosol, and several authors have demonstrated that fatty acids used for the biosynthesis of VLDL are derived from TG stored in cytosolic lipid droplets (Olofsson *et al.*, 2009). Other potential sources of fatty acids for VLDL synthesis include: 1) peripheral fats stored in adipose tissue that flow to the liver via the plasma pool of fatty acids linked to serum albumin; 2) fatty acids synthetized within the liver trough DNL; 3) dietary fatty acids transported via chylomicrons; 4) uptake of chylomicron remnants by the liver (Boren *et al.*, 1993).

Nascent VLDL assembled in the liver contain apolipoproteins, TG, cholesterol and phospholipids. TG constitute the primary component (up to 60%). The assembly of VLDL involves a stepwise lipidation of the structural protein apolipoprotein B100 (Apo B100) in the liver. The initialing step is a lipidation of Apo B100 by microsomal triglyceride transfer protein (MTP) in the rough ER. This results in the formation of a primordial pre-VLDL lipoprotein particle, which is converted in a TG-poor VLDL by additional lipidation. The TG-

poor VLDL, also called light VLDL, can either be secreted from the cells or furthered lipidated to form a mature TG-rich VLDL particle, also known as dense or large VLDL (Olofsson *et al.*, 2000).

Among the apolipoproteins, nascent VLDL contain one molecule of Apo B100 per particle, and several other apolipoproteins, such as apoliprotein CI (Apo CI) and apolipoprotein E (Apo E); however, they can enrich this pool after exchanging with other lipoproteins in the bloodstream. Once in the circulation, VLDL pick also apolipoprotein CII (Apo CII) and apolipoprotein CIII (Apo CIII) from other lipoproteins.

Apo B100 can interact with the VLDL receptor (VLDLR) that mediates lipid entry into the cell, while Apo E is necessary for hepatic uptake. In fact, VLDLR is highly expressed in adipose tissue, heart and skeletal muscle but is virtually absent in liver (Adiels *et al.*, 2008b).

Apo CII is responsible for the activation of lipoprotein lipase (LPL), an enzyme attached to the luminal surface of endothelial cells in capillaries of different tissues. LPL hydrolyzes TG in the VLDL and releases them (Olofsson and Boren, 2012; Olofsson *et al.*, 2007). Consequently, the VLDL lose part of their TG and the proportion of cholesterol in the lipoprotein increases. The VLDL remnant is called intermediate-density lipoprotein (IDL) and can be further delipidated to generate low-density lipoproteins (LDL) (Adiels *et al.*, 2008a).

Apo CIII is the most abundant apolipoprotein in diabetic and hypertrigliceridemic patients and seems to play a role in insulin resistance (Hiukka *et al.*, 2005).

I. 1.2.2.1.1. Apo CIII

Apo CIII is synthetized in the liver and freely exchanged between lipoprotein particles. It is found in association with chylomicrons, VLDL, and high-density lipoproteins (HDL). Is a protein composed of 79 amino acids with a molecular weight of 8,8 KDa. Apo CIII has been identified as a key modulator of plasma TG concentration (Ooi *et al.*, 2008). It has three actions that can impair plasma lipoprotein metabolism and lead to hypertriglyceridemia: 1) Apo CIII dampens clearance of lipoproteins from the circulation by interfering with their binding to hepatic Apo B100/Apo E receptor masking the binding site. 2) Apo CIII inhibits LPL that hydrolyzes TG in the VLDL and facilitates their clearance from plasma. As a result, TG are accumulated and contribute to the development of hypertriglyceridemia. 3) Apo CIII stimulates VLDL synthesis and secretion by the liver.

Recent studies have shown that loss of function in Apo CIII leads to a decrease in serum TG levels and a reduced risk of CVD (Digenio *et al.*, 2016; Pollin *et al.*, 2008). On the contrary, mice overexpressing Apo CIII show high plasma TG and display increased insulin resistance (Lee *et al.*, 2011). It has also been reported that Apo CIII itself can directly affect

atherogenic mechanisms in vascular cells increasing the adhesion of human monocytes to vascular endothelial cells.

I. 1.2.2.2. IDL

IDL are formed when VLDL particles lose many of their TG after interacting with the LPL. They are characterized by an intermediate density and contain up to 40% of cholesterol. IDLs have two metabolic fates: to be up-taken by hepatocytes in an Apo E-mediated process, or to continue losing TG and become LDL (Soutar *et al.*, 1982).

I. 1.2.2.3. LDL

LDL represent the major cholesterol-carrying lipoproteins in humans and constitute the fraction most strongly implicated in atherogenesis.

LDL particles are approximately 20 nm to 28 nm in diameter. Each particle contains a single Apo B100 molecule, along with 80 to 100 additional apolipoproteins, such as the Apo E. LDL can interact with their receptor through the Apo B100. This protein binds to its receptor and form a complex, which is endocytosed by the cell. The binding is enhanced by the presence of the Apo E (Dergunov *et al.*, 2005). For this reason, the LDL receptor is also sometimes referred to as the Apo B100/Apo E receptor. The lack of Apo B100 or its alteration drastically reduces LDL uptake from tissues, thus increasing blood cholesterol levels (Boren *et al.*, 1993). The longer LDL remain in the blood, the greater the protein and lipid components will become oxidized, thus increasing risk for intravascular inflammation and atherogenesis. Insulin increases the binding of LDL to their receptor in liver cells. The precise mechanism for this effect is unclear, but might be mediated through the regulation of Apo B100 degradation. The effects of insulin on hepatic LDL binding may explain the hypercholesterolemia and increased risk of atherosclerosis that have been shown to be associated with uncontrolled diabetes (Castelli *et al.*, 1986; Mahley *et al.*, 1984).

I. 1.2.2.4. HDL

HDL represent a heterogeneous population of lipoproteins, possessing different sizes, protein content, and lipid composition. One of the major functions of HDL is to acquire cholesterol from peripheral tissues and transport this cholesterol back to the liver, where it can ultimately be excreted following conversion to bile acids. This function is referred to as reverse cholesterol transport (RCT). The role of HDL in RCT represents the major atheroprotective function of this class of lipoprotein. In addition to RCT, HDLs exert anti-inflammatory, antioxidant, and vasodilatory effects that together represent additional atheroprotective functions of HDL. Of note, the levels of this atheroprotective lipoprotein are decreased in diabetic dyslipidemia (Adiels *et al.*, 2008a).

The primary apolipoproteins of HDLs are Apo AI, Apo AII, Apo CI, Apo CII and Apo E, but they contain many others. In fact, a major function of HDL is to act as a circulating store

of Apo CI, Apo CII and Apo E to exchange with other lipoproteins, such as VLDL. Apo AI is the most abundant protein in HDLs, constituting over 70% of the total protein mass (Gordon *et al.*, 1989; Mahley *et al.*, 1984).

Apo AI is an activator of lecithin/cholesterol acyltransferase (LCAT), the enzyme responsible for cholesterol esterification in the HDL particles.

Apo AII is synthesized in the liver and is the second most abundant protein on HDL accounting for approximately 20% of HDL protein.

Table I.1. shows the lipid and apolipoprotein distribution between the different types of apolipoproteins.

	VLDL	IDL	LDL
E-C-			
TG	44.7 ± 19.5	48.9 ± 49.6	85.8 ± 20.0
Cholesterol	22.5 ± 15.0	16.5 ± 6.6	629 ± 130
ApoB	14.0 ± 12.0	19.6 ± 12.1	832 ± 345
E+C-			
TG	16.2 ± 11.8	5.6 ± 5.3	2.5 ± 3.1
Cholesterol	3.3 ± 2.2	0.4 ± 0.6	2.6 ± 1.2
ApoB	2.5 ± 1.1	0.6 ± 0.3	1.3 ± 0.3
ApoE	29.9 ± 25.2	13.3 ± 10.5	17.3 ± 10.9
E+C+			
TG	125.1 ± 76.8	27.7 ± 11.8	27.7 ± 18.8
Cholesterol	24.2 ± 10.6	2.6 ± 1.4	4.6 ± 2.4
ApoB	12.6 ± 5.7	2.8 ± 1.8	2.1 ± 2.1
ApoE	204 ± 110	15.2 ± 9.3	22.3 ± 10.2
ApoCIII	238 ± 170	nd	nd
E-C+			
TG	108.7 ± 46.4	51.5 ± 34.1	30.8 ± 12.1
Cholesterol	10.3 ± 4.0	3.1 ± 1.4	6.2 ± 2.0
ApoB	3.8 ± 1.2	2.8 ± 1.2	4.1 ± 4.3
ApoCIII	108.5 ± 107.6	18.4 ± 13.7	nd

Table I.1. Lipid and apolipoprotein distribution in VLDL, IDL and LDL subfractions in healthy subjects (Khoo *et al.*, 1999). Lipoproteins contain one molecule of Apo B100 per particle, but they differ for their content of Apo E and Apo C: lipoproteins not containing Apo E nor Apo C (E-C-), lipoproteins containing Apo E but not Apo C (E+C-), lipoproteins containing both Apo E and Apo C (E+C+), lipoproteins containing Apo C but not Apo E (E-C+). TG and cholesterol concentrations are expressed in µM; apolipoproteins concentrations are expressed in nM; nd: not determined.

I. 2. Insulin resistance

Insulin resistance is the pathological condition in which cells fail to respond properly to the hormone insulin. It develops in multiple organs and predicts and precedes T2D (Grundy, 2008). Often, insulin resistance is secondary to obesity and develops in obese patients because of the increase in TG and fatty acids levels and the accumulation of lipids in non-adipose tissues (Boden, 2002b). In fact, obesity is associated with a dysfunctional adipose tissue, which is not able to properly handle the normal lipid metabolism and is responsible for several abnormalities, including an excessive accumulation of lipids in the adipose tissue, increased levels of TG and fatty acids in blood, and increased release of adipokines (Boden and Shulman, 2002). Several studies have correlated obesity with insulin resistance (Arner, 2002; Coughlan *et al.*, 2013; de Ferranti and Mozaffarian, 2008). However, insulin resistance also develop in non-obese subjects (DeFronzo and Tripathy, 2009), showing that insulin resistance depends on many other factors, including life style, genetic causes and hormonal changes (Guo, 2014).

What is certainly known is that impaired lipid metabolism and increased fatty acid levels play a pivotal role in the development of insulin resistance (Arner, 2002; Sears and Perry, 2015). The inverse correlation between high fatty acid concentrations and decreased insulin sensitivity suggested that altered fatty acid metabolism may have a primary role in causing insulin resistance in T2D (Petersen and Shulman, 2002).
On the other hand, insulin resistance can drive an increase in TG and fatty acids levels (Yazici and Sezer, 2017). In fact, insulin plays a pivotal role in the regulation of lipid metabolism and consequently any impairment in insulin functions would lead to alteration in the lipid content.

At present, the mechanisms that lead to the development of insulin resistance have not been completely elucidated. Many authors have suggested a new intriguing point of view that considers T2D not only a glucose-related disease but also a lipid-related disease, since insulin dysfunction not only results in high serum glucose but also in high serum TG levels (Shafrir and Raz, 2003).

I. 2.1. Insulin resistance and adipose tissue

The adipose tissue plays an important role in buffering the flux of dietary fat into the circulation in the postprandial period. This buffering action limits an abnormal increase in plasma lipids and protects other tissues from exposure to excessive lipid fluxes (Frayn, 2002). When the adipose tissue faces dysfunction, lipolysis is enhanced and consequently provokes a greater release of fatty acids (de Ferranti and Mozaffarian, 2008).
The causes of this dysfunction are currently unclear but can include genetic factors and hormonal changes (de Ferranti and Mozaffarian, 2008). For instance, changes in leptin and adiponectin levels are typical in obesity and provoke an over release of fatty acids in

the bloodstream (Cortes *et al.*, 2014). Moreover, transgenic (Tg) mice with a dysfunctional adipose tissue and severe lipodystrophy have very high plasma fatty acids and typically develop diabetes (Parker *et al.*, 2011).

The excess of fatty acids accumulates in the adipocyte and contributes to the development of insulin resistance. As previously mentioned, insulin promotes DNL and TG synthesis in adipose tissue, while inhibits lipolysis (Mayer *et al.*, 2007). As consequence, when the adipose tissue becomes insulin resistant, the insulin-induced inhibition of HSL is blunted. The result is an additional increase in lipolysis, which further contributes to a greater release of fatty acids in the bloodstream and to other tissues (Frayn, 2002). Moreover, insulin resistance in adipose tissue is characterized by a reduction in glucose uptake and glucose metabolism, which in turn increases the lipolysis ratio (Yazici and Sezer, 2017) (Figure I.7.).

Since most diabetic patients are also obese and show increased circulating levels of both TG and fatty acids, it is difficult to say whether insulin resistance in adipose tissue is a consequence, rather than a cause, of elevated circulating lipids.

Of note, the impairment in adipose tissue functions seems to generate an insidious pathologic loop in which lipid excess represents at the same time the cause and the consequence of insulin resistance.

I. 2.2. Insulin resistance and skeletal muscle

Many evidences suggest that in non-obese subjects insulin resistance first occurs in skeletal muscle and is therefore central to systemic insulin resistance and the development of T2D (Petersen *et al.*, 2007; Petersen and Shulman, 2002).

Skeletal muscle is the most important organ for whole-body glucose homeostasis and is responsible for approximately 80% of insulin-stimulate glucose disposal under normal conditions (Abdul-Ghani and DeFronzo, 2010).
In a physiological fed status, muscle converts 75% of glucose into glycogen and store it, whereas drives the remaining 25% into glycolysis. In a fasting status or during exercise, skeletal muscle switches to fatty acid oxidation to produce energy and starts to mobilize glycogen (Boden, 2002a).

In contrast to other tissues, the rate-limiting step for glucose metabolism in skeletal muscle is glucose uptake from blood (Petersen *et al.*, 2007).
Under insulin resistance conditions, skeletal muscle cannot uptake glucose even if its circulating levels are high; thus, it begins to metabolize fatty acids through the fatty acid oxidation process (DeFronzo and Tripathy, 2009) (Figure I.7.).

Many authors pointed that the cause of reduced glucose uptake in skeletal muscle during insulin resistance is the impairment of GLUT4 functionality. They demonstrated that GLUT4 translocation is altered in insulin resistance conditions, limiting the rate of sugar that enter into skeletal muscle (Kahn, 1992; Randle *et al.*, 1964). There are several different mechanisms responsible for GLUT4 failure, which are discussed further. The consequence of the reduction in GLUT4 functionality is an increase in lipid metabolism and a defect in glycogen synthesis (Petersen and Shulman, 2002).

Impaired glycogen synthesis is another of the primary defects observed in insulin resistance in muscle (DeFronzo and Tripathy, 2009)(Figure I.7.). Insulin inhibits GSK3 through an Akt-mediated phosphorylation. GSK3 is the enzyme responsible for the inactivation of GS. If GSK3 is inactivated by insulin, its inhibitory effect on GS is removed; consequently, GS starts to synthetize glycogen. When the insulin signaling pathway is altered, GSK3 does not respond to insulin, GS is inhibited, and glycogen synthesis is blunted.

The mechanisms that lead to the development of insulin resistance in skeletal muscle are not completely understood. Intracellular lipid accumulation and subsequent lipotoxicity have been reported to play an important role (Schaffer, 2003; Tumova *et al.*, 2016). In contrast to the liver and adipose tissue, skeletal muscle cannot synthetize fatty acids from carbon precursors (Tumova *et al.*, 2016). Thus, intramyocellular lipid accumulation is mainly caused by elevated levels of circulating fatty acids. Once accumulated into the cells, fatty acids can trigger inflammation in myocytes and provokes a release of a variety of inflammatory mediators into the vessels (de Ferranti and Mozaffarian, 2008; Tumova *et al.*, 2016). Recent studies (Gregor and Hotamisligil, 2011) have shown that the inflammatory process might be responsible for the development of insulin resistance in skeletal muscle, since some obese patients who are not insulin resistant do not show inflammation in myocytes, compared with obese patients with insulin resistance (Barbarroja *et al.*, 2010). In addition, accumulation of excessive amounts of fatty acids in skeletal muscle induces ER stress and mitochondrial dysfunction and further contribute to the development of insulin resistance (Shinjo *et al.*, 2017; Yilmaz, 2017).
The molecular mechanisms responsible for fatty acid-induced insulin resistance in skeletal muscle will be extensively analyzed in next sections.

I. 2.3. Insulin resistance and the liver

The impaired response in glucose uptake from tissues is not the only characteristic of insulin resistance. The failure of the liver to switch from glucose production (gluconeogenesis) to glucose disposal and the consequent uncontrolled hepatic glucose production is also an important hallmark of impaired insulin action and, in turn, contributes to exaggerated hyperglycemia. In fact, while hepatic gluconeogenesis is

enhanced, glycogen synthesis and glycolysis are inhibited, thus leading to increased glucose levels (Figure I.7.). Extrahepatic factors contribute to enhance hepatic gluconeogenesis during an insulin resistant status: for instance, insulin fails to suppress glucagon secretion from the pancreas, and the increased release of glucagon in the bloodstream subsequently activates hepatic gluconeogenesis (Moore *et al.*, 2003).

The effect of insulin resistance regarding hepatic lipid metabolism is more complex. Insulin is required for hepatic lipid synthesis and inhibits hepatic lipolysis (de Ferranti and Mozaffarian, 2008). Thus, one might hypothesize that hepatic insulin resistance would decrease hepatic TG synthesis and therefore plasma TG. In contrast, liver and plasma TG are increased in insulin resistant states. This paradox might be due to a pathway-selective insulin resistance that independently modulate glucose and lipid metabolism in different tissues (Brown and Goldstein, 2008). With selective insulin resistance, insulin fails to adequately suppress hepatic glucose production or to adequately augment hepatic glucose uptake and yet still sustains hepatic lipogenesis or TG accumulation, contributing to hypertriglyceridemia (Otero *et al.*, 2014). Compensatory hyperinsulinemia might be responsible for this effect and possibly contributes to maintain normal lipogenesis, even if gluconeogenesis and glucose uptake are impaired and the tissue is already insulin resistant (Corkey, 2012).

Moreover, since hepatic glucose disposal is decreased, glycogen synthesis is inhibited. This condition diverts carbohydrate carbon flux to DNL provoking hepatic lipid accumulation. Palmitate is the primary product of DNL and it is esterified to form TG. TG accumulated into the liver are subsequently released in the circulation, exacerbating hypertriglyceridemia (Irimia *et al.*, 2010).

Collectively, these findings suggest that, in contrast to skeletal muscle, lipid accumulation in the liver might be a consequence of insulin resistance, rather than a cause.

This confirms the theory of pathway-selective insulin resistance and suggests that, in most cases, insulin resistance manifests first in skeletal muscle and adipose tissue and then in liver (Brown and Goldstein, 2008).

In conclusion, alterations in hepatic lipid metabolism are not simply due to selective defects in insulin action, but to a large extent are driven by changes in substrate delivery to the liver that arise from impaired insulin signaling in muscle and adipose tissue (Otero *et al.*, 2014).

I. 2.4. Insulin resistance and the β-cell. Hyperinsulinemia.

When the body produces insulin under conditions of insulin resistance, the cells are resistant to the effect of this hormone and are unable to use it as effectively, leading to high blood glucose level. β-cells in the pancreas subsequently increase their production of insulin, thus provoking a high blood insulin level (hyperinsulinemia). This often remains undetected and can contribute to the development of T2D (Chiu *et al.*, 2007). Koopmans *et al.* showed that chronic hyperinsulinemia in conscious rats for 7 days resulted in a reduction in insulin-mediated total-body glucose uptake and glucose storage. Hepatic glucose production was also suppressed after 7 days of hyperinsulinemia. Taken together, these findings indicate that hyperinsulinemia is not only a compensatory response to insulin resistance, but also a self-perpetuating cause of the defect in insulin action (Koopmans *et al.*, 1997). There are many mechanisms by which hyperinsulinemia can exacerbate insulin resistance: 1) prolonged insulin treatment reduces GLUT4 membrane trafficking; 2) insulin inhibits IRS gene transcription and promotes IRS protein ubiquitination or degradation; 3) insulin activates many kinases, which in turn inhibit insulin downstream signaling in a negative feedback; 4) prolonged hyperinsulinemia provokes β-cells failure (Guo, 2014).

In fact, the persistent stimulus to the β-cell to over-secrete insulin leads to a progressive loss of β-cell function. This dysfunction results in the partial loss of cell capacity to secrete insulin, thus triggering the development of T2D. The mechanisms that cause β-cell impairment are not completely clear: some studies report that β-cells can be damaged by high blood glucose itself, a condition called glucose toxicity (Del Prato *et al.*, 1994), although genetic factors can be also involved (Elizabeth *et al.*, 2017; Stoehr *et al.*, 2000).

Elegant studies by De Fronzo and Groop (DeFronzo, 1988; Eriksson *et al.*, 1989) demonstrated that insulin resistance was also present in normal glucose tolerant humans with diabetes family history, but that insulin resistance was subclinical, as plasma glucose levels were maintained within the normal range by increased insulin secretion by pancreatic β-cells. In fact, initial compensatory hyperinsulinemia can mask specific abnormalities in the metabolism of target tissues, and can itself exacerbates insulin resistance (Shanik *et al.*, 2008). De Fronzo and colleagues (1988) proposed the concept of the initial increase and subsequent decrease in insulin secretion over time with sustained insulin resistance. Time-dependent loss of insulin secretion would ultimately lead to increased glucose levels and the clinical onset of impaired glucose tolerance (Ferrannini *et al.*, 2005).

In individuals with obesity who are mildly glucose intolerant but do not have diabetes, fasting hyperinsulinemia occurs without the detectable increases in blood glucose that would theoretically be required to stimulate β-cells to secrete additional insulin. The above confounding considerations gave rise to the hypothesis that hyperinsulinemia is

the initial, primary effect of a high-fat diet (HFD) feeding and an obesity status (Corkey, 2012). Indeed, it has been reported that HFD feeding can cause primary hyperinsulinemia by directly stimulating islet β-cells to produce insulin, in the absence of insulin resistance or increased blood glucose levels (Boden *et al.*, 1995). Potential mediators of increased insulin secretion are the elevated circulating free fatty acids that are typically present in obesity (van der Kolk *et al.*, 2016). In fact, although insulin secretion is glucose-dependent, it has been shown that fatty acids acutely enhance insulin secretion in human islets (Cen *et al.*, 2016). Physiological increases in plasma fatty acids potentiate insulin secretion from β-cells and support between 30-50% of basal insulin levels (Cen *et al.*, 2016). However, when the increase in circulating fatty acids is prolonged and become pathological, fatty acids overstimulate β-cells to secrete insulin and can account for the hyperinsulinemia in patients who have raised fatty acids, but normal blood glucose (Boden *et al.*, 1998; Cen *et al.*, 2016). Moreover, it has been reported that HFD decreases insulin clearance, and that in obese individuals insulin metabolism is reduced (Kim *et al.*, 2015), thus contributing to maintain elevated insulin levels in the blood.

Taken together, these findings indicate that it is difficult to establish whether hyperinsulinemia is a consequence or a cause of impaired lipid metabolism and insulin resistance. Surely, all these pathways are tightly linked, and reciprocally regulate each other (Corkey, 2012; Shanik *et al.*, 2008).

Figure I.7. shows some of the effects of insulin resistance in the target organs.

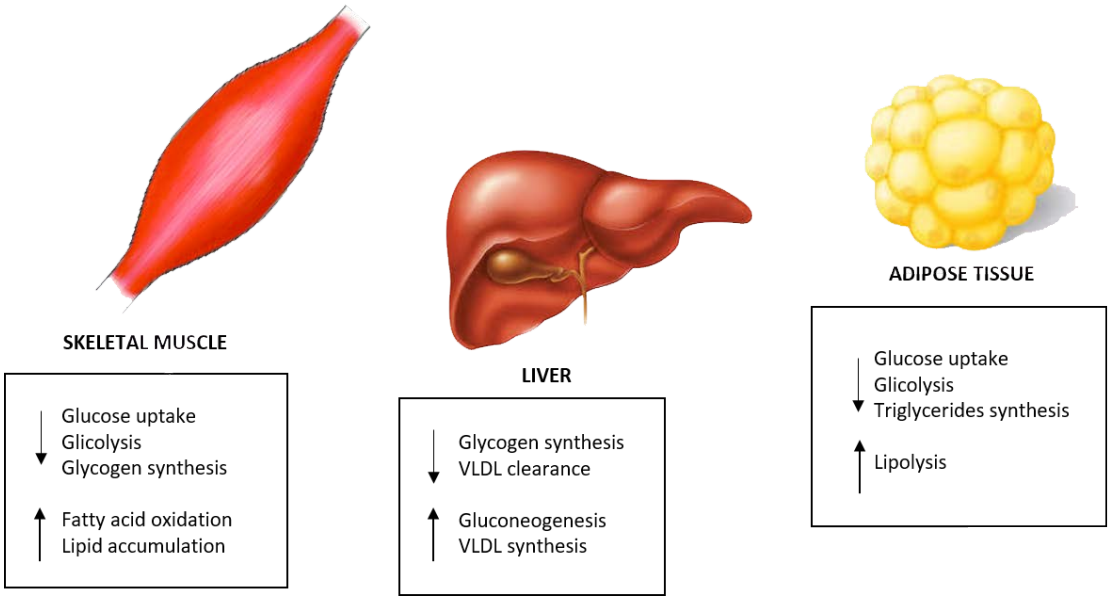

Figure I.7. Insulin resistant status in the organism. Glucose uptake and glycogen synthesis are reduced in skeletal muscle, that starts to metabolize lipids instead of glucose. Cells are starved of energy, despite the high levels of glucose in the blood. Hepatic gluconeogenesis is increased because the inhibitory effect of insulin is blunted. VLDL synthesis is also increased. In adipose tissue, lipolysis is enhanced while glucose uptake and glycolysis are reduced (Adiels *et al.*, 2008b)

I. 2.5. Metabolic mechanisms involved in the development of insulin resistance

In an insulin resistant state, the insulin signaling pathway is compromised (Boucher *et al.*, 2014) and, as a result, downstream effects of insulin on lipid and glucose metabolism are partially or totally blunted.

Next, some of the main molecular mechanisms involved in insulin resistance development will be described.

I. 2.5.1. Attenuation of the insulin signaling pathway

Several studies have reported that a defect in the insulin receptor tyrosine kinase activity, or the impairment of functions and levels of IRS proteins are involved in the development of insulin resistance in many tissues (Boucher *et al.*, 2014). For example, Tg mice lacking insulin receptor rapidly develop diabetes (Bruning *et al.*, 1998). Likewise, IRS1-deficient mice are insulin resistant and have impaired glucose tolerance (Guo, 2014).

I. 2.5.1.1. Insulin receptor and insulin receptor substrates

In insulin resistant conditions, characterized by elevated levels of circulating insulin, the insulin receptor expression is downregulated. Thus, the number of insulin receptor proteins on the membrane surface is lower than normal (DeFronzo and Tripathy, 2009).

Although insulin receptor number is decreased, it still maintains its tyrosine kinase activity. Tyrosine phosphorylation is essential for both insulin receptor and IRS activation. On the other hand, when these proteins are phosphorylated on serine residues, their activity is blocked. Many studies have demonstrated that serine and threonine phosphorylation of the IRS proteins is primary involved in turning the insulin signaling down (Taniguchi *et al.*, 2006). Increased inhibitory Ser/Thr phosphorylation of insulin receptor and IRS occurs in response to inflammatory cytokines, fatty acids, hyperglycemia, mitochondrial dysfunction, hyperinsulinemia and ER stress via activation of multiple kinases, predominantly c-Jun-terminal kinase (JNK), Inhibitor of Kappa B Kinase (IKK) (Schubert *et al.*, 2003), conventional and novels PKCs and MAPK (Aguirre *et al.*, 2000; De Fea and Roth, 1997; Gao *et al.*, 2002). An increase in cAMP concentration also induces inhibitory serine phosphorylation of the insulin receptor in a PKA-dependent manner (Roth and Beaudoin, 1987). Increased serine phosphorylation on insulin receptor, associated with decreased tyrosine kinase activity, has been observed in insulin resistant states, both in rodents and humans (Shao *et al.*, 2000). Although inhibitory IRS serine phosphorylation occurs at many different sites, the best studied of these modifications takes place at Ser^{307}. IRS1 Ser^{307} phosphorylation is increased in obese and diabetic mice (Um *et al.*, 2004). The activation of the NFκB-mediated pathway has also been shown to inhibit insulin signaling through enhanced serine phosphorylation of IRS1 (Cai *et al.*, 2005) (Figure I.8.).

I. 2.5.1.2. PI3K and Akt

Activation of PI3K by IRS proteins is necessary for the downstream insulin pathway. Specific inhibitors of PI3K block almost all of insulin metabolic actions, highlighting the pivotal role of this enzyme in the metabolic actions of this hormone (Taniguchi *et al.*, 2006). PI3K is activated by the interaction between its SH2 domain and the tyrosine-phosphorylated IRS proteins. The regulatory subunit p85 maintains the PI3K in its inactivated status. It has been demonstrated that in insulin resistance p85 subunit is overexpressed, thus PI3K activity is reduced. Furthermore, the p85 subunit can enhance the activity of many kinases, such as JNK, that phosphorylate on serine residues and subsequently inactivate IRS proteins (Taniguchi *et al.*, 2006).

Phosphorylation of Akt is also critical for the physiological insulin signaling pathway. It has been reported that during insulin resistance phosphorylation of Akt is strongly reduced. Protein phosphatase 2A (PP2A) has been shown to dephosphorylate Akt and several studies indicate that PP2A is hyperactivated in diabetic states (Kowluru and Matti, 2012). The reduction in Akt phosphorylation leads to an increase in GSK3 activity, which in turn blocks glycogen synthesis. On the other hand, Akt-mediated phosphorylation of AS160 protein is decreased, thus inhibiting GLUT4 translocation to the membrane surface.

Moreover, TRB3 expression is induced in diabetes and disrupts insulin signaling by binding to Akt and blocking its activation. In agreement with this, TRB3 knockdown in mice leads to improved glucose tolerance (Koo *et al.*, 2004) (Figure I.8.).

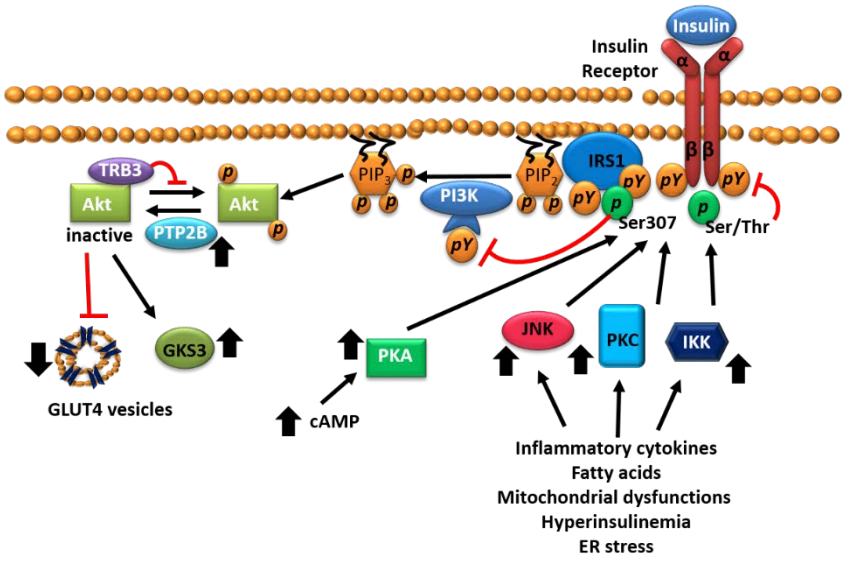

Figure I.8. Molecular pathways that impair insulin signaling. Several kinases are responsible for the phosphorylation of the insulin receptor in serine and threonine residues, and for the phosphorylation of IRS proteins on Ser^{307}, which impairs the downstream insulin signaling. Other kinases directly blunt the phosphorylation and activation of Akt. The result is a hyperactivation of GSK3 and the subsequent reduction of glycogen synthesis in liver and skeletal muscle, as well as a reduction of GLUT4 translocation and glucose uptake in skeletal muscle and adipose tissue (Taniguchi *et al.*, 2006).

I. 2.5.2. ER stress and insulin resistance

The ER is a central organelle entrusted with lipid synthesis, calcium homeostasis, protein folding, maturation, and trafficking. Most secreted and integral membrane proteins of eukaryotic cells are translocated into the lumen of ER. The ER lumen provides a specialized environment for post-translational modification and folding of proteins. Various factors, such as oxidative stress, can interfere with ER function and lead to accumulation of unfolded proteins. This process is called ER stress and further activates a molecular cascade called unfolding protein response (UPR). The initial aim of the UPR is to restore the normal function of the cell by halting protein translation and increasing the production of chaperones responsible for the correct protein folding. If this objective is not achieved and the protein disruption is prolonged, the UPR turns on apoptotic pathway (Xu *et al.*, 2012). Interestingly, the ER stress may intersect with a variety of inflammatory and stress signaling systems, including the NFκB and the JNK pathways.

The canonical UPR include three branches, that are mediated by three ER membrane-associated proteins: the inositol-requiring kinase 1 (IRE1), the activating transcription factor 6 (ATF6) and the protein kinase R-like ER kinase (PERK) (Figure I.9.). In a well-functioning and stress-free ER, these three transmembrane proteins are bound by a chaperone, the glucose-regulated protein 78 also called immunoglobulin binding protein (GRP78/BiP), in their intraluminal domains and rendered inactive (Back and Kaufman, 2012). Accumulation of improperly folded proteins and increased protein cargo in the ER results in the recruitment of BiP away from these UPR sensors. Consequently, BiP separates from the transmembrane proteins, which are now free to be activated. This event triggers the oligomerization and activation of the two kinase IRE1 and PERK and engage a complex downstream signaling pathway. Activation of the third branch of the UPR requires translocation of ATF6 to the Golgi apparatus, where is processed by specific proteases and transformed in the active transcription factor. In a situation of persistent ER stress, the levels of BiP/GRP78 are highly increased (Hotamisligil, 2010).

I. 2.5.2.1. IRE1

The endoribonuclease activity of IRE1 cleaves a 26 base-pair segment to form the mRNA of the X-box binding protein 1 (XBP1), creating an alternative message that is translated into the active (or spliced) form of the transcription factor (sXBP1). sXBP1, alone or in conjunction with ATF6, launches a transcriptional program to produce chaperones and proteins involved in ER biogenesis, phospholipid synthesis, ER-associated protein degradation and secretion. Thus, sXBP1 activates one of the mayor pathways for enhancing the folding capacity of the ER and for dealing with the ER stress. IRE1 can also trigger the activation of the JNK kinase and induce the activation of pro-inflammatory, pro-apoptotic pathway (Hotamisligil, 2010).

I. 2.5.2.2. ATF6

When activated, ATF6 moves to the nucleus to stimulate the expression of genes containing ER stress elements (ERSE) and cAMP response elements (CRE) (Scheuner *et al.*, 2005) in their promoters. ATF6 fosters the expression of the chaperone C/EBP homologous protein (CHOP) that is involved in apoptotic pathways. CHOP in turn can activate the kinase JNK. ATF6 can also interact directly with the XBP1 protein to target UPR control genes and it can contribute to the activation of the NFκB pathway.

I. 2.5.2.3. PERK

The activation of PERK results in phosphorylation of eukaryotic translational initiation factor 2α (eIF2α) at Ser^{51}, which converts eIF2α in the activated form. Phosphorylated eIF2α interacts with the activating transcription factor 4 (ATF4) and promotes the expression of genes encoding for chaperones, such as CHOP and BiP/GRP78 (Hotamisligil, 2010).

Since the ER is the principal site of protein synthesis and maturation, its biology is relevant to substrate metabolism. The ER can be view as a 'nutrient-sensing' apparatus that can coordinate metabolic responses through its ability to control the synthetic and catabolic pathways of various nutrients. Defects in the ER function can be responsible for metabolic alteration at systemic levels. Many studies have confirmed that the UPR is tightly engaged with alterations in glucose and lipid metabolism and is now well established that the ER stress plays an important role in the development of insulin resistance (Ron and Walter, 2007). In agreement with this, it has been described that obesity results in chronic ER stress in adipose tissue. Indeed, increased activation of IRE1 and JNK, and upregulation of XBP1s expression are observed in adipose tissue from obese patients (Boden *et al.*, 2008). Interestingly, the loss of fat in obese patients following gastric bypass surgery reduces XBP1s and BiP expression in white adipose tissue, as well as the phosphorylation levels of eIF2α and JNK, whereas exercise training decreases ER stress in white adipose tissue of obese rodents (Gregor *et al.*, 2009). What causes ER stress in obese patients remains unclear. Studies in human beings suggest that hyperinsulinemia, which is often observed in obesity, causes ER stress in adipose tissue, possibly via enhancement of protein biosynthesis and post-translational protein modification that leads to the accumulation of unfolded/misfolded proteins (Kawasaki *et al.*, 2012). Other studies indicate that the increased release of fatty acids, typical of obese status, is responsible for triggering ER stress in adipose tissue (Jiao *et al.*, 2011). However, what is certain is that ER stress represents an important risk factor for the development of insulin resistance in different tissues. Several i*n vivo* experiments have examined the molecular mechanisms by which increased ER stress can contribute to insulin resistance. For instance, PERK activation increases the expression of cytokines that can inhibit GLUT4 translocation (Jiao *et al.*, 2011), and also reduces insulin responsiveness in adipose tissue (Bobrovnikova-Marjon *et al.*, 2012). Moreover, the activation of IRE1 in adipose tissue of obese patients is responsible for JNK activation, which in turn can phosphorylate IRS1 on serine residues to promote insulin resistance (Salvado *et al.*, 2015). In addition, it has been reported that ER stress in adipose tissue provokes the downregulation of insulin receptor proteins, thus attenuating the insulin signaling pathway (Zhou *et al.*, 2009). In liver, ER stress contributes to insulin resistance by activating transcription factors that regulate the expression of gluconeogenic genes. ER stress-induced hepatic insulin resistance may also be the result of increased lipogenesis, which favors intracellular accumulation of intermediary complex lipids and triggers inflammation (Salvado *et al.*, 2015). In fact, ER stress contributes to lipid accumulation through several mechanisms, including the activation of the transcription factor sterol regulatory element-binding protein (SREBP)-1, which is regulated by the PERK–eIF2α pathway and enhances lipogenesis (Zhang *et al.*, 2012) by increasing the

transcription of lipogenic genes, including fatty acid synthase and stearoyl-CoA desaturase (SCD) (Kammoun *et al.*, 2009).

In skeletal muscle, ER stress can contribute to insulin resistance through phosphorylation of IRS proteins via the IRE1/JNK pathway (Hirosumi *et al.*, 2002). Alterations in the ER may also contribute to the development of an inflammatory status. Hotamisligil and colleagues demonstrated that the ER stress plays and important role in promoting inflammation and consequently leading to insulin resistance in skeletal muscle of obese patients (Hotamisligil, 2010).

The involvement of ER stress in β-cell apoptosis and failure has also been observed (Han *et al.*, 2013). In fact, it has been described that humans and mice with altered levels of PERK have profound β-cell dysfunction and are severely diabetic, whereas mice with a mutation in the PERK phosphorylation site in eIF2α have fewer β-cells and are diabetic as a result of insulin deficiency (Harding *et al.*, 2001; Scheuner *et al.*, 2001). There are many potential mechanisms by which ER stress can contribute to β-cell dysfunction in T2D, including lipotoxicity, glucotoxicity, inflammatory challenge, and the accumulation of proinsulin and amyloid. In this regard, several studies suggest a pathway by which chronic exposure of islets to increased nutrient levels could cause the gradual demise of β-cells (Back and Kaufman, 2012; Salvado *et al.*, 2015). In fact, it is known that ingestion of excess calories will require an increase in insulin biosynthesis and secretion to maintain fuel homeostasis. If this condition becomes chronic, the biosynthetic demand may eventually overload the protein folding capacity of the ER, leading to the activation of the UPR. Consistent with this hypothesis, it has been described that misfolded protein (e.g., proinsulin) accumulation in the ER leads to β-cell death through PERK-mediated phosphorylation of eIF2α and ensuing transcriptional induction of ATF4 and the proapoptotic gene CHOP (Scheuner *et al.*, 2005).

Several strategies have been proposed to target ER stress as a therapeutic approach for pharmacological intervention in insulin resistance and T2D. Reducing chronic ER stress by the administration of 4-phenylbutyrate (PBA), which is known to be a strong ER stress inhibitor, increased systemic insulin sensitivity, normalized hyperglycemia and reduced hepatosteatosis in murine models of obesity and T2D. In humans, PBA prevents lipid-induced insulin resistance and restores β-cell functionality, and ameliorates insulin sensitivity in skeletal muscle and liver, thus suggesting that ER stress inhibition by these drugs might be a viable therapeutic strategy towards increasing insulin sensitivity (Xiao *et al.*, 2011).

Figure I.9. shows some of the molecular links between ER stress and insulin resistance.

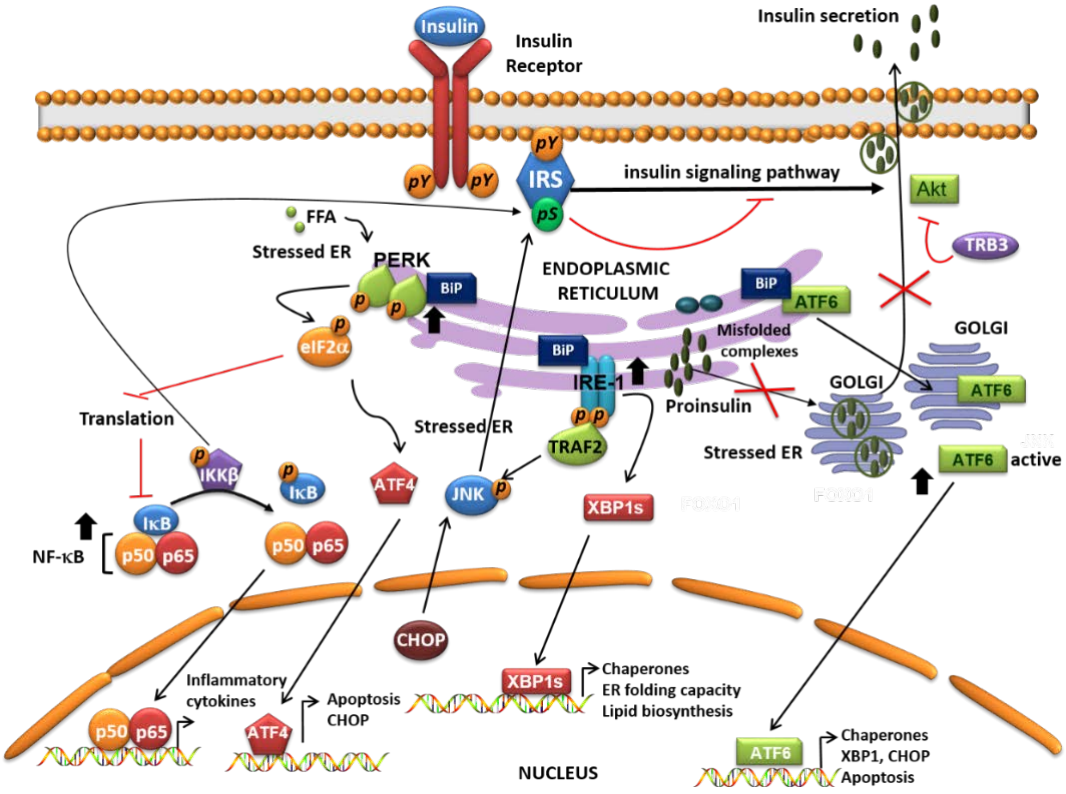

Figure I.9. Endoplasmic reticulum stress and insulin resistance: molecular links. The activation of the IRE complex leads to increased activity of JNK, which is responsible for the phosphorylation of IRS on Ser^{307}. The unfolded protein response impairs the insulin assembly and secretion from the Golgi. The activation of the NFκB complex through PERK-eIF2α mechanism triggers the inflammatory response, which in turn exacerbates insulin resistance (Salvado *et al.*, 2015).

I. 2.5.3. Inflammation and insulin resistance

Different studies have reported that a chronical low-level inflammatory process can contribute to insulin resistance in many tissues. In fact, many evidences indicate that metabolic and inflammatory pathways are closely inter-related and that nutrients themselves, if chronically in excess, can activate the inflammatory response (Gregor and Hotamisligil, 2011).

Thus, inflammation often occurs as consequence of a caloric overload that leads to accumulation of nutrients in the body and induces toxicity (Boucher *et al.*, 2014). For example, an uncontrolled hyperglycemia increases the influx through the polyol pathway and triggers the activation of JNK pathway. Elevated levels of blood glucose also increase the production of advanced glycation end products (AGE) that are linked to oxidative stress and induce inflammation (Evans *et al.*, 2005; Kim *et al.*, 2001; Riboulet-Chavey *et al.*, 2006).

Adipose tissue expansion occurs in response to HFD and caloric overload, and it is associated with an accumulation of reactive oxygen species (ROS), increase in immune cell infiltration and subsequent pro-inflammatory response (Sun *et al.*, 2011).

Obesity-induced inflammation can be provoked by the elevated levels of fatty acids and TG that are a typical characteristic in obesity, and is the result of a dysfunction in the adipose tissue, which not only serves as fat storage but also constitutes an endocrine and secretory organ able to release many inflammatory cytokines and chemokines. In fact, an impairment of adipocyte function accelerates fat (TG and fatty acids) spillover from adipose tissue to the circulation and additionally causes secretion of many endocrine pro-inflammatory mediators (Lumeng and Saltiel, 2011). Through fatty acids, adipokines and inflammatory mediators the adipose tissue communicates with peripheral tissues, such as liver, skeletal muscle or pancreas, and causes metabolic adverse effects (de Ferranti and Mozaffarian, 2008).

There are many possible molecular mechanisms by which inflammation can contribute to insulin resistance (Figure I.10.).

I. 2.5.3.1. The NFκB pathway

NFκB is a transcription factor that regulates the expression of genes related with stress and inflammatory response. The NFκB family has five subunits: p65, RelB, p50 and p52 that associate and form homo- or heterodimers. The most common heterodimer is formed by the p50/p65 subunits. Under resting conditions, inactive NFκB dimers are bound to inhibitor of κB (IκB) proteins in the cytoplasm. There are many isoforms of IκB proteins, being IκBα the most common. After an inflammatory stimulus, a specific kinase, called IκB kinase (IKK) (Schubert *et al.*, 2003), phosphorylates the IκBα inhibitory protein on Ser^{32} and Ser^{36} residues, thus inactivating this protein and promoting its degradation. This event removes the inhibitory effect of the IκBα protein on the NFκB dimer and breaks the union between them. The dimer is now free to translocate into the nucleus where it binds to the promoter region of its target genes and triggers the transcription process (Kumar *et al.*, 2004).

NFκB enhances the expression of many pro-inflammatory cytokines, such as interleukin-6 (IL6), tumor necrosis factor α (TNFα), and monocyte chemotactic protein 1 (MCP1). TNFα in turn stimulates NFκB activity, generating a positive feedback (Green *et al.*, 2011). The NFκB-induced expression of MCP1 is responsible for macrophage and lymphocyte accumulation in adipose tissue, which is related to insulin resistance (Shi *et al.*, 2006); (Nguyen *et al.*, 2007). In fact, it has been reported that, in rodents, 1 week of HFD increases MCP1 levels and promotes macrophage infiltration and insulin resistance in adipose tissue, while the deletion of MCP1 or its receptor prevents such response and improves insulin sensitivity (Kanda *et al.*, 2006).

The other cytokines produced after NFκB activation, once released into the cytosol, can impair the insulin signaling pathway by phosphorylating IRS proteins on serine residues and also by downregulating the expression of IR, IRS1 and GLUT4 genes (Boucher *et al.*, 2014). Moreover, cytokines are also able to decrease GLUT4 translocation on the membrane surface (Hamid Akash *et al.*, 2017).
On the other hand, the activation of IKK itself triggers the phosphorylation of IRS1 on Ser^{307}, thus decreasing the insulin signaling pathway (Gao *et al.*, 2002).
Several studies have described the involvement of the NFκB pathway in the development of insulin resistance. For instance, it has been reported that overexpression of NFκB in the liver of normal rodents results in liver and muscle insulin resistance and diabetes, whereas antibody-mediated neutralization of IL6 in animals fed on a HFD partially restores insulin sensitivity (Cai *et al.*, 2005). In addition, higher TNFα levels were observed in skeletal muscle of rats fed a fructose-rich diet and contribute to insulin resistance in myocytes. Consistent with this, targeting TNFα with a neutralizing antibody alleviates insulin resistance in rats with hyperglycemia (Qu *et al.*, 2017; Togashi *et al.*, 2000).
On the other hand, NFκB is negatively regulated by AMPK that prevents its trans-activation induced by the cytokine TNFα, and also reduces its expression (Cacicedo *et al.*, 2004; Salminen *et al.*, 2011).

Collectively, these findings confirm that NFκB activation plays an important role in the impairment of insulin signaling and in the subsequent development of insulin resistance.

I. 2.5.3.2. <u>The MAPK pathway</u>

As mentioned above, MAPK are a wide family of serine/threonine kinases mostly involved in cellular proliferation. However, some of them also play a role in metabolic pathways.
Among these, JNK is strongly involved in the inflammatory response and in insulin resistance. Many evidence confirm that JNK directly phosphorylates IRS1 on Ser^{307}, turning the insulin signaling down (Hirosumi *et al.*, 2002; Taniguchi *et al.*, 2006). In addition, JNK activates the AP1 transcription factor, which is known to promote the expression of many pro-inflammatory genes (Hirosumi *et al.*, 2002). Thus, JNK also contributes to insulin resistance by inducing the inflammatory response (Wu and Ballantyne, 2017). Many studies have confirmed the role of JNK in insulin resistance. For example, it has been reported that JNK activity is increased in the liver of obese mice and deletion of JNK gene prevents HFD-induced insulin resistance in rodents (Hirosumi *et al.*, 2002; Kaneto *et al.*, 2004). Moreover, in cultured myocytes, fatty acid-induced insulin resistance is accompanied by increased JNK activity, whereas JNK knockdown attenuates insulin resistance (Senn, 2006; Vijayvargia *et al.*, 2010)
The ERK1/2 protein has also been shown to be involved in the insulin metabolic effects. As previously mentioned, ERK1/2 participates in a negative feedback loop in the insulin

pathway. In fact, ERK1/2 is activated by insulin downstream cascade, which in turn phosphorylates IRS1 on serine residues, thus switching off the insulin signaling pathway (Taniguchi *et al.*, 2006).

Some studies also pointed that ERK1/2 can contribute to insulin resistance by inducing the inflammatory response. In fact, ERK1/2 promotes the NFκB pathway by phosphorylating and activating the IKK (Zhang *et al.*, 2014). Moreover, the activation of ERK1/2 stimulates the AP1 transcription factor, which in turn promotes the expression of many genes related with inflammation (Chalmers *et al.*, 2007; Takata *et al.*, 2009).

Interestingly, it has been reported that ERK1/2 is implicated in a negative cross-talk with the AMPK protein. In fact, it seems that AMPK activation inhibits the ERK1/2 phosphorylation and vice versa (Du *et al.*, 2008). Some studies have shown that the reduction of AMPK activity in the liver of mice fed a HFD is accompanied by a simultaneous increase in ERK1/2 phosphorylation (Barroso *et al.*, 2011). Based on these findings, it is possible that ERK1/2 might contribute to insulin resistance also by inhibiting AMPK activity.

I. 2.5.3.3. <u>The JAK/STAT pathway</u>

The Janus kinase (Goedert *et al.*, 1989) receptor is a surface tyrosine kinase receptor that is activated by cytokines. During the inflammatory process, cytokines are released from many tissues and bind the JAK receptor. This binding triggers the downstream signal, which involves two STAT proteins. The receptor phosphorylates and activates the STAT proteins, which subsequently form hetero- or homodimers and translocate to the cell nucleus where they induce transcription of target genes. There are many isoforms of STAT proteins. The phosphorylation of the STAT3 isoform is increased in insulin resistance, suggesting that this pathway might be involved in development of insulin resistance (McGillicuddy *et al.*, 2009).

Activation of JAK-STAT pathways potently induces suppressor of cytokine signaling molecules 1 and 3 (SOCS1 and 3), which have been implicated in TNFα-induced insulin resistance in adipocytes and hepatic insulin resistance *in vitro* and *in vivo* (McGillicuddy *et al.*, 2009). SOCS proteins inhibit STAT phosphorylation by competing with STATs for phospho-tyrosine binding sites on JAK receptors and are therefore involved in a negative feedback loop that leads to termination of the JAK/STAT pathway. Interestingly, SOCS proteins, particularly SOCS3 subtype, negatively regulate insulin signaling by several mechanisms: the inhibition of tyrosine kinase activity of the insulin receptor, the competition for the binding-site of the IRS proteins on the receptor, and the induction of IRS proteins degradation (Rui *et al.*, 2002; Ueki *et al.*, 2004). Overexpression of SOCS3 in cultured myocytes decreased insulin-stimulated glycogen synthesis (Ueki *et al.*, 2004). In addition, the expression and protein levels of SOCS3 are increased in obesity and

metabolic syndrome, confirming the link between cytokine signaling and insulin resistance (Boucher *et al.*, 2014; McGillicuddy *et al.*, 2009).

I. 2.5.3.4. TLRs

Toll-like receptors (TLRs) are a class of proteins that play a critical role in the early innate immune response, since they are involved in sensing invading pathogens and endogenous danger signals. They recognize highly conserved structural motifs known as pathogen-associated microbial patterns (PAMPs), which are exclusively expressed by microbial pathogens, or danger-associated molecular patterns (DAMPs) that are endogenous molecules released from necrotic or dying cells (Takeda *et al.*, 2003).

Structurally, they are transmembrane receptors usually expressed on sentinel cells such as leukocytes, macrophages, natural killer cells, but widely distributed also in other cell types. TLRs proteins are characterized by an extracellular domain containing leucine-rich repeats (LRRs) and a cytoplasmic tail that contains a conserved region called the Toll/Interleukin-1 receptor (TIR) domain. The TLR family is known to consist of 10 members (TLR1-TLR10): TLR2 is essential for the recognition of a variety of PAMPs from Gram-positive bacteria; TLR3 is implicated in recognizing virus-derived double-stranded RNA; TLR4 is predominantly activated by lipopolysaccharide; TLR5 detects bacterial flagellin; TLR9 is required for response to unmethylated DNA, and TLR7-8 recognize small synthetic antiviral molecules (Delneste *et al.*, 2007; Takeda *et al.*, 2003). TLR2 and TLR4 are abundant in adipose tissue and skeletal muscle.

Upon activation, TLRs recruit adapter proteins within the cytosol of the cell to propagate the antigen-induced signal transduction pathway. These recruited proteins are then responsible for the subsequent activation of other downstream proteins, including protein kinases that further amplify the signal and ultimately lead to the upregulation of genes that orchestrate inflammatory responses. TLRs downstream signaling leads to the activation of the IKK complex, which in turn phosphorylates IκBα and induce the subsequent nuclear localization of NFκB. Activation of NFκB triggers the production of pro-inflammatory cytokines such as TNFα, IL6, and IL1 among many others. TLRs also enhance JNK activity that is involved in serine phosphorylation of IRS proteins (Konner and Bruning, 2011).

Apart from exogenous ligands, TLRs also bind endogenous ligands related with the inflammatory response. Among these, many fatty acids have been shown to activate TLRs (Hwang *et al.*, 2016; Nicholas *et al.*, 2017; Yang *et al.*, 2015).

The role of TLRs in the cross-talk between inflammatory and metabolic signaling is now emerging and requires to be further investigated (Shi *et al.*, 2006) (Himes and Smith, 2010). Shi *et al*. (Shi *et al.*, 2006) demonstrated that $TLR4^{-/-}$ knockout mice fed a HFD were protected against obesity and lipid-induced insulin resistance compared to control mice.

Other authors also showed that mice deficient in hepatocyte Tlr4 (Tlr4LKO) exhibited improved glucose tolerance, enhanced insulin sensitivity and ameliorated hepatic steatosis after a HFD challenge. Furthermore, Tlr4LKO mice have reduced macrophage content in white adipose tissue, as well as decreased tissue and circulating inflammatory markers (Jia *et al.*, 2014). Studies on rodents with the PPARγ agonist pioglitazone indicated that this drug strongly decreases TLR4 mRNA expression, hepatic cholesterol and TG levels. Pioglitazone also significantly decreased blood glucose levels and improved insulin resistance and these effects were mediated through TLR4 modulation (Eraky *et al.*, 2017). Moreover, Reyna *et al.* (Reyna *et al.*, 2008) reported that individuals with obesity and T2D have increased TLR4 expression and signaling. Collectively, these data indicate that TLRs activation contributes to obesity-associated inflammation and insulin resistance.

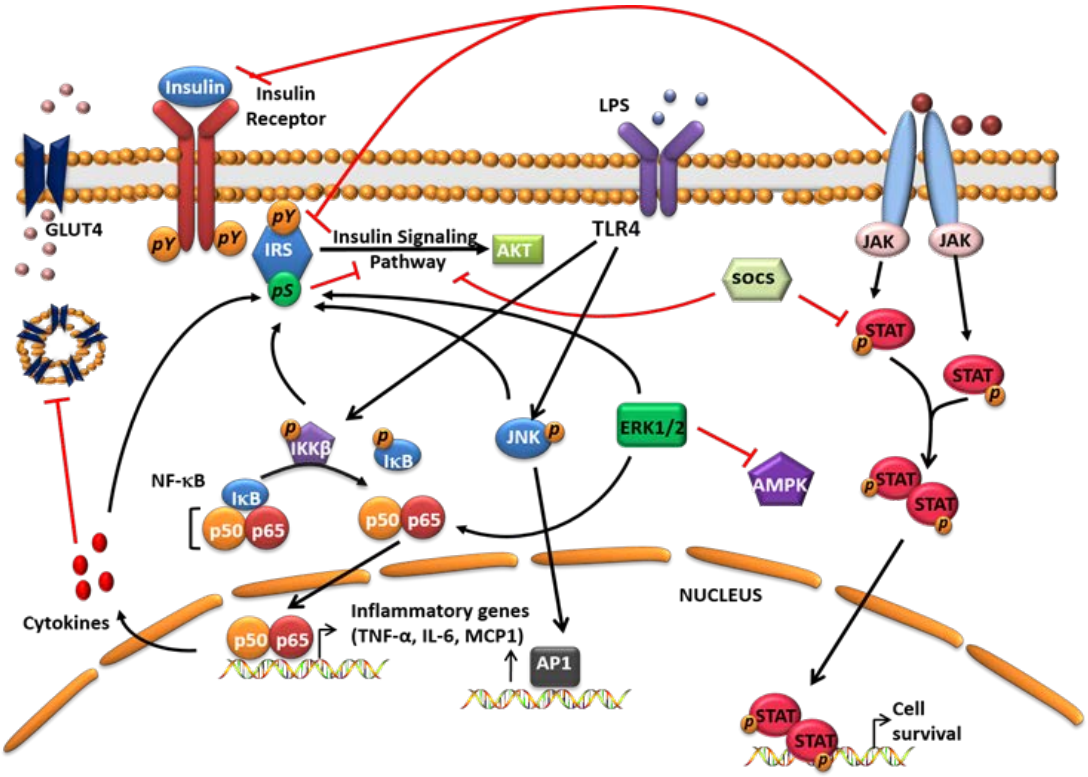

Figure I.10. Inflammation and insulin resistance: molecular links. Several kinases involved in the inflammatory process, such as IKK, JNK, and ERK1/2, are responsible for the phosphorylation of IRS protein on Ser^{307}, thus inhibiting the insulin signaling pathway. Moreover, enhanced cytokine production impairs GLUT4 translocation and glucose uptake. The activation of the JAK/STAT/SOCS pathway inhibits insulin signaling by impairing insulin receptor and IRS activity (Hotamisligil, 2006).

I. 2.5.4. Lipids and insulin resistance

In overnutrition, insulin initially drives the body to store the excess calories in the adipose tissue. This process breaks down at some stage and lipids start to accumulate in non-adipose tissues, such as liver and skeletal muscle, where they contribute to the development of insulin resistance.

I. 2.5.4.1. Free fatty acids and insulin resistance

Excessive amounts of free fatty acids accumulated in peripheral tissues have adverse effects on cellular signaling functions. The relationship between fatty acids and insulin resistance has been broadly studied and discussed (Bergman and Ader, 2000; Randle *et al.*, 1963). Fatty acids have been shown to reduce insulin-dependent glucose uptake in skeletal muscle by decreasing GLUT4 translocation (Boden and Shulman, 2002). Elevated levels of fatty acids also attenuate insulin effect by inhibiting glycogen synthesis and glucose metabolism, both in skeletal muscle and liver, while they sustain gluconeogenesis in liver (Sears and Perry, 2015). In addition, it has been reported that chronically elevated free fatty acids elicit a lipotoxic effect in the pancreas and reduce β-cell function (Bergman and Ader, 2000; Pankow *et al.*, 2004; Tumova *et al.*, 2016) .

Not only the amount, but also the quality of dietary fatty acids is important to determine their effect in the body (Lottenberg *et al.*, 2012). Different type of fatty acids, defined by the degree of saturation and length of carbon chain, may induce diverse metabolic responses in cells and tissues. The most common fatty acids found in human plasma are saturated palmitic acid, monounsaturated oleic acid and polyunsaturated linoleic acid. Saturated fats significantly worsen insulin sensitivity, whereas monounsaturated and polyunsaturated fats have less pronounced effect or even improve insulin sensitivity (Lottenberg *et al.*, 2012; Salvado *et al.*, 2013). The role of palmitate in impairing glucose disposal and insulin sensitivity in many tissues, especially skeletal muscle, has been extensively studied and is now well recognized (Calvo-Ochoa *et al.*, 2017; Makinen *et al.*, 2017).

Fatty acids can induce insulin resistance by many molecular mechanisms that include: 1) increased synthesis of deleterious lipids [diacylglycerol (DAG) and ceramide]; 2) activation of the inflammatory process; 3) dysfunction of cellular organelles (ER stress and mitochondrial dysfunction). All these pathways are inter-connected and lead to fatty acid-induced insulin resistance (Rachek, 2014), as summarized in figure I.11.

Following, we will discuss some of the main molecular mechanisms involved in the development of lipid-induced insulin resistance.

I. 2.5.4.1.1. DAG and ceramides

When the amount of fatty acids that enter into the cell [by diffusion, or through the binding to fatty acid transporter protein (FATP) and fatty acid translocase (FAT/CD36)]

overcomes the oxidation capability of the tissue, fatty acids are redirected to other metabolic pathways, such as the production of DAG and ceramides (Petersen and Shulman, 2017).

DAG are glycerides consisting of two fatty acid chains covalently bound to a glycerol molecule through ester linkages that are the intermediate of TG synthesis. DAG are synthetized from glycerol 3 phosphate by the enzyme glycerol 3 phosphate acyltransferase (GPAT) and they ate transformed into TG by the enzyme diglyceride acyltransferase (DGAT). DAG are also released when TG are hydrolyzed by lipases during the first step of lipolysis (Itani *et al.*, 2002).

DAG exert many functions in physiological cell metabolism since they work as secondary messengers of GTP-coupled receptors. However, when their levels are increased, they contribute to lipid-induced insulin resistance.

In biochemical signaling, DAG work as second messengers, and are a product of the hydrolysis of the phospholipid phosphatidylinositol 4,5-bisphosphate (PIP2) by the enzyme phospholipase C (PLC), a membrane-bound enzyme that, through the same reaction, simultaneously produces inositol trisphosphate (IP3). Although IP3 diffuses into the cytosol, DAG remain within the plasma membrane where they work as activators of protein kinase C (PKC). Activation of PKC triggers a cascade of many downstream signaling pathways (Szendroedi *et al.*, 2014).

When DAG levels are increased because of lipid accumulation in liver and skeletal muscle, DAG activate the novel PKCs, especially isoforms ε, δ and θ. These isoforms have been shown to phosphorylate serine residues on insulin receptor and its substrates (IRS proteins), thereby impairing insulin receptor-mediated tyrosine phosphorylation and, therefore, interfering with insulin signaling pathway. In fact, it has been established that DAG-mediated activation of PKCs drastically reduces GLUT4 translocation on membrane surface (Li *et al.*, 2004b; Perseghin *et al.*, 2003; Saltiel and Pessin, 2002). PKCs also block AMPK activation contributing to further impair lipid metabolism (Coughlan *et al.*, 2013; Szendroedi *et al.*, 2014). Moreover, the inactivation of AMPK mediated by PKC prevents AMPK anti-inflammatory effects on NFκB and ERK1/2 pathways and consequently increases the inflammatory process (Salminen *et al.*, 2011) (Figure I.11.).

Many evidences confirm that DAG are involved in lipid-induced insulin resistance. In humans, raising plasma fatty acids levels by lipid infusion results in increased DAG content, which is associated to PKCθ activation and provokes an acute muscle insulin resistance (Itani *et al.*, 2002). Obese subjects with T2D show increased DAG levels and PKCθ activity (Itani *et al.*, 2001). On the other end, inhibition or ablation of PKCθ in mice protects against lipid-induced insulin resistance (Kim *et al.*, 2004). Recently, a novel DGAT inhibitor has been shown to improve insulin resistance in adipose tissue, as well as systemic glucose metabolism in mice (Tomimoto *et al.*, 2015).

Several genetically modified mouse models have been generated to examine the role of DAG in lipid-induced insulin resistance. Mice with loss of function of GPAT accumulate less intracellular DAG that control mice on a HFD and are protected against insulin resistance. In mice overexpressing GPAT the converse was true: increased intracellular DAG and insulin resistance were observed on regular chow diet (Petersen and Shulman, 2017).

Lipid accumulation and impaired lipid metabolism also result in redirection of long chain acyl-CoA into synthesis of ceramides. Ceramides are composed of sphingosines and fatty acids. They are found in high concentrations within the cell membranes, since they are part of sphingomyelin, one of the major lipids in the lipid bilayer. Contrary to previous assumptions that ceramides and other sphingolipids found in cell membrane were purely supporting structural elements, ceramides can participate in a variety of cellular signaling. Palmitate is the precursor of *de novo* synthesis of ceramides, thus ceramides concentration depends on palmitate levels in blood. Actually, an increase in the saturated/unsaturated fatty acids ratio is observed in type 2 diabetic patients and is thought to reduce membrane fluidity and insulin sensitivity (Field *et al.*, 1990). It has been reported that pharmacological inhibition of serine-palmitoyltransferase 1 (SPT1), the enzyme that catalyzes the first step of ceramide synthesis, prevents hepatic insulin resistance in rodents (Aerts *et al.*, 2007; Holland *et al.*, 2007). Other evidence confirms the role of ceramides in lipid-induced insulin resistance: increased plasma concentration of ceramides was observed in obese and diabetic patients (Haus *et al.*, 2009) as well as in leptin-deficient mice (Holland *et al.*, 2011); the ceramide inhibitor myriocin prevents impaired insulin sensitivity in rodents fed a HFD (Holland *et al.*, 2007).

Several mechanisms have been proposed to explain how ceramides might induce cellular insulin resistance. Early work with cultured myocytes and adipocytes suggested that ceramides impair insulin activation of Akt through two mechanisms: 1) they increase protein phosphatase 2A (PP2A) activity that dephosphorylates and inactivates Akt (Teruel *et al.*, 2001); 2) they activate atypical PKCζ, which in turn phosphorylates Akt at Thr^{34}, resulting in reduced binding of PI3P to Akt (Powell *et al.*, 2003; Schmitz-Peiffer *et al.*, 1999). In addition, ceramides have been show to activate the JNK pathway (Westwick *et al.*, 1995) and to induce ER stress (Boslem *et al.*, 2011). Likewise, it has been reported that ceramide-induced ER stress strongly contributes to β-cell dysfunction and induces β-cell apoptosis (Boslem *et al.*, 2011). Moreover, in pancreatic β-cells, ceramides mediate palmitate-induced repression of insulin gene transcription (Lang *et al.*, 2011).

Recently, ceramides have been shown to reduce the β-oxidation rate and to impair mitochondrial homeostasis, through the inhibition of mitochondrial electron transport chain activity. In fact, treating mice with myriocin increased mitochondrial activity, enhanced oxygen consumption rates and raised insulin sensitivity (Chaurasia and Summers, 2015) (Figure I.11.).

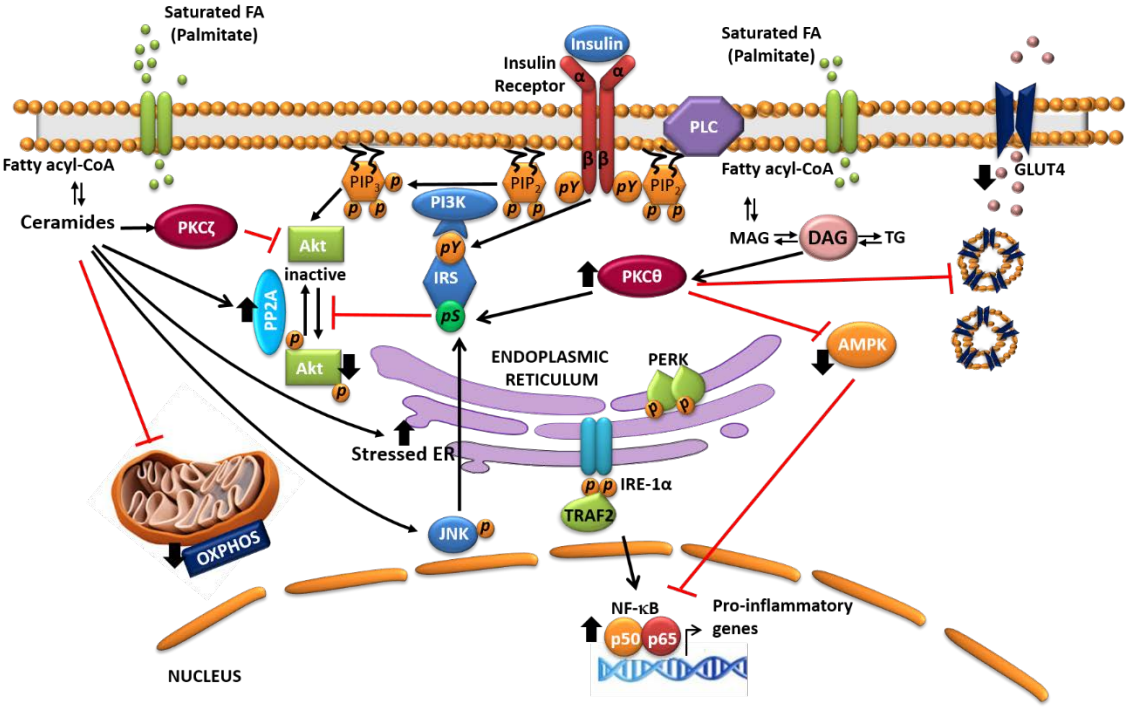

Figure I.11. Lipid-induced insulin resistance: molecular mechanisms. DAG and ceramides contribute to insulin resistance by activating PKC and by dephosphorylating Akt, respectively. PKC phosphorylates IRS on Ser^{307} and inhibits AMPK activity, thus enhancing inflammation. Ceramides also induce mitochondrial dysfunction and ER stress (Boden and Shulman, 2002; Boren *et al.*, 2013)

I. 2.5.4.1.2. Fatty acid-induced inflammation

It has been well established that excessive amounts of fatty acids can impair insulin action and glucose metabolism by inducing a chronic low-grade inflammatory process (Boden and Shulman, 2002). The fatty acid-induced inflammatory process plays a key role in the development of insulin resistance (Gregor and Hotamisligil, 2011)(Figure I.12.).

Accumulated fatty acids activate the inflammatory response by two ways: indirectly through the synthesis of complex lipids, which in turn activate the NFκB pathway, as mentioned above (Haversen *et al.*, 2009); and directly through the interaction with TLR2 and TLR4 (Maloney *et al.*, 2009).

The fatty acid-induced activation of the NFκB pathway leads to the subsequent secretion of several pro-inflammatory cytokines, including TNFα, IL1 and IL6 (Wu and Ballantyne, 2017). For example, it has been reported that palmitate infusion highly increases plasma concentration of TNFα in mice (Hamid Akash *et al.*, 2017). As previously mentioned, cytokines contribute to impair the insulin signaling by downregulating IRS1 expression and by reducing GLUT4 translocation (Lumeng and Saltiel, 2011).

The fatty acid-induced activation of NFκB also leads to the increase in IKK activity, which in turn phosphorylates IRS1 on serine residues, thus impairing the insulin signaling pathway.
Moreover, palmitate itself has been shown to directly activate the MAPK cascade in skeletal muscle, promoting the phosphorylation of ERK1/2 and contributing to insulin resistance (Macrae *et al.*, 2013) (Figure I.12.).

Fatty acids activate TLRs pathway through binding the TLRs endogenous ligand Fetuin A. In fact, it has been demonstrated that fatty acids do not directly bind to TLRs and that the presence of fetuin A is needed to trigger the downstream cascade (Pal *et al.*, 2012).
The fatty acid-induced activation of TLRs ultimately leads to the stimulation of NFκB system and the MAPK cascade (Brachmann *et al.*, 2005). Moreover, fatty acid-induced activation of TLRs increases the oxidative stress and the production of ROS. This event exacerbates the inflammatory response and promotes additional secretion of inflammatory cytokines, thus triggering a positive-feedback loop that contributes to the deleterious effects of saturated fatty acids on insulin sensitivity (Dasu and Jialal, 2011) (Figure I.12.).

I. 2.5.4.1.3. Fatty acid-induced organelle dysfunction

Elevated intracellular levels of fatty acids are also involved in development of ER stress and mitochondrial dysfunction. Increasing evidence indicates that both these phenomena are implicated in fatty acid-induced insulin resistance (Anderson *et al.*, 2009; Bonnard *et al.*, 2008) (Figure I.12.). In fact, when elevated levels of fatty acids accumulate into the cell, the ER progressively loses its capacity of properly managing the process of protein folding. This results in the accumulation of unfolded proteins and the development of ER stress. Several studies have reported that palmitic acid triggers the UPR and increases the expression of many ER stress markers such as CHOP, ATF4 and BiP, which in turn lead to the impairment of insulin signaling in liver (Kim *et al.*, 2010; Wei *et al.*, 2006; Xu *et al.*, 2015). Other study described that direct exposure of myotubes to palmitate also induces ER stress and contributes to fatty acid-induced insulin resistance in skeletal muscle (Salvado *et al.*, 2015).
In addition to ER stress, many other different mitochondrial abnormalities have been reported in liver and skeletal muscle of obese and insulin resistant subjects, such as a deficiency of mitochondrial electron transport chain proteins, decreased expression of genes involved in oxidative metabolism and mitochondrial biogenesis, decreased fatty acid oxidation and/or less abundant mitochondria with changed morphology (Tumova *et al.*, 2016).

Since ER and mitochondria are closely connected organelles, the ER stress contributes to mitochondrial dysfunction by increasing calcium release, which is directed toward the

mitochondria via domains shared by ER and mitochondria, and induce depolarization on mitochondrial membrane and subsequent impairment of the respiratory chain (Shinjo *et al.*, 2017). In addition, ER stress itself downregulates genes involved in mitochondrial function through the AP1 and ATF6 transcription factors (Zhang and Ren, 2011).

An additional mechanism by which elevated fatty acids contribute to mitochondrial dysfunction is the production of ROS species and the increase in oxidative stress. ROS can impair the activity of many enzymes involved in fatty acid oxidation, thus provoking a reduction in mitochondrial oxidative capability and subsequently leading to mitochondrial failure (Seifert *et al.*, 2010). To highlight the importance of oxidative stress in mitochondrial dysfunction and insulin resistance, a study by Houstis reported that insulin resistance can be prevented by blocking the increase in ROS levels induced by lipid overload (Houstis *et al.*, 2006). Additionally, mitochondrial superoxide production is an unifying element of insulin resistance, thus confirming the role of oxidative stress in lipid-induced insulin resistance (Hoehn *et al.*, 2009).

When fatty acids accumulate into the cell, mitochondria start to oxidize them and, in the first place, β-oxidation rate increases. However, if accumulation of intracellular lipids is prolonged, and overcomes the mitochondrial oxidation capability, the organelle faces dysfunction and begins to fail. The consequence is a decrease in β-oxidation rate and an incomplete fat oxidation, which in turn leads to further accumulation of lipid metabolites (Koves *et al.*, 2008).

Interestingly, plasma fatty acids levels are negatively correlated with the expression of PGC1α, that is involved in the regulation of mitochondrial function (Richardson *et al.*, 2005). The reduction of PGC1α expression, induced by increased levels of fatty acids, is believed to underlie some of these metabolic dysfunctions, since it is involved in mitochondrial biogenesis (Kang and Li Ji, 2012).

Fatty acids downregulate PGC1α expression through the activation of the NFκB pathway. Alternatively, they modulate its activity at translational level through the activation of JNK and ERK1/2 that directly phosphorylate and inactivate PGC1α protein (Coll *et al.*, 2006). In agreement with these findings, a reduction of PGC1α and some of its target genes involved in oxidative phosphorylation, such as ACOX and MCAD, was observed in skeletal muscle of T2D patients with increased plasma fatty acids (Mootha *et al.*, 2003; Patti *et al.*, 2003). Since PGC1α is a co-activator of PPARs, its reduction induced by elevated levels of fatty acids can also be responsible for PPARs downregulation. In fact, there is evidence that some saturated fatty acids can induce PPARs downregulation by decreasing PGC1α (Barroso *et al.*, 2011) and that this mechanism exacerbates mitochondrial dysfunction and insulin resistance in adipose tissue and skeletal muscle (Lee *et al.*, 2003a). These findings are also consistent with the evidence that palmitate and other saturated fatty acids are involved in the downregulation of genes encoding for mitochondrial respiratory

complexes OXPHOS I-V, which are targets of PPARs, resulting in impaired mitochondrial function in subjects with T2D (Razak and Anand, 2004).

It is well known that the β-oxidation is under the control of many kinases, such as ACC and AMPK (He *et al.*, 2016). Saturated fatty acids have been shown to drastically reduced AMPK activity, possibly through the activation of ERK1/2 signaling, since a negative cross-talk between AMPK and ERK1/2 has been described (Du *et al.*, 2008). AMPK has been identified as an upstream regulator of PGC1α, thus its inhibition further downregulates the coactivator activity (Lira *et al.*, 2010). Our group showed that the unsaturated fatty acid oleate prevented palmitate-induced insulin resistance through an AMPK-dependent mechanism, thus confirming the role of this kinase in lipid-induced insulin resistance (Salvado *et al.*, 2013). Colletta *et al.* have demonstrate that the PPARγ agonist pioglitazone activates AMPK in human muscle of patients with T2D, leading to expression of genes involved in mitochondrial function and fat oxidation and reduced toxic burden of intracellular lipid metabolites (Coletta *et al.*, 2009).

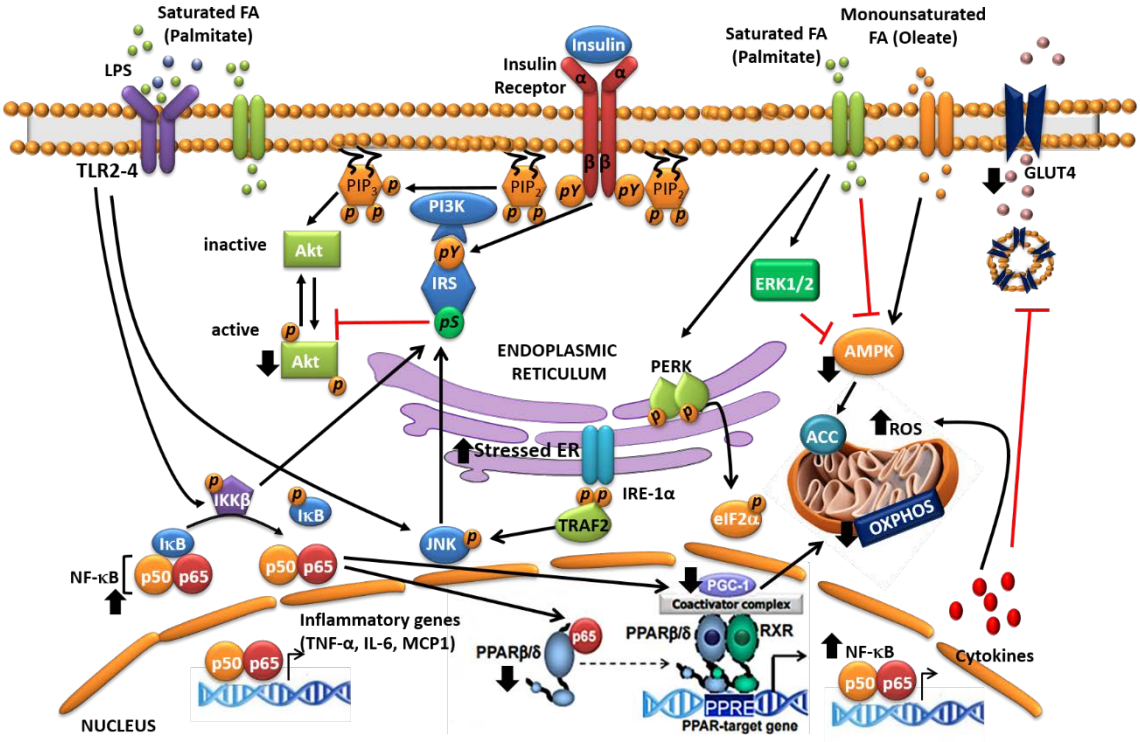

Figure I.12. Lipid-induced insulin resistance: molecular mechanisms. Fatty acids increase ER stress and induce inflammation by activating TLRs and the NFkB pathway and by inhibiting AMPK activity. Fatty acids also induce mitochondrial dysfunction by downregulating PGC1α activity and PPARs levels (Boden and Shulman, 2002; Boren *et al.*, 2013).

I. 2.5.4.2. Lipoproteins and insulin resistance

As broadly discussed, an increase in circulating levels of TG occurs in obesity because adipose tissue function is altered and its lipid handling impaired; as a result, VLDL particles that carry those TG are also increased. It has recently been reported that levels of TG rich-VLDL are higher in patients with obesity and T2D compared to healthy subjects, and a significant linear association between TG rich-VLDL levels and insulin resistance has been described (Andersen *et al.*, 2017). Furthermore, higher postprandial levels of TG-rich VLDL were found not only in the blood but also in skeletal muscle of obese patients and they were accompanied by decreased insulin sensitivity (van der Kolk *et al.*, 2016). The increase of VLDL levels in subjects with obesity and T2D might be due to hepatic overproduction, higher secretion and/or decreased clearance (Ginsberg and Huang, 2000).

Hepatic overproduction of VLDL initiates a sequence of lipoprotein changes that leads to atherogenic dyslipidemia. In particular, the dyslipidemia seen in insulin resistance and T2D is characterized by the presence TG-rich VLDL. When these particles are delipidated by LPL the final product is a small, dense LDL (sdLDL). The VLDL-TG level is the major predictor of LDL size in individuals with or without T2D (Adiels *et al.*, 2008a; Ginsberg and Huang, 2000).

Atherogenic dyslipidemia can precede the diagnosis of T2D by several years and is believed to be responsible for the cardiovascular complications of T2D (Adiels *et al.*, 2008a).

In subjects with T2D hepatic uptake of VLDL, IDL and LDL is decreased, resulting in increased plasma residence of these lipoproteins, which further contributes to their accumulation (Watts *et al.*, 2003). In addition, insulin transcriptionally regulates the expression of the LDL receptor and contributes to hepatic lipoprotein uptake. As a consequence, in insulin resistant tissues, LDL uptake is impaired and lipoproteins accumulate (Ginsberg and Huang, 2000). Moreover, increased free fatty acid influx to the liver, as seen in obesity, drives assembly of VLDL in the hepatocytes and enhances their secretion (Adiels *et al.*, 2008b).

Insulin has been shown to decreased VLDL formation by regulating the amount of fatty acids into the circulation (Lewis *et al.*, 1993). Insulin also contributes to VLDL clearance by activating LPL in adipose tissue and by stimulating their degradation in the cells. Thus, in an insulin resistance status, VLDL production is overstimulated and clearance is inhibited; this situation leads to increased levels of these lipoproteins that exacerbate hypertriglyceridemia (Adiels *et al.*, 2008b).

Whereas the effect of insulin resistance on lipoprotein metabolism has been extensively studied, little is known about the effect of elevated circulating lipoproteins in the development of insulin resistance. Recently, a study in mice showed that elevated VLDL

stimulate cytokine secretion from macrophages in adipose tissue through their binding with the VLDLR (Shin *et al.*, 2017). Since it has been well established that cytokines produced from macrophages can impair insulin signaling in adipocytes (Berg *et al.*, 2002), it is plausible than VLDL contribute to insulin resistance through this mechanism. Nguyen *et al*. also described that exposure of adipocytes to VLDL during 24 hours markedly increased the phosphorylation of JNK and p38 MAPK as well as the expression of IL6 and MCP1, thus confirming the possibility that VLDL contribute to insulin resistance by enhancing the inflammatory response (Nguyen *et al.*, 2014)(Figure I.13.).
In a recent study, Shin *et al.* reported that elevated levels of VLDL also increase *de novo* synthesis of ceramides in macrophages, which in turn promote insulin resistance in adipose tissue. The authors suggest that VLDL can contribute to insulin resistance by stimulating ceramide production and subsequent PKC activation (Shin *et al.*, 2017) (Figure I.13.).
Other evidence suggests that elevated VLDL or oxidized products of LDL can impair β-cell function through the activation of an apoptotic pathway that involves JNK. This situation leads to insulin deficiency and subsequent insulin resistance in peripheral tissues (Musso *et al.*, 2010; Roehrich *et al.*, 2003).

Not only the increase in the levels of VLDL, but also the impairment in their apolipoprotein composition is a characteristic of diabetic dyslipidemia (Tomkin and Owens, 2017). Insulin strongly increases the rate of Apo B degradation, thus inhibiting VLDL assembly and secretion by the liver. In insulin resistant settings, Apo B degradation is decreased. This situation leads to elevated levels of circulating VLDL, which can exchange their pool of apolipoproteins (Mark and Dani, 2016). In addition, it has been reported that elevated levels of circulating fatty acids stimulate the synthesis of Apo B100 and Apo B48, thus contributing to increase the levels of circulating lipoproteins (Tomkin and Owens, 2017).
Several studies described that in plasma of diabetic and hypertriglyceridemic patients the amount of Apo CIII contained in VLDL particles is increased compared to non-diabetic patients (Wyler von Ballmoos *et al.*, 2015). Therefore, it is possible that Apo CIII may be important in the development of obesity-associated diabetes. In this regard, it has been reported that insulin decreases Apo CIII expression by binding to an insulin response element located on Apo CIII gene. Therefore, during insulin resistant states, Apo CIII expression is enhanced, resulting in an increase of encoded Apo CIII protein and a subsequent increase in lipoproteins levels (Wyler von Ballmoos *et al.*, 2015).
Further, a high positive correlation has been described between TG levels and Apo CIII levels. In fact, many studies reported that Apo CIII inhibits TG hydrolysis contributing to increase TG circulating levels and exacerbating lipid toxicity (Gaudet *et al.*, 2014; Graham *et al.*, 2013; Ooi *et al.*, 2008). Consistent with this, it has been described that mice carrying

a null mutation in the gene encoding for Apo CIII showed lower TG levels compared to wild-type mice and seemed to have a favorable plasma lipid profile (Pollin *et al.*, 2008). On the contrary, mice overexpressing Apo CIII not only have high plasma TG, but also displayed increased insulin resistance (Lee *et al.*, 2011). Moreover, Apo CIII contributes to increase lipoproteins and TG levels by inhibiting LPL and by blocking the binding of lipoproteins to their receptor, thus limiting their clearance (Ginsberg and Huang, 2000) (Figure I.13.). Other evidences suggest that Apo CIII might have a role in insulin resistance by inducing β-cell dysfunction. In fact, it has been reported that Apo CIII enhances the activity of voltage-gated Ca^{2+} channels in pancreatic cells, resulting in increased cytoplasmic free Ca^{2+} concentration and apoptosis (Holmberg *et al.*, 2011). In addition, Kawakami *et al.* reported that Apo CIII alone can activate PKCα and NFκB and subsequently induce inflammation and monocyte adhesion on vascular endothelial cells (Kawakami *et al.*, 2007)(Figure I.13.). Collectively, these data suggest that Apo CIII might contribute to exacerbate insulin resistance in peripheral tissues, and make it a good candidate to further investigations.

However, Apo CIII is not the only apolipoprotein that seems to be involved in the development of insulin resistance and T2D. In fact, elevated levels of Apo E have also been related with insulin resistance (Gao *et al.*, 2007; Wang *et al.*, 2012). A recent *in vivo* study showed that Apo E overexpressing mice exhibit an impaired insulin signaling in brain and reduced peripheral insulin sensitivity (Zhao *et al.*, 2017). Conversely, Apo E deficiency in mice prevented obesity, glucose intolerance, and insulin resistance (Gao *et al.*, 2007). Moreover, Apo E deficient mice were protected against HFD-induced insulin resistance compared to wild type mice, and when injected with VLDL showed a reduction of many inflammatory markers compared to control mice (Wang *et al.*, 2012). It has been established that Apo E significantly reduces insulin signaling in neurons through binding to the insulin receptor protein and promoting its internalization in the endosomal compartment (Zhao *et al.*, 2017). Moreover, Apo E reduces the phosphorylation of Akt in the brain, possibly by activating MAPK pathway and inducing serine phosphorylation of IRS1 (Ong *et al.*, 2014). It is not clear if these molecular mechanisms apply also in liver, adipose tissue and skeletal muscle, but previous studies with Apo E overexpressing mice not only showed impairment of insulin signaling in the brain, but also indicated peripheral insulin resistance (Zhao *et al.*, 2017). Thus, it is possible that Apo E might also be involved in the development of peripheral insulin resistance.

Further investigations are required to get deeper inside into the mechanisms that link lipoprotein metabolism with insulin resistance and examine whether these mechanisms might be useful to prevent or to treat insulin resistance in skeletal muscle.

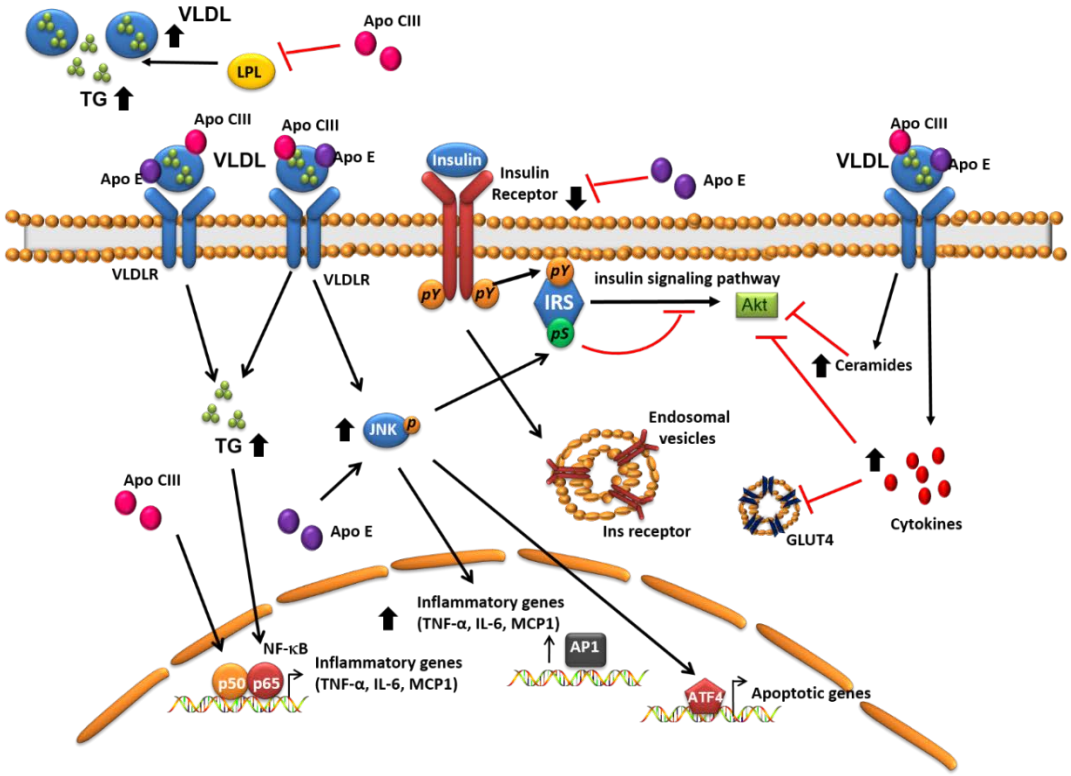

Figure I.13. Lipoproteins and insulin resistance: molecular links. VLDL and LDL have been reported to induce inflammation and cytokine production. Apo E reduces the insulin signaling pathway possibly through JNK activation. Apo CIII increases VLDL and TG levels, induces inflammation and impairs β-cell function (Ginsberg *et al.*, 2006).

I. 3. Alzheimer's disease, insulin resistance and T2D

It has been established that T2D is associated with cognitive dysfunction (Barbagallo and Dominguez, 2014). The incidence of both T2D and dementia increases in later life, which raises the prevalence of the comorbidity of these pathologies with age. Moreover, several studies have generated epidemiological, clinical and pathological evidence of the relationship between T2D and Alzheimer's Disease (AD) (Leibson *et al.*, 1997; McCrimmon *et al.*, 2012; Ott *et al.*, 1999). One of the earliest findings that indicates that older people with T2D have a higher risk of cognitive dysfunction is the Rotterdam Study (Ott *et al.*, 1999), in which longitudinal epidemiological follow-up of several diabetic patients have revealed that the risk of developing late-onset AD is 2-fold higher among those patients with T2D.

The mechanistic links between AD and T2D are still unclear, although many evidences indicate that the two diseases share several molecular abnormalities, such as impaired mitochondrial function, increased low-grade inflammation, and altered glucose and lipid metabolism (Correia *et al.*, 2012). The revaluation of the literature revealed that impairments in cerebral insulin function, glucose utilization and energy metabolism represent very early abnormalities in AD patients, that precede or accompany the initial stage of cognitive dysfunction and suggested the hypothesis that AD can be considered a type 3 diabetes (de la Monte and Wands, 2008). However, some authors reported that increased levels of typical markers of AD precede and prompt glucose intolerance and insulin resistance both in the central nervous system (CNS) and in the periphery (Jimenez-Palomares *et al.*, 2012; Plucinska *et al.*, 2016; Sato and Morishita, 2013). In agreement with this, the Mayo Clinic AD Patient registry revealed that 80% of AD patients have either T2D or an impaired fasting glucose level (Janson *et al.*, 2004), indicating that AD represents an important risk factor for T2D.

It is still controversial whether insulin resistance represents a hallmark for AD or, conversely, abnormalities of AD can contribute to peripheral insulin resistance. Although it is impossible to discriminate which abnormality occurs first, the tight connection between the two diseases highlights the importance to go further inside the molecular mechanisms, to discover new therapeutic strategies.

In the following sections, the principle hallmarks of AD and their involvement in insulin resistance will be described.

I. 3.1. Alzheimer's hallmarks: neurofibrillary tangles and amyloid plaques

Recently, newer clinical criteria for the diagnosis of AD have been accepted and include analysis of abnormal cerebrospinal fluid (CSF) markers and positive brain imaging obtained by positron emission tomography (PET)(Baker *et al.*, 2011). However, AD can only be diagnosed with certainty by post mortem demonstration of abundant

neurofibrillary tangles and β-amyloid deposits in vessel walls and other selected regions of the brain (Lewczuk *et al.*, 2010). Thus, according to classical criteria, the two principal hallmarks of AD are neurofibrillary tangles formed by hyper-phosphorylated tau protein and β-amyloid (Aβ) plaques.

I. 3.1.1. Tau proteins

Tau proteins are proteins that stabilize microtubules. They are abundant in neurons of the CNS but are also expressed at very low levels in astrocytes and oligodendrocytes. Pathologies and dementias of the nervous system such as AD and Parkinson's disease are associated with tau proteins that have become defective and no longer stabilize microtubules properly (Gotz *et al.*, 2006).

Tau proteins are highly soluble microtubule-associated proteins (Lee *et al.*, 2008) and interact with tubulin to stabilize microtubules. Six tau isoforms exist in human brain tissue, and they are distinguished by their number of microtubule-binding domains. Three isoforms have three binding domains and the other three have four binding domains. The binding domains are located in the carboxy-terminus of the protein and are positively charged (allowing it to bind to the negatively charged microtubule). The isoforms with four binding domains are better at stabilizing microtubules than those with three binding domains (Goedert *et al.*, 1989).

Tau contains 79 potential serine and threonine phosphorylation sites that are only half-phosphorylated in normal physiological condition. Phosphorylation of tau is under the control of a host of kinases and phosphatases, including GSK3 and PP2A (Avila, 2008). Hyper-phosphorylation of the tau proteins result in self-assembly into paired helical filaments, leading to the formation of neurofibrillary tangles that accumulate and exert toxic effects on neuronal survival (Gotz *et al.*, 2006).

I. 3.1.2. Amyloid Precursor Protein (APP) and Aβ synthesis

The amyloid precursor protein (APP) is one member of a family of related proteins that includes the amyloid precursor-like proteins 1 and 2 (APLP1 and APLP2). All are single-pass transmembrane proteins with large extracellular domains and a short cytoplasmic domain. Only APP generates amyloidogenic Aβ fragments owing to a sequence divergence at the internal cleavage site (Tharp and Sarkar, 2013).

Once in the endosome compartment, APP can be cleaved by different enzymes (Figure I.14.). The principal proteolytic cleavage of APP is performed by a protease designated as α-secretase. The α-secretase is a member of the a disintegrin and metalloproteinase (ADAM) family (Adamovich *et al.*, 2013), which includes the TNFα-converting enzyme (TACE) and the meltrin γ (or MDC9). The most common isoform of α-secretase is the ADAM10 protein, which is responsible for the APP cleavage between Lys^{16} and Leu^{17} amino acids (residues 612 and 613 of APP). These residues are located in the sequence

that produces for the Aβ peptide itself and therefore such specific cleavage precludes generation of Aβ peptide. Initially it was believed that this cleavage is the physiological one (Esch *et al.*, 1990; Sisodia, 1992) and that it prevents amyloidogenesis in AD. However, this is an oversimplification, because only a fraction of the total pool of APP is cleaved by α-secretase, leaving most of the APP protein intact. Furthermore, other kinds of APP cleavage also occur under physiological conditions. This indicates that all fragments of APP, including the Aβ peptide, are part of normal physiology (Haass *et al.*, 1992; Seubert *et al.*, 1992). The cleavage of APP by α-secretase results in the generation of a 100 KDa soluble APP fragment (sAPPα), which is released into the cytosol and might have biological functions in growth regulation and neuroprotection, and a C-terminal 83-residue APP fragment (C83), which remains bounded to the cell membrane (Oltersdorf *et al.*, 1990). The α-secretase cleavage is stimulated by many transduction signaling, including the activation of PKC protein (Buxbaum *et al.*, 1993).

The alternative proteolytic cleavage of APP is carried out by a protease called β-secretase. The β-secretase cleaves APP at the N-terminus of the Aβ-peptide sequence and generates a soluble N-terminal fragment called sAPPβ and a membrane-bounded C-terminal fragment of 99 residues (C99) (Vassar *et al.*, 2014). The most common β-secretase is the β-site APP Cleaving Enzyme (BACE) which is highly expressed in several tissues.

After both the α-secretase and the β-secretase cleavages, the γ-secretase enzyme then cuts the C83 or the C99 fragment, thus producing the non-toxic p3 fragment or the Aβ peptide, respectively (Vassar *et al.*, 2014). The γ-secretase is a multi-subunit complex composed of four transmembrane proteins: presenilin, nicastrin, presenilin enhancer 2 (PEN2) and anterior pharynx-defective 1 (APH1) and exists in many isoforms. Depending on the γ-secretase isoform, the sAPPβ fragment might undergo different cleavages on different sites. Thus, Aβ peptides with different length are produced, from 38 up to 42 residues. The most common Aβ peptides generated by the γ-secretase cleavage are the Aβ40 and the Aβ42, respectively composed by 40 and 42 amino acids. These short peptides are the most toxic and can assembly and accumulate to form amyloid plaques (Dislich and Lichtenthaler, 2012; Tharp and Sarkar, 2013) (Figure I.14.).

Insulin has been reported to efficiently regulate APP trafficking from the endosome compartment, which is the main site for cleavage, to the membrane surface. This effect allows to lower the amount of APP available for cleavage and to subsequently reduce the Aβ production (Gasparini *et al.*, 2001). Therefore, in insulin resistant states, APP cleavage and Aβ production are increased.

In the next sections, a brief description of the enzymatic products of the APP cleaving process (the sAPPα, sAPPβ and Aβ fragments) and of BACE1 activity will be given.

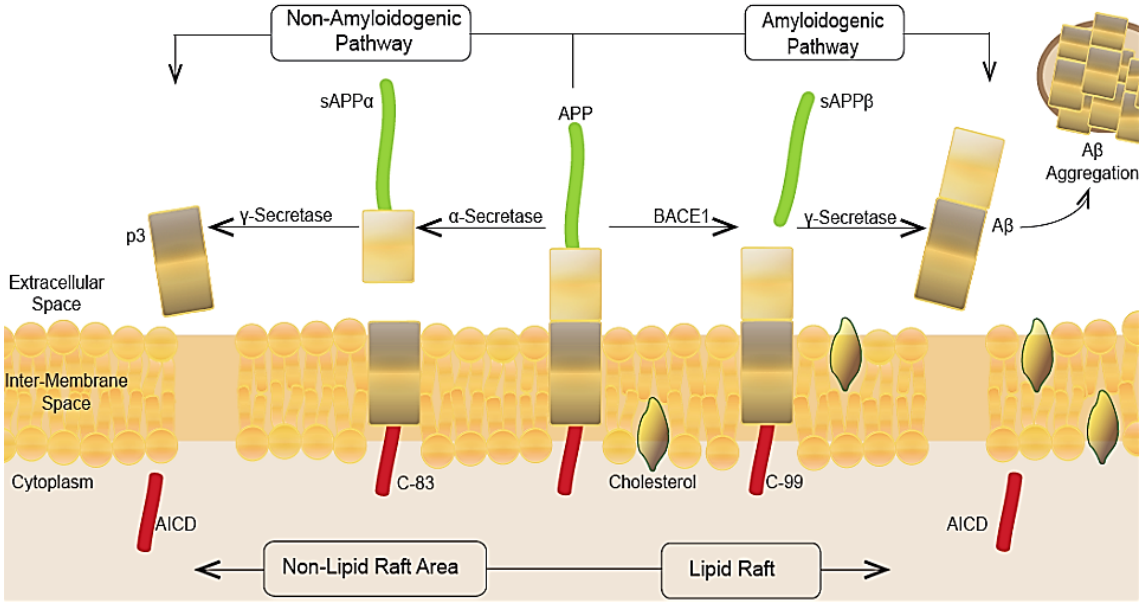

Figure I.14. Amyloidogenic and non-amyloidogenic pathways. When APP is cleaved by the α-secretase the proteolytic products are the soluble N-terminal fragment sAPPα and the membrane-bound C83 fragment. Subsequently, the γ-secretase cleaves the C83 peptide, forming the short p3 fragment and the APP intracellular domain (AICD). This cleavage precludes the Aβ formation. On the other hand, when APP is cleaved by the β-secretase BACE1, the soluble sAPPβ fragment and the C-terminal C99 peptide are produced. The subsequent cleavage of C99 by the γ-secretase produces the Aβ fragment that can aggregates into amyloid plaques (Read J., 2013).

I. 3.2. sAPPα and sAPPβ

While the role of Aβ fragments in the pathogenesis of AD is well established and has been extensively studied, little is known about the physiological functions of the intermediate soluble fragment sAPPα and β. sAPPβ differs from sAPPα by lacking a region of 16 amino acids at the C-terminus (Chasseigneaux and Allinquant, 2012).

It has been shown that sAPPα possesses neurotrophic effects; for example, it promotes neurite outgrowth *in vitro* (Mattson, 1997) and protects neural tissue after brain injury (Thornton *et al.*, 2006). Moreover, sAPPα regulates neural progenitor cell proliferation in the adult brain and it has been reported that intraventricular injection of recombinant sAPPα can rescue age-associated decline of neurogenesis (Demars *et al.*, 2013).

Recently, a receptor for sAPPα has been identified, the p75 neurotrophin receptor (p75NTR). p75NTR mediates a diverse set of functions, including neurite outgrowth, axonal elongation, neuronal survival, and modulation of synaptic transmission through the cAMP-PKA pathway (Hasebe *et al.*, 2013). sAPPα binds to p75NTR and promotes its downstream cascade. It has been reported that sAPPβ also binds to p75NTR but with much lesser affinity than sAPPα and has no effects on neurite outgrowth (Hasebe *et al.*, 2013).

The physiological functions of sAPPβ are still unclear (Jiang *et al.*, 2003). Nikolaev *et al.* showed that it binds to a death receptor (death receptor 6, DR6) and mediates neuronal

apoptosis by activating distinct caspases (Nikolaev *et al.*, 2009). Other studies reported that sAPPβ is also involved in maintaining cortical thickness (Alcolea *et al.*, 2017).

Several studies have measured sAPPα and β concentration in the CSF and have assessed their kinetics. Dobrowolska *et al.* (Dobrowolska *et al.*, 2014a) described a circadian production for both sAPPα and β and also for Aβ40-42 peptides, supporting the hypothesis that APP is diurnally regulated in the human CNS. This diurnal pattern diminishes with increased age and the sAPPs production tents to become constant. Moreover, the authors demonstrated that the four APP metabolites (sAPPα, sAPPβ, Aβ40, and Aβ42) were positively correlated in all healthy participants. This positive correlation suggests that the α- and β- APP pathways are non-competitive under normal physiologic conditions, where APP availability may be the limiting factor that determines sAPPα over sAPPβ production (Dobrowolska *et al.*, 2014a). However, in patients with AD, the physiologic regulation of amyloid production in the CSF is impaired and Aβ levels are higher than in control subjects. In addition, the ratio of sAPPβ to sAPPα is also significantly higher in subjects with cerebral Aβ deposits *vs.* those without deposits (Dobrowolska *et al.*, 2014b). This might indicate that only in pathological conditions the two pathways become mutually exclusive, being the pro-amyloidogenic pathway predominant and shunting down the non-amyloidogenic pathways. Therefore, the sAPPβ to sAPPα ratio may be a useful biomarker for cerebral amyloidosis. Consistent with these results, several studies revealed increased sAPPβ levels in the CSF of patients with AD compared to controls (Araki *et al.*, 2017; Lewczuk *et al.*, 2010). On the other hand, some authors did not observed any change in sAPPβ or sAPPα concentration in subjects with AD *vs.* healthy subjects (Olsson *et al.*, 2003; Zetterberg *et al.*, 2008).

Interestingly, other authors also found a positive correlation between elevated levels of sAPPβ and increased levels of phospho-tau in patients with AD, suggesting a pathological association between tau metabolism and β-secretase activity, although the molecular mechanism remains unknown (Araki *et al.*, 2017).

Of note, it is important to remark that in physiological conditions, the concentration of sAPPα and β in the CSF is significantly higher than the concentration of Aβ42 (sAPPα: 114.4 ng/ml; sAPPβ: 141±47 ng/ml; Aβ42: 886±230 pg/ml)(Araki *et al.*, 2017; Oikonomidi *et al.*, 2016). The reason could be the reduced clearance for these larger APP metabolites when compared with Aβ. In fact, Dobrowolska *et al.* described that total sAPPα and β are metabolized 2-fold slower than Aβ in young, healthy humans. The slower turnover rates for these larger APP metabolites may be driven by delayed transport out of the brain (Dobrowolska *et al.*, 2014b). The mechanism for the efflux of brain sAPPα and β into periphery remains unknown (Xiang *et al.*, 2015). However, it has been well established that sAPPα and sAPPβ are not only produced in the brain, but also in the peripheral tissues. For instance, platelets, leucocytes, endothelial cells, skeletal muscle, pancreas,

kidney, spleen, heart, liver and many other tissues possess the proteolytic machinery to produce sAPPβ (Kitazume *et al.*, 2012; Vignini *et al.*, 2011). Recently, plasma concentrations of sAPPβ were shown to differ between patients with AD and healthy elderly individuals (Alexopoulos *et al.*, 2017; Perneczky *et al.*, 2013; Wu *et al.*, 2011). However, the results are inconclusive since some authors showed a reduction of sAPPβ plasma levels in patients with AD (Alexopoulos *et al.*, 2017), while others observed increased levels (Wu *et al.*, 2011). An example is depicted in Table I.2.

Since β-secretase activity has been also reported to be increased in the peripheral compartment in subjects with dementia (Jiang *et al.*, 2003; Xiang *et al.*, 2015), it is feasible that sAPPβ plasma levels might be higher in AD patients than in healthy subjects, thus becoming a potential marker of the disease.

Groups	Age	Gender (M/F)	sAPPα (ng/ml)	sAPPβ (ng/ml)	p-tau (pg/ml)	Aβ42 (pg/ml)
AD	75.5 ± 1.5	15/18	320.6 ± 22.6	594.9 ± 39.7	89.1 ± 5.8	677.8 ± 34.0
MCI-AD	70.6 ± 2.1	7/10	468.0 ± 66.4	785.4 ± 101.2	91.7 ± 9.5	562.0 ± 60.8
Non-AD	72.6 ± 1.6	14/13	235.5 ± 24.9	417.6 ± 33.6	43.9 ± 3.8	844.3 ± 55.2
Dis. control	67.5 ± 1.9	12/7	222.8 ± 25.0	383.6 ± 34.3	36.1 ± 2.7	1013.0 ± 71.2

Table I.2. Concentration in the CSF of sAPPα, sAPPβ, p-Tau and Aβ42 in healthy subjects (Dis. Control) or in patients with AD, Mild Cognitive Impairment (MCI) (Burgess *et al.*, 2006) or others non-Alzheimer dementias (non-AD) (Araki *et al.*, 2017).

I. 3.3. BACEs

BACE is a 501-amino acid transmembrane aspartic protease of 70 KDa molecular weight that exists in two homologs: BACE1 and BACE2. BACE1 is widely expressed in many tissues, including brain, skeletal muscle, liver, and adipose tissue. BACE2 is predominantly expressed in pancreatic β-cells and only at a very low level in neurons.

The BACEs proteins are paralogous to pepsins and cathepsins and, similar to other aspartic proteases, undergo many post-translational modifications (Rawlings and Bateman, 2009; Southan and Hancock, 2013).

BACE1 is synthetized as a zymogen in which its pre- and pro-peptide domains are removed in the ER and in the Golgi apparatus by specific peptidases. BACE1 also undergoes N-glycosylation at four asparagine residues (N153, N172, N223, N354) in the ER and the Golgi. During its transit to the ER, the BACE1 catalytic domain is folded and cross-linked with three disulfide bonds (C216-C420, C278-C443, C330-C380). The BACE1 catalytic domain contains two signature aspartic-acid active site motifs that are spaced approximately 200 residues apart; both aspartates (position 93 and 89) are required for the proteolytic activity of BACE1. The cytosolic domain of BACE1 can undergo

phosphorylation at Ser^{498}, an event that influences BACE1 trafficking in the endosome system; in addition, Lys^{501} in the cytosolic domain can be ubiquitinated, a process that affects BACE1 degradation. BACE1 also exhibits S-palmitoylation at four cysteine residues (C474, C478, C482, C485) at the junction of the transmembrane and the cytosolic domains that determines its localization into lipids raft of the endosomes membrane (Dislich and Lichtenthaler, 2012). In agreement with the BACE1 localization into phospholipidic endosome bilayer, a direct effect of the lipid sphingosine-1-phosphate on BACE1 has been shown: the sphingosine binds to the C-terminal and transmembrane region activating the proteolytic activity of BACE1 (Takasugi *et al.*, 2011).

Being an aspartyl protease, BACE1 requires low pH for its activity and this correlates with the endosome intraluminal pH. Thus, BACE1 cleavage of APP and other substrates mostly occurs in endosome. Many proteins regulate the sorting of BACE1 from endosomes; among these, the most important are the Golgi-localized γ-ear containing ADP-ribosylation factor binding 1 and 3 (GGA1 and GGA3). They interact with BACE1 via an acidic dileucine binding motif and negatively regulate BACE1 residence in the endosome, thus reducing its proteolytic activity (Kang *et al.*, 2010).

I. 3.3.1. <u>The BACE1 cleavage of APP</u>

BACE1 cleaves the APP on the amino acids Asp^{1} and Glu^{11} of the Aβ-peptide sequence, which correspond to the residues 671 and 672, and produce the membrane-bounded C-terminal fragment of 99 amino acids (C99) and the N-terminal soluble sAPPβ peptide with a molecular weight of approximately 100-110 KDa. Unless BACE2 can cut at the same level, it predominantly cuts at Phe^{19} and Phe^{20} residues, thus precluding Aβ formation. Well established lines of APP Tg mice have been generated that develop amyloid plaques with age. Several of these APP Tg lines were crossed with BACE1 knockout models to produce APP Tg/$BACE1^{-/-}$ bigenic mice. These mice were shown to lack Aβ production, amyloid deposition and Aβ-dependent memory deficits, confirming that BACE1 cleavage is necessary for Aβ production (Ohno *et al.*, 2006) (Luo *et al.*, 2001).

Several studies have tried to determine whether BACE1 levels are increased in brain of patients with AD or not. However, the results are controversial. In fact, some authors showed no differences in BACE1 expression between AD patients and healthy subjects (Perneczky *et al.*, 2013; Savage *et al.*, 2015), while others found a significant increase (more than 2-fold) of BACE1 levels in the CSF of AD patients compared to controls (Hampel and Shen, 2009; Olsson *et al.*, 2003). In subjects with sporadic AD, an increase in BACE1 enzymatic activity was observed in frontal cortex from postmortem specimens, as compared to control subjects, and it appears correlated with amyloid load (Fukumoto *et al.*, 2002; Johnston *et al.*, 2005; Li *et al.*, 2004a). Some authors also found increased BACE1 protein levels in brain of patients with sporadic AD (Yang *et al.*, 2003). Moreover, Wu *et*

al. reported that BACE1 enzymatic activity increases with age (Wu *et al.*, 2011), while other studies revealed that BACE1 levels are upregulated under stress conditions, such as cerebral ischemia, hypoxia and oxidative stress. Both age and stress conditions represent a risk factor for the development of AD. Animal models overexpressing BACE1 showed impaired learning/memory and marked cognitive deficiency, suggesting that BACE1 upregulation might contribute to the development of the disease (Rockenstein *et al.*, 2005).

I. 3.3.2. Other BACE1 substrates

Initially, APP was the only known BACE1 substrate. However, now it is recognized that BACE1 cleaves many other substrates, different from APP, and this provides new insights into important BACE1 physiological functions. One of the best understood effects of BACE1 is its proteolytic processing and activation of neuroregulin 1 (NRG1) type III, a protein that plays a pivotal role in post-natal myelination. $BACE1^{-/-}$ animals show prominent hypomyelination in the peripheral nervous system (Willem *et al.*, 2009). Moreover, a recent study showed that BACE1 processing of NRG1 is required for formation and maintenance of muscle spindle. In fact, inhibition of BACE1 activity or ablation of NRG1 expression in adult mice result in a massive reduction of the muscle spindle pool and impaired coordination of movement (Cheret *et al.*, 2013).

The β-subunits 2 and 4 of the voltage-gated sodium channels (VGSCs) are also known to be processed by BACE1 under physiological conditions (Isom, 2001). Other BACE1 substrates have been identified and are related with the inflammatory process: the β-galactoside-6-sialyltransferase (ST6Gal1), which is released from liver during acute phase reactions; the P-selectin glycoprotein ligand 1 (PSGL1), which mediates the adhesion to endothelial cells during inflammation; and the interleukin1 receptor II that is responsible for IL1 effects. Currently is not known whether the shedding of these substrates occurs under physiological conditions. However, $BACE1^{-/-}$ mice show a favorable anti-inflammatory profile, compared to wild-type mice (Dislich and Lichtenthaler, 2012).

The low-density lipoprotein receptor-related protein (LRP) has been shown to coimmunoprecipitate with BACE1 in human brain tissue, although no endogenous processing of LRP by BACE1 has been demonstrated so far (von Arnim *et al.*, 2005).

BACE1 also cleaves many proteins that are involved in axon neurogenesis and outgrowth, axoglial interactions and synapsis functions (Vassar *et al.*, 2014).

Recently, Chen e*t al.* reported that BACE1 allosterically binds to adenylate cyclase (AC), through its transmembrane domain (Chen *et al.*, 2012b). AC is the transmembrane enzyme responsible for the production of the secondary messenger cAMP, which is involved in learning and memory processes (Brunelli *et al.*, 1976). The authors demonstrated that AC is not a substrate for BACE1 proteolytic activity, but their

interaction impairs AC downstream signaling pathway, the cAMP/PKA/CREB pathway, thus contributing to induce deficits in learning and memory processes (Chen *et al.*, 2012b). Since the cAMP response binding protein (CREB) is an important transcription factor also involved in many metabolic processes, the cAMP/PKA/CREB pathway might be considered an important molecular link between AD and T2D. Thus, it is feasible that BACE1 contributes to metabolic and peripheral effects, not only by the cleavage of APP, but also through its modulation of AC/cAMP/CREB pathway.
The CREB pathway will be extensively described in the next section.

I. 3.3.2.1. The cAMP/PKA/CREB pathway

CREB belongs to the family of leucine zipper transcription factors, which are expressed in a variety of tissues (Ortega-Martinez, 2015). CREB binds to conserved DNA sequences called cAMP response elements (CRE) that are present within the regulatory regions of several genes. The binding of CREB and other transcription factors to the promoter sequence CRE regulates RNA polymerase activity, thereby controlling gene expression (Ortega-Martinez, 2015). The CREB family of transcription factors includes CREB, CRE modulator (CREM), and activating transcription factor 1 (ATF1). CREB and ATF1 are expressed ubiquitously, whereas CREM is mainly expressed in the neuroendocrine system (Ortega-Martinez, 2015).
The transcriptional activity of CREB depends on its phosphorylation status, which is determined by opposing actions of protein kinases and phosphatases. The cAMP-dependent PKA is the main kinase that phosphorylates CREB at Ser^{133} and promotes its transcriptional activity. When a stimulus gets to the membrane surface and, for instance, binds to the transmembrane G-protein-coupled receptor, the enzyme AC is activated and produces the second messenger cAMP. The accumulation of cAMP induces PKA activation. In fact, in the basal state, PKA resides in the cytoplasm as an inactive heterotetramer of paired regulatory subunits and catalytic subunits. When the levels of cAMP rise into the cell, the cAMP binds to the regulatory subunits causing them to undergo a conformational change that liberates the catalytic subunits. Thus, the catalytic subunits are free to passively diffuse into the nucleus where phosphorylate CREB at Ser^{133}.
Phosphorylation of CREB promotes the recruitment of two coactivators, the CREB binding protein (CBP) and the paralogue p300, which are required for gene transcription since they directly interact with the RNA polymerase and have intrinsic histone acetyltransferase activity. Target gene activation is terminated by the protein phosphatase 1 (PPA1), which mediates CREB dephosphorylation (Mayr and Montminy, 2001) (Figure I.15.).
There are many signaling cascades upstream the CREB phosphorylation. For example, the pro-inflammatory and stress-induced MAPK pathway, as well as grow factor receptors

signaling, the Ca^{2+}/calmodulin-dependent protein kinase signaling or the phophoinositide 3 kinase/Akt pathway have been shown to induce CREB activity (Lonze and Ginty, 2002). On the other hand, CREB has a widely range of target genes that are involved in metabolism (PDK4, hexokinase, PGC1α, CPT1), cell proliferation and growth (somatostatin, glucagon, insulin), memory and plasticity [c-fos, brain derived neurotropic factor (BDNF), activity regulated cytoskeleton associated protein (Arc)], and several other processes (Ortega-Martinez, 2015).

Chen *et al.* recently reported that BACE1 overexpressing mice exhibit dramatically decreased levels of phosphorylated CREB, thus pointing BACE1 as a potential negative modulator of CREB activity (Chen *et al.*, 2012b). Moreover, exposure of neuronal cells to low concentrations of Aβ toxic peptide heavily decreased CREB phosphorylation and activity (Tong *et al.*, 2001). It is well established that Aβ deposition causes oxidative stress in the brain (Yang *et al.*, 2004) and can contribute to neuronal death through this pathway. CREB is involved in the oxidative-stress response since is activated by several stress kinases, such as MAPK. CREB also participates in mitochondrial oxidative metabolism by enhancing the expression of the transcriptional coactivator PGC1α, which is one of its most important target genes (Mayr and Montminy, 2001). As discussed below, mitochondrial dysfunction and oxidative stress are a common feature between AD and T2D and accumulating evidences suggest that the impairment of the PKA/CREB pathway could be a molecular link between the two diseases. In fact, cAMP is the major modulator of CREB activity but it also enhances AMPK phosphorylation that is involved in PGC1α activation and is considered the principal sensor of energy status in the cells (Kim *et al.*, 2014).

Figure I.15 summarizes the AC/cAMP/PKA/CREB pathway.

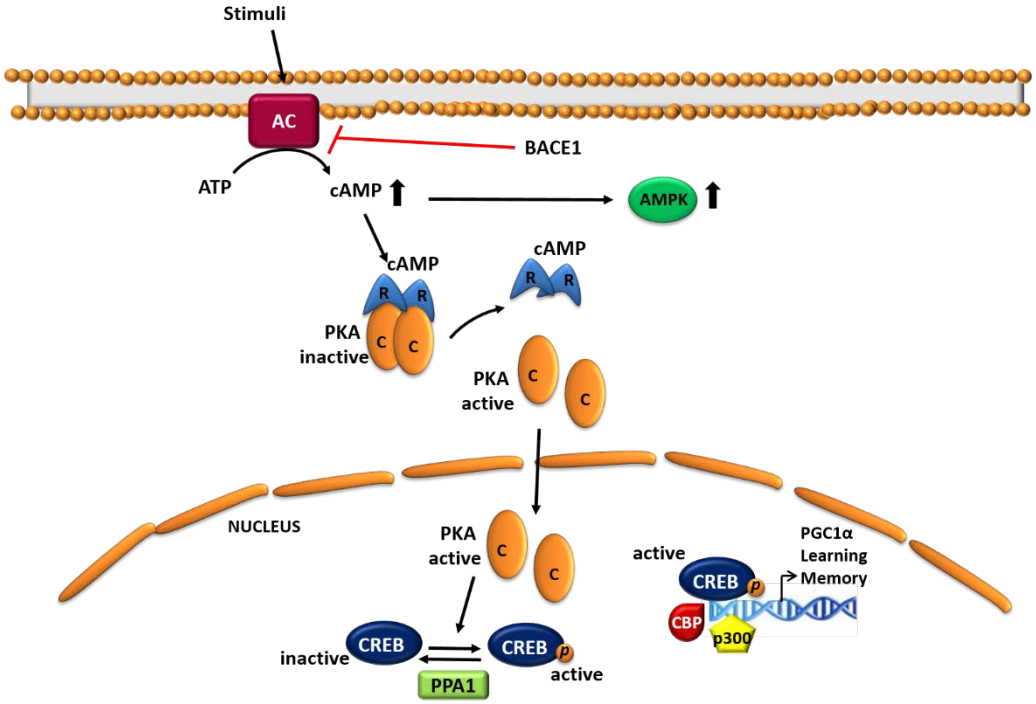

Figure I.15. CREB/PKA pathway. When the stimuli get to the membrane surface, adenylate cyclase (AC) is activated and the intracellular concentration of cyclic AMP increases. cAMP binds to the regulatory subunits of PKA, thus inducing a conformational change that frees the catalytic subunits and activates PKA. Once in the nucleus, PKA phosphorylates CREB on Ser^{133} promoting its activity as transcription factor (Mayr and Montminy, 2001).

I. 3.3.3. Transcriptional and translational regulation of BACE1

BACE1 expression and enzymatic activity are strictly regulated at both transcriptional and translational level (Rossner *et al.*, 2006) (Figure I.16.).

A number of transcription factors have been identify that positively or negatively regulate BACE1 expression in both basal and cell stress conditions (Guglielmotto *et al.*, 2012; Sun *et al.*, 2005). For example, it has been reported that PPARγ and its coactivator PGC1α strongly reduce BACE1 expression in neurons. AMPK stimulation also decreases BACE1 expression, possibly by directly activating PGC1α (Wang *et al.*, 2013), while nitric oxide (NO) has been reported to strongly reduce BACE1 expression through a cGMP-PKG signaling (Kwak *et al.*, 2011). Sastre *et al.* demonstrated that PPARγ depletion in fibroblasts potentiated BACE1 gene promoter activity and that, conversely, upregulation of PPARγ reduced BACE1 expression (Sastre *et al.*, 2006). In the same study, the authors also reported that non-steroidal anti-inflammatory drugs (NSAIDs) were able to decrease BACE1 expression by activating PPARγ (Sastre *et al.*, 2006). Consistent with this, another study from Wang *et al.* reported that cycloxygenase 2 (COX2), which is the main target of the inhibitory action of NSAIDs, increases BACE1 expression in neurons, through a mechanism that involves NFκB activation (Wang *et al.*, 2014).

Indeed, during inflammation and stress conditions, the NFκB pathway has been reported to heavily upregulate BACE1 expression (Chen *et al.*, 2012a). In fact, two functional NFκB binding elements were identified in the human BACE1 promoter region and their activity was increased by NFκB stimulation and TNFα secretion. On the contrary, disruption of the p65 gene in mice blunted BACE1 gene transcription (Wang *et al.*, 2013). Guglielmotto *et al.* reported that AGEs, formed during a hyperglycemic status, can induce oxidative stress and the subsequent activation of the NFκB pathway, thus increasing BACE1 expression in diabetic rat (Guglielmotto *et al.*, 2012). It has also been described that the activation of the JNK pathway during stress and inflammation leads to the stimulation of the transcriptional factor AP1, which in turn increases BACE1 expression. Moreover, ER stress induction in human cultured myocytes significantly increases BACE1 transcript and mRNA levels, suggesting that ER stress can participate in upregulating BACE1 expression (Nogalska *et al.*, 2010; Rozpedek *et al.*, 2015).

Regarding the post-transcriptional modifications, many molecules have been shown to regulate BACE1 activity and trafficking. PGC1α promotes BACE degradation by enhancing its ubiquitination in cardiac and skeletal muscle (Gong *et al.*, 2010). The translational regulator S6 kinase (S6K) protein, which is activated by the antidiabetic drug metformin, decreases BACE1 protein levels by stopping its translation (Hettich *et al.*, 2014). Moreover, the activation of PERK and the subsequent phosphorylation of eIF2α during ER stress promotes BACE1 translation and increases its protein levels (O'Connor *et al.*, 2008).

An *in vitro* experiment also showed that the lipid second messenger C6 ceramide post-translationally stabilizes BACE1 protein, thus reducing its turnover and maintaining its levels higher than normal (Puglielli *et al.*, 2003). Consistent with these findings, feeding a HFD has been reported to increase BACE1 activity, possibly promoting its subcellular trafficking from the cell surface to the endosomal compartments and therefore increasing APP cleavage (Maesako *et al.*, 2015).

Finally, it has also been reported that the soluble fragment sAPPα directly associates with BACE1 protein and interferes with BACE1/APP interaction, thus decreasing BACE1 enzymatic activity and Aβ production (Obregon *et al.*, 2012).

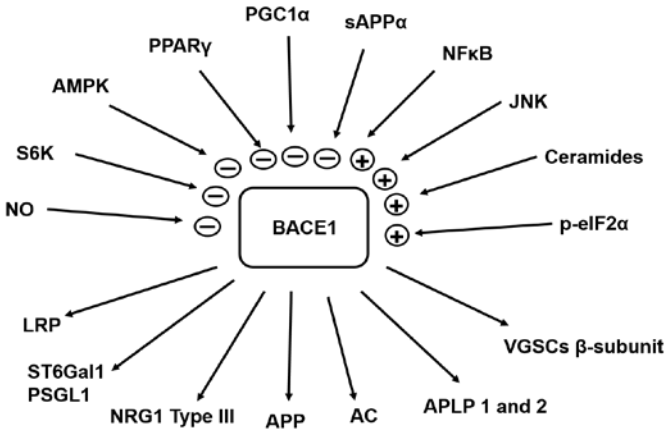

Figure I.16. Schematic portrayal of BACE1 substrates and regulation. APP is not the only BACE1 substrate. In fact, BACE1 can cleave or interact with several proteins, such as Neuroregulin 1 (NRG1), adenylate cyclase (AC) or the Voltage Gate Sodium Channels (VGSCs). BACE1 activity and expression are strictly regulated. PGC1α and AMP negatively regulate BACE1, while inflammatory and ER stress pathway up-regulate BACE1 (Vassar *et al.*, 2014).

I. 3.3.4. The role of BACE1 and Aβ in glucose and lipids homeostasis

Recent studies have demonstrated that BACE1 has also a role in energy metabolism. Meakin and colleagues showed that BACE1 knockout mice are leaner, with decreased adiposity, higher energy expenditure, improved glucose disposal and better peripheral insulin sensitivity than wild type littermates. BACE1 knockout mice were also protected from diet-induced obesity. These findings suggest the idea that BACE1 may play a critical role in glucose and lipid homeostasis, not only in physiological conditions, but also in a condition of chronic overnutrition (Meakin *et al.*, 2012).

As previously mentioned, BACE1 is widely expressed in several tissues, including liver, skeletal muscle and adipose tissue and many evidences suggest that BACE1 cleavage of APP takes place also in tissues different from brain. BACE1 cleavage of APP has been tested in skeletal muscle and the concentration of its proteolytic products has been measured in myocytes. Hamilton *et al.* detected the presence of both BACE1 and APP in C2C12 myoblast and myotubes and demonstrated that BACE1 was proteolytically active on APP by detecting the presence of the sAPPβ fragment in the incubation medium (Hamilton *et al.*, 2014). HFD feeding significantly increased the protease activity of BACE1 on APP in skeletal muscle and liver of wild-type mice. Consistent with these results, treatment of myotubes with palmitic acid or ceramides strongly increased BACE1 expression and protein levels (Hamilton *et al.*, 2014). Pharmacological inhibition of BACE1 activity in myotubes, using a high selective BACE1 inhibitor, significantly increased Akt phosphorylation and GLUT4 translocation, confirming the role of BACE1 in peripheral insulin signaling (Meakin *et al.*, 2012).

A recent study in rodents showed that overexpression of BACE1 in neurons induced systemic glucose intolerance in mice from 4 months of age onward and that the diabetic phenotype was associated with advanced ER stress. The animals also showed dysregulated central and plasma lipid composition (Plucinska *et al.*, 2016).

Many evidences also suggest that the fragment Aβ, especially the Aβ40 and Aβ42 peptides, might be involved in the development of central and peripheral insulin resistance. Lee and colleagues showed that Aβ inhibits both insulin-induced Akt phosphorylation and activity. Aβ also blocks the association between PDK and Akt, specifically interrupting the PDK-dependent activation of Akt *in vitro* (Lee *et al.*, 2009). In addition, Zhang *et al.* reported that mice intraperitoneally injected with Aβ42 exhibit increased fasting blood glucose level, impaired insulin tolerance, and hepatic insulin signaling. The authors demonstrated that the fragment Aβ was able to impair insulin signaling through the activation of the JAK/STAT pathway. In fact, the injection of Aβ42 activates hepatic JAK2/STAT3/SOCS1 signaling, and neutralization of Aβ in mice inhibits liver JAK2/STAT3/SOCS1 signaling. Furthermore, knockdown of hepatic JAK2 by tail vein injection of adenovirus inhibits JAK2/STAT3/SOCS1 signaling and improves glucose/insulin tolerance and hepatic insulin sensitivity in mice (Zhang *et al.*, 2013). An additional *in vivo* study also showed that Aβ accumulation preceded and prompted onset of glucose intolerance and insulin resistance in APP Tg mice, unless the molecular mechanism was not elucidated (Jimenez-Palomares *et al.*, 2012). Pancreatic amyloid is produced in β-cells and is co-released with insulin. A study of Tg mice found that excess accumulation of pancreatic amyloid led to β-cell dysfunction, disruption in glucose homeostasis and T2D (Janson *et al.*, 1996).

Several authors also reported that elevated levels of Aβ peptide cause the abnormal activation of the JNK pathway and the secretion of the TNFα cytokine, possibly contributing to insulin resistance through this mechanism (Bomfim *et al.*, 2012; Ma *et al.*, 2009). Moreover, a very recent work showed that Aβ impairs insulin sensitivity in neurons by downregulating AMPK (Chang *et al.*, 2017) (Figure I.17.).

Furthermore, it has been established that the Aβ peptide is degraded by the insulin degrading enzyme (IDE), the same enzyme that degrades insulin (Fernandez-Gamba *et al.*, 2009). Aβ peptides and insulin compete for the binding to IDE catalytic domain, although the enzyme binds insulin with greater affinity than Aβ. Consequently, in a condition of hyperinsulinemia or insulin resistance, the enzyme is completely saturated with insulin. The result is a reduction in Aβ clearance and a subsequent accumulation of Aβ aggregates, which can further impair the insulin signaling (Qiu and Folstein, 2006).

Extracellular Aβ also exists as soluble oligomers, known as Aβ-derived diffusible ligands (ADDLs), which are toxic to neurons and are reported to decrease insulin signaling by

inhibition of insulin binding to its receptor or by mediating insulin receptor internalization and downregulation (De Felice *et al.*, 2009; Xie *et al.*, 2002). Moreover, ADDLs can trigger oxidative stress and disturb Ca^{2+} homeostasis, thus provoking ER stress (De Felice *et al.*, 2009; Hoozemans *et al.*, 2009; Ikezoe *et al.*, 2009) and contributing to impair insulin signaling.

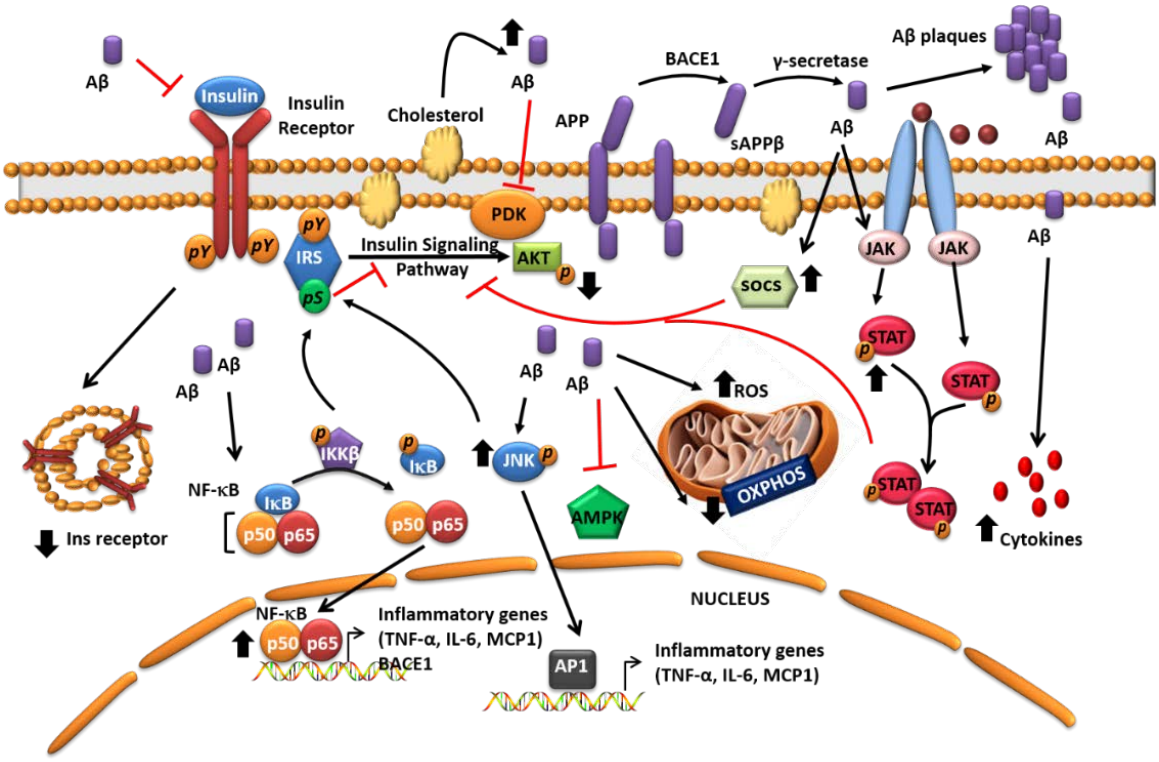

Figure I.17. Possible role of Aβ peptide in insulin resistance: molecular mechanisms. Aβ has been reported to block Akt phosphorylation by inhibiting its interaction with PDK. Aβ also induces inflammation through the JAK/STAT/SOCS and the NFκB pathways. Finally, Aβ can induce mitochondrial oxidative stress (Akter *et al.*, 2011).

I. 3.3.5. BACE1 inhibitors

Aspartic proteases are a therapeutically important class of enzyme that includes the HIV protease and the renin enzyme, which possess structural homology with the BACEs active site. Their inhibitors have presented major medicinal chemistry challenges and, only after decades of effort, clinically effective molecules were designed. Recently, novel biological approaches consented to obtain very high selective BACE1 inhibitors that are able to pass the blood-brain barrier (BBB) and are currently on study for the therapy of AD. The laboratory Merck first developed the cyclic isothiourea LY2811376 that presented a good pharmacokinetic and lowered the Aβ production up to 75% in brain of dogs and rodents.

However, the development of this compound was recently terminated, owing to observation of retinal and glial cell degeneration and liver toxicity (Vassar, 2014).
The most important BACE1 inhibitor currently on study is the compound MK-8931 (Merck 3 or M3) that is progressing into a long-term clinical efficacy study in patients. Structurally, M3 is a pyridinecarboxamide that achieves a substantial selectivity for BACE1 over its homologous BACE2 (>100 fold) and over other humans aspartyl proteases (Kennedy *et al.*, 2016). The study, started in November 2013, contained a lead-in safety cohort of 200 patients with mild-moderate AD that received daily doses of M3. The preliminary phase 3 results indicate a 50-75% reduction of Aβ production in the CSF of the patients; effects of M3 on metabolic parameters will be assess (Vassar *et al.*, 2014). *In vitro* studies showed that M3 improved insulin signaling and glucose uptake in skeletal muscle cells (Hamilton *et al.*, 2014; Meakin *et al.*, 2012), thus suggesting a potential role of this compound not only in the therapy of AD but also in the treatment of T2D and its complication on cognitive functions.

II. Objectives

The mechanisms responsible for the development of insulin resistance in skeletal muscle are not completely unveiled. The discovery of new factors that contribute to insulin resistance, might provide new clues about the development of this disease, especially in skeletal muscle, since skeletal muscle is the primary site of insulin-stimulated glucose disposal and is therefore central to systemic insulin resistance and the development of T2D (Petersen *et al.*, 2007; Petersen and Shulman, 2002).

In addition, drugs currently available for the management of T2D have limited efficacy, limited tolerability, and significant mechanism-based side effects and, as a result, only a small percentage of all patients with T2DM achieve adequate disease control (Nichols *et al.*, 2012). Therefore, there is a need for new drugs to prevent and treat T2D. Consequently, the discovery of new mechanisms involved in the development of insulin resistance might provide new targets for new pharmacological strategies and lead to the development of innovative drugs for the treatment of T2D and its complications.

In this doctoral thesis, we have investigated new potential mechanisms that contribute to the development of ER stress, inflammation and insulin resistance in skeletal muscle.

Whereas the effect of insulin resistance on lipoprotein metabolism has been extensively studied, very little was known about the involvement of lipoproteins in the development of T2D. Since dyslipidemia is frequently associated to T2D and precedes the disease by several years (Adiels *et al.*, 2008b), we hypothesized that the increase in VLDL might contribute to the development of ER stress, inflammation and insulin resistance in skeletal muscle.

On the other hand, since it has been reported that BACE1 knockout mice present improved glucose tolerance and are protected from HFD-induced insulin resistance (Meakin *et al.*, 2012), we hypothesized that BACE1 might be involved in lipid-induced ER, inflammation and insulin resistance in skeletal muscle.

Considering all these facts, the objectives of the present doctoral thesis were the following:

1. To examine whether VLDL and its apolipoprotein Apo CIII can impair insulin signaling in skeletal muscle and to analyze the molecular mechanisms involved.
2. To examine whether BACE1 inhibition prevents saturated fatty acid-induced ER stress, inflammation and insulin resistance in skeletal muscle.
3. To determine the molecular mechanisms by which BACE1 activity contributes to lipid-induced insulin resistance in skeletal muscle.

III. Materials and methods

III. 1. Subjects

Subjects were recruited by the Endocrinology Department at the University Hospital Joan XXIII (Tarragona, Spain) in accordance with the Helsinki Declaration (2008). All participants gave their informed consent and the study was approved by the respective local Ethic Committee review board of the participating Hospital. Donors were classified as lean or obese based on body mass index (BMI) following World Health Organization criteria (WHO). T2D subjects were diagnosed according WHO criteria. All patients had fasted overnight before collection of blood samples. Anthropometric and biochemical variables from the two cohorts used are presented in Table III.1.

	LEAN (n=4)	OBESE (n=8)	T2D (n=5)	P
Age	45 ± 14	58 ± 11	61 ± 16	NS
Sex (male/female)	2/2	4/4	3/2	NS
BMI (kg/m^2)	21 ± 1.7	31 ± 3.3*	29 ± 2.0$^{\#}$	----
Glucose (mg/dl)	109 (87-176)	97 (79-103)	145 (88-218)	NS
Cholesterol (mg/dl)	176 (126-230)	215 (186-250)	150 (142-377)	NS
HDL (mg/dl)	42 ± 10	50 ± 11	39 ± 5	NS
TG (mg/dl)	143 (71-355)	124 (85-144)	152 (102-417)	NS
Insulin (µIU/ml)	7.1 ± 3.1	12 ± 4.7	16 ± 5.7$^{\#}$	----
HOMA-IR	1.9 (1.7-2.2)	2.5 (1.9-2.8)	3.9 (2.9-11)	0.034

Table III.1. Anthropometric and plasma parameters of patients used in the study. HOMA-IR: homeostasis model assessment index-insulin resistance. *p<0.01 (*vs* lean), $^{\#}$p<0.05 (*vs* lean), NS: no significant.

All subjects were of white origin and reported that their body weight had been stable for at least 3 months prior to the study. They had no systemic disease other than obesity, and all had been free of infection in the previous month before the study. Primary liver disease, CVD, arthritis, acute inflammatory disease, infectious disease, neoplastic and renal diseases were specifically excluded by biochemical evaluation. Serum was immediately separated by centrifugation and stored at −80º C until analysis. Subjects were stratified according to age, gender and BMI. The hospital ethics committee approved the study and informed consent for biobanking surgically removed tissue was obtained from all participants in accordance with the Declaration of Helsinki. All patients had fasted overnight before collection of adipose tissue and blood. Visceral (VAT) and subcutaneous (SAT) adipose tissue was obtained during scheduled non-acute surgical procedures including laparoscopic surgery for hiatus hernia repair or cholecystectomies. Serum fasting glucose, insulin, triglycerides, total cholesterol and high-density lipoprotein were determined by standard enzymatic methods. Insulin resistance was estimated using homeostasis model assessment index-insulin resistance (HOMA-IR).

For western blot analysis of sAPPβ in human serum samples, serum albumin and the major subclasses of gamma globulin (Gibbons *et al.*) were removed using Amicon Ultra-0.5 centrifugal Filter devices (Millipore) following Pierce Albumin/IgG Removal Kit (Pierce Biotechnology).

III. 2. Animals

C57BL/6J background mice, male, 2 months age, were maintained at standard laboratory conditions (22ºC temperature, 12 hours light), constantly supplied with water and fed a standard diet. Mice were then divided into two different experimental groups (n=6 per group), and treated with a standard diet or a HFD (Research diet D08061110) respectively, for 12 weeks. Gastrocnemius skeletal muscle was obtained, and stored at -80^{o} C for further analysis. For quantification of sAPPβ and Aβ42, plasma was collected and concentrated (30 kDa Amicon Ultra 15 ml filter) by centrifugation and subjected to SDS-PAGE western blot, as described further.

All animal care, experimental protocols and procedures were performed in accordance to the Animal Scientific Procedures Act (1986), with approval of the University of Barcelona and Dundee ethics committees.

III. 2.1. apoCIII Tg

Wild type and Tg mice overexpressing human Apo CIII (apoCIII Tg) (C57BL/6J background) were anesthetized with inhaled isoflurane (ISOFLO®, Esteve) and then sacrificed. Skeletal muscle (gastrocnemius) samples were frozen in liquid nitrogen during the extraction, and then stored at -80ºC for further analysis, such as mRNA and protein extraction described in the next sections.

III. 2.2. *Ex vivo* assay with VLDL

Skeletal muscles (soleus) were isolated from male C57BL/6J mice (8 weeks old), incubated with MEM 199 medium (SIGMA-Aldrich), and subsequently mounted on an incubation apparatus consisting of a circulating water bath at 37°C with constant oxygenation (95% O_2 and 5% CO_2) (Alkhateeb *et al.*, 2006). After 30 minutes, vehicle or VLDL (500 µg/mL) solutions were added to the control and the treated group, respectively. Temperature, oxygen levels and tissue viability were constantly monitored for 6 hours. At the end of the incubation, skeletal muscles were immediately frozen in liquid nitrogen and stored at -80ºC.

III. 2.3. BACE1 knock out mice

Wild type and BACE1-null mice (C57BL/6J background) were fed a standard diet or a HFD containing, by energy, 45% fat, 20% protein and 35% carbohydrate (catalogue number 58V8, TestDiet®, Purina Mills) for 20 weeks. Mice were then anesthetized with inhaled isoflurane (ISOFLO®, Esteve) and sacrificed. Skeletal muscle (gastrocnemius) samples

were frozen in liquid nitrogen during the extraction, and then stored at -80ºC for further analysis. For quantification of sAPPβ and Aβ42, plasma of wild type mice fed a standard diet (Control group) or a HFD (HFD group) was collected and concentrated (30 kDa Amicon Ultra 15 ml filter) by centrifugation and subjected to SDS-PAGE western blot, as described further.

III. 2.4. *In situ* injection of sAPPβ

C57BL/6 mice were randomly distributed into two groups (n=6 each) and, after a temporal anesthesia with inhaled isoflurane (ISOFLO®, Esteve), intramuscular (gastrocnemius) injection of vehicle (PBS plus 4% urea) or 5 µg of recombinant sAPPβ (Thermo-fisher Scientific) was performed. Twelve hours later, animals were sacrificed and the skeletal muscle gastrocnemius was excised.

III. 2.5. Intraperitoneal injection of sAPPβ

C57BL/6 mice were randomly distributed into two groups (n=6 each) and vehicle (PBS plus 4% urea) or 10 µg of sAPPβ (Thermo-fisher Scientific) were administered (i.p.) twice, before (at 20.00 h) and after (at 8.00 h) an over-night fasting (sAPPβ final dose: 20µg/mice). Two hours later the last injection, either a glucose tolerance test (GTT) or an insulin tolerance test (ITT) were performed. In the GTT animals received 2 g/Kg body weight of glucose by i.p. injection, and blood was collected from the tail vein after 0, 15, 30, 60 and 120 min. In the ITT each animal received 0.5 IU/Kg of body weight of insulin.

III. 3. Cell culture

Mouse C2C12 myoblasts (ATCC Laboratory) were maintained in Dulbecco's modified Eagle's medium (DMEM, Thermo-Fisher Scientific) supplemented with 10% fetal bovine serum (FBS), 50 units/ml penicillin and 50 µg/ml streptomycin. 6-well plates (final volume per well 2 ml) were used for RNA extraction, 10 cm plates (final volume 10 ml) were used for protein extraction, and 25 cm flasks (final volume 2 ml) were used for fatty acid oxidation and glucose uptake assay. When cells reached 80-90% confluence, the medium was switched to the differentiation medium containing DMEM and 2% horse serum, which was changed every other day. After 4 additional days, the differentiated C2C12 cells had fused into myotubes.

Human LHCN-M2 myoblasts (ATCC) were maintained in DMEM (Thermo-Fisher Scientific) supplemented with 15% FBS, vitamin B12 (1.4 µg/mL), dexamethasone (0.055 µg/mL), hepatocyte growth factor (2.5ng/mL) and basic fibroblast growth factor 2 (FGF2). When cells reached 80-90 % confluences, the medium was switched to differentiation medium MEM 199 (SIGMA-Aldrich), and supplemented also with porcine skin gelatin, 60 units/mL penicillin and 60 µg/mL streptomycin. After 4 additional days, the differentiated LHCNM2 cells had fused into myotubes.

III. 3.1. Incubation with VLDL and Apo CIII

VLDL particles (*d*<1.006 g/mL) were isolated by ultracentrifugation at 100,000 *g* for 24 hours from normolipidemic human plasma obtained in EDTA-containing vacutainer tubes (total cholesterol ≤5.2 mmol/L, TG ≤1 mmol/L). To obtain VLDL particles with low or high amounts of Apo CIII, we further isolated light VLDL from normolipidemic (TG < 1 mmol/L) and hypertriglyceridemic (TG ≥2.5 mmol/L) human plasma by ultracentrifugation at 56,000 *g* for 1 hour. VLDL preparations were extensively dialyzed in phosphate buffer solution (PBS) and then TG and Apo B concentrations were measured using a commercial kit adapted to a COBAS c501 autoanalyzer (Roche Diagnostics, Rotkreuz, Switzerland). Apo B/TG ratios were similar in both light VLDL preparations. Apo CIII levels were determined using a nephelometric commercial kit (Kamiya, Biomedical Company, Seattle, WA) adapted to COBAS c501 autoanalyzer. C2C12 myotubes were incubated in serum free DMEM and treated with 300 µg/mL of filtered VLDL, based on TG concentration, for 24 hours. PBS was used as vehicle. Table III.2. shows lipids and apolipoprotein concentrations of light VLDL fractions used in our study.

	TG (g/L)	Cholesterol (g/L)	Apo B (g/L)	Apo CIII (g/L)
Light VLDL NL	0.779	0.985	0.2	0.010
Light VLDL HT	2.575	0.997	0.21	0.112

Table III.2. Apolipoprotein and lipid composition of light VLDL. NL: plasma from normolipemic subjects. HT: plasma from hypertriglyceridemic subjects.

C2C12 myotubes were also incubated in the presence or absence of 100 µg/ml of human recombinant Apo CIII (Abcam) for 24 hours. Apo CI (final concentration 100 µg/ml, SIGMA-Aldrich) was used as control to verify that Apo CIII effects were specific. The selective ERK1/2 inhibitor U0126 (final concentration 10µM, SIGMA-Aldrich) was added 1 hour before the treatment with VLDL or Apo CIII. Treatment with TLR2 neutralizing antibody (final concentration 50 µg/ml, Invivogen) was also performed 1 hour before the incubation with Apo CIII, as specified in the protocol. Nonimmune IgG (final concentration 50 µg/ml, Invivogen) was used as control.

III. 3.2. Incubation with palmitate and sAPPβ

Lipid-containing media were prepared by conjugation of non-esterified fatty acids (NEFA) with NEFA-free bovine serum albumin (BSA). Palmitic acid was dissolved in ethanol (96 % v/v) and diluted 1:100 in DMEM containing 2% (w/v) NEFA-free BSA. Differentiated myotubes were incubated in serum-free DMEM containing 2% BSA in either the presence

(palmitate-treated cells) or absence (control cells) of NEFA for16 hours. Palmitate final concentration was 0.5 mM. Treatment with M3 (final concentration 100 nM, Merck) was performed 24 hours before the incubation with palmitate, reaching a total duration of 24+16=40 hours.

Differentiated myotubes were also incubated in serum free DMEM with 20 nM of recombinant sAPPβ (Termo- fisher Scientific) for 24 hours.

III. 3.3. SiRNA transfection

C2C12 cells were plated in a 6-well plate, grown and differentiated as described above. One day before transfection, medium was changed to an incubation medium without penicillin/streptomycin. According to the manufacturer instructions 5µl/well of Lipofectamine 2000 (Invitrogen) were used for transfection. Lipofectamine 2000 was conjugated with SiRNA oligomers (100 pmol/well, Santa Cruz Biotechnology) in the Opti-MEM medium (500µl/well, SIGMA-Aldrich) and the complex incubated at room temperature for 20 minutes. Next, cells were transfected with the lipofectamine-oligomer complexes for 48 hours. Medium was changed after 6 hours from the initial step of transfection and serum free medium containing penicillin/streptomycin was added. SiRNA oligomers against ERK1/2 and BACE1 genes were used. A non-targeting Control SiRNA was used as negative control. A 48-hours SiRNA transfection guaranteed a ≈70% knocking down of gene expression, as showed in Figure III.1.

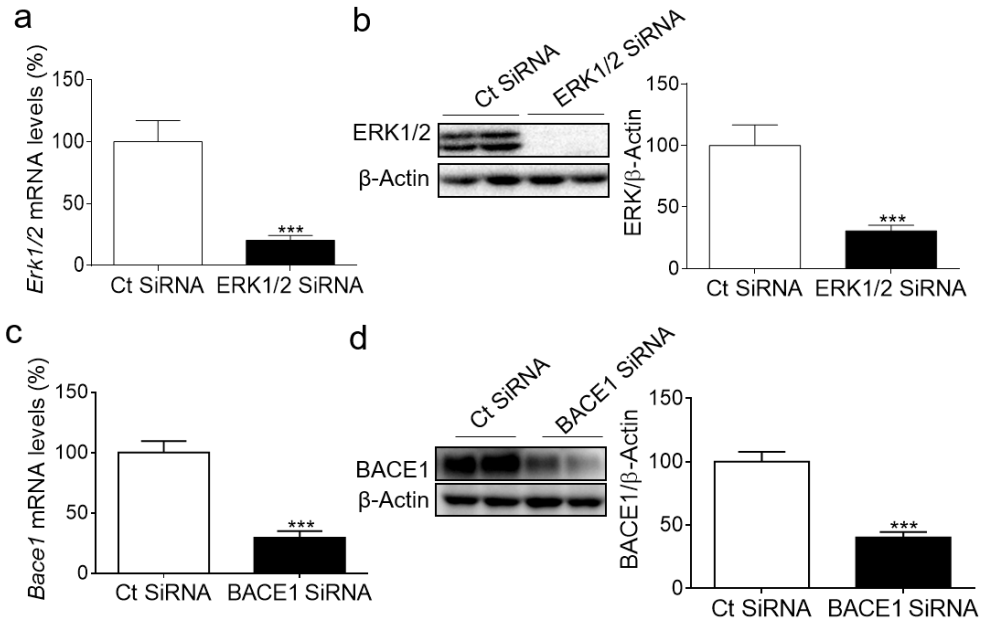

Figure III.1. SiRNA transfection decreases over 70% of gene expression. **a-c)** *Erk1/2* and *Bace1* mRNA levels. **b-d)** ERK1/2, BACE1 and β-actin protein levels. The graphs show quantification of the *aprt*-normalized mRNA levels, expressed as a % of control samples ± SD of five independent experiments. ***p<0.001*vs.* control.

Treatment with biochemical compounds and inhibitors were performed within the last 24 hours of transfection.

III. 3.4. PGC1α overexpression

LHCNM2 cells were plated in a 6-well plate, grown and differentiated as described above, until the optimal confluence. One day before the virus-infection, medium was changed to an incubation medium without penicillin/streptomycin. According to the manufacturer instructions (Abm Materials), cells were infected with 70 µL of the vector adenovirus, carrying the green fluorescent protein (GFP) gene, or the human PGC1α transcript (Ad-h-PPARGC1A, Vector BIOLAB), for the control and the treated group, respectively. Cells were incubated for 1 hour at 37° C and then the medium was changed. Gene transduction was evaluated after 48 hours from the infection and a 4/5-fold increase in PGC1α gene expression was observed (Figure III.2.)

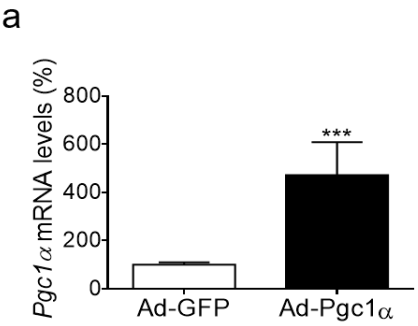

Figure III.2. PGC1α overexpression in LHCNM2 cells. **a)** *Pgc1α mRNA levels.* Graphs show quantification of the *18S*-normalized mRNA levels, expressed as a % of control samples ± SD of five independent experiments. ***p<0.001*vs.* control.

III. 4. Real-time poly chain reaction (Rt-PCR)

For human samples, total RNA was extracted from adipose tissue using the RNeasy Lipid Tissue Midi Kit (Qiagen Science). For mice tissue samples (skeletal muscle, liver and adipose tissue) and cell cultures, total RNA was extracted using TRISURE™ (Bioline).

Total RNA quantity was measured at 260 nm and purity was assessed by the OD260/OD280 ratio. One microgram of RNA was reverse transcribed to copy DNA (cDNA) using random primers (Random Hexamers, Thermo-Fisher Scientific), deoxynucleotide (dNTP) mix and retro-transcriptase enzyme (Invitrogen) in the Reverse Transcription System (Applied Byosistems). The protocol consisted of several subsequent steps at different temperatures (65° C x 5 min, 4° C x 5 min, 37° C x 2 min, 25° C x 10 min, 37° C x 50 min, and 70° C x 15 min). For human samples, quantitative gene expression was

evaluated by RT-PCR on a 7900HT Fast Real-Time PCR System, using TaqMan Low Density Arrays (Applied Biosystem, BACE1 probe Hs01121195_m1 and PPARGC1A probe Hs01016719_m1). For mice and cell culture samples, quantitative gene expression was evaluated by RT-PCR on a Mini-48 well T100^{TM} BioRAD thermal cycler (BIORAD) using SYBR Green Master Mix (Thermo-Fisher Scientific). For each sample, 10 nanograms of copy-DNA and 900 nM of primers and/or Taqman probes were used. The real-time protocol included two first steps (50^{o} C x 2 min, 95^{o} C x 10 min) and 40 repetitive cycles, one of each consisting of 3 subsequent steps (95^{o} C x 15 s, 60^{o} C x 30 s, 72^{o} C x 30 s). One additional final step, determining the melting curve, was added to the real-time protocol for SYBR Green. The 60^{o} C temperature was adjusted based on the primer annealing temperature (which was 2-5 degrees higher, in order to pledge the specific union of primers to the cDNA). Table III.3. shows all the primer sequences used in the assays.

Gene		**Primers**
h18S	for	5'-GCCGCTAGAGGTGAAATTCTTG-3'
	rev	5'-CATTCTTGGCAAATGCTTTCG-3'
mAcox	for	5'-TCTGGAGATCACGGGCACTT-3'
	rev	5'-TTTCCAAGCCTCGAAGATGAG-3'
mAprt	for	5'-CAGCGGCAAGATCGACTACA-3'
	rev	5'-AGCTAGGGAAGGGCCAAACA-3'
mAtf3	for	5'-CTGGAGATGTCAGTCACCAAGTCT-3'
	rev	5'-TTTCTCGCCGCCTCCTTT-3'
hBACE1	for	5'-CCCGAAAACGAATTGGCTTT-3'
	rev	5'-GCTGCCGTCCTGAACTCATC-3'
mBace1	for	5'-CGGCGGGAGTGGTATTATGAAGT-3'
	rev	5'-ATGGTGATGCGGAAGGACTGATT-3'
mBip	for	5`-CAGATCTTCTCCACGGCTTC-3`
	rev	5`-GCAGGAGGAATTCCAGTCAG-3`
mChop	for	5`-CGAAGAGGAAGAATCAAAAACCTT-3`
	rev	5`-GCCCTGGCTCCTCTGTCA-3`
mCpt1α	for	5`-GCAGAGCACGGCAAAATGA-3`
	rev	5`-GGCTTTCGACCCGAGAAGAC-3`
mG6p	for	5'-CGACTCGCTATCTCCAAGTGA-3'

	rev	5’-GTTGAACCAGTCTCCGACCA-3’
mIκBα	for	5’-CTCACGGAGGACGGAGACTC-3’
	rev	5’-CTCTTCGTGGATGATTGCCA-3’
mIl6	for	5’-ACACATGTTCTCTGGGAAATCGT-3’
	rev	5’-AAGTGCATCATCGTTGTTCATACA-3’
mMcad	for	5`-TGACGGAGCAGCCAATGA-3`
	rev	5`-ATGGCCGCCACATCAGA-3`
mMcp1	for	5’-GCTGGAGAGCTACAAGAGGATCA-3’
	rev	5’-CTCTCTCTTGAGCTTGGTGACAAA-3’
mPepck	for	5’-AAGCATTCAACGCCAGGTTC-3’
	rev	5’-GGGCGAGTCTGTCAGTTCAAT-3’
mNq01	for	5’-TATCCTTCCGAGTCATCTCTAGCA-3’
	rev	5’-TCTGCAGCTTCCAGCTTCTTG-3’
hPGC1α	for	5’-CCCAAGGGTTCCCCATTT-3’
	rev	5’-TTAGGCCTGCAGTTCCAGAGA-3’
mPgc1α	for	5’-AACCACACCCACAGGATCAGA-3’
	rev	5’-TCTTCGCTTTATTGCTCCATGA-3’
mPparα	for	5`-CAAGGCCTCAGGGTACCACTAC-3`
	rev	5`-GCCGAATAGTTCGCCGAAA-3`
mPparβ/δ	for	5`-GCCACAACGCACCCTTTG-3`
	rev	5`-CCACACCAGGCCCTTCTCT-3`
mSocs1	for	5`-GCTGTGCCGCAGCATTAAG-3`
	rev	5`-CCAGAAGTGGGAGGCATCTC-3`
mSocs3	for	5’-TTCCCATGCCGCTCACA-3’
	rev	5’-CCCACCCAGCCCCATAC-3’
mTnfα	for	5’-AGCCGATGGGTTGTACCTTGT-3’
	rev	5’-TGAGATAGCAAATCGGCTGAC-3’

Table III.3. Primer sequences used for RT-PCR on T100^{TM} BIORAD thermal cycler using SYBR Green master mix. h: human genes, used for LHCNM2 cell samples, m: mouse genes, used for C2C12 cell samples and mice tissues. for: forward primer. rev: reverse primer.

Results were calculated using the comparative Ct method (2- ΔΔ Ct), and expressed relative to the expression of the housekeeping genes cyclophilin 1A (PPIA) (probe Hs 04194521_s1) and 18S (probe Hs 03928985_g1) in the case of human samples, or relative to the expression of the housekeeping gene APRT, in the case of mice and cell culture samples.

III. 5. PCR and DNA electrophoresis

Amplification of cDNA expressing the XBP1 gene was performed in the mini 48-well MJ BIORAD thermal cycler, using 0.25µg of cDNA per sample, spliced XBP1 primers forward and reverse (2µM each), $MgCl_2$ 2.5µM, dNTP mix 0.2 µM and the Taq polymerase enzyme (Invivogen). The PCR protocol included an initial step at 95° C for 15 minutes and 35 repetitive cycles consisting in three subsequent steps (94° C x 1min, 58° C x 1 min, 72° C x 1 min). The sequences of sXBP1 primers were: for 5'-TGAGAACCAGGAGTTAAGAACACGC-3', rev 5'-TTCTGGGTAGACCTCTGGGAGTTCC-3'.

Once DNA was amplified, a qualitative electrophoresis on a 1.5% agarose gel was performed during 1 hour at 100 Volt. Red-Safe™ nucleic acid staining solution (JH Science) was used as chemiluminescent reagent; a 50 base-pair DNA Step-ladder (SIGMA-Aldrich) served as molecular weight marker. Imaging was obtained after exposing the gel for 1 sec-5 min in the UV-light Gel Documentation system (BIORAD).

III. 6. Immunoblotting

Cell culture and tissue samples were homogenized in PBS 1X (Thermo-Fisher Scientific) and centrifuged at 4° C (8000 g x 2 min for cell cultures, 10000 g for 15 min for tissue samples). For total protein extraction, the pellet was re-suspended in a solution of RIPA buffer (SIGMA-Aldrich) supplemented with protease and phosphatase inhibitors [phenylmethylsulfonyl fluoride (PMSF) 0.2 mM, sodium orthovanadate (OvNa) 1 mM, sodium fluoride (NaF) 5 mM, aprotinin 2.78ml/ml, and leupeptin 20µg/ml], and incubated for 1 hour (*in vitro*) or 2 hours (*in vivo*) on a rotating system (25 rpm). After centrifugation 10000 g x 20 min at 4° C the supernatant containing the total protein extract was collected. For nuclear protein extraction, the pellet was re-suspended in an aqueous solution containing the protease and phosphatase inhibitors described above plus 10 mM of HEPES [4-(2-hydroxyethyl)-1-piperazineethanesulfonic acid], 1.5 mM of magnesium chloride ($MgCl_2$), 10 mM of potassium chloride (KCl) and 0.5 mM of DTT [1-(4)-dithiothreitol]. After a 10 minutes incubation in ice and a centrifugation 8000 g x 5 min at 4° C, the pellet was re-suspended in a second buffer containing 25% glycerol, sodium chloride (NaCl) 420 mM and ethylenediaminetetraacetic acid (EDTA) 0.2 mM. The final step of the extraction consisted in a 20 minutes incubation in ice and a centrifugation 10000 g x 10 min. At the end, the supernatant contained the nuclear proteins.

Protein quantification was performed using the Bradford Reagent (BIORAD). Absorbance was red at 595 nM, and the protein concentration was determined by extrapolation from a BSA standard curve.

For the sodium-dodecyl-sulfate polyacrylamide gel electrophoresis (SDS-PAGE), a 10% polyacrylamide gel containing SDS was used, and 30 µg of the protein extract were run into the gel during an electrophoresis at 100 Volts for 1 hour and 30 min. The proteins contained in the gel were then transferred to a polyvinylidene difluoride (PVDF) membrane (BIORAD) which was incubated in a tris-buffered saline (TBS) solution, containing 5% of BSA and 0.01% of the Tween 20® tensioactive (SIGMA-Aldrich). The membrane was incubated over night at 4° C with the primary antibody (1:1000 or 1:500 dilution, according to the manufacturer data sheet), and subsequently incubated at room temperature for 1 hour with the secondary, specie-specific antibody (1:5000 dilution). After a series of 5-min washes with the TBS solution, the protein content in the membrane was assessed. Detection was achieved using the Western Lightning® Plus-ECL chemiluminescence kit (PerkinElmer). The equal loading of proteins was assessed by Ponceau S staining. The size of detected proteins was estimated using protein molecular-mass standards. For validation, we used a protein marker (Precision Plus Protein Dual Color Standards 1610374; BIORAD), on the same blots. Imaging was obtained with the BioRad ChemiDoc XRS system (BIORAD), after exposing the membrane for 5 sec-5 min.

III. 7. Co-Immunoprecipitation

The cell culture and tissue samples were homogenized in PBS 1X (Thermo-Fisher Scientific) supplemented with 50 mM KCl, 0.05 mM EDTA, 2.5 mM $MgCl_2$, DTT 1mM, 18.5% of glycerol and 2% of BSA. The suspension was then incubated over night with the primary antibody (1:1000 or 1:500 dilution, according to the manufacturer data sheet), using a rotating system (25 rpm) at 4° C. The antibody/antigen complex was then pull out of the sample using protein A/G-coupled agarose beads (Santa Cru Technology) that physically isolate the protein of interest from the rest of the sample. The beads were conjugated with the samples containing the antibody/antigen complex by an overnight incubation at 4° C on a rotating system. The elution of the complexes was obtained by washing the pellet with PBS supplemented with protease and phosphatase inhibitors and by centrifugation (10000 g x 3 min at 4° C). Finally, the samples were separated by SDS-PAGE for western blot analysis, and incubated with the antibody of interest that binds the complexes. As negative control, few samples were incubated with the un-specific antibody Oct1.

Table III.4. shows the list of antibodies used for western blot and co-immunoprecipitation.

Antibody	**Reference**
Aβ42	Abcam (catalogue n. ab10148)
AC	Abcam (catalogue n. ab69597)
ACC	Cell Signaling Technology (catalogue n. #3662)
p-ACC Ser^{79}	Cell Signaling Technology (catalogue n. #3661)
AKT	Cell Signaling Technology (catalogue n. #9272)
p-AKT Ser^{473}	Cell Signaling Technology (catalogue n. #9271)
AMPK	Cell Signaling Technology (catalogue n. #2532)
p-AMPK Thr^{172}	Cell Signaling Technology (catalogue n. #2535)
Anti-mouse (secondary Ab)	ThermoFisher Scientific (catalogue n. A-11001)
Anti-rabbit (secondary Ab)	ThermoFisher Scientific (catalogue n. A-11034)
Anti-goat (secondary Ab)	Santa Cruz Biotechnology (catalogue n. sc-2020)
Anti-rat	Santa Cruz Biotechnology (catalogue n. sc-2065)
β-Actin	ThermoFischer Scientific (catalogue n. #2535)
BACE1	Cell Signaling Technology (catalogue n. #5606)
BiP	Cell Signaling Technology (catalogue n. #3177)
CHOP	Cell Signaling Technology (catalogue n. #2895)
CREB	Cell Signaling Technology (catalogue n. #4820)
p-CREB Ser^{133}	Cell Signaling Technology (catalogue n. #9198)
eIf2α	Cell Signaling Technology (catalogue n. #9722)
p-eIF2α Ser^{51}	Cell Signaling Technology (catalogue n. #9721)
ERK1/2	Cell Signaling Technology (catalogue n. #9102)
p-ERK1/2 Thr^{202}/Tyr^{204}	Cell Signaling Technology (catalogue n. #9101)
GAPDH	Santa Cruz Biotechnology (catalogue n. sc-32233)
IgG	Cell Signaling Technology (catalogue n. #2729)
IκBα	Cell Signaling Technology (catalogue n. #9242)
IRβ	Cell Signaling Technology (catalogue n. #3025)
IRS1	Cell Signaling Technology (catalogue n. #2382)
p-IRS1 Ser^{307}	Cell Signaling Technology (catalogue n. #2381)

Lamin B	Santa Cruz Biotechnology (catalogue n. sc-6216)
p65	Santa Cruz Biotechnology (catalogue n. sc-372)
NQO1	Santa Cruz Biotechnology (catalogue n. sc-16464)
NRF1	Cell Signaling Technology (catalogue n. #69432)
NRF2	Cell Signaling Technology (catalogue n. #4399)
Oct1	Santa Cruz Biotechnology (catalogue n. sc-232)
OXPHOS	Abcam (catalogue n. ab110413)
PGC1α	Abcam (catalogue n. ab54481)
PKA	Cell Signaling Technology (catalogue n. #4782)
p-PKA Thr^{197}	Cell Signaling Technology (catalogue n. #4781)
PPARα	Santa Cruz Biotechnology (catalogue n. sc-9000)
PPARβ/δ	Santa Cruz Biotechnology (catalogue n. sc-7197)
Prohibitin	Santa Cruz Biotechnology (catalogue n. sc-28259)
sAPPβ	BioLegend (catalogue n. #813401)
SOCS3	Santa Cruz Biotechnology (catalogue n. sc-9023)
STAT3	Cell Signaling Technology (catalogue n. #30835)
p-STAT3 Tyr^{705}	Cell Signaling Technology (catalogue n. #9131)
TRB3	Santa Cruz Biotechnology (catalogue n. sc-365842)

Table III.4. List of antibodies used for immunoblotting and co-immunoprecipitation

III. 8. Electrophoretic mobility shift assay (EMSA)

For the EMSA assay, 5µg of the nuclear protein extract were conjugated with a ^{32}P-labelled probe using a binding buffer containing 10 mM of tris hydrochloric acid (tris-HCL, pH 8.0), 25 mM of KCl, 0.5 mM of EDTA 50% glycerol, 0.5 mM of DTT, and water. Preliminary, the unlabeled probe was marked with ^{32}P-ATP (3000 Ci/mM, Perkin Elmer) by an incubation at 37^{o} C for 2 hours, and subsequently purified by filtration through a NICK^{TM} column (GE Healthcare) using the Tris-EDTA (TE) buffer, containing 10 mM of Tris-HCl and 1 mM of EDTA. After a 30 minutes incubation in ice, the samples were run through a 7.5 % polyacrylamide gel with an electrophoresis at 190 Volts for 2 hours and 30 minutes. The gel was then transferred to Whatman paper, and dried at 80 °C in vacuum dryer for 1-2 hours. The paper was subsequently placed in a cassette with an imaging-screen (KODAK) and exposed in dark condition from 12 hours up to 7 days. After the exposition, the

imagine was captured using the Quantity One Program® (BIORAD). As negative control, a sample without nuclear extract was used. For the competition assay, the unlabeled probe was added to the sample, while for the supershift assay 2 µg of PPARα, PPARβ/δ or NFκB antibody were added to the respective samples. To determine that the DNA-binding was specific, an extra sample was added, containing the un-specific antibody Oct1.

III. 9. Total fatty acid oxidation (FAO)

Cells were grown and differentiated as previously described. One day before the experiment medium was changed to FBS-free medium, in order to avoid the effect of fatty acid eventually contained in the FBS. Cells were treated with the different biochemical compounds (palmitate, sAPPβ and/or M3) as previously described. After the treatment, cells were washed with the Krebs-Ringer bicarbonate HEPES buffer (KRBH, SIGMA-Aldrich) supplemented with 1% of NEFA-free BSA and incubated at 37° C for 30 minutes. Next, the incubation solution was eliminated, and cells were treated with 2ml/flask of the reaction solution. The reaction solution was prepared right before the experiment, in DMEM-Glutamax with low glucose concentration (Thermo-Fischer scientific) by adding 1% of NEFA-free BSA, 1 mM carnitine, 0.25 mM of unlabeled palmitic acid, and 1µCi/ml of ^{14}C-labeled palmitic acid (Perkin-Elmer). The flasks were hermetically closed with a rubber cup connected to a small poly vinyl chloride (PVC) tube contained a Wathman paper previously drenched with 100 µl of 0.1 M potassium hydroxide (KOH). Flasks were incubated for 3 hours at 37° C. At the end of the incubation, the oxidative reaction was blocked by adding perchloric acid 60% (w/v) using a syringe that injected the liquid trough the rubber cups. After an overnight incubation at 4° C, the production of radioactive CO_2 derived from the fatty acid oxidation and captured on the Wathman paper was detected. The counts per minute (cpm) of each sample were measured by adding the Wathman paper to a vial containing 5 ml of the scintillation liquid. A blank sample containing only the scintillation liquid without the paper was also included, as well as a positive control representing the total cpm, obtained by adding directly to the vial the initial amount of labeled palmitate added to each flask (1 µCi). Results were standardized with milligrams of total protein, and expressed as nmol of oxidized palmitic acid per hour, according to the formula:

nmol of oxidized palm/mg of total protein per hour = [(cpm sample – cpm blank) x nmol of labeled palmitate initially added to each flask]/(total cpm x mg of total protein x hour)

III. 10. Glucose uptake

Cells were grown and differentiated as previously described. One day before the experiment medium was changed to FBS-free medium and cells were treated with the

different biochemical compounds as indicated in the previous sections. After the treatment, cells were washed with HEPES buffer (pH 7.4), containing HEPES 20 nM, magnesium sulfate ($MgSO_4$) 2.5 mM, KCl 5 mM and calcium chloride ($CaCl_2$) 1 mM, and incubated at 37° C for 1 hour. Next, a 15 minutes stimulation with 100 nM insulin was performed. At the end of the stimulation, 2µCi per flask of ^{3}H-Deoxy-D-glucose (Perkin Elmer) were added to each group, and cells were incubated at 37° C. After 20 minutes, the glucose uptake reaction was stopped by adding to each flask cytochalasin B 10 µM (SIGMA-Aldrich). Finally, cells were washed in sterile physiologic solution (NaCl 0.9% w/v) and lysated with sodium hydroxide (NaOH) 0.2 M. The cpm of each sample were measured by adding 500 µl of the cellular lysate to a vial containing 5 ml of scintillation liquid. In the negative control group, cytochalasin B was added right after the labeled glucose, in order to immediately blunt the insulin-stimulated glucose uptake. The group was used as reference for the basal glucose uptake, and its cpm value was subtracted to all other groups. A positive control representing the total cpm was also included. Results were standardized with milligrams of total protein, and expressed as pmol of glucose uptaken per minute, according to the formula:

pmol of uptaken glucose/mg of total protein per min = [(cpm sample – cpm cytochalasin) x pmol of labeled glucose initially added to each flask]/(total cpm x mg of total protein x min)

III. 11. Quantification of IL6, PKA activity, and cAMP levels

Detection of IL6 and cAMP levels in the medium of treated C2C12 cells was achieved by using mouse IL6 ELISA Kit (Novex by life-technologies) and cAMP Direct Immunoassay Colorimetric Kit (BIOVISION), respectively, according to the manufacturer's instruction. PKA activity was determined using the PKA kinase activity kit (Enzo Lifescience), following the manufacturer's instructions. Absorbance was read at wavelength of 450 nm using a UV-Vis Spectrophotomer (Systronics).

III. 12. Statistical analysis

For clinical and anthropometrical variables, normal distributed data were expressed as mean value±SD, and variables with no Gaussian distribution values were expressed as median (25th–75th quartiles). For analysis of expression variables that do not follow a Gaussian distribution, values were analyzed by non-parametrical tests (Kruskal-Wallis). When data were normally distributed, differences in clinical variables, laboratory parameters or expression variables between groups were compared by ANOVA with post hoc Scheffe correction.

Results were normalised to levels in control groups and are expressed as means ± S.D. Significant differences were established by either the Student's t test or one-way and two-way ANOVA, according to the number of groups compared, using GraphPad Prism software (GraphPad Software). When significant variations were found by one or two-way ANOVA, the Tukey-Kramer multiple comparison post-test was performed. Differences were considered significant at $p<0.05$.

IV. Results

IV. 1. VLDL and apolipoprotein CIII induce ER stress and inflammation and attenuate insulin signalling via Toll-like receptor 2 in mouse skeletal muscle cells.

IV. 1.1. VLDL induce ER stress and inflammation and attenuate the insulin signaling pathway in myotubes

We first evaluated weather VLDL can induce ER stress and inflammation in C2C12 murine myotubes. After a 24 hours incubation, we observed that VLDL exposure (300 µg/ml) significantly increased the expression of the ER stress markers BiP, CHOP, and NQO1 (Figure IV.1. a). Consistent with the presence of VLDL-induced ER stress the protein levels of BiP, phospho-eIF2α and TRB3 were increased by VLDL (Figure IV.1. b). VLDL exposure also increased the mRNA levels of inflammatory genes such as IL6, MCP1, and TNFα, whereas the expression of the NFκB inhibitor IκBα was reduced (Figure IV.1. c-d). IL6 induces insulin resistance by activating STAT3, which in turn upregulates the transcription of SOCS3. SOCS3 inhibits insulin signaling through several distinct mechanisms, including IRS degradation (Rui *et al.*, 2002). In agreement with the increase in IL6 expression, the mRNA levels of SOCS3 were also increased after VLDL exposure (Figure IV.1. c). The activation of the NFκB pathway by VLDL was confirmed by the presence of reduced protein levels of IκBα and enhanced levels of the p65 subunit of NFκB (Figure IV.1. d). Similarly, increased protein levels of phosphorylated STAT3 at Tyr^{705} and SOCS3 demonstrated the activation of the STAT3-SOCS3 pathway by VLDL (Figure IV.1. e). Collectively, these data show that VLDL induce ER stress and inflammation in skeletal muscle cells.

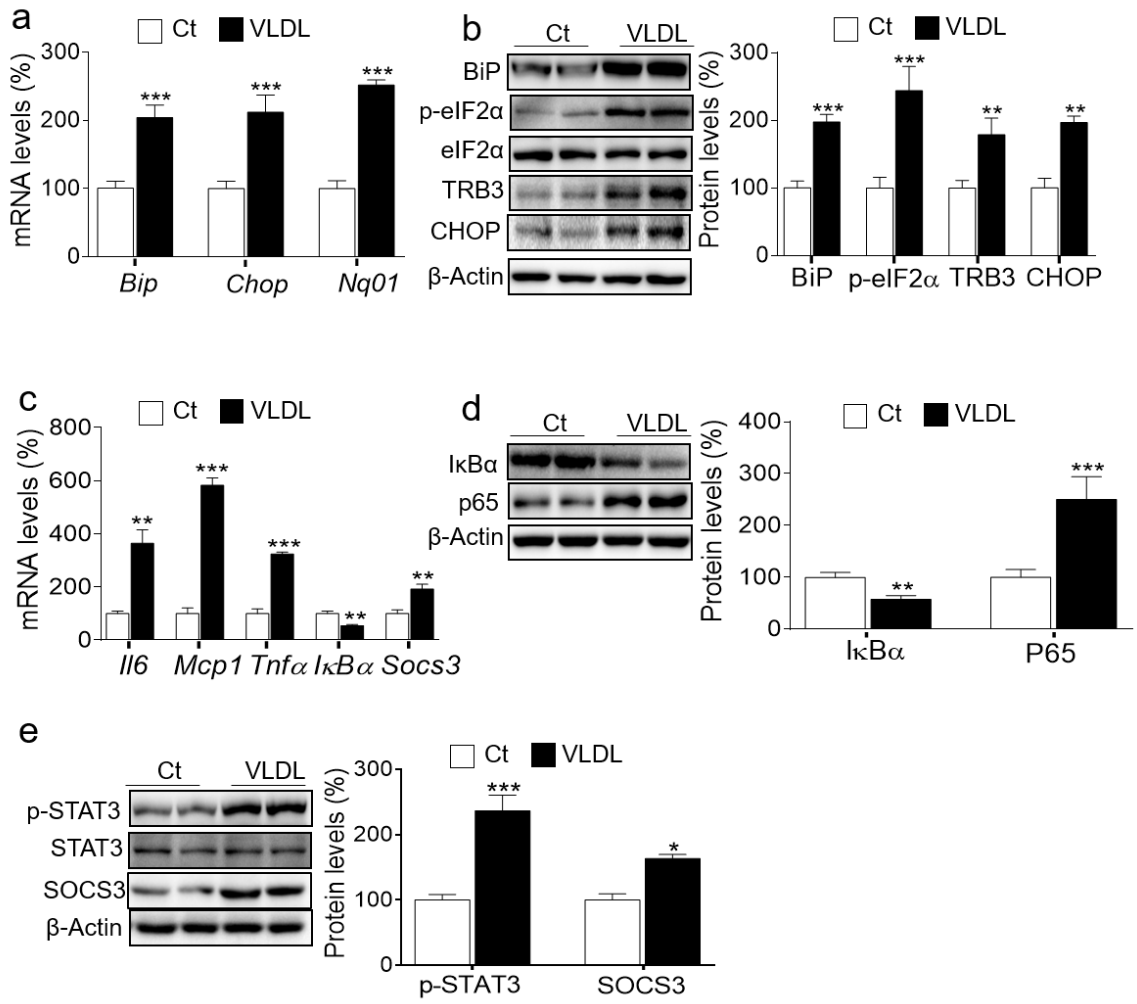

Figure IV.1. VLDL induce ER stress and inflammation. C2C12 myotubes were incubated in the presence or absence (Ct: control) of 300 μg/mL VLDL for 24 h. **a)** mRNA abundance of *Bip*, *Chop* and *Nqo1*. **b)** BiP, phosphorylated eIF2α (Ser^{51}), TRB3, CHOP, and β-actin protein levels. **c)** mRNA abundance of *Il6*, *Mcp1, Tnfα, IκBα* and *Socs3*. **d)** IκBα, p65 and α-actin protein levels. **e)** phosphorylated STAT3 (Tyr^{705}), SOCS3, and β-actin protein levels. The graphs show quantification expressed as a percentage of control samples ± SD of five independent experiments. ***p<0.001, **p<0.01 and *p<0.05 *vs.* control.

Since ER stress and inflammation are often accompanied by mitochondrial dysfunction and mitochondrial dysfunction has been related with insulin resistance in skeletal muscle (Coletta and Mandarino, 2011), we evaluated the expression and the protein levels of several mitochondrial markers. As previously described, PGC1α transcriptionally regulate mitochondrial biogenesis and play a critical role in skeletal muscle metabolic function. Myotubes exposed to VLDL showed a reduction in PGC1α expression (Figure IV.2. a). Since PGC1α is the major co-activator of the PPARs, also the expression of these transcription factors and many of their target genes involved in fatty acid oxidation, such as ACOX and

MCAD, was decreased by VLDL (Figure IV.2. a). In addition, PGC1α protein levels were downregulated by VLDL, and consistent with this reduction, the protein levels of its downstream transcription factor NRF1 were also decreased, indicating that VLDL impairs mitochondrial function in skeletal muscle (Figure IV.2. b-c).

PGC1α is also under the control of AMPK, whose activation upregulates PGC1α levels and increases fatty acid oxidation by phosphorylating ACC. In addition, AMPK exerts multiple protective effects, including inhibition of inflammation and insulin resistance (Day *et al.*, 2017). We observed that VLDL exposure reduced the levels of both phospho-AMPK and phospho-ACC in myotubes, whereas it increased the protein levels of the redox transcription factor NRF2, and its target gene NQO1 (Figure IV.2. c).

Taken together, these preliminary data clearly indicate that VLDL not only induce ER stress, and inflammation, but also impair mitochondrial function in skeletal muscle cells.

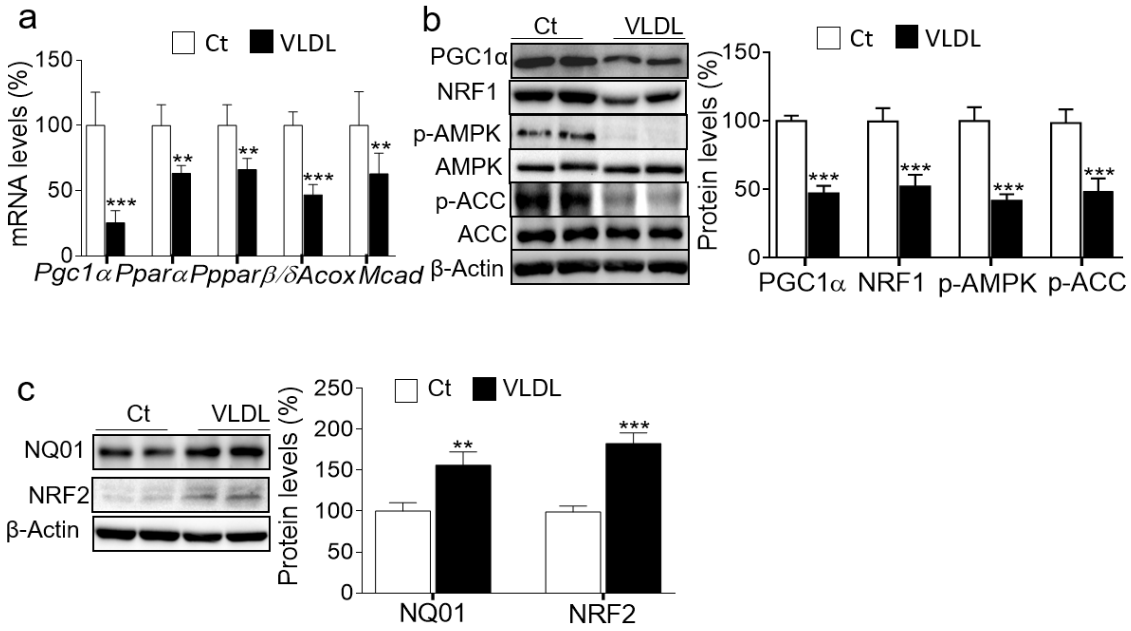

Figure IV.2. VLDL reduce PGC1α and AMPK levels. Mouse C2C12 myotubes were incubated in the presence or absence (Ct: control) of 300 μg/mL VLDL for 24 h. **a)** *Pgc1*, *Pparα*, *Pparβ/δ, Acox,* and *Mcad* mRNA levels. **b)** PGC1α, NRF1, phosphorylated AMPK (Thr^{172}), phosphorylated ACC (Ser^{79}), and β-actin protein levels. **c)** NQO1, NRF2 and β-actin protein levels. The graphs show quantification expressed as a percentage of control samples ± SD of five independent experiments. ***p<0.001, **p<0.01 and *p<0.05 *vs.* control.

When we evaluated the levels of proteins involved in the insulin signaling pathway, we observed that, in agreement with a previous study reporting that ER stress reduced insulin receptor levels in adipocytes (Zhou *et al.*, 2009), protein levels of the β-subunit of insulin receptor (IRβ) were reduced in VLDL-exposed cells (Figure IV.3. a). In addition, VLDL increased IRS1 phosphorylation at Ser^{307} and blunted the increase in insulin-stimulated AKT phosphorylation (Figure IV.3. b). These data suggest that VLDL are able themselves to impair the insulin signaling pathway in skeletal muscle cells.

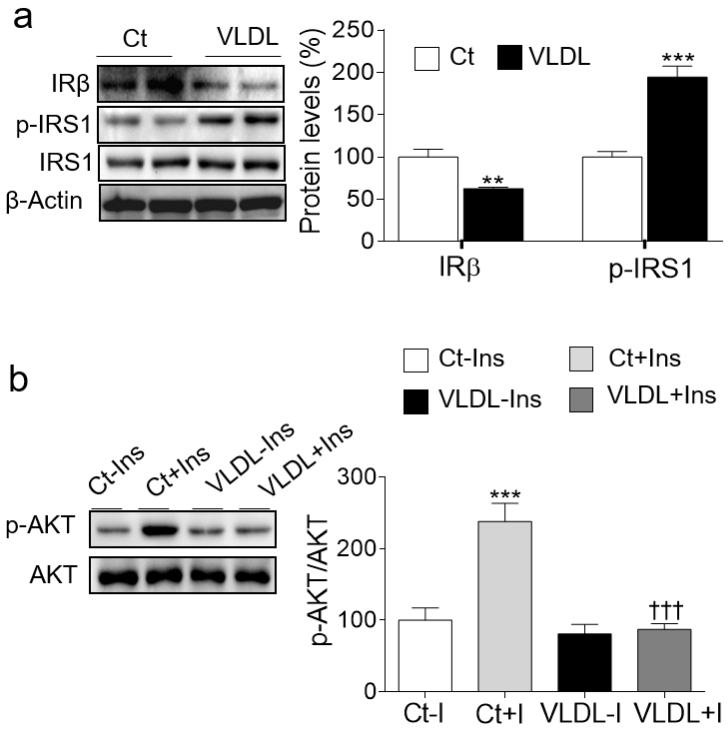

Figure IV.3. VLDL induce insulin resistance. Mouse C2C12 myotubes were incubated in the presence or absence (Ct: control) of 300 μg/mL VLDL for 24 h. **a)** IRβ, phosphorylated IRS1 (Ser^{307}), and β-actin protein levels. **b)** Phosphorylated AKT (Ser^{473}) protein levels. The graphs show quantification expressed as a percentage of control samples ± SD of five independent experiments. Where indicated, cells were incubated with 100 nM insulin (Ins) for the last 10 min. ***p<0.001, **p<0.01 and *p<0.05 *vs.* control. †††p<0.001 *vs.* control cells incubated with insulin.

IV. 1.2. VLDL increase ER stress, mitochondrial dysfunction and inflammation and attenuate the insulin signaling pathway in isolated skeletal muscle

Next, we examined whether VLDL cause similar effects in skeletal muscle. We first determined the levels of ER stress and inflammatory markers. Isolated muscles were incubated with VLDL for 6 h, which resulted in an increase in the expression and protein levels of BiP and in phospho-eIF2α, whereas no changes were observed in CHOP (Figure IV.4. a-b). Muscles exposed to VLDL also showed a significant increase in the mRNA levels of IL6, MCP1, SOCS3 and TNFα, which was consistent with the reduction in IκBα caused by VLDL (Figure IV.4. c).

We then evaluated some of the proteins involved in the insulin signaling pathway and, in agreement with our results *in vitro,* a reduction in the protein levels of insulin receptor was observed in muscle incubated with VLDL (Figure IV.4. d). In addition, the phosphorylation of IRS1 at Ser^{307} was significantly increased in skeletal muscles exposed to VLDL (Figure IV.4. d), confirming the role of these lipoproteins in the development of insulin resistance.

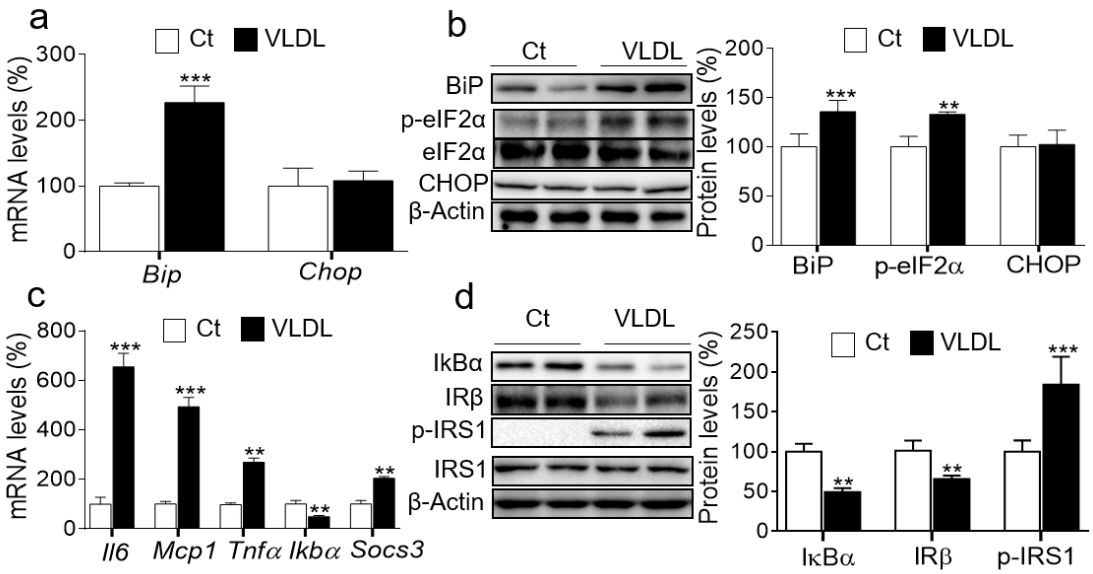

Figure IV.4. VLDL induce ER stress and inflammation, and attenuate the insulin signaling pathway in isolated skeletal muscle. Muscles were incubated in the presence or absence (Control: Ct) of 500 μg/mL VLDL for 6 h. **a)** mRNA abundance of *Bip* and *Chop.* **b)** phosphorylated eIF2α (Ser^{51}), BiP, CHOP, and β-actin protein levels. **c)** mRNA abundance of *Il6*, *Mcp1*, *Tnfα, IκBα* and *Socs3*. **d)** IκBα, IRβ, phosphorylated IRS1 (Ser^{307}), and β-actin protein levels. The graphs show quantification expressed as a percentage of control samples ± SD of five independent experiments. Where indicated, cells were incubated with 100 nM insulin (Ins) for the last 10 min. ***p<0.001, **p<0.01 and *p<0.05 *vs.* control.

Next, we assessed the levels of mitochondrial markers and genes involved in fatty acid oxidation. Similarly to what we observed *in vitro*, VLDL caused a marked reduction in the expression of PGC1α, PPARα PPARβ/δ and their target genes involved in fatty acid oxidation (ACOX and MCAD) (Figure IV.5. a).

As previously explained, PGC1α regulates the expression of mitochondrial OXPHOS genes and NRF1 (Handschin, 2009). Consistent with this, the reduction in the protein levels of this transcriptional co-activator caused by VLDL was accompanied by a reduction in NRF1 and the different OXPHOS complexes (Figure IV.5. b). In addition, a reduction was detected in phospho-AMPK and phospho-ACC in muscles exposed to VLDL (Figure IV.5. c).

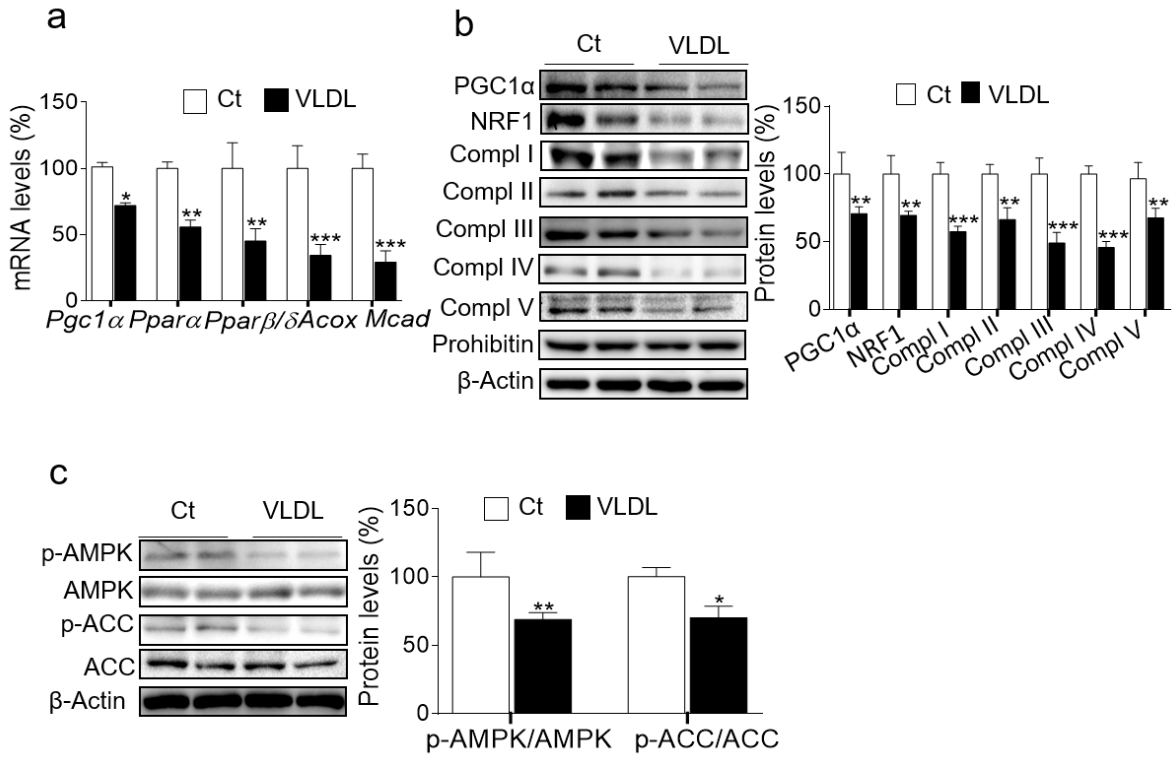

Figure IV.5. VLDL reduce the levels of mitochondrial proteins in isolated skeletal muscle. Muscles were incubated in the presence or absence (Control: Ct) of 500 μg/mL VLDL for 6 h. **a)** *Pgc1α*, *Pparα*, *Pparβ/δ, Acox,* and *Mcad* mRNA levels. **b)** PGC1α, NRF1, OXPHOS complexes, prohibitin, and β-actin protein levels. **c)** phosphorylated AMPK (Thr^{172}), phosphorylated ACC (Ser^{79}), and β-actin protein levels. The graphs show quantification expressed as a percentage of control samples ± SD of five independent experiments. ***p<0.001, **p<0.01 and *p<0.05 *vs.* control.

IV. 1.3. ERK1/2 inhibition prevents the effects of VLDL

Interestingly, NFκB activation requires MAPK–ERK1/2 (Ozaki *et al.*, 2016) and activation of both ERK1/2 and NFκB results in the downregulation of PGC1α in myotubes (Ozaki *et al.*, 2016). Likewise, an inhibitory crosstalk between AMPK and ERK1/2 has been reported (Du *et al.*, 2008) and inhibition of ERK1/2 was found to improve AMPK and Akt pathways and reversed ER stress-induced insulin resistance in myotubes (Coll *et al.*, 2006).

These data prompted us to evaluate whether the ERK1/2-MAPK cascade was involved in the effects mediated by VLDL. This possibility was supported by the fact that VLDL increased phospho-ERK1/2 levels in both cultured myotubes and isolated muscle (Figure IV.6. a). Next, we used U0126, a potent and specific ERK1/2 inhibitor which binds to MEK, thereby inhibiting its catalytic activity and phosphorylation of ERK1/2, to investigate whether inhibition of this kinase prevented the effects caused by VLDL. U0126 prevented the increase in the expression of ER stress and inflammatory markers (Figure IV.6. b) and the reduction in PGC1α levels and in genes involved in fatty acid oxidation (Figure IV.6. c). Knockdown of ERK1/2 by siRNA transfection confirmed that this kinase was responsible for the effects of VLDL on ER stress and inflammation (Figure IV.6. d) and the reduction in genes involved in fatty acid oxidation (Figure IV.6.e).

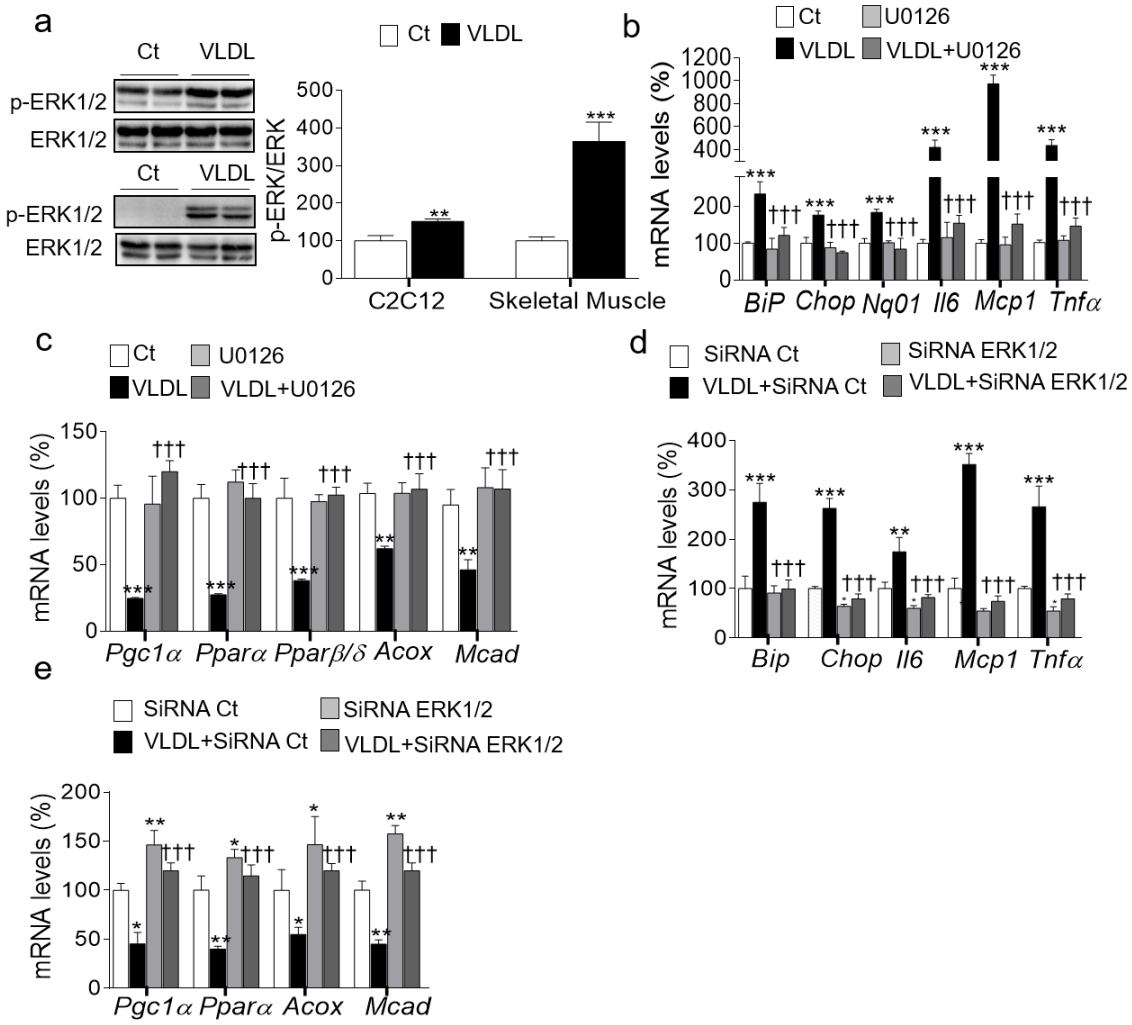

Figure IV.6. ERK1/2 inhibition and knockdown prevents the effects of VLDL. **a)** C2C12 myotubes and isolated skeletal muscles were incubated in the presence or absence (Ct: control) of 300 (cells) or 500 (muscle) μg/mL VLDL and the protein levels of phosphorylated ERK1/2 (Thr^{202}/Tyr^{204}) were analyzed. C2C12 myotubes were incubated in the presence or absence (Ct: control) of 300 μg/mL VLDL, 10 μM U0126, or 10 μM U0126 plus VLDL for 24 h. **b)** mRNA abundance of *BiP*, *Chop*, *Nqo1, Il6, Mcp1,* and *Tnfα*. **c)** mRNA abundance of *Pgc1α*, *Pparα*, *Pparβ/δ, Acox,* and *Mcad* mRNA levels. C2C12 cells were transfected with control or ERK1/2 siRNA and the mRNA abundance of **d)** *Bip*, *Chop*, *Nqo1*, *Il6*, *Mcp1*, and *Tnfα* and **e)** *Pgc1α*, *Pparα*, *Acox,* and *Mcad* was evaluated. The graphs show quantification expressed as a % of control samples ± SD of five independent experiments. ***p<0.001, **p<0.01 and *p<0.05 *vs.* control. †††p<0.001 *vs.* VLDL-exposed cells.

IV. 1.4. Apo CIII mimics the effects of VLDL

Given that Apo CIII is the most abundant apolipoprotein in VLDL of diabetic and hypertriglyceridemic patients (Hiukka *et al.*, 2005), we next examined whether this apolipoprotein was responsible for the effects of VLDL in myotubes. Exposure of myotubes to VLDL with high or low Apo CIII content isolated from plasma of either hypertriglyceridemic or normolipidemic subjects showed that light VLDL with low levels of Apo CIII did not cause the effects observed with VLDL with high Apo CIII content (Figure IV.7. a-b). These data clearly indicate the involvement of Apo CIII in the effects of VLDL.

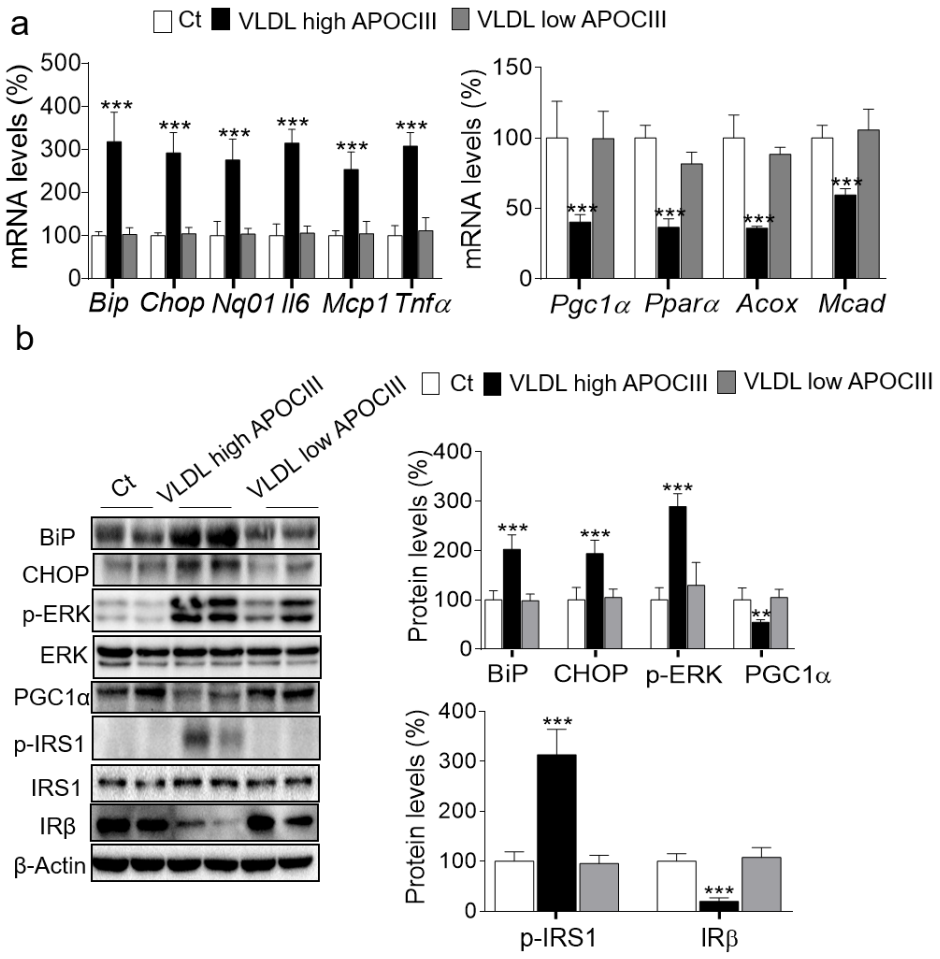

Figure IV.7. Apo CIII mediates the effects of VLDL. C2C12 myotubes were incubated during 24 hours in the presence or absence (Control: Ct) of 300 μg/mL VLDL containing high or low amount of Apo CIII, respectively. **a)** mRNA abundance of *BiP*, *Chop*, *Nqo1, Il6, Mcp1, Tnfα, Pgc1α*, *Pparα*, *Pparβ/δ, Acox,* and *Mcad*. **b)** BiP, CHOP, p-ERK1/2, PGC1α, IRβ, phosphorylated IRS1 (Ser^{307}), and β-actin protein levels. The graphs show quantification expressed as a % of control samples ± SD of five independent experiments. ***p<0.001, **p<0.01 and *p<0.05 *vs.* control.

To confirm the role of Apo CIII in VLDL-induced ER stress, inflammation and insulin resistance we then incubated myotubes with purified Apo CIII. Exposure of cells to Apo CIII led to a significant increase in ERK1/2 phosphorylation (Figure IV.8. a), BiP, phospho-eIF2α and TRB3 protein levels (Figure IV.8. b) as well as in the secretion of IL6 (Figure IV.8. c), indicating that this apolipoprotein induces ER stress and inflammation in skeletal muscle cells. In addition, Apo CIII exposure reduced the expression of PGC1α, PPARα, and PPARβ/δ (Figure IV.8. d), and the protein levels of PGC1α and NRF1 (Figure IV.8. e), indicating that Apo CIII is also involved in VLDL-induced reduction of fatty acid oxidation and in mitochondrial dysfunction.

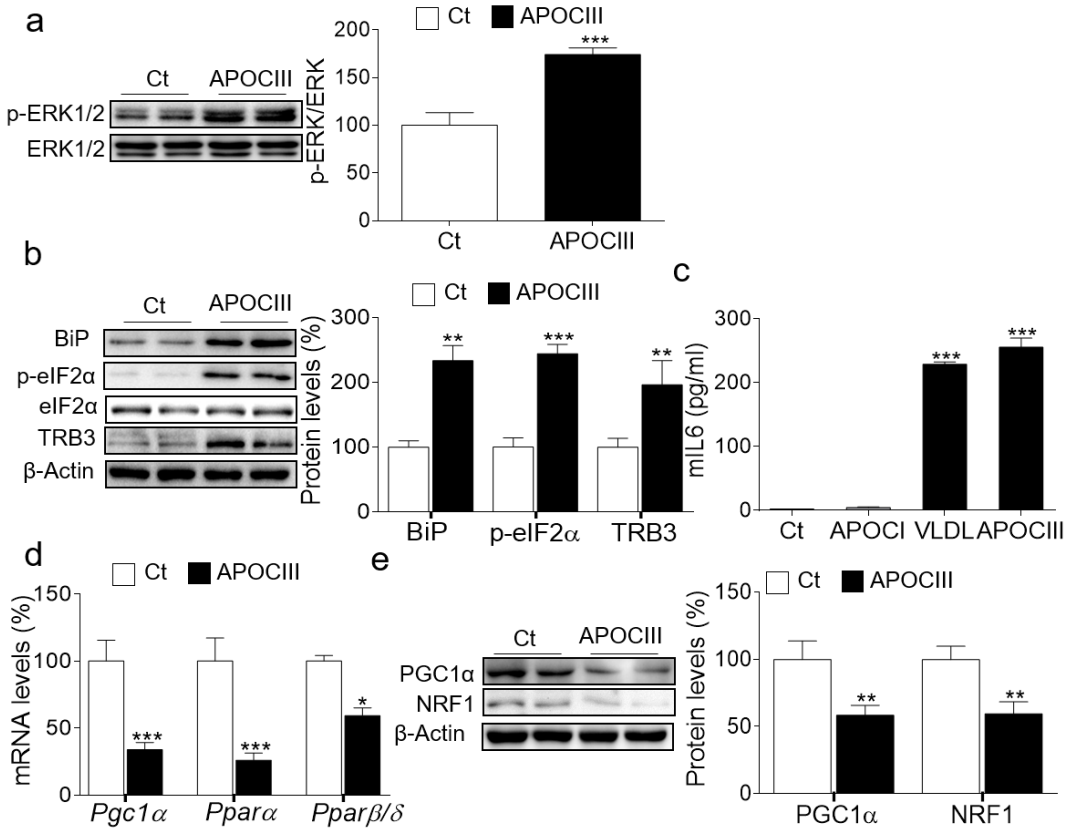

Figure IV.8. ApoCIII activates ERK1/2 and induces ER stress, inflammation, and mitochondrial dysfunction. C2C12 myotubes were incubated in the presence or absence (Ct: control) of 100 μg/mL Apo CIII for 24 h. Were indicated, C2C12 myotubes were incubated with 100 μg/mL of Apo CI or 300 μg/mL of VLDL for 24 h. **a)** phosphorylated ERK1/2 (Thr^{202}/Tyr^{204}) protein levels. **b)** TRB3, phosphorylated eIF2α (Ser^{51}), BiP, and β-actin protein levels. **c)** IL6 secretion in the cultured medium. **d)** mRNA abundance of *Pgc1α*, *Pparα*, *Pparβ/δ*. **e)** PGC1α, NRF1 and β-actin protein levels. The graphs show quantification expressed as a % of control samples ± SD of five independent experiments. ***p<0.001, **p<0.01 and *p<0.05 *vs.* control.

In agreement with the reduction of PGC1α and its target genes, Apo CIII reduced the DNA-binding activity of the transcription factor PPARβ/δ (Figure IV.9. a).

Interestingly, we observed that the effects Apo CIII on PGC1α downregulation were concentration-dependent (Figure IV.9. b).

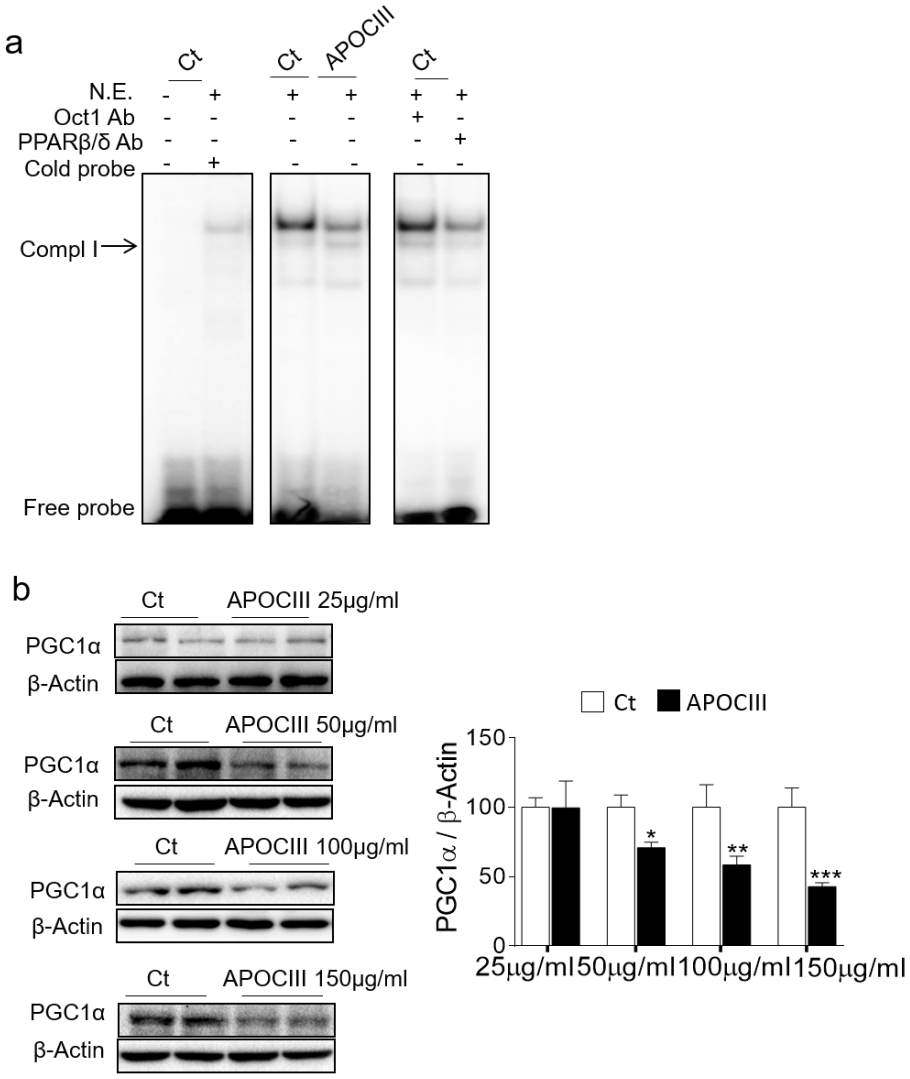

Figure IV.9. Apo CIII reduces PPARβ/δ DNA-binding activity and decrease PGC1α levels in a dose-dependent manner. C2C12 myotubes were incubated with **a)** 100µg/mL and **b)** 25-50-100-150 µg/mL of Apo CIII for 24 h. **a)** Autoradiograph of EMSA performed with a ^{32}P-labeled PPAR nucleotide and crude nuclear protein extract (NE) from C2C12 myotubes. One main specific complex (I) based on competition with a molar excess of unlabeled probe is shown. The supershift assay performed by incubating NE with an antibody (Ab) directed against PPARβ/δ shows a reduction in the band, whereas the band is observed with the unrelated antibody against Oct1. **b)** PGC1α protein levels. The graphs show quantification expressed as a % of control samples ± SD of five independent experiments. ***p<0.001, **p<0.01 and *p<0.05 *vs.* control.

The induction of ER stress caused by Apo CIII was accompanied by a reduction in the protein levels of insulin receptor and an increase in IRS1 phosphorylated at Ser^{307} (Figure IV.10. a), whereas insulin-stimulated Akt phosphorylation was mitigated (Figure IV.10. b).

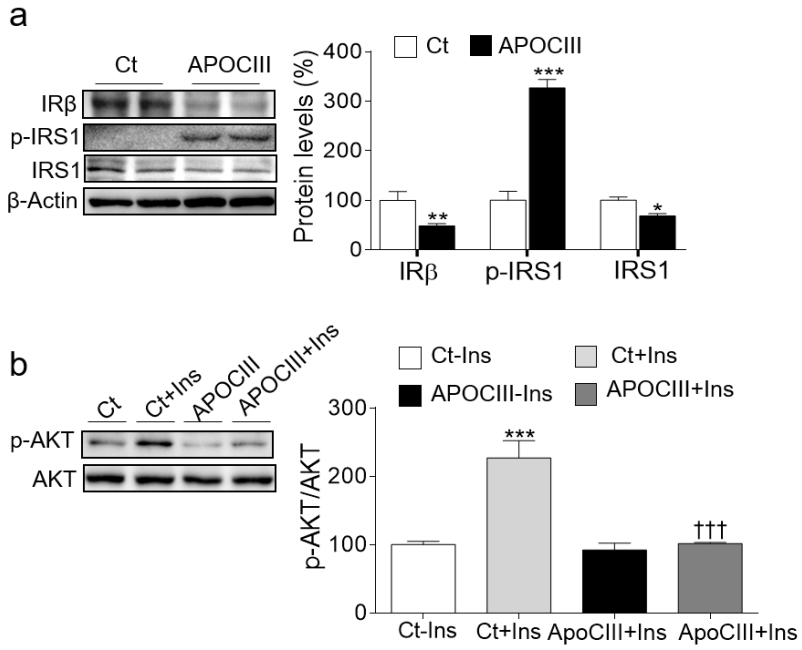

Figure IV.10. ApoCIII induce insulin resistance. C2C12 myotubes were incubated in the presence or absence (Ct: control) of 100 μg/mL Apo CIII for 24 h. Were indicated, C2C12 myotubes were incubated with 100 nM Insulin (Ins) for the last 10 minutes. **a)** IRβ and phosphorylated IRS1 (Ser^{307}) protein levels. **b)** phosphorylated AKT (Ser^{473}) protein levels. The graphs show quantification expressed as a % of control samples ± SD of five independent experiments. ***p<0.001, **p<0.01 and *p<0.05 *vs.* control, †††p<0.001 *vs.* control cells incubated with insulin.

No changes were observed in ER stress and inflammatory markers or in the protein levels of PGC1α and phospho-ERK1/2 when cells were incubated with Apo CI, indicating that the effects of Apo CIII were specific (Figure IV.11. a-b). In addition, both VLDL and Apo CIII reduced insulin-stimulated glucose uptake in myotubes, whereas VLDL low in Apo CIII did not (Figure IV.11. c).

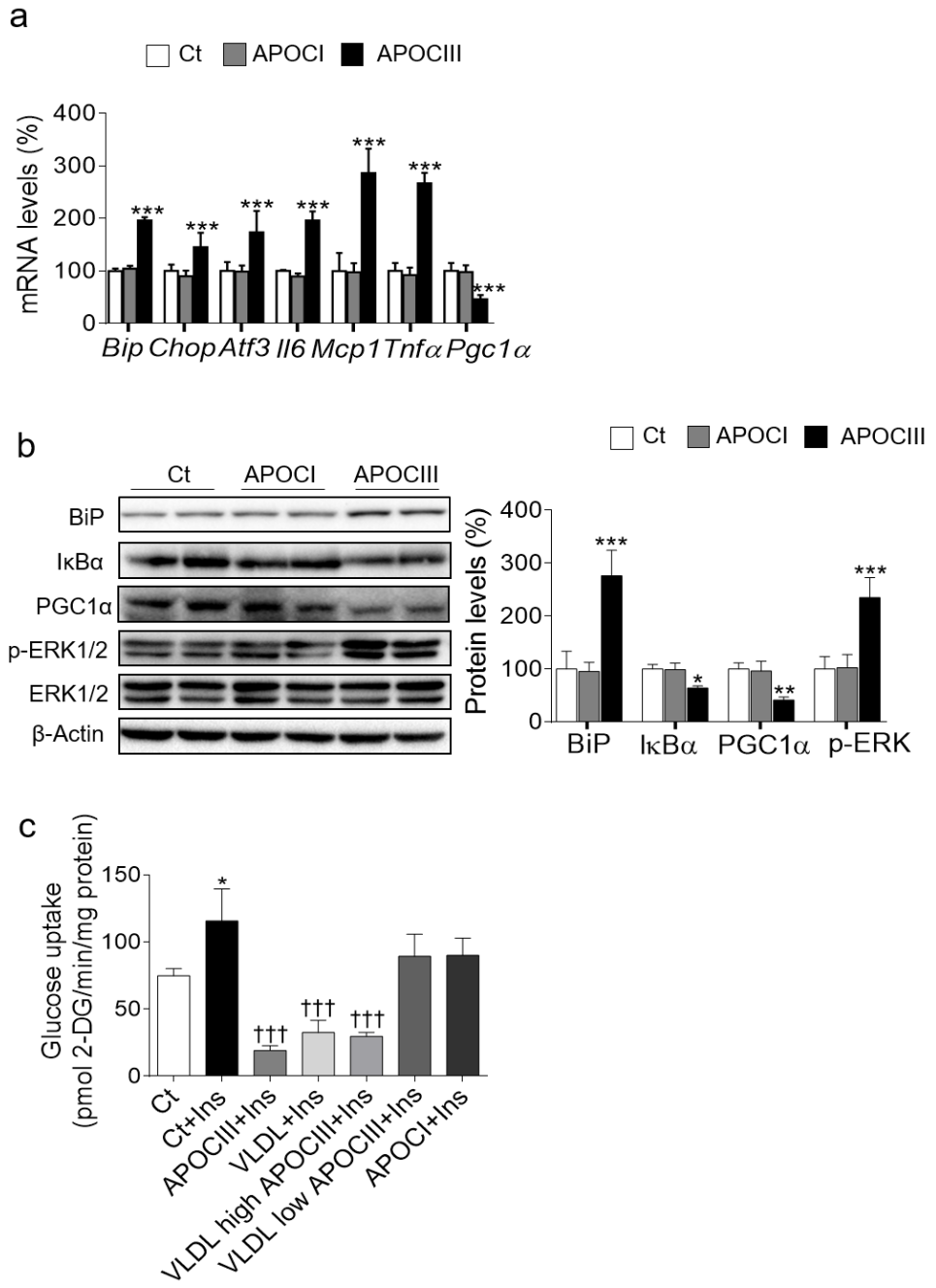

Figure IV.11. The effects of ApoCIII are specific. C2C12 myotubes were incubated in the presence or absence (Ct: control) of 100 µg/mL of Apo CIII and Apo CI and of 300µg/mL of VLDL with low or high amount of Apo CIII during 24 h. When indicated cells were stimulated with 100 nM insulin (Ins) **a)** mRNA abundance of *BiP, Chop, Atf3, Il6, Mcp1, Tnfα, Pgc1α*. **b)** BiP, IκBα, PGC1α, phosphorylated ERK1/2 (Thr^{202}/Tyr^{204}) and β-actin protein levels. **c)** Insulin-dependent glucose-uptake performed using ^{3}H-labelled glucose. Results are expressed as pmol of glucose uptaken per minute and standardized to mg of total protein. The graphs show quantification expressed as a % of control samples ± SD of five independent experiments. ***p<0.001, **p<0.01 and *p<0.05 *vs.* control, †††p<0.001 *vs.* control cells incubated with insulin.

Collectively, these data clearly show the involvement of Apo CIII in the effects of VLDL. However, some authors have raised the possibility that the release of fatty acids from VLDL particles might be responsible for some of the effects of these lipoproteins on ER stress and inflammation (Pedrini *et al.*, 2005). To avoid this interference, we did not use BSA when we incubated myotubes with VLDL or purified Apo CIII, thus preventing fatty acid uptake from the cells. However, we also incubated cells with both palmitic acid and Apo CIII to examine whether the effects of this apolipoprotein could be observed also in presence of the saturated fatty acid. Indeed, Apo CIII significantly intensified the effects of palmitate on the levels of ER stress markers, ERK1/2 phosphorylation, PGC1α and insulin signaling pathway (Figure IV.12. a), indicating that the increase in Apo CIII might exacerbate the effects of lipids on insulin resistance.

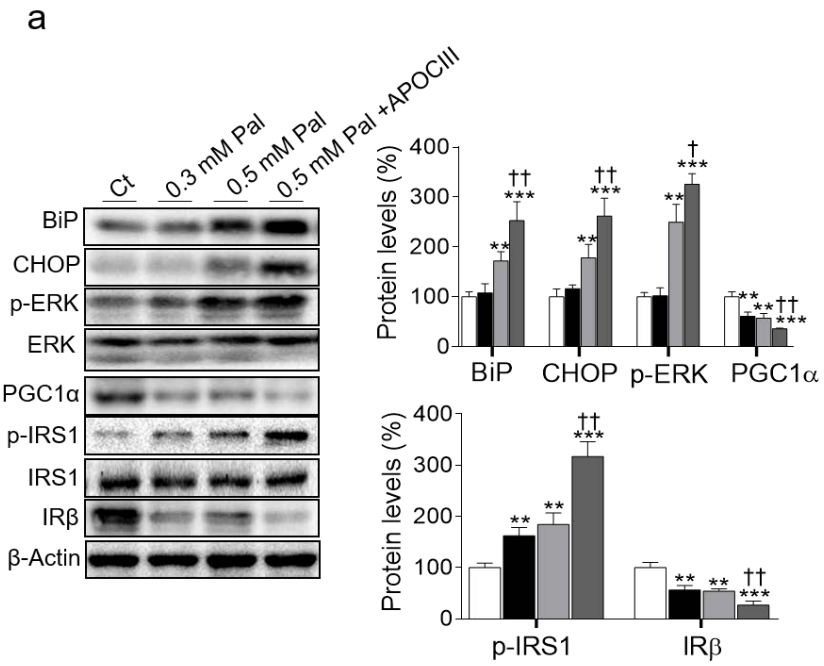

Figure IV.12. ApoCIII exacerbates the effects of palmitic acid. C2C12 myotubes were incubated in the presence or absence (Ct: control) of 100 µg/mL of Apo CIII and different concentrations (0.3 mM and 0.5 mM) of palmitic acid. **a)** BiP, CHOP, phosphorylated ERK1/2 (Thr^{202}/Tyr^{204}), PGC1α, phosphorylated IRS1 (Ser^{307}), IRβ and β-actin protein levels. The graphs show quantification expressed as a % of control samples ± SD of five independent experiments. ***p<0.001, **p<0.01 and *p<0.05 *vs.* control, †p<0.5 *vs.* cells incubated with pamitate, ††p<0.01 *vs.* cells incubated with pamitate.

IV. 1.5. The effects of Apo CIII were prevented by ERK1/2 inhibition

The increase in the expression of ER stress and inflammatory markers caused by Apo CIII was blunted by U0126 co-incubation (Figure IV.13. a). Likewise, U0126 prevented the increase in the protein levels of BiP, phospho-eIF2α and phospho-ERK1/2 caused by Apo CIII (Figure IV.13. b). Inhibition of the MAPK-ERK1/2 pathway also prevented the reduction in IκBα and the increase in the DNA-binding activity of NFκB (Figure IV.13. c-d), as well as the increase in NRF2 and phospho-STAT3 at Tyr^{705} levels (Figure IV.13. d) observed in cells exposed only to Apo CIII. Incubation with U0126 also abolished the Apo CIII-induced reduction in the expression of PGC1α, PPARα, PPARβ/δ and their target genes involved in fatty acid oxidation (Figure IV.14. a). Likewise, the decrease in the protein levels of PGC1α, phospho-AMPK, and phospho-ACC was reversed by U0126 (Figure IV.14. b). siRNA knockdown of ERK1/2 confirmed that this kinase was responsible for the increase in ER stress and inflammation (Figure IV.14. c) and the reduction in fatty acids genes (Figure IV.14. d) caused by Apo CIII.

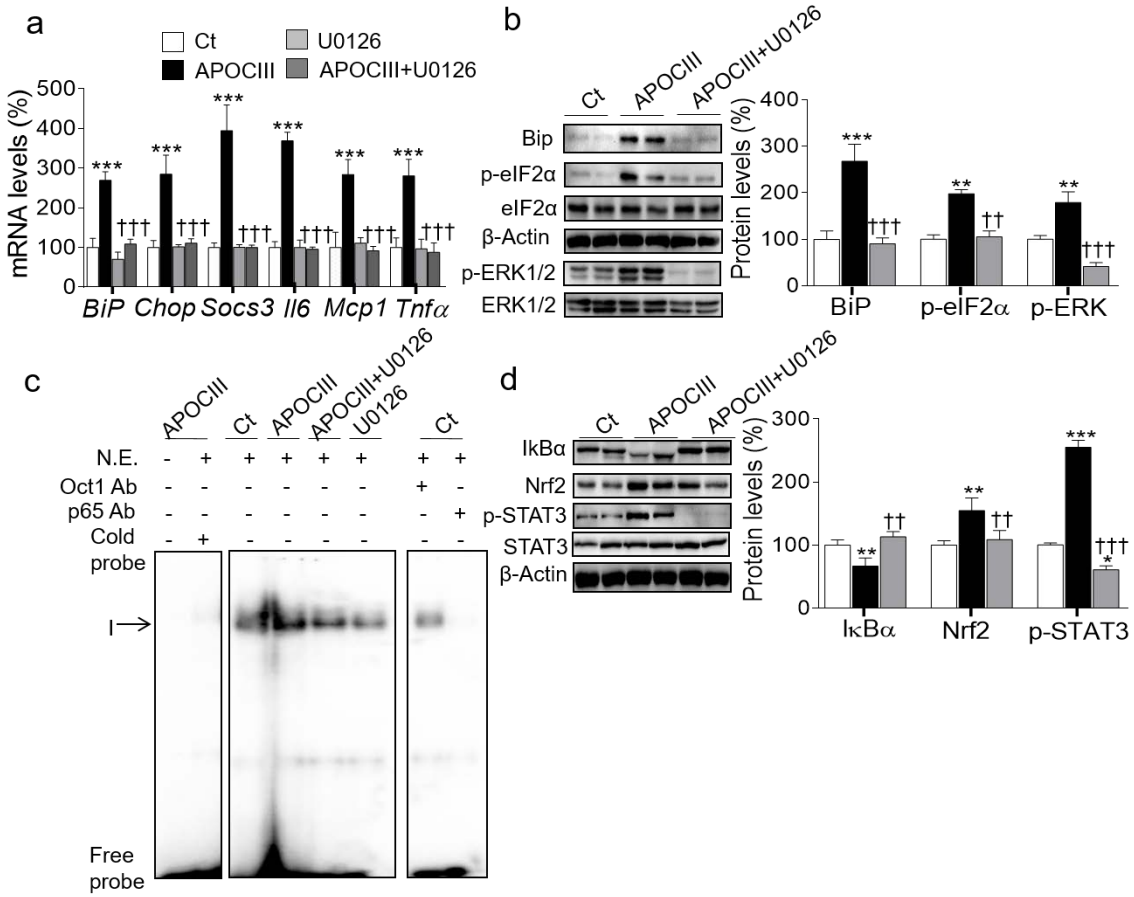

Figure IV.13. The effect of Apo CIII are prevented by ERK1/2 inhibition. C2C12 myotubes were incubated in the presence or absence (Ct: control) of 100 µg/mL of Apo CIII for 24 h. **a)** mRNA abundance of *BiP, Chop, Socs3, Il6, Mcp1, Tnfα.* **b)** phosphorylated eIF2α (Ser^{51}), phosphorylated ERK1/2 (Thr^{202}/Tyr^{204}), and β-actin protein levels. **c)** Autoradiograph of EMSA performed with a ^{32}P-labeled NFκB nucleotide and crude nuclear protein extract (NE) from C2C12 myotubes. One main specific complex (I) based on competition with a molar excess of unlabeled probe is shown. The supershift assay performed by incubating NE with an antibody (Ab) directed against the p65 subunit of NFκB shows a reduction in the band, whereas the band is observed with the unrelated antibody against Oct1. **d)** IκBα, NRF2, phosphorylated STAT3 (Tyr^{705}) and β-actin protein levels. The graphs show quantification expressed as a % of control samples ± SD of five independent experiments. ***p<0.001, **p<0.01 and *p<0.05 *vs.* control, ††p<0.01 vs Apo CIII-exposed cells, †††p<0.001 *vs.* Apo CIII-exposed cells.

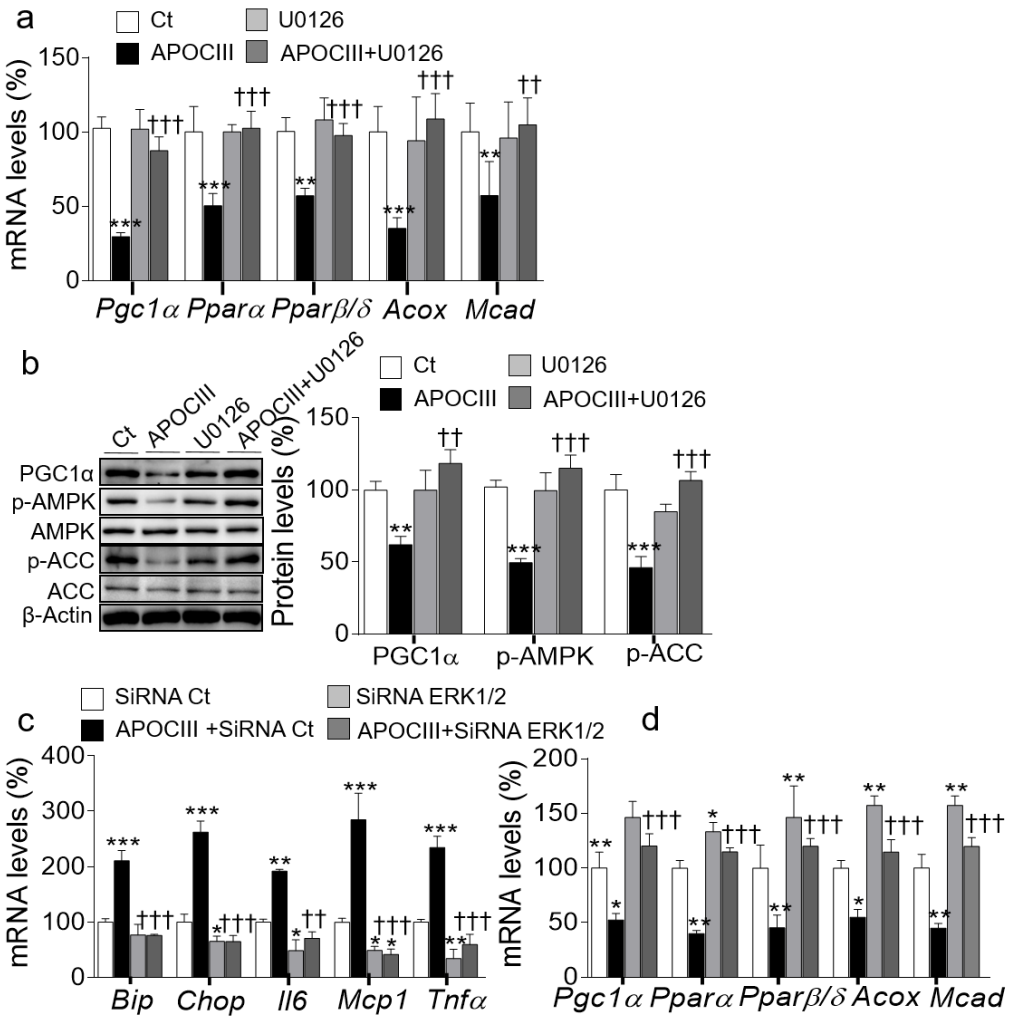

Figure IV.14. The effect of Apo CIII are prevented by ERK1/2 inhibition. C2C12 myotubes were incubated in the presence or absence (Ct: control) of 100 μg/mL of Apo CIII, 10 μM U0126, or 10 μM U0126 plus 100 μg/mL Apo CIII for 24 h. **a)** mRNA abundance of *Pgc1α, Pparα, Pparβ/δ, Acox, Mcad.* **b)** PGC1α, phosphorylated AMPK (Thr^{172}), phosphorylated ACC (Ser^{79}), and β-actin protein levels. C2C12 cells were transfected with control or ERK1/2 siRNA and the mRNA abundance of **c)** *Bip*, *Chop*, *Il6*, *Mcp1*, and *Tnfα*, and **d)** *Pgc1α*, *Pparα*, *Acox,* and *Mcad* was evaluated**.** The graphs show quantification expressed as a % of control samples ± SD of five independent experiments. ***p<0.001, **p<0.01 and *p<0.05 *vs.* control, †††p<0.001 *vs.* Apo CIII-exposed cells.

Next, we examined whether some of the changes caused by Apo CIII *in vitro* were also observed in skeletal muscle of Tg mice with human Apo CIII overexpression (ApoCIIITg) (Figure IV.15.). It has been reported that these mice have marked elevations in plasma TG, but no impairment of glucose tolerance (Reaven *et al.*, 1994). However, ApoCIIITg mice fed a HFD show hepatic insulin resistance (Lee *et al.*, 2011) and are more susceptible to develop diabetes (Salerno *et al.*, 2007). In skeletal muscle of ApoCIIITg mice fed a standard

diet we observed increased CHOP, IL6 and TNFα expression compared to non-transgenic (Ntg) littermate mice, whereas no changes were observed in BiP mRNA levels (Figure IV.15. a). Moreover, we detected a marked increase in the protein levels of phospho-ERK1/2, that was accompanied by a reduction in PGC1α protein levels (Figure IV.15. b-c).

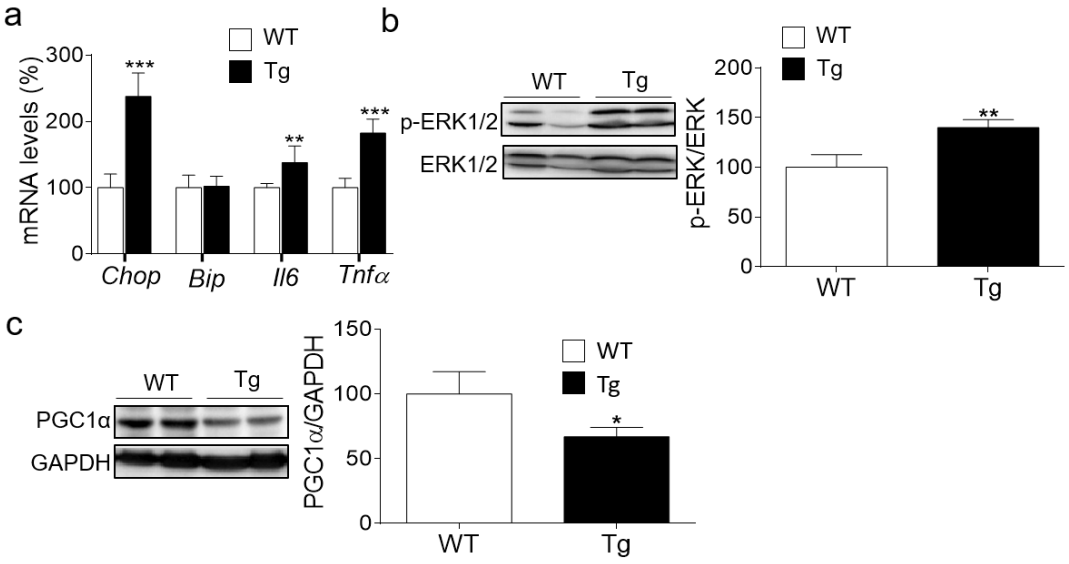

Figure IV.15. Skeletal muscle from ApoCIIITg mice shows increased ER stress and inflammatory markers, increased phosphorylated ERK1/2 levels, and reduced PGC1α levels. Skeletal muscle from male non-transgenic (wild type: WT) and apoCIIITg mice was used (n=5 per group). **a)** mRNA abundance of *Chop, Bip*, *Tnfα* and *Il6.* **b)** phosphorylated ERK1/2 (Thr^{202}/Tyr^{204}), and **c)** PGC1α and GAPDH protein levels. The graphs show quantification expressed as a % of control samples ± SD of five independent experiments. ***p<0.001, **p<0.01 and *p<0.05 *vs.* wild type mice.

IV. 1.6. Apo CIII activates ERK1/2 through TLR2

Since TLRs activate ERK1/2 and cause inflammation (Chung *et al.*, 2006), we examined whether Apo CIII acted through these receptors. To study this possibility, we incubated cells exposed to Apo CIII with a selective neutralizing antibody against either TLR2 or IgG. In the presence of this neutralizing antibody, the increase in phospho-ERK1/2 levels caused by Apo CIII alone was blunted (Figure IV.16. a). Consistent with a crucial role for ERK1/2 in the effects caused by Apo CIII, the TLR2 neutralizing antibody prevented the changes in the mRNA and protein levels of ER stress and inflammatory markers (Figure IV.16. b-c). Likewise, TLR2 neutralization partially reversed the reduction in the protein levels of insulin receptor, blunted the increase in IRS1-Ser^{307} (Figure IV.16. d) and

prevented the reduction in PGC1α, PPARα, and NRF1 (Figure IV.17. a-b). Blocking TLR2 also prevented the reduction in the expression of genes involved in fatty acid oxidation, such as ACOX and MCAD (Figure IV.17. a).

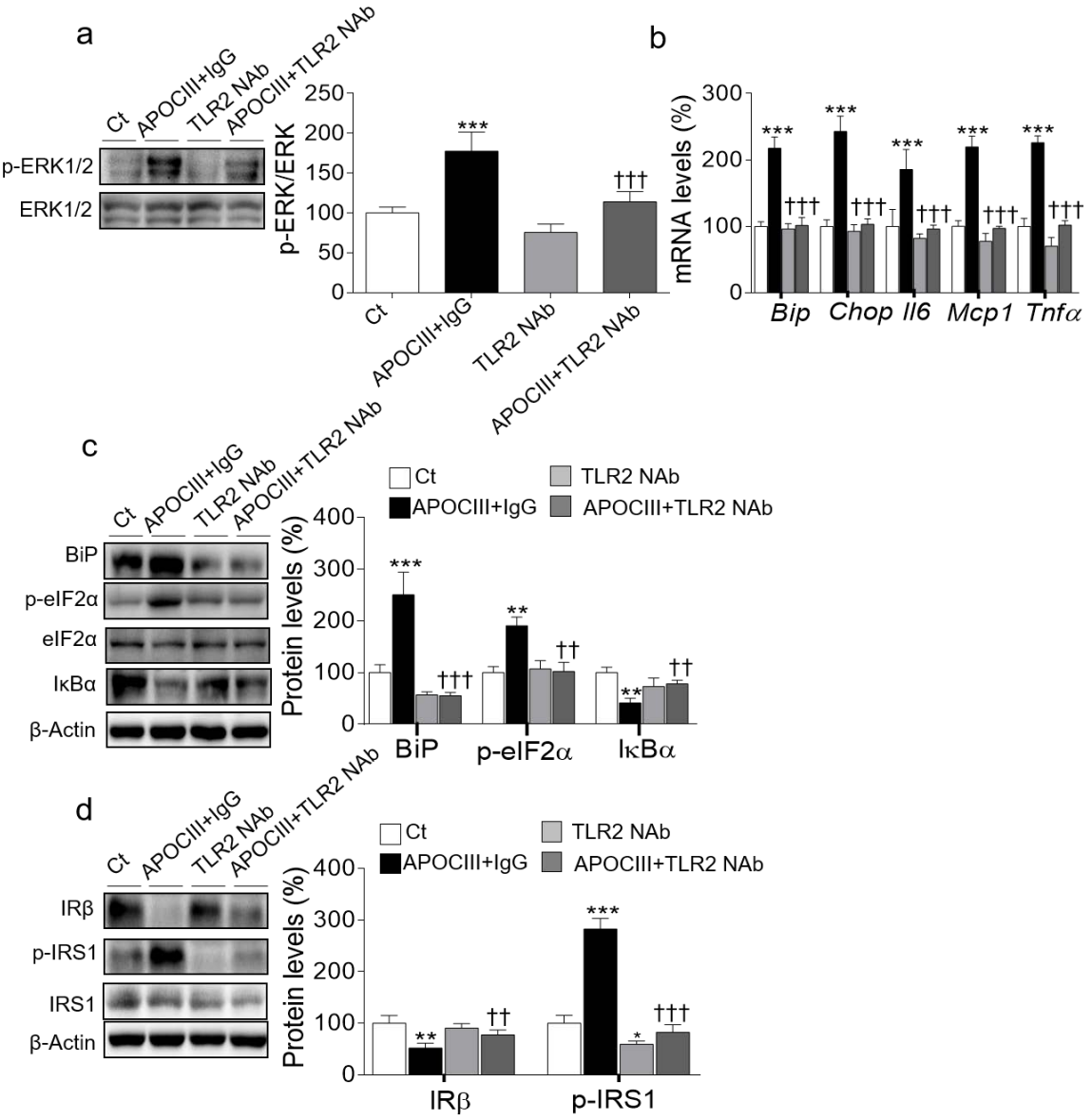

Figure IV.16. TLR2 mediates the effects of Apo CIII on ERK1/2, ER stress, and inflammation. C2C12 myotubes were incubated in the presence or absence (Ct: control) of 100 μg/mL Apo CIII plus 50 μg/mL of IgG, 50 μg/mL of the neutralizing antibody against TLR2 (TLR2NAb), or 100 μg/mL Apo CIII plus 50 μg/mL of the TLR2NAb for 24 h. **a)** phosphorylated ERK1/2 (Thr^{202}/Tyr^{204}) protein levels. **b)** mRNA abundance of *Bip*, *Chop*, *Il6*, *Mcp1*, and *Tnfα* **c)** BiP, phosphorylated eIF2α (Ser^{51}), IκBα, and β-actin protein levels. **d)** IRβ, phosphorylated IRS1 (Ser^{307}), and β-actin protein levels. The graphs show quantification expressed as a % of control samples ± SD of five independent experiments. ***p<0.001, **p<0.01 and *p<0.05 *vs.* control. ††p<0.01 *vs.* Apo CIII+IgG exposed cells, †††p<0.001 *vs.* Apo CIII+IgG exposed cells.

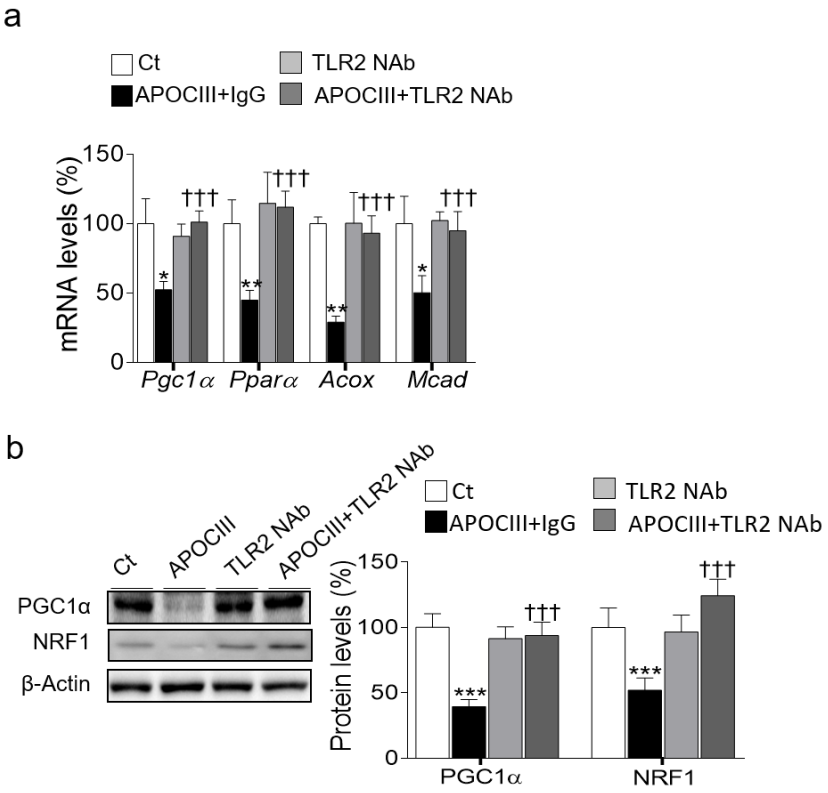

Figure IV.17. TLR2 mediates the effects of Apo CIII on PGC1α and fatty acid oxidation. C2C12 myotubes were incubated in the presence or absence (Ct: control) of 100 μg/mL Apo CIII plus 50 μg/mL of IgG, 50 μg/mL of the neutralizing antibody against TLR2 (TLR2NAb), or 100 μg/mL Apo CIII plus 50 μg/mL of the TLR2NAb for 24 h. **a)** mRNA abundance of *Pgc1α*, *Pparα*, *Acox,* and *Mcad* **b)** PGC1α, NRF1 and β-actin protein levels. The graphs show quantification expressed as a % of control samples ± SD of five independent experiments. ***p<0.001, **p<0.01 and *p<0.05 *vs.* control. ††p<0.01 *vs.* Apo CIII+IgG exposed cells, †††p<0.001 *vs.* Apo CIII+IgG exposed cells.

Collectively, our results clearly indicate that VLDL and Apo CIII can induce ER stress, inflammation and attenuate the insulin signaling pathway in skeletal muscle by activating the TLR2 and the ERK1/2 pathway.

IV. 2. The BACE1 product sAPPβ induces ER stress and inflammation and impairs insulin signaling

IV. 2.1. Palmitate increases BACE1 expression through an NFκB-dependent mechanism

As mentioned in the introduction, it has been previously reported that palmitate treatment increases BACE1 protein levels in C2C12 myotubes through post-translational stabilization of BACE1 protein caused by palmitate and ceramides (Hamilton *et al.*, 2014; Puglielli *et al.*, 2003). However, it was unknown whether transcriptional mechanisms were also involved. Interestingly, palmitate exposure increased BACE1 mRNA levels in C2C12 myotubes (Figure IV.18. a). Since palmitate increases NFκB activity in myotubes (Chaurasia and Summers, 2015) and BACE1 is under the transcriptional control of NFκB (Buggia-Prevot *et al.*, 2008), we evaluated whether palmitate-induced NFκB activation was responsible for the increase in BACE1 expression by using the NFκB inhibitor parthenolide (Hehner *et al.*, 1998). Parthenolide prevented the palmitate-induced increase in BACE1 mRNA levels (Figure IV.18. b), suggesting that palmitate increases its expression by activating NFκB. Therefore, the observed increase in BACE1 protein levels following palmitate exposure (Figure IV.18. c) might be the result of both the reported post-translational stabilization of BACE1 protein (Hamilton *et al.*, 2014; Puglielli *et al.*, 2003), and also of BACE1 increased expression. When mice were fed a HFD we also observed an increase in the mRNA and protein levels of BACE1 in the skeletal muscle of these mice compared to those fed a standard diet (Figure IV.18. d-e), suggesting that the transcriptional mechanism may also operate *in vivo*.

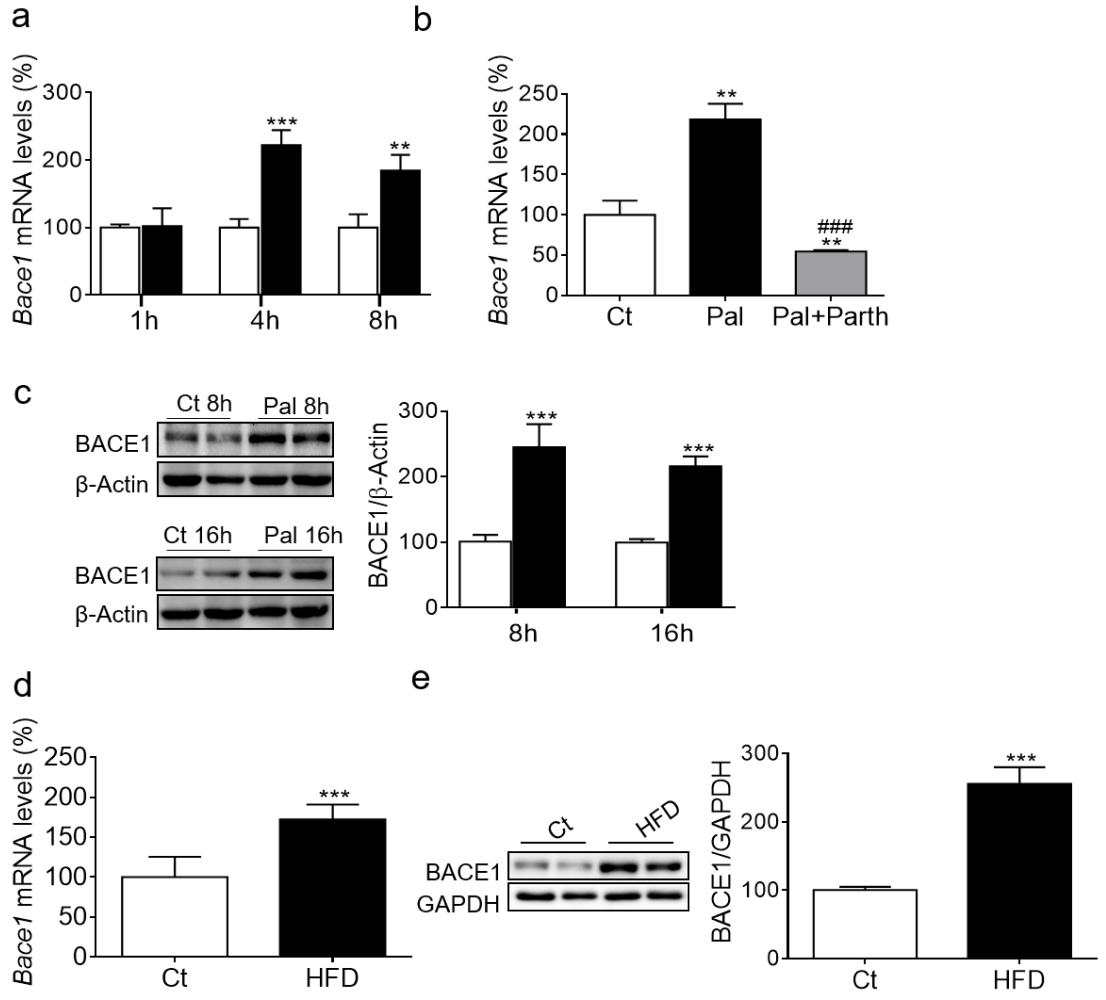

Figure IV.18. Palmitate modulates *Bace1* mRNA expression in skeletal muscle cells. C2C12 myotubes were incubated in the presence or absence (Ct: control) of 0.5mM of the saturated fatty acid palmitate (Pal), or 0.5 mM Pal plus 10 μM parthenolide (Parth) for different times (1h, 4h, 8h, 16h). ***a-b)*** mRNA abundance of *Bace1* ***c)*** BACE1 and β-actin protein levels. Skeletal muscle from male mice fed a standard diet (Control, Ct) or an high-fat diet (HFD) (n=5 per group) for 12 weeks. **d)** mRNA abundance and **e)** protein levels of BACE1. The graphs show quantification expressed as a % of control samples ± SD of five independent experiments. ***p<0.001, **p<0.01 and *p<0.05 *vs.* control. ###p<0.001 *vs.* palmitate-exposed cells.

IV. 2.2. BACE1 inhibition prevents palmitate-induced ER stress, inflammation and insulin resistance in skeletal muscle cells

Next, we hypothesized that BACE1 might contribute to some of the deleterious effects of palmitate, including ER stress, inflammation, and insulin resistance. To elucidate this, we used the high selective BACE1 inhibitor M3, which has been reported to inhibit BACE1 activity in C2C12 cells (Puglielli *et al.*, 2003; Vassar, 2014). M3 treatment significantly attenuated the palmitate-mediated increase in the expression of ER stress markers (sXBP1, ATF3, CHOP, and BiP) and inflammatory markers (TNFα, IL6) (Figure IV.19. a-b). As

expected, palmitate exposure reduced protein levels of the NFκB inhibitor IκBα, whereas in the myotubes co-incubated with palmitate in the presence of M3, this reduction was blunted (Figure IV.19. c). Consistent with this, the nuclear protein levels of the NFκB subunit p65 were raised by palmitate, but this increase was abolished when cells were co-incubated with both palmitate and M3 (Figure IV.19. c). Likewise, NFκB DNA-binding activity increased (complex I) in nuclear extracts from palmitate-exposed cells, whereas the binding activity in cells co-incubated with palmitate and M3 was similar to that observed in control cells (Figure IV.19.d).

Collectively, these data suggest that BACE1 is involved in the effects of palmitate on ER stress and inflammation in skeletal muscle cells.

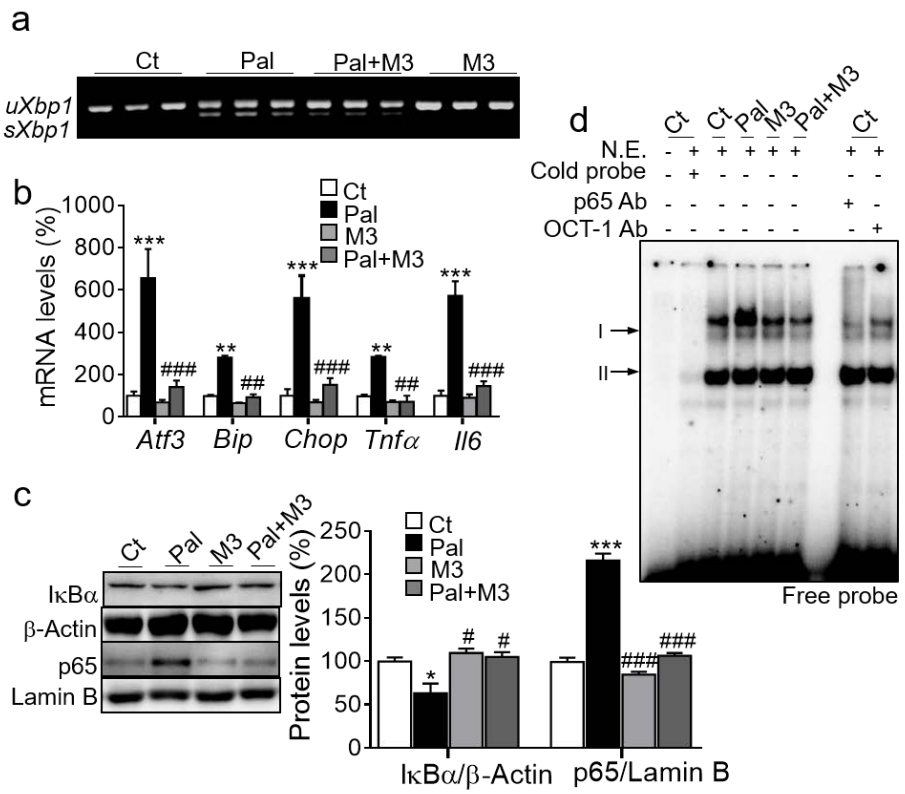

Figure IV.19. BACE1 inhibition attenuates palmitate-induced ER stress and inflammation in myotubes. C2C12 myotubes were incubated in the presence or absence (Ct: control) of 0.5 mM palmitate (Pal) or Pal 0.5 mM plus 100 nM M3 for 16 h. **a)** spliced *Xbp1* (*sXbp1*) mRNA levels. uXBP1, unspliced XBP1. **b)** *Atf3*, *Chop*, *Tnfα*, *Il-6,* and *BiP* mRNA levels. **c)** IκBα, p65 and β-actin protein levels. **d)** Autoradiograph of EMSA performed with a ^{32}P-labeled NFκB nucleotide and crude nuclear protein extract (NE) from C2C12 myotubes. Two main specific complexes (I and II) based on competition with a molar excess of unlabeled probe is shown. The supershift assay performed by incubating NE with an antibody (Ab) directed against the p65 subunit of NFκB shows a reduction in the complex I band, whereas the band is observed with the unrelated antibody against Oct1. ***p<0.001, **p<0.01 and *p<0.05 *vs.* control. $^{###}$p<0.001 *vs.* palmitate-exposed cells.

When we evaluated the insulin signaling pathway, we observed that protein levels of insulin receptor were reduced in palmitate-exposed cells, but this reduction was prevented by M3 (Figure IV.20. a). In addition, the palmitate-induced increase in IRS1 phosphorylation at Ser^{307} was also blocked in cells incubated with M3 (Figure IV.20. a). Finally, palmitate reduced insulin-stimulated Akt phosphorylation, whereas this reduction was completely reversed in cells co-incubated with palmitate and M3 (Figure IV.20. b). Taken together, our findings suggest that BACE1 might also mediate the palmitate-induced impairment of insulin signaling pathway in myotubes.

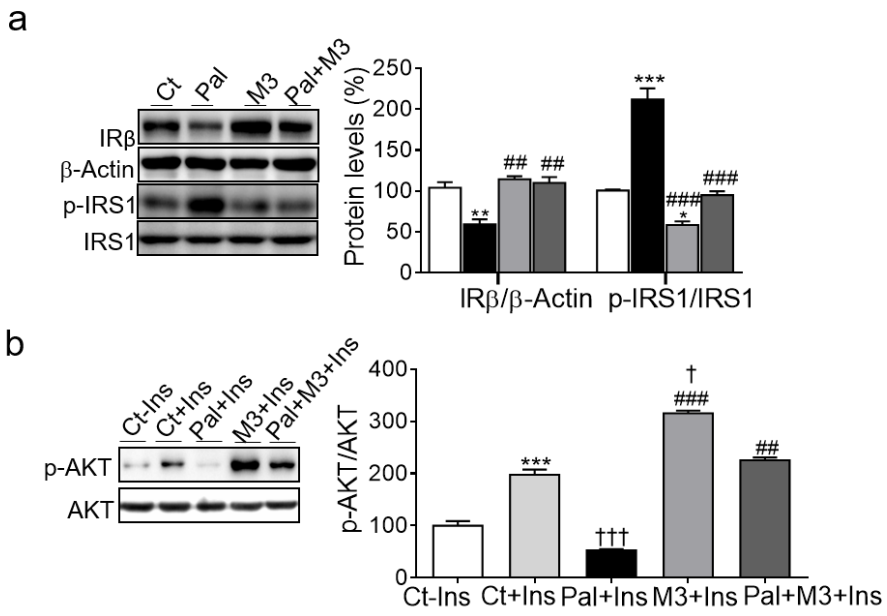

Figure IV.20. BACE1 inhibition attenuates palmitate-induced insulin resistance in myotubes. C2C12 myotubes were incubated in the presence or absence (Ct: control) of 0.5 mM palmitate (Pal) or Pal 0.5 mM plus 100 nM M3 for 16 h. Were indicated, myotubes were stimulated with 10 nM insulin (Ins) during the last 10 minutes. **a)** IRβ, phosphorylated IRS1 (Ser^{307}) and β-actin protein levels. **b)** Phosphorylated AKT (Ser^{473}) protein levels. The graphs show quantification expressed as a % of control samples ± SD of five independent experiments. ***p<0.001, **p<0.01 and *p<0.05 *vs.* control. $^{\#\#}$p<0.001 *vs.* palmitate-exposed cells. $^{\#\#\#}$p<0.001 *vs.* palmitate-exposed cells. †††p<0.001 *vs.* control plus Ins.

IV. 2.3. BACE1 inhibition prevents the reduction in PGC1α levels caused by palmitate

Since palmitate increases BACE1 protein levels and we reported that this saturated fatty acid reduces the expression of PGC1α (Coll *et al.*, 2006) we next evaluated whether BACE1 inhibition prevented the reduction in PGC1α levels. Interestingly, palmitate caused a reduction in PGC1α mRNA levels that was prevented by M3 (Figure IV.21. a). Similarly, PGC1α protein levels showed a significant reduction in palmitate-exposed cells, but this reduction was not observed when cells where co-incubated with palmitate plus M3 (Figure IV.21. b). In agreement with these changes, palmitate induced a reduction in the

mRNA and protein levels of PPARα and PPARβ/δ, but their levels were restored in cells co-incubated with palmitate in the presence of M3 (Figure IV.21. a-b). The expression of PPAR-target genes such as ACOX, CPT1 and MCAD, as well as IκBα, which is also under the transcriptional control of PPARα (Buroker *et al.*, 2009) was reduced by palmitate (with the exception of CPT1) and restored when cells were incubated with the fatty acid plus M3 (Figure IV.21. c). Given that PGC1α regulates PPARα transcriptional activity (Vega *et al.*, 2000), we assessed the DNA-binding activity of this transcription factor by performing EMSA. PPARα DNA-binding activity (complex I) was reduced by palmitate, in agreement with the reduction in PGC1α protein levels, whereas this reduction was partially prevented in cells co-incubated with both palmitate and M3 (Figure IV.21. d). It is worth pointing out that incubation of the cells only with the M3 compound significantly increased mRNA levels of PPARα, PPARβ/δ, PGC1α, and the PPAR target gene CPT1 (Figure IV.21. e), suggesting that basal expression of these genes may be repressed by BACE1 activity. In this regard, some authors reported that BACE1 expression is downregulated by PGC1α and PPARγ in neurons (Wang *et al.*, 2013), leading to the speculation that a mutual control between BACE1 and PGC1α might exist. To examine whether this mechanism also occurs in skeletal muscle, we overexpressed PGC1α in human myotubes. No changes were observed in BACE1 expression or protein levels (Figure IV.21. f-g), thus ruling out the possibility that BACE1 is under the transcriptional control of PGC1α in skeletal muscle cells.

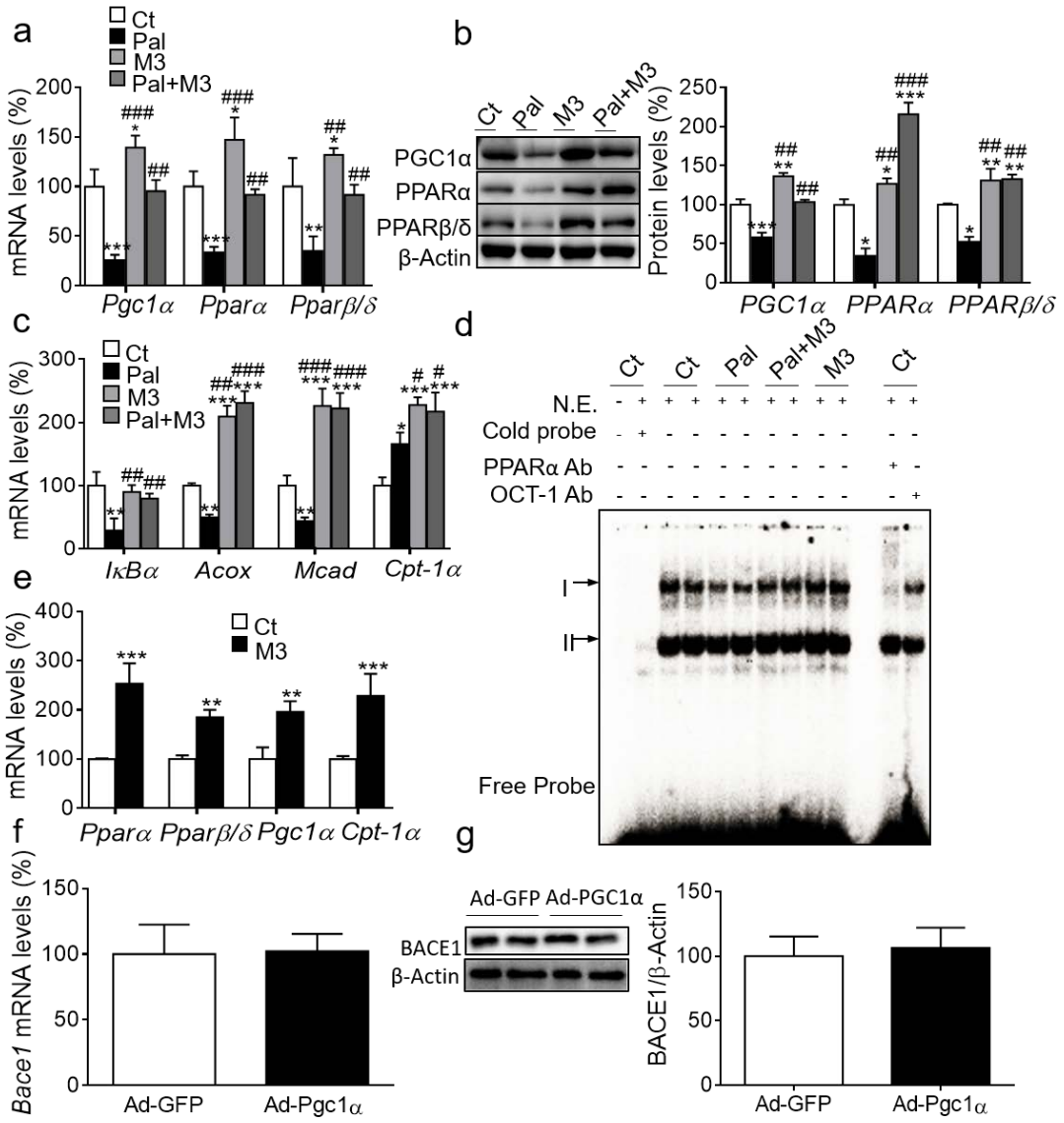

Figure IV.21. BACE1 inhibition attenuates palmitate-induced downregulation of PGC1α in myotubes. Mouse C2C12 myotubes were incubated in the presence or absence (Ct: control) of 0.5 mM palmitate (Pal) or 100 nM M3, or Pal 0.5 mM plus 100 nM M3 for 16 h. **a)** mRNA abundance of *Pgc1α, Pparα* and *Pparβ/δ.* **b)** PGC1α, PPARα, PPARβ/δ and β-actin protein levels. **c)** mRNA abundance of *IκBα, Acox, Mcad* and *Cpt1α.* Human LHCNM2 myotubes were transfected with GFP- or PGC1α-expressing Adenovirus (Ad-GFP and Ad-Pgc1α), respectively. **d)** Autoradiograph of EMSA performed with a ^{32}P-labeled PPAR nucleotide and crude nuclear protein extract (NE) from C2C12 myotubes. One main specific complex (I) based on competition with a molar excess of unlabeled probe is shown. The supershift assay performed by incubating NE with an antibody (Ab) directed against PPARα shows a reduction in the band, whereas the band is observed with the unrelated antibody against Oct1. **e)** mRNA abundance of *Pgc1α, Pparα*, *Pparβ/δ* and *Cpt1α.* **f)** mRNA abundance and **g)** protein levels of BACE1. The graphs show quantification expressed as a % of control samples ± SD of five independent experiments. ***p<0.001, **p<0.01 and *p<0.05 *vs.* control. $^{\#\#}$p<0.001 *vs.* palmitate-exposed cells. $^{\#\#\#}$p<0.001 *vs.* palmitate-exposed cells.

IV. 2.4. BACE1 knockdown increases PGC1α in myotubes and skeletal muscle

To clearly demonstrate that BACE1 modulates PGC1α we used genetic approaches. Knockdown of BACE1 by siRNA transfection in C2C12 cells led to a significant increase in the expression and the protein levels of PGC1α, PPARα and PPARβ/δ (Figure IV.22. a-b). In addition, expression of the PPAR-target genes CPT1, ACOX and MCAD was significantly increased by BACE1 knockdown, whereas expression of CHOP, TNFα and MCP1 were reduced (Figure IV.22. c). Moreover, IκBα and insulin receptor protein levels were also increased by BACE1 knockdown, whereas phospho-IRS1 (Ser^{307}) levels were decreased (Figure IV.22. d).

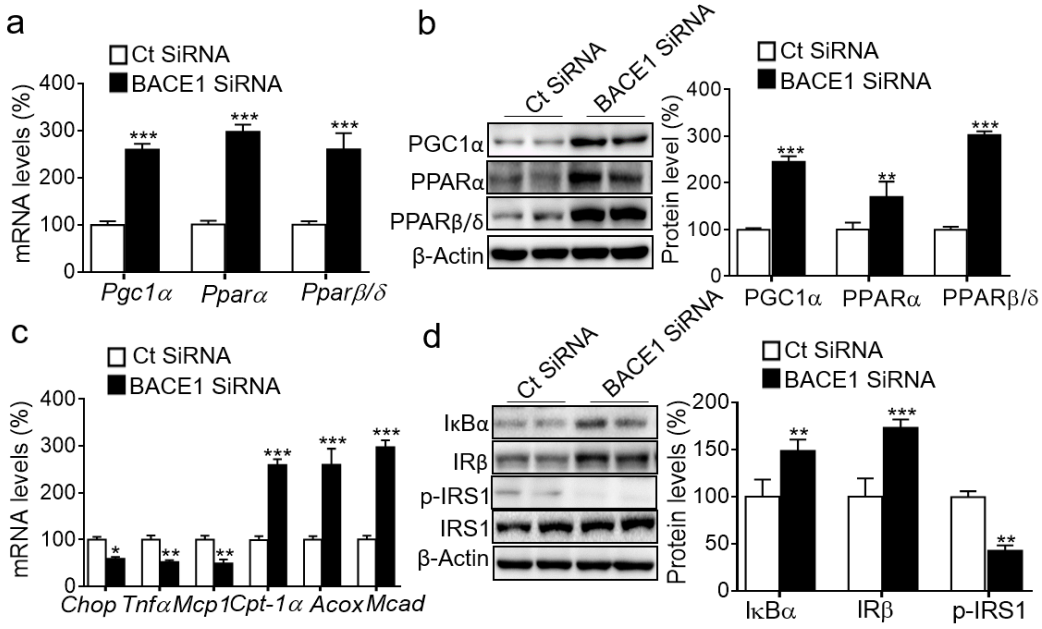

Figure IV.22. BACE1 knockdown increases PGC1α levels, reduces ER stress and inflammation and attenuates insulin resistance in myotubes. C2C12 cells were transfected with control or BACE1 siRNA for 48 hours and the expression **a)** and protein levels **b)** of PGC1α, PPARα and PPARβ/δ were examined**. c)** mRNA abundance of *Chop, Tnfα, Mcp1, Cpt1α, Acox and Mcad.* **d)** IκBα, IRβ, phosphorylated IRS1 (Ser^{307}) and β-actin protein levels. The graphs show quantification expressed as a % of control samples ± SD of five independent experiments. ***p<0.001, **p<0.01 and *p<0.05 *vs.* control. $^{\#\#}$p<0.001 *vs.* palmitate-exposed cells.

In agreement with the results *in vitro*, a significant increase in PGC1α expression and protein levels was observed in skeletal muscle from BACE1 deficient mice (Figure IV.23 a-b). Moreover, PPARα and PPARβ/δ expression and protein levels were also enhanced in BACE1 knockout mice (Figure IV.23. a-b). Consistent with this, the expression of IκBα, CPT1, ACOX, and MCAD was increased in BACE1-deficient mice, whereas MCP1, TNFα and CHOP expression was decreased compared with wild-type littermates (Figure IV.23. c). Similarly, the protein levels of IκBα and insulin receptor were increased in the skeletal muscle of BACE1-deficient mice compared with wild-type littermates, whereas phospho-eIF2α, which induces CHOP levels, and phospho-IRS1 (Ser^{307}) were decreased (Figure IV.23. d).

Collectively, these data clearly indicate that BACE1 activity is involved in the modulation of several ER stress and inflammatory markers as well as in the insulin signaling pathway, and that its effect might be mediated by the downregulation of PGC1α.

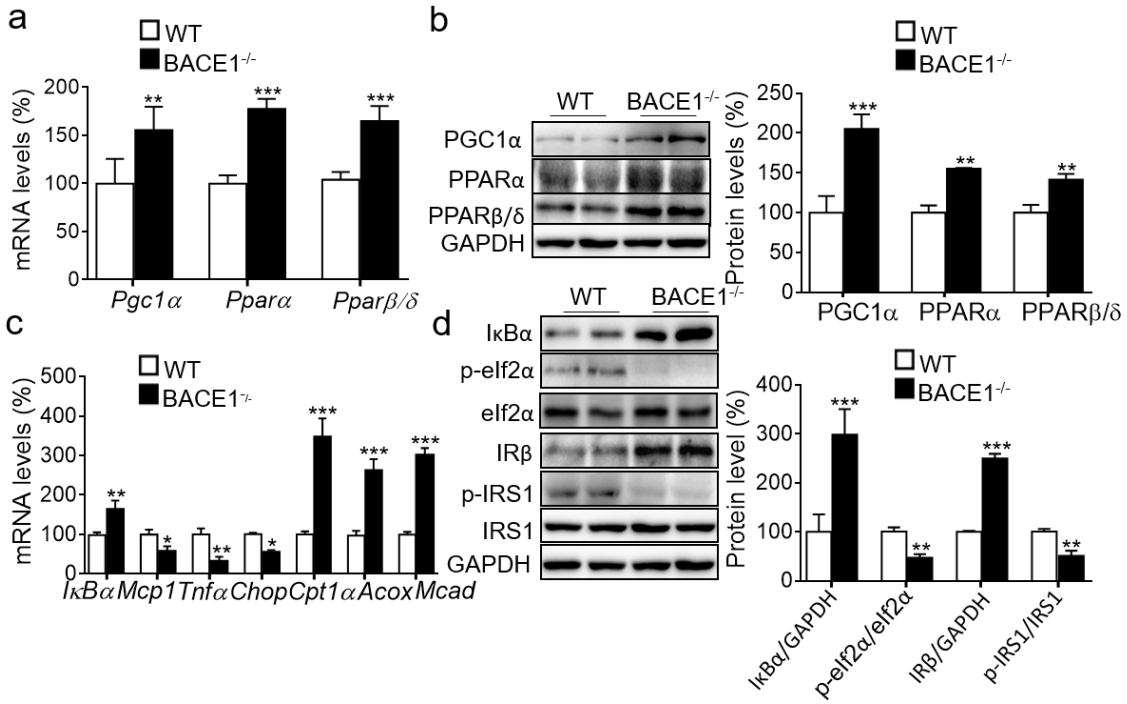

Figure IV.23. BACE1 knockdown increases PGC1α levels, ameliorates ER stress and inflammation, and attenuates insulin resistance in skeletal muscle. Skeletal muscle from male wild type and BACE1-null mice ($BACE1^{-/-}$) was used (n=6 per group). **a)** mRNA abundance of *Pgc1α, Pparα* and *Pparβ/δ.* **b)** PGC1α, PPARα, PPARβ/δ and GAPDH protein levels. **c)** mRNA abundance of of *IκBα*, *Mcp1*, *Tnfα*, *Chop, Cpt1α*, *Acox* and *Mcad*. **d)** IκBα, phospho-eIF2α (Ser^{51}), IRβ and phospho-IRS1 (Ser^{307}) protein levels. The graphs show quantification expressed as a % of control samples ± SD of five independent experiments. ***p<0.001, **p<0.01 and *p<0.05 *vs.* control. $^{\#\#}$p<0.001 *vs.* palmitate-exposed cells. $^{\#\#\#}$p<0.001 *vs.* palmitate-exposed

IV. 2.5. BACE1 knockdown prevents the reduction in PGC1α expression and the inflammatory process caused by a HFD in skeletal muscle

When we evaluated the effects of a HFD in the skeletal muscle of wild-type and BACE1-deficient mice, a reduction in PGC1α expression was observed in wild-type mice fed a HFD, but the increase in the expression of this co-activator displayed in BACE1$^{-/-}$ mice prevented the reduction in PGC1α mRNA levels when these mice were fed a HFD (Figure IV.24. a). Consistent with the reduction in PGC1α expression, PPARα mRNA levels were also down-regulated in the skeletal muscle of wild-type mice fed a HFD, whereas this reduction was prevented in BACE1$^{-/-}$ mice fed the HFD. Likewise, the HFD significantly increased some of the inflammatory markers, such as TNFα and IL6 and reduced IκBα expression in wild-type mice, whereas these changes were prevented in BACE1-deficient mice fed a HFD (Figure IV. 24. a). The protective effect of BACE1 inhibition on the inflammatory process might be due to the increase of PGC1α which in turn downregulate NFκB and exerts an anti-inflammatory effect in skeletal muscle (Alvarez-Guardia *et al.*, 2010).

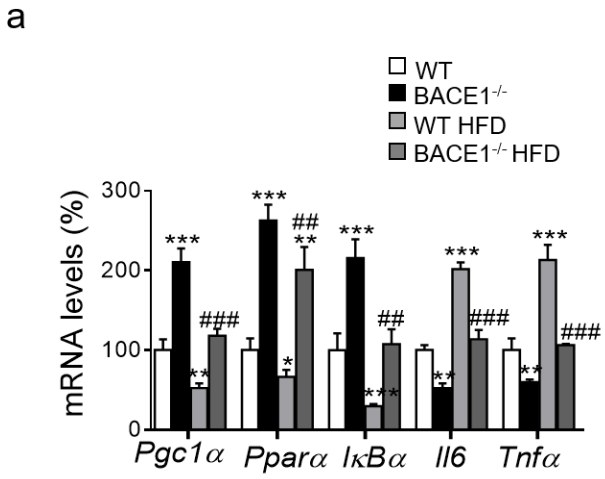

Figure IV.24. BACE1 knockdown prevents the reduction in PGC1α expression and the increase in ER stress and inflammation caused by an HFD in skeletal muscle. Skeletal muscle from male wild type and BACE1-null mice (BACE1$^{-/-}$) fed with a regular chow diet and HFD for 20 weeks was used (n=6 per group). **a)** mRNA abundance of *Pgc1α, Pparα IκBα*, *Il6 and Tnfα.* The graphs show quantification expressed as a % of control samples ± SD of five independent experiments. ***p<0.001, **p<0.01 and *p<0.05 *vs.* control. $^{\#\#}$p<0.001 *vs.* palmitate-exposed cells. $^{\#\#\#}$p<0.001 *vs.* palmitate-exposed cells.

IV. 2.6. sAPPβ mimics the effects of palmitate on ER stress, inflammation and insulin signaling pathway

We next hypothesized whether the BACE1 enzymatic product sAPPβ might be responsible for the effects caused by BACE1 in palmitate-exposed cells. sAPPβ concentration was selected after performing curve-concentration studies in which the levels of some ER stress and inflammatory markers were assessed. Both the concentration of 20nM and 40 nM significantly increased the expression and protein levels of BiP and IL6 and reduced the levels of PGC1α, whereas the concentration of 5 nM and 10 nM did not (Figure IV.25. a-d). To compare the effects of sAPPβ with the effects of palmitate we then separately incubated myotubes with both those compounds. sAPPβ caused a reduction similar to that caused by palmitate in PGC1α mRNA (Figure IV.25. e) and protein levels (Figure IV.25. f). In agreement with this, the mRNA levels of PPARα and PPARβ/δ and several of their target genes involved in fatty acid oxidation, including CPT1, ACOX and MCAD were decreased by sAPPβ (Figure IV.25. e). The effect of sAPPβ on the expression of these genes differed from that of palmitate only in the case of CPT1 expression. No changes were observed in the expression levels of CPT1α, ACOX, MCAD and PPARβ/δ when myotubes were exposed to sAPPα (Figure IV.26. a). Conversely, sAPPα increased the expression of PGC1α and PPARα expression, in contrast to sAPPβ (Figure IV.26. a). Consistent with the reported regulation of mitochondrial oxidative phosphorylation (OXPHOS) genes by PGC1α, palmitate and sAPPβ also reduced the protein levels of complexes I, II, III, IV and V (Figure IV.26. b). In addition, sAPPβ itself elicited a significant increase in the expression of ATF3, CHOP, TNFα and IL6, whereas IκBα expression was reduced (Figure IV.26. c). Likewise, sAPPβ caused an increase in nuclear p65 protein levels (Figure IV.26. d). No changes were observed in the expression or protein levels of ER stress and inflammation markers following sAPPα treatment (Figure IV.26. e-f).

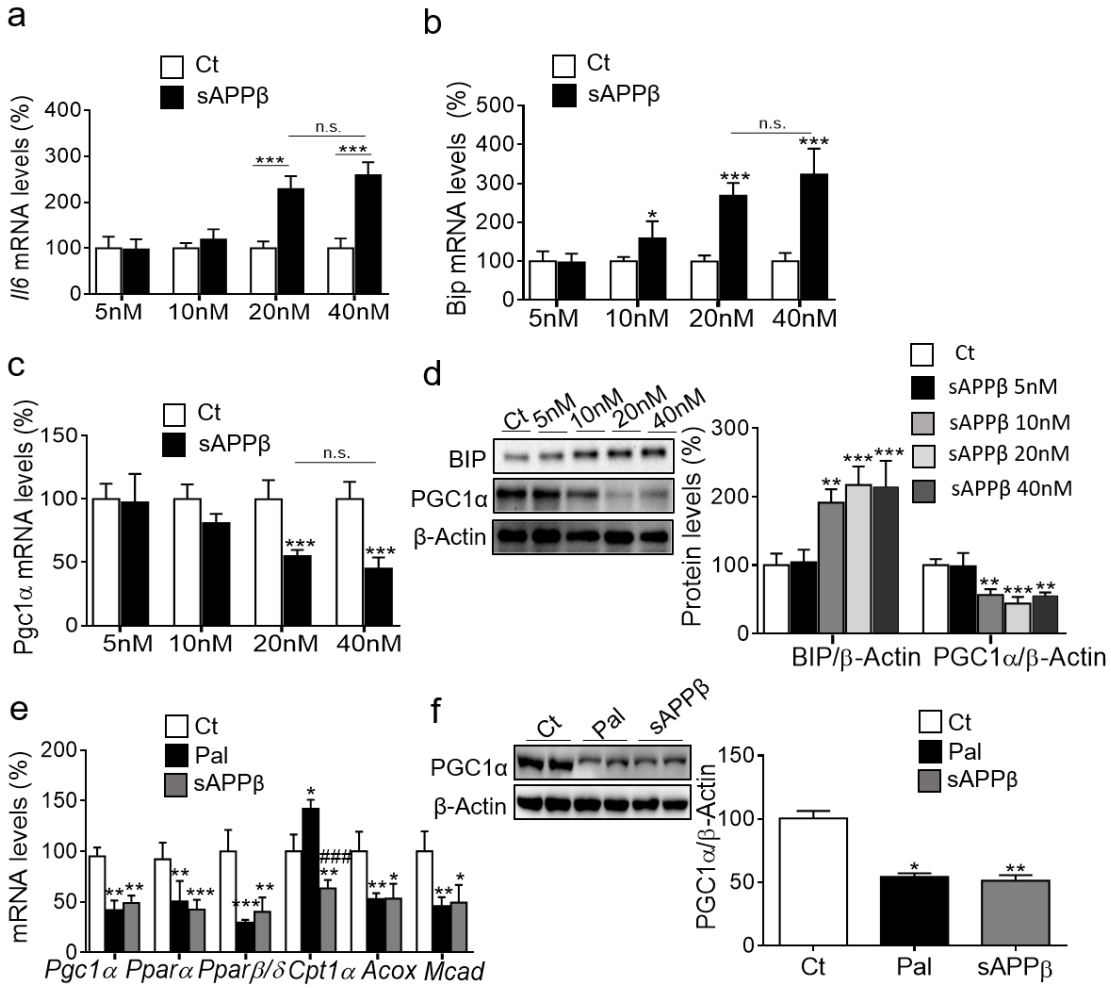

Figure IV.25. sAPPβ mimics the effects of palmitate exposure on ER stress and inflammation. C2C12 myotubes were incubated with different concentrations of sAPPβ and the **a,b,c)** expression and **d)** protein levels of IL6, BiP and PGC1α was determined. C2C12 myotubes were incubated in the presence or absence (Ct: control) of 0.5 mM palmitate (Pal) or 20 nM sAPPβ for 16 h. **e)** mRNA abundance of *Pgc1α, Pparα, Cpt1α, Acox and Mcad.* **f)** PGC1α and β-actin protein levels. The graphs show quantification expressed as a % of control samples ± SD of five independent experiments. ***p<0.001, **p<0.01 and *p<0.05 *vs.* control. $^{\#\#}$p<0.001 *vs.* palmitate-exposed cells. $^{\#\#\#}$p<0.001 *vs.* palmitate-exposed cells.

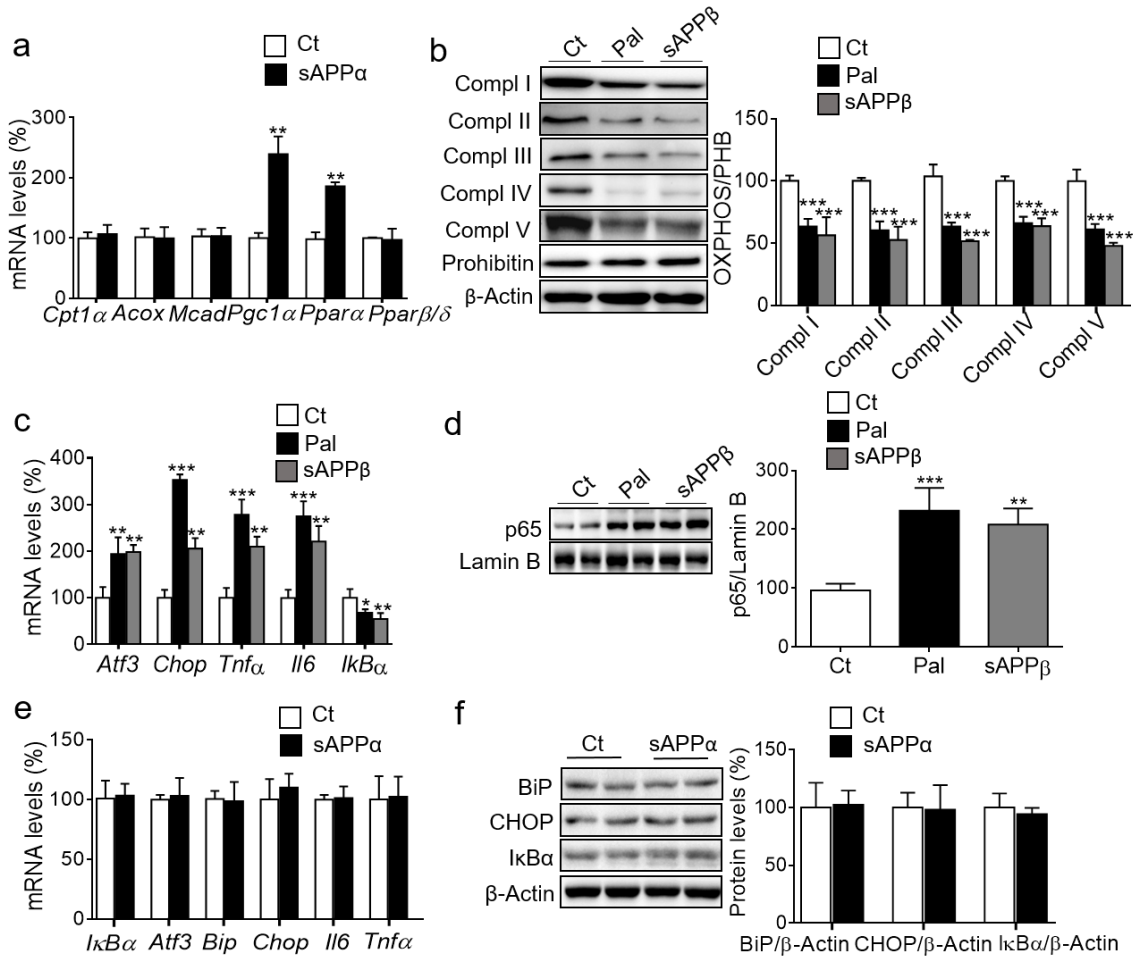

Figure IV.26. sAPPβ mimics the effects of palmitate exposure on ER stress, inflammation and mitochondrial function, wherease sAPPα does not. C2C12 myotubes were incubated in the presence or absence (Ct: control) of 0.5 mM palmitate (Pal), 20 nM sAPPβ, or 20 nM of sAPPα for 16 h. **a)** mRNA abundance of *Cpt1α, Acox, Mcad Pgc1α*, *Pparα* and *Pparβ/δ.* **b)** OXPHOS complexes, prohibitin (PHB) and β-actin protein levels. **c)** mRNA abundance of *Atf3, Chop, Tnfα, Il6 and IκBα.* **d)** p65 and Lamin B protein levels. **e)** mRNA abundance of *IκBα, Atf3, Bip, Chop, Il6 and Tnfα.* **f)** BiP, CHOP, IκBα and β-actin protein levels. The graphs show quantification expressed as a % of control samples ± SD of five independent experiments. ***p<0.001, **p<0.01 and *p<0.05 *vs.* control.

Regarding the insulin signaling pathway, myotubes exposed to sAPPβ showed a reduction in insulin receptor protein levels (Figures IV.27. a), an increase in IRS1 phosphorylation at Ser^{307} (Figures IV.27. b), and a consequent reduction in insulin-stimulated Akt phosphorylation, identical to that observed with palmitate (Figures IV.27. c). Consistent with the attenuation of the insulin signaling pathway, sAPPβ also reduced insulin-stimulated glucose uptake in C2C12 myotubes, whereas sAPPα did not (Figure IV.27. d). Since our findings indicate that BACE1 activity and sAPPβ regulate the expression of genes involved in fatty acid oxidation, we next determined whether the changes in the

expression of these genes affected the β-oxidation in myotubes exposed to palmitate in the presence or absence of M3 and to sAPPβ. Palmitate significantly reduced fatty acid oxidation and this effect was blunted by co-incubation with M3, while sAPPβ caused a reduction in fatty acid oxidation similar to that observed for palmitate (Figure IV.27. e). Taken together, our findings allow us to speculate that BACE1 might be involved in palmitate-induced ER stress, inflammation and impairment of insulin signaling pathway in skeletal muscle cells and that its product sAPPβ might be responsible for such effects.

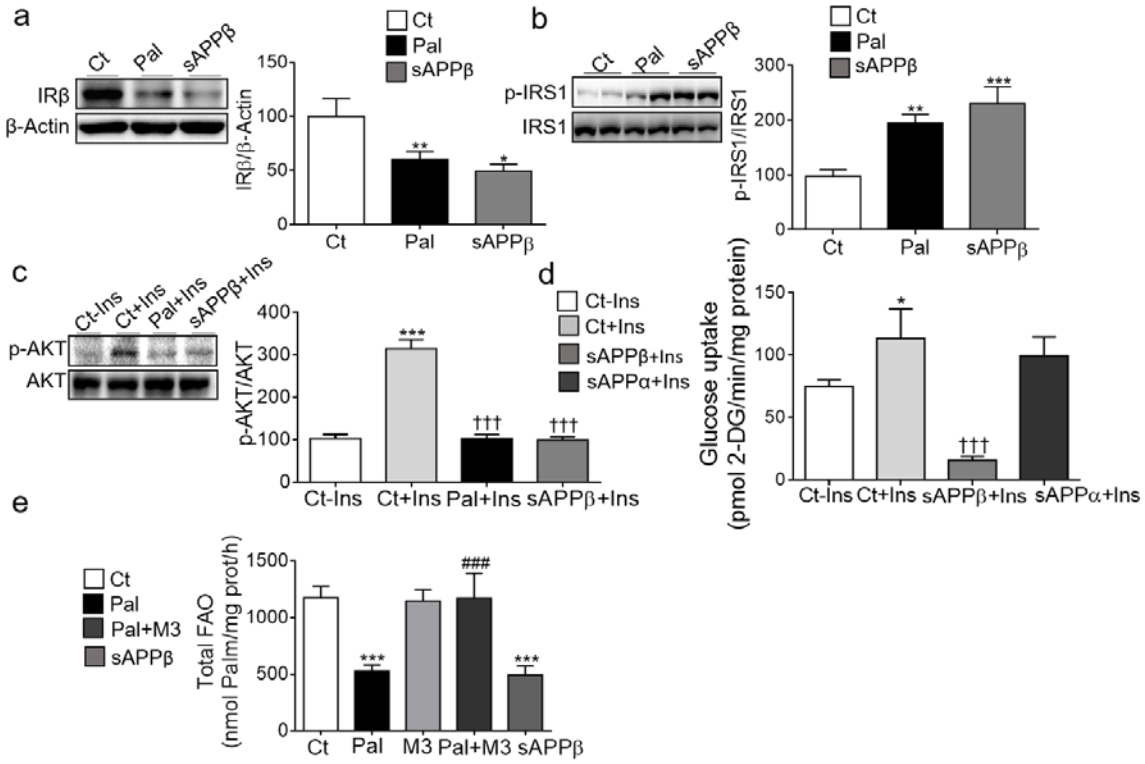

Figure IV.27. sAPPβ mimics the effects of palmitate exposure on insulin resistance in myotubes. C2C12 myotubes were incubated in the presence or absence (Ct: control) of 0.5 mM palmitate (Pal) or 20 nM sAPPβ. Where indicated cells were incubated with 100nM of M3, or 0.5 mM Pal plus M3, or 20 nM of sAPPα. Where indicated cells were stimulated with 100 nM insulin (Ins) **a)** IRβ and β-actin protein levels. **b)** phosphorylated IRS1 (Ser^{307}) protein levels. **c)** phosphorylated Akt (Ser^{473}) protein levels. The graphs show quantification expressed as a % of control samples ± SD of five independent experiments. **d)** Total fatty acid oxidation (FAO) performed using ^{14}C-labelled palmitate. Results are expressed as nmol of oxidized palmitate per hour, and standardized to mg of total protein. **e)** Insulin-dependent glucose-uptake performed using ^{3}H-labelled glucose. Results are expressed as pmol of glucose uptaken per minute, and standardized to mg of total protein. ***p<0.001, **p<0.01 and *p<0.05 *vs.* control. $^{###}$p<0.001 *vs.* palmitate-exposed cells.

IV. 2.7. BACE1 expression and sAPPβ levels are increased in type 2 diabetic patients

Next, we explored whether the relationship between BACE1 and PGC1α was also observed in humans. In subcutaneous adipose tissue (SAT) BACE1 expression was increased in obese and especially in type 2 diabetic patients compared with lean subjects (Figure IV.28. a). Interestingly, this increase was accompanied by a significant reduction in PGC1α mRNA levels (Figure IV.28. b). These changes were not observed in visceral adipose tissue (VAT), where the basal expression of BACE1 was higher than that one observed in SAT of lean subjects, possibly disguising the increase of BACE1 levels in the T2D group (Figure IV.28. c-d). Interestingly, mice fed a HFD exhibited higher plasma sAPPβ levels compared to mice fed a standard diet, whereas no changes were observed in Aβ42 (Figure IV.28. e). In humans, although no changes were observed between obese and lean subjects (Figure IV.28. f), a significant increase was observed in plasma sAPPβ levels from type 2 diabetic patients compared with obese non-diabetic subjects (Figure IV.28. g), suggesting that this peptide might be involved in peripheral insulin resistance.

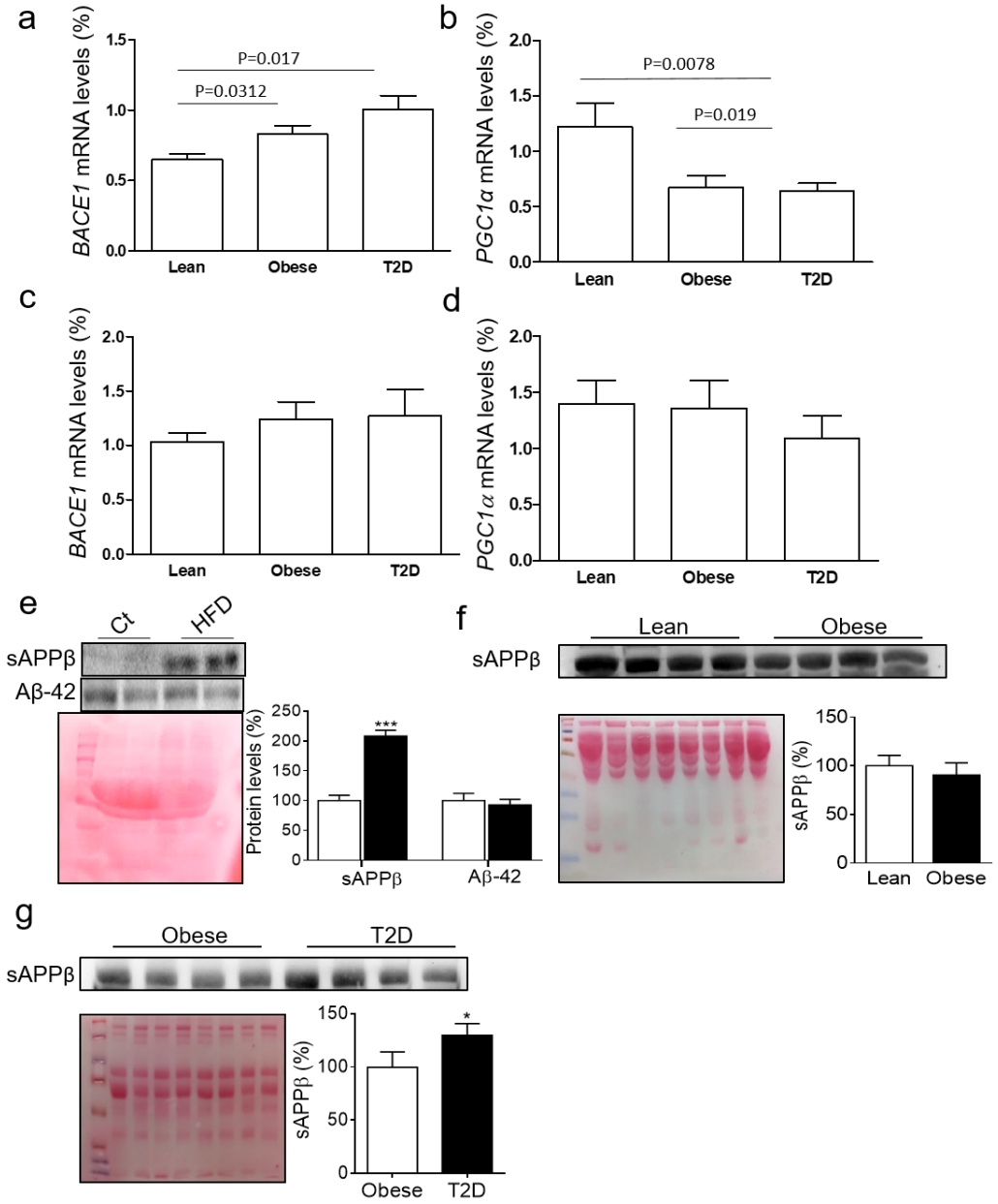

Figure IV.28. Increased BACE1 expression in SAT is accompanied by enhanced plasma levels of sAPPβ in type 2 diabetic patients. SAT and VAT of lean, obese and type 2 diabetic patients were used. Basal expression in VAT of lean subjects was taken as reference (1.0). **a-b)** mRNA abundance of *Bace1* and *Pgc1α* in SAT. **c-d)** mRNA abundance of *Bace1* and *Pgc1α* in VAT. Plasma of mice fed a standard diet (Control: Ct, white bars) or a HFD (black bars) for 12 weeks was collected and analyzed by western blot. Ponceau S staining served as loading control. **e)** sAPPβ and Aβ42 protein levels. Plasma of lean, obese and type 2 diabetic patients was collected and analyzed by western blot. Ponceau S staining served as loading control. **f-g)** sAPPβ protein levels. The graphs show quantification expressed as a % of control samples ± SD of three different experiments. ***p<0.001, **p<0.01 and *p<0.05 *vs.* control.

IV. 2.8. sAPPβ administration to mice induces ER stress, inflammation and reduces PGC1α

To go further inside the metabolic effects of sAPPβ we treated wild type mice with this peptide, using two different approach: we performed a unique *in situ* injection in the gastrocnemius muscle, or we administered it through a double intraperitoneal injection. Interestingly, the unique intramuscular injection of sAPPβ in gastrocnemius muscle resulted in an increase in the expression of CHOP and ATF3, although BiP levels were not affected (Figure IV.29. a). sAPPβ also upregulated TNFα and IL6 expression (Figure IV.29. a), whereas a reduction in PGC1α and PPARα mRNA levels was observed (Figure IV.29. b). Likewise, PGC1α and IκBα protein levels were decreased in skeletal muscle following *in situ* administration of sAPPβ, while phospho-eIF2α and BiP protein levels were enhanced (Figure IV.29. c), confirming the potential role of sAPPβ in inducing ER stress and inflammation in skeletal muscle.

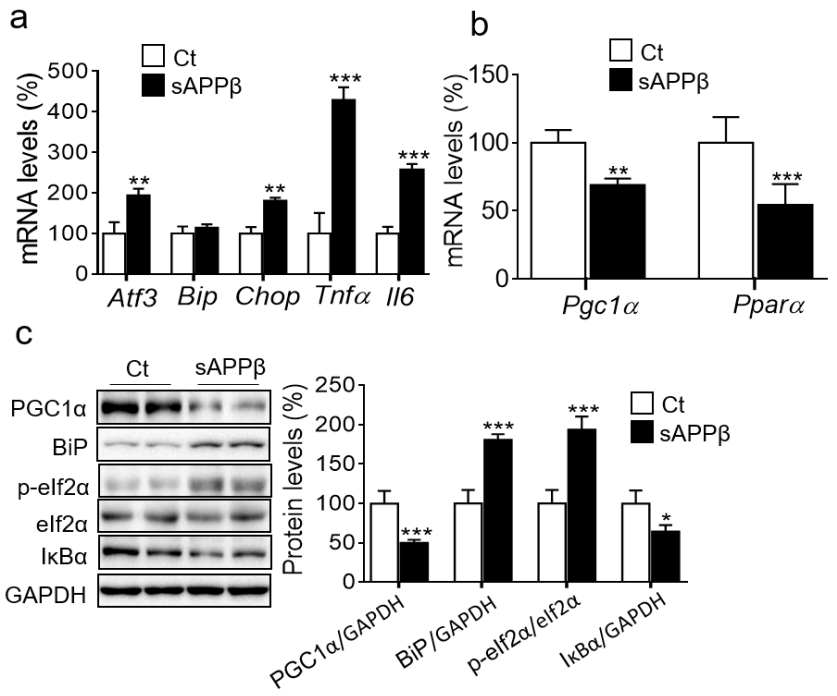

Figure IV.29. Intramuscular (i.m.) injection of sAPPβ in the gastrocnemius muscle of mice reduces PGC1α, and induces ER stress and inflammation. 2-months-old mice were injected with vehicle (Control: Ct, white bars) or with 5µg of sAPPβ (black bars) and the gastrocnemius skeletal muscle was obtained. **a)** mRNA abundance of *Atf3, Bip, Chop, Tnfα and Il6.* **b)** mRNA abundance of *Pgc1α* and *Pparα.* **c)** PGC1α, BiP, phosphorylated eIF2α (Ser[51]), IκBα and GAPDH protein levels. The graphs show quantification expressed as a % of control samples ± SD of five different experiments. ***p<0.001, **p<0.01 and *p<0.05 *vs.* control.

Similarly, intraperitoneal administration of sAPPβ caused an increase in the plasma levels of this peptide (Figure IV.30. a) comparable to that caused by HFD and this led to upregulation of ATF3, TNFα and IL6 expression in skeletal muscle, whereas no significant changes were observed in BiP and CHOP (Figure IV.30. b). Consistent with the increased expression of inflammatory markers, the protein levels of IκBα were decreased by sAPPβ administration, whereas BiP protein abundance was increased (Figure IV.30. c). sAPPβ administration also reduced PGC1α expression and protein levels as well as the mRNA levels of PPARα in skeletal muscle (Figures IV.30. d-e).

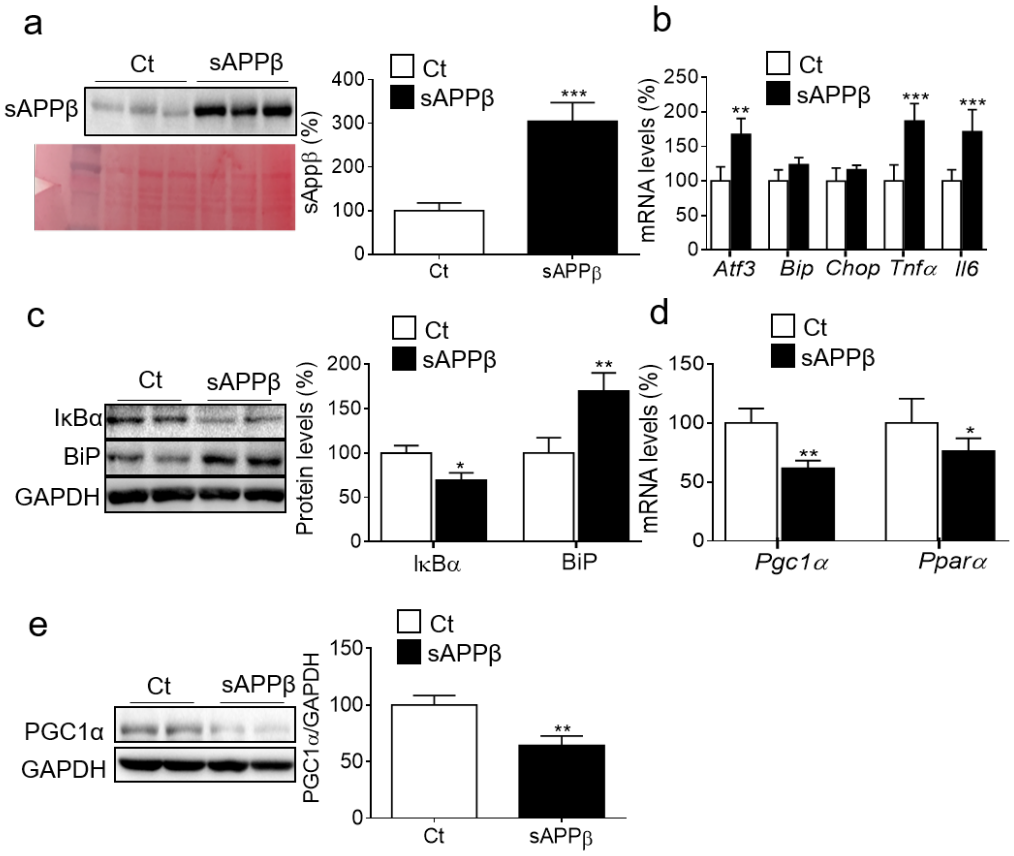

Figure IV.30. Intraperitoneal (i.p.) injection of sAPPβ in mice reduces PGC1α, and induces ER stress and inflammation. 2-months-old mice (n=6 per group) were injected with vehicle (Control: Ct, white bars) or with 20µg of sAPPβ (black bars), respectively. Plasma was collected and analyzed by western blot. Ponceau S staining served as loading control **a)** sAPPβ protein levels. **b)** mRNA abundance of *Atf3, Bip, Chop, Tnfα and Il6.* **c)** IκBα, BiP and GAPH protein levels. **d)** mRNA abundance of *Pgc1α* and *Pparα.* **e)** PGC1α, and GAPDH protein levels. The graphs show quantification expressed as a % of control samples ± SD of five different experiments. ***p<0.001, **p<0.01 and *p<0.05 *vs.* control.

We then performed a GTT test on mice treated with sAPPβ (20 µg/mice) before (20.00 h) and after (8.00 h) an overnight fasting. Given the inhibitory effect of sAPPβ on insulin signaling pathway and glucose uptake that we have observed *in vitro*, we expected increased glucose levels during the GTT. Surprisingly, intraperitoneal acute administration of sAPPβ resulted in a reduction in basal glucose levels (Figure IV.31. a) and decreased the AUC of plasma glucose levels in the GTT (Figure IV.32. b).

In contrast, the AUC of plasma glucose levels was increased by sAPPβ in the ITT, indicating a reduction in insulin sensitivity (Figure IV.31. c).

Consistent with the reduction in insulin sensitivity suggested by the ITT, the insulin receptor protein levels were reduced and the levels of phospho-IRS1 (Ser^{307}) were enhanced by sAPPβ in skeletal muscle (Figure IV.31. d). In adipose tissue, we observed similar changes to those reported in skeletal muscle following sAPPβ treatment (Figure IV.31. e).

Given the discrepancy between the GTT and the ITT, we then examined sAPPβ effects in liver. In fact, liver is responsible for maintaining the adequate glucose levels in fasting condition, through the gluconeogenesis process. We observed that hepatic expression of PGC1α, PPARα and IκBα (Figure IV.31. f) and protein levels of PGC1α and NRF1 (Figure IV.31. g) were drastically reduced by sAPPβ administration. In contrast, expression of BiP, CHOP and TNFα was significantly upregulated in mice treated with sAPPβ (Figure IV.31. f).

As explained in the introductive part, PGC1α promotes hepatic gluconeogenesis by regulating the expression of rate-limiting gluconeogenic genes such as PEPCK and G6Pase (Yoon *et al.*, 2001). Thus, we determined the levels of these enzymes in the liver of mice treated with sAPPβ and we observed that, in agreement with the decrease in hepatic expression of PGC1α and with the reduction of plasma glucose concentration, the hepatic expression of PEPCK and G6Pase was also decreased (Figure IV.31. f).

Thus, it is plausible that the decrease in glucose levels observed in mice treated with sAPPβ during the GTT, may be due to a reduction in hepatic gluconeogenesis after the overnight fasting.

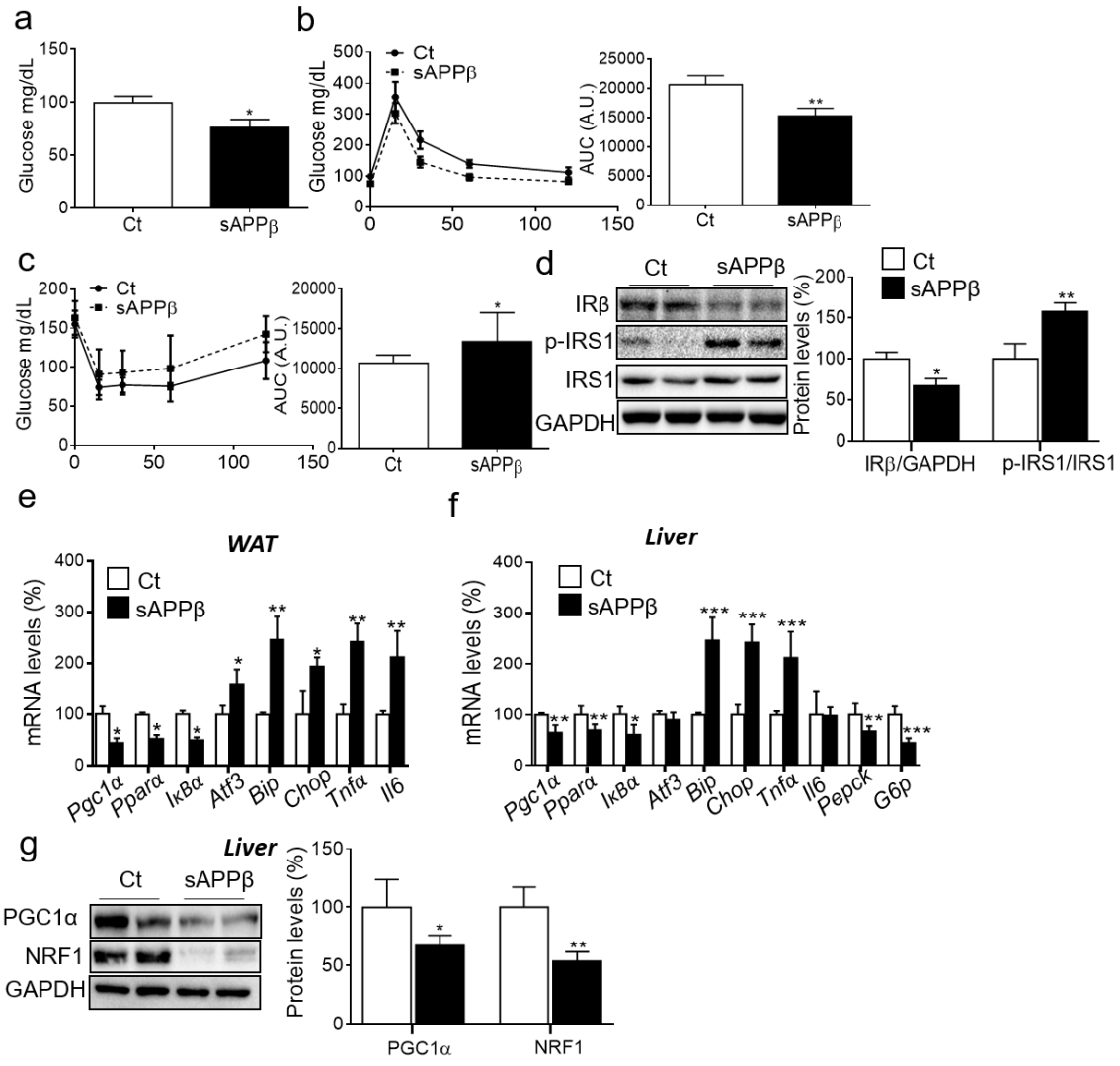

Figure IV.31. sAPPβ administration to mice reduces PGC1α in skeletal muscle and liver, reduces insulin sensitivity and lowers basal glucose levels. sAPPβ (20 μg/mouse, black bars) or vehicle (Control: Ct, white bars) was administered intraperitoneal (i.p.) to mice (n=6 per group) before (20.00 h) and after (8.00 h) an overnight fasting to conduct either a GTT or a ITT. **a)** plasma basal glucose levels 2 hours later the last administration of sAPPβ. **b-c)** GTT and ITT and area under the curve (AUC). Data are presented as the mean ± S.D. (n=6 per group). Intraperitoneal (i.p.) injection of sAPPβ in mice reduces PGC1α, and induces ER stress and inflammation. Skeletal muscle from control and treated mice was collected and analyzed. **d)** IRβ, phosphorylated IRS1 (Ser^{307}) and GAPDH protein levels. White adipose tissue (WAT) was collected and analyzed. **e)** mRNA abundance of *Pgc1α, Pparα, IκBα, Atf3, Bip, Chop, Tnfα and Il6.* Liver was collected and analyzed **f)** mRNA abundance of *Pgc1α, Pparα, IκBα, Atf3, Bip, Chop, Tnfα Il6, Pepck and G6pase.* **g)** PGC1α, NRF1 and GAPDH protein levels. The graphs show quantification expressed as a % of control samples ± SD of five different experiments. ***p<0.001, **p<0.01 and *p<0.05 *vs.* control.

IV. 2.9. BACE1 downregulates CREB phosphorylation

Next, we focused on the potential mechanisms by which BACE1 and sAPPβ regulate the expression of PGC1α, since its reduction seems to be the main step driving the changes caused by palmitate-induced up-regulation of β-secretase. We have already mentioned that PGC1α expression is regulated by the transcription factor CREB (Herzig *et al.*, 2001) which in turn is activated following phosphorylation at Ser^{133} by PKA, which is allosterically activated by cAMP (Mayr and Montminy, 2001). Phosphorylated CREB then interacts with the transcription co-activator CBP to initiate the transcription and translation of CREB-target genes, such as PGC1α (Vercauteren *et al.*, 2006). Of note, it has previously been reported that elevated BACE1 protein levels reduce CREB phosphorylation, PKA activity, and cAMP levels in neuroblastoma cells and rat primary cortical neurons, contributing to memory and cognitive deficits typical of AD (Chen *et al.*, 2012b). We hypothesized that palmitate-induced increase in BACE1 protein levels might affect CREB phosphorylation, leading to decreased PGC1α expression, which contributes to reduce fatty acid oxidation, thereby exacerbating inflammation and insulin resistance. We also speculate that sAPPβ might be the responsible for PGC1α downregulation. To assess our hypothesis, we first examined whether BACE1 inhibition and sAPPβ affected the PKA/CREB pathway. Exposure to palmitate and sAPPβ reduced phospho-CREB (Ser^{133}) levels, whereas the reduction caused by palmitate was prevented by pre-treatment with M3 (Figures IV.32. a-b). Consistent with this, increased levels of phospho-CREB were observed following BACE1 knockdown in myotubes and in skeletal muscle of $BACE1^{-/-}$ mice (Figures IV.32. c-d). Exposure to palmitate reduced phospho-protein levels (Thr^{197}) of the catalytic subunit of PKA, which is required for full catalytic activity of this kinase (Lonze and Ginty, 2002), and this reduction was blunted by M3 (Figure IV.32. e). In addition, sAPPβ caused a stronger reduction in phospho-PKA protein levels than that observed for palmitate (Figure IV.32. f). Similarly, BACE1 knockdown in myotubes and BACE1-deficiency in skeletal muscle resulted in increased levels of phospho-PKA (Figure IV.32. g-h). Moreover, PKA activity was reduced following exposure to sAPPβ and palmitate, the latter being reversed by pre-treatment with M3 (Figure IV.32. i). Finally, cells exposed to palmitate and sAPPβ also showed a reduction in cAMP levels, whereas M3 pre-treatment prevented the reduction caused by the saturated fatty acid (Figure IV.32. l).

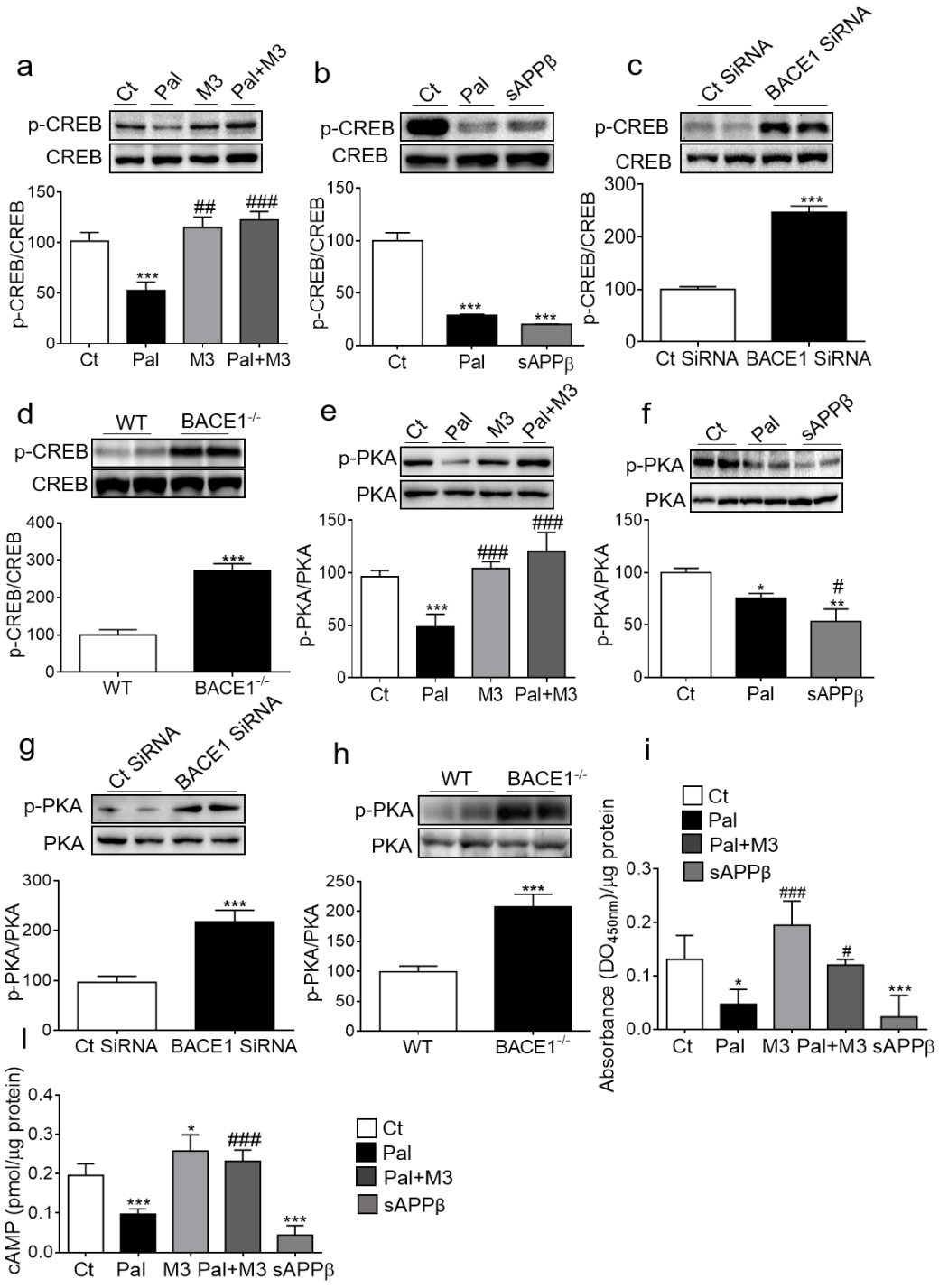

Figure IV.32. BACE1 regulates the cAMP-PKA-CREB pathway in myotubes. C2C12 myotubes were incubated in the presence or absence (Ct: control) of 0.5 mM palmitate (Pal), or 0.5 mM Pal plus 100 nM M3, or 20 nM sAPPβ. Were indicated, C2C12 myotubes were transfected wit SiRNA Control (SRNA Ct) or SiRNA against BACE1 (SirNA BACE1) during 48h. Skeletal muscle of BACE1-null mice was also used. **a-b-c)** phosphorylated CREB (Ser^{133}) protein levels in myotubes **d)** phosphorylated CREB (Ser^{133}) protein levels in skeletal muscle of BACE1-deficient mice **e-f-g)** phosphorylated PKA (Thr^{197}) protein levels in myotubes **h)** phosphorylated PKA (Thr^{197}) protein levels in skeletal muscle of BACE1-deficien mice. The graphs show quantification expressed as a % of control samples ± SD of five different experiments. **i)** PKA activity. Results are expressed as absorbance standardized to µg of total protein. **l)** cAMP levels expressed as pmol standardized to µg of total protein. ***p<0.001, **p<0.01 and *p<0.05 *vs.* control. $^{\#}$p<0.1 *vs.* palmitate-exposed cells, $^{\#\#}$p<0.01 *vs.* palmitate-exposed cells, $^{\#\#\#}$p<0.001 *vs.* palmitate-exposed cells.

As previously mentioned, Chen *et al.* (Chen *et al.*, 2012b) demonstrated that BACE1 may also reduce the cAMP/PKA/CREB pathway by interacting with adenylate cyclase. To examine whether palmitate affects the interaction between BACE1 and adenylate cyclase, we performed protein co-immunoprecipitation. In agreement with the increase in protein levels caused by palmitate, this fatty acid raised the interaction between adenylate cyclase and BACE1, whereas this increase was prevented in cells exposed to palmitate plus M3 (Figure IV.33. a).

We then examined whether sAPPβ also affected the interaction between BACE1 and AC. Interestingly, mice treated with sAPPβ showed an increase in the expression and the protein levels of BACE1 in skeletal muscle (Figure IV.33. b-c), suggesting a positive feedback of sAPPβ on its enzyme. As expected, the increase in BACE1 levels caused by the treatment with sAPPβ (both *in vitro* and *in vivo*) subsequently enhanced the interaction between BACE1 and AC (Figure IV.33. d-e). Of note, this interaction was reduced by parthenolide (Figure IV.33. e), suggesting that sAPPβ contributes to increase BACE1 levels through the activation of NFκB.

In summary, we can speculate that the BACE1-induced downregulation of PGC1α is mediated by the previous downregulation of the cAMP/PKA/CREB pathway and is responsible for many of the deleterious effects of palmitate. sAPPβ itself would exert its effects through this mechanism.

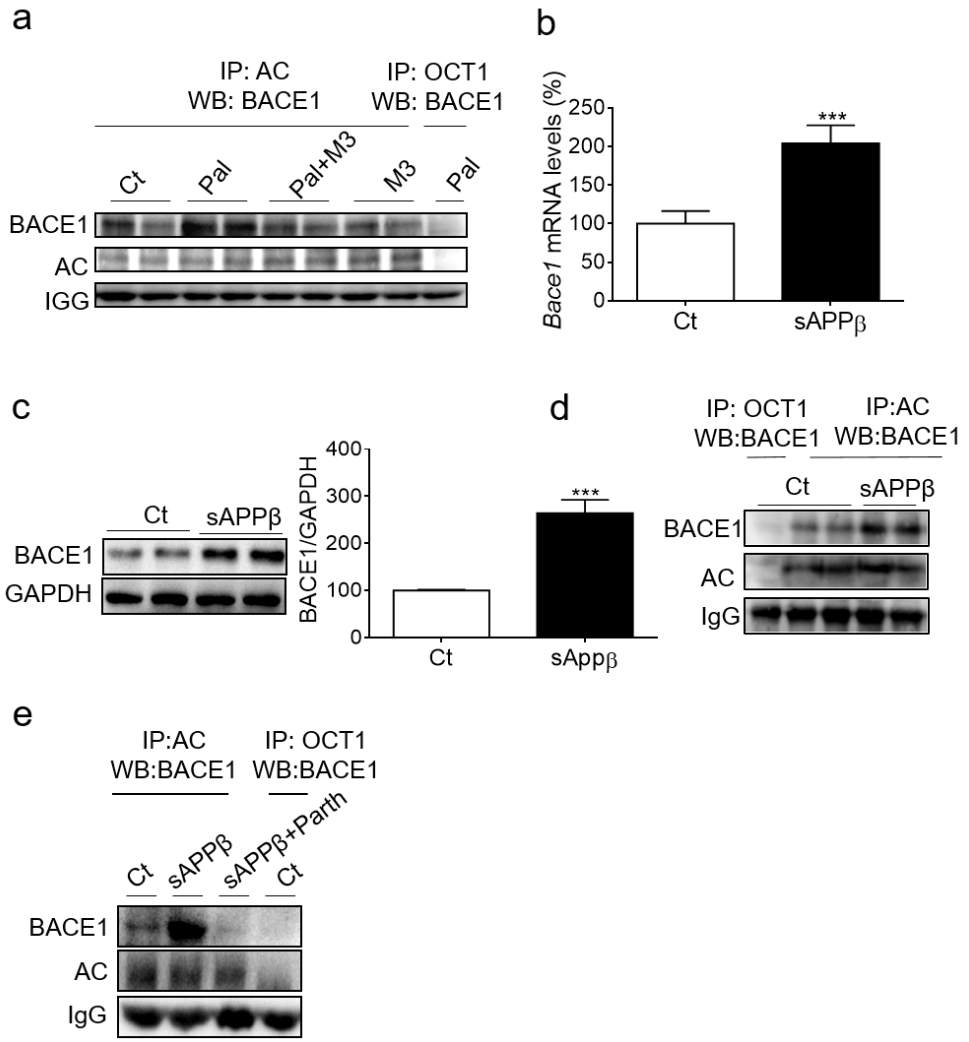

Figure IV.33. BACE1 interacts with AC and this interaction is attenuated by M3. sAPPβ increases BACE1 levels and its interaction with AC, possibly through the activation of NFκB. C2C12 myotubes were incubated in presence or absence (Control: Ct) of 0.5 mM palmitate (Pal), or 100 nM M3, or 0.5 mM Pal plus 100 nM M3. **a)** C2C12 protein extracts were immunoprecipitated using an AC antibody and then subjected to SDS-PAGE and immunoblotted with an anti-BACE1 antibody. No immunoprecipitation was observed with the unrelated antibody OCT1, indicating that the effect of the anti-BACE1 antibody was specific. Skeletal muscle from mice treated i.p. with vehicle (Control: Ct, white bars) or sAPPβ 20 µg/mouse (black bars) was used. **b)** mRNA abundance of *Bace1*. **c)** BACE1 and GAPDH protein levels. **d)** Protein extracts were immunoprecipitated using an AC antibody and then subjected to SDS-PAGE and immunoblotted with an anti-BACE1 antibody. No immunoprecipitation was observed with the unrelated antibody OCT1, indicating that the effect of the anti-BACE1 antibody was specific. C2C12 myotubes were incubated in presence or absence (Control: Ct) of 20 nM sAPPβ, or 20 nM sAPPβ plus 10 µM parthenolide (Parth). **e)** Protein extracts were immunoprecipitated using an AC antibody and then subjected to SDS-PAGE and immunoblotted with an anti-BACE1 antibody. No immunoprecipitation was observed with the unrelated antibody OCT1, indicating that the effect of the anti-BACE1 antibody was specific. The graphs show quantification expressed as a % of control samples ± SD of four different experiments***p<0.001, **p<0.01 and *p<0.05 *vs.* control.

V. Discussion

The prevalence of T2D is increasing at an alarming rate and the current worldwide diabetic population is expected to almost double by 2030 (IDF, 2015). This disturbing trend is partly the result of an epidemic increase in obesity, which is a major cause of T2D and is spreading also among young subjects (Gray and Kim, 2011; Lascar *et al.*, 2017). In fact, T2D and obesity are intimately linked, and together they increase the risk of cardiovascular events, a leading cause of death in patients with diabetes (Gray and Kim, 2011). Epidemiologic studies report that over 80% of diabetic patients are obese and present a condition of sub-acute chronic inflammation, possibly due to elevated levels of circulating TG and fatty acids (Goldfine and Shoelson, 2017). In fact, it is well established that increased levels of fatty acids induce inflammation and contribute to the development of insulin resistance in T2D (Boden, 2002b).

Atherogenic dyslipidemia is a typical characteristic of both obesity and T2D and emerged as an important risk factor for myocardial infarction and CVD in these patients. It is characterized by high levels of plasma TG, low levels of HDL and appearance of sdLDL. Diabetic dyslipidemia frequently precedes T2D by several years, indicating that the disturbance of lipid metabolism is an early event in the development of T2D (Adiels *et al.*, 2008b).

Indeed, it is now recognized that the different components of dyslipidemia, obesity and T2D are closely linked to each other metabolically.

Moreover, T2D has been associated with an increased risk of cognitive impairment, dementia and AD (Akter *et al.*, 2011; Arvanitakis *et al.*, 2004). Patients with T2D show double risk to develop AD in elderly. Many common features are shared between T2D, obesity and AD, such as impaired insulin signaling, inflammation and mitochondrial dysfunction (Correia *et al.*, 2012; Kim and Feldman, 2015).

Therefore, is of primary importance to go further inside the molecular mechanisms that link metabolic disorders, with the aim of discovering novel potential strategies to treat diabetes and its latter complications, such as AD and CVD.

In the present work, we investigated the molecular pathways that link lipoprotein metabolism with insulin resistance and examined the role of amyloidogenic components in peripheral insulin resistance.

We focused on skeletal muscle because it accounts for up to 80% of insulin-dependent glucose disposal and it has been established that skeletal muscle insulin resistance precedes and is responsible for systemic insulin resistance, thus being critical for the pathogenesis of T2D (DeFronzo and Tripathy, 2009).

V. 1. VLDL and Apo CIII contribute to ER stress, inflammation and insulin resistance in skeletal muscle

Although it is well established that insulin resistance drives atherogenic dyslipidemia (Adiels *et al.*, 2008b), there is little evidence on whether the increase in VLDL particles associated with insulin resistant states exacerbates insulin resistance in skeletal muscle. In other words, it is still controversial whether the increase in VLDL levels can just be considered a consequence rather than one of the causes of insulin resistance.

It is known that, in physiological conditions, insulin inhibits VLDL secretion and advances their clearance. Moreover, insulin promotes LPL activity, thus increasing VLDL metabolism into remnants particles (Ginsberg and Huang, 2000). *In vivo* and *in vitro* studies have provided convincing data that insulin-resistant obese subjects and type 2 diabetic patients do not show an insulin-induced inhibition of VLDL secretion, resulting in elevated levels of these lipoproteins (Lewis *et al.*, 1993; Taskinen, 2003).

However, the increase in VLDL levels might be the result not only of the impaired insulin action on VLDL synthesis and clearance, but also of a greater influx of free fatty acids into the liver, a typical condition in obese and insulin resistant states. Several evidences correlate an increased fatty acids influx to the liver with increased VLDL levels (Bennacer *et al.*, 2017; Ginsberg *et al.*, 2006).

Thus, it has been established that both obesity and insulin resistance provoke an increase in VLDL circulating levels. However, whether this increase in VLDL levels contributes to exacerbate insulin resistance in peripheral tissue was unknown.

A previous study from Pedrini *et al.* (Pedrini *et al.*, 2005) reported that the exposure of L6 skeletal myotubes to TG-rich lipoproteins (TGRLs) significantly impaired glycogen synthesis, glucose uptake and insulin signaling, suggesting that increased levels of TGRLs might not only be a consequence of insulin resistance but could also be a cause for it. Consistent with this study, our findings demonstrate that exposure of myotubes and isolated skeletal muscle to VLDL strongly impairs the insulin signaling pathway, by reducing Akt phosphorylation and insulin receptor protein levels and by phosphorylating IRS1 on serine residues. However, Pedrini *et al.* did not find any evidence of serine phosphorylation of IRS1. This discrepancy might be due to the time of incubation. In fact, even though the authors used concentrations higher than ours, they exposed cells to TGRLs during a maximum of 16 hours, while our incubation lasted 24 hours. Nevertheless, all these data indicate that VLDL play a role in the impairment of insulin signaling pathway.

Our findings also demonstrate that VLDL exposure induces ER stress and inflammation in skeletal muscle cells, in agreement with previous studies reporting that elevated levels of VLDL stimulate cytokine secretion from macrophages in adipose tissue (Ebtehaj *et al.*,

2017; Nguyen *et al.*, 2014). Since both ER stress and inflammation are involved in the development of insulin resistance in skeletal muscle, it is feasible that VLDL might contribute to insulin resistance also through these mechanisms.

Collectively, our findings indicate that VLDL are involved in ER stress, inflammation and insulin resistance in skeletal muscle and that they represent not only a consequence of peripheral insulin resistance, but also a cause. This is an important change of the point of view, and adds a new perspective to the treatment of T2D.

However, another unresolved matter was to elucidate the molecular mechanism implicated in VLDL effects. It is known that VLDL exert many of their actions through the binding to the VLDLR. For instance, Nguyen *et al.* reported that VLDLR is a determinant factor in adipose tissue inflammation and adipocytes macrophage infiltration (Nguyen *et al.*, 2014). In fact, the authors showed that when adipocytes were stimulated with VLDL from hyperlipidemic mice the inflammatory response was strongly increased, while the VLDL-induced inflammation was partially reduced in mice lacking VLDLR (Nguyen *et al.*, 2014). Consistent with this, Pedrini *et al.* (Pedrini *et al.*, 2005) demonstrated that the effects of TGRLs on glycogen synthesis and insulin signaling pathway were at least partially mediated by receptors of the LDLR family, of which VLDLR belongs. However, both studies mentioned above reported that the effects of VLDL and/or TGRLs were only partially blunted by knocking down VLDLR in mice or by pharmacological inhibition of the LDL receptor, respectively. Thus, these findings confirm the intriguing idea that alternative mechanisms are involved in the effects of VLDL on inflammation and insulin signaling.

In this regard, our findings demonstrate that Apo CIII might be the VLDL component responsible for the changes caused by VLDL exposure, since we observed that VLDL containing high amounts of Apo CIII induced ER stress, inflammation and impairment of insulin signaling in myotubes, whereas VLDL fractions containing very low amounts of Apo CIII did not.

We decided to examine the potential role of Apo CIII in skeletal muscle insulin resistance based on some studies that reported increased levels of Apo CIII in plasma of diabetic and hypertriglyceridemic patients compared to healthy controls (Hu *et al.*, 2014; Lee *et al.*, 2003b), suggesting a role for this apolipoprotein in T2D. Indeed, our results clearly show that Apo CIII itself impairs insulin signaling pathway and drastically reduces glucose uptake in C2C12 myotubes and that its effects are concentration-dependent. These results are consistent with the *in vivo* study of Lee *et al*. who demonstrated that mice overexpressing Apo CIII gene manifest severe hepatic insulin resistance compared to wild type mice (Lee *et al.*, 2011).

The findings of our study are consistent with the evidence that Apo CIII expression is increased by insulin deficiency (Chen *et al.*, 1994), insulin resistance (Altomonte *et al.*, 2004) and hyperglycemia (Caron *et al.*, 2011), converting Apo CIII in the most abundant VLDL apolipoprotein in individuals with diabetes (Hiukka *et al.*, 2005), and suggesting that the increase in Apo CIII levels in diabetic patients may contribute to exacerbate these conditions. In this regard, it is interesting to note that humans with a mutation in the Apo CIII gene that results in a reduction in the half-life of Apo CIII, show a favorable lipoprotein pattern, increased insulin sensitivity and protection against CVD (Jorgensen *et al.*, 2014). Several additional evidences seem to confirm that Apo CIII plays a key role in metabolic syndrome (Pollex *et al.*, 2007) and diabetes (Avall *et al.*, 2015). Thus, decreasing Apo CIII in mice results in improved glucose tolerance. In agreement with this, antisense-mediated lowering of plasma Apo CIII improves dyslipidemia and insulin sensitivity in humans with T2D (Digenio *et al.*, 2016), and delays the onset of T1D in prediabetic rats (Holmberg *et al.*, 2011), thus confirming the role of Apo CIII as a diabetogenic factor.

However, some results are controversial since Raeven *et al.* sustained that hypertriglyceridemic mice overexpressing Apo CIII were not insulin resistant (Reaven *et al.*, 1994), while Pollin *et al.* showed that a null mutation in human Apo CIII gene confers a favorable plasma lipid profile, although it does not improve insulin sensitivity (Pollin *et al.*, 2008). The explanation for such discrepancies might lie on the fact that, in the plasma, circulating VLDL containing Apo CIII would be in the presence of other lipoproteins, cells and molecules that can attenuate their effects. For instance, several authors have reported that HDL directly enhance glucose metabolism and exerts an anti-inflammatory effect (Ebtehaj *et al.*, 2017; Lehti *et al.*, 2013). Thus, it is possible that the protective effect of circulating HDL counteracts the VLDL-induced inflammation and insulin signaling impairment. Therefore, the effects of lipoproteins on insulin sensitivity would be the result of a balance between different lipoprotein levels and the contribution of additional factors.

Of note, it is important to remark that we did not use high concentrations of VLDL or Apo CIII, and that direct exposure of myotubes to such concentrations is enough to impair the insulin signaling pathway in myotubes. It is feasible that, *in vivo*, the concentrations required to induce a significant impairment of insulin signaling are higher than in our model, since, as previously discussed, the deleterious effects of VLDL might be counteracted by other lipoproteins and components present in the circulation. However, the goal of our study was to assess the role of VLDL and Apo CIII on skeletal muscle insulin resistance and this model allowed us to examine their molecular mechanism without the confounding effects of other lipoproteins.

For the same reason, we did not fed Apo CIII Tg mice with a HFD, in order to uniquely examined the role of Apo CIII in skeletal muscle. In fact, a previous study from Lee *et al.* (Lee *et al.*, 2011) showed that feeding Apo CIII Tg mice with a HFD reduced the circulating levels of Apo CIII and TG, thus possibly affecting Apo CIII action on skeletal muscle and leading to a much more complicated model that would make difficult to obtain a clear interpretation of the changes exclusively caused by Apo CIII in skeletal muscle.

In this regard, it would be interesting to treat healthy, glucose-normal tolerant, no hyperglycemic or hypertriglyceridemic mice directly with Apo CIII to check the effect on the insulin signaling pathway in skeletal muscle. For instance, our Tg mice were not hyperinsulinemic, although they did show significantly increased levels of TG, thus constituting a good model for studying the effect of Apo CIII overexpression in skeletal muscle.

The mechanism by which VLDL and Apo CIII increase ER stress and inflammation and attenuate insulin signaling in myotubes seems to involve ERK1/2 activation. This kinase has been implicated in the development of insulin resistance associated with obesity and T2D (Ozaki *et al.*, 2016). In fact, *Erk1*$^{-/-}$ mice challenged with a HFD are resistant to obesity and are protected from insulin resistance (Bost *et al.*, 2005). In addition, hyperinsulinemic-euglycemic clamp studies have demonstrated an increase in whole-body insulin sensitivity in *ob/ob- Erk1*$^{-/-}$ mice associated with an increase in both insulin-stimulated glucose disposal and adipose tissue insulin sensitivity (Jager *et al.*, 2011).

As broadly explained in the introductive part, the increase in ERK1/2 can induce insulin resistance through different mechanisms. First, ERK1/2 itself is able to phosphorylate IRS1 on serine residues and attenuate insulin signaling (Nguyen *et al.*, 2014; Taniguchi *et al.*, 2006). Second, an inhibitory cross-talk exists between AMPK and ERK1/2 (Du *et al.*, 2008) so that activation of ERK1/2 inhibits AMPK activity and promotes ER stress-induced insulin resistance in skeletal muscle (Coll *et al.*, 2006). In fact, AMPK activation inhibits ER stress (Dong *et al.*, 2010b), whereas the reduction in its activity promotes ER stress (Dong *et al.*, 2010a).

In the present study, we showed that both VLDL and Apo CIII exposure increases ERK1/2 phosphorylation and activation in myotubes and isolated skeletal muscle. As expected, ERK1/2 activation was accompanied by a reduction in AMPK activity. Hence, VLDL and Apo CIII-induced ER stress might be the result of the reduction in AMPK activity. Moreover, VLDL- and Apo CIII-induced ER stress ultimately results in the activation of the IKK-NFκB pathway, which attenuates the insulin signaling pathway by phosphorylating IRS1 in serine residues and increases the transcription of inflammatory genes such as TNFα, IL6 and many other cytokines.

In agreement with a role for ERK1/2 in the changes observed, we found that ERK1/2 inhibition or knockdown in skeletal muscle cells prevented the changes in ER stress and inflammation and the attenuation in insulin signaling pathway caused by VLDL and Apo CIII.
Moreover, ERK1/2 inhibition prevented the reduction in AMPK caused by VLDL and Apo CIII, confirming the negative feedback between AMPK and ERK1/2.
Similarly, the reduction of AMPK caused by VLDL/Apo CIII-induced ERK1/2 activation might contribute to decrease PGC1α levels, since AMPK activation regulates PGC1α transcription (Canto and Auwerx, 2009).
Given the key role of PGC1α in regulating the activity of transcription factors involved in fatty acid oxidation, such as the PPARs (Miura *et al.*, 2003), the reduction in PGC1α following treatment with VLDL or Apo CIII might be responsible for the decrease in the expression of genes involved in fatty acid oxidation. This would ultimately lead to a decrease in fatty acid oxidation, and consequently, in fatty acid accumulation, suggesting that PGC1α down regulation caused by VLDL and Apo CIII exposure can promote the deleterious effects of fatty acids (Schenk *et al.*, 2008).

In addition, it is known that TG contained in VLDL can be hydrolyzed to release fatty acids (Furtado *et al.*, 2008), further contributing to their intracellular accumulation. Thus, one might raise the question whether the effects of VLDL on ER stress, inflammation and insulin signaling are due to released fatty acids or not. Several evidences have ruled out this possibility, since studies have been conducted with lipoproteins in presence of LPL inhibitors, thus blocking TG hydrolysis and subsequent fatty acid release (Pedrini *et al.*, 2005). For example, Pedrini *et al*., incubated myotubes with TGRLs in presence of orlistat, an LPL inhibitor, and did not observe a reduction in the deleterious effects of TGRLs on insulin signaling. These authors also measured the concentration of fatty acids released in the cultured medium, and no difference were observed between myotubes exposed to TGRLs and the control group (Pedrini *et al.*, 2005). To avoid any interference with the potential fatty acids effects, our experiments were performed using a medium devoid of BSA, which is a carrier of fatty acids and is responsible for their entrance into the cell. However, other studies are in contrast with these evidences. In this regard, it is notable to mention the study of Lee *et al*., showing that overexpression of Apo CIII gene in mice increased hepatic TG and fatty acids content and this was associated with an increase in cytosolic DAG. The authors also found an increase in PKC activity that was responsible for the reduction of Akt phosphorylation and for the subsequent impairment of insulin signaling pathway (Lee *et al.*, 2011). In our study, we did not measure the levels of DAG in skeletal muscle cells or isolated muscle exposed to Apo CIII or VLDL, nor in Tg mice, thus

we cannot discard the contribution of this mechanism to VLDL/Apo CIII-induced impairment of insulin signaling.
However, when we also evaluated the combination of palmitate and Apo CIII on the expression of inflammatory and ER stress markers as well as on the insulin signaling pathway, we observed that the addition of Apo CIII exacerbated the effects of palmitate. Consequently, even if we cannot discard that part of the effect of VLDL and Apo CIII on ER stress, inflammation and insulin signaling in myotubes is mediated by intracellular fatty acids or DAG, we can certainly assume that Apo CIII itself is able to further induce inflammation and impair insulin signaling pathway.

Next, we analyzed the potential molecular mechanisms by which Apo CIII increases ERK1/2 activity, induces inflammation and ER stress and impairs insulin signaling in myotubes. We observed that Apo CIII effects were mediated by TLR2.
As mentioned in the introductive part, TLR2 not only recognizes numerous lipid-containing molecules, but also it recognizes endogenous proteins (Takeda *et al.*, 2003). Moreover, activation of TLR2 ultimately leads to NFκB and ERK1/2 activation (Konner and Bruning, 2011), thus mediating the inflammatory process and contributing to insulin resistance. Likewise, TLR2 deficiency improves insulin sensitivity and attenuates cytokine expression (Kuo *et al.*, 2011). We showed that the blockade of TLR2 almost completely prevented the effect of Apo CIII on ER stress, inflammation and insulin signaling pathway.

Collectively, our findings confirm the importance of TLR2 in insulin resistance and indicate that its activation by VLDL and Apo CIII induces ER stress, inflammation and insulin resistance in skeletal muscle by activating the ERK1/2 pathway.

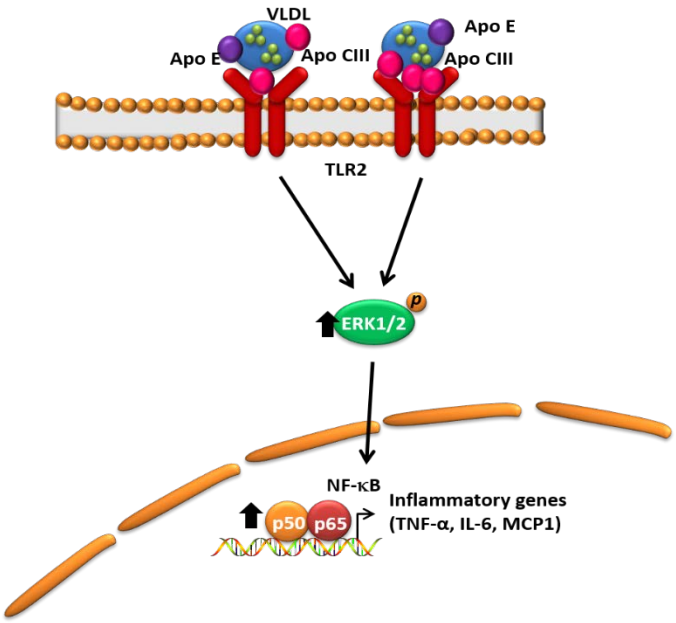

Figure V.1. Potential molecular mechanism of Apo CIII. The binding to TLR2 would activate a downstream signaling that leads to the activation of MAPK-ERK pathways. ERK induces IKK activity and enhances the NFκB pathway (Chung *et al.*, 2006).

V. 2. BACE1 and sAPPβ contribute to palmitate-induced ER stress, inflammation and insulin resistance in skeletal muscle

To explore new molecular mechanisms that can contribute to the development of insulin resistance in skeletal muscle, we examined the role of BACE1, based on recent findings that showed that BACE1 knockout mice showed better glucose tolerance and insulin sensitivity (Meakin *et al.*, 2012) and that inhibition of muscle BACE1 activity increases glucose uptake and GLUT4 translocation (Hamilton *et al.*, 2014). Other studies also showed that both saturated fatty acids and its derivatives ceramides increase BACE1 levels in muscle (Puglielli *et al.*, 2003). Collectively, these evidences suggest that BACE1 might be involved in fatty acid-induced insulin resistance in myotubes.

Indeed, our results clearly show that BACE1 expression in skeletal muscle cells is sensitive to changes in palmitate levels, since it increases in a concentration-dependent manner after palmitate exposure.

Whilst previous work has suggested that BACE1 protein expression is controlled by increased fatty acids and ceramides through post-translational stabilization (Puglielli *et al.*, 2003), our findings also indicate that transcriptional mechanisms are, at least, partially responsible for the increase in BACE1 levels following palmitate exposure. These findings suggest that, in addition to post-translational mechanisms, the increase in BACE1 expression might also contribute to an increase in its protein levels in cells exposed to palmitate.

It is worth mentioning that the increase in BACE1 expression in palmitate-exposed cells seem to be dependent on palmitate-induced NFκB activation, since the inhibition of the transcription factor with the specific inhibitor parthenolide prevented the increase in BACE1 mRNA levels.

This is consistent with previous findings showing that BACE1 expression and activity increase in situation of stress and inflammation (Guglielmotto *et al.*, 2012; Nogalska *et al.*, 2010; Wang *et al.*, 2013). Therefore, it is possible that a condition of metabolic stress generates a vicious circle in which ER stress and inflammation induced by elevated levels of fatty acid contribute to increase BACE1 levels, which in turn participate in the deleterious effects of fatty acids on ER stress, inflammation and insulin signaling pathway.

In this regard, and consistent with the *in vitro* results, the findings of the present study clearly show that BACE1 is increased in subcutaneous adipose tissue (SAT) of obese and diabetic patients, as well as in skeletal muscle of mice fed a HFD. We observed a trend to increase in the expression levels of BACE1 also in visceral adipose tissue (VAT) of obese subjects compared to lean controls, although differences did not reach statistical significance, probably because the basal expression of BACE1 in VAT was much higher

than in SAT. We do not have an explanation for this, but our results are consistent with another study reporting the same evidence in a small cohort of patients, where APP expression was significantly higher in VAT compared to SAT (Lee *et al.*, 2008).

In addition, our results indicate that the increase in BACE1 levels caused by palmitate can contribute to lipid-induced ER stress, inflammation and insulin resistance in skeletal muscle cells. In other words, we demonstrate that the deleterious effects of palmitate also depend upon BACE1 activity. In fact, BACE1 inhibition with M3 reduced palmitate-induced ER stress and inflammation and prevented attenuation of the insulin signaling pathway. This is the first time that these network interactions have been demonstrated in skeletal muscle, and our results add an important dimension to the mechanisms driving insulin resistance in myotubes.

To our knowledge, there are not previous studies about BACE1 expression in peripheral tissue of diabetic and obese patients, even though some authors reported that APP expression is up-regulated in subcutaneous abdominal adipocytes from obese and hyperinsulinemic subjects (Lee *et al.*, 2008) and that plasma Aβ levels are positively correlated with body fat in healthy individuals (Balakrishnan *et al.*, 2005). However, these authors did not directly assessed the BACE1 activity nor the sAPPβ levels.

Recently, Meakin *et al*. reported that BACE1 knockout mice were protected against diet-induced obesity and showed an enhanced insulin sensitivity (Meakin *et al.*, 2012). Moreover, the authors demonstrated that a reduction in BACE1 activity *per se* increased glucose uptake and cell surface GLUT4 translocation in an insulin-independent manner. Conversely, overexpressing BACE1 decreased glucose uptake and oxidation in skeletal muscle cells. Our results are only partially consistent with those of Meakin's group, since we observed an increase in Akt phosphorylation in cells exposed to M3 inhibitor, both in presence or absence of insulin. This would suggest that a reduction of BACE1 activity *per se* increases the insulin signaling pathway also in an insulin dependent manner. Moreover, cells exposed to the BACE1 product sAPPβ showed impaired insulin signaling, indicating that the development of insulin resistance mediated by overexpression of BACE1 not only depends on BACE1-induced downregulation of GLUT4 and subsequent decrease of glucose uptake, but also depends on sAPPβ-induced impairment of insulin signaling.

Indeed, it has been well established that BACE1 is proteolytically active in skeletal muscle. Hamilton *et al.* reported that BACE1 cleaves APP in C2C12 myotubes and this cleavage leads to the production of the soluble fragment sAPPβ (Hamilton *et al.*, 2014).

In our study, we demonstrate a role of sAPPβ in the development of peripheral insulin resistance. To our knowledge, this is the first study that evaluates the contribution of sAPPβ to the development of skeletal muscle insulin resistance. In fact, until now, most

of the studies focused on Aβ peptide instead of sAPPβ. This is understandable, since Aβ peptide is responsible for the amyloid deposits that lead to AD. Many studies reported that Aβ is able to impair insulin signaling and to induce oxidative stress and mitochondrial dysfunctions in neurons and peripheral system (De Felice *et al.*, 2007; Zhang *et al.*, 2013). However, it has been reported that both in the CSF and in the bloodstream of healthy subjects, the levels of sAPPβ are much higher than the levels of Aβ (Alexopoulos *et al.*, 2017; Araki *et al.*, 2017; Oikonomidi *et al.*, 2016). In addition, the clearance of sAPPβ is slower compared to the clearance of Aβ peptides. Thus sAPPβ resides longer than Aβ in the peripheral circulation (Dobrowolska *et al.*, 2014b).

Based on these findings, we hypothesized that sAPPβ might be responsible for BACE1 effects on ER stress, inflammation and insulin signaling pathway, at least in the peripheral system.

To verify our hypothesis, we analyzed the circulating levels of sAPPβ in plasma of diabetic patients and they were significantly increased compared to healthy subjects, suggesting the potential role of this compound on peripheral insulin resistance. Our results showed that sAPPβ is increased in plasma of diabetic patients but not in obese subjects. This could be in contrast with the study of Lee *et al.* showing that APP is upregulated in adipocytes of obese patients (Lee *et al.*, 2008) and with the study of Balakrishnan *et al.* (Balakrishnan *et al.*, 2005), which shows that plasma levels of Aβ42 positively correlate with increased body fat in healthy individuals. Likewise, Aβ levels are not only dependent on BACE1 activity since Aβ fragment is not the direct product of BACE1 enzymatic cleavage.

Of note, Lee *et al.* did not measured the levels of circulating sAPPβ in the subjects involved in the study. Moreover, the obese group presented hyperinsulinemia and impaired glucose tolerance, suggesting that the obese patients were in a pre-diabetic status. It is now recognized that insulin and Aβ compete for the binding to IDE (Qiu and Folstein, 2006; Xie *et al.*, 2002). Thus, in a condition of hyperinsulinemia, the enzyme is almost completely saturated with insulin, to which binds with much greater affinity, and, as consequence, the clearance of Aβ is reduced. This situation does not occur with sAPPβ and could contribute to explain why Aβ levels are increased in obese, hyperinsulinemic patients, while sAPPβ levels possibly are not.
Regarding the study of Balakrishnan *et al.,* the authors not only reported a positive correlation between increased body fat mass and the levels of Aβ42, but also between the insulin levels and the Aβ42 concentration in plasma. Thus, again, the increase of Aβ42 levels observed in subjects with higher body mass index (BMI) and hyperinsulinemia might be due to a reduced clearance of Aβ. Moreover, the study found a positive correlation only with the levels of Aβ42, but not Aβ40. This suggest that γ-secretase activity, but not

β-secretase, is involved and that the increase in Aβ levels in obese patients does not necessary entail a previous similar increase in sAPPβ levels.

The increase of sAPPβ levels uniquely in diabetic patients but not in obese subjects compared to lean ones, suggests that the increase in levels of sAPPβ might be associated with the transition from obesity to T2D. In other words, obesity is necessary, but not sufficient to significantly increase sAPPβ levels. A possible explanation for this would be that most of the obese subjects, despite of increased levels of TG and fatty acids, present normal glucose tolerance and higher levels of circulating insulin, compared to lean healthy subjects. It has been established that insulin enhances sAPPα secretion (Solano *et al.*, 2000) and that sAPPα blocks the sAPPβ production by interacting with BACE1 (Obregon *et al.*, 2012) and reducing its expression (Donmez *et al.*, 2010). Thus, it is conceivable that until insulin sensitivity in obese subjects remains unaltered and the levels of circulating insulin are high, sAPPα contributes to maintain low levels of circulating sAPPβ, counteracting the enhancing effect of fatty acids on BACE1 activity. Conversely, when β-cell failure occurs and obese patients become insulin resistant and diabetic, then the secretion of sAPPα is no longer increased, the lipid-induced enhancement of BACE1 activity is no longer counteracted and the levels of sAPPβ possibly start to raise.

However, our results show increased levels of sAPPβ in plasma of mice fed a HFD. The discrepancy with the results in obese humans might be explained considering the fact that rodents are much more sensitive than men to a HFD. Moreover, it is possible that many of the obese subjects recruited in the study were controlling their diet to reduce calorie and fat intake. Finally, mice fed a HFD presented impaired glucose tolerance and reduced insulin sensitivity, thus resembling a prediabetic status, whereas obese patients did not.
Interestingly, we did not observe an increase of Aβ42 levels in plasma of mice fed with HFD. This is consistent with some studies (Mayeux *et al.*, 2003; Mayeux *et al.*, 1999) and in contrast with others discussed above (Balakrishnan *et al.*, 2005; Galloway *et al.*, 2007). It is possible that we were not able to detect increased levels of Aβ42 in plasma because its clearance is significantly quicker than sAPPβ clearance.

Overall, the fact that sAPPβ increases in diabetic subjects suggest a role for this compound in peripheral insulin resistance. To further corroborate our hypothesis, we treated skeletal muscle cells with sAPPβ. Our findings demonstrated that sAPPβ mimicked most of the effects of palmitate exposure. In fact, sAPPβ had the capacity to increase ER stress and inflammation and to impair insulin signaling pathway in C2C12 myotubes. We then directly injected low doses of sAPPβ in healthy mice. Acute administration of sAPPβ to mice elicited similar effects to those observed in myoubes. Moreover, mice injected with sAPPβ presented worse response to the ITT, thus showing reduced insulin sensitivity compared to control mice.

The changes caused by palmitate and sAPPβ on skeletal muscle might be the result of the reduction in PGC1α levels. In fact, we observed that PGC1α levels were drastically decrease in cells exposed to palmitate or sAPPβ. Conversely, PGC1α levels were increase in BACE1 KO mice, confirming that BACE1 contributes to reduce PGC1α levels. It is worth noting that previous works reported that PGC1α transcriptionally regulates BACE1 expression in neurons (Wang *et al.*, 2013). However, when we overexpressed PGC1α in skeletal muscle cells, we did not observe a reduction in BACE1 levels, suggesting that this mechanism does not operate in skeletal muscle.

As previously discussed, PGC1α preserves OXPHOS genes (Patti *et al.*, 2003), and co-activates transcription factors involved in FAO, such as the PPARs (Kang and Li Ji, 2012). Therefore, the reduction in PGC1α levels caused by palmitate and sAPPβ may reduce FAO and further increase the amount of palmitate that accumulates into the cell. This would ultimately exacerbate ER stress, inflammation and insulin resistance in skeletal muscle cells. In addition, PGC1α itself plays an anti-inflammatory role in skeletal muscle by inducing the PPARs-dependent expression of the inhibitory protein IκBα, which exerts an inhibitory effect on NFκB transcription factor (Buroker *et al.*, 2009). For instance, PGC1α knockout mice show higher basal mRNA expression of TNFα and IL6 in skeletal muscle compared to wild type mice (Arnold *et al.*, 2011; Handschin, 2009). Therefore, the decrease in PGC1α levels caused by palmitate or sAPPβ leads to a reduction in IκBα levels, intensifying NFκB activity. This would generate a positive feedback between NFκB and BACE1. In fact, the sAPPβ- or palmitate-induced increase in NFκB would enhance BACE1 levels, which in turn downregulate PGC1α and contribute to intensify NFκB activity.

Our results are consistent with previous studies, showing that Aβ peptides induce inflammation, mitochondrial dysfunction and reduce PGC1α and AMPK levels in neurons (Chang *et al.*, 2017; Tong *et al.*, 2001). However, any of these studies examined the role of soluble sAPPβ. Other findings also reported that amyloid peptides contribute to inflammation and ER stress in the CNS by activating the JAK/STAT/SOCS pathway (Zhang *et al.*, 2013). Therefore, we wonder whether the soluble sAPPβ had the same effect in myotubes. We did not observe any increase in JAK/STAT/SOCS pathway after cell exposure to sAPPβ, suggesting that different molecular mechanisms are involved in skeletal muscle (Figure V.2.).

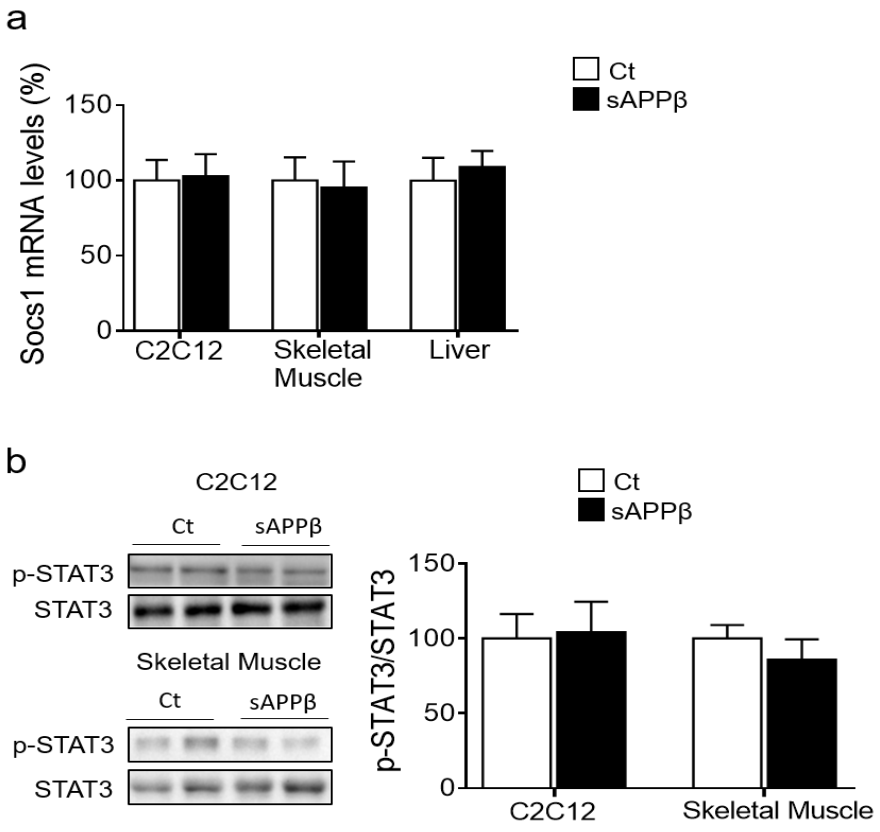

Figure V.2. sAPPβ does not regulate the JAK/STAT/SOCS pathway in skeletal muscle. C2C12 myotubes were incubated in presence or absence (Control: Ct) of 20 nM sAPPβ for 24 h. Skeletal muscle and liver of mice injected i.p. with 10μg of sAPPβ. The graphs show quantification expressed as a % of control samples ± SD of five different experiments***p<0.001, **p<0.01 and *p<0.05 *vs.* control.

The reduction in PGC1α induced by sAPPβ might also be responsible for the decreased levels of blood glucose observed in mice after an overnight fasting. In fact, acute administration of sAPPβ to mice provoked a reduction in fasting glucose levels in treated mice compared to control. This was surprisingly, considering that the ITT showed impaired insulin sensitivity in mice treated with sAPPβ. A possible explanation for this is that the treatment induced a strong reduction of PGC1α in liver. PGC1α controls and promotes hepatic gluconeogenesis (Yoon *et al.*, 2001), which is the predominant mechanism responsible for maintaining euglycemia during prolonged fasting. Thus, a reduction in PGC1α levels, drastically diminishes hepatic gluconeogenesis and, consequently, blood glucose levels. It is also well established that PGC1α exerts opposite effects on hepatic and muscle insulin sensitivity, since its overexpression in mice promotes hepatic insulin resistance while improves muscle insulin sensitivity (Liang *et al.*, 2009). As a consequence, the net result of PGC1α downregulation induced by sAPPβ in mice in fasting conditions is

a reduction in plasma glucose levels, being preponderant the reduction in hepatic gluconeogenesis over the reduction in muscle glucose uptake. This is consistent with our results, showing that sAPPβ reduces glucose uptake in skeletal muscle cells, and at the same time downregulates genes related with gluconeogenesis in liver. This would be the possible reason why the impairment in glucose tolerance and insulin sensitivity induced by sAPPβ in skeletal muscle is only appreciable during ITT test, but not in the fasting status, since is counteracted by the decrease in hepatic gluconeogenesis.

Furthermore, our results showed that sAPPβ alters PGC1α expression and fatty acid metabolism by inhibiting the PKA-CREB pathway. CREB binding to PGC1α promoter plays a key role in activating PGC1α expression in skeletal muscle (Kang and Li Ji, 2012; Mayr and Montminy, 2001). In addition, CREB is phosphorylated by PKA following activation by cAMP. We observed that palmitate and sAPPβ reduced cAMP, phospho-PKA and phospho-CREB levels, and PKA activity, suggesting that this pathway could be the responsible for PGC1α reduction. Moreover, palmitate effects were blunted by the BACE1 inhibitor M3, suggesting that BACE itself plays a role in impairing the PKA-CREB pathway. Actually, a recent study from Chen *et al.* reported that BACE1 alters CREB transcription activity in neurons, although its effect is independent from Aβ production (Chen *et al.*, 2012b). These findings agree with our results, since only sAPPβ but not Aβ is the direct product of BACE1 enzymatic activity and its levels are more abundant than Aβ in the circulation. Thus, it is feasible that in skeletal muscle cells sAPPβ directly impairs CREB activity, leading to a reduction in PGC1α levels. However, other authors reported that Aβ42 directly suppresses CREB phosphorylation in cortical neurons (Tong *et al.*, 2001).

Consistent with this, genetic approaches using SiRNA against BACE1 in myotubes and skeletal muscle from BACE1 deficient mice demonstrated that knockdown of this gene increased phopsho-CREB levels and PKA phosphorylation. Moreover, *in vivo* administration of sAPPβ also downregulated PKA and CREB levels in skeletal muscle (data not shown).

To go further inside the molecular mechanism, we tested whether BACE1 or sAPPβ directly interact with one of the component of the cAMP/PKA/CREB pathway. Chen *et al.* reported that BACE1 interacts via its transmembrane domain to AC to inactivate CREB phosphorylation (Chen *et al.*, 2012a). Consistent with this, our results showed that palmitate exposure, likely as the result of the increase in BACE1 protein levels, enhanced BACE1 interaction with AC, in a mechanism that may also contribute to reduce cAMP levels, as previously reported (Chen *et al.*, 2012a). It is worth mentioning that when cells were incubated with palmitate in the presence of the inhibitor M3, the increased interaction between BACE1 and AC, induced by palmitate, was reduced. This suggests that the interaction between AC and BACE1 not only depends on BACE1 protein levels, but also

on BACE1 activity and that, consequently, a reduction in BACE1 activity ultimately contributes to improve AC function in skeletal muscle cells. Moreover, sAPPβ itself enhances BACE1 interaction with adenylate cyclase, setting a positive feedback that further impairs the cAMP/PKA/CREB pathway. The molecular mechanism by which sAPPβ increases BACE1 interaction with AC remains unclear, although it might depend on an increase in BACE1 protein levels induced by sAPPβ itself or, more likely, by the sAPPβ-induced activation of NFκB pathway. In fact, the inhibition of NFκB induced by parthenolide decreased the BACE1-AC interaction in skeletal muscle cells.

Of course, it is well known that NFκB itself also reduces PGC1α expression (Alvarez-Guardia *et al.*, 2010; Coll *et al.*, 2006). Thus, this pathway could contribute to PGC1α downregulation induced by palmitate and sAPPβ. Although we do not discard this mechanism, our results clearly show that BACE1 drastically reduces CREB phosphorylation. Since CREB is probably the most important transcription factor that promotes PGC1α expression in muscle (Arnold *et al.*, 2011), a reduction in its activity subsequently leads to decreased levels of PGC1α. Moreover, we demonstrated that BACE1 interacts with AC, and that M3 reduces this interaction and recovers the negative effect of BACE1 on PKA activity and CREB phosphorylation, thus corroborating our hypothesis. We obtained the same results using a genetic approach, since knocking down BACE1 strongly increased PKA activity, CREB phosphorylation and PGC1α levels, confirming that PKA/CREB pathway is involved in PGC1α downregulation. In addition, sAPPβ itself drastically decreases PKA activity, CREB phosphorylation and PGC1α levels.

In conclusion, we hypothesize that sAPPβ induces PGC1α downregulation through impairing the cAMP/PKA/CREB pathway. The reduction in PGC1α levels would ultimately contribute to exacerbate insulin resistance in skeletal muscle cells. Since palmitate and its derivatives increase BACE1 levels, and consequently sAPPβ production, this mechanism would be involved in lipid-induced insulin resistance. sAPPβ itself might generate an insidious vicious loop by upregulating BACE1 levels (Figure V.3.).

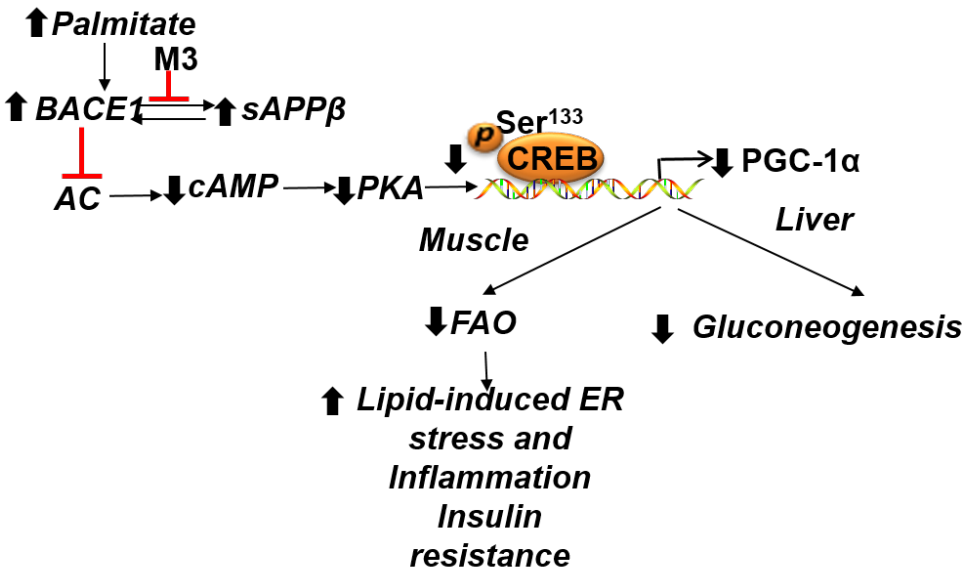

Figure V.3. Potential molecular mechanism of BACE1 and sAPPβ on PKA/CREB/PGC1α pathway. Effects in skeletal muscle and liver.

VI. Conclusions

1. VLDL induce ER stress and inflammation in skeletal muscle.
2. Apo CIII is responsible for the effects of VLDL on ER stress, inflammation and the attenuation of the insulin signaling pathway in skeletal muscle.
3. The ERK1/2 pathway is involved in VLDL and Apo CIII molecular mechanism on ER stress, inflammation and the attenuation of the insulin signaling pathway.
4. VLDL and Apo CIII activate ERK1/2 through TLR2.

5. BACE1 is involved in lipid-induced ER stress, inflammation and the attenuation of the insulin signaling pathway in skeletal muscle.
6. BACE1 contributes to lipid-induce insulin resistance by reducing PGC1α and impairing mitochondrial function.
7. The BACE1 product sAPPβ reduces PGC1α expression and induces ER stress, inflammation and attenuates the insulin signaling pathway.
8. sAPPβ impairs glucose uptake and fatty acid oxidation in skeletal muscle, thus contributing to the development of insulin resistance.
9. BACE1 and sAPPβ reduce PGC1α by downregulating the cAMP/PKA/CREB pathway.

10. Apo CIII and sAPPβ might be considered novel determinants in the development of insulin resistance and new potential pharmacological targets in the treatment of T2D.

VII. Bibliography

Abdul-Ghani, M. A., & DeFronzo, R. A. (2010). Pathogenesis of insulin resistance in skeletal muscle. *J Biomed Biotechnol, 2010*, 476279. doi: 10.1155/2010/476279

Adamovich, Y., Shlomai, A., Tsvetkov, P., Umansky, K. B., Reuven, N., Estall, J. L., et al. (2013). The protein level of PGC-1alpha, a key metabolic regulator, is controlled by NADH-NQO1. *Mol Cell Biol, 33*(13), 2603-2613. doi: 10.1128/mcb.01672-12

Adiels, M., Olofsson, S. O., Taskinen, M. R., & Boren, J. (2008a). Overproduction of very low-density lipoproteins is the hallmark of the dyslipidemia in the metabolic syndrome. *Arterioscler Thromb Vasc Biol, 28*(7), 1225-1236. doi: 10.1161/atvbaha.107.160192

Adiels, M., Taskinen, M. R., & Boren, J. (2008b). Fatty liver, insulin resistance, and dyslipidemia. *Curr Diab Rep, 8*(1), 60-64.

Aerts, J. M., Ottenhoff, R., Powlson, A. S., Grefhorst, A., van Eijk, M., Dubbelhuis, P. F., et al. (2007). Pharmacological inhibition of glucosylceramide synthase enhances insulin sensitivity. *Diabetes, 56*(5), 1341-1349. doi: 10.2337/db06-1619

Aguirre, V., Uchida, T., Yenush, L., Davis, R., & White, M. F. (2000). The c-Jun NH(2)-terminal kinase promotes insulin resistance during association with insulin receptor substrate-1 and phosphorylation of Ser(307). *J Biol Chem, 275*(12), 9047-9054.

Akter, K., Lanza, E. A., Martin, S. A., Myronyuk, N., Rua, M., & Raffa, R. B. (2011). Diabetes mellitus and Alzheimer's disease: shared pathology and treatment? *Br J Clin Pharmacol, 71*(3), 365-376. doi: 10.1111/j.1365-2125.2010.03830.x

Alcolea, D., Vilaplana, E., Suarez-Calvet, M., Illan-Gala, I., Blesa, R., Clarimon, J., et al. (2017). CSF sAPPbeta, YKL-40, and neurofilament light in frontotemporal lobar degeneration. *Neurology, 89*(2), 178-188. doi: 10.1212/wnl.0000000000004088

Alessi, D. R., James, S. R., Downes, C. P., Holmes, A. B., Gaffney, P. R., Reese, C. B., et al. (1997). Characterization of a 3-phosphoinositide-dependent protein kinase which phosphorylates and activates protein kinase Balpha. *Curr Biol, 7*(4), 261-269.

Alexopoulos, P., Gleixner, L. S., Werle, L., Buhl, F., Thierjung, N., Giourou, E., et al. (2017). Plasma levels of soluble amyloid precursor protein beta in symptomatic Alzheimer's disease. *Eur Arch Psychiatry Clin Neurosci*. doi: 10.1007/s00406-017-0815-9

Ali, A., Hoeflich, K. P., & Woodgett, J. R. (2001). Glycogen synthase kinase-3: properties, functions, and regulation. *Chem Rev, 101*(8), 2527-2540.

Alkhateeb, H., Chabowski, A., & Bonen, A. (2006). Viability of the isolated soleus muscle during long-term incubation. *Appl Physiol Nutr Metab, 31*(4), 467-476. doi: 10.1139/h06-022

Altomonte, J., Cong, L., Harbaran, S., Richter, A., Xu, J., Meseck, M., et al. (2004). Foxo1 mediates insulin action on apoC-III and triglyceride metabolism. *J Clin Invest, 114*(10), 1493-1503. doi: 10.1172/jci19992

Alvarez-Guardia, D., Palomer, X., Coll, T., Davidson, M. M., Chan, T. O., Feldman, A. M., et al. (2010). The p65 subunit of NF-kappaB binds to PGC-1alpha, linking inflammation and metabolic disturbances in cardiac cells. *Cardiovasc Res, 87*(3), 449-458. doi: 10.1093/cvr/cvq080

Andersen, I. R., Sondergaard, E., Sorensen, L. P., Nellemann, B., Gormsen, L. C., Jensen, M. D., et al. (2017). Increased VLDL-TG Fatty Acid Storage in Skeletal Muscle in Men With Type 2 Diabetes. *J Clin Endocrinol Metab, 102*(3), 831-839. doi: 10.1210/jc.2016-2979

Anderson, E. J., Lustig, M. E., Boyle, K. E., Woodlief, T. L., Kane, D. A., Lin, C. T., et al. (2009). Mitochondrial H2O2 emission and cellular redox state link excess fat intake to insulin resistance in both rodents and humans. *J Clin Invest, 119*(3), 573-581. doi: 10.1172/jci37048

Anez-Bustillos, L., Dao, D. T., Fell, G. L., Baker, M. A., Gura, K. M., Bistrian, B. R., et al. (2017). Redefining essential fatty acids in the era of novel intravenous lipid emulsions. *Clin Nutr*. doi: 10.1016/j.clnu.2017.07.004

Araki, W., Hattori, K., Kanemaru, K., Yokoi, Y., Omachi, Y., Takano, H., et al. (2017). Re-evaluation of soluble APP-alpha and APP-beta in cerebrospinal fluid as potential biomarkers for early diagnosis of dementia disorders. *Biomark Res, 5*, 28. doi: 10.1186/s40364-017-0108-5

Arner, P. (2002). Insulin resistance in type 2 diabetes: role of fatty acids. *Diabetes Metab Res Rev, 18 Suppl 2*, S5-9.

Arnold, A. S., Egger, A., & Handschin, C. (2011). PGC-1alpha and myokines in the aging muscle - a mini-review. *Gerontology, 57*(1), 37-43. doi: 10.1159/000281883

Arvanitakis, Z., Wilson, R. S., Bienias, J. L., Evans, D. A., & Bennett, D. A. (2004). Diabetes mellitus and risk of Alzheimer disease and decline in cognitive function. *Arch Neurol, 61*(5), 661-666. doi: 10.1001/archneur.61.5.661

Avall, K., Ali, Y., Leibiger, I. B., Leibiger, B., Moede, T., Paschen, M., et al. (2015). Apolipoprotein CIII links islet insulin resistance to beta-cell failure in diabetes. *Proc Natl Acad Sci U S A, 112*(20), E2611-2619. doi: 10.1073/pnas.1423849112

Avila, J. (2008). Tau kinases and phosphatases. *J Cell Mol Med, 12*(1), 258-259. doi: 10.1111/j.1582-4934.2007.00214.x

Baar, K., Wende, A. R., Jones, T. E., Marison, M., Nolte, L. A., Chen, M., et al. (2002). Adaptations of skeletal muscle to exercise: rapid increase in the transcriptional coactivator PGC-1. *Faseb j, 16*(14), 1879-1886. doi: 10.1096/fj.02-0367com

Back, S. H., & Kaufman, R. J. (2012). Endoplasmic reticulum stress and type 2 diabetes. *Annu Rev Biochem, 81*, 767-793. doi: 10.1146/annurev-biochem-072909-095555

Baker, L. D., Cross, D. J., Minoshima, S., Belongia, D., Watson, G. S., & Craft, S. (2011). Insulin resistance and Alzheimer-like reductions in regional cerebral glucose metabolism for cognitively normal adults with prediabetes or early type 2 diabetes. *Arch Neurol, 68*(1), 51-57. doi: 10.1001/archneurol.2010.225

Balakrishnan, K., Verdile, G., Mehta, P. D., Beilby, J., Nolan, D., Galvao, D. A., et al. (2005). Plasma Abeta42 correlates positively with increased body fat in healthy individuals. *J Alzheimers Dis, 8*(3), 269-282.

Barbagallo, M., & Dominguez, L. J. (2014). Type 2 diabetes mellitus and Alzheimer's disease. *World J Diabetes, 5*(6), 889-893. doi: 10.4239/wjd.v5.i6.889

Barbarroja, N., Lopez-Pedrera, R., Mayas, M. D., Garcia-Fuentes, E., Garrido-Sanchez, L., Macias-Gonzalez, M., et al. (2010). The obese healthy paradox: is inflammation the answer? *Biochem J, 430*(1), 141-149. doi: 10.1042/bj20100285

Barish, G. D., Narkar, V. A., & Evans, R. M. (2006). PPAR delta: a dagger in the heart of the metabolic syndrome. *J Clin Invest, 116*(3), 590-597. doi: 10.1172/jci27955

Barroso, E., Rodriguez-Calvo, R., Serrano-Marco, L., Astudillo, A. M., Balsinde, J., Palomer, X., et al. (2011). The PPARbeta/delta activator GW501516 prevents the down-regulation of AMPK caused by a high-fat diet in liver and amplifies the PGC-1alpha-Lipin 1-PPARalpha pathway leading to increased fatty acid oxidation. *Endocrinology, 152*(5), 1848-1859. doi: 10.1210/en.2010-1468

Bayascas, J. R., Wullschleger, S., Sakamoto, K., Garcia-Martinez, J. M., Clacher, C., Komander, D., et al. (2008). Mutation of the PDK1 PH domain inhibits protein kinase B/Akt, leading to small size and insulin resistance. *Mol Cell Biol, 28*(10), 3258-3272. doi: 10.1128/mcb.02032-07

Becker, A. B., & Roth, R. A. (1990). Insulin receptor structure and function in normal and pathological conditions. *Annu Rev Med, 41*, 99-115. doi: 10.1146/annurev.me.41.020190.000531

Bennacer, A. F., Haffaf, E., Kacimi, G., Oudjit, B., & Koceir, E. A. (2017). Association of polyunsaturated/saturated fatty acids to metabolic syndrome cardiovascular risk factors and lipoprotein (a) in hypertensive type 2 diabetic patients. *Ann Biol Clin (Paris), 75*(3), 293-304. doi: 10.1684/abc.2017.1244

Berg, A. H., Combs, T. P., & Scherer, P. E. (2002). ACRP30/adiponectin: an adipokine regulating glucose and lipid metabolism. *Trends Endocrinol Metab, 13*(2), 84-89.

Berg J, S. L. (2008). *Biochemistry* (F. a. Company Ed. 6th ed.).

Bergman, R. N., & Ader, M. (2000). Free fatty acids and pathogenesis of type 2 diabetes mellitus. *Trends Endocrinol Metab, 11*(9), 351-356.

Bobrovnikova-Marjon, E., Pytel, D., Riese, M. J., Vaites, L. P., Singh, N., Koretzky, G. A., et al. (2012). PERK utilizes intrinsic lipid kinase activity to generate phosphatidic acid, mediate Akt activation, and promote adipocyte differentiation. *Mol Cell Biol, 32*(12), 2268-2278. doi: 10.1128/mcb.00063-12

Boden, G. (2002a). Interaction between free fatty acids and glucose metabolism. *Curr Opin Clin Nutr Metab Care, 5*(5), 545-549.

Boden, G. (2002b). Obesity and diabetes mellitus--how are they linked? *West Indian Med J, 51 Suppl 1*, 51-54.

Boden, G., Chen, X., & Iqbal, N. (1998). Acute lowering of plasma fatty acids lowers basal insulin secretion in diabetic and nondiabetic subjects. *Diabetes, 47*(10), 1609-1612.

Boden, G., Chen, X., Rosner, J., & Barton, M. (1995). Effects of a 48-h fat infusion on insulin secretion and glucose utilization. *Diabetes, 44*(10), 1239-1242.

Boden, G., Duan, X., Homko, C., Molina, E. J., Song, W., Perez, O., et al. (2008). Increase in endoplasmic reticulum stress-related proteins and genes in adipose tissue of obese, insulin-resistant individuals. *Diabetes, 57*(9), 2438-2444. doi: 10.2337/db08-0604

Boden, G., & Shulman, G. I. (2002). Free fatty acids in obesity and type 2 diabetes: defining their role in the development of insulin resistance and beta-cell dysfunction. *Eur J Clin Invest, 32 Suppl 3*, 14-23.

Bomfim, T. R., Forny-Germano, L., Sathler, L. B., Brito-Moreira, J., Houzel, J. C., Decker, H., et al. (2012). An anti-diabetes agent protects the mouse brain from defective insulin signaling caused by Alzheimer's disease- associated Abeta oligomers. *J Clin Invest, 122*(4), 1339-1353. doi: 10.1172/jci57256

Bonnard, C., Durand, A., Peyrol, S., Chanseaume, E., Chauvin, M. A., Morio, B., et al. (2008). Mitochondrial dysfunction results from oxidative stress in the skeletal muscle of diet-induced insulin-resistant mice. *J Clin Invest, 118*(2), 789-800. doi: 10.1172/jci32601

Boren, J., Taskinen, M. R., Olofsson, S. O., & Levin, M. (2013). Ectopic lipid storage and insulin resistance: a harmful relationship. *J Intern Med, 274*(1), 25-40. doi: 10.1111/joim.12071

Boren, J., Wettesten, M., Rustaeus, S., Andersson, M., & Olofsson, S. O. (1993). The assembly and secretion of apoB-100-containing lipoproteins. *Biochem Soc Trans, 21*(2), 487-493.

Boslem, E., MacIntosh, G., Preston, A. M., Bartley, C., Busch, A. K., Fuller, M., et al. (2011). A lipidomic screen of palmitate-treated MIN6 beta-cells links sphingolipid metabolites with endoplasmic reticulum (ER) stress and impaired protein trafficking. *Biochem J, 435*(1), 267-276. doi: 10.1042/bj20101867

Bost, F., Aouadi, M., Caron, L., Even, P., Belmonte, N., Prot, M., et al. (2005). The extracellular signal-regulated kinase isoform ERK1 is specifically required for in vitro and in vivo adipogenesis. *Diabetes, 54*(2), 402-411.

Boucher, J., Kleinridders, A., & Kahn, C. R. (2014). Insulin receptor signaling in normal and insulin-resistant states. *Cold Spring Harb Perspect Biol, 6*(1). doi: 10.1101/cshperspect.a009191

Bouzakri, K., Roques, M., Gual, P., Espinosa, S., Guebre-Egziabher, F., Riou, J. P., et al. (2003). Reduced activation of phosphatidylinositol-3 kinase and increased serine 636 phosphorylation of insulin receptor substrate-1 in primary culture of skeletal muscle cells from patients with type 2 diabetes. *Diabetes, 52*(6), 1319-1325.

Brachmann, S. M., Ueki, K., Engelman, J. A., Kahn, R. C., & Cantley, L. C. (2005). Phosphoinositide 3-kinase catalytic subunit deletion and regulatory subunit deletion have opposite effects on insulin sensitivity in mice. *Mol Cell Biol, 25*(5), 1596-1607. doi: 10.1128/mcb.25.5.1596-1607.2005

Brown, M. S., & Goldstein, J. L. (2008). Selective versus total insulin resistance: a pathogenic paradox. *Cell Metab, 7*(2), 95-96. doi: 10.1016/j.cmet.2007.12.009

Brownsey, R. W., Zhande, R., & Boone, A. N. (1997). Isoforms of acetyl-CoA carboxylase: structures, regulatory properties and metabolic functions. *Biochem Soc Trans, 25*(4), 1232-1238.

Brunelli, M., Castellucci, V., & Kandel, E. R. (1976). Synaptic facilitation and behavioral sensitization in Aplysia: possible role of serotonin and cyclic AMP. *Science, 194*(4270), 1178-1181.

Bruning, J. C., Michael, M. D., Winnay, J. N., Hayashi, T., Horsch, D., Accili, D., et al. (1998). A muscle-specific insulin receptor knockout exhibits features of the metabolic syndrome of NIDDM without altering glucose tolerance. *Mol Cell, 2*(5), 559-569.

Bryant, N. J., Govers, R., & James, D. E. (2002). Regulated transport of the glucose transporter GLUT4. *Nat Rev Mol Cell Biol, 3*(4), 267-277. doi: 10.1038/nrm782

Buggia-Prevot, V., Sevalle, J., Rossner, S., & Checler, F. (2008). NFkappaB-dependent control of BACE1 promoter transactivation by Abeta42. *J Biol Chem, 283*(15), 10037-10047. doi: 10.1074/jbc.M706579200

Burgess, B. L., McIsaac, S. A., Naus, K. E., Chan, J. Y., Tansley, G. H., Yang, J., et al. (2006). Elevated plasma triglyceride levels precede amyloid deposition in Alzheimer's disease mouse models with abundant A beta in plasma. *Neurobiol Dis, 24*(1), 114-127. doi: 10.1016/j.nbd.2006.06.007

Buroker, N. E., Barboza, J., & Huang, J. Y. (2009). The IkappaBalpha gene is a peroxisome proliferator-activated receptor cardiac target gene. *Febs j, 276*(12), 3247-3255. doi: 10.1111/j.1742-4658.2009.07039.x

Buxbaum, J. D., Koo, E. H., & Greengard, P. (1993). Protein phosphorylation inhibits production of Alzheimer amyloid beta/A4 peptide. *Proc Natl Acad Sci U S A, 90*(19), 9195-9198.

Cacicedo, J. M., Yagihashi, N., Keaney, J. F., Jr., Ruderman, N. B., & Ido, Y. (2004). AMPK inhibits fatty acid-induced increases in NF-kappaB transactivation in cultured human umbilical vein endothelial cells. *Biochem Biophys Res Commun, 324*(4), 1204-1209. doi: 10.1016/j.bbrc.2004.09.177

Cahill, G. F., Jr. (2006). Fuel metabolism in starvation. *Annu Rev Nutr, 26*, 1-22. doi: 10.1146/annurev.nutr.26.061505.111258

Cai, D., Yuan, M., Frantz, D. F., Melendez, P. A., Hansen, L., Lee, J., et al. (2005). Local and systemic insulin resistance resulting from hepatic activation of IKK-beta and NF-kappaB. *Nat Med, 11*(2), 183-190. doi: 10.1038/nm1166

Calvo-Ochoa, E., Sanchez-Alegria, K., Gomez-Inclan, C., Ferrera, P., & Arias, C. (2017). Palmitic acid stimulates energy metabolism and inhibits insulin/PI3K/AKT signaling in differentiated human neuroblastoma cells: The role of mTOR activation and mitochondrial ROS production. *Neurochem Int, 110*, 75-83. doi: 10.1016/j.neuint.2017.09.008

Canto, C., & Auwerx, J. (2009). PGC-1alpha, SIRT1 and AMPK, an energy sensing network that controls energy expenditure. *Curr Opin Lipidol, 20*(2), 98-105. doi: 10.1097/MOL.0b013e328328d0a4

Caron, S., Verrijken, A., Mertens, I., Samanez, C. H., Mautino, G., Haas, J. T., et al. (2011). Transcriptional activation of apolipoprotein CIII expression by glucose may contribute to diabetic dyslipidemia. *Arterioscler Thromb Vasc Biol, 31*(3), 513-519. doi: 10.1161/atvbaha.110.220723

Castelli, W. P., Garrison, R. J., Wilson, P. W., Abbott, R. D., Kalousdian, S., & Kannel, W. B. (1986). Incidence of coronary heart disease and lipoprotein cholesterol levels. The Framingham Study. *Jama, 256*(20), 2835-2838.

Cen, J., Sargsyan, E., & Bergsten, P. (2016). Fatty acids stimulate insulin secretion from human pancreatic islets at fasting glucose concentrations via mitochondria-dependent and -independent mechanisms. *Nutr Metab (Lond), 13*(1), 59. doi: 10.1186/s12986-016-0119-5

Clarke, S. D., Thuillier, P., Baillie, R. A., & Sha, X. (1999). Peroxisome proliferator-activated receptors: a family of lipid-activated transcription factors. *Am J Clin Nutr, 70*(4), 566-571.

Coletta, D. K., & Mandarino, L. J. (2011). Mitochondrial dysfunction and insulin resistance from the outside in: extracellular matrix, the cytoskeleton, and mitochondria. *Am J Physiol Endocrinol Metab, 301*(5), E749-755. doi: 10.1152/ajpendo.00363.2011

Coletta, D. K., Sriwijitkamol, A., Wajcberg, E., Tantiwong, P., Li, M., Prentki, M., et al. (2009). Pioglitazone stimulates AMP-activated protein kinase signalling and increases the expression of genes involved in adiponectin signalling, mitochondrial function and fat oxidation in human skeletal muscle in vivo: a randomised trial. *Diabetologia, 52*(4), 723-732. doi: 10.1007/s00125-008-1256-9

Coll, T., Jove, M., Rodriguez-Calvo, R., Eyre, E., Palomer, X., Sanchez, R. M., et al. (2006). Palmitate-mediated downregulation of peroxisome proliferator-activated receptor-gamma coactivator 1alpha in skeletal muscle cells involves MEK1/2 and nuclear factor-kappaB activation. *Diabetes, 55*(10), 2779-2787. doi: 10.2337/db05-1494

Corkey, B. E. (2012). Banting lecture 2011: hyperinsulinemia: cause or consequence? *Diabetes, 61*(1), 4-13. doi: 10.2337/db11-1483

Correia, S. C., Santos, R. X., Carvalho, C., Cardoso, S., Candeias, E., Santos, M. S., et al. (2012). Insulin signaling, glucose metabolism and mitochondria: major players in Alzheimer's disease and diabetes interrelation. *Brain Res, 1441*, 64-78. doi: 10.1016/j.brainres.2011.12.063

Cortes, V. A., Cautivo, K. M., Rong, S., Garg, A., Horton, J. D., & Agarwal, A. K. (2014). Leptin ameliorates insulin resistance and hepatic steatosis in Agpat2-/- lipodystrophic mice independent of hepatocyte leptin receptors. *J Lipid Res, 55*(2), 276-288. doi: 10.1194/jlr.M045799

Coughlan, K. A., Valentine, R. J., Ruderman, N. B., & Saha, A. K. (2013). Nutrient Excess in AMPK Downregulation and Insulin Resistance. *J Endocrinol Diabetes Obes, 1*(1), 1008.

Chaban, Y., Boekema, E. J., & Dudkina, N. V. (2014). Structures of mitochondrial oxidative phosphorylation supercomplexes and mechanisms for their stabilisation. *Biochim Biophys Acta, 1837*(4), 418-426. doi: 10.1016/j.bbabio.2013.10.004

Chalmers, C. J., Gilley, R., March, H. N., Balmanno, K., & Cook, S. J. (2007). The duration of ERK1/2 activity determines the activation of c-Fos and Fra-1 and the composition and quantitative transcriptional output of AP-1. *Cell Signal, 19*(4), 695-704. doi: 10.1016/j.cellsig.2006.09.001

Chang, C. C., Li, H. H., Chang, Y. T., Ho, Y. J., Hsieh, L. J., Chiu, P. Y., et al. (2017). Abeta exacerbates alpha-synuclein-induced neurotoxicity through impaired insulin signaling in alpha-synuclein-overexpressed human SK-N-MC neuronal cells. *CNS Neurosci Ther*. doi: 10.1111/cns.12772

Chasseigneaux, S., & Allinquant, B. (2012). Functions of Abeta, sAPPalpha and sAPPbeta : similarities and differences. *J Neurochem, 120 Suppl 1*, 99-108. doi: 10.1111/j.1471-4159.2011.07584.x

Chaurasia, B., & Summers, S. A. (2015). Ceramides - Lipotoxic Inducers of Metabolic Disorders. *Trends Endocrinol Metab, 26*(10), 538-550. doi: 10.1016/j.tem.2015.07.006

Chen, C. H., Zhou, W., Liu, S., Deng, Y., Cai, F., Tone, M., et al. (2012a). Increased NF-kappaB signalling up-regulates BACE1 expression and its therapeutic potential in Alzheimer's disease. *Int J Neuropsychopharmacol, 15*(1), 77-90. doi: 10.1017/s1461145711000149

Chen, M., Breslow, J. L., Li, W., & Leff, T. (1994). Transcriptional regulation of the apoC-III gene by insulin in diabetic mice: correlation with changes in plasma triglyceride levels. *J Lipid Res, 35*(11), 1918-1924.

Chen, Y., Huang, X., Zhang, Y. W., Rockenstein, E., Bu, G., Golde, T. E., et al. (2012b). Alzheimer's beta-secretase (BACE1) regulates the cAMP/PKA/CREB pathway independently of beta-amyloid. *J Neurosci, 32*(33), 11390-11395. doi: 10.1523/jneurosci.0757-12.2012

Cheret, C., Willem, M., Fricker, F. R., Wende, H., Wulf-Goldenberg, A., Tahirovic, S., et al. (2013). Bace1 and Neuregulin-1 cooperate to control formation and maintenance of muscle spindles. *Embo j, 32*(14), 2015-2028. doi: 10.1038/emboj.2013.146

Chiu, H. K., Tsai, E. C., Juneja, R., Stoever, J., Brooks-Worrell, B., Goel, A., et al. (2007). Equivalent insulin resistance in latent autoimmune diabetes in adults (LADA) and type 2 diabetic patients. *Diabetes Res Clin Pract, 77*(2), 237-244. doi: 10.1016/j.diabres.2006.12.013

Choi, R. H., McConahay, A., Jeong, H. W., McClellan, J. L., Hardee, J. P., Carson, J. A., et al. (2017). Tribbles 3 regulates protein turnover in mouse skeletal muscle. *Biochem Biophys Res Commun, 493*(3), 1236-1242. doi: 10.1016/j.bbrc.2017.09.134

Chung, S., Lapoint, K., Martinez, K., Kennedy, A., Boysen Sandberg, M., & McIntosh, M. K. (2006). Preadipocytes mediate lipopolysaccharide-induced inflammation and insulin resistance in primary cultures of newly differentiated human adipocytes. *Endocrinology, 147*(11), 5340-5351. doi: 10.1210/en.2006-0536

Dasu, M. R., & Jialal, I. (2011). Free fatty acids in the presence of high glucose amplify monocyte inflammation via Toll-like receptors. *Am J Physiol Endocrinol Metab, 300*(1), E145-154. doi: 10.1152/ajpendo.00490.2010

Day, E. A., Ford, R. J., & Steinberg, G. R. (2017). AMPK as a Therapeutic Target for Treating Metabolic Diseases. *Trends Endocrinol Metab, 28*(8), 545-560. doi: 10.1016/j.tem.2017.05.004

De Fea, K., & Roth, R. A. (1997). Protein kinase C modulation of insulin receptor substrate-1 tyrosine phosphorylation requires serine 612. *Biochemistry, 36*(42), 12939-12947. doi: 10.1021/bi971157f

De Felice, F. G., Velasco, P. T., Lambert, M. P., Viola, K., Fernandez, S. J., Ferreira, S. T., et al. (2007). Abeta oligomers induce neuronal oxidative stress through an N-methyl-D-aspartate receptor-dependent mechanism that is blocked by the Alzheimer drug memantine. *J Biol Chem, 282*(15), 11590-11601. doi: 10.1074/jbc.M607483200

De Felice, F. G., Vieira, M. N., Bomfim, T. R., Decker, H., Velasco, P. T., Lambert, M. P., et al. (2009). Protection of synapses against Alzheimer's-linked toxins: insulin signaling prevents the pathogenic binding of Abeta oligomers. *Proc Natl Acad Sci U S A, 106*(6), 1971-1976. doi: 10.1073/pnas.0809158106

de Ferranti, S., & Mozaffarian, D. (2008). The perfect storm: obesity, adipocyte dysfunction, and metabolic consequences. *Clin Chem, 54*(6), 945-955. doi: 10.1373/clinchem.2007.100156

De Groot LJ, C. G., Dungan K, et al., editors. (2015). Endocrinology

de la Monte, S. M., & Wands, J. R. (2008). Alzheimer's disease is type 3 diabetes-evidence reviewed. *J Diabetes Sci Technol, 2*(6), 1101-1113. doi: 10.1177/193229680800200619

DeFronzo, R. A. (1988). Lilly lecture 1987. The triumvirate: beta-cell, muscle, liver. A collusion responsible for NIDDM. *Diabetes, 37*(6), 667-687.

DeFronzo, R. A., & Tripathy, D. (2009). Skeletal muscle insulin resistance is the primary defect in type 2 diabetes. *Diabetes Care, 32 Suppl 2*, S157-163. doi: 10.2337/dc09-S302

Del Prato, S., Leonetti, F., Simonson, D. C., Sheehan, P., Matsuda, M., & DeFronzo, R. A. (1994). Effect of sustained physiologic hyperinsulinaemia and hyperglycaemia on insulin secretion and insulin sensitivity in man. *Diabetologia, 37*(10), 1025-1035.

Delneste, Y., Beauvillain, C., & Jeannin, P. (2007). [Innate immunity: structure and function of TLRs]. *Med Sci (Paris), 23*(1), 67-73. doi: 10.1051/medsci/200723167

Demars, M. P., Hollands, C., Zhao Kda, T., & Lazarov, O. (2013). Soluble amyloid precursor protein-alpha rescues age-linked decline in neural progenitor cell proliferation. *Neurobiol Aging, 34*(10), 2431-2440. doi: 10.1016/j.neurobiolaging.2013.04.016

Dergunov, A. D., Novoselov, A. V., Visvikis, S., Siest, G., Yakushkin, V. V., & Tsibulsky, V. (2005). The composition, structural properties and binding of very-low-density and low-density lipoproteins to the LDL receptor in normo- and hypertriglyceridemia: relation to the apolipoprotein E phenotype. *Biol Chem, 386*(5), 441-452. doi: 10.1515/bc.2005.053

Digenio, A., Dunbar, R. L., Alexander, V. J., Hompesch, M., Morrow, L., Lee, R. G., et al. (2016). Antisense-Mediated Lowering of Plasma Apolipoprotein C-III by Volanesorsen Improves Dyslipidemia and Insulin Sensitivity in Type 2 Diabetes. *Diabetes Care, 39*(8), 1408-1415. doi: 10.2337/dc16-0126

Dimitriadis, G., Mitrou, P., Lambadiari, V., Maratou, E., & Raptis, S. A. (2011). Insulin effects in muscle and adipose tissue. *Diabetes Res Clin Pract, 93 Suppl 1*, S52-59. doi: 10.1016/s0168-8227(11)70014-6

Dislich, B., & Lichtenthaler, S. F. (2012). The Membrane-Bound Aspartyl Protease BACE1: Molecular and Functional Properties in Alzheimer's Disease and Beyond. *Front Physiol, 3*, 8. doi: 10.3389/fphys.2012.00008

Dobrowolska, J. A., Kasten, T., Huang, Y., Benzinger, T. L., Sigurdson, W., Ovod, V., et al. (2014a). Diurnal patterns of soluble amyloid precursor protein metabolites in the human central nervous system. *PLoS One, 9*(3), e89998. doi: 10.1371/journal.pone.0089998

Dobrowolska, J. A., Michener, M. S., Wu, G., Patterson, B. W., Chott, R., Ovod, V., et al. (2014b). CNS amyloid-beta, soluble APP-alpha and -beta kinetics during BACE inhibition. *J Neurosci, 34*(24), 8336-8346. doi: 10.1523/jneurosci.0540-14.2014

Dong, Y., Zhang, M., Liang, B., Xie, Z., Zhao, Z., Asfa, S., et al. (2010a). Reduction of AMP-activated protein kinase alpha2 increases endoplasmic reticulum stress and atherosclerosis in vivo. *Circulation, 121*(6), 792-803. doi: 10.1161/circulationaha.109.900928

Dong, Y., Zhang, M., Wang, S., Liang, B., Zhao, Z., Liu, C., et al. (2010b). Activation of AMP-activated protein kinase inhibits oxidized LDL-triggered endoplasmic reticulum stress in vivo. *Diabetes, 59*(6), 1386-1396. doi: 10.2337/db09-1637

Donmez, G., Wang, D., Cohen, D. E., & Guarente, L. (2010). SIRT1 suppresses beta-amyloid production by activating the alpha-secretase gene ADAM10. *Cell, 142*(2), 320-332. doi: 10.1016/j.cell.2010.06.020

Dourlen, P., Sujkowski, A., Wessells, R., & Mollereau, B. (2015). Fatty acid transport proteins in disease: New insights from invertebrate models. *Prog Lipid Res, 60*, 30-40. doi: 10.1016/j.plipres.2015.08.001

Du, J., Guan, T., Zhang, H., Xia, Y., Liu, F., & Zhang, Y. (2008). Inhibitory crosstalk between ERK and AMPK in the growth and proliferation of cardiac fibroblasts. *Biochem Biophys Res Commun, 368*(2), 402-407. doi: 10.1016/j.bbrc.2008.01.099

Duncan, R. E., Ahmadian, M., Jaworski, K., Sarkadi-Nagy, E., & Sul, H. S. (2007). Regulation of lipolysis in adipocytes. *Annu Rev Nutr, 27*, 79-101. doi: 10.1146/annurev.nutr.27.061406.093734

Ebtehaj, S., Gruppen, E. G., Parvizi, M., Tietge, U. J. F., & Dullaart, R. P. F. (2017). The anti-inflammatory function of HDL is impaired in type 2 diabetes: role of hyperglycemia, paraoxonase-1 and low grade inflammation. *Cardiovasc Diabetol, 16*(1), 132. doi: 10.1186/s12933-017-0613-8

Elizabeth, M. M., Alarcon, A., J, F., Clara, O. C., Escobar, V., & Del Carmen, M. (2017). Pancreatic beta-Cells and Type 2 Diabetes Development. *Curr Diabetes Rev, 13*(2), 108-121. doi: 10.2174/1573399812666151020101222

Engelgau, M. M., Narayan, K. M., & Herman, W. H. (2000). Screening for type 2 diabetes. *Diabetes Care, 23*(10), 1563-1580.

Eraky, S. M., Abdel-Rahman, N., & Eissa, L. A. (2017). Modulating effects of omega-3 fatty acids and pioglitazone combination on insulin resistance through toll-like receptor 4 in type 2 diabetes mellitus. *Prostaglandins Leukot Essent Fatty Acids*. doi: 10.1016/j.plefa.2017.06.009

Eriksson, J., Franssila-Kallunki, A., Ekstrand, A., Saloranta, C., Widen, E., Schalin, C., et al. (1989). Early metabolic defects in persons at increased risk for non-insulin-dependent diabetes mellitus. *N Engl J Med, 321*(6), 337-343. doi: 10.1056/nejm198908103210601

Esch, F. S., Keim, P. S., Beattie, E. C., Blacher, R. W., Culwell, A. R., Oltersdorf, T., et al. (1990). Cleavage of amyloid beta peptide during constitutive processing of its precursor. *Science, 248*(4959), 1122-1124.

Evans, J. L., Maddux, B. A., & Goldfine, I. D. (2005). The molecular basis for oxidative stress-induced insulin resistance. *Antioxid Redox Signal, 7*(7-8), 1040-1052. doi: 10.1089/ars.2005.7.1040

Farese, R. V. (2002). Function and dysfunction of aPKC isoforms for glucose transport in insulin-sensitive and insulin-resistant states. *Am J Physiol Endocrinol Metab, 283*(1), E1-11. doi: 10.1152/ajpendo.00045.2002

Fernandez-Gamba, A., Leal, M. C., Morelli, L., & Castano, E. M. (2009). Insulin-degrading enzyme: structure-function relationship and its possible roles in health and disease. *Curr Pharm Des, 15*(31), 3644-3655.

Ferrannini, E., Gastaldelli, A., Miyazaki, Y., Matsuda, M., Mari, A., & DeFronzo, R. A. (2005). beta-Cell function in subjects spanning the range from normal glucose tolerance to overt diabetes: a new analysis. *J Clin Endocrinol Metab, 90*(1), 493-500. doi: 10.1210/jc.2004-1133

Field, C. J., Ryan, E. A., Thomson, A. B., & Clandinin, M. T. (1990). Diet fat composition alters membrane phospholipid composition, insulin binding, and glucose metabolism in adipocytes from control and diabetic animals. *J Biol Chem, 265*(19), 11143-11150.

Fillmore, N., Mori, J., & Lopaschuk, G. D. (2014). Mitochondrial fatty acid oxidation alterations in heart failure, ischaemic heart disease and diabetic cardiomyopathy. *Br J Pharmacol, 171*(8), 2080-2090. doi: 10.1111/bph.12475

Finck, B. N., & Kelly, D. P. (2006). PGC-1 coactivators: inducible regulators of energy metabolism in health and disease. *J Clin Invest, 116*(3), 615-622. doi: 10.1172/jci27794

Fisher, E. A. (2012). The degradation of apolipoprotein B100: multiple opportunities to regulate VLDL triglyceride production by different proteolytic pathways. *Biochim Biophys Acta, 1821*(5), 778-781. doi: 10.1016/j.bbalip.2012.02.001

Frayn, K. N. (2002). Adipose tissue as a buffer for daily lipid flux. *Diabetologia, 45*(9), 1201-1210. doi: 10.1007/s00125-002-0873-y

Fukumoto, H., Cheung, B. S., Hyman, B. T., & Irizarry, M. C. (2002). Beta-secretase protein and activity are increased in the neocortex in Alzheimer disease. *Arch Neurol, 59*(9), 1381-1389.

Furtado, J. D., Campos, H., Appel, L. J., Miller, E. R., Laranjo, N., Carey, V. J., et al. (2008). Effect of protein, unsaturated fat, and carbohydrate intakes on plasma apolipoprotein B and VLDL and LDL containing apolipoprotein C-III: results from the OmniHeart Trial. *Am J Clin Nutr, 87*(6), 1623-1630.

Galloway, S., Jian, L., Johnsen, R., Chew, S., & Mamo, J. C. (2007). beta-amyloid or its precursor protein is found in epithelial cells of the small intestine and is stimulated by high-fat feeding. *J Nutr Biochem, 18*(4), 279-284. doi: 10.1016/j.jnutbio.2006.07.003

Gao, J., Katagiri, H., Ishigaki, Y., Yamada, T., Ogihara, T., Imai, J., et al. (2007). Involvement of apolipoprotein E in excess fat accumulation and insulin resistance. *Diabetes, 56*(1), 24-33. doi: 10.2337/db06-0144

Gao, Z., Hwang, D., Bataille, F., Lefevre, M., York, D., Quon, M. J., et al. (2002). Serine phosphorylation of insulin receptor substrate 1 by inhibitor kappa B kinase complex. *J Biol Chem, 277*(50), 48115-48121. doi: 10.1074/jbc.M209459200

Garofalo, R. S., Orena, S. J., Rafidi, K., Torchia, A. J., Stock, J. L., Hildebrandt, A. L., et al. (2003). Severe diabetes, age-dependent loss of adipose tissue, and mild growth deficiency in mice lacking Akt2/PKB beta. *J Clin Invest, 112*(2), 197-208. doi: 10.1172/jci16885

Gasparini, L., Gouras, G. K., Wang, R., Gross, R. S., Beal, M. F., Greengard, P., et al. (2001). Stimulation of beta-amyloid precursor protein trafficking by insulin reduces intraneuronal beta-amyloid and requires mitogen-activated protein kinase signaling. *J Neurosci, 21*(8), 2561-2570.

Gaudet, D., Brisson, D., Tremblay, K., Alexander, V. J., Singleton, W., Hughes, S. G., et al. (2014). Targeting APOC3 in the familial chylomicronemia syndrome. *N Engl J Med, 371*(23), 2200-2206. doi: 10.1056/NEJMoa1400284

Gibbons, G. F., Wiggins, D., Brown, A. M., & Hebbachi, A. M. (2004). Synthesis and function of hepatic very-low-density lipoprotein. *Biochem Soc Trans, 32*(Pt 1), 59-64. doi: 10.1042/

Ginsberg, H. N., & Huang, L. S. (2000). The insulin resistance syndrome: impact on lipoprotein metabolism and atherothrombosis. *J Cardiovasc Risk, 7*(5), 325-331.

Ginsberg, H. N., Zhang, Y. L., & Hernandez-Ono, A. (2006). Metabolic syndrome: focus on dyslipidemia. *Obesity (Silver Spring), 14 Suppl 1*, 41s-49s. doi: 10.1038/oby.2006.281

Goedert, M., Spillantini, M. G., Jakes, R., Rutherford, D., & Crowther, R. A. (1989). Multiple isoforms of human microtubule-associated protein tau: sequences and localization in neurofibrillary tangles of Alzheimer's disease. *Neuron, 3*(4), 519-526.

Goldfine, A. B., & Shoelson, S. E. (2017). Therapeutic approaches targeting inflammation for diabetes and associated cardiovascular risk. *J Clin Invest, 127*(1), 83-93. doi: 10.1172/jci88884

Gong, B., Chen, F., Pan, Y., Arrieta-Cruz, I., Yoshida, Y., Haroutunian, V., et al. (2010). SCFFbx2-E3-ligase-mediated degradation of BACE1 attenuates Alzheimer's disease amyloidosis and improves synaptic function. *Aging Cell, 9*(6), 1018-1031. doi: 10.1111/j.1474-9726.2010.00632.x

Gordon, D. J., Probstfield, J. L., Garrison, R. J., Neaton, J. D., Castelli, W. P., Knoke, J. D., et al. (1989). High-density lipoprotein cholesterol and cardiovascular disease. Four prospective American studies. *Circulation, 79*(1), 8-15.

Gotz, J., Ittner, L. M., & Kins, S. (2006). Do axonal defects in tau and amyloid precursor protein transgenic animals model axonopathy in Alzheimer's disease? *J Neurochem, 98*(4), 993-1006. doi: 10.1111/j.1471-4159.2006.03955.x

Graham, M. J., Lee, R. G., Bell, T. A., 3rd, Fu, W., Mullick, A. E., Alexander, V. J., et al. (2013). Antisense oligonucleotide inhibition of apolipoprotein C-III reduces plasma triglycerides in rodents, nonhuman primates, and humans. *Circ Res, 112*(11), 1479-1490. doi: 10.1161/circresaha.111.300367

Gray, S., & Kim, J. K. (2011). New insights into insulin resistance in the diabetic heart. *Trends Endocrinol Metab, 22*(10), 394-403. doi: 10.1016/j.tem.2011.05.001

Green, C. J., Pedersen, M., Pedersen, B. K., & Scheele, C. (2011). Elevated NF-kappaB activation is conserved in human myocytes cultured from obese type 2 diabetic patients and attenuated by AMP-activated protein kinase. *Diabetes, 60*(11), 2810-2819. doi: 10.2337/db11-0263

Gregor, M. F., & Hotamisligil, G. S. (2011). Inflammatory mechanisms in obesity. *Annu Rev Immunol, 29*, 415-445. doi: 10.1146/annurev-immunol-031210-101322

Gregor, M. F., Yang, L., Fabbrini, E., Mohammed, B. S., Eagon, J. C., Hotamisligil, G. S., et al. (2009). Endoplasmic reticulum stress is reduced in tissues of obese subjects after weight loss. *Diabetes, 58*(3), 693-700. doi: 10.2337/db08-1220

Grundy, S. M. (2008). Metabolic syndrome pandemic. *Arterioscler Thromb Vasc Biol, 28*(4), 629-636. doi: 10.1161/atvbaha.107.151092

Guglielmotto, M., Aragno, M., Tamagno, E., Vercellinatto, I., Visentin, S., Medana, C., et al. (2012). AGEs/RAGE complex upregulates BACE1 via NF-kappaB pathway activation. *Neurobiol Aging, 33*(1), 196.e113-127. doi: 10.1016/j.neurobiolaging.2010.05.026

Guo, S. (2014). Insulin signaling, resistance, and the metabolic syndrome: insights from mouse models into disease mechanisms. *J Endocrinol, 220*(2), T1-t23. doi: 10.1530/joe-13-0327

Haass, C., Schlossmacher, M. G., Hung, A. Y., Vigo-Pelfrey, C., Mellon, A., Ostaszewski, B. L., et al. (1992). Amyloid beta-peptide is produced by cultured cells during normal metabolism. *Nature, 359*(6393), 322-325. doi: 10.1038/359322a0

Hamid Akash, M. S., Rehman, K., & Liaqat, A. (2017). Tumor necrosis factor-alpha: Role in development of insulin resistance and pathogenesis of type 2 diabetes mellitus. *J Cell Biochem*. doi: 10.1002/jcb.26174

Hamilton, D. L., Findlay, J. A., Montagut, G., Meakin, P. J., Bestow, D., Jalicy, S. M., et al. (2014). Altered amyloid precursor protein processing regulates glucose uptake and oxidation in cultured rodent myotubes. *Diabetologia, 57*(8), 1684-1692. doi: 10.1007/s00125-014-3269-x

Hampel, H., & Shen, Y. (2009). Beta-site amyloid precursor protein cleaving enzyme 1 (BACE1) as a biological candidate marker of Alzheimer's disease. *Scand J Clin Lab Invest, 69*(1), 8-12. doi: 10.1080/00365510701864610

Han, J., Back, S. H., Hur, J., Lin, Y. H., Gildersleeve, R., Shan, J., et al. (2013). ER-stress-induced transcriptional regulation increases protein synthesis leading to cell death. *Nat Cell Biol, 15*(5), 481-490. doi: 10.1038/ncb2738

Handschin, C. (2009). Peroxisome proliferator-activated receptor-gamma coactivator-1alpha in muscle links metabolism to inflammation. *Clin Exp Pharmacol Physiol, 36*(12), 1139-1143. doi: 10.1111/j.1440-1681.2009.05275.x

Harada, M., Nattel, S. N., & Nattel, S. (2012). AMP-activated protein kinase: potential role in cardiac electrophysiology and arrhythmias. *Circ Arrhythm Electrophysiol, 5*(4), 860-867. doi: 10.1161/circep.112.972265

Harding, H. P., Zeng, H., Zhang, Y., Jungries, R., Chung, P., Plesken, H., et al. (2001). Diabetes mellitus and exocrine pancreatic dysfunction in perk-/- mice reveals a role for translational control in secretory cell survival. *Mol Cell, 7*(6), 1153-1163.

Hasebe, N., Fujita, Y., Ueno, M., Yoshimura, K., Fujino, Y., & Yamashita, T. (2013). Soluble beta-amyloid Precursor Protein Alpha binds to p75 neurotrophin receptor to promote neurite outgrowth. *PLoS One, 8*(12), e82321. doi: 10.1371/journal.pone.0082321

Haus, J. M., Kashyap, S. R., Kasumov, T., Zhang, R., Kelly, K. R., Defronzo, R. A., et al. (2009). Plasma ceramides are elevated in obese subjects with type 2 diabetes and correlate with the severity of insulin resistance. *Diabetes, 58*(2), 337-343. doi: 10.2337/db08-1228

Haversen, L., Danielsson, K. N., Fogelstrand, L., & Wiklund, O. (2009). Induction of proinflammatory cytokines by long-chain saturated fatty acids in human macrophages. *Atherosclerosis, 202*(2), 382-393. doi: 10.1016/j.atherosclerosis.2008.05.033

He, L., Zhou, X., Huang, N., Li, H., Tian, J., Li, T., et al. (2016). The Mechanism of AMPK Regulation on Glucose, Lipid and Protein Metabolic Homeostasis and Its Related Physiologically Nutritional Significance. *Curr Protein Pept Sci*.

Hehner, S. P., Heinrich, M., Bork, P. M., Vogt, M., Ratter, F., Lehmann, V., et al. (1998). Sesquiterpene lactones specifically inhibit activation of NF-kappa B by preventing the degradation of I kappa B-alpha and I kappa B-beta. *J Biol Chem, 273*(3), 1288-1297.

Hellerstein, M. K. (2001). No common energy currency: de novo lipogenesis as the road less traveled. *Am J Clin Nutr, 74*(6), 707-708.

Herzig, S., Long, F., Jhala, U. S., Hedrick, S., Quinn, R., Bauer, A., et al. (2001). CREB regulates hepatic gluconeogenesis through the coactivator PGC-1. *Nature, 413*(6852), 179-183. doi: 10.1038/35093131

Hettich, M. M., Matthes, F., Ryan, D. P., Griesche, N., Schroder, S., Dorn, S., et al. (2014). The anti-diabetic drug metformin reduces BACE1 protein level by interfering with the MID1 complex. *PLoS One, 9*(7), e102420. doi: 10.1371/journal.pone.0102420

Himes, R. W., & Smith, C. W. (2010). Tlr2 is critical for diet-induced metabolic syndrome in a murine model. *Faseb j, 24*(3), 731-739. doi: 10.1096/fj.09-141929

Hirosumi, J., Tuncman, G., Chang, L., Gorgun, C. Z., Uysal, K. T., Maeda, K., et al. (2002). A central role for JNK in obesity and insulin resistance. *Nature, 420*(6913), 333-336. doi: 10.1038/nature01137

Hiukka, A., Fruchart-Najib, J., Leinonen, E., Hilden, H., Fruchart, J. C., & Taskinen, M. R. (2005). Alterations of lipids and apolipoprotein CIII in very low density lipoprotein subspecies in type 2 diabetes. *Diabetologia, 48*(6), 1207-1215. doi: 10.1007/s00125-005-1753-z

Hoehn, K. L., Salmon, A. B., Hohnen-Behrens, C., Turner, N., Hoy, A. J., Maghzal, G. J., et al. (2009). Insulin resistance is a cellular antioxidant defense mechanism. *Proc Natl Acad Sci U S A, 106*(42), 17787-17792. doi: 10.1073/pnas.0902380106

Holmberg, R., Refai, E., Hoog, A., Crooke, R. M., Graham, M., Olivecrona, G., et al. (2011). Lowering apolipoprotein CIII delays onset of type 1 diabetes. *Proc Natl Acad Sci U S A, 108*(26), 10685-10689. doi: 10.1073/pnas.1019553108

Holland, W. L., Brozinick, J. T., Wang, L. P., Hawkins, E. D., Sargent, K. M., Liu, Y., et al. (2007). Inhibition of ceramide synthesis ameliorates glucocorticoid-, saturated-fat-, and obesity-induced insulin resistance. *Cell Metab, 5*(3), 167-179. doi: 10.1016/j.cmet.2007.01.002

Holland, W. L., Miller, R. A., Wang, Z. V., Sun, K., Barth, B. M., Bui, H. H., et al. (2011). Receptor-mediated activation of ceramidase activity initiates the pleiotropic actions of adiponectin. *Nat Med, 17*(1), 55-63. doi: 10.1038/nm.2277

Holloszy, J. O. (1967). Biochemical adaptations in muscle. Effects of exercise on mitochondrial oxygen uptake and respiratory enzyme activity in skeletal muscle. *J Biol Chem, 242*(9), 2278-2282.

Hoozemans, J. J., van Haastert, E. S., Nijholt, D. A., Rozemuller, A. J., Eikelenboom, P., & Scheper, W. (2009). The unfolded protein response is activated in pretangle neurons in Alzheimer's disease hippocampus. *Am J Pathol, 174*(4), 1241-1251. doi: 10.2353/ajpath.2009.080814

Hotamisligil, G. S. (2006). Inflammation and metabolic disorders. *Nature, 444*(7121), 860-867. doi: 10.1038/nature05485

Hotamisligil, G. S. (2010). Endoplasmic reticulum stress and the inflammatory basis of metabolic disease. *Cell, 140*(6), 900-917. doi: 10.1016/j.cell.2010.02.034

Houstis, N., Rosen, E. D., & Lander, E. S. (2006). Reactive oxygen species have a causal role in multiple forms of insulin resistance. *Nature, 440*(7086), 944-948. doi: 10.1038/nature04634

Hu, Z. J., Ren, L. P., Wang, C., Liu, B., & Song, G. Y. (2014). Associations between apolipoprotein CIII concentrations and microalbuminuria in type 2 diabetes. *Exp Ther Med, 8*(3), 951-956. doi: 10.3892/etm.2014.1830

Hwang, D. H., Kim, J. A., & Lee, J. Y. (2016). Mechanisms for the activation of Toll-like receptor 2/4 by saturated fatty acids and inhibition by docosahexaenoic acid. *Eur J Pharmacol, 785*, 24-35. doi: 10.1016/j.ejphar.2016.04.024

IDF. (2015). International Diabetes Federation. https://www.idf.org/

Ikezoe, K., Furuya, H., Arahata, H., Nakagawa, M., Tateishi, T., Fujii, N., et al. (2009). Amyloid-beta accumulation caused by chloroquine injections precedes ER stress and autophagosome formation in rat skeletal muscle. *Acta Neuropathol, 117*(5), 575-582. doi: 10.1007/s00401-009-0488-1

Imamura, T., Huang, J., Usui, I., Satoh, H., Bever, J., & Olefsky, J. M. (2003). Insulin-induced GLUT4 translocation involves protein kinase C-lambda-mediated functional coupling between Rab4 and the motor protein kinesin. *Mol Cell Biol, 23*(14), 4892-4900.

Irimia, J. M., Meyer, C. M., Peper, C. L., Zhai, L., Bock, C. B., Previs, S. F., et al. (2010). Impaired glucose tolerance and predisposition to the fasted state in liver glycogen synthase knock-out mice. *J Biol Chem, 285*(17), 12851-12861. doi: 10.1074/jbc.M110.106534

Isom, L. L. (2001). Sodium channel beta subunits: anything but auxiliary. *Neuroscientist, 7*(1), 42-54. doi: 10.1177/107385840100700108

Itani, S. I., Pories, W. J., Macdonald, K. G., & Dohm, G. L. (2001). Increased protein kinase C theta in skeletal muscle of diabetic patients. *Metabolism, 50*(5), 553-557. doi: 10.1053/meta.2001.22512

Itani, S. I., Ruderman, N. B., Schmieder, F., & Boden, G. (2002). Lipid-induced insulin resistance in human muscle is associated with changes in diacylglycerol, protein kinase C, and IkappaB-alpha. *Diabetes, 51*(7), 2005-2011.

Jager, J., Corcelle, V., Gremeaux, T., Laurent, K., Waget, A., Pages, G., et al. (2011). Deficiency in the extracellular signal-regulated kinase 1 (ERK1) protects leptin-deficient mice from insulin resistance without affecting obesity. *Diabetologia, 54*(1), 180-189. doi: 10.1007/s00125-010-1944-0

Janson, J., Laedtke, T., Parisi, J. E., O'Brien, P., Petersen, R. C., & Butler, P. C. (2004). Increased risk of type 2 diabetes in Alzheimer disease. *Diabetes, 53*(2), 474-481.

Janson, J., Soeller, W. C., Roche, P. C., Nelson, R. T., Torchia, A. J., Kreutter, D. K., et al. (1996). Spontaneous diabetes mellitus in transgenic mice expressing human islet amyloid polypeptide. *Proc Natl Acad Sci U S A, 93*(14), 7283-7288.

Jeon, S. M. (2016). Regulation and function of AMPK in physiology and diseases. *Exp Mol Med, 48*(7), e245. doi: 10.1038/emm.2016.81

Jia, L., Vianna, C. R., Fukuda, M., Berglund, E. D., Liu, C., Tao, C., et al. (2014). Hepatocyte Toll-like receptor 4 regulates obesity-induced inflammation and insulin resistance. *Nat Commun, 5*, 3878. doi: 10.1038/ncomms4878

Jiang, S., Zhang, M., Ren, D., Tang, G., Lin, S., Qian, Y., et al. (2003). Enhanced production of amyloid precursor protein mRNA by peripheral mononuclear blood cell in Alzheimer's disease. *Am J Med Genet B Neuropsychiatr Genet, 118b*(1), 99-102. doi: 10.1002/ajmg.b.10067

Jiao, P., Ma, J., Feng, B., Zhang, H., Diehl, J. A., Chin, Y. E., et al. (2011). FFA-induced adipocyte inflammation and insulin resistance: involvement of ER stress and IKKbeta pathways. *Obesity (Silver Spring), 19*(3), 483-491. doi: 10.1038/oby.2010.200

Jimenez-Palomares, M., Ramos-Rodriguez, J. J., Lopez-Acosta, J. F., Pacheco-Herrero, M., Lechuga-Sancho, A. M., Perdomo, G., et al. (2012). Increased Abeta production prompts the onset of glucose intolerance and insulin resistance. *Am J Physiol Endocrinol Metab, 302*(11), E1373-1380. doi: 10.1152/ajpendo.00500.2011

Johnston, J. A., Liu, W. W., Todd, S. A., Coulson, D. T., Murphy, S., Irvine, G. B., et al. (2005). Expression and activity of beta-site amyloid precursor protein cleaving enzyme in Alzheimer's disease. *Biochem Soc Trans, 33*(Pt 5), 1096-1100. doi: 10.1042/bst20051096

Jorgensen, A. B., Frikke-Schmidt, R., Nordestgaard, B. G., & Tybjaerg-Hansen, A. (2014). Loss-of-function mutations in APOC3 and risk of ischemic vascular disease. *N Engl J Med, 371*(1), 32-41. doi: 10.1056/NEJMoa1308027

Kahn, B. B. (1992). Facilitative glucose transporters: regulatory mechanisms and dysregulation in diabetes. *J Clin Invest, 89*(5), 1367-1374. doi: 10.1172/jci115724

Kammoun, H. L., Chabanon, H., Hainault, I., Luquet, S., Magnan, C., Koike, T., et al. (2009). GRP78 expression inhibits insulin and ER stress-induced SREBP-1c activation and reduces hepatic steatosis in mice. *J Clin Invest, 119*(5), 1201-1215. doi: 10.1172/jci37007

Kanda, H., Tateya, S., Tamori, Y., Kotani, K., Hiasa, K., Kitazawa, R., et al. (2006). MCP-1 contributes to macrophage infiltration into adipose tissue, insulin resistance, and hepatic steatosis in obesity. *J Clin Invest, 116*(6), 1494-1505. doi: 10.1172/jci26498

Kane, S., Sano, H., Liu, S. C., Asara, J. M., Lane, W. S., Garner, C. C., et al. (2002). A method to identify serine kinase substrates. Akt phosphorylates a novel adipocyte protein with a Rab GTPase-activating protein (GAP) domain. *J Biol Chem, 277*(25), 22115-22118. doi: 10.1074/jbc.C200198200

Kaneto, H., Nakatani, Y., Miyatsuka, T., Kawamori, D., Matsuoka, T. A., Matsuhisa, M., et al. (2004). Possible novel therapy for diabetes with cell-permeable JNK-inhibitory peptide. *Nat Med, 10*(10), 1128-1132. doi: 10.1038/nm1111

Kang, C., & Li Ji, L. (2012). Role of PGC-1alpha signaling in skeletal muscle health and disease. *Ann N Y Acad Sci, 1271*, 110-117. doi: 10.1111/j.1749-6632.2012.06738.x

Kang, E. L., Cameron, A. N., Piazza, F., Walker, K. R., & Tesco, G. (2010). Ubiquitin regulates GGA3-mediated degradation of BACE1. *J Biol Chem, 285*(31), 24108-24119. doi: 10.1074/jbc.M109.092742

Kawaguchi, M., Tamura, Y., Kakehi, S., Takeno, K., Sakurai, Y., Watanabe, T., et al. (2014). Association between expression of FABPpm in skeletal muscle and insulin sensitivity in intramyocellular lipid-accumulated nonobese men. *J Clin Endocrinol Metab, 99*(9), 3343-3352. doi: 10.1210/jc.2014-1896

Kawakami, A., Aikawa, M., Nitta, N., Yoshida, M., Libby, P., & Sacks, F. M. (2007). Apolipoprotein CIII-induced THP-1 cell adhesion to endothelial cells involves pertussis toxin-sensitive G protein- and protein kinase C alpha-mediated nuclear factor-kappaB activation. *Arterioscler Thromb Vasc Biol, 27*(1), 219-225. doi: 10.1161/01.ATV.0000249620.68705.0d

Kawasaki, N., Asada, R., Saito, A., Kanemoto, S., & Imaizumi, K. (2012). Obesity-induced endoplasmic reticulum stress causes chronic inflammation in adipose tissue. *Sci Rep, 2*, 799. doi: 10.1038/srep00799

Kennedy, M. E., Stamford, A. W., Chen, X., Cox, K., Cumming, J. N., Dockendorf, M. F., et al. (2016). The BACE1 inhibitor verubecestat (MK-8931) reduces CNS beta-amyloid in animal models and in Alzheimer's disease patients. *Sci Transl Med, 8*(363), 363ra150. doi: 10.1126/scitranslmed.aad9704

Kerner, J., & Hoppel, C. (2000). Fatty acid import into mitochondria. *Biochim Biophys Acta, 1486*(1), 1-17.

Khoo, C., Campos, H., Judge, H., & Sacks, F. M. (1999). Effects of estrogenic oral contraceptives on the lipoprotein B particle system defined by apolipoproteins E and C-III content. *J Lipid Res, 40*(2), 202-212.

Kim, B., & Feldman, E. L. (2015). Insulin resistance as a key link for the increased risk of cognitive impairment in the metabolic syndrome. *Exp Mol Med, 47*, e149. doi: 10.1038/emm.2015.3

Kim, D. S., Jeong, S. K., Kim, H. R., Kim, D. S., Chae, S. W., & Chae, H. J. (2010). Metformin regulates palmitate-induced apoptosis and ER stress response in HepG2 liver cells. *Immunopharmacol Immunotoxicol, 32*(2), 251-257. doi: 10.3109/08923970903252220

Kim, H. K., Song, I. S., Lee, S. Y., Jeong, S. H., Lee, S. R., Heo, H. J., et al. (2014). B7-H4 downregulation induces mitochondrial dysfunction and enhances doxorubicin sensitivity via the cAMP/CREB/PGC1-alpha signaling pathway in HeLa cells. *Pflugers Arch, 466*(12), 2323-2338. doi: 10.1007/s00424-014-1493-3

Kim, J. K., Fillmore, J. J., Sunshine, M. J., Albrecht, B., Higashimori, T., Kim, D. W., et al. (2004). PKC-theta knockout mice are protected from fat-induced insulin resistance. *J Clin Invest, 114*(6), 823-827. doi: 10.1172/jci22230

Kim, J. K., Zisman, A., Fillmore, J. J., Peroni, O. D., Kotani, K., Perret, P., et al. (2001). Glucose toxicity and the development of diabetes in mice with muscle-specific inactivation of GLUT4. *J Clin Invest, 108*(1), 153-160. doi: 10.1172/jci10294

Kim, M. K., Reaven, G. M., Chen, Y. D., Kim, E., & Kim, S. H. (2015). Hyperinsulinemia in individuals with obesity: Role of insulin clearance. *Obesity (Silver Spring), 23*(12), 2430-2434. doi: 10.1002/oby.21256

Kitazume, S., Yoshihisa, A., Yamaki, T., Oikawa, M., Tachida, Y., Ogawa, K., et al. (2012). Soluble amyloid precursor protein 770 is released from inflamed endothelial cells and activated platelets: a novel biomarker for acute coronary syndrome. *J Biol Chem, 287*(48), 40817-40825. doi: 10.1074/jbc.M112.398578

Konner, A. C., & Bruning, J. C. (2011). Toll-like receptors: linking inflammation to metabolism. *Trends Endocrinol Metab, 22*(1), 16-23. doi: 10.1016/j.tem.2010.08.007

Koo, S. H., Satoh, H., Herzig, S., Lee, C. H., Hedrick, S., Kulkarni, R., et al. (2004). PGC-1 promotes insulin resistance in liver through PPAR-alpha-dependent induction of TRB-3. *Nat Med, 10*(5), 530-534. doi: 10.1038/nm1044

Koopmans, S. J., Ohman, L., Haywood, J. R., Mandarino, L. J., & DeFronzo, R. A. (1997). Seven days of euglycemic hyperinsulinemia induces insulin resistance for glucose metabolism but not hypertension, elevated catecholamine levels, or increased sodium retention in conscious normal rats. *Diabetes, 46*(10), 1572-1578.

Koves, T. R., Ussher, J. R., Noland, R. C., Slentz, D., Mosedale, M., Ilkayeva, O., et al. (2008). Mitochondrial overload and incomplete fatty acid oxidation contribute to skeletal muscle insulin resistance. *Cell Metab, 7*(1), 45-56. doi: 10.1016/j.cmet.2007.10.013

Kowluru, A., & Matti, A. (2012). Hyperactivation of protein phosphatase 2A in models of glucolipotoxicity and diabetes: potential mechanisms and functional consequences. *Biochem Pharmacol, 84*(5), 591-597. doi: 10.1016/j.bcp.2012.05.003

Kumar, A., Takada, Y., Boriek, A. M., & Aggarwal, B. B. (2004). Nuclear factor-kappaB: its role in health and disease. *J Mol Med (Berl), 82*(7), 434-448. doi: 10.1007/s00109-004-0555-y

Kuo, L. H., Tsai, P. J., Jiang, M. J., Chuang, Y. L., Yu, L., Lai, K. T., et al. (2011). Toll-like receptor 2 deficiency improves insulin sensitivity and hepatic insulin signalling in the mouse. *Diabetologia, 54*(1), 168-179. doi: 10.1007/s00125-010-1931-5

Kurtz, J. E., & Ray-Coquard, I. (2012). PI3 kinase inhibitors in the clinic: an update. *Anticancer Res, 32*(7), 2463-2470.

Kwak, Y. D., Wang, R., Li, J. J., Zhang, Y. W., Xu, H., & Liao, F. F. (2011). Differential regulation of BACE1 expression by oxidative and nitrosative signals. *Mol Neurodegener, 6*, 17. doi: 10.1186/1750-1326-6-17

Lang, F., Ullrich, S., & Gulbins, E. (2011). Ceramide formation as a target in beta-cell survival and function. *Expert Opin Ther Targets, 15*(9), 1061-1071. doi: 10.1517/14728222.2011.588209

Lascar, N., Brown, J., Pattison, H., Barnett, A. H., Bailey, C. J., & Bellary, S. (2017). Type 2 diabetes in adolescents and young adults. *Lancet Diabetes Endocrinol*. doi: 10.1016/s2213-8587(17)30186-9

Lee, C. H., Olson, P., & Evans, R. M. (2003a). Minireview: lipid metabolism, metabolic diseases, and peroxisome proliferator-activated receptors. *Endocrinology, 144*(6), 2201-2207. doi: 10.1210/en.2003-0288

Lee, H. K., Kumar, P., Fu, Q., Rosen, K. M., & Querfurth, H. W. (2009). The insulin/Akt signaling pathway is targeted by intracellular beta-amyloid. *Mol Biol Cell, 20*(5), 1533-1544. doi: 10.1091/mbc.E08-07-0777

Lee, H. Y., Birkenfeld, A. L., Jornayvaz, F. R., Jurczak, M. J., Kanda, S., Popov, V., et al. (2011). Apolipoprotein CIII overexpressing mice are predisposed to diet-induced hepatic steatosis and hepatic insulin resistance. *Hepatology, 54*(5), 1650-1660. doi: 10.1002/hep.24571

Lee, S. J., Moye, L. A., Campos, H., Williams, G. H., & Sacks, F. M. (2003b). Hypertriglyceridemia but not diabetes status is associated with VLDL containing apolipoprotein CIII in patients with coronary heart disease. *Atherosclerosis, 167*(2), 293-302.

Lee, T. W., Bai, K. J., Lee, T. I., Chao, T. F., Kao, Y. H., & Chen, Y. J. (2017). PPARs modulate cardiac metabolism and mitochondrial function in diabetes. *J Biomed Sci, 24*(1), 5. doi: 10.1186/s12929-016-0309-5

Lee, Y. H., Tharp, W. G., Maple, R. L., Nair, S., Permana, P. A., & Pratley, R. E. (2008). Amyloid precursor protein expression is upregulated in adipocytes in obesity. *Obesity (Silver Spring), 16*(7), 1493-1500. doi: 10.1038/oby.2008.267

Lefebvre, P., Chinetti, G., Fruchart, J. C., & Staels, B. (2006). Sorting out the roles of PPAR alpha in energy metabolism and vascular homeostasis. *J Clin Invest, 116*(3), 571-580. doi: 10.1172/jci27989

Lehmann, J. M., Moore, L. B., Smith-Oliver, T. A., Wilkison, W. O., Willson, T. M., & Kliewer, S. A. (1995). An antidiabetic thiazolidinedione is a high affinity ligand for peroxisome proliferator-activated receptor gamma (PPAR gamma). *J Biol Chem, 270*(22), 12953-12956.

Lehti, M., Donelan, E., Abplanalp, W., Al-Massadi, O., Habegger, K. M., Weber, J., et al. (2013). High-density lipoprotein maintains skeletal muscle function by modulating cellular respiration in mice. *Circulation, 128*(22), 2364-2371. doi: 10.1161/circulationaha.113.001551

Leibson, C. L., Rocca, W. A., Hanson, V. A., Cha, R., Kokmen, E., O'Brien, P. C., et al. (1997). Risk of dementia among persons with diabetes mellitus: a population-based cohort study. *Am J Epidemiol, 145*(4), 301-308.

Leick, L., Lyngby, S. S., Wojtaszewski, J. F., & Pilegaard, H. (2010). PGC-1alpha is required for training-induced prevention of age-associated decline in mitochondrial enzymes in mouse skeletal muscle. *Exp Gerontol, 45*(5), 336-342. doi: 10.1016/j.exger.2010.01.011

Lewczuk, P., Kamrowski-Kruck, H., Peters, O., Heuser, I., Jessen, F., Popp, J., et al. (2010). Soluble amyloid precursor proteins in the cerebrospinal fluid as novel potential biomarkers of Alzheimer's disease: a multicenter study. *Mol Psychiatry, 15*(2), 138-145. doi: 10.1038/mp.2008.84

Lewis, G. F., Uffelman, K. D., Szeto, L. W., & Steiner, G. (1993). Effects of acute hyperinsulinemia on VLDL triglyceride and VLDL apoB production in normal weight and obese individuals. *Diabetes, 42*(6), 833-842.

Li, R., Lindholm, K., Yang, L. B., Yue, X., Citron, M., Yan, R., et al. (2004a). Amyloid beta peptide load is correlated with increased beta-secretase activity in sporadic Alzheimer's disease patients. *Proc Natl Acad Sci U S A, 101*(10), 3632-3637. doi: 10.1073/pnas.0205689101

Li, Y., Soos, T. J., Li, X., Wu, J., Degennaro, M., Sun, X., et al. (2004b). Protein kinase C Theta inhibits insulin signaling by phosphorylating IRS1 at Ser(1101). *J Biol Chem, 279*(44), 45304-45307. doi: 10.1074/jbc.C400186200

Liang, H., Balas, B., Tantiwong, P., Dube, J., Goodpaster, B. H., O'Doherty, R. M., et al. (2009). Whole body overexpression of PGC-1alpha has opposite effects on hepatic and muscle insulin sensitivity. *Am J Physiol Endocrinol Metab, 296*(4), E945-954. doi: 10.1152/ajpendo.90292.2008

Liao, Y., & Hung, M. C. (2010). Physiological regulation of Akt activity and stability. *Am J Transl Res, 2*(1), 19-42.

Lira, V. A., Benton, C. R., Yan, Z., & Bonen, A. (2010). PGC-1alpha regulation by exercise training and its influences on muscle function and insulin sensitivity. *Am J Physiol Endocrinol Metab, 299*(2), E145-161. doi: 10.1152/ajpendo.00755.2009

Lonze, B. E., & Ginty, D. D. (2002). Function and regulation of CREB family transcription factors in the nervous system. *Neuron, 35*(4), 605-623.

Lottenberg, A. M., Afonso Mda, S., Lavrador, M. S., Machado, R. M., & Nakandakare, E. R. (2012). The role of dietary fatty acids in the pathology of metabolic syndrome. *J Nutr Biochem, 23*(9), 1027-1040. doi: 10.1016/j.jnutbio.2012.03.004

Lumeng, C. N., & Saltiel, A. R. (2011). Inflammatory links between obesity and metabolic disease. *J Clin Invest, 121*(6), 2111-2117. doi: 10.1172/jci57132

Luo, Y., Bolon, B., Kahn, S., Bennett, B. D., Babu-Khan, S., Denis, P., et al. (2001). Mice deficient in BACE1, the Alzheimer's beta-secretase, have normal phenotype and abolished beta-amyloid generation. *Nat Neurosci, 4*(3), 231-232. doi: 10.1038/85059

Ma, Q. L., Yang, F., Rosario, E. R., Ubeda, O. J., Beech, W., Gant, D. J., et al. (2009). Beta-amyloid oligomers induce phosphorylation of tau and inactivation of insulin receptor substrate via c-Jun N-terminal kinase signaling: suppression by omega-3 fatty acids and curcumin. *J Neurosci, 29*(28), 9078-9089. doi: 10.1523/jneurosci.1071-09.2009

Macrae, K., Stretton, C., Lipina, C., Blachnio-Zabielska, A., Baranowski, M., Gorski, J., et al. (2013). Defining the role of DAG, mitochondrial function, and lipid deposition in palmitate-induced proinflammatory signaling and its counter-modulation by palmitoleate. *J Lipid Res, 54*(9), 2366-2378. doi: 10.1194/jlr.M036996

Maesako, M., Uemura, M., Tashiro, Y., Sasaki, K., Watanabe, K., Noda, Y., et al. (2015). High Fat Diet Enhances beta-Site Cleavage of Amyloid Precursor Protein (APP) via Promoting beta-Site APP Cleaving Enzyme 1/Adaptor Protein 2/Clathrin Complex Formation. *PLoS One, 10*(9), e0131199. doi: 10.1371/journal.pone.0131199

Mahley, R. W., Innerarity, T. L., Rall, S. C., Jr., & Weisgraber, K. H. (1984). Plasma lipoproteins: apolipoprotein structure and function. *J Lipid Res, 25*(12), 1277-1294.

Makinen, S., Nguyen, H. Y., Skrobuk, P., & Koistinen, H. A. (2017). Palmitate and oleate exert differential effects on insulin signalling and glucose uptake in human skeletal muscle cells. *Endocr Connect*. doi: 10.1530/ec-17-0039

Maloney, E., Sweet, I. R., Hockenbery, D. M., Pham, M., Rizzo, N. O., Tateya, S., et al. (2009). Activation of NF-kappaB by palmitate in endothelial cells: a key role for NADPH oxidase-derived superoxide in response to TLR4 activation. *Arterioscler Thromb Vasc Biol, 29*(9), 1370-1375. doi: 10.1161/atvbaha.109.188813

Mark, L., & Dani, G. (2016). [Diabetic dyslipidaemia and the atherosclerosis]. *Orv Hetil, 157*(19), 746-752. doi: 10.1556/650.2016.30441

Mattson, M. P. (1997). Cellular actions of beta-amyloid precursor protein and its soluble and fibrillogenic derivatives. *Physiol Rev, 77*(4), 1081-1132.

Mayer, J. P., Zhang, F., & DiMarchi, R. D. (2007). Insulin structure and function. *Biopolymers, 88*(5), 687-713. doi: 10.1002/bip.20734

Mayeux, R., Honig, L. S., Tang, M. X., Manly, J., Stern, Y., Schupf, N., et al. (2003). Plasma A[beta]40 and A[beta]42 and Alzheimer's disease: relation to age, mortality, and risk. *Neurology, 61*(9), 1185-1190.

Mayeux, R., Tang, M. X., Jacobs, D. M., Manly, J., Bell, K., Merchant, C., et al. (1999). Plasma amyloid beta-peptide 1-42 and incipient Alzheimer's disease. *Ann Neurol, 46*(3), 412-416.

Mayr, B., & Montminy, M. (2001). Transcriptional regulation by the phosphorylation-dependent factor CREB. *Nat Rev Mol Cell Biol, 2*(8), 599-609. doi: 10.1038/35085068

McCrimmon, R. J., Ryan, C. M., & Frier, B. M. (2012). Diabetes and cognitive dysfunction. *Lancet, 379*(9833), 2291-2299. doi: 10.1016/s0140-6736(12)60360-2

McGarry, J. D., & Brown, N. F. (1997). The mitochondrial carnitine palmitoyltransferase system. From concept to molecular analysis. *Eur J Biochem, 244*(1), 1-14.

McGillicuddy, F. C., Chiquoine, E. H., Hinkle, C. C., Kim, R. J., Shah, R., Roche, H. M., et al. (2009). Interferon gamma attenuates insulin signaling, lipid storage, and differentiation in human adipocytes via activation of the JAK/STAT pathway. *J Biol Chem, 284*(46), 31936-31944. doi: 10.1074/jbc.M109.061655

Meakin, P. J., Harper, A. J., Hamilton, D. L., Gallagher, J., McNeilly, A. D., Burgess, L. A., et al. (2012). Reduction in BACE1 decreases body weight, protects against diet-induced obesity and enhances insulin sensitivity in mice. *Biochem J, 441*(1), 285-296. doi: 10.1042/bj20110512

Mellor, H., & Parker, P. J. (1998). The extended protein kinase C superfamily. *Biochem J, 332 (Pt 2)*, 281-292.

Michael, L. F., Wu, Z., Cheatham, R. B., Puigserver, P., Adelmant, G., Lehman, J. J., et al. (2001). Restoration of insulin-sensitive glucose transporter (GLUT4) gene expression in muscle cells by the transcriptional coactivator PGC-1. *Proc Natl Acad Sci U S A, 98*(7), 3820-3825. doi: 10.1073/pnas.061035098

Miinea, C. P., Sano, H., Kane, S., Sano, E., Fukuda, M., Peranen, J., et al. (2005). AS160, the Akt substrate regulating GLUT4 translocation, has a functional Rab GTPase-activating protein domain. *Biochem J, 391*(Pt 1), 87-93. doi: 10.1042/bj20050887

Minokoshi, Y., Alquier, T., Furukawa, N., Kim, Y. B., Lee, A., Xue, B., et al. (2004). AMP-kinase regulates food intake by responding to hormonal and nutrient signals in the hypothalamus. *Nature, 428*(6982), 569-574. doi: 10.1038/nature02440

Miura, S., Kai, Y., Ono, M., & Ezaki, O. (2003). Overexpression of peroxisome proliferator-activated receptor gamma coactivator-1alpha down-regulates GLUT4 mRNA in skeletal muscles. *J Biol Chem, 278*(33), 31385-31390. doi: 10.1074/jbc.M304312200

Moore, M. C., Cherrington, A. D., & Wasserman, D. H. (2003). Regulation of hepatic and peripheral glucose disposal. *Best Pract Res Clin Endocrinol Metab, 17*(3), 343-364.

Mootha, V. K., Lindgren, C. M., Eriksson, K. F., Subramanian, A., Sihag, S., Lehar, J., et al. (2003). PGC-1alpha-responsive genes involved in oxidative phosphorylation are coordinately downregulated in human diabetes. *Nat Genet, 34*(3), 267-273. doi: 10.1038/ng1180

Mora, A., Komander, D., van Aalten, D. M., & Alessi, D. R. (2004). PDK1, the master regulator of AGC kinase signal transduction. *Semin Cell Dev Biol, 15*(2), 161-170.

Musso, G., Gambino, R., & Cassader, M. (2010). Lipoprotein metabolism mediates the association of MTP polymorphism with beta-cell dysfunction in healthy subjects and in nondiabetic normolipidemic patients with nonalcoholic steatohepatitis. *J Nutr Biochem, 21*(9), 834-840. doi: 10.1016/j.jnutbio.2009.06.007

Nguyen, A., Tao, H., Metrione, M., & Hajri, T. (2014). Very low density lipoprotein receptor (VLDLR) expression is a determinant factor in adipose tissue inflammation and adipocyte-macrophage interaction. *J Biol Chem, 289*(3), 1688-1703. doi: 10.1074/jbc.M113.515320

Nguyen, M. T., Favelyukis, S., Nguyen, A. K., Reichart, D., Scott, P. A., Jenn, A., et al. (2007). A subpopulation of macrophages infiltrates hypertrophic adipose tissue and is activated by free fatty acids via Toll-like receptors 2 and 4 and JNK-dependent pathways. *J Biol Chem, 282*(48), 35279-35292. doi: 10.1074/jbc.M706762200

Nicholas, D. A., Zhang, K., Hung, C., Glasgow, S., Aruni, A. W., Unternaehrer, J., et al. (2017). Palmitic acid is a toll-like receptor 4 ligand that induces human dendritic cell secretion of IL-1beta. *PLoS One, 12*(5), e0176793. doi: 10.1371/journal.pone.0176793

Nichols, G. A., Kimes, T. M., Harp, J. B., Kou, T. D., & Brodovicz, K. G. (2012). Glycemic response and attainment of A1C goals following newly initiated insulin therapy for type 2 diabetes. *Diabetes Care, 35*(3), 495-497. doi: 10.2337/dc11-1171

Nikolaev, A., McLaughlin, T., O'Leary, D. D., & Tessier-Lavigne, M. (2009). APP binds DR6 to trigger axon pruning and neuron death via distinct caspases. *Nature, 457*(7232), 981-989. doi: 10.1038/nature07767

Nogalska, A., Engel, W. K., & Askanas, V. (2010). Increased BACE1 mRNA and noncoding BACE1-antisense transcript in sporadic inclusion-body myositis muscle fibers--possibly caused by endoplasmic reticulum stress. *Neurosci Lett, 474*(3), 140-143. doi: 10.1016/j.neulet.2010.03.023

O'Connor, T., Sadleir, K. R., Maus, E., Velliquette, R. A., Zhao, J., Cole, S. L., et al. (2008). Phosphorylation of the translation initiation factor eIF2alpha increases BACE1 levels and promotes amyloidogenesis. *Neuron, 60*(6), 988-1009. doi: 10.1016/j.neuron.2008.10.047

Obregon, D., Hou, H., Deng, J., Giunta, B., Tian, J., Darlington, D., et al. (2012). Soluble amyloid precursor protein-alpha modulates beta-secretase activity and amyloid-beta generation. *Nat Commun, 3*, 777. doi: 10.1038/ncomms1781

Ohno, M., Chang, L., Tseng, W., Oakley, H., Citron, M., Klein, W. L., et al. (2006). Temporal memory deficits in Alzheimer's mouse models: rescue by genetic deletion of BACE1. *Eur J Neurosci, 23*(1), 251-260. doi: 10.1111/j.1460-9568.2005.04551.x

Oikonomidi, A., Lewczuk, P., Kornhuber, J., Smulders, Y., Linnebank, M., Semmler, A., et al. (2016). Homocysteine metabolism is associated with cerebrospinal fluid levels of soluble amyloid precursor protein and amyloid beta. *J Neurochem, 139*(2), 324-332. doi: 10.1111/jnc.13766

Olofsson, S. O., & Boren, J. (2012). Apolipoprotein B secretory regulation by degradation. *Arterioscler Thromb Vasc Biol, 32*(6), 1334-1338. doi: 10.1161/atvbaha.112.251116

Olofsson, S. O., Bostrom, P., Andersson, L., Rutberg, M., Perman, J., & Boren, J. (2009). Lipid droplets as dynamic organelles connecting storage and efflux of lipids. *Biochim Biophys Acta, 1791*(6), 448-458. doi: 10.1016/j.bbalip.2008.08.001

Olofsson, S. O., Stillemark-Billton, P., & Asp, L. (2000). Intracellular assembly of VLDL: two major steps in separate cell compartments. *Trends Cardiovasc Med, 10*(8), 338-345.

Olofsson, S. O., Wiklund, O., & Boren, J. (2007). Apolipoproteins A-I and B: biosynthesis, role in the development of atherosclerosis and targets for intervention against cardiovascular disease. *Vasc Health Risk Manag, 3*(4), 491-502.

Olsson, A., Hoglund, K., Sjogren, M., Andreasen, N., Minthon, L., Lannfelt, L., et al. (2003). Measurement of alpha- and beta-secretase cleaved amyloid precursor protein in cerebrospinal fluid from Alzheimer patients. *Exp Neurol, 183*(1), 74-80.

Oltersdorf, T., Ward, P. J., Henriksson, T., Beattie, E. C., Neve, R., Lieberburg, I., et al. (1990). The Alzheimer amyloid precursor protein. Identification of a stable intermediate in the biosynthetic/degradative pathway. *J Biol Chem, 265*(8), 4492-4497.

Ong, Q. R., Chan, E. S., Lim, M. L., Cole, G. M., & Wong, B. S. (2014). Reduced phosphorylation of brain insulin receptor substrate and Akt proteins in apolipoprotein-E4 targeted replacement mice. *Sci Rep, 4*, 3754. doi: 10.1038/srep03754

Ooi, E. M., Barrett, P. H., Chan, D. C., & Watts, G. F. (2008). Apolipoprotein C-III: understanding an emerging cardiovascular risk factor. *Clin Sci (Lond), 114*(10), 611-624. doi: 10.1042/cs20070308

Ortega-Martinez, S. (2015). A new perspective on the role of the CREB family of transcription factors in memory consolidation via adult hippocampal neurogenesis. *Front Mol Neurosci, 8*, 46. doi: 10.3389/fnmol.2015.00046

Otero, Y. F., Stafford, J. M., & McGuinness, O. P. (2014). Pathway-selective insulin resistance and metabolic disease: the importance of nutrient flux. *J Biol Chem, 289*(30), 20462-20469. doi: 10.1074/jbc.R114.576355

Ott, A., Stolk, R. P., van Harskamp, F., Pols, H. A., Hofman, A., & Breteler, M. M. (1999). Diabetes mellitus and the risk of dementia: The Rotterdam Study. *Neurology, 53*(9), 1937-1942.

Ozaki, K. I., Awazu, M., Tamiya, M., Iwasaki, Y., Harada, A., Kugisaki, S., et al. (2016). Targeting the ERK signaling pathway as a potential treatment for insulin resistance and type 2 diabetes. *Am J Physiol Endocrinol Metab, 310*(8), E643-e651. doi: 10.1152/ajpendo.00445.2015

Pal, D., Dasgupta, S., Kundu, R., Maitra, S., Das, G., Mukhopadhyay, S., et al. (2012). Fetuin-A acts as an endogenous ligand of TLR4 to promote lipid-induced insulin resistance. *Nat Med, 18*(8), 1279-1285. doi: 10.1038/nm.2851

Pankow, J. S., Duncan, B. B., Schmidt, M. I., Ballantyne, C. M., Couper, D. J., Hoogeveen, R. C., et al. (2004). Fasting plasma free fatty acids and risk of type 2 diabetes: the atherosclerosis risk in communities study. *Diabetes Care, 27*(1), 77-82.

Parker, V. E., Savage, D. B., O'Rahilly, S., & Semple, R. K. (2011). Mechanistic insights into insulin resistance in the genetic era. *Diabet Med, 28*(12), 1476-1486. doi: 10.1111/j.1464-5491.2011.03463.x

Patti, M. E., Butte, A. J., Crunkhorn, S., Cusi, K., Berria, R., Kashyap, S., et al. (2003). Coordinated reduction of genes of oxidative metabolism in humans with insulin resistance and diabetes: Potential role of PGC1 and NRF1. *Proc Natl Acad Sci U S A, 100*(14), 8466-8471. doi: 10.1073/pnas.1032913100

Pedrini, M. T., Kranebitter, M., Niederwanger, A., Kaser, S., Engl, J., Debbage, P., et al. (2005). Human triglyceride-rich lipoproteins impair glucose metabolism and insulin signalling in L6 skeletal muscle cells independently of non-esterified fatty acid levels. *Diabetologia, 48*(4), 756-766. doi: 10.1007/s00125-005-1684-8

Perneczky, R., Guo, L. H., Kagerbauer, S. M., Werle, L., Kurz, A., Martin, J., et al. (2013). Soluble amyloid precursor protein beta as blood-based biomarker of Alzheimer's disease. *Transl Psychiatry, 3*, e227. doi: 10.1038/tp.2013.11

Perseghin, G., Petersen, K., & Shulman, G. I. (2003). Cellular mechanism of insulin resistance: potential links with inflammation. *Int J Obes Relat Metab Disord, 27 Suppl 3*, S6-11. doi: 10.1038/sj.ijo.0802491

Petersen, K. F., Dufour, S., Savage, D. B., Bilz, S., Solomon, G., Yonemitsu, S., et al. (2007). The role of skeletal muscle insulin resistance in the pathogenesis of the metabolic syndrome. *Proc Natl Acad Sci U S A, 104*(31), 12587-12594. doi: 10.1073/pnas.0705408104

Petersen, K. F., & Shulman, G. I. (2002). Pathogenesis of skeletal muscle insulin resistance in type 2 diabetes mellitus. *Am J Cardiol, 90*(5a), 11g-18g.

Petersen, M. C., & Shulman, G. I. (2017). Roles of Diacylglycerols and Ceramides in Hepatic Insulin Resistance. *Trends Pharmacol Sci*. doi: 10.1016/j.tips.2017.04.004

Pilegaard, H., Saltin, B., & Neufer, P. D. (2003). Exercise induces transient transcriptional activation of the PGC-1alpha gene in human skeletal muscle. *J Physiol, 546*(Pt 3), 851-858.

Plucinska, K., Dekeryte, R., Koss, D., Shearer, K., Mody, N., Whitfield, P. D., et al. (2016). Neuronal human BACE1 knockin induces systemic diabetes in mice. *Diabetologia, 59*(7), 1513-1523. doi: 10.1007/s00125-016-3960-1

Pollex, R. L., Ban, M. R., Young, T. K., Bjerregaard, P., Anand, S. S., Yusuf, S., et al. (2007). Association between the -455T>C promoter polymorphism of the APOC3 gene and the metabolic syndrome in a multi-ethnic sample. *BMC Med Genet, 8*, 80. doi: 10.1186/1471-2350-8-80

Pollin, T. I., Damcott, C. M., Shen, H., Ott, S. H., Shelton, J., Horenstein, R. B., et al. (2008). A null mutation in human APOC3 confers a favorable plasma lipid profile and apparent cardioprotection. *Science, 322*(5908), 1702-1705. doi: 10.1126/science.1161524

Powell, D. J., Hajduch, E., Kular, G., & Hundal, H. S. (2003). Ceramide disables 3-phosphoinositide binding to the pleckstrin homology domain of protein kinase B (PKB)/Akt by a PKCzeta-dependent mechanism. *Mol Cell Biol, 23*(21), 7794-7808.

Price, N. L., Gomes, A. P., Ling, A. J., Duarte, F. V., Martin-Montalvo, A., North, B. J., et al. (2012). SIRT1 is required for AMPK activation and the beneficial effects of resveratrol on mitochondrial function. *Cell Metab, 15*(5), 675-690. doi: 10.1016/j.cmet.2012.04.003

Puglielli, L., Ellis, B. C., Saunders, A. J., & Kovacs, D. M. (2003). Ceramide stabilizes beta-site amyloid precursor protein-cleaving enzyme 1 and promotes amyloid beta-peptide biogenesis. *J Biol Chem, 278*(22), 19777-19783. doi: 10.1074/jbc.M300466200

Qiu, W. Q., & Folstein, M. F. (2006). Insulin, insulin-degrading enzyme and amyloid-beta peptide in Alzheimer's disease: review and hypothesis. *Neurobiol Aging, 27*(2), 190-198. doi: 10.1016/j.neurobiolaging.2005.01.004

Qu, W., Han, C., Li, M., Zhang, J., & Jiang, Z. (2017). Anti-TNF-alpha antibody alleviates insulin resistance in rats with sepsis-induced stress hyperglycemia. *J Endocrinol Invest*. doi: 10.1007/s40618-017-0742-7

Rachek, L. I. (2014). Free fatty acids and skeletal muscle insulin resistance. *Prog Mol Biol Transl Sci, 121*, 267-292. doi: 10.1016/b978-0-12-800101-1.00008-9

Randle, P. J., Garland, P. B., Hales, C. N., & Newsholme, E. A. (1963). The glucose fatty-acid cycle. Its role in insulin sensitivity and the metabolic disturbances of diabetes mellitus. *Lancet, 1*(7285), 785-789.

Randle, P. J., Newsholme, E. A., & Garland, P. B. (1964). Regulation of glucose uptake by muscle. 8. Effects of fatty acids, ketone bodies and pyruvate, and of alloxan-diabetes and starvation, on the uptake and metabolic fate of glucose in rat heart and diaphragm muscles. *Biochem J, 93*(3), 652-665.

Rawlings, N. D., & Bateman, A. (2009). Pepsin homologues in bacteria. *BMC Genomics, 10*, 437. doi: 10.1186/1471-2164-10-437

Razak, F., & Anand, S. S. (2004). Impaired mitochondrial activity in the insulin-resistant offspring of patients with type 2 diabetes. Petersen KF, Dufour S, Befroy D, Garcia R, Shulman GI. N Engl J Med 2004; 350: 664-71. *Vasc Med, 9*(3), 223-224. doi: 10.1191/1358863x04vm568xx

Read J., S. C. (2013). *Dropping the BACE: Beta Secretase (BACE1) as an Alzheimer's Disease Intervention Target*.

Reaven, G. M., Mondon, C. E., Chen, Y. D., & Breslow, J. L. (1994). Hypertriglyceridemic mice transgenic for the human apolipoprotein C-III gene are neither insulin resistant nor hyperinsulinemic. *J Lipid Res, 35*(5), 820-824.

Reyna, S. M., Ghosh, S., Tantiwong, P., Meka, C. S., Eagan, P., Jenkinson, C. P., et al. (2008). Elevated toll-like receptor 4 expression and signaling in muscle from insulin-resistant subjects. *Diabetes, 57*(10), 2595-2602. doi: 10.2337/db08-0038

Riboulet-Chavey, A., Pierron, A., Durand, I., Murdaca, J., Giudicelli, J., & Van Obberghen, E. (2006). Methylglyoxal impairs the insulin signaling pathways independently of the formation of intracellular reactive oxygen species. *Diabetes, 55*(5), 1289-1299.

Richardson, D. K., Kashyap, S., Bajaj, M., Cusi, K., Mandarino, S. J., Finlayson, J., et al. (2005). Lipid infusion decreases the expression of nuclear encoded mitochondrial genes and increases the expression of extracellular matrix genes in human skeletal muscle. *J Biol Chem, 280*(11), 10290-10297. doi: 10.1074/jbc.M408985200

Rioux, V., & Legrand, P. (2007). Saturated fatty acids: simple molecular structures with complex cellular functions. *Curr Opin Clin Nutr Metab Care, 10*(6), 752-758. doi: 10.1097/MCO.0b013e3282f01a75

Rockenstein, E., Mante, M., Alford, M., Adame, A., Crews, L., Hashimoto, M., et al. (2005). High beta-secretase activity elicits neurodegeneration in transgenic mice despite reductions in amyloid-beta levels: implications for the treatment of Alzheimer disease. *J Biol Chem, 280*(38), 32957-32967. doi: 10.1074/jbc.M507016200

Roehrich, M. E., Mooser, V., Lenain, V., Herz, J., Nimpf, J., Azhar, S., et al. (2003). Insulin-secreting beta-cell dysfunction induced by human lipoproteins. *J Biol Chem, 278*(20), 18368-18375. doi: 10.1074/jbc.M300102200

Rogers, G. W., Nadanaciva, S., Swiss, R., Divakaruni, A. S., & Will, Y. (2014). Assessment of fatty acid beta oxidation in cells and isolated mitochondria. *Curr Protoc Toxicol, 60*, 25.23.21-19. doi: 10.1002/0471140856.tx2503s60

Ron, D., & Walter, P. (2007). Signal integration in the endoplasmic reticulum unfolded protein response. *Nat Rev Mol Cell Biol, 8*(7), 519-529. doi: 10.1038/nrm2199

Rossner, S., Sastre, M., Bourne, K., & Lichtenthaler, S. F. (2006). Transcriptional and translational regulation of BACE1 expression--implications for Alzheimer's disease. *Prog Neurobiol, 79*(2), 95-111. doi: 10.1016/j.pneurobio.2006.06.001

Roth, R. A., & Beaudoin, J. (1987). Phosphorylation of purified insulin receptor by cAMP kinase. *Diabetes, 36*(1), 123-126.

Rozpedek, W., Markiewicz, L., Diehl, J. A., Pytel, D., & Majsterek, I. (2015). Unfolded Protein Response and PERK Kinase as a New Therapeutic Target in the Pathogenesis of Alzheimer's Disease. *Curr Med Chem, 22*(27), 3169-3184.

Rui, L., Yuan, M., Frantz, D., Shoelson, S., & White, M. F. (2002). SOCS-1 and SOCS-3 block insulin signaling by ubiquitin-mediated degradation of IRS1 and IRS2. *J Biol Chem, 277*(44), 42394-42398. doi: 10.1074/jbc.C200444200

Salerno, A. G., Silva, T. R., Amaral, M. E., Alberici, L. C., Bonfleur, M. L., Patricio, P. R., et al. (2007). Overexpression of apolipoprotein CIII increases and CETP reverses diet-induced obesity in transgenic mice. *Int J Obes (Lond), 31*(10), 1586-1595. doi: 10.1038/sj.ijo.0803646

Salminen, A., Hyttinen, J. M., & Kaarniranta, K. (2011). AMP-activated protein kinase inhibits NF-kappaB signaling and inflammation: impact on healthspan and lifespan. *J Mol Med (Berl), 89*(7), 667-676. doi: 10.1007/s00109-011-0748-0

Saltiel, A. R., & Pessin, J. E. (2002). Insulin signaling pathways in time and space. *Trends Cell Biol, 12*(2), 65-71.

Salvado, L., Coll, T., Gomez-Foix, A. M., Salmeron, E., Barroso, E., Palomer, X., et al. (2013). Oleate prevents saturated-fatty-acid-induced ER stress, inflammation and insulin resistance in skeletal muscle cells through an AMPK-dependent mechanism. *Diabetologia, 56*(6), 1372-1382. doi: 10.1007/s00125-013-2867-3

Salvado, L., Palomer, X., Barroso, E., & Vazquez-Carrera, M. (2015). Targeting endoplasmic reticulum stress in insulin resistance. *Trends Endocrinol Metab, 26*(8), 438-448. doi: 10.1016/j.tem.2015.05.007

Sarbassov, D. D., Guertin, D. A., Ali, S. M., & Sabatini, D. M. (2005). Phosphorylation and regulation of Akt/PKB by the rictor-mTOR complex. *Science, 307*(5712), 1098-1101. doi: 10.1126/science.1106148

Sastre, M., Dewachter, I., Rossner, S., Bogdanovic, N., Rosen, E., Borghgraef, P., et al. (2006). Nonsteroidal anti-inflammatory drugs repress beta-secretase gene promoter activity by the activation of PPARgamma. *Proc Natl Acad Sci U S A, 103*(2), 443-448. doi: 10.1073/pnas.0503839103

Sato, N., & Morishita, R. (2013). Plasma abeta: a possible missing link between Alzheimer disease and diabetes. *Diabetes, 62*(4), 1005-1006. doi: 10.2337/db12-1549

Savage, M. J., Holder, D. J., Wu, G., Kaplow, J., Siuciak, J. A., & Potter, W. Z. (2015). Soluble BACE-1 Activity and sAbetaPPbeta Concentrations in Alzheimer's Disease and Age-Matched Healthy Control Cerebrospinal Fluid from the Alzheimer's Disease Neuroimaging Initiative-1 Baseline Cohort. *J Alzheimers Dis, 46*(2), 431-440. doi: 10.3233/jad-142778

Schaffer, J. E. (2003). Lipotoxicity: when tissues overeat. *Curr Opin Lipidol, 14*(3), 281-287. doi: 10.1097/01.mol.0000073508.41685.7f

Schenk, S., Saberi, M., & Olefsky, J. M. (2008). Insulin sensitivity: modulation by nutrients and inflammation. *J Clin Invest, 118*(9), 2992-3002. doi: 10.1172/jci34260

Scheuner, D., Song, B., McEwen, E., Liu, C., Laybutt, R., Gillespie, P., et al. (2001). Translational control is required for the unfolded protein response and in vivo glucose homeostasis. *Mol Cell, 7*(6), 1165-1176.

Scheuner, D., Vander Mierde, D., Song, B., Flamez, D., Creemers, J. W., Tsukamoto, K., et al. (2005). Control of mRNA translation preserves endoplasmic reticulum function in beta cells and maintains glucose homeostasis. *Nat Med, 11*(7), 757-764. doi: 10.1038/nm1259

Schmitz-Peiffer, C., Craig, D. L., & Biden, T. J. (1999). Ceramide generation is sufficient to account for the inhibition of the insulin-stimulated PKB pathway in C2C12 skeletal muscle cells pretreated with palmitate. *J Biol Chem, 274*(34), 24202-24210.

Schubert, M., Brazil, D. P., Burks, D. J., Kushner, J. A., Ye, J., Flint, C. L., et al. (2003). Insulin receptor substrate-2 deficiency impairs brain growth and promotes tau phosphorylation. *J Neurosci, 23*(18), 7084-7092.

Sears, B., & Perry, M. (2015). The role of fatty acids in insulin resistance. *Lipids Health Dis, 14*, 121. doi: 10.1186/s12944-015-0123-1

Seifert, E. L., Estey, C., Xuan, J. Y., & Harper, M. E. (2010). Electron transport chain-dependent and -independent mechanisms of mitochondrial H2O2 emission during long-chain fatty acid oxidation. *J Biol Chem, 285*(8), 5748-5758. doi: 10.1074/jbc.M109.026203

Senn, J. J. (2006). Toll-like receptor-2 is essential for the development of palmitate-induced insulin resistance in myotubes. *J Biol Chem, 281*(37), 26865-26875. doi: 10.1074/jbc.M513304200

Seubert, P., Vigo-Pelfrey, C., Esch, F., Lee, M., Dovey, H., Davis, D., et al. (1992). Isolation and quantification of soluble Alzheimer's beta-peptide from biological fluids. *Nature, 359*(6393), 325-327. doi: 10.1038/359325a0

Shafrir, E., & Raz, I. (2003). Diabetes: mellitus or lipidus? *Diabetologia, 46*(3), 433-440. doi: 10.1007/s00125-003-1052-5

Shanik, M. H., Xu, Y., Skrha, J., Dankner, R., Zick, Y., & Roth, J. (2008). Insulin resistance and hyperinsulinemia: is hyperinsulinemia the cart or the horse? *Diabetes Care, 31 Suppl 2*, S262-268. doi: 10.2337/dc08-s264

Shao, J., Catalano, P. M., Yamashita, H., Ruyter, I., Smith, S., Youngren, J., et al. (2000). Decreased insulin receptor tyrosine kinase activity and plasma cell membrane glycoprotein-1 overexpression in skeletal muscle from obese women with gestational diabetes mellitus (GDM): evidence for increased serine/threonine phosphorylation in pregnancy and GDM. *Diabetes, 49*(4), 603-610.

Shaw, L. M. (2011). The insulin receptor substrate (IRS) proteins: at the intersection of metabolism and cancer. *Cell Cycle, 10*(11), 1750-1756. doi: 10.4161/cc.10.11.15824

Shi, H., Kokoeva, M. V., Inouye, K., Tzameli, I., Yin, H., & Flier, J. S. (2006). TLR4 links innate immunity and fatty acid-induced insulin resistance. *J Clin Invest, 116*(11), 3015-3025. doi: 10.1172/jci28898

Shin, K. C., Hwang, I., Choe, S. S., Park, J., Ji, Y., Kim, J. I., et al. (2017). Macrophage VLDLR mediates obesity-induced insulin resistance with adipose tissue inflammation. *Nat Commun, 8*(1), 1087. doi: 10.1038/s41467-017-01232-w

Shinjo, S., Jiang, S., Nameta, M., Suzuki, T., Kanai, M., Nomura, Y., et al. (2017). Disruption of the mitochondria-associated ER membrane (MAM) plays a central role in palmitic acid-induced insulin resistance. *Exp Cell Res, 359*(1), 86-93. doi: 10.1016/j.yexcr.2017.08.006

Sisodia, S. S. (1992). Beta-amyloid precursor protein cleavage by a membrane-bound protease. *Proc Natl Acad Sci U S A, 89*(13), 6075-6079.

Solano, D. C., Sironi, M., Bonfini, C., Solerte, S. B., Govoni, S., & Racchi, M. (2000). Insulin regulates soluble amyloid precursor protein release via phosphatidyl inositol 3 kinase-dependent pathway. *Faseb j, 14*(7), 1015-1022.

Soutar, A. K., Myant, N. B., & Thompson, G. R. (1982). The metabolism of very low density and intermediate density lipoproteins in patients with familial hypercholesterolaemia. *Atherosclerosis, 43*(2-3), 217-231.

Southan, C., & Hancock, J. M. (2013). A tale of two drug targets: the evolutionary history of BACE1 and BACE2. *Front Genet, 4*, 293. doi: 10.3389/fgene.2013.00293

Stapleton, D., Mitchelhill, K. I., Gao, G., Widmer, J., Michell, B. J., Teh, T., et al. (1996). Mammalian AMP-activated protein kinase subfamily. *J Biol Chem, 271*(2), 611-614.

Stoehr, J. P., Nadler, S. T., Schueler, K. L., Rabaglia, M. E., Yandell, B. S., Metz, S. A., et al. (2000). Genetic obesity unmasks nonlinear interactions between murine type 2 diabetes susceptibility loci. *Diabetes, 49*(11), 1946-1954.

Sun, K., Kusminski, C. M., & Scherer, P. E. (2011). Adipose tissue remodeling and obesity. *J Clin Invest, 121*(6), 2094-2101. doi: 10.1172/jci45887

Sun, X., Wang, Y., Qing, H., Christensen, M. A., Liu, Y., Zhou, W., et al. (2005). Distinct transcriptional regulation and function of the human BACE2 and BACE1 genes. *Faseb j, 19*(7), 739-749. doi: 10.1096/fj.04-3426com

Szendroedi, J., Yoshimura, T., Phielix, E., Koliaki, C., Marcucci, M., Zhang, D., et al. (2014). Role of diacylglycerol activation of PKCtheta in lipid-induced muscle insulin resistance in humans. *Proc Natl Acad Sci U S A, 111*(26), 9597-9602. doi: 10.1073/pnas.1409229111

Tadaishi, M., Miura, S., Kai, Y., Kano, Y., Oishi, Y., & Ezaki, O. (2011). Skeletal muscle-specific expression of PGC-1alpha-b, an exercise-responsive isoform, increases exercise capacity and peak oxygen uptake. *PLoS One, 6*(12), e28290. doi: 10.1371/journal.pone.0028290

Takasugi, N., Sasaki, T., Suzuki, K., Osawa, S., Isshiki, H., Hori, Y., et al. (2011). BACE1 activity is modulated by cell-associated sphingosine-1-phosphate. *J Neurosci, 31*(18), 6850-6857. doi: 10.1523/jneurosci.6467-10.2011

Takata, H., Ikeda, Y., Suehiro, T., Ishibashi, A., Inoue, M., Kumon, Y., et al. (2009). High glucose induces transactivation of the alpha2-HS glycoprotein gene through the ERK1/2 signaling pathway. *J Atheroscler Thromb, 16*(4), 448-456.

Takeda, K., Kaisho, T., & Akira, S. (2003). Toll-like receptors. *Annu Rev Immunol, 21*, 335-376. doi: 10.1146/annurev.immunol.21.120601.141126

Taniguchi, C. M., Emanuelli, B., & Kahn, C. R. (2006). Critical nodes in signalling pathways: insights into insulin action. *Nat Rev Mol Cell Biol, 7*(2), 85-96. doi: 10.1038/nrm1837

Taskinen, M. R. (2003). Diabetic dyslipidaemia: from basic research to clinical practice. *Diabetologia, 46*(6), 733-749. doi: 10.1007/s00125-003-1111-y

Teruel, T., Hernandez, R., & Lorenzo, M. (2001). Ceramide mediates insulin resistance by tumor necrosis factor-alpha in brown adipocytes by maintaining Akt in an inactive dephosphorylated state. *Diabetes, 50*(11), 2563-2571.

Tharp, W. G., & Sarkar, I. N. (2013). Origins of amyloid-beta. *BMC Genomics, 14*, 290. doi: 10.1186/1471-2164-14-290

Thornton, E., Vink, R., Blumbergs, P. C., & Van Den Heuvel, C. (2006). Soluble amyloid precursor protein alpha reduces neuronal injury and improves functional outcome following diffuse traumatic brain injury in rats. *Brain Res, 1094*(1), 38-46. doi: 10.1016/j.brainres.2006.03.107

Thorpe, C., & Kim, J. J. (1995). Structure and mechanism of action of the acyl-CoA dehydrogenases. *Faseb j, 9*(9), 718-725.

Togashi, N., Ura, N., Higashiura, K., Murakami, H., & Shimamoto, K. (2000). The contribution of skeletal muscle tumor necrosis factor-alpha to insulin resistance and hypertension in fructose-fed rats. *J Hypertens, 18*(11), 1605-1610.

Tomimoto, D., Okuma, C., Ishii, Y., Kobayashi, A., Ohta, T., Kakutani, M., et al. (2015). JTT-553, a novel Acyl CoA:diacylglycerol acyltransferase (DGAT) 1 inhibitor, improves glucose metabolism in diet-induced obesity and genetic T2DM mice. *J Pharmacol Sci, 129*(1), 51-58. doi: 10.1016/j.jphs.2015.08.005

Tomkin, G. H., & Owens, D. (2017). Diabetes and dyslipidemia: characterizing lipoprotein metabolism. *Diabetes Metab Syndr Obes, 10*, 333-343. doi: 10.2147/dmso.s115855

Tong, L., Thornton, P. L., Balazs, R., & Cotman, C. W. (2001). Beta -amyloid-(1-42) impairs activity-dependent cAMP-response element-binding protein signaling in neurons at concentrations in which cell survival Is not compromised. *J Biol Chem, 276*(20), 17301-17306. doi: 10.1074/jbc.M010450200

Tumova, J., Andel, M., & Trnka, J. (2016). Excess of free fatty acids as a cause of metabolic dysfunction in skeletal muscle. *Physiol Res, 65*(2), 193-207.

Tyagi, S., Gupta, P., Saini, A. S., Kaushal, C., & Sharma, S. (2011). The peroxisome proliferator-activated receptor: A family of nuclear receptors role in various diseases. *J Adv Pharm Technol Res, 2*(4), 236-240. doi: 10.4103/2231-4040.90879

Ueki, K., Kondo, T., & Kahn, C. R. (2004). Suppressor of cytokine signaling 1 (SOCS-1) and SOCS-3 cause insulin resistance through inhibition of tyrosine phosphorylation of insulin receptor substrate proteins by discrete mechanisms. *Mol Cell Biol, 24*(12), 5434-5446. doi: 10.1128/mcb.24.12.5434-5446.2004

Um, S. H., Frigerio, F., Watanabe, M., Picard, F., Joaquin, M., Sticker, M., et al. (2004). Absence of S6K1 protects against age- and diet-induced obesity while enhancing insulin sensitivity. *Nature, 431*(7005), 200-205. doi: 10.1038/nature02866

van der Kolk, B. W., Goossens, G. H., Jocken, J. W., & Blaak, E. E. (2016). Altered skeletal muscle fatty acid handling is associated with the degree of insulin resistance in overweight and obese humans. *Diabetologia, 59*(12), 2686-2696. doi: 10.1007/s00125-016-4104-3

Varanasi, U., Chu, R., Chu, S., Espinosa, R., LeBeau, M. M., & Reddy, J. K. (1994). Isolation of the human peroxisomal acyl-CoA oxidase gene: organization, promoter analysis, and chromosomal localization. *Proc Natl Acad Sci U S A, 91*(8), 3107-3111.

Vassar, R. (2014). BACE1 inhibitor drugs in clinical trials for Alzheimer's disease. *Alzheimers Res Ther, 6*(9), 89. doi: 10.1186/s13195-014-0089-7

Vassar, R., Kuhn, P. H., Haass, C., Kennedy, M. E., Rajendran, L., Wong, P. C., et al. (2014). Function, therapeutic potential and cell biology of BACE proteases: current status and future prospects. *J Neurochem, 130*(1), 4-28. doi: 10.1111/jnc.12715

Vega, R. B., Huss, J. M., & Kelly, D. P. (2000). The coactivator PGC-1 cooperates with peroxisome proliferator-activated receptor alpha in transcriptional control of nuclear genes encoding mitochondrial fatty acid oxidation enzymes. *Mol Cell Biol, 20*(5), 1868-1876.

Vercauteren, K., Pasko, R. A., Gleyzer, N., Marino, V. M., & Scarpulla, R. C. (2006). PGC-1-related coactivator: immediate early expression and characterization of a CREB/NRF-1 binding domain associated with cytochrome c promoter occupancy and respiratory growth. *Mol Cell Biol, 26*(20), 7409-7419. doi: 10.1128/mcb.00585-06

Vignini, A., Sartini, D., Morganti, S., Nanetti, L., Luzzi, S., Provinciali, L., et al. (2011). Platelet amyloid precursor protein isoform expression in Alzheimer's disease: evidence for peripheral marker. *Int J Immunopathol Pharmacol, 24*(2), 529-534. doi: 10.1177/039463201102400229

Vijayvargia, R., Mann, K., Weiss, H. R., Pownall, H. J., & Ruan, H. (2010). JNK deficiency enhances fatty acid utilization and diverts glucose from oxidation to glycogen storage in cultured myotubes. *Obesity (Silver Spring), 18*(9), 1701-1709. doi: 10.1038/oby.2009.501

von Arnim, C. A., Kinoshita, A., Peltan, I. D., Tangredi, M. M., Herl, L., Lee, B. M., et al. (2005). The low density lipoprotein receptor-related protein (LRP) is a novel beta-secretase (BACE1) substrate. *J Biol Chem, 280*(18), 17777-17785. doi: 10.1074/jbc.M414248200

Wang, H., Knaub, L. A., Jensen, D. R., Young Jung, D., Hong, E. G., Ko, H. J., et al. (2009). Skeletal muscle-specific deletion of lipoprotein lipase enhances insulin signaling in skeletal muscle but causes insulin resistance in liver and other tissues. *Diabetes, 58*(1), 116-124. doi: 10.2337/db07-1839

Wang, J., Perrard, X. D., Perrard, J. L., Mukherjee, A., Rosales, C., Chen, Y., et al. (2012). ApoE and the role of very low density lipoproteins in adipose tissue inflammation. *Atherosclerosis, 223*(2), 342-349. doi: 10.1016/j.atherosclerosis.2012.06.003

Wang, P., Guan, P. P., Wang, T., Yu, X., Guo, J. J., & Wang, Z. Y. (2014). Aggravation of Alzheimer's disease due to the COX-2-mediated reciprocal regulation of IL-1beta and Abeta between glial and neuron cells. *Aging Cell, 13*(4), 605-615. doi: 10.1111/acel.12209

Wang, R., Li, J. J., Diao, S., Kwak, Y. D., Liu, L., Zhi, L., et al. (2013). Metabolic stress modulates Alzheimer's beta-secretase gene transcription via SIRT1-PPARgamma-PGC-1 in neurons. *Cell Metab, 17*(5), 685-694. doi: 10.1016/j.cmet.2013.03.016

Watts, G. F., Barrett, P. H., Ji, J., Serone, A. P., Chan, D. C., Croft, K. D., et al. (2003). Differential regulation of lipoprotein kinetics by atorvastatin and fenofibrate in subjects with the metabolic syndrome. *Diabetes, 52*(3), 803-811.

Wei, Y., Wang, D., Topczewski, F., & Pagliassotti, M. J. (2006). Saturated fatty acids induce endoplasmic reticulum stress and apoptosis independently of ceramide in liver cells. *Am J Physiol Endocrinol Metab, 291*(2), E275-281. doi: 10.1152/ajpendo.00644.2005

Wende, A. R., Schaeffer, P. J., Parker, G. J., Zechner, C., Han, D. H., Chen, M. M., et al. (2007). A role for the transcriptional coactivator PGC-1alpha in muscle refueling. *J Biol Chem, 282*(50), 36642-36651. doi: 10.1074/jbc.M707006200

Westwick, J. K., Bielawska, A. E., Dbaibo, G., Hannun, Y. A., & Brenner, D. A. (1995). Ceramide activates the stress-activated protein kinases. *J Biol Chem, 270*(39), 22689-22692.

White, M. F., Shoelson, S. E., Keutmann, H., & Kahn, C. R. (1988). A cascade of tyrosine autophosphorylation in the beta-subunit activates the phosphotransferase of the insulin receptor. *J Biol Chem, 263*(6), 2969-2980.

Willem, M., Lammich, S., & Haass, C. (2009). Function, regulation and therapeutic properties of beta-secretase (BACE1). *Semin Cell Dev Biol, 20*(2), 175-182. doi: 10.1016/j.semcdb.2009.01.003

Witters, L. A., & Kemp, B. E. (1992). Insulin activation of acetyl-CoA carboxylase accompanied by inhibition of the 5'-AMP-activated protein kinase. *J Biol Chem, 267*(5), 2864-2867.

Witters, L. A., Watts, T. D., Daniels, D. L., & Evans, J. L. (1988). Insulin stimulates the dephosphorylation and activation of acetyl-CoA carboxylase. *Proc Natl Acad Sci U S A, 85*(15), 5473-5477.

Wu, G., Sankaranarayanan, S., Hsieh, S. H., Simon, A. J., & Savage, M. J. (2011). Decrease in brain soluble amyloid precursor protein beta (sAPPbeta) in Alzheimer's disease cortex. *J Neurosci Res, 89*(6), 822-832. doi: 10.1002/jnr.22618

Wu, H., & Ballantyne, C. M. (2017). Skeletal muscle inflammation and insulin resistance in obesity. *J Clin Invest, 127*(1), 43-54. doi: 10.1172/jci88880

Wyler von Ballmoos, M. C., Haring, B., & Sacks, F. M. (2015). The risk of cardiovascular events with increased apolipoprotein CIII: A systematic review and meta-analysis. *J Clin Lipidol, 9*(4), 498-510. doi: 10.1016/j.jacl.2015.05.002

Xiang, Y., Bu, X. L., Liu, Y. H., Zhu, C., Shen, L. L., Jiao, S. S., et al. (2015). Physiological amyloid-beta clearance in the periphery and its therapeutic potential for Alzheimer's disease. *Acta Neuropathol, 130*(4), 487-499. doi: 10.1007/s00401-015-1477-1

Xiao, C., Giacca, A., & Lewis, G. F. (2011). Sodium phenylbutyrate, a drug with known capacity to reduce endoplasmic reticulum stress, partially alleviates lipid-induced insulin resistance and beta-cell dysfunction in humans. *Diabetes, 60*(3), 918-924. doi: 10.2337/db10-1433

Xie, L., Helmerhorst, E., Taddei, K., Plewright, B., Van Bronswijk, W., & Martins, R. (2002). Alzheimer's beta-amyloid peptides compete for insulin binding to the insulin receptor. *J Neurosci, 22*(10), Rc221. doi: 20026383

Xu, J., Zhou, Q., Xu, W., & Cai, L. (2012). Endoplasmic reticulum stress and diabetic cardiomyopathy. *Exp Diabetes Res, 2012*, 827971. doi: 10.1155/2012/827971

Xu, S., Nam, S. M., Kim, J. H., Das, R., Choi, S. K., Nguyen, T. T., et al. (2015). Palmitate induces ER calcium depletion and apoptosis in mouse podocytes subsequent to mitochondrial oxidative stress. *Cell Death Dis, 6*, e1976. doi: 10.1038/cddis.2015.331

Yang, L. B., Lindholm, K., Yan, R., Citron, M., Xia, W., Yang, X. L., et al. (2003). Elevated beta-secretase expression and enzymatic activity detected in sporadic Alzheimer disease. *Nat Med, 9*(1), 3-4. doi: 10.1038/nm0103-3

Yang, S. P., Bae, D. G., Kang, H. J., Gwag, B. J., Gho, Y. S., & Chae, C. B. (2004). Co-accumulation of vascular endothelial growth factor with beta-amyloid in the brain of patients with Alzheimer's disease. *Neurobiol Aging, 25*(3), 283-290. doi: 10.1016/s0197-4580(03)00111-8

Yang, X., Haghiac, M., Glazebrook, P., Minium, J., Catalano, P. M., & Hauguel-de Mouzon, S. (2015). Saturated fatty acids enhance TLR4 immune pathways in human trophoblasts. *Hum Reprod, 30*(9), 2152-2159. doi: 10.1093/humrep/dev173

Yazici, D., & Sezer, H. (2017). Insulin Resistance, Obesity and Lipotoxicity. *Adv Exp Med Biol, 960*, 277-304. doi: 10.1007/978-3-319-48382-5_12

Yilmaz, E. (2017). Endoplasmic Reticulum Stress and Obesity. *Adv Exp Med Biol, 960*, 261-276. doi: 10.1007/978-3-319-48382-5_11

Yoon, J. C., Puigserver, P., Chen, G., Donovan, J., Wu, Z., Rhee, J., et al. (2001). Control of hepatic gluconeogenesis through the transcriptional coactivator PGC-1. *Nature, 413*(6852), 131-138. doi: 10.1038/35093050

Zetterberg, H., Andreasson, U., Hansson, O., Wu, G., Sankaranarayanan, S., Andersson, M. E., et al. (2008). Elevated cerebrospinal fluid BACE1 activity in incipient Alzheimer disease. *Arch Neurol, 65*(8), 1102-1107. doi: 10.1001/archneur.65.8.1102

Zhang, C., Chen, X., Zhu, R. M., Zhang, Y., Yu, T., Wang, H., et al. (2012). Endoplasmic reticulum stress is involved in hepatic SREBP-1c activation and lipid accumulation in fructose-fed mice. *Toxicol Lett, 212*(3), 229-240. doi: 10.1016/j.toxlet.2012.06.002

Zhang, R., Liu, S., Guo, B., Chang, L., & Li, Y. (2014). Chemerin induces insulin resistance in rat cardiomyocytes in part through the ERK1/2 signaling pathway. *Pharmacology, 94*(5-6), 259-264. doi: 10.1159/000369171

Zhang, W., Wu, M., Kim, T., Jariwala, R. H., Garvey, W. J., Luo, N., et al. (2016). Skeletal Muscle TRIB3 Mediates Glucose Toxicity in Diabetes and High- Fat Diet-Induced Insulin Resistance. *Diabetes, 65*(8), 2380-2391. doi: 10.2337/db16-0154

Zhang, Y., & Ren, J. (2011). Thapsigargin triggers cardiac contractile dysfunction via NADPH oxidase-mediated mitochondrial dysfunction: Role of Akt dephosphorylation. *Free Radic Biol Med, 51*(12), 2172-2184. doi: 10.1016/j.freeradbiomed.2011.09.005

Zhang, Y., Zhou, B., Deng, B., Zhang, F., Wu, J., Wang, Y., et al. (2013). Amyloid-beta induces hepatic insulin resistance in vivo via JAK2. *Diabetes, 62*(4), 1159-1166. doi: 10.2337/db12-0670

Zhao, N., Liu, C. C., Van Ingelgom, A. J., Martens, Y. A., Linares, C., Knight, J. A., et al. (2017). Apolipoprotein E4 Impairs Neuronal Insulin Signaling by Trapping Insulin Receptor in the Endosomes. *Neuron, 96*(1), 115-129.e115. doi: 10.1016/j.neuron.2017.09.003

Zhou, L., Zhang, J., Fang, Q., Liu, M., Liu, X., Jia, W., et al. (2009). Autophagy-mediated insulin receptor down-regulation contributes to endoplasmic reticulum stress-induced insulin resistance. *Mol Pharmacol, 76*(3), 596-603. doi: 10.1124/mol.109.057067

VIII. Annex

Diabetologia (2017) 60:2262–2273
DOI 10.1007/s00125-017-4401-5

ARTICLE

VLDL and apolipoprotein CIII induce ER stress and inflammation and attenuate insulin signalling via Toll-like receptor 2 in mouse skeletal muscle cells

Gaia Botteri[1,2,3] · Marta Montori[1,2,3] · Anna Gumà[2,4] · Javier Pizarro[1,2,3] · Lídia Cedó[2,5] · Joan Carles Escolà-Gil[2,5,6] · Diana Li[7] · Emma Barroso[1,2,3] · Xavier Palomer[1,2,3] · Alison B. Kohan[7] · Manuel Vázquez-Carrera[1,2,3]

Received: 15 May 2017 / Accepted: 30 June 2017 / Published online: 23 August 2017

Abstract

Aim/hypothesis Here, our aim was to examine whether VLDL and apolipoprotein (apo) CIII induce endoplasmic reticulum (ER) stress, inflammation and insulin resistance in skeletal muscle.

Methods Studies were conducted in mouse C2C12 myotubes, isolated skeletal muscle and skeletal muscle from transgenic mice overexpressing apoCIII.

Results C2C12 myotubes exposed to VLDL showed increased levels of ER stress and inflammatory markers whereas peroxisome proliferator-activated receptor γ co-activator 1α (PGC-1α) and AMP-activated protein kinase (AMPK) levels were reduced and the insulin signalling pathway was attenuated. The effects of VLDL were also observed in isolated skeletal muscle incubated with VLDL. The changes caused by VLDL were dependent on extracellular signal-regulated kinase (ERK) 1/2 since they were prevented by the ERK1/2 inhibitor U0126 or by knockdown of this kinase by siRNA transfection. ApoCIII mimicked the effects of VLDL and its effects were also blocked by ERK1/2 inhibition, suggesting that this apolipoprotein was responsible for the effects of VLDL. Skeletal muscle from transgenic mice overexpressing apoCIII showed increased levels of some ER stress and inflammatory markers and increased phosphorylated ERK1/2 levels, whereas PGC-1α levels were reduced, confirming apoCIII effects in vivo. Finally, incubation of myotubes with a neutralising antibody against Toll-like receptor 2 abolished the effects of apoCIII on ER stress, inflammation and insulin resistance, indicating that the effects of apoCIII were mediated by this receptor.

Conclusions/interpretation These results imply that elevated VLDL in diabetic states can contribute to the exacerbation of insulin resistance by activating ERK1/2 through Toll-like receptor 2.

Keywords AMPK · apoCIII · ERK1/2 · TLR2 · VLDL

Abbreviations

ACC	Acetyl-CoA carboxylase
AMPK	AMP-activated protein kinase
Apo	Apolipoprotein
apoCIII Tg	Transgenic mice overexpressing human apoCIII
BiP	Binding immunoglobulin protein
CPT-1	Carnitine palmitoyltransferase 1

Electronic supplementary material The online version of this article (doi:10.1007/s00125-017-4401-5) contains peer-reviewed but unedited supplementary material, which is available to authorised users.

✉ Manuel Vázquez-Carrera
mvazquezcarrera@ub.edu

1 Pharmacology Unit, Department of Pharmacology, Toxicology and Therapeutic Chemistry, Faculty of Pharmacy and Food Sciences, Institut de Biomedicina de la Universidad de Barcelona (IBUB), University of Barcelona, Diagonal 643, E-08028 Barcelona, Spain

2 Centro de Investigación Biomédica en Red de Diabetes y Enfermedades Metabólicas Asociadas (CIBERDEM), Instituto de Salud Carlos III, Barcelona, Spain

3 Institut de Recerca Sant Joan de Déu (IR-SJD), Esplugues de Llobregat, Barcelona, Spain

4 Department of Biochemistry and Molecular Biology and IBUB, University of Barcelona, Barcelona, Spain

5 Institut d'Investigacions Biomèdiques (IIB) Sant Pau, Barcelona, Spain

6 Department of Biochemistry and Molecular Biology, Autonomous University of Barcelona, Barcelona, Spain

7 Department of Nutritional Sciences, University of Connecticut, Storrs, CT, USA

CHOP	CCAAT-enhancer-binding protein homologous protein
eIF2α	Eukaryotic initiation factor 2α
EMSA	Electrophoretic mobility shift assay
ER	Endoplasmic reticulum
ERK	Extracellular signal-regulated kinase
FAO	Fatty acid oxidation
GRP78	Glucose-regulated protein 78
IκB	Inhibitor of κB
IKK-β	IκB kinase β
IRβ	Insulin receptor β-subunit
IRE-1α	Inositol-requiring 1 transmembrane kinase/endonuclease-1α
MAPK	Mitogen-activated protein kinase
MCAD	Medium chain acyl-CoA dehydrogenase
MCP-1	Monocyte chemoattractant protein 1
MEK	MAPK–ERK
NRF1	Nuclear respiratory factor 1
NRF2	Nuclear factor-E2-related factor 2
OXPHOS	Oxidative phosphorylation
PERK	Eukaryotic translation initiation factor-2α kinase 3
PGC-1α	Peroxisome proliferator-activated receptor γ coactivator 1α
PPAR	Peroxisome proliferator-activated receptor
SOCS	Suppressor of cytokine signalling 3
STAT3	Signal transducer and activator of transcription 3
TLR	Toll-like receptor
TRB3	Tribbles 3
UPR	Unfolded protein response
XBP1	X-box binding protein-1

Introduction

Insulin resistance and type 2 diabetes mellitus are characterised by the presence of atherogenic dyslipidaemia, which includes the following cluster of abnormalities: high levels of triacylglycerols, low levels of HDL-cholesterol and the appearance of small, dense LDLs [1]. Atherogenic dyslipidaemia frequently precedes type 2 diabetes mellitus by several years, indicating that derangement of lipid metabolism is an early event in the development of this disease [2]. It is now well accepted that the different components of atherogenic dyslipidaemia are closely linked and are initiated by insulin resistance through overproduction of triacylglycerol-rich VLDL [1, 2]. In addition to triacylglycerols, VLDLs also contain apolipoproteins, of which apolipoprotein (apo) CIII is one of the most abundant [3] with levels that are closely correlated with serum triacylglycerol levels [4]. Plasma apoCIII increases plasma triacylglycerols predominantly through the inhibition of VLDL hydrolysis by lipoprotein lipase and by inhibiting chylomicron and VLDL clearance by the liver [5], but it also causes inflammation in endothelial cells [6]. Furthermore, some studies have associated elevated circulating apoCIII with insulin resistance [7], although others did not find a relationship [8].

Whereas the effects of insulin resistance on lipoprotein metabolism have been studied extensively [1, 2], little is known about the effects of elevated VLDL and apoCIII on the molecular mechanism of insulin resistance in skeletal muscle cells. This is important, since the primary site of insulin-stimulated glucose disposal is skeletal muscle and this can account for up to 90% of glucose clearance [9]. As a result, loss of skeletal muscle insulin sensitivity is believed to be critical in the pathogenesis of type 2 diabetes [10]. The mechanisms involved in the development of insulin resistance are currently unclear, but accumulating evidence points to the presence of a chronic low-level inflammatory process [11]. Among other mechanisms, endoplasmic reticulum (ER) stress [12] and Toll-like receptors (TLRs) [13] can activate proinflammatory signalling pathways, including inhibitor of κB (IκB) kinase β (IKK-β)–NF-κB. Thus, IKK-β phosphorylates IRS-1 on serine residues, attenuating the insulin signalling pathway whereas, once activated, NF-κB regulates the expression of multiple inflammatory mediators, which also contribute to insulin resistance [11].

In the present study, we examined whether VLDL and apoCIII induce ER stress, inflammation and insulin resistance in skeletal muscle cells.

Methods

Materials *Escherichia coli* (K12 strain) lipopolysaccharide (ultrapure) and PAM3CSK4 (tripalmitoylated cysteine-, serine- and lysine-containing peptide) were purchased from InvivoGen (San Diego, CA, USA). LDH Cytotoxicity Assay Kit (88953) was from Thermo Scientific (Waltham, MA, USA) and the Elisa kit for measuring IL-6 secretion (Novex, KMC0061) was from Life Technologies (Carlsbad, CA, USA).

Plasma VLDL isolation VLDL particles (< 1.006 g/ml) were isolated by ultracentrifugation at 100,000*g* for 24 h from normolipidaemic human plasma obtained in EDTA-containing vacutainer tubes (total cholesterol ≤ 5.2 mmol/l, triacylglycerols ≤ 1 mmol/l). To obtain VLDL particles containing low or high amounts of apoCIII, we further isolated light VLDL (Svedberg flotation units 60–400) from normolipidaemic and hypertriacylglycerolaemic (triacylglycerols ≥ 2.5 mmol/l) human plasma by ultracentrifugation at 56,000*g* for 1 h. VLDL preparations were extensively dialysed in PBS and then triacylglycerol and apoB concentrations were measured using a commercial kit adapted to a

COBAS c501 autoanalyser (Roche Diagnostics, Rotkreuz, Switzerland). ApoB/triacylglycerol ratios were similar in both light VLDL preparations. ApoCIII levels were determined using a nephelometric commercial kit (Kamiya Biomedical Company, Seattle, WA, USA) adapted to COBAS c501 autoanalyser. Cells were treated with 300 μg/ml of filtered VLDL, based on triacylglycerol concentration, as previously described [14].

Cell culture Mouse mycoplasma free C2C12 cells (ATCC, Manassas, VA, USA) were maintained, grown and differentiated to myotubes as previously described [15]. ATCC provided authentication of the cells. Where indicated, cells were treated with 10 μmol/l U0126, 100 μg/ml apoCIII (purity > 95%) (Abcam, Cambridge, UK), 50 μg/ml TLR2 neutralising antibody (InvivoGen) or control non-immune IgG for 24 h. Cells were transiently transfected with 50 nmol/l siRNA against extracellular signal-regulated kinase (ERK) 1/2 (Santa Cruz, Dallas, TX, USA) and siRNA control using Lipofectamine 2000 (Life Technologies) according to the manufacturer's instructions.

Animals Skeletal muscle (gastrocnemius) samples from male wild-type and transgenic mice overexpressing human apoCIII (apoCIII Tg; C57BL/6J background) were frozen in liquid nitrogen and then stored at − 80°C. For ex vivo experiments, skeletal muscles were isolated from male C57BL/6J mice (6–8 weeks old) and mounted in an incubation bath as previously described [16] in the presence or absence of 500 μg/ml VLDL. Experimenters were not blind to group assignment or outcome assessment. For further details, please refer to the electronic supplementary material (ESM) Methods.

RNA preparation and quantitative RT-PCR Relative levels of specific mRNAs were assessed by real-time PCR, as previously described [15]. For details, see ESM Methods. The primer sequences used are shown in ESM Table 1.

Immunoblotting Isolation of total and nuclear protein extracts was performed as described elsewhere [15]. Western blot analysis was performed using antibodies against total (1:1000, 9272) and phospho-Akt (Ser^{473}) (1:1000, 9271), glucose-regulated protein78 (GRP78)/binding immunoglobulin protein (BiP) (1:1000, 3177), insulin receptor β-subunit (IRβ) (1:1000, 3020), CCAT-enhancer-binding protein homologous protein (CHOP) (1:1000, 5554), total eukaryotic initiation factor 2α (eIF2α) (1:1000, 9722) and phospho-eIF2α (Ser^{51}) (1:1000, 9721S), total signal transducer and activator of transcription 3 (STAT3) (1:1000, 9132) and phospho-STAT3 (Tyr^{705}) (1:1000, 9131), total extracellular signal-regulated kinase (ERK) 1/2 (1:1000, 9102) and phospho-ERK1/2 (Thr^{202}/Tyr^{204}) (1:1000, 9101), total

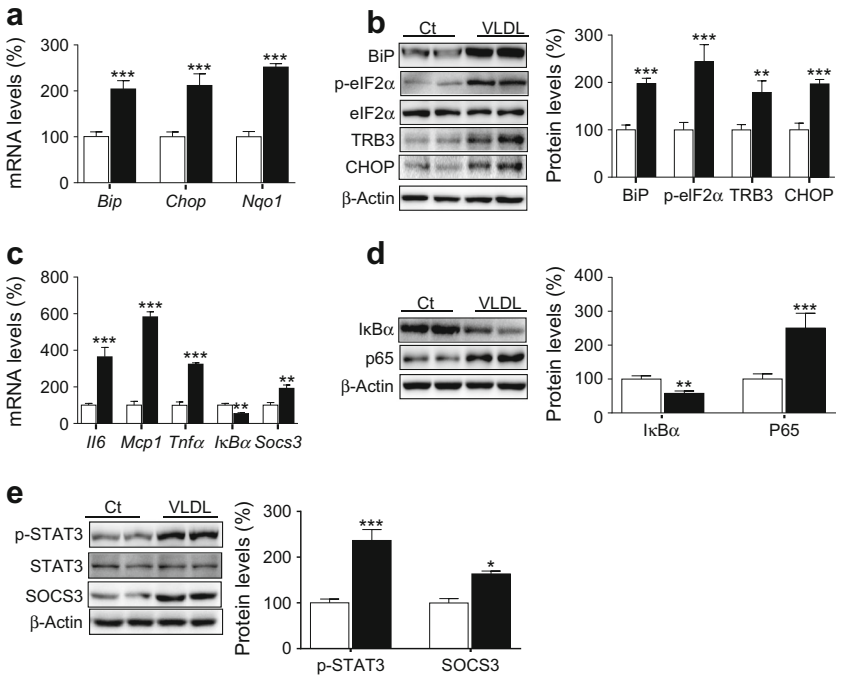

Fig. 1 VLDL induces ER stress and inflammation. Mouse C2C12 myotubes were incubated in the presence (black bars) or absence (control, Ct, white bars) of 300 μg/ml VLDL for 24 h. (**a**) mRNA abundance of *Bip*, *Chop* and *Nqo1*. mRNA levels are normalised to *Aprt* (n = 8–10, five independent C2C12 cultures were used). (**b**) BiP, phospho-eIF2α (Ser^{51}), TRB3, CHOP and β-actin protein levels. (**c**), mRNA abundance of *Il6*, *Mcp1*, *Tnfα* , *IκBα* and *Socs3*. (**d**) IκBα, p65 and β-actin protein levels. (**e**) Phospho-STAT3 (Tyr^{705}), SOCS3 and β-actin protein levels. The graphs show quantification expressed as a percentage of control samples. Data are means ± SD of five independent experiments and were compared by Student's t test. *$p < 0.05$, **$p < 0.01$ and ***$p < 0.001$ vs control

acetyl-CoA carboxylase (ACC) (1:1000, 3662) and phospho-ACC (Ser^{79}) (1:1000, 3661), NQO1 (1:500, 62,262), nuclear respiratory factor 1 (NRF1) (1:500, 12,381), nuclear factor-E2-related factor 2 (NRF2) (1:500, 4399), phospho-IRS-1 (Ser^{307}) (1:500, 2381), IκBα (1:500, 9242), p65 (1:500, 3034), total AMP-activated protein kinase (AMPK) (1:1000, 2532) and phospho-AMPK (Thr^{172}) (1:1000, 2531) (all from Cell Signaling Technology, Danvers, MA, USA; numbers indicate catalogue number), oxidative phosphorylation (1:1000, ab110413) (OXPHOS), peroxisome proliferator-activated receptor γ co-activator 1α (PGC-1α; (1:1000, ab54481) (Abcam), OCT-1 (1:500, sc-8024X), peroxisome proliferator-activated receptor (PPAR)β/δ (1:500, sc-7197), prohibitin (1:500, sc-377037), suppressor of cytokine signalling 3 (SOCS3) (1:500, sc-51699), Tribbles 3 (TRB3) (1:500, sc-365842), glyceraldehyde 3-phosphate dehydrogenase (1:500, sc-32233), total IRS-1 (1:500, sc-560) and β-actin (1:500, sc-47778) (all from Santa Cruz; numbers indicate catalogue number). Detection was achieved using the Western Lightning Plus-ECL chemiluminescence kit (PerkinElmer, Waltham, MA, USA). The equal loading of proteins was assessed by Ponceau S staining. For validation, we used a protein marker (Precision Plus Protein Dual Color Standards 1610374; Bio-Rad, Hercules, CA, USA), on the same blots. All of these commercially available antibodies showed a single distinct band at the molecular weight indicated in the datasheets.

Electrophoretic mobility shift assay The electrophoretic mobility shift assay (EMSA) was performed as described in ESM Methods.

2-Deoxy-D-(1,2-[^{3}H]N)glucose uptake Glucose uptake experiments were performed as described in ESM Methods.

Image analysis The chemiluminescent blots were imaged using the ChemiDoc MP imager (Bio-Rad). Image acquisition and subsequent densitometric analysis of the corresponding blots were performed using ImageLab software version 4.1 (Bio-Rad). For further details, see ESM Methods.

Statistical analyses Results were normalised to levels in control groups and are expressed as mean ± SD. Significant differences were established by either Student's *t* test or two-way ANOVA, according to the number of groups compared, using GraphPad Prism V4.03 software (GraphPad Software, San Diego, CA, USA). When significant variations were found by two-way ANOVA, the Tukey–Kramer multiple comparison post hoc test was performed. Differences were considered significant at $p < 0.05$.

Results

VLDL induces ER stress, inflammation and insulin resistance in myotubes VLDL exposure significantly increased expression of the ER stress markers *Bip* (also known as *Hspa5*), *Chop* (*Ddit3*) and *Nqo1*, the latter being an NRF2-target gene activated by ER stress (Fig. 1a). Consistent with

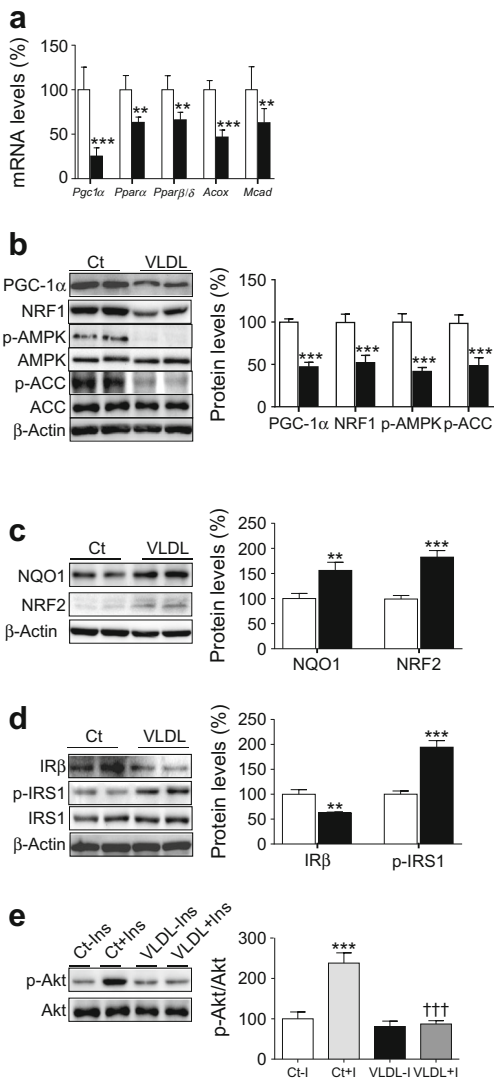

Fig. 2 VLDL reduces PGC-1α and AMPK levels and induces insulin resistance. Mouse C2C12 myotubes were incubated in the presence (black bars) or absence (control, Ct, white bars) of 300 μg/ml VLDL for 24 h. (**a**) *Pgc1α*, *Pparα* (*Ppara*), *Pparβ/δ* (*Pparb*/*Ppard*), *Acox* and *Mcad* mRNA levels (n = 8–10, five independent C2C12 cultures were used). (**b**) PGC-1α, NRF1, phospho-AMPK (Thr^{172}), phospho-ACC (Ser^{79}) and β-actin protein levels. (**c**) NQO1, NRF2 and β-actin protein levels. (**d**) IRβ, phospho-IRS-1 (Ser^{307}), and β-actin protein levels. (**e**) Phospho-Akt (Ser^{473}) protein levels. Where indicated, cells were incubated with 100 nmol/l insulin (Ins, I) for the last 10 min. The graphs show quantification expressed as a percentage of control samples. Data are means ± SD of five independent experiments and compared by Student's *t* test (**a**–**d**) or two-way ANOVA followed by Tukey post hoc test (**e**). $^{**}p < 0.01$ and $^{***}p < 0.001$ vs control; $^{\dagger\dagger\dagger}p < 0.001$ vs control cells incubated with insulin

the presence of VLDL-induced ER stress, the protein levels of BiP, phospho-eIF2α, CHOP and TRB3, a pseudokinase that mediates ER stress-induced insulin resistance in myotubes [17], were increased by VLDL (Fig. 1b). VLDL exposure also increased the mRNA levels of inflammatory genes such as *Il6*, *Mcp1* (also known as *Ccl2*) and *Tnfα* (*Tnf*), whereas the mRNA expression of the NF-κB inhibitor *IκBα* (*Nfkbia*) was reduced (Fig. 1c). IL-6 induces insulin resistance by activating STAT3, which in turn upregulates the transcription of SOCS3. SOCS3 inhibits insulin signalling through several distinct mechanisms, including IRS degradation [18]. In agreement with the increase in IL-6 expression, the mRNA levels of *Socs3* were also increased after VLDL exposure (Fig. 1c). The potential activation of the NF-κB pathway by VLDL was confirmed by the presence of reduced protein levels of IκBα and enhanced levels of the p65 subunit of NF-κB (Fig. 1d). Similarly, increased protein levels of phospho-STAT3 (phosphorylated at Tyr^{705}) and SOCS3 demonstrated the activation of the STAT3–SOCS3 pathway by VLDL (Fig. 1e).

Mitochondrial function is transcriptionally controlled by PGC-1α [19], which plays a critical role in skeletal muscle metabolic function. In fact, some studies indicate that the reported reduction in PGC-1α expression and/or function in the skeletal muscle of individuals who have diabetes or are at risk for diabetes [20, 21] induces insulin resistance by reducing oxidative phosphorylation and lipid oxidation, leading to accumulation of lipid derivatives in skeletal muscle [22]. Myotubes exposed to VLDL showed a reduction in the mRNA expression of *Pgc1α* (also known as *Ppargc1a*) (Fig. 2a). This transcriptional co-activator regulates the activity of several transcription factors, including PPARα and PPARβ/δ, which control the expression/function of genes involved in fatty acid oxidation (FAO) [23]. The expression of these transcription factors and that of their target genes involved in FAO, such as those encoding acyl-coA oxidase (*Acox*, also known as *Acox1*) and medium chain acyl-CoA dehydrogenase (*Mcad*, also known as *Acadm*), was also decreased by VLDL (Fig. 2a). In addition, PGC-1α protein levels were downregulated by VLDL and, consistent with this reduction, the protein levels of its downstream transcription factor NRF1 [24] were also reduced (Fig. 2b). FAO is also under the control of AMPK, whose activation exerts multiple protective effects, including inhibition of inflammation and insulin resistance [25]. Activation of this kinase upregulates PGC-1α levels and

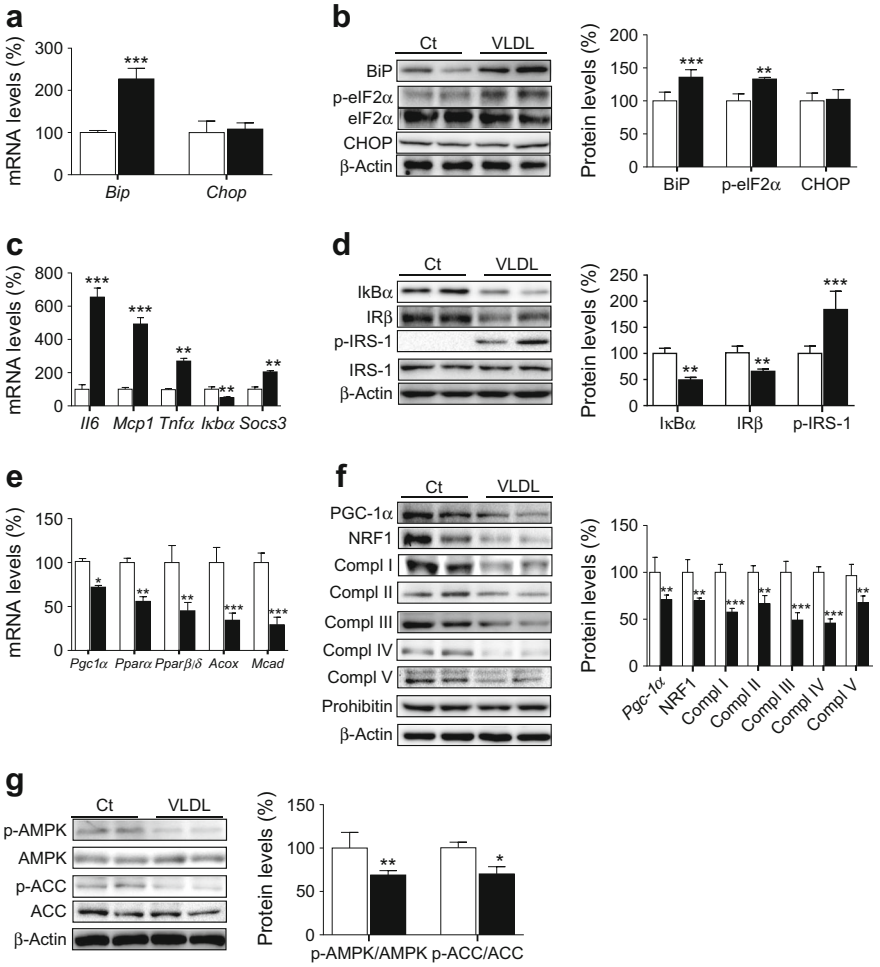

Fig. 3 VLDL induces ER stress and inflammation, reduces the levels of mitochondrial proteins and attenuates the insulin signalling pathway in isolated skeletal muscle. Mouse gastrocnemius muscles were incubated in the presence (black bars) or absence (control, Ct, white bars) of 500 μg/ml VLDL for 6 h. (**a**) mRNA abundance of *Bip* and *Chop*. (**b**) BiP, Phospho-eIF2α (Ser^{51}), CHOP and β-actin protein levels. (**c**) mRNA abundance of *Il6*, *Mcp1*, *Tnfα*, *Ikbα* and *Socs3*. (**d**) IκBα, IRβ, phospho-IRS-1 (Ser^{307}), and β-actin protein levels. (**e**) *Pgc1α*, *Pparα*, *Pparβ/δ*, *Acox* and *Mcad* mRNA levels. (**f**) PGC-1α, NRF1, OXPHOS complexes (Compl), prohibitin and β-actin protein levels. (**g**) Phospho-AMPK (Thr^{172}), phospho-ACC (Ser^{79}) and β-actin protein levels. The graphs show quantification expressed as a percentage of control. Data are means ± SD of five independent experiments and were compared by Student's *t* test. $^{*}p < 0.05$, $^{**}p < 0.01$ and $^{***}p < 0.001$ and vs control

increases FAO by phosphorylating ACC at Ser^{79}, leading to inhibition of ACC's activity and decreased malonyl-CoA content, which inhibits carnitine palmitoyltransferase (CPT-1), the rate-limiting step in FAO in mitochondria [25]. VLDL reduced the levels of both phospho-AMPK and phospho-ACC in myotubes (Fig. 2b), whereas it increased the protein levels of the redox transcription factor NRF2 and the protein encoded by its target gene *Nqo1* (Fig. 2c).

When we examined proteins involved in the insulin signalling pathway, we observed that in agreement with a previous study reporting that ER stress reduced insulin receptor levels in adipocytes [26], protein levels of IRβ were reduced in VLDL-exposed cells (Fig. 2d). In addition, VLDL increased IRS-1 phosphorylation at Ser^{307} (Fig. 2d) and blunted insulin-stimulated Akt phosphorylation (Fig. 2e).

VLDL increases ER stress, mitochondrial dysfunction and inflammation in isolated skeletal muscle Next, we examined the effects of VLDL on skeletal muscle. Gastrocnemius muscles isolated from mice were incubated with VLDL for 6 h, which resulted in an increase in the mRNA expression and protein levels of BiP and phospho-eIF2α, whereas no changes were observed in CHOP (Fig. 3a, b). Muscles exposed to VLDL also showed a significant increase in the mRNA levels of *Il6*, *Mcp1* and *Tnfα* (Fig. 3c), consistent with the reduction in IκBα (Fig. 3d). VLDL also reduced IRβ protein levels and increased IRS phosphorylation at Ser^{307} (Fig. 3d). Similar to what we observed in vitro, VLDL caused a marked reduction in the expression of *Pgc1α*, *Pparα*, *Pparβ/δ*, and their target genes involved in FAO (Fig. 3e). Consistent with the reported regulation of mitochondrial OXPHOS genes [27] and NRF1 [24] by PGC-1α, the reduction in the protein levels of this transcriptional co-activator caused by VLDL was accompanied by a reduction in NRF1 and the different OXPHOS complexes (Fig. 3f). In addition, a reduction was detected in phospho-AMPK and phospho-ACC in muscles exposed to VLDL (Fig. 3g).

ERK1/2 inhibition prevents the effects of VLDL Interestingly, TLR-mediated NF-κB activation requires mitogen-activated protein kinase (MAPK)–ERK (MEK) 1/2 [28] and activation of both MEK1/2 and NF-κB results in the

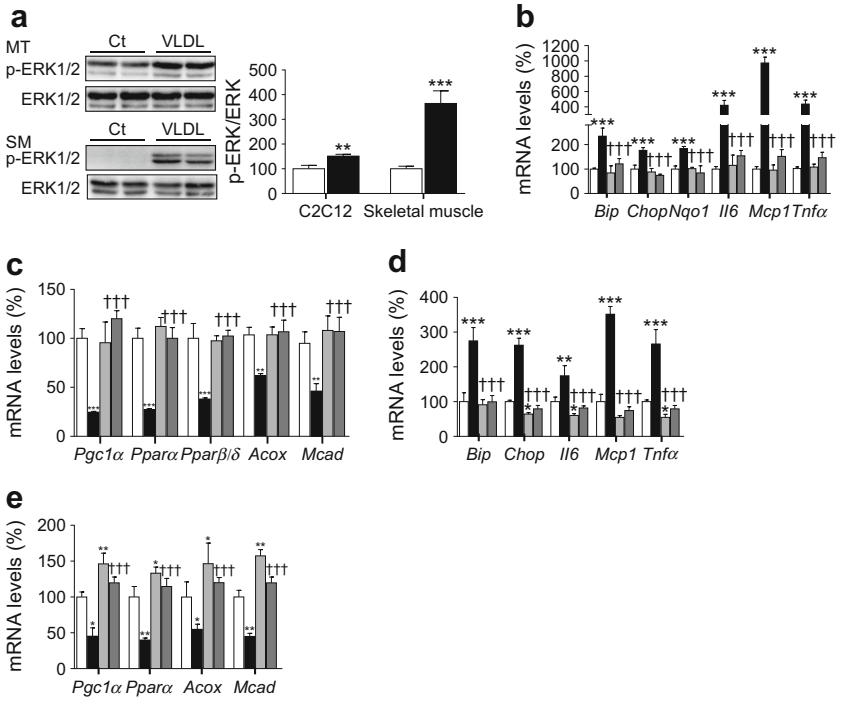

Fig. 4 ERK1/2 inhibition and knockdown prevents the effects of VLDL. (**a**) C2C12 myotubes (MT) and isolated skeletal muscles (SM) were incubated in the presence (black bars) or absence (control, Ct, white bars) of 300 μg/ml VLDL (myotubes) or 500 μg/ml VLDL (muscle) and the protein levels of phospho-ERK1/2 (Thr^{202}/Tyr^{204}) were analysed. (**b**, **c**) C2C12 myotubes were incubated in the presence (black bars) or absence (control, white bars) of 300 μg/ml VLDL for 24 h; 10 μmol/l U0126 was added to control (light grey bars) or VLDL-treated (dark grey bars) myotubes and the mRNA abundance of *Bip*, *Chop*, *Nqo1*, *Il6*, *Mcp1* and *Tnfα* (**b**) and *Pgc1α*, *Pparα*, *Pparβ/δ*, *Acox* and *Mcad* (**c**) was evaluated. (**d**, **e**) C2C12 cells were transfected with control siRNA or ERK1/2 siRNA and incubated in the presence or absence of 300 μg/ml VLDL. The mRNA abundance of *Bip*, *Chop*, *Il6*, *Mcp1* and *Tnfα* (**d**) and *Pgc1α*, *Pparα*, *Acox* and *Mcad* (**e**) was evaluated. White bars, control siRNA; light grey bars ERK1/2 siRNA; black bars VLDL + control siRNA; dark grey bars VLDL+ERK1/2 siRNA. The graphs show quantification expressed as a percentage of control. Data are means ± SD of five independent experiments and were compared by Student's *t* test (**a**) or two-way ANOVA followed by Tukey post hoc test (**b**–**e**). *$p < 0.05$, **$p < 0.01$ and ***$p < 0.001$ vs control; $^{\dagger\dagger\dagger}p < 0.001$ vs VLDL-exposed cells

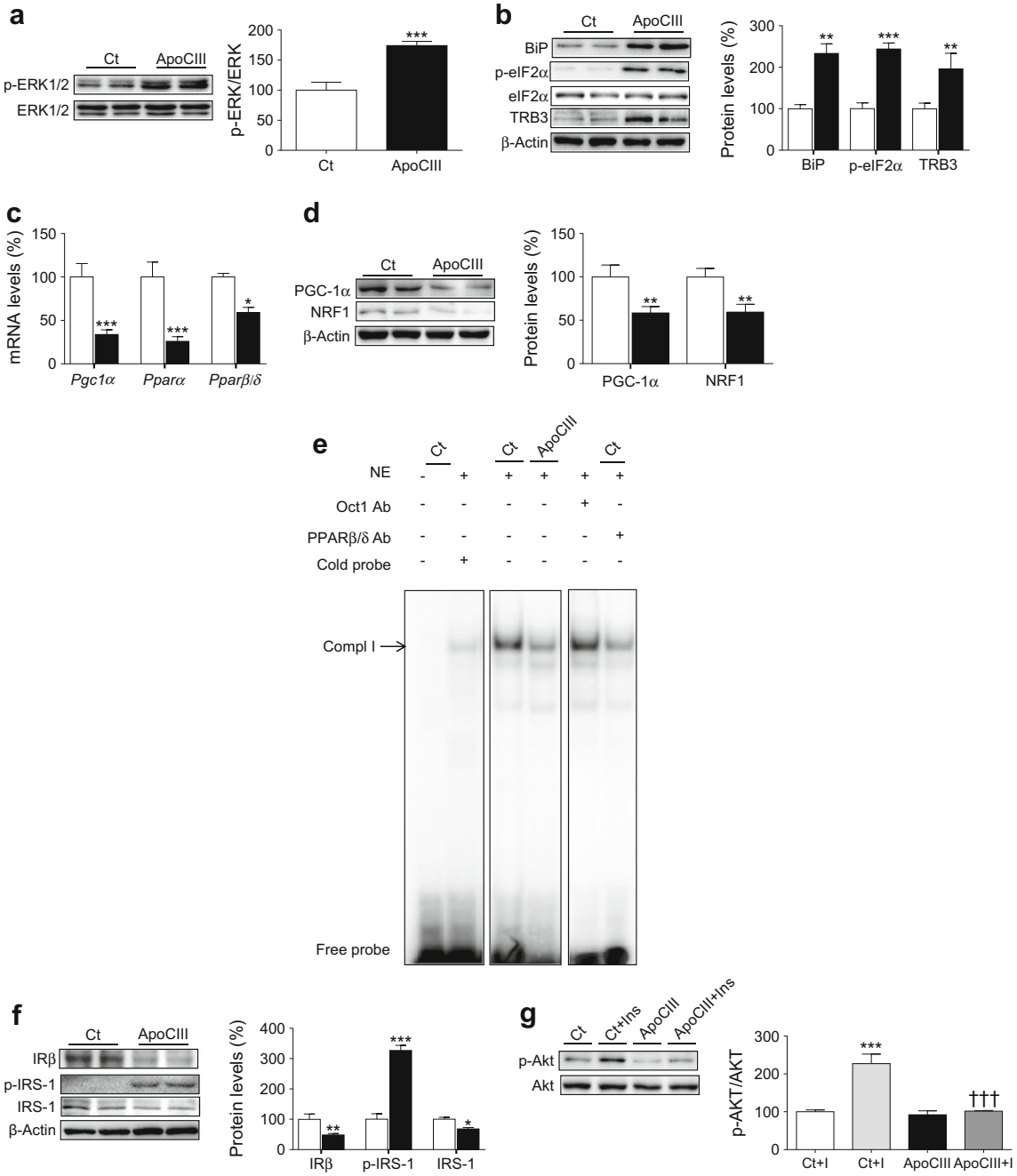

Fig. 5 ApoCIII activates ERK1/2 and induces ER stress, inflammation and insulin resistance. C2C12 myotubes were incubated in the presence (black bars) or absence (control, Ct, white bars) of 100 μg/ml apoCIII for 24 h. (**a**) Phospho-ERK1/2 (Thr^{202}/Tyr^{204}) protein levels. (**b**) BiP, phospho-eIF2α (Ser^{51}), TRB3 and β-actin protein levels. (**c**) mRNA abundance of *Pgc1α*, *Pparα* and *Pparβ/δ*. (**d**) PGC-1α, NRF1 and β-actin protein levels. (**e**) Autoradiograph of EMSA performed with a ^{32}P-labelled PPAR nucleotide and crude nuclear protein extract (NE) from C2C12 myotubes. One main specific complex (Compl I) based on competition with a molar excess of unlabelled probe is shown. The supershift assay performed by incubating NE with an antibody (Ab) directed against PPARβ/δ shows a reduction in the band, whereas the band is unchanged by an unrelated antibody against Oct1. (**f**) IRβ, phospho-IRS-1 (Ser^{307}) and β-actin protein levels. (**g**) Phosphorylated Akt (Ser^{473}) protein levels. Where indicated, cells were incubated with 100 nmol/l insulin (Ins, I) for the last 10 min. The graphs show quantification expressed as a percentage of control. Data are means ± SD of five independent experiments and were compared by Student's *t* test (**a**–**f**) or two-way ANOVA followed by Tukey post hoc test (**g**). $^{*}p < 0.05$, $^{**}p < 0.01$ and $^{***}p < 0.001$ vs control; $^{†††}p < 0.001$ vs control cells incubated with insulin

downregulation of PGC-1α in myotubes [29]. Similarly, an inhibitory crosstalk between AMPK and ERK1/2 has been reported and inhibition of ERK1/2 was found to improve AMPK and Akt pathways and to reverse ER stress-induced insulin resistance in myotubes [30]. These data prompted us to investigate whether the ERK–MAPK cascade was involved in

the effects mediated by VLDL. This possibility was supported by the fact that VLDL increased phospho-ERK1/2 levels in both cultured myotubes and isolated muscle (Fig. 4a). Next, we used U0126, a potent and specific ERK1/2 inhibitor that binds to MEK, thereby inhibiting its catalytic activity and phosphorylation of ERK1/2, to investigate whether inhibition of this kinase prevented the effects caused by VLDL. U0126 prevented the increase in the expression of ER stress and inflammatory markers (Fig. 4b) and the reduction in genes involved in FAO (Fig. 4c). Knockdown of ERK1/2 by siRNA transfection (ESM Fig. 1) confirmed that this kinase was responsible for the effects of VLDL on ER stress and inflammation (Fig. 4d) and the reduction in genes involved in FAO (Fig. 4e).

ApoCIII mimics the effects of VLDL through TLR2 Given that apoCIII is the most abundant apolipoprotein in VLDL in individuals with diabetes [3], we next investigated whether this apolipoprotein was responsible for the effects of VLDL in myotubes. Exposure of myotubes to light VLDL with high or low apoCIII content isolated from plasma of hypertriacylglycerolaemia or normolipidaemic individuals, respectively, showed that light VLDL with low levels of apoCIII did not cause the effects observed with VLDL with high apoCIII content (ESM Fig. 2a,b). Incubation of myotubes with apoCIII did not cause toxicity (ESM Fig. 2c) and led to a significant increase in phospho-ERK1/2 (Fig. 5a), TRB3, phospho-eIF2α and BiP protein levels (Fig. 5b), as well as secretion of IL-6 (ESM Fig. 2d), indicating that this apolipoprotein induces ER stress and inflammation. In contrast, apoCIII exposure reduced the expression of *Pgc1α*, *Pparα* and *Pparβ/δ* (Fig. 5c) and reduced the protein levels of PGC-1α and NRF1 (Fig. 5d). In agreement with this, apoCIII reduced the DNA-binding activity of PPARβ/δ (Fig. 5e). Moreover, the effects of apoCIII were concentration dependent (ESM Fig. 3). The induction of ER stress caused by apoCIII was accompanied by a reduction in the protein levels of IRβ and an increase in IRS-1 phosphorylated at Ser^{307} (Fig. 5f), whereas insulin-stimulated Akt phosphorylation was mitigated (Fig. 5g). No changes were observed in ER stress and inflammatory markers or in the protein levels of PGC-1α and phospho-

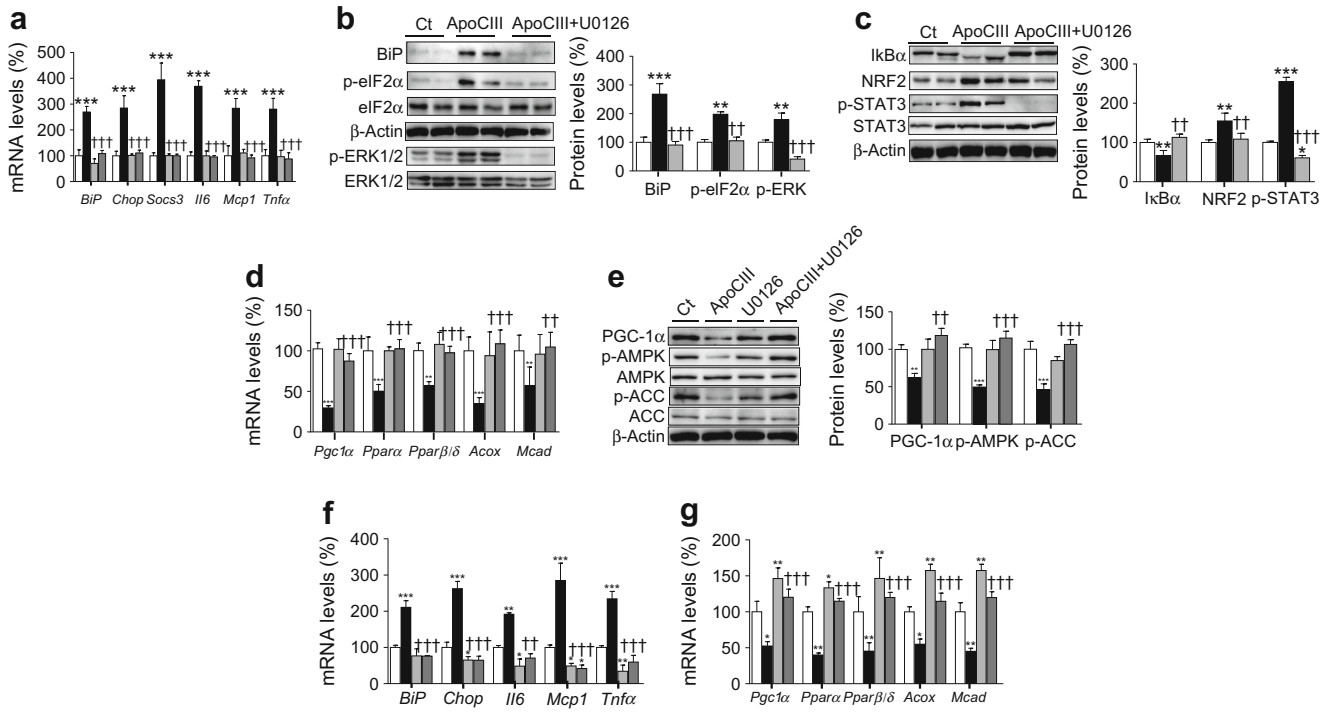

Fig. 6 ERK1/2 inhibition prevents the effects of apoCIII on ER stress and inflammation. (**a**–**e**) C2C12 myotubes were incubated in the presence (black bars) or absence (control, Ct, white bars) of 100 μg/ml apoCIII for 24 h; 10 μmol/l U0126 was added to control myotubes (light grey bars) or apoCIII-treated myotubes (dark grey bars). (**a**) mRNA abundance of *Bip*, *Chop*, *Socs3*, *Il6*, *Mcp1* and *Tnfα*. (**b**) BiP, phospho-eIF2α (Ser^{51}), phospho-ERK1/2 (Thr^{202}/Tyr^{204}) and β-actin protein levels. (**c**) IκBα, NRF2, phospho-STAT3 (Tyr^{705}) and β-actin protein levels. (**d**) mRNA abundance of *Pgc1α*, *Pparα*, *Pparβ/δ*, *Acox* and *Mcad*. (**e**) PGC-1α, phospho-AMPK (Thr^{172}), phospho-ACC (Ser^{79}) and β-actin protein levels. (**f**, **g**) C2C12 myotubes were transfected with control or ERK1/2 siRNA and incubated in the presence or absence of 100 μg/ml apoCIII for 24 h. The mRNA abundance of *Bip*, *Chop*, *Il6*, *Mcp1* and *Tnfα* (**f**) and *Pgc-1α*, *Pparα*, *Pparβ/δ*, *Acox* and *Mcad* (**g**) was evaluated. White bars, control siRNA; light grey bars ERK1/2 siRNA; black bars, apoCIII+ control siRNA; dark grey bars, apoCIII+ERK1/2 siRNA The graphs show quantification expressed as a percentage of control. Data are means ± SD of five independent experiments and were compared by two-way ANOVA followed by Tukey post hoc test. *$p < 0.05$, **$p < 0.01$ and ***$p < 0.001$ vs control; $^{††}p < 0.01$ and $^{†††}p < 0.001$ vs apoCIII-exposed cells

ERK1/2 when cells were incubated with apoCI, indicating that the effects of apoCIII were specific (ESM Fig. 4a,b). In addition, VLDL and apoCIII reduced insulin-stimulated glucose uptake, whereas light VLDL low in apoCIII did not (ESM Fig. 4c). Moreover, apoCIII intensified the effects of the saturated fatty acid palmitate on the levels of ER stress markers, ERK1/2 phosphorylation, PGC-1α and insulin signalling pathway (ESM Fig. 4d), indicating that the increase in apoCIII might exacerbate the effects of lipids on insulin resistance.

The increase in the expression of ER stress and inflammatory markers caused by apoCIII was blunted by co-incubation with U0126 (Fig. 6a). Likewise, U0126 prevented the increase in the protein levels of BiP, phospho-eIF2α and phospho-ERK1/2 caused by apoCIII (Fig. 6b). Inhibition of the MAPK–ERK1/2 pathway also prevented the reduction in IκBα and the increase in the DNA-binding activity of NF-κB (ESM Fig. 5a) and the increase in NRF2 and phospho-STAT3 (Tyr^{705}) (Fig. 6c) observed in cells exposed only to apoCIII. ApoCIII also reduced the expression of *Pgc1α*, *Pparα* and *Pparβ/δ* and their target genes involved in FAO–changes that were abolished by U0126 (Fig. 6d). Additionally, the reduction in the protein levels of PGC-1α, phospho-AMPK and phospho-ACC was reversed by U0126 (Fig. 6e). siRNA knockdown of ERK1/2 confirmed that this kinase was responsible for the increase in ER stress and inflammation (Fig. 6f) and the reduction in FAO genes (Fig. 6g) caused by apoCIII.

Next, we examined whether some of the changes caused by apoCIII in vitro were observed in skeletal muscle of transgenic mice with human apoCIII overexpression (apoCIII Tg) (Fig. 7a). These mice have marked elevations in plasma triacylglycerols but no impairment of glucose tolerance [31]. However, apoCIII Tg mice fed a high-fat diet show hepatic insulin resistance [7] and are more susceptible to development of diabetes [32]. In skeletal muscle of apoCIII Tg mice fed a standard diet, increased *Chop*, *Il6* and *Tnfα* expression was detected when these mice were compared with non-transgenic littermates, whereas no changes were observed in *Bip* mRNA levels (Fig. 7b). Moreover, the marked increase in the protein levels of phospho-ERK1/2 in skeletal muscle from apoCIII Tg mice was accompanied by a reduction in PGC-1α protein levels (Fig. 7c, d).

Since TLRs activate ERK1/2 and cause inflammation [28], we examined whether apoCIII acted through these receptors. We incubated mouse C2C12 myotubes exposed to apoCIII with a selective neutralising antibody against either TLR2 or IgG (ESM Fig. 5b). In the presence of this neutralising antibody, the increase in phospho-ERK1/2 levels caused by apoCIII alone was blunted (Fig. 8a). Consistent with a crucial role for ERK1/2 in the effects caused by apoCIII, the TLR2 neutralising antibody prevented the apoCIII-induced changes in the mRNA (Fig. 8b) and protein (Fig. 8c) levels of ER stress

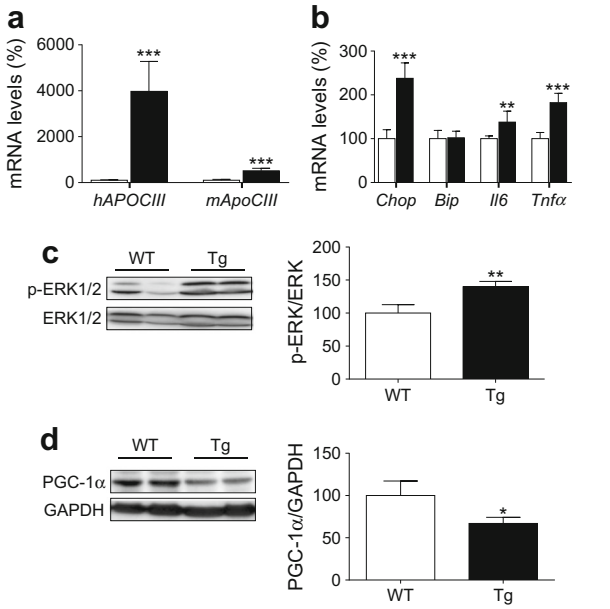

Fig. 7 Skeletal muscle from apoCIII Tg mice shows increased levels of phospho-ERK1/2. Skeletal muscle from male non-transgenic (WT, white bars) and apoCIII Tg mice (Tg, black bars) was used. (**a**) mRNA abundance of human *APOCIII* and mouse *ApoCIII* (*Apoc3*). (**b**) mRNA abundance of *Chop*, *Bip*, *Il6* and *Tnfα*. (**c**) Phospho-ERK1/2 (Thr^{202}/Tyr^{204}) protein level. (**d**) PGC-1α protein levels. The graphs show quantification expressed as a percentage of WT value. Data are means ± SD ($n = 5$ per group) and were compared by Student's *t* test. $^{*}p < 0.05$, $^{**}p < 0.01$ and $^{***}p < 0.001$ vs WT mice

and inflammatory markers. Likewise, TLR2 neutralisation partially reversed the reduction in the protein levels of IRβ (Fig. 8d), blunted the increase in phospho-IRS-1 (Ser^{307}) (Fig. 8d) and prevented the reduction in PGC-1α and NRF1 (Fig. 8e). Blocking TLR2 also prevented the apoCIII-induced reduction in the expression of genes involved in FAO (Fig. 8f).

Discussion

Although it is well established that insulin resistance drives atherogenic dyslipidaemia, there is little evidence on whether the increase in VLDL particles associated with insulin-resistant states exacerbates the insulin resistance. Our findings demonstrate that exposure of myotubes and isolated skeletal muscle to VLDL increases the levels of ER stress and inflammatory markers and attenuates the insulin signalling pathway. These data indicate that increased levels of VLDL particles may contribute towards exacerbation of insulin resistance. Our findings also demonstrate that apoCIII may be the VLDL component responsible for the changes caused by VLDL exposure. This is interesting, since apoCIII expression is increased by insulin deficiency, insulin resistance [33, 34] and hyperglycaemia [35], converting apoCIII into the most abundant VLDL apolipoprotein in individuals with diabetes [3], suggesting that the increase in apoCIII levels in diabetic

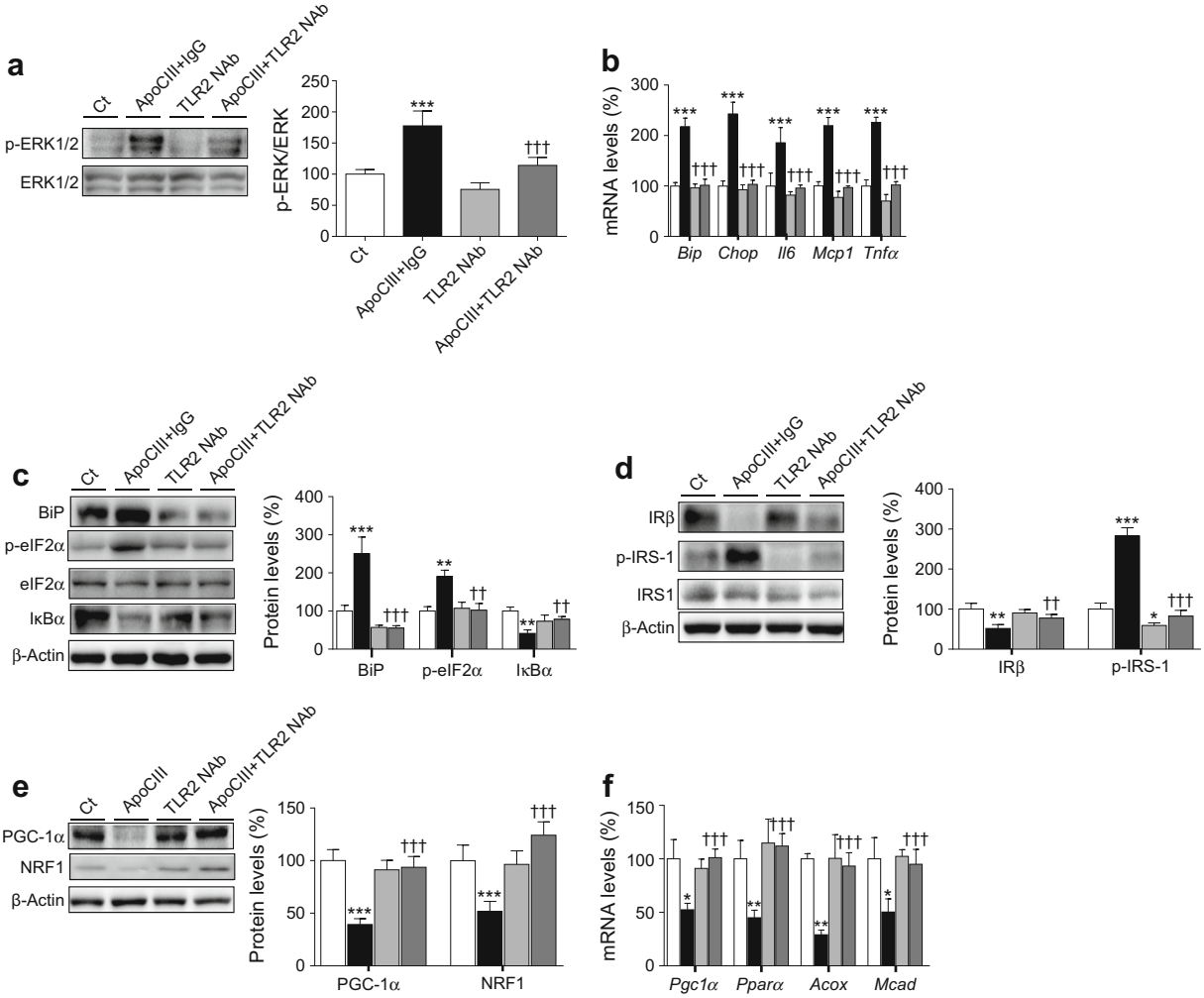

Fig. 8 TLR2 mediates the effects of apoCIII on ERK1/2, ER stress and inflammation. Mouse C2C12 myotubes were incubated in the presence or absence (control, Ct, white bars) of 100 μg/ml apoCIII for 24 h; 50 μg/ml of IgG was added to apoCIII-treated myotubes (black bars) or 50 μg/ml of the neutralising antibody against TLR2 (TLR2NAb) was added to the control (light grey bars) or apoCIII-treated (dark grey bars) myotubes. (**a**) Phospho-ERK1/2 (Thr^{202}/Tyr^{204}) protein levels. (**b**) mRNA abundance of *Bip*, *Chop*, *Il6*, *Mcp1* and *Tnfα*. (**c**) BiP, phospho-eIF2α (Ser^{51}), IκBα, and β-actin protein levels. (**d**) IRβ, phospho-IRS-1 (Ser^{307}) and β-actin protein levels. (**e**) PGC-1α, NRF1 and β-actin protein levels. (**f**) mRNA abundance of *Pgc1α*, *Pparα*, *Acox* and *Mcad* mRNA. The graphs show quantification expressed as a percentage of control. Data are means ± SD of five independent experiments and were compared by two-way ANOVA followed by Tukey post hoc test. $^{*}p < 0.05$, $^{**}p < 0.01$ and $^{***}p < 0.001$ vs control; $^{\dagger\dagger}p < 0.01$ and $^{\dagger\dagger\dagger}p < 0.001$ vs apoCIII-exposed cells

states may contribute to exacerbation of these conditions. In this regard, it is interesting to note that humans with a mutation in the *APOCIII* gene (also known as *APOC3*) that results in a reduction in the half-life of apoCIII, show a favourable lipoprotein pattern, increased insulin sensitivity and longevity and protection against cardiovascular diseases [36, 37]. Recent evidence seems to confirm that apoCIII plays a key role in diabetes. Thus, decreasing apoCIII in mice results in improved glucose tolerance [38]. In agreement with this, antisense-mediated lowering of plasma apoCIII improves dyslipidaemia and insulin sensitivity in humans with type 2 diabetes [39] and a null mutation in human *APOCIII* confers a favourable plasma lipid profile, although it does not improve insulin sensitivity [8].

The mechanism by which VLDL and apoCIII increase ER stress and inflammation and attenuate insulin signalling in myotubes seems to involve ERK1/2 activation. This kinase has been implicated in the development of insulin resistance associated with obesity and type 2 diabetes [40]. In fact, $Erk1^{-/-}$ mice (also known as $Mapk3^{-/-}$ mice) challenged with a high-fat diet are resistant to obesity and are protected from insulin resistance [41]. In addition, hyperinsulinaemic–euglycaemic clamp studies have demonstrated an increase in whole-body insulin sensitivity in *ob*/*ob*-$Erk1^{-/-}$ mice associated with an increase in both insulin-stimulated glucose disposal in skeletal muscles and adipose tissue insulin sensitivity [42].

In the present study, apoCIII-induced ERK1/2 activation was accompanied by a reduction in AMPK activity. An

inhibitory crosstalk exists between AMPK and ERK1/2 and activation of ERK1/2 inhibits AMPK and promotes ER stress-induced insulin resistance in skeletal muscle cells [14, 29]. Hence, VLDL and apoCIII-induced ER stress might be a result of the reduction in AMPK activity. In fact, AMPK activation inhibits ER stress [14, 43], whereas the reduction in its activity promotes ER stress [44]. Moreover, VLDL- and apoCIII-induced ER stress ultimately results in activation of the IKKβ–NF-κB pathway, which attenuates the insulin signalling pathway by phosphorylating IRS-1 in serine residues and increases the transcription of inflammatory genes. In agreement with this, we found that ERK1/2 inhibition or knockdown prevented the changes in ER stress and inflammation and the attenuation of the insulin signalling pathway caused by VLDL. Moreover, ERK1/2 inhibition prevented the reduction in AMPK caused by apoCIII, confirming the negative crosstalk between ERK1/2 and AMPK.

Similarly, the reduction in AMPK caused by apoCIII-induced ERK1/2 activation may contribute to reduced PGC-1α levels, since PGC-1α is an important mediator of AMPK-induced gene expression and AMPK activation regulates PGC-1α transcription [45]. Given the key role of PGC-1α in regulating the activity of transcription factors involved in FAO, such as PPARs [22], the reduction in PGC-1α following treatment with VLDL or apoCIII leads to a decrease in the expression of genes involved in FAO, suggesting that it can promote the deleterious effects of saturated fatty acids [11].

VLDLs also bind to the VLDL receptor, which is a determinant factor in adipose tissue inflammation and adipocyte macrophage infiltration when stimulated with VLDL from hyperlipidaemic mice [13]. Although we cannot discount a role for this receptor, the fact that the effects of VLDL from normolipidaemic individuals are mimicked by apoCIII seems to suggest that most of the effects of these lipoproteins are caused by the presence of apoCIII in these particles.

Interestingly, our findings indicate that the effects of apoCIII are mediated by TLR2. TLR2 not only recognises numerous lipid-containing molecules but also it recognises endogenous proteins [46]. It is expressed in skeletal muscle cells and is involved in fatty acid-induced insulin resistance [47]. Moreover, activation of the TLR2 pathway ultimately leads to NF-κB and ERK1/2 activation [48]. Likewise, TLR2 deficiency improves insulin sensitivity and attenuates cytokine expression [49]. Our findings confirm the importance of TLR2 in insulin resistance and indicate that its activation by VLDL and apoCIII induces ER stress, inflammation and insulin resistance.

In conclusion, our findings show that VLDL- and apoCIII-induced TLR2 activation results in ER stress, inflammation and insulin resistance by activating ERK1/2 in skeletal muscle cells. These results imply that elevated VLDL in diabetic states can contribute to the exacerbation of insulin resistance.

Acknowledgements We thank the University of Barcelona's Language Advisory Service for revising the manuscript.

Data availability Data are available on request from the authors.

Funding This study was partly supported by funds from the Spanish Ministerio de Economía y Competitividad (SAF2012-30708 and SAF2015-64146-R to MVC), the Generalitat de Catalunya (2014SGR-0013 to MVC), NIH NIDDK (DK101663 to ABK), USDA NIFA (11874590 to ABK) and USDA NIFA Hatch Formula Funds (2015-31200-06009 to ABK), an Instituto de Salud Carlos III grant (PI16-00139 to JCE-G) and European Union ERDF funds. CIBER de Diabetes y Enfermedades Metabólicas Asociadas (CIBERDEM) is an Instituto de Salud Carlos III project (Grant CB07/08/0003 to MVC). GB was supported by an FPI grant from the Spanish Ministerio de Economía y Competitividad.

Duality of interest The authors declare that there is no duality of interest associated with this manuscript.

Contribution statement All authors processed the samples, analysed and prepared the data and were involved in drafting the article. GB, AG, JCEG, XP and ABK contributed to data interpretation and revised the article. MVC designed the experiments, interpreted the data and was primarily responsible for writing the manuscript. All authors approved the final version of the manuscript. MVC is the guarantor of this work.

References

1. Xiao C, Dash S, Morgantini C, Hegele RA, Lewis GF (2016) Pharmacological targeting of the atherogenic dyslipidemia complex: the next frontier in CVD prevention beyond lowering LDL cholesterol. Diabetes 65:1767–1778
2. Adiels M, Olofsson SO, Taskinen MR, Borén J (2008) Overproduction of very low-density lipoproteins is the hallmark of the dyslipidemia in the metabolic syndrome. Arterioscler Thromb Vasc Biol 28:1225–1236
3. Hiukka A, Fruchart-Najib J, Leinonen E, Hilden H, Fruchart JC, Taskinen MR (2005) Alterations of lipids and apolipoprotein CIII in very low density lipoprotein subspecies in type 2 diabetes. Diabetologia 48:1207–1215
4. Campos H, Perlov D, Khoo C, Sacks FM (2001) Distinct patterns of lipoproteins with apoB defined by presence of apoE or apoC-III in hypercholesterolemia and hypertriglyceridemia. J Lipid Res 42:1239–1249
5. Aalto-Setälä K, Fisher EA, Chen X et al (1992) Mechanism of hypertriglyceridemia in human apolipoprotein (apo) CIII transgenic mice. Diminished very low density lipoprotein fractional catabolic rate associated with increased apo CIII and reduced apo E on the particles. J Clin Invest 90:1889–1900
6. Kawakami A, Aikawa M, Alcaide P, Luscinskas FW, Libby P, Sacks FM (2006) Apolipoprotein CIII induces expression of vascular cell adhesion molecule-1 in vascular endothelial cells and increases adhesion of monocytic cells. Circulation 114:681–687
7. Lee HY, Birkenfeld AL, Jornayvaz FR et al (2011) Apolipoprotein CIII overexpressing mice are predisposed to diet-induced hepatic steatosis and hepatic insulin resistance. Hepatology 54:1650–1660
8. Pollin TI, Damcott CM, Shen H et al (2008) A null mutation in human APOC3 confers a favorable plasma lipid profile and apparent cardioprotection. Science 332:1702–1705

9. DeFronzo RA, Gunnarsson R, Björkman O, Olsson M, Wahren J (1985) Effects of insulin on peripheral and splanchnic glucose metabolism in noninsulin-dependent (type II) diabetes mellitus. J Clin Invest 76:149–155
10. Abdul-Ghani MA, DeFronzo RA (2010) Pathogenesis of insulin resistance in skeletal muscle. J Biomed Biotechnol 2010:476279
11. Schenk S, Saberi M, Olefsky JM (2008) Insulin sensitivity: modulation by nutrients and inflammation. J Clin Invest 118:2992–3002
12. Salvadó L, Palomer X, Barroso E, Vázquez-Carrera M (2015) Targeting endoplasmic reticulum stress in insulin resistance. Trends Endocrinol Metab 26:438–448
13. Könner AC, Brüning JC (2011) Toll-like receptors: linking inflammation to metabolism. Trends Endocrinol Metab 22:16–23
14. Nguyen A, Tao H, Metrione M, Hajri T (2014) Very low density lipoprotein receptor (VLDLR) expression is a determinant factor in adipose tissue inflammation and adipocyte-macrophage interaction. J Biol Chem 289:1688–1703
15. Salvadó L, Barroso E, Gómez-Foix AM et al (2014) PPARβ/δ prevents endoplasmic reticulum stress-associated inflammation and insulin resistance in skeletal muscle cells through an AMPK-dependent mechanism. Diabetologia 57:2126–2135
16. Alkhateeb H, Chabowski A, Bonen A (2006) Viability of the isolated soleus muscle during long-term incubation. Appl Physiol Nutr Metab 31:467–476
17. Koh HJ, Toyoda T, Didesch MM et al (2013) Tribbles 3 mediates endoplasmic reticulum stress-induced insulin resistance in skeletal muscle. Nat Commun 4:1871
18. Howard JK, Flier JS (2006) Attenuation of leptin and insulin signaling by SOCS proteins. Trends Endocrinol Metab 17:365–371
19. Handschin C, Spiegelman BM (2006) Peroxisome proliferator-activated receptor gamma coactivator 1 coactivators, energy homeostasis, and metabolism. Endocr Rev 27:728–735
20. Patti ME, Butte AJ, Crunkhorn S et al (2003) Coordinated reduction of genes of oxidative metabolism in humans with insulin resistance and diabetes: potential role of *PGC1* and *NRF1*. Proc Natl Acad Sci U S A 100:8466–8471
21. Mootha VK, Lindgren CM, Eriksson KF et al (2003) PGC-1α-responsive genes involved in oxidative phosphorylation are coordinately downregulated in human diabetes. Nat Genet 34:267–273
22. Miura S, Kai Y, Ono M, Ezaki O (2003) Overexpression of peroxisome proliferator-activated receptor γ coactivator-1α down-regulates GLUT4 mRNA in skeletal muscles. J Biol Chem 278:31385–31390
23. Vega RB, Huss JM, Kelly DP (2000) The coactivator PGC-1 cooperates with peroxisome proliferator-activated receptor α in transcriptional control of nuclear genes encoding mitochondrial fatty acid oxidation enzymes. Mol Cell Biol 20:1868–1876
24. Wu Z, Puigserver P, Andersson U et al (1999) Mechanisms controlling mitochondrial biogenesis and respiration through the thermogenic coactivator PGC-1. Cell 98:115–124
25. Zhang BB, Zhou G, Li C (2009) AMPK: an emerging drug target for diabetes and the metabolic syndrome. Cell Metab 9:407–416
26. Zhou L, Zhang J, Fang Q et al (2009) Autophagy-mediated insulin receptor down-regulation contributes to endoplasmic reticulum stress-induced insulin resistance. Mol Pharmacol 76:596–603
27. Wenz T, Rossi SG, Rotundo RL, Spiegelman BM, Moraes CT (2009) Increased muscle PGC-1α expression protects from sarcopenia and metabolic disease during aging. Proc Natl Acad Sci U S A 106:20405–20410
28. Chung S, Lapoint K, Martinez K et al (2006) Preadipocytes mediate lipopolysaccharide-induced inflammation and insulin resistance in primary cultures of newly differentiated human adipocytes. Endocrinology 147:5340–5351
29. Coll T, Jové M, Rodríguez-Calvo R et al (2006) Palmitate-mediated downregulation of peroxisome proliferator-activated receptor-gamma coactivator 1α in skeletal muscle cells involves MEK1/2 and nuclear factor-κB activation. Diabetes 55:2779–2787
30. Hwang SL, Jeong YT, Li X et al (2013) Inhibitory cross-talk between the AMPK and ERK pathways mediates endoplasmic reticulum stress-induced insulin resistance in skeletal muscle. Br J Pharmacol 169:69–81
31. Reaven GM, Mondon CE, Chen YD, Breslow JL (1994) Hypertriglyceridemic mice transgenic for the human apolipoprotein C-III gene are neither insulin resistant nor hyperinsulinemic. J Lipid Res 35:820–824
32. Salerno AG, Silva TR, Amaral ME et al (2007) Overexpression of apolipoprotein CIII increases and CETP reverses diet-induced obesity in transgenic mice. Int J Obes 31:1586–1595
33. Chen M, Breslow JL, Li W, Leff T (1994) Transcriptional regulation of the apoC-III gene by insulin in diabetic mice: correlation with changes in plasma triglyceride levels. J Lipid Res 35:1918–1924
34. Altomonte J, Cong L, Harbaran S et al (2004) Foxo1 mediates insulin action on apoC-III and triglyceride metabolism. J Clin Invest 114:1493–1503
35. Caron S, Verrijken A, Mertens I et al (2011) Transcriptional activation of apolipoprotein CIII expression by glucose may contribute to diabetic dyslipidemia. Arterioscler Thromb Vasc Biol 31:513–519
36. Atzmon G, Rincon M, Schechter CB et al (2006) Lipoprotein genotype and conserved pathway for exceptional longevity in humans. PLoS Biol 4:e113
37. Jørgensen AB, Frikke-Schmidt R, Nordestgaard BG, Tybjærg-Hansen A (2014) Loss-of-function mutations in *APOC3* and risk of ischemic vascular disease. N Engl J Med 371:32–41
38. Åvall K, Ali Y, Leibiger IB et al (2015) Apolipoprotein CIII links islet insulin resistance to β-cell failure in diabetes. Proc Natl Acad Sci U S A A112:E2611–E2619
39. Digenio A, Dunbar RL, Alexander VJ et al (2016) Antisense-mediated lowering of plasma apolipoprotein C-III by volanesorsen improves dyslipidemia and insulin sensitivity in type 2 diabetes. Diabetes Care 39:1408–1415
40. Ozaki KI, Awazu M, Tamiya M et al (2016) Targeting the ERK signaling pathway as a potential treatment for insulin resistance and type 2 diabetes. Am J Physiol Endocrinol Metab 310:E643–E651
41. Bost F, Aouadi M, Caron L et al (2005) The extracellular signal-regulated kinase isoform ERK1 is specifically required for in vitro and in vivo adipogenesis. Diabetes 54:402–411
42. Jager J, Corcelle V, Grémeaux T et al (2011) Deficiency in the extracellular signal-regulated kinase 1 (ERK1) protects leptin-deficient mice from insulin resistance without affecting obesity. Diabetologia 54:180–189
43. Dong Y, Zhang M, Wang S et al (2010) Activation of AMP-activated protein kinase inhibits oxidized LDL-triggered endoplasmic reticulum stress in vivo. Diabetes 59:1386–1396
44. Dong Y, Zhang M, Liang B et al (2010) Reduction of AMP-activated protein kinase α2 increases endoplasmic reticulum stress and atherosclerosis in vivo. Circulation 121:792–803
45. Cantó C, Auwerx J (2009) PGC-1α, SIRT1 and AMPK, an energy sensing network that controls energy expenditure. Curr Opin Lipidol 20:98–105
46. Rubartelli A, Lotze MT (2007) Inside, outside, upside down: damage-associated molecular-pattern molecules (DAMPs) and redox. Trends Immunol 28:429–436
47. Senn JJ (2006) Toll-like receptor-2 is essential for the development of palmitate-induced insulin resistance in myotubes. J Biol Chem 281:26865–26875
48. Ninomiya-Tsuji J, Kishimoto K, Hiyama A, Inoue J, Cao Z, Matsumoto K (1999) The kinase TAK1 can activate the NIK-IκB as well as the MAP kinase cascade in the IL-1 signalling pathway. Nature 398:252–256
49. Kuo LH, Tsai PJ, Jiang MJ et al (2011) Toll-like receptor 2 deficiency improves insulin sensitivity and hepatic insulin signalling in the mouse. Diabetologia 54:168–179

International Journal of Cardiology 174 (2014) 110–118

Contents lists available at ScienceDirect

International Journal of Cardiology

journal homepage: www.elsevier.com/locate/ijcard

PPARβ/δ attenuates palmitate-induced endoplasmic reticulum stress and induces autophagic markers in human cardiac cells

Xavier Palomer [a], Eva Capdevila-Busquets [a], Gaia Botteri [a], Laia Salvadó [a], Emma Barroso [a], Mercy M. Davidson [b], Liliane Michalik [c], Walter Wahli [c,d], Manuel Vázquez-Carrera [a,*]

[a] Department of Pharmacology and Therapeutic Chemistry, IBUB (Institut de Biomedicina de la Universitat de Barcelona), CIBER de Diabetes y Enfermedades Metabólicas Asociadas (CIBERDEM), Faculty of Pharmacy, University of Barcelona, Diagonal 643, Barcelona E-08028, Spain
[b] Department of Radiation Oncology, Columbia University, P&S 11-451, 630 West 168th Street, New York, NY 10032, USA
[c] Center for Integrative Genomics, National Research Center Frontiers in Genetics, University of Lausanne, Quartier UNIL-Sorge, Bâtiment Génopode, CH-1015 Lausanne, Switzerland
[d] Lee Kong Chian School of Medicine, Nanyang Technological University, School of Nursing Building, SGH, Block C, #01-01, 9 Hospital Drive, Singapore 169612, Singapore

ARTICLE INFO

Article history:
Received 23 December 2013
Received in revised form 24 March 2014
Accepted 29 March 2014
Available online 8 April 2014

Keywords:
Autophagy
Diabetic cardiomyopathy
Endoplasmic reticulum stress
PPARβ/δ

ABSTRACT

Background: Chronic endoplasmic reticulum (ER) stress contributes to the apoptotic cell death in the myocardium, thereby playing a critical role in the development of cardiomyopathy. ER stress has been reported to be induced after high-fat diet feeding in mice and also after saturated fatty acid treatment in vitro. Therefore, since several studies have shown that peroxisome proliferator-activated receptor (PPAR)β/δ inhibits ER stress, the main goal of this study consisted in investigating whether activation of this nuclear receptor was able to prevent lipid-induced ER stress in cardiac cells.
Methods and results: Wild-type and transgenic mice with reduced PPARβ/δ expression were fed a standard diet or a high-fat diet for two months. For in vitro studies, a cardiomyocyte cell line of human origin, AC16, was treated with palmitate and the PPARβ/δ agonist GW501516. Our results demonstrate that palmitate induced ER stress in AC16 cells, a fact which was prevented after PPARβ/δ activation with GW501516. Interestingly, the effect of GW501516 on ER stress occurred in an AMPK-independent manner. The most striking result of this study is that GW501516 treatment also upregulated the protein levels of beclin 1 and LC3II, two well-known markers of autophagy. In accordance with this, feeding on a high-fat diet or suppression of PPARβ/δ in knockout mice induced ER stress in the heart. Moreover, PPARβ/δ knockout mice also displayed a reduction in autophagic markers.
Conclusion: Our data indicate that PPARβ/δ activation might be useful to prevent the harmful effects of ER stress induced by saturated fatty acids in the heart by inducing autophagy.

1. Introduction

If uncorrected, type 2 diabetes and obesity are among the major risk factors for the development of cardiovascular diseases. Plasma free fatty acid levels are often elevated in patients with type 2 diabetes mellitus or obesity, and are responsible for several harmful effects on the heart, such as the activation of endoplasmic reticulum (ER) stress and chronic low-level inflammatory processes. In fact, it has been suggested that saturated fatty acids induce insulin resistance by causing ER stress in pancreatic β-cells [1,2], hepatocytes [3] and muscle cells [4,5] of human and murine origin. ER is the organelle responsible for protein folding and maturation in eukaryotic cells. Any physiological or pathological perturbation that interferes with the folding process will cause the accumulation of unfolded or misfolded proteins, thus leading to the activation of the unfolded protein response (UPR) by the ER [6]. Initiation of the UPR involves three key signaling proteins: activating transcription factor 6 (ATF6), inositol-requiring enzyme (IRE)-1α, and PKR-like ER kinase (PERK). In the absence of stress, the N-termini of these trans-membrane proteins are bound to the intra-luminal BiP/GRP78 (binding immunoglobulin protein/glucose-regulated protein 78) protein. On stress exposure, the large excess of unfolded proteins sequesters BiP/GRP78 from trans-membrane ER proteins, thereby inducing the UPR. In particular, ATF6 is transported from the ER to the Golgi complex, where proteolytic cleavage releases a soluble fragment that translocates to the nucleus, in which it acts as a transcription factor for ER chaperones [7]. In addition, the endoribonuclease activity of IRE-1α cleaves a 26 base-pair segment from the mRNA of the X-box binding protein-1 (*XBP1*), creating an alternative message that is translated into the spliced and active form of this transcription factor, sXBP1. Finally, PERK phosphorylates and inhibits the eukaryotic initiation factor 2α (eIF2α), and by this means inhibits the translation of most mRNAs [8]. However, some mRNAs escape this translational control, for example transcription factor *ATF4*, a master regulator of the ER stress response

* Corresponding author at: Department of Pharmacology and Therapeutic Chemistry, Faculty of Pharmacy, University of Barcelona, Diagonal 643, E-08028 Barcelona, Spain. Tel.: +34 934024531; fax: +34 934035982.
E-mail address: mvazquezcarrera@ub.edu (M. Vázquez-Carrera).

http://dx.doi.org/10.1016/j.ijcard.2014.03.176
0167-5273/

that is capable of inducing the expression of *ATF3*, *BiP/GRP78*, *CHOP* (CCAAT/enhancer binding protein homologous protein) and genes involved in autophagy, antioxidant responses, and apoptosis [9].

Activation of the UPR initially aims to mitigate adverse effects of ER stress and thus enhance cell survival by halting general mRNA translation, facilitating protein degradation via the ER-associated degradation (ERAD) pathway and enhancing the production of molecular chaperones involved in protein folding. If ER stress is limited, the UPR will potentiate autophagy to protect the cells [10]. This pro-survival pathway has evolved as an alternate mechanism for saving nutrients, recycling intracellular components and eliminating abnormal protein aggregates and misfolded proteins formed during the ER stress that cannot be removed through the ERAD pathway. However, if ER stress is not mitigated within a certain time period or the disturbance is prolonged, then, the UPR will turn on apoptosis for removing cells that threaten the integrity of the organism [11]. Cardiomyocytes rarely proliferate within the adult heart and, as a consequence, their loss due to apoptosis may play an essential pathogenic role during cardiovascular diseases [7]. In consonance with this, ER stress is involved in the pathogenesis of diabetic cardiomyopathy by enhancing cell death in the myocardium of streptozotocin-induced diabetic rats [12]. The myocardium of two rat models of type 2 diabetes mellitus also displays ER stress [13,14]. For this reason, inhibition of ER stress has been suggested as a potential therapeutic target for preventing and treating diabetic cardiomyopathy.

Peroxisome proliferator-activated receptor (PPAR)β/δ is a transcription factor that regulates cardiac metabolism and can limit myocardial inflammation and hypertrophy via inhibition of nuclear factor (NF)-κB [15]. NF-κB is a pro-inflammatory transcription factor that is activated in the heart during prolonged ER stress, and is responsible for the induction of apoptosis [16]. Cardiomyocyte-restricted deletion of PPARβ/δ decreases basal myocardial fatty acid oxidation, thus leading to lipotoxic cardiomyopathy and subsequent cardiac dysfunction, cardiac hypertrophy and congestive heart failure [17,18]. Interestingly, activation of PPARβ/δ with the GW501516 agonist rescues ER stress induced by palmitate in pancreatic β-cells [19], while another agonist, L165041, attenuates ER stress in the liver [20], although the mechanisms involved remain unknown. Therefore, the present study was designed to gain a better understanding of the mechanisms by which exposure to the saturated fatty acid palmitate results in ER stress in cardiac cells. In addition, since PPARβ/δ is the most prevalent PPAR isoform in the heart [15], we also aimed to elucidate whether the PPARβ/δ agonist GW501516 could prevent saturated fatty acid-induced ER stress in cardiac myocytes, as well as the mechanisms involved.

2. Methods

2.1. Cell culture and mice

Human cardiac AC16 cells were maintained and grown as previously described [21]. Palmitate-containing medium was prepared by conjugation with fatty acid-free bovine serum albumin [22]. After incubation, RNA or protein was extracted from cardiac cells as described below.

Male PPARβ/δ-null mice and their control wild-type littermates with the same genetic background (C57BL/6X129/SV) were used (aged 3–5 months old) [23]. Each strain was randomized into two groups. One group was fed with a standard chow diet, and the other was fed with a Western-type high-fat diet (HFD, 45% kcal from fat, 91.5% saturated fatty acid content) for 8 weeks. Mice were housed under standard light–dark cycle (12-h light/dark cycle) and temperature (21 ± 1 °C) conditions, and food and water were provided ad libitum. At the end of the treatment, mice were anesthetized with 5% isoflurane and, after monitoring the adequacy of anesthesia by testing rear foot reflexes, they were euthanized by cervical dislocation. After this, the heart was excised, rinsed in ice-cold phosphate buffer saline and snap-frozen in liquid nitrogen. All procedures were approved by the University of Barcelona Bioethics Committee, as stated in Law 5/21 July 1995 passed by the Generalitat de Catalunya.

2.2. RNA preparation and quantitative real-time RT-PCR analysis

Relative levels of specific mRNAs were assessed by real-time reverse transcription polymerase chain reaction (RT-PCR), as previously described [24]. The sequences of the forward and reverse primers are shown in Supplemental Table S1. For measurement of *XBP1* splicing, cDNA was used for PCR amplification using *XBP1* primers spanning the 26-bp intron splicing site (forward: 5′-TGAGAACCAGGAGTTAAGAACACGC-3′ and reverse: 5′-TTCTGGGTAGACCTCTGGGAGTTCC-3′). The PCR cycle consisting of 94 °C for 1 min, 62 °C for 1 min, and 72 °C for 1 min was repeated 30 times. This gave a PCR product of 326 bp for unspliced and 300 bp for spliced XBP1. The PCR products were separated by electrophoresis with a 2% agarose gel and visualized by ethidium bromide staining.

2.3. Immunoblot analysis

To obtain total protein extracts, AC16 cardiac cells and the heart tissue were lysed in cold RIPA buffer (Sigma, St Louis, MO, USA) with phosphatase and protease inhibitors (0.2 mmol/L phenylmethylsulfonyl fluoride, 1 mmol/L sodium orthovanadate, 5.4 μg/mL aprotinin). The homogenate was then centrifuged at 10,000 ×*g* for 30 min at 4 °C, and protein concentration contained in the supernatant was determined using the Bradford method [25]. Protein extracts were separated by SDS-PAGE on 10% separation gels and transferred to Immobilon polyvinylidene difluoride membranes (Millipore, Bedford, MA, USA) [26]. Proteins were detected using the Western Lightning® Plus-ECL chemiluminescence kit (PerkinElmer, Waltham, MA, USA) and their size was estimated using protein molecular mass standards (Life Technologies, S.A., Spain). All antibodies used throughout the study were purchased from Cell Signaling Technology (Danvers, MA, USA), except actin (Sigma).

2.4. Statistical analysis

Results are expressed as the mean ± SD of three independent experiments for the in vitro studies, each consisting of three culture plates (n = 9), and of four mice for the in vivo experiments. Significant differences were established by one-way ANOVA using the GraphPad Prism (GraphPad Software Inc. V4.03, San Diego, CA, USA) software. When significant variations were found by one-way ANOVA, the Tukey–Kramer multiple comparison post-test was performed. Differences were considered significant at $P < 0.05$.

3. Results

3.1. PPARβ/δ activation prevents palmitate-induced ER stress in cardiac cells of human origin

As a first approach, we aimed to determine whether palmitate (0.25 mM for 18 h) was capable of inducing the expression of several ER stress markers in human cardiac AC16 cells. Real-time RT-PCR analyses demonstrated that palmitate significantly induced the expression of *sXBP1*, *ATF3* (approximately 2-fold, $P < 0.001$), *BiP/GRP78* (4.5-fold, $P < 0.001$) and *CHOP* (4.5-fold, $P < 0.001$), compared to cells exposed only to BSA (Fig. 1). To investigate whether PPARβ/δ activation prevented ER stress, human cardiac cells were co-incubated with palmitate and GW501516 (10 μM). As shown in Fig. 2A, the PPARβ/δ agonist completely abolished the increase in *ATF3* and attenuated the rise in *CHOP* expression caused by the saturated fatty acid, but did not prevent the splicing of *XBP1* or the induction of *BiP/GRP78* expression. In agreement with the above results, BiP/GRP78 and CHOP protein levels were increased in cells exposed to palmitate (Fig. 2B). Since activation of IRE-1α promotes the splicing of *XBP1*, we also evaluated whether palmitate upregulated IRE-1α phosphorylation at Ser724 residues, which is indicative of its activity. As expected, palmitate treatment also enhanced the phosphorylation of IRE-1α with regard to control non-treated cells (2-fold, $P < 0.05$, Fig. 2B). On the contrary, no changes were observed in the phosphorylation levels at the Ser51 residue of eIF2α (see Supplemental Fig. 1A). Consistent with changes in mRNA levels, GW501516 abrogated the increase in CHOP protein levels induced by palmitate, but not those of the BiP/GRP78 chaperone. Surprisingly, GW501516 prevented IRE-1α phosphorylation induced by palmitate as well, although *sXBP1* was not downregulated. Incubation with GW501516 alone had no effect on *sXBP1* levels, but prevented IRE-1α phosphorylation in palmitate-treated cells. On the other hand, co-incubation of cells with palmitate, GW501516 and the PPARβ/δ antagonist GSK0660 (10 μM) reversed the effects of GW501516 on the expression of *ATF3*, but not on *CHOP* (Fig. 2A), therefore demonstrating that PPARβ/δ activation was involved, at least in part, in the effects of GW501516 on ER stress.

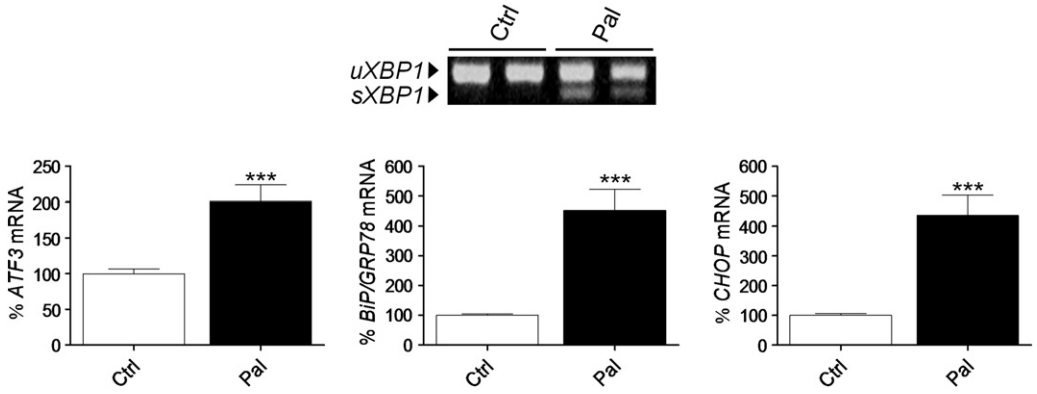

Fig. 1. Palmitate induces endoplasmic reticulum stress markers in human cardiac cells. *sXBP1*, *ATF3*, *BiP/GRP78* and *CHOP* mRNA levels in AC16 cells incubated for 18 h with palmitate (Pal, 0.25 mmol/L). The graphs represent the quantification of the *18S*-normalized mRNA levels, expressed as a percentage of control samples ± SD. $^{***}P < 0.001$ vs. control (Ctrl).

3.2. The preventive effect of PPARβ/δ activation on palmitate-induced ER stress is AMPK-independent

To investigate the role of 5′ AMP-activated protein kinase (AMPK) in palmitate-induced ER stress in human cardiac cells, as well as the preventive effects of GW501516, we took advantage of the AMPK activator AICAR (5-aminoimidazole-4-carboxamide ribonucleotide) and the AMPK inhibitor compound C. As shown in Fig. 3A, the increase in the expression of the ER markers *sXBP1*, *BiP/GRP78* and *CHOP* caused by palmitate was abolished in cells co-incubated with palmitate plus AICAR. In contrast, AICAR further induced *ATF3* mRNA transcript levels (3.5-fold, $P < 0.001$ vs. control cells). In accordance with these data, AICAR prevented IRE-1α phosphorylation and the induction of BiP/GRP78 and CHOP protein levels stimulated by the saturated fatty acid (Fig. 3B), but appeared to up-regulate eIF2α phosphorylation on Ser51 residues (3-fold, $P < 0.01$ vs. control cells, Supplemental Fig. 1B). The outcome observed after co-incubation with compound C demonstrated the involvement of AMPK in ER stress induced by palmitate, since compound C abolished the effects of AMPK activation on *XBP1* splicing, ATF3 and CHOP mRNA expression and protein accumulation, and the

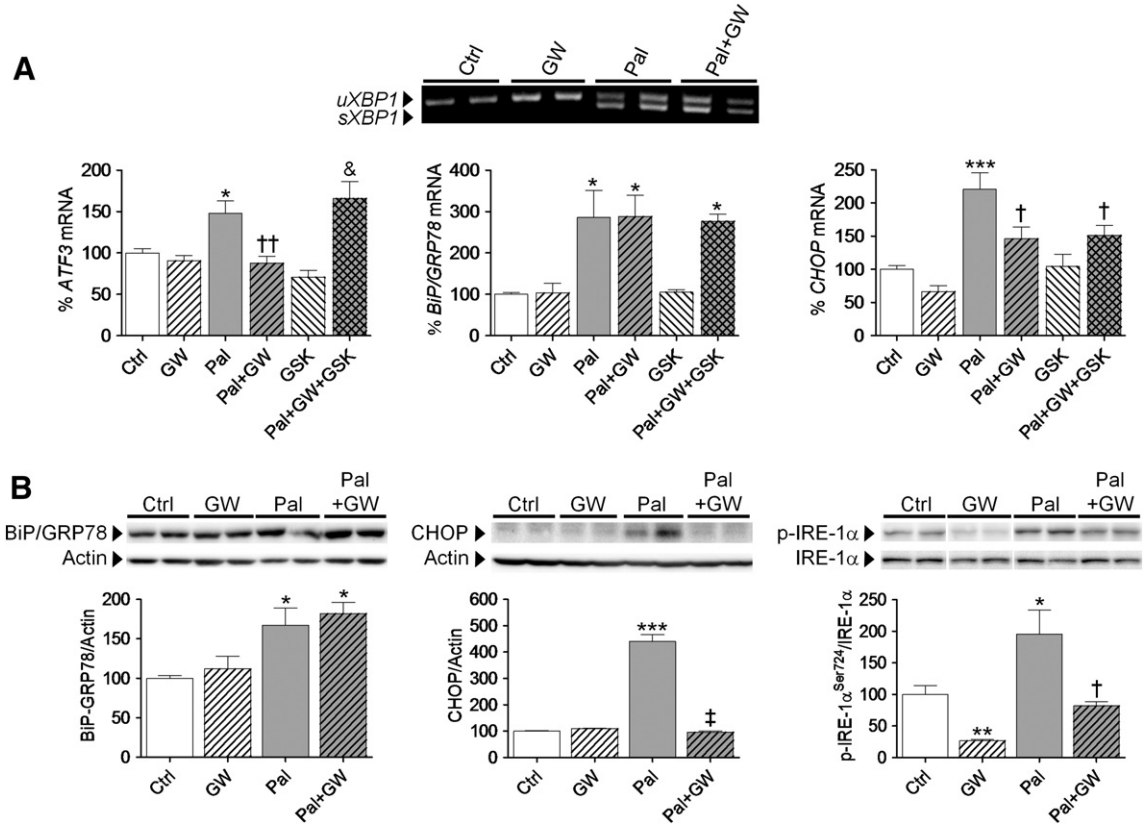

Fig. 2. PPARβ/δ activation prevents palmitate-induced ER stress in human cardiac cells. AC16 cells were incubated for 18 h with palmitate (Pal, 0.25 mmol/L) in the presence or absence of GW501516 (GW, 10 μmol/L) or GSK0660 (GSK, 10 μmol/L). (A) *sXBP1*, *ATF3*, *BiP/GRP78* and *CHOP* mRNA levels. The graphs represent the quantification of the *18S*-normalized mRNA levels, expressed as a percentage of control samples ± SD. (B) Western-blot analysis showing protein levels of BiP/GRP78, CHOP and the ratio phosphorylated IRE-1α^{Ser724}/IRE-1α in total protein extracts. To show equal loading of protein, the actin signal is included from the same blot. The graphs represent the quantification of the normalized protein levels expressed as a percentage of control samples ± SD. All autoradiograph data are representative of two separate experiments. $^{*}P < 0.05$, $^{**}P < 0.01$ and $^{***}P < 0.001$ vs. Ctrl; $^{\dagger}P < 0.05$, $^{\dagger\dagger}P < 0.01$ and $^{\ddagger}P < 0.001$ vs. Pal; $^{\&}P < 0.05$ vs. Pal + GW.

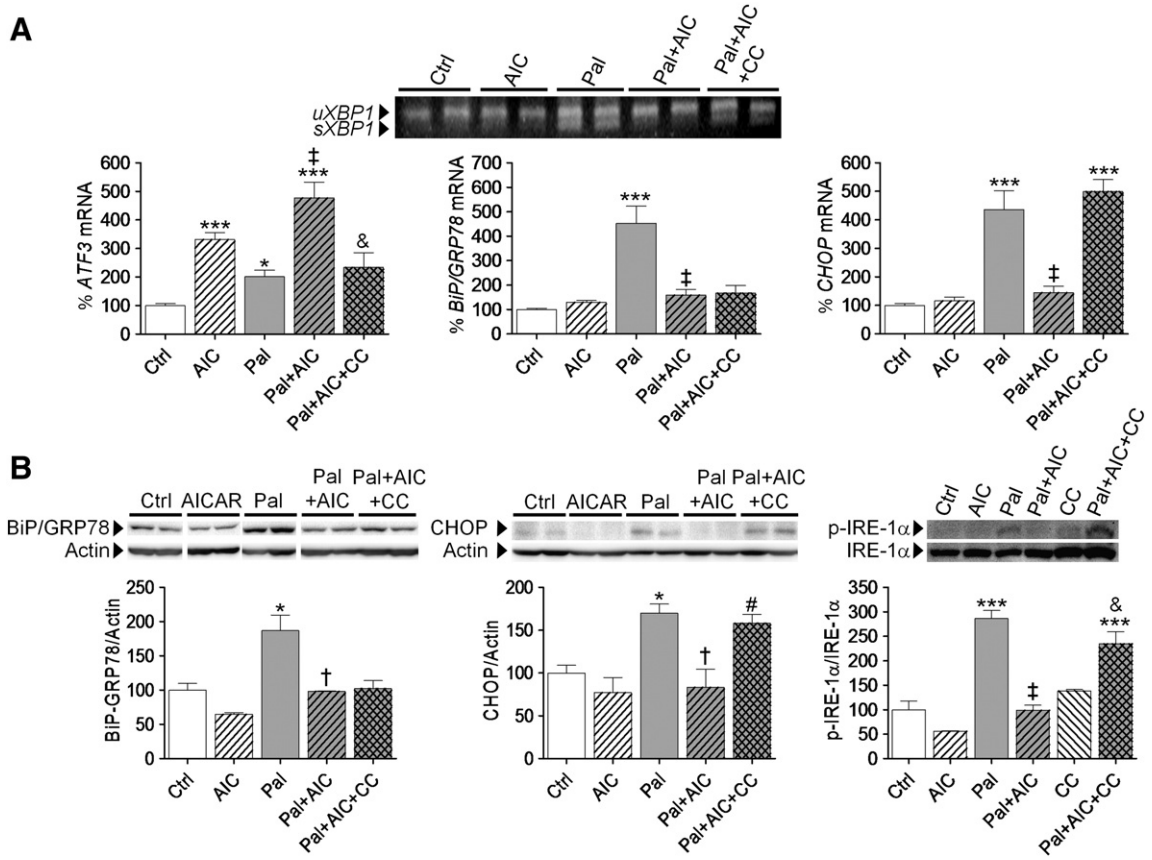

Fig. 3. AMPK activation avoids palmitate-induced ER stress in human cardiac cells. AC16 cells were incubated for 18 h with palmitate (Pal, 0.25 mmol/L) in the presence or absence of AICAR (AIC, 2 mmol/L) or compound C (CC, 30 μmol/L). (A) *sXBP1*, *ATF3*, *BiP/GRP78* and *CHOP* mRNA levels. The graphs represent the quantification of the *18S*-normalized mRNA levels, expressed as a percentage of control samples ± SD. (B) Western-blot analysis showing protein levels of BiP/GRP78, CHOP and the ratio phosphorylated IRE-1α^{Ser724}/IRE-1α in total protein extracts. To show equal loading of protein, the actin signal is included from the same blot. The graphs represent the quantification of the normalized protein levels expressed as a percentage of control samples ± SD. All autoradiograph data are representative of two separate experiments. $^{*}P < 0.05$, $^{**}P < 0.01$ and $^{***}P < 0.001$ vs. Ctrl; $^{\dagger}P < 0.05$, $^{\dagger\dagger}P < 0.01$ and $^{\ddagger}P < 0.001$ vs. Pal; $^{\#}P < 0.05$ and $^{\&}P < 0.01$ vs. Pal + AIC.

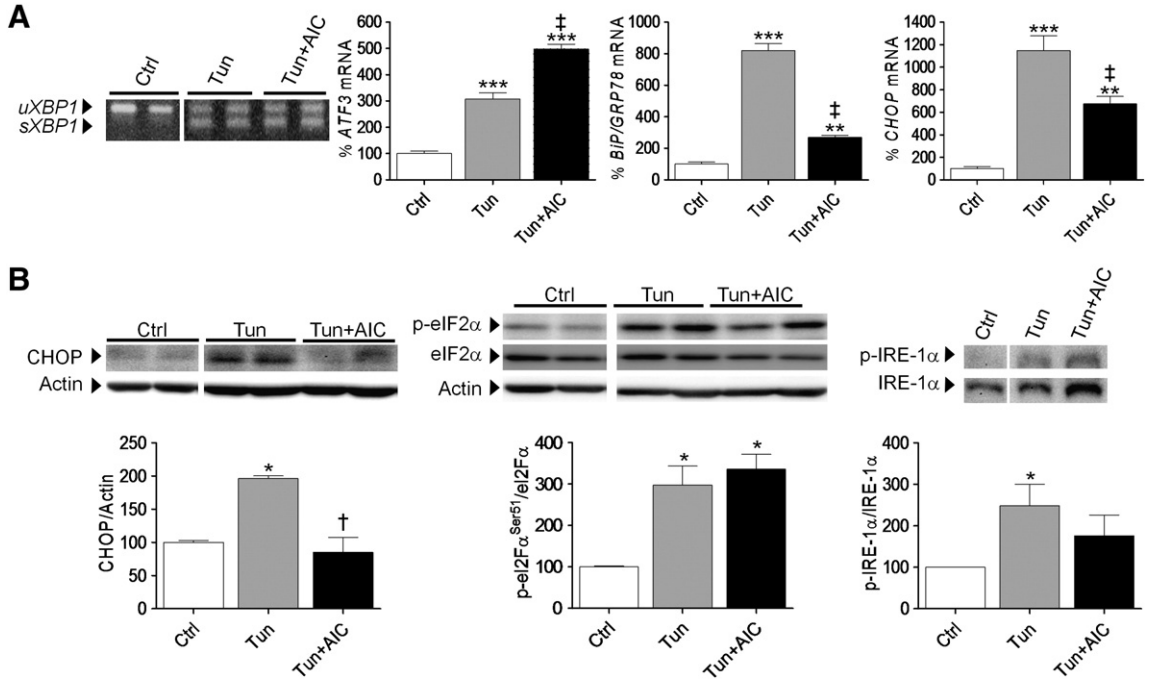

Fig. 4. Tunicamycin elicits ER stress in human cardiac cells. AC16 cells were incubated for 4 h with tunicamycin (Tun, 5 μg/mL) and AICAR (AIC, 2 mmol/L). (A) *sXBP1*, *ATF3*, *BiP/GRP78* and *CHOP* mRNA levels. The graphs represent the quantification of the *18S*-normalized mRNA levels, expressed as a percentage of control samples ± SD. (B) Western-blot analysis showing protein levels of CHOP, phosphorylated eIF2α^{Ser51}/eIF2α and phosphorylated IRE-1α^{Ser724}/IRE-1α in total protein extracts. To show equal loading of protein, the actin signal is included from the same blot. The graphs represent the quantification of the normalized protein levels expressed as a percentage of control samples ± SD. All autoradiograph data are representative of two separate experiments. $^{*}P < 0.05$, $^{**}P < 0.01$ and $^{***}P < 0.001$ vs. Ctrl; $^{\dagger}P < 0.05$, $^{\dagger\dagger}P < 0.01$ and $^{\ddagger}P < 0.001$ vs. Tun.

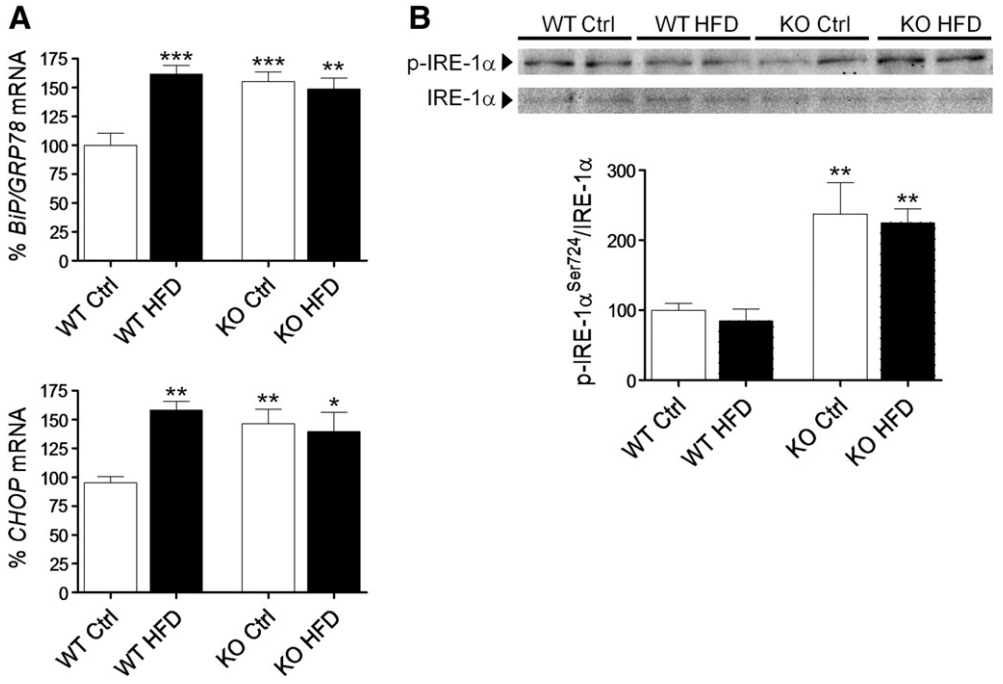

Fig. 5. ER stress induced by an HFD in the heart of mice is exacerbated in PPARβ/δ knockout mice. (A) Relative quantification of *BiP/GRP78* and *CHOP* mRNA levels assessed by real-time RT-PCR of samples obtained from the heart of wild-type (WT) or knockout PPARβ/δ (KO) mice fed a standard chow diet (Ctrl) or a saturated fatty acid-rich diet (HFD) for two months. The graphs represent the quantification of the *APRT*-normalized mRNA levels, expressed as a percentage of control samples ± SD. (B) Western-blot analysis showing the levels of phosphorylated IRE-1α^{Ser724}/IRE-1α in total protein extracts obtained from the samples depicted in panel A. The graphs represent the quantification of the normalized protein levels expressed as a percentage of control samples ± SD. All autoradiograph data are representative of two separate experiments. $^{*}P < 0.05$, $^{**}P < 0.01$ and $^{***}P < 0.001$ vs. WT Ctrl.

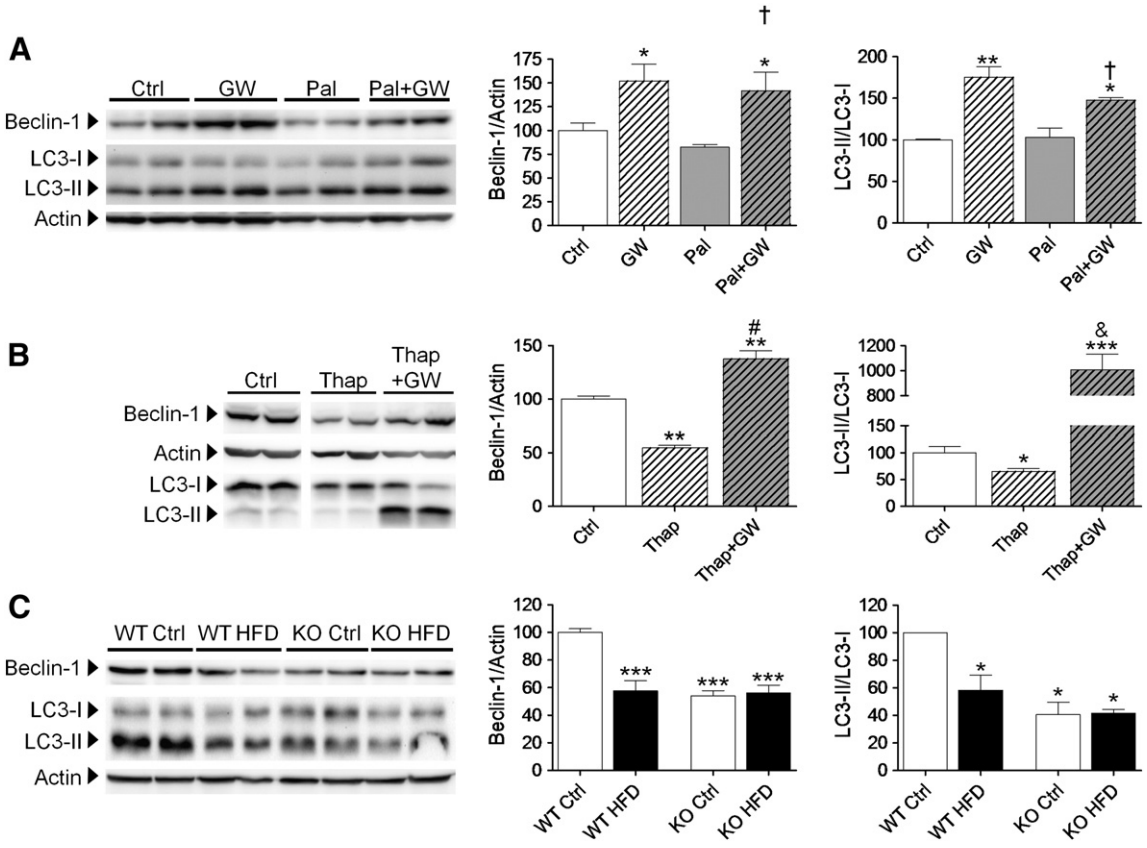

Fig. 6. PPARβ/δ activity regulates autophagy in cardiac cells. Western-blot analysis showing protein levels of beclin-1 and the LC3-II/LC3-I ratio in total protein extracts obtained from human cardiac AC16 cells incubated for (A) 18 h with palmitate (Pal, 0.25 mmol/L) or (B) 18 h with thapsigargin (Thap, 1 μmol/L), both in the presence or absence of GW501516 (GW, 10 μmol/L). (C) Western-blot analysis showing protein levels of beclin-1 and the LC3-II/LC3-I ratio in total protein extracts isolated from the heart of wild-type (WT) or knockout PPARβ/δ (KO) mice fed a standard chow diet (Ctrl) or a saturated fatty acid-rich diet (HFD) for two months. The graphs represent the quantification of the normalized protein levels expressed as a percentage of control samples ± SD. All autoradiograph data are representative of two separate experiments. (A) and (B) $^{*}P < 0.05$, $^{**}P < 0.01$ and $^{***}P < 0.001$ vs. Ctrl; $^{\dagger}P < 0.05$ vs. Pal; $^{\&}P < 0.01$, $^{\#}P < 0.001$ vs. Thap. (C) $^{*}P < 0.05$, $^{**}P < 0.01$ and $^{***}P < 0.001$ vs. WT Ctrl.

phosphorylation of eIF2α and IRE-1α (Fig. 3 and Supplemental Fig. 1B). To further confirm the role of AMPK in regulating ER stress in our cells, we monitored AMPK phosphorylation at Thr172, which is essential for its activity. As expected, compound C reduced AMPK phosphorylation (~90% reduction, $P < 0.05$ vs. control cells) in human AC16 cardiac cells but, strikingly, both AICAR (2-fold, $P < 0.05$ vs. control cells) and palmitate (3.5-fold, $P < 0.001$) enhanced this phosphorylation (Supplemental Fig. 2A). We also explored the phosphorylation of the cardiac-specific acetyl-CoA carboxylase (ACC) isoform, ACC2, a substrate for AMPK that serves as a surrogate for determining its activity. In contrast to AMPK phosphorylation, phospho-ACC2 levels were slightly reduced in cells exposed to palmitate or compound C, whereas in the presence of AICAR, they were significantly raised (2-fold, $P < 0.05$, Supplemental Fig. 2A).

ER stress inhibition after AMPK activation was also demonstrated after cardiac AC16 cells had been induced with tunicamycin, a mixture of homologous nucleoside antibiotics that acts as a potent pharmacologic ER-stress inducer. Tunicamycin elicited a huge increase in *sXBP1*, *ATF3* (3-fold, $P < 0.001$), *BiP/GRP78* (8-fold, $P < 0.001$) and *CHOP* (11-fold, $P < 0.001$) expression, as well as IRE-1α phosphorylation (2.5-fold, $P < 0.05$) (Fig. 4A). Co-incubation of tunicamycin-treated cells with AICAR prevented the rise of some of these ER stress markers, such as *BiP/GRP78* and *CHOP* expression, but not all (*sXBP1* and *ATF3*). Western-blot analyses revealed that AICAR also abolished the increase in CHOP protein induced by tunicamycin, as observed by mRNA levels, but not eIF2α or IRE-1α phosphorylation (Fig. 4B). Activation of AMPK by AICAR was again monitored by determination of ACC2 phosphorylation (Supplemental Fig. 2B).

Therefore, given that GW501516 can induce AMPK phosphorylation at Thr172 independently of PPARβ/δ activation, and we had observed that AMPK activation prevented palmitate-induced ER stress, we next examined whether this kinase was involved in the effects of GW501516. However, we found that compound C did not prevent GW501516-mediated effects on any of the ER stress markers examined (*ATF3*, *BiP/GRP78* and *CHOP* expression, Supplemental Fig. 3A). This indicates that AMPK did not mediate the beneficial effects of GW501516 on ER stress, and may be explained by the fact that, in contrast to previously reported data [27], GW501516 did not enhance AMPK and ACC2 phosphorylation in AC16 cells (Supplemental Fig. 3B). Likewise, GW501516 did not prevent either the effects of tunicamycin on the expression of *sXBP1*, *BiP/GRP78* and *CHOP*, or the phosphorylation of IRE-1α (Supplemental Fig. 4). Overall, this reinforces the notion that the effects of GW501516 are not dependant on AMPK activation.

3.3. ER stress induced by an HFD in the heart of mice is exacerbated in PPARβ/δ knockout mice

To corroborate the results obtained with cultured human cardiac cells, we also conducted in vivo studies with mice fed an HFD rich in saturated fatty acids. Consistent with the in vitro studies, an HFD significantly induced *BiP/GRP78* and *CHOP* expression in the heart of male wild type mice (1.5-fold, $P < 0.001$, and 1.5-fold, $P < 0.01$, respectively, vs. wild type control diet) (Fig. 5A). To further confirm the protective role of PPARβ/δ, we took advantage of PPARβ/δ knockout mice. Interestingly, *BiP/GRP78* (1.5-fold, $P < 0.01$ vs. wild type mice) and *CHOP* (1.5-fold, $P < 0.05$) expression was also higher in PPARβ/δ knockout mice than in wild type mice (Fig. 5A). This indicates that PPARβ/δ somehow prevented ER stress in the heart of these mice. Western-blot analysis revealed that PPARβ/δ suppression also enhanced IRE-1α phosphorylation (2.5-fold, $P < 0.01$) (Fig. 5B), although no splicing of *XBP1* was detected (Supplemental Fig. 5A). All these changes coincided with diminished AMPK and ACC2 activity, as revealed by western-blot (Supplemental Fig. 5B). This suggests that there was reduced fatty acid β-oxidation in mice fed an HFD and in PPARβ/δ knockout mice.

3.4. PPARβ/δ activity regulates autophagy in cardiac cells

As reported above, when ER stress becomes chronically activated, apoptosis is induced to remove affected cells. Therefore, the next goal of this study was to evaluate the presence of apoptosis in human cardiac cells treated with palmitate. This was attained by determining different apoptotic markers that are essential for the elimination of irreversibly damaged cells under chronic ER stress, such as α-spectrin breakdown and Bcl-2 protein levels, by means of western-blot analysis, or *Bax*, *Bim* and *Puma* mRNA levels by real-time RT-PCR. As observed in Supplemental Fig. 6, 0.25 mM palmitate treatment for 18 h did not induce apoptosis in human cardiac AC16 cells. GW501516 did not display any effect on apoptosis, except for a slight but interesting decrease of *Bim* expression after co-incubation with palmitate (40% reduction, $P < 0.01$ vs. palmitate-treated cells).

After that, we examined the occurrence of autophagy in human cardiac cells by checking two well-established autophagic markers in eukaryotes, the LC3-II/LC3-I ratio and the protein levels of beclin-1, which are both required for the formation of the autophagosome during autophagy. LC3 is considered a marker for autophagy when it is proteolytically processed to form LC3-II. In spite of beclin-1 and LC3 expression (Supplemental Fig. 7A) and the fact that protein levels (Fig. 6A) were not modified in palmitate-treated cells, we found that GW501516, alone or in combination with palmitate, significantly enhanced both markers of autophagy, beclin-1 (1.5-fold, $P < 0.05$) and the LC3-II/LC3-I ratio (1.75-fold, $P < 0.01$, Fig. 6A). GW501516 also induced autophagy in the presence of tunicamycin, which indicates that its effect was not dependent on the type of ER stress inducer (Supplemental Fig. 7B). On the contrary, autophagy was not observed after treatment with AICAR (Supplemental Fig. 7C). These results suggest that GW501516 induces autophagy by post-transcriptional mechanisms, and in an AMPK-independent manner. To further corroborate the effect of GW501516 on autophagy, we next incubated human cardiac cells with thapsigargin. Thapsigargin is a sesquiterpene lactone that is experimentally used to specifically inhibit the last step in the autophagic process, which also raises cytosolic calcium concentration, thereby inducing ER-stress. As shown in Fig. 6B, thapsigargin down-regulated the protein levels of beclin-1 (45% reduction, $P < 0.01$ vs. control cells) and the LC3-II/LC3-I ratio (35% reduction, $P < 0.05$), a fact which was not only prevented, but also further increased, after GW501516 co-incubation. Besides inhibiting autophagy, thapsigargin triggers expression of *CHOP*, a transcription factor involved in ER stress-induced apoptosis [10,28]. In accordance with this, we found that thapsigargin up-regulated BiP/GRP78 (3.5-fold, $P < 0.01$) and CHOP protein levels (7.5-fold, $P < 0.001$). The PPARβ/δ agonist GW501516 did not prevent the increase in BiP/GRP78 protein levels, but did attenuate those of CHOP (Supplemental Fig. 8), which suggests that this drug also down-regulated the ER stress induced by thapsigargin. Last, but not least, we demonstrated that HFD feeding or PPARβ/δ suppression clearly down-regulated beclin-1 and the LC3-II/LC3-I ratio in the heart of mice (Fig. 6C), which indicates that this nuclear receptor plays a key role in the control of the autophagic process in cardiac cells.

4. Discussion

In recent years, activation of the UPR during ER stress has evolved as a new mechanism involved in the association between saturated free fatty acid-induced inflammation and chronic metabolic diseases, such as obesity, insulin resistance, and type 2 diabetes [6,29]. Studies performed in muscle [4,30] and pancreatic β-cells [28] have demonstrated that palmitate induces the splicing of *XBP1* and enhances the expression of ER stress markers such as *ATF3*, *BiP/GRP78* and *CHOP*, as well as the phosphorylation of IRE-1α [4,30]. In agreement with this, we report that palmitate induces *XBP1* splicing and IRE-1α phosphorylation, as well as ATF3, BiP/GRP78 and CHOP gene expression and protein accumulation in human cardiac cells. However, and in contrast to muscle

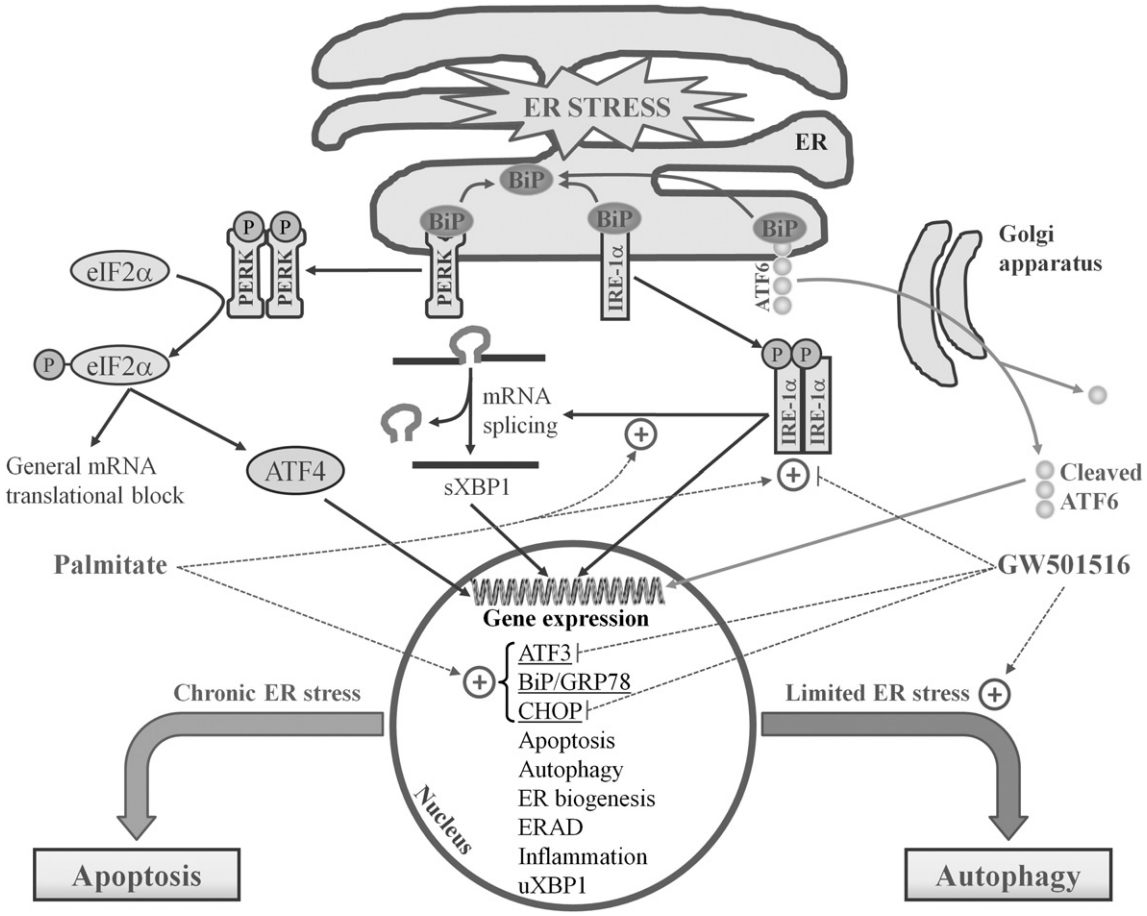

Fig. 7. PPARβ/δ attenuates palmitate-induced endoplasmic reticulum stress and induces autophagy. Initiation of the UPR involves the activation of ATF6, IRE-1α and PERK pathways. In the absence of stress, these trans-membrane proteins are bound to the intra-luminal BiP/GRP78 protein. On stress exposure, the large excess of unfolded proteins sequesters BiP/GRP78 from trans-membrane ER proteins, thereby inducing the UPR. After proteolytically processing at the Golgi complex, ATF6 translocates to the nucleus, in which it acts as a transcription factor for ER chaperones and ERAD-related genes. On the other hand, the endoribonuclease activity of IRE-1α cleaves the mRNA of *XBP1*, creating an alternative message that is translated into the spliced and active form of this transcription factor (sXBP1). Active IRE-1α also regulates responses mediated by mitogen-activated protein kinases (MAPKs) and NF-κB, which are relevant factors for the induction of apoptosis and inflammatory processes by ER stress. Finally, PERK phosphorylates and inhibits eIF2α, and by this means inhibits the translation of most mRNAs. However, some mRNAs escape this translational control, for example transcription factor *ATF4* (and its target genes *ATF3*, *BiP/GRP78* and *CHOP*) and genes involved in autophagy and apoptosis. If ER stress is limited, the UPR will potentiate autophagy to protect the cells. However, if ER stress is prolonged, the UPR will turn on apoptosis for removing cells that threaten the integrity of the organism. Palmitate induces *XBP1* splicing and IRE-1α phosphorylation, as well as ATF3, BiP/GRP78 and CHOP gene expression and protein accumulation in human cardiac cells. PPARβ/δ activation with GW501516 prevents saturated fatty acid-induced ER stress, since it abolishes the rise in ATF3 and CHOP levels and prevents IRE-1α phosphorylation in palmitate-treated cells. ATF, activating transcription factor; BiP/GRP78, binding immunoglobulin protein/glucose-regulated protein 78; CHOP, CCAAT/enhancer binding protein homologous protein; eIF2α, eukaryotic initiation factor 2α; ERAD, ER-associated degradation; IRE-1α, inositol-requiring enzyme; PERK, PKR-like ER kinase.

cells [4,5,31], the PERK/eIF2α branch of the UPR pathway was not activated in human cardiac cells, since eIF2α phosphorylation at Ser51 remained unaltered after palmitate treatment. In addition, we demonstrate here for the first time in cardiac cells that PPARβ/δ activation with GW501516 prevents saturated fatty acid-induced ER stress, since it abolishes the rise in ATF3 and CHOP levels. Strikingly, GW501516 prevented IRE-1α phosphorylation, but this was not accompanied by *sXBP1* downregulation. This suggests that in human cardiac cells *XBP1* splicing depends on the action of a yet to uncover endoribonuclease or that the time chosen for analyses was too short. sXBP1 up-regulates many essential UPR genes involved in folding, organelle biogenesis, ERAD, autophagy, and protein quality control, but its specific target genes may vary depending on the cell type and the nature of the stressor stimulus [8]. Although *BiP/GRP78* expression may be transcriptionally controlled by the three UPR branches, and given that the effects of GW501516 on *XBP1* splicing fairly correlated with those of *BiP/GRP78* expression, our results suggest that, at least in human cardiac cells, *BiP/GRP78* might be transcriptionally controlled by sXBP1.

Owing to its high fat content, the Western-type diet is known to cause insulin resistance and type 2 diabetes mellitus, besides inducing ER stress and inflammation [30,32]. Our studies conducted in vivo with mice also demonstrate that saturated fatty acid-rich HFD feeding induces *BiP/GRP78* and *CHOP* expression in the heart. More importantly, the expression of these ER stress markers was also enhanced in PPARβ/δ knockout mice, thus indicating that PPARβ/δ somehow prevented ER stress in the heart of mice. In agreement to what happened in vitro, PPARβ/δ suppression enhanced IRE-1α phosphorylation, but not *XBP1* splicing. Unlike human cardiac cells in vitro, we found that eIF2α phosphorylation was enhanced in the heart of mice fed an HFD and also in PPARβ/δ knockout mice (Supplemental Fig. 9).

AMPK activation brings about multiple protective effects, including inhibition of inflammation, oxidative stress and insulin resistance, which result in a diminution of the risk for developing obesity and type 2 diabetes [33]. Recently, it has been reported that AMPK protects against cardiomyocyte hypoxic injury [34] and atherosclerosis [35] by reducing ER stress. When we examined the potential mechanisms responsible for the increase in ER stress following palmitate exposure, we observed that this saturated fatty acid reduced AMPK activity. In consonance with this, AICAR prevented the rise of most palmitate-induced ER stress markers. Similar results were obtained after induction of ER stress with tunicamycin. In contrast, our results clearly indicate that the preventive effects of GW501516 on palmitate- and

tunicamycin-induced ER stress are AMPK-independent. On the contrary, results obtained in both mice fed an HFD and in PPARβ/δ knockout mice suggest that reduced fatty acid β-oxidation occurs in the heart. Nevertheless, our in vivo results match with those obtained in the liver and muscle of rodents after HFD feeding, in which saturated fatty acids appear to contribute to AMPK inhibition [36].

Prolonged or severe ER stress during diabetic cardiomyopathy leads to apoptotic cell death of cardiomyocytes [14] and, because myocytes rarely proliferate in the adult heart, the loss of cardiomyocytes will compromise cardiac function. The initiation of the caspase cascade during intrinsic apoptosis is mediated by BH3-only domain proteins such as Bim (B-cell lymphoma-2 [Bcl-2]-like 11) and Puma (Bcl-2 binding component 3), which are responsible for transmitting death signals by either inhibiting the Bcl-2 anti-apoptotic members (Bcl-2; Bcl-xL, B-cell lymphoma-extra large) or activating the pro-apoptotic Bcl-2 multi-domain proteins (Bax, Bcl-2-associated × protein; Bak, Bcl-2 homologous antagonist/killer) at the mitochondria. The UPR promotes the expression of CHOP, a pro-apoptotic transcription factor that has a critical role in cardiac cell death caused by chronic ER stress during heart failure [11] and cardiac hypertrophy [37]. The UPR, possibly through CHOP, down-regulates the anti-apoptotic Bcl-2 family of proteins, but transcriptionally up-regulates Bim and Puma. Overall, this contributes to apoptosis in cells undergoing irreversible ER stress [8]. However, although we had found a significant increase in CHOP protein levels after palmitate treatment, no changes in any of the apoptotic markers examined were detected in human cardiac cells. In accordance with this, Quentin et al. [38] demonstrated that CHOP is not necessarily a mediator of apoptosis in rat cardiomyocytes. Nevertheless, our results contrast with those obtained in diverse hepatoma cell lines [39,40], in which palmitic acid was found to induce ER stress and subsequent apoptosis. Although GW501516 prevented the rise in CHOP protein levels after palmitate treatment in human cardiac cells, it did not reduce apoptosis. The relatively short duration of palmitate treatment might account for the lack of apoptotic activation in human cardiac cells, since several authors have speculated that the transition between adaptive UPR and apoptosis depends, at least in part, on the duration of ER stress stimulation [8].

It is widely accepted that, when ER stress is limited, the UPR potentiates autophagy as a short-term strategy to protect cells. Thus, suppression of autophagy favors the development of heart failure during diabetes [41], whereas its induction may reduce myocardial ischemia/reperfusion-induced lethal injury [10]. The most striking result of our study is the enhancement of two well-known markers of autophagy in cardiac cells after GW501516 treatment and in the heart of mice fed an HFD. More importantly, we also report here that PPARβ/δ suppression down-regulates autophagic markers in the heart of mice, hence suggesting that this nuclear receptor is crucial in regulating the autophagic process in cardiac cells. However, and unlike a previous study performed with rat heart [10], we did not find any correlation between eIF2α phosphorylation and the conversion of LC3-II from LC3-I. This suggests that the PERK/eIF2α pathway is not essential for autophagy in our model. In fact, our results better fit with those obtained by Ogata et al. [42] in mouse embryonic fibroblasts, which demonstrated that activation of autophagy by ER stress depends on the kinase domain of IRE-1α, but not on its endoribonuclease activity on *XBP1* nor on the PERK/eIF2α pathway. A recent study demonstrated that activation of AMPK restores cardiac autophagy and protects against cardiac cell apoptosis, which ultimately improves cardiac function in diabetic mice [41]. In contrast, our results indicate that GW501516 induces autophagy by post-transcriptional mechanisms in an AMPK-independent manner. This discrepancy might be explained by the fact that He and collaborators investigated autophagy in the context of high glucose conditions, and AMPK is a well-recognized regulator of glucose homeostasis. However, recent studies performed in mice fed an HFD reported that autophagy is down-regulated in adipose tissue [43] and in the heart [44]. The former study also demonstrates that autophagy suppression induces inflammatory responses via ER stress activation, while the opposite, that is activation of autophagy with rapamycin, decreases inflammatory gene expression [43]. Overall, and taking into account our previous data demonstrating that PPARβ/δ can limit myocardial inflammation by NF-κB inhibition [15], we hypothesize that GW501516 might prevent ER stress in human cardiac cells by means of autophagy activation. This is supported by our results demonstrating that the NF-κB inhibitor parthenolide prevented the up-regulation of *ATF3* and *CHOP* expression induced by palmitate in human cardiac cells (Supplemental Fig. 10).

Given its causative role in cardiovascular diseases associated with metabolic disorders such as obesity and diabetes, ER stress has been suggested as a useful therapeutic target. With this aim, several chemical chaperones have been examined in a number of disease models as potential tools for preventing ER stress and the activation of the UPR, since they play a similar role to endogenous chaperones, stabilizing proteins and assisting in their proper folding [45]. For instance, 4-phenylbutyric acid (PBA) and tauroursodeoxycholic acid (TUDCA) have had beneficial effects on insulin resistance, obesity and diabetes in several in vitro [4,5] and in vivo [46] models. However, chemical chaperones have major drawbacks: their null specificity and a high-dose are required to obtain effective protein folding properties. Therefore, the research and development of new drugs that target ER stress during metabolic diseases without the undesired effects of chemical chaperones are of great interest.

5. Study limitations

A major drawback of the study might be the origin of the AC16 cell line itself, since it consists of a fusion of primary ventricular cells with SV-40-transformed fibroblasts. However, this cell line develops many of the biochemical and morphological properties characteristic of cardiac muscle cells, even though it does not form completely differentiated cardiomyocytes [47]. Furthermore, the more relevant findings obtained in this study with AC16 human cardiac cells have been further corroborated later in the heart of mice.

6. Conclusions

Results herein reported demonstrate that PPARβ/δ activation with GW501516 attenuates palmitate-induced ER stress and induces autophagy in human cardiac cells (Fig. 7), thereby adding a new beneficial mechanism for this drug. In this context, activation of autophagy has already been suggested as a useful therapeutic approach for diabetes, owing to its ability to reduce ER stress in pancreatic β-cells [48]. PPARβ/δ has many valuable physiological functions ranging from enhanced fatty acid catabolism and improved insulin sensitivity, to inflammation inhibition, thus displaying a potential therapeutic role for the prevention and treatment of diseases including diabetes, dyslipidemias or metabolic syndrome. Since chronic low-grade inflammation and ER stress play a significant role in cardiac hypertrophy and heart failure, and GW501516 has been shown to ameliorate metabolic disturbances in heart caused by high-fat diets [15], it is tempting to speculate that PPARβ/δ might serve as a therapeutic target to prevent cardiac hypertrophy and heart failure induced by ER stress during metabolic disorders.

Supplementary data to this article can be found online at http://dx.doi.org/10.1016/j.ijcard.2014.03.176.

Acknowledgments

This study was supported by funds from the *Ministerio de Economía y Competitividad* of the Spanish Government (SAF2009-06939 and SAF2012-30708). *CIBER de Diabetes y Enfermedades Metabólicas Asociadas* (CIBERDEM) is an initiative of the *Instituto de*

Salud Carlos III (ISCIII) — *Ministerio de Economía y Competitividad*. We thank the University of Barcelona's Language Advisory Service for their assistance.

The authors of this manuscript have certified that they comply with the Principles of Ethical Publishing in the International Journal of Cardiology.

References

[1] Diakogiannaki E, Welters HJ, Morgan NG. Differential regulation of the endoplasmic reticulum stress response in pancreatic beta-cells exposed to long-chain saturated and monounsaturated fatty acids. J Endocrinol 2008;197:553–63.
[2] Karaskov E, Scott C, Zhang L, Teodoro T, Ravazzola M, Volchuk A. Chronic palmitate but not oleate exposure induces endoplasmic reticulum stress, which may contribute to INS-1 pancreatic beta-cell apoptosis. Endocrinology 2006;147:3398–407.
[3] Jung TW, Lee KT, Lee MW, Ka KH. SIRT1 attenuates palmitate-induced endoplasmic reticulum stress and insulin resistance in HepG2 cells via induction of oxygen-regulated protein 150. Biochem Biophys Res Commun 2012;422:229–32.
[4] Salvadó L, Coll T, Gomez-Foix AM, et al. Oleate prevents saturated-fatty-acid-induced ER stress, inflammation and insulin resistance in skeletal muscle cells through an AMPK-dependent mechanism. Diabetologia 2013;56:1372–82.
[5] Peng G, Li L, Liu Y, et al. Oleate blocks palmitate-induced abnormal lipid distribution, endoplasmic reticulum expansion and stress, and insulin resistance in skeletal muscle. Endocrinology 2011;152:2206–18.
[6] Hotamisligil GS. Endoplasmic reticulum stress and the inflammatory basis of metabolic disease. Cell 2010;140:900–17.
[7] Xu J, Zhou Q, Xu W, Cai L. Endoplasmic reticulum stress and diabetic cardiomyopathy. Exp Diabetes Res 2012;2012:827971.
[8] Hetz C, Martinon F, Rodriguez D, Glimcher LH. The unfolded protein response: integrating stress signals through the stress sensor IRE1α. Physiol Rev 2011;91:1219–43.
[9] Ma Y, Brewer JW, Diehl JA, Hendershot LM. Two distinct stress signaling pathways converge upon the CHOP promoter during the mammalian unfolded protein response. J Mol Biol 2002;318:1351–65.
[10] Petrovski G, Das S, Juhasz B, Kertesz A, Tosaki A, Das DK. Cardioprotection by endoplasmic reticulum stress-induced autophagy. Antioxid Redox Signal 2011;14:2191–200.
[11] Zhao H, Liao Y, Minamino T, et al. Inhibition of cardiac remodeling by pravastatin is associated with amelioration of endoplasmic reticulum stress. Hypertens Res 2008;31:1977–87.
[12] Li Z, Zhang T, Dai H, et al. Involvement of endoplasmic reticulum stress in myocardial apoptosis of streptozocin-induced diabetic rats. J Clin Biochem Nutr 2007;41:58–67.
[13] Lakshmanan AP, Meilei H, Suzuki K, et al. The hyperglycemia stimulated myocardial endoplasmic reticulum (ER) stress contributes to diabetic cardiomyopathy in the transgenic non-obese type 2 diabetic rats: a differential role of unfolded protein response (UPR) signaling proteins. Int J Biochem Cell Biol 2012;45:438–47.
[14] Takada A, Miki T, Kuno A, et al. Role of ER stress in ventricular contractile dysfunction in type 2 diabetes. PLoS ONE 2012;7:e39893.
[15] Álvarez-Guardia D, Palomer X, Coll T, et al. PPARbeta/delta activation blocks lipid-induced inflammatory pathways in mouse heart and human cardiac cells. Biochim Biophys Acta 1811;2011:59–67.
[16] Hamid T, Guo SZ, Kingery JR, Xiang X, Dawn B, Prabhu SD. Cardiomyocyte NF-kappaB p65 promotes adverse remodelling, apoptosis, and endoplasmic reticulum stress in heart failure. Cardiovasc Res 2011;89:129–38.
[17] Cheng L, Ding G, Qin Q, et al. Cardiomyocyte-restricted peroxisome proliferator-activated receptor-delta deletion perturbs myocardial fatty acid oxidation and leads to cardiomyopathy. Nat Med 2004;10:1245–50.
[18] Wang P, Liu J, Li Y, et al. Peroxisome proliferator-activated receptor delta is an essential transcriptional regulator for mitochondrial protection and biogenesis in adult heart. Circ Res 2010;106:911–9.
[19] Cao M, Tong Y, Lv Q, et al. PPARdelta activation rescues pancreatic beta-cell line INS-1E from palmitate-induced endoplasmic reticulum stress through enhanced fatty acid oxidation. PPAR Res 2012;2012:680684.
[20] Ramirez T, Tong M, Chen WC, Nguyen QG, Wands JR, de la Monte SM. Chronic alcohol-induced hepatic insulin resistance and ER stress ameliorated by PPAR-delta agonist treatment. J Gastroenterol Hepatol 2013;28:179–87.
[21] Palomer X, Álvarez-Guardia D, Rodriguez-Calvo R, et al. TNF-alpha reduces PGC-1alpha expression through NF-kappaB and p38 MAPK leading to increased glucose oxidation in a human cardiac cell model. Cardiovasc Res 2009;81:703–12.
[22] Coll T, Palomer X, Blanco-Vaca F, et al. Cyclooxygenase 2 inhibition exacerbates palmitate-induced inflammation and insulin resistance in skeletal muscle cells. Endocrinology 2010;151:537–48.
[23] Nadra K, Anghel SI, Joye E, et al. Differentiation of trophoblast giant cells and their metabolic functions are dependent on peroxisome proliferator-activated receptor beta/delta. Mol Cell Biol 2006;26:3266–81.
[24] Palomer X, Capdevila-Busquets E, Álvarez-Guardia D, et al. Resveratrol induces nuclear factor-kappaB activity in human cardiac cells. Int J Cardiol 2013;167:2507–16.
[25] Bradford MM. A rapid and sensitive method for the quantitation of microgram quantities of protein utilizing the principle of protein-dye binding. Anal Biochem 1976;72:248–54.
[26] Álvarez-Guardia D, Palomer X, Coll T, et al. The p65 subunit of NF-kappaB binds to PGC-1alpha, linking inflammation and metabolic disturbances in cardiac cells. Cardiovasc Res 2010;87:449–58.
[27] Kramer DK, Al Khalili L, Guigas B, Leng Y, Garcia-Roves PM, Krook A. Role of AMP kinase and PPARdelta in the regulation of lipid and glucose metabolism in human skeletal muscle. J Biol Chem 2007;282:19313–20.
[28] Kharroubi I, Ladriere L, Cardozo AK, Dogusan Z, Cnop M, Eizirik DL. Free fatty acids and cytokines induce pancreatic beta-cell apoptosis by different mechanisms: role of nuclear factor-kappaB and endoplasmic reticulum stress. Endocrinology 2004;145:5087–96.
[29] Zhang K, Kaufman RJ. From endoplasmic-reticulum stress to the inflammatory response. Nature 2008;454:455–62.
[30] Rieusset J, Chauvin MA, Durand A, et al. Reduction of endoplasmic reticulum stress using chemical chaperones or Grp78 overexpression does not protect muscle cells from palmitate-induced insulin resistance. Biochem Biophys Res Commun 2011;417:439–45.
[31] Hage Hassan R, Hainault I, Vilquin JT, et al. Endoplasmic reticulum stress does not mediate palmitate-induced insulin resistance in mouse and human muscle cells. Diabetologia 2012;55:204–14.
[32] Panzhinskiy E, Hua Y, Culver B, Ren J, Nair S. Endoplasmic reticulum stress upregulates protein tyrosine phosphatase 1B and impairs glucose uptake in cultured myotubes. Diabetologia 2012;56:598–607.
[33] Shaw RJ, Lamia KA, Vasquez D, et al. The kinase LKB1 mediates glucose homeostasis in liver and therapeutic effects of metformin. Science 2005;310:1642–6.
[34] Yeh CH, Chen TP, Wang YC, Lin YM, Fang SW. AMP-activated protein kinase activation during cardioplegia-induced hypoxia/reoxygenation injury attenuates cardiomyocytic apoptosis via reduction of endoplasmic reticulum stress. Mediators Inflamm 2010;2010:130636.
[35] Dong Y, Zhang M, Liang B, et al. Reduction of AMP-activated protein kinase alpha2 increases endoplasmic reticulum stress and atherosclerosis in vivo. Circulation 2010;121:792–803.
[36] Muse ED, Obici S, Bhanot S, et al. Role of resistin in diet-induced hepatic insulin resistance. J Clin Invest 2004;114:232–9.
[37] Ni L, Zhou C, Duan Q, et al. Beta-AR blockers suppresses ER stress in cardiac hypertrophy and heart failure. PLoS ONE 2011;6:e27294.
[38] Quentin T, Steinmetz M, Poppe A, Thoms S. Metformin differentially activates ER stress signaling pathways without inducing apoptosis. Dis Model Mech 2011;5:259–69.
[39] Zhang Y, Xue R, Zhang Z, Yang X, Shi H. Palmitic and linoleic acids induce ER stress and apoptosis in hepatoma cells. Lipids Health Dis 2012;11:1.
[40] Cao J, Dai DL, Yao L, et al. Saturated fatty acid induction of endoplasmic reticulum stress and apoptosis in human liver cells via the PERK/ATF4/CHOP signaling pathway. Mol Cell Biochem 2012;364:115–29.
[41] He C, Zhu H, Li H, Zou MH, Xie Z. Dissociation of Bcl-2–Beclin1 complex by activated AMPK enhances cardiac autophagy and protects against cardiomyocyte apoptosis in diabetes. Diabetes 2012;62:1270–81.
[42] Ogata M, Hino S, Saito A, et al. Autophagy is activated for cell survival after endoplasmic reticulum stress. Mol Cell Biol 2006;26:9220–31.
[43] Yoshizaki T, Kusunoki C, Kondo M, et al. Autophagy regulates inflammation in adipocytes. Biochem Biophys Res Commun 2012;417:352–7.
[44] Guo R, Zhang Y, Turdi S, Ren J. Adiponectin knockout accentuates high fat diet-induced obesity and cardiac dysfunction: role of autophagy. Biochim Biophys Acta 1832;2013:1136–48.
[45] Basseri S, Austin RC. Endoplasmic reticulum stress and lipid metabolism: mechanisms and therapeutic potential. Biochem Res Int 2012;2012:841362.
[46] Ozcan U, Yilmaz E, Ozcan L, et al. Chemical chaperones reduce ER stress and restore glucose homeostasis in a mouse model of type 2 diabetes. Science 2006;313:1137–40.
[47] Davidson MM, Nesti C, Palenzuela L, et al. Novel cell lines derived from adult human ventricular cardiomyocytes. J Mol Cell Cardiol 2005;39:133–47.
[48] Bachar-Wikstrom E, Wikstrom JD, Ariav Y, et al. Stimulation of autophagy improves endoplasmic reticulum stress-induced diabetes. Diabetes 2012;62:1227–37.

Glossary

ACC: acetyl-CoA carboxylase
ACO: acyl-CoA oxidase
AICAR: 5-aminoimidazole-4-carboxamide ribonucleotide
AMPK: 5′ AMP-activated protein kinase
ATF: activating transcription factor
Bax: Bcl-2-associated X protein
Bcl-2: B-cell lymphoma 2
Bim: Bcl-2-like 11
BiP/GRP78: binding immunoglobulin protein/glucose-regulated protein
CHOP: CCAAT/enhancer binding protein (C/EBP) homologous protein
CPT-1b: carnitine palmitoyltransferase 1b
ER: endoplasmic reticulum
ERAD: ER-associated degradation
HFD: high-fat diet
IRE-1α: inositol-requiring enzyme-1α
LC3: microtubule-associated protein 1A/1B-light chain 3
NF-κB: nuclear factor-κB
PERK: PKR-like ER kinase
PPARβ/δ: peroxisome proliferator-activated receptor β/δ
Puma: Bcl-2 binding component 3
UPR: unfolded protein response
XBP1: X-box binding protein 1

© 2015. Published by The Company of Biologists Ltd | Disease Models & Mechanisms (2015) 8, 1081-1091 doi:10.1242/dmm.020768

RESEARCH ARTICLE

miR-146a targets *Fos* expression in human cardiac cells

Xavier Palomer[1], Eva Capdevila-Busquets[1], Gaia Botteri[1], Mercy M. Davidson[2], Cristina Rodríguez[3], José Martínez-González[3], Francisco Vidal[4], Emma Barroso[1], Tung O. Chan[5], Arthur M. Feldman[6] and Manuel Vázquez-Carrera[1,*]

ABSTRACT

miR-146a is a microRNA whose transcript levels are induced in the heart upon activation of NF-κB, a transcription factor induced by pro-inflammatory molecules (such as TNF-α) that is strongly related to the pathogenesis of cardiac disorders. The main goal of this study consisted of studying new roles of miR-146a in cardiac pathological processes caused by the pro-inflammatory cytokine TNF-α. Our results demonstrate that miR-146a transcript levels were sharply increased in cardiac ventricular tissue of transgenic mice with specific overexpression of TNF-α in the heart, and also in a cardiomyocyte cell line of human origin (AC16) exposed to TNF-α. Among all the *in silico* predicted miR-146a target genes, Fos mRNA and protein levels notably decreased after TNF-α treatment or miR-146a overexpression. These changes correlated with a diminution in the DNA-binding activity of AP-1, the Fos-containing transcription factor complex. Interestingly, AP-1 inhibition was accompanied by a reduction in matrix metalloproteinase (*MMP*)*-9* mRNA levels in human cardiac cells. The specific regulation of this MMP by miR-146a was further confirmed at the secretion and enzymatic activity levels, as well as after anti-miR-mediated miR-146a inhibition. The results reported here demonstrate that *Fos* is a direct target of miR-146a activity and that downregulation of the Fos–AP-1 pathway by miR-146a has the capacity to inhibit MMP-9 activity. Given that *MMP-9* is an AP-1 target gene involved in cardiac remodeling, myocardial dysfunction and progression of heart failure, these findings suggest that miR-146a might be a new and promising therapeutic tool for treating cardiac disorders associated with enhanced inflammation in the heart.

KEY WORDS: Fos, Cardiac remodeling, Inflammation, miR-146a, Matrix metalloproteinase-9

INTRODUCTION

The myocardium responds to various pathological stimuli by expressing and secreting several pro-inflammatory cytokines and chemokines such as interleukin-6 (IL-6), monocyte chemoattractant protein-1 (MCP-1) and tumor necrosis factor-α (TNF-α) (Palomer et al., 2013a,b). These pro-inflammatory mediators, which are transcriptionally regulated by the ubiquitous and inducible nuclear factor-κB (NF-κB), exert their pleiotropic autocrine effects via downstream activation of activator protein-1 (AP-1) and NF-κB itself, thereby contributing to myocardial inflammation, dilated cardiomyopathy, cardiac hypertrophy and heart failure (Gupta et al., 2008; Palomer et al., 2013a,b). Myocardial injury caused by these pathologies leads to myocyte function failure, fibrosis and ensuing ventricular remodeling, which can eventually trigger heart failure. In this regard, TNF-α production is enhanced in the heart of spontaneously hypertensive rats and in the failing human heart; this then contributes to cardiac remodeling and malfunction, thereby speeding up heart failure progression (Bergman et al., 1999). Likewise, continual intra-cardiac expression of TNF-α promotes the development of cardiac allograft hypertrophy (Stetson et al., 2001). Therefore, it is not surprising that pharmacological inhibition of TNF-α activity improves myocardial function during heart failure (Isic et al., 2008).

A recent study performed in rats has revealed an essential role for NF-κB and AP-1 in the pathogenesis of cardiac hypertrophy (Wang et al., 2009). AP-1 is a heterodimeric transcription factor composed of members belonging to the Jun, Fos, activating transcription factors (ATFs) and Jun-dimerization partner families. AP-1 regulates a number of cellular processes, including differentiation, proliferation and apoptosis. In the heart, AP-1 causes changes in the extracellular matrix and decreases contractility and cell permeability, inducing hypertrophy of cardiomyocytes and fibrosis of the interstitial substance, which eventually lead to heart failure (Wang et al., 2009).

The last decade has seen a plethora of studies reporting a critical role of microRNAs (miRNAs) as regulators of cardiac development, function and performance, as well as in the development of cardiac disease. miRNAs are endogenous non-coding small RNAs that modulate gene expression by targeting mRNAs for post-transcriptional repression through imperfect base-pairing, thereby participating in many essential biological processes. To date, more than 900 mature miRNAs have been identified in the human genome, which alter the translation of up to 50% of all genes (van de Vrie et al., 2011). Furthermore, a single miRNA could target multiple mRNAs, and most mRNAs can be regulated by different miRNAs, hence bringing enormous complexity to the regulation of gene expression. Chronic immune activation and anomalous miRNA expression have been regarded as important players in the pathological molecular mechanisms underlying cardiac disease. As an example, microarray studies have shed some light on the specific miRNAs that are aberrantly downregulated (miR-1, -29, -30, -133 and -150) or upregulated (miR-21, -23a, -125, -146, -195, -199 and -214) in heart failure patients (van de Vrie et al., 2011). However, little is known at present about the function of specific miRNAs

[1]Department of Pharmacology and Therapeutic Chemistry, IBUB (Institut de Biomedicina de la Universitat de Barcelona) and CIBER de Diabetes y Enfermedades Metabólicas Asociadas (CIBERDEM), Faculty of Pharmacy, University of Barcelona, Diagonal 643, Barcelona E-08028, Spain. [2]Department of Radiation Oncology, Columbia University, P&S 11-451, 630 West 168th Street, New York, NY 10032, USA. [3]Centro de Investigación Cardiovascular, CSIC-ICCC, IIB-Sant Pau, Avda. Sant Antoni Maria Claret 167, Barcelona 08025, Spain. [4]Unitat de Diagnòstic i Teràpia Molecular, Banc de Sang i Teixits, Passeig Vall d'Hebron 119-129, Barcelona 08035, Spain. [5]Department of Medicine, The Center for Translational Medicine, Jefferson Medical College, 1025 Walnut Street, Philadelphia, PA 19107, USA. [6]Departments of Medicine and Physiology, Cardiovascular Research Center, Temple University School of Medicine, 3500 N, Broad Street, Philadelphia, PA 19140, USA.

*Author for correspondence (mvazquezcarrera@ub.edu)

Received 11 March 2015; Accepted 12 June 2015

Disease Models & Mechanisms (2015) 8, 1081-1091 doi:10.1242/dmm.020768

TRANSLATIONAL IMPACT

Clinical issue

Heart disease is the leading cause of death in diabetic patients. Diabetic cardiomyopathy is characterized by concentric left ventricular hypertrophy, dilated cardiomyopathy, myocardial fibrosis and subsequent ventricular remodeling, eventually leading to heart failure. However, despite the added burden that diabetes poses on the heart, current therapeutic strategies do not specifically address diabetic cardiomyopathy. An increasing body of evidence suggests a potential link between chronic low-grade inflammation and metabolic disorders such as insulin resistance and type 2 diabetes. Chronic immune activation and aberrant microRNA (miRNA) expression have been regarded as important players in the pathological molecular mechanisms underlying cardiac disease, although little is known at present about the function of specific miRNAs during inflammatory responses in the heart.

Results

In this study, the authors investigate the role of miR-146a in the pathological processes induced by the pro-inflammatory cytokine TNF-α in the heart. They find a huge increase in miR-146a levels in the heart of transgenic mice with cardiac-specific overexpression of TNF-α and in human cardiac AC16 cells exposed to TNF-α. The authors demonstrate that *Fos* is a direct target of miR-146a activity: overexpression of the latter results in a notable decrease in both Fos mRNA and protein levels, which correlated with a diminution in the DNA-binding activity of AP-1, the Fos-containing transcription factor complex. The authors also report that AP-1 inhibition is accompanied by a reduction in matrix metalloproteinase (MMP)-9 secretion and enzymatic activity in human cardiac cells.

Implications and future directions

In the heart, AP-1 causes changes in the extracellular matrix and decreases contractility, inducing hypertrophy of cardiomyocytes and fibrosis of the interstitial substance, which ultimately lead to heart failure. The results reported here demonstrate that Fos is a direct target of miR-146a activity and that downregulation of the Fos–AP-1 pathway by miR-146a has the capacity to inhibit MMP-9 activity. These results are very appealing because upregulation of MMP-9 expression correlates fairly well with heart failure, whereas its downregulation suppresses ventricular remodeling, myocardial dysfunction and progression of heart failure. The recently developed antisense-oligonucleotide-mediated knockdown and miRNA overexpression techniques have become very attractive pharmacological strategies in the treatment of cardiovascular disease. In this respect, miR-146a emerges as a new and promising therapeutic tool for preventing cardiac disorders associated with inflammatory states in the heart.

during inflammatory responses in the heart. For this reason, the main goal of the present study was to investigate the potential role of miRNAs in the pathological processes induced by TNF-α in cardiac cells.

RESULTS

TNF-α induces miR-146a expression and reduces Fos in cardiac cells

As a first approach, we assessed the effects of TNF-α on the expression of a panel of miRNAs previously related to heart disease, obesity, type 2 diabetes and inflammation. Of these, only miR-146a expression was significantly induced by TNF-α [approximately sixfold, $P<0.01$ vs control (Ctrl), Fig. 1A] in human cardiac AC16 cells, whereas the remaining miRNAs were not modified or simply not detected (see supplementary material Fig. S1). To further confirm these results, neonatal rat cardiomyocytes were cultured *in vitro* and treated with TNF-α; as shown in Fig. 1B, miR-146a was also significantly upregulated by this pro-inflammatory cytokine (1.5-fold, $P<0.05$ vs Ctrl). Consistent with this finding, miR-146a was also hugely stimulated in left ventricular tissue of TNF1.6 transgenic mice with cardiac-specific TNF-α overexpression [tenfold, $P<0.01$ vs wild type (WT), Fig. 1C].

The miRGator analysis tool (available at http://genome.ewha.ac.kr/miRGator/miRNAexpression.html), an online interface that uses multiple target prediction algorithms, was then used to identify unknown downstream targets of miR-146a. Of all the predicted genes, *Fos* (FBJ murine osteosarcoma viral oncogene homolog; also known as *c-Fos*) displayed a notable decrease in its mRNA levels in human cardiac AC16 cells after TNF-α treatment, which was sustained over time and with different TNF-α concentrations (Fig. 1D,E). Interestingly, there was a time-dependent significant negative correlation between *Fos* mRNA levels and miR-146a expression in human cardiac AC16 cells (Fig. 1D, Spearman rank correlation $r=-0.8929$, $P<0.05$).

After that, we examined the effects of TNF-α on neonatal rat cardiomyocytes cultured *in vitro* and, in agreement with the enhanced miR-146a levels, TNF-α partially inhibited *Fos* expression (~50% reduction, $P<0.05$ vs Ctrl, Fig. 1F). Fos is a leucine zipper protein that forms the transcription factor AP-1 and, for this reason, we next carried out an electrophoretic mobility shift assay (EMSA) to assess the transcriptional activity of AP-1. AP-1 formed one specific DNA-binding complex (I) with nuclear proteins in human cardiac cells (Fig. 1G). The competitor lane demonstrated that this complex was specific for the AP-1 probe, whereas addition of a Fos-specific antibody to the binding reaction disrupted the protein:DNA interaction, hence suggesting that complex I contained the Fos subunit. More importantly, treatment of AC16 cells with TNF-α inhibited AP-1 DNA-binding activity compared with control cells.

miR-146a is directly responsible for Fos downregulation in cardiac cells

To determine whether *Fos* was a direct target of miR-146a activity, human AC16 cardiac cells were transfected with a plasmid carrying pre-miR-146a in the absence of TNF-α, which yielded an important increase in miR-146a expression (15-fold, $P<0.05$ vs *lacZ*, Fig. 2A). Compatible with our hypothesis, real-time RT-PCR analysis revealed that this miRNA was inhibiting *Fos* expression (~45% reduction, $P<0.01$, Fig. 2B). Such inhibition resulted in a significant downregulation of Fos protein levels at both the cytoplasm (CP fraction, ~50% reduction, $P<0.05$) and the nucleus (NE fraction, ~50% reduction, $P<0.05$) of miR-146a-transfected cells (Fig. 2C), and caused a significant decrease in the DNA-binding activity of the AP-1 transcription factor (Fig. 2D). In agreement with this, downregulation of miR-146a levels (~98% reduction, Fig. 3A) by transfecting AC16 cells with a human anti-miR-146a inhibitor coincided with a significant increase in *Fos* expression (1.9-fold, $P<0.001$ vs Ctrl anti-miR, Fig. 3B). In addition, the anti-miR-146a inhibitor partially reversed the effects of TNF-α on *Fos* expression (1.7-fold, $P<0.001$ vs anti-miR+TNF-α). In agreement with gene expression data, Fos protein levels were enhanced by 1.4-fold ($P<0.05$ vs Ctrl anti-miR+TNF-α) in the nucleus of AC16 cells transfected with anti-miR-146a (NE fraction, Fig. 3C). In order to demonstrate the specificity of Fos regulation by miR-146a, the protein levels of Jun and the p65 subunit of NF-κB were also determined in cytoplasmic and nuclear extracts of cells overexpressing miR-146a (Fig. 2C) and after downregulation of miR-146a with an anti-miR-146a inhibitor (Fig. 3C). It is worth mentioning that p65 and Jun were not altered after modulation of miR-146a levels. As expected, p65 protein levels were increased in the nucleus after TNF-α treatment, owing to NF-κB activation. In

Disease Models & Mechanisms (2015) 8, 1081-1091 doi:10.1242/dmm.020768

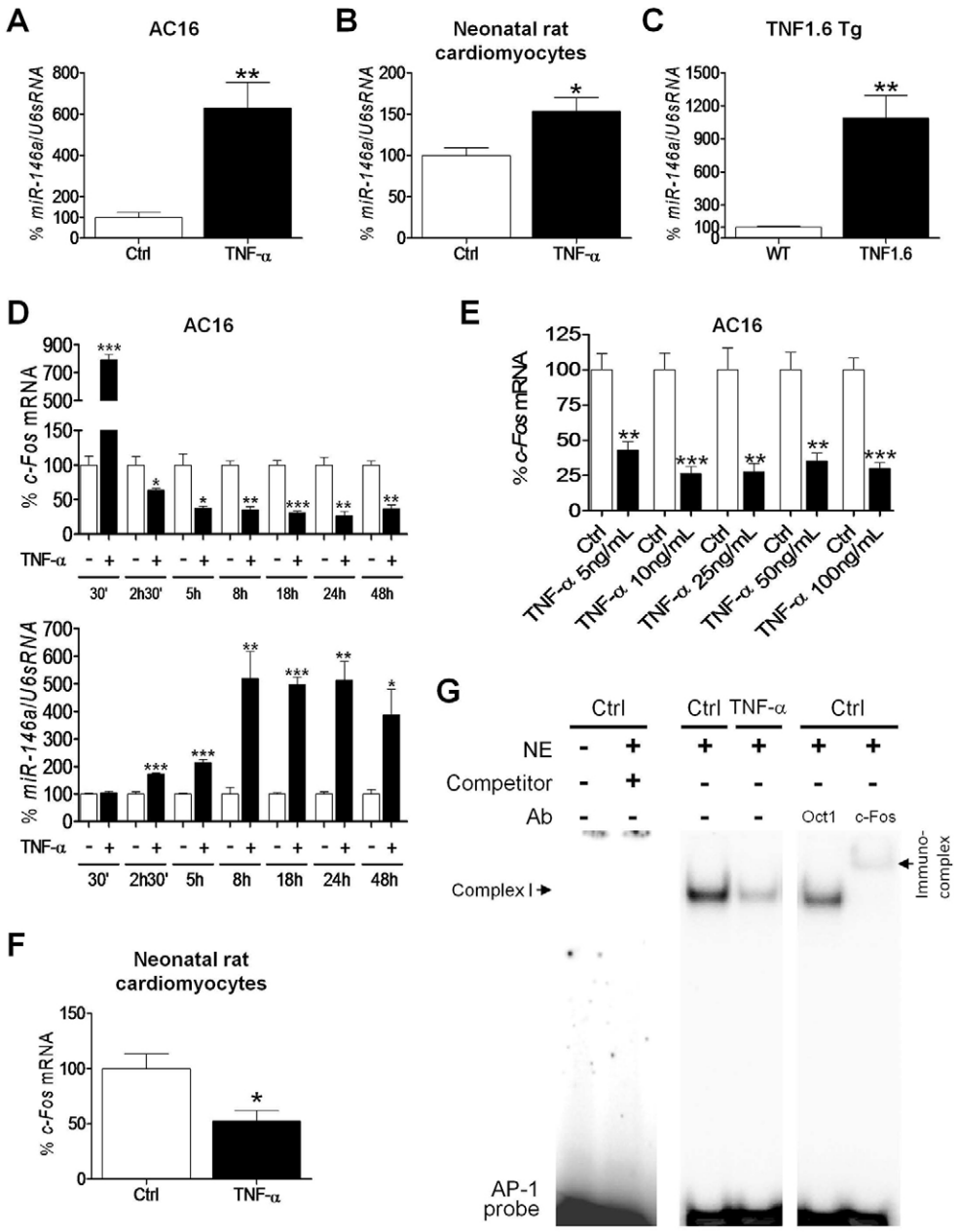

Fig. 1. TNF-α upregulates miR-146a and reduces *Fos* expression in cardiac cells. Relative quantification of miR-146a levels in samples obtained from: (A) non-differentiated AC16 cells treated with TNF-α (100 ng/ml, 24 h); (B) neonatal rat cardiomyocytes treated with TNF-α (10 ng/ml, 6 h); and (C) left ventricle tissue of transgenic TNF1.6 or control wild-type (WT) mice. Relative quantification of *Fos* and miR-146a expression in: (D) non-differentiated AC16 cells treated with 100 ng/ml TNF-α for 30 min to 48 h; (E) non-differentiated AC16 cells treated with 5, 10, 25, 50 and 100 ng/ml TNF-α for 24 h; and (F) neonatal rat cardiomyocytes treated with TNF-α (10 ng/ml, 6 h). Graphs represent the quantification of (A-C) U6sRNA-, (D,E) 18S- or (F) APRT-normalized mRNA levels, expressed as a percentage of control (Ctrl) or wild-type (WT) samples ±s.d. **P*<0.05, ***P*<0.01 and ****P*<0.001 vs Ctrl. (G) EMSA assay showing AP-1 DNA-binding activity in non-differentiated AC16 cells treated with TNF-α. Ab, antibody; NE, nuclear extracts.

non-stimulated cells, NF-κB remains inactive in the cytoplasm owing to its heterodimerization with the inhibitor protein IκB. In the presence of a stimulus (e.g. TNF-α), the IκB kinase (IKK) complex phosphorylates IκB, which induces ubiquitylation and ensuing proteasome-mediated degradation of the latter. The subsequent release of the NF-κB heterodimer makes possible its translocation to the nucleus, where it can begin the transcription of its target genes.

miR-146a modulates inflammation in human cardiac cells

After dimerization with Jun family members and by binding to the so-called TPA-responsive elements (TREs; TGAC/GTCA) in the promoter region of target genes, Fos regulates the expression of genes involved in multiple processes, including inflammation, endoplasmic reticulum stress, metabolism, fibrosis, proliferation and survival (Chinenov and Kerppola, 2001; Durchdewald et al., 2009). Dysregulation of Fos has been linked with a variety of pathological conditions. In the heart, for instance, AP-1 stimulates the expression of inflammatory genes, endothelin, fibronectin, matrix metalloproteinases (MMPs), transforming growth factor (TGF)-β and collagen, thereby displaying potent effects on matrix remodeling and favoring cardiac fibroblast proliferation (Wang et al., 2009; Takimoto and Kass, 2007; Pan et al., 2012). Therefore, in order to determine the pathophysiological relevance of AP-1 down-modulation in human cardiac cells, we next analyzed the expression of various genes that had been reportedly demonstrated to be targeted by the AP-1 transcription factor and also be involved in cardiac disease. As shown in supplementary material Fig. S2, no significant variation was observed in the expression of genes such as *ATF4* (activating transcription factor 4), *BiP/GRP78* (binding immunoglobulin protein/glucose-regulated protein 78), endothelin 1 (*ET-1*), fibronectin 1 (*FN1*), lipin 1, lipoprotein lipase (*LPL*), *TGF-β1*, type I collagen or type IV collagen.

On the other hand, miR-146a has been shown to modulate NF-κB activity through the direct targeting of well-established mediators of

Disease Models & Mechanisms (2015) 8, 1081-1091 doi:10.1242/dmm.020768

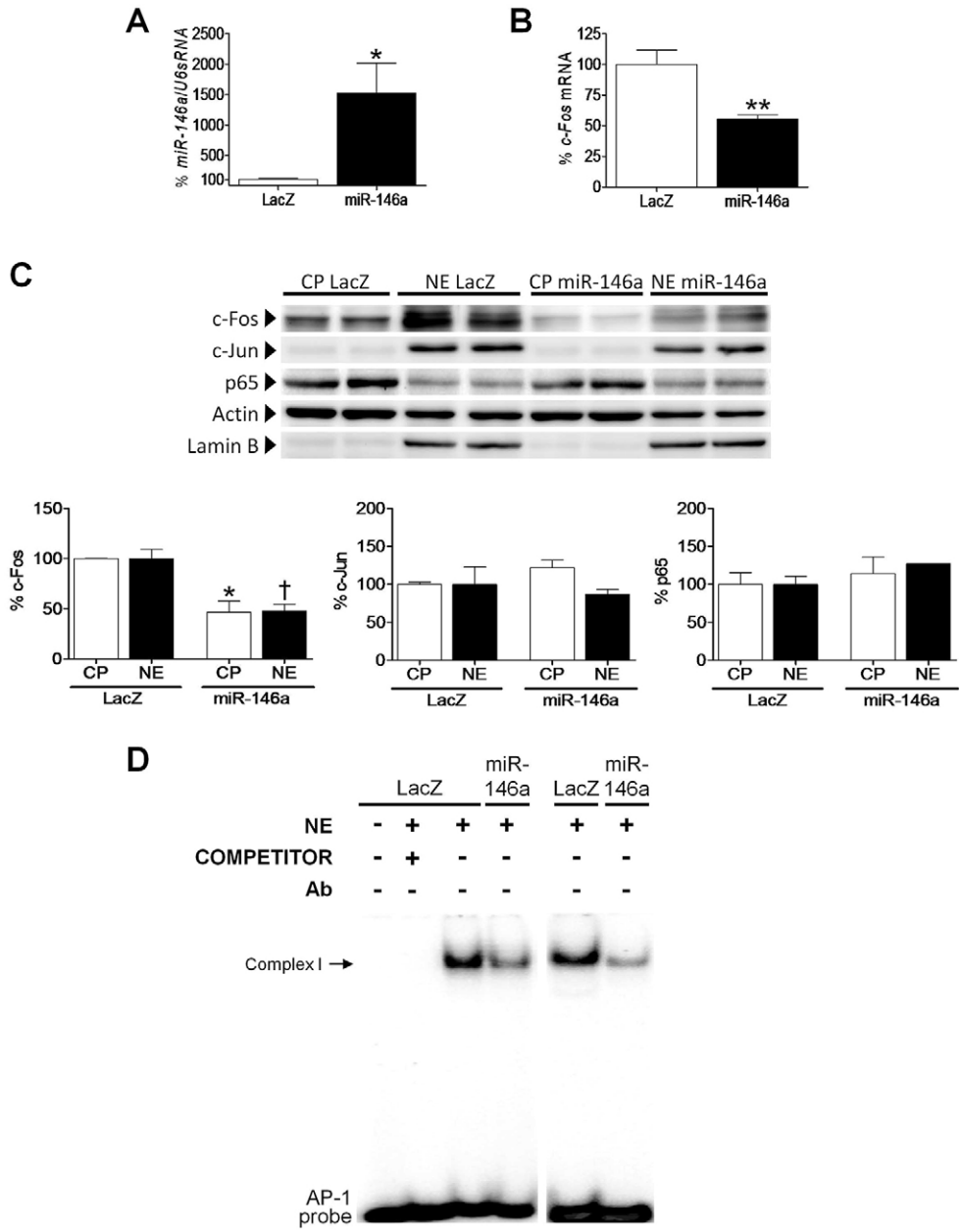

Fig. 2. miR-146a overexpression inhibits Fos in human cardiac cells. Relative quantification of miR-146a (A) and *Fos* (B) mRNA levels in human cardiac AC16 cells transfected with *lacZ*- or miR-146a-carrying plasmids. The graph represents the quantification of (A) U6sRNA- or (B) 18S-normalized mRNA levels, expressed as a percentage of control samples ±s.d. **P*<0.05 and ***P*<0.01 vs *lacZ*. (C) Western-blot analysis showing the protein levels of Fos, Jun and p65 in cytosolic (CP) and nuclear (NE) protein fractions obtained from human cardiac AC16 cells as described in panel A. To show equal loading of protein, the actin and lamin B signals from the same blot are included. The graphs at the bottom of panel C represent the quantification of protein levels normalized to actin (CP) or lamin B (NE), expressed as a percentage of CP or NE control samples ±s.d. The blot data are representative of two separate experiments. **P*<0.05 vs *lacZ* CP; †*P*<0.05 vs *lacZ* NE. (D) EMSA assay showing AP-1 DNA-binding activity after transfection of AC16 cells as described in panel A. Ab, antibody; NE, nuclear extracts.

its activation, including interleukin-1 receptor-associated kinase (IRAK)1, IRAK2, TNF receptor-associated factor (TRAF)2 and TRAF6 (Wang et al., 2013; Tanic et al., 2012). However, none of the transcript levels for these genes was found to be modified after miR-146a overexpression or inhibition, thus indicating that they were not regulated by this miRNA in human cardiac AC16 cells (see supplementary material Fig. S3). However, miR-146a overexpression inhibited *IL-6* (~40% reduction, $P<0.05$ vs *lacZ*) and *MCP-1* (~50% reduction, $P<0.01$) transcript levels, although *TNF-α* levels remained unaltered (Fig. 4A). In consonance with this, transfection of AC16 cells with the anti-miR-146a inhibitor upregulated the expression of *IL-6* (1.3-fold, $P<0.05$ vs anti-miR+TNF-α), although only when the pro-inflammatory stimulus TNF-α was added to the medium (Fig. 4B). As previously reported (Palomer et al., 2009), treatment of AC16 cells with TNF-α (100 ng/ml for 24 h) significantly induced the expression of *IL-6*, *MCP-1* and *TNF-α*, regardless of miR-146a levels. After that, an EMSA was carried out to verify whether modulation of miR-146a levels in AC16 cells led to changes in NF-κB activity. As shown in Fig. 4C, NF-κB formed four specific DNA-binding complexes (I to IV) with nuclear proteins. The competitor lane confirmed that all four complexes were specific for the NF-κB probe, and supershift analyses provided evidence that only complexes I and II contained the p65 subunit of NF-κB. Interestingly, complexes I, II and III were increased in TNF-α-treated cells, but no variations were detected after miR-146a modulation. These results suggest that *IL-6* and *MCP-1* gene expression might be regulated by transcription factors other than NF-κB.

Inhibition of AP-1 activity by miR-146a coincides with a reduction in MMP-9 activity

Examination of *MMP-9* expression in human cardiac cells transfected with miR-146a revealed that, unlike *MMP-2*, its transcript levels were downregulated (~40% reduction, $P<0.05$, Fig. 5A). According to these results, anti-miR-146a stimulated *MMP-9* expression regardless of the presence (1.5-fold, $P<0.001$) or

Disease Models & Mechanisms (2015) 8, 1081-1091 doi:10.1242/dmm.020768

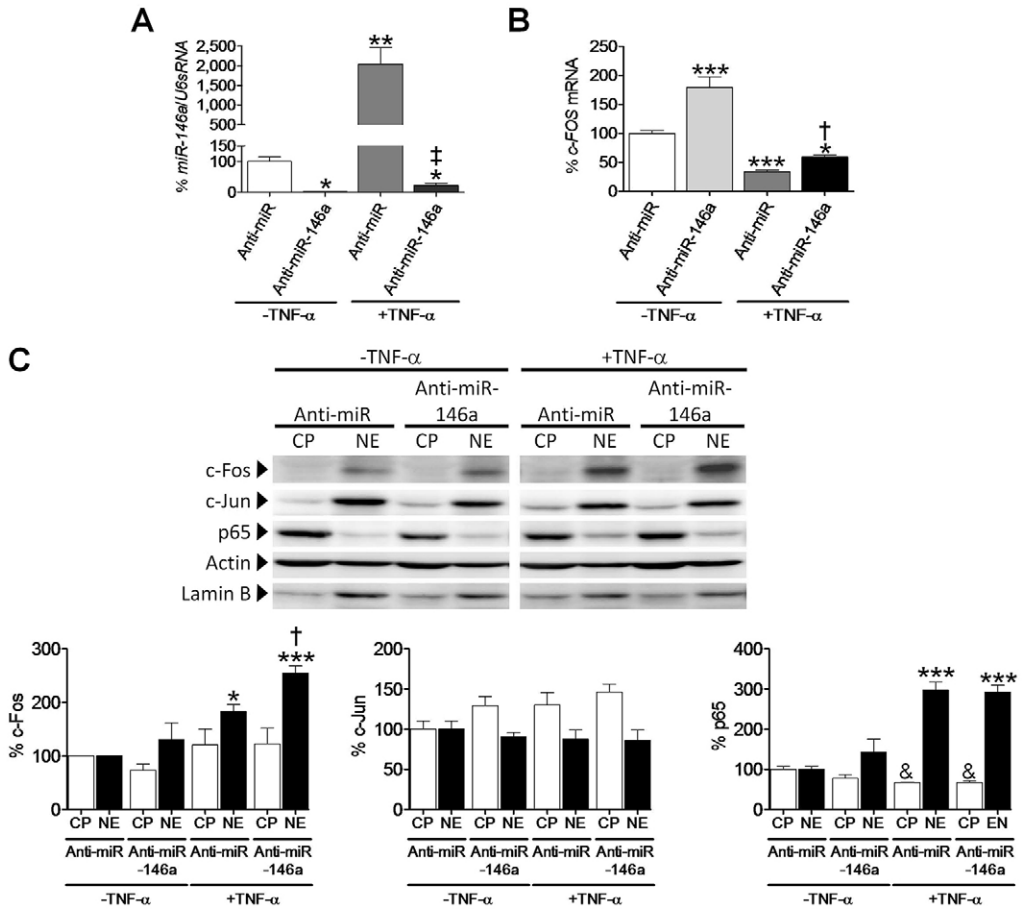

Fig. 3. miR-146a inhibition induces Fos in human cardiac cells. Relative quantification of miR-146a (A) and *Fos* (B) mRNA levels in human cardiac AC16 cells after transfection with a human anti-miR-146a inhibitor or an anti-miR negative control (Anti-miR). The graph represents the quantification of (A) U6sRNA- or (B) 18S-normalized mRNA levels, expressed as a percentage of control samples ±s.d. **P*<0.05, ***P*<0.01 and ****P*<0.001 vs Anti-miR–TNF-α; †*P*<0.05 and ‡*P*<0.001 vs Anti-miR +TNF-α. (C) Western-blot analysis showing the protein levels of Fos, Jun and p65 in cytosolic (CP) and nuclear (NE) protein fractions obtained from human cardiac AC16 cells as described in panel A. To show equal loading of protein, the actin and lamin B signals from the same blot are included. The graphs at the bottom of panel C represent the quantification of protein levels normalized to actin (CP) or lamin B (NE), expressed as a percentage of CP or NE control samples ±s.d. The blot data are representative of two separate experiments. **P*<0.05 and ****P*<0.001 vs NE Anti-miR–TNF-α; †*P*<0.05 vs NE Anti-miR+TNF-α; &*P*<0.05 vs CP Anti-miR–TNF-α.

absence (1.5-fold, $P<0.001$) of TNF-α (Fig. 5B). We next examined this issue in left ventricular tissue obtained from patients undergoing heart transplantation. The relative expression of miR-146a positively correlated with that of *TNF-α* (Fig. 5C, top panel, Spearman rank correlation $r=0.5480$), a finding that, despite being only marginally significant ($P=0.08$), matched the previous results obtained in AC16 cells fairly closely. Of note, miR-146a levels negatively correlated with the expression of *Fos* (Fig. 5C, middle panel, Spearman rank correlation $r=-0.6208$, $P<0.05$) and *MMP-9* (Fig. 5C, bottom panel, $r=-0.5659$, $P<0.05$) in these patients. Finally, we aimed to examine the effects of *MMP-9* downregulation by miR-146a on its enzymatic activity. As expected, miR-146a overexpression elicited a reduction in MMP-9 secretion to the media (~25% reduction, $P<0.001$, Fig. 5D) and MMP-9 activity (~35% reduction, $P<0.05$, Fig. 5E). The zymogram also yielded a stronger gelatinolytic activity band, which was concentrated in the area corresponding to the molecular mass of MMP-2 (62 kDa), which was not modified under our conditions.

DISCUSSION

The molecular mechanisms that lie behind the development of heart failure induced by cytokines remain, at least in part, elusive, but there are consistent observations indicating that chronic immune activation and anomalous miRNA expression come together in the failing heart (van de Vrie et al., 2011). Our results demonstrate that miR-146a is strongly induced in human cardiac cells and neonatal rat cardiomyocytes exposed to TNF-α *in vitro*, as well as in the heart of transgenic mice with cardiac-specific overexpression of TNF-α. This is not surprising, given that this miRNA has already been shown to be transcriptionally upregulated after NF-κB activation by TNF-α and IL-1β in other cell types (Taganov et al., 2006; Perry et al., 2008; Schroen and Heymans, 2012; Li et al., 2012). This regulatory mechanism is fundamental because continuous NF-κB activation aggravates cardiac remodeling, worsens cardiac function, and hastens progression to heart failure and cardiac hypertrophy (Bergman et al., 1999; Stetson et al., 2001). In agreement with this, miR-146a, which is abundantly expressed in the heart (van de Vrie et al., 2011), protects the myocardium from ischemia-reperfusion injury in a process that involves attenuation of NF-κB activation (Wang et al., 2013).

Owing to the crucial function of miRNAs in controlling mRNA expression, the discovery of currently unknown targets of specific miRNAs is paramount, but the fact that most miRNAs are only partially complementary to their target genes hinders this identification. Therefore, the chief finding of this study is the identification of a new miR-146a target, *Fos*, an AP-1 subunit that is rapidly activated upon cardiac stress to mediate changes in gene expression (Shieh et al., 2011). Validation of new miRNA targets is often complicated because many putative targets display little or indeed no detectable modification when tested *in vitro* (Small et al., 2010), and this might account for the relatively modest effect of miR-146a on *Fos* mRNA levels, despite the huge miR-146a changes observed in transfected cells. The lack of any change in Jun protein levels indicated the specificity of miR-146a over the Fos subunit of the AP-1 transcription factor.

The next logical step in this study consisted of finding out which genes were regulated by Fos–AP-1 under our conditions. AP-1 protein typically binds to TREs in target promoter regions often

Disease Models & Mechanisms (2015) 8, 1081-1091 doi:10.1242/dmm.020768

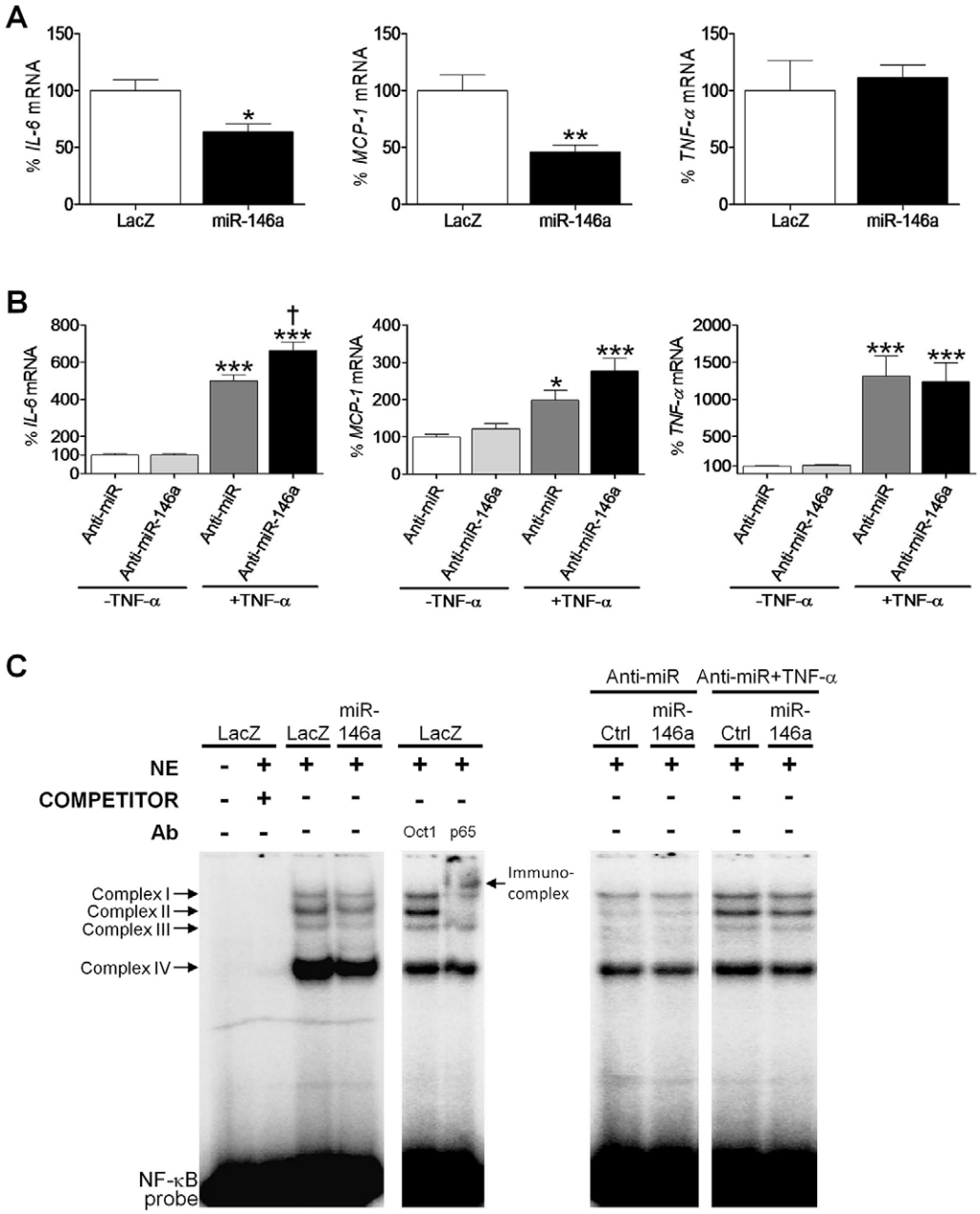

Fig. 4. miR-146a regulates IL-6 and MCP-1 expression in human cardiac cells. Relative quantification of *IL-6*, *MCP-1* and *TNF-α* mRNA levels in non-differentiated human cardiac AC16 cells transfected with: (A) *lacZ*- or miR-146a-carrying plasmids, or (B) a human anti-miR-146a inhibitor or an anti-miR negative control (Anti-miR). The graphs represent the quantification of 18S-normalized mRNA levels, expressed as a percentage of control samples ±s.d. (A) **P*<0.05 and ***P*<0.01 vs *lacZ*; (B) **P*<0.05 and ****P*<0.001 vs Anti-miR–TNF-α; †*P*<0.05 vs Anti-miR+TNF-α. (C) EMSA assay showing NF-κB DNA-binding activity after transfection of AC16 cells as described in panels A and B. Ab, antibody; Ctrl, control; NE, nuclear extracts.

adjacent to NF-κB or nuclear factor of activated T-cells (NFAT) to coordinately regulate transcription in response to immune and inflammatory stimuli (Chinenov and Kerppola, 2001). Gene expression assessment revealed that miR-146a was modulating mRNA levels of *IL-6* and *MCP-1* in AC16 cells. Taking into account that this was not accompanied by changes in the DNA-binding activity of NF-κB, and bearing in mind that *in silico* data indicate that these pro-inflammatory genes are not direct targets of miR-146a, our results suggest that AP-1 might be regulating their expression. In support of this, we can cite our previous data demonstrating that, besides NF-κB, other transcription factors are controlling *IL-6* and *MCP-1* mRNA levels in human cardiac cells (Palomer et al., 2014; Álvarez-Guardia et al., 2011). In fact, other studies have demonstrated the involvement of AP-1 but not NF-κB in the transcriptional control of *IL-6* in other cell types (Lu et al., 2010). In contrast, the expression of other genes such as *ATF4*, *BiP/GRP78*, *IRAK1*, *IRAK2*, *TRAF2*, *TRAF6*, *ET-1*, *FN1*, lipin 1, *LPL*, *TGF-β1*, type I collagen or type IV collagen did not seem to be regulated by miR-146a. In fact, the expression of AP-1 target genes depends on the cell type and is also influenced by the particular signals that trigger their expression (Chinenov and Kerppola, 2001). Besides regulation at the transcriptional level, additional mechanisms might contribute to the target gene specificity of AP-1, including mRNA translation and turnover, post-translational

Disease Models & Mechanisms (2015) 8, 1081-1091 doi:10.1242/dmm.020768

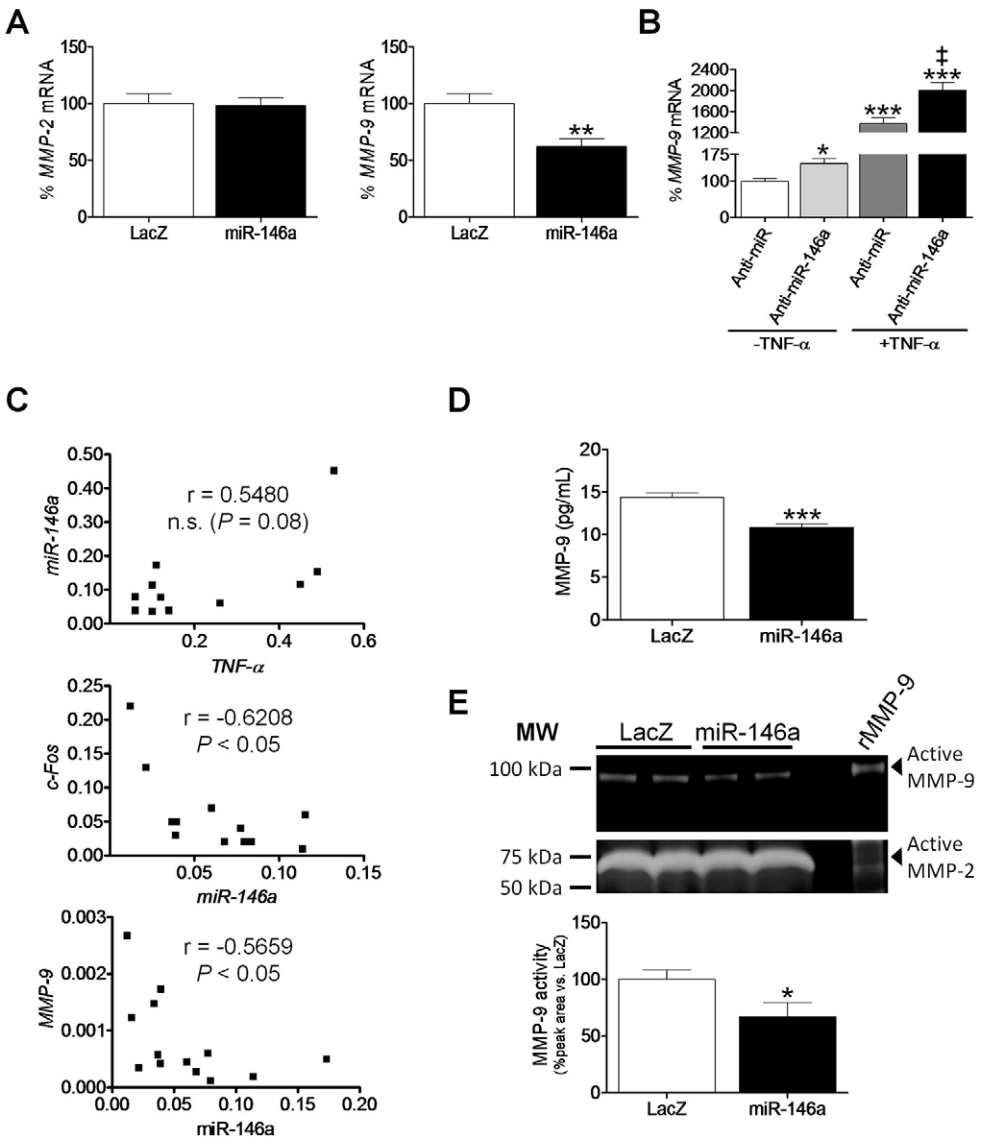

Fig. 5. miR-146a downregulates MMP-9 expression, secretion and activity in human cardiac cells. Relative quantification of *MMP-2* and *MMP-9* mRNA levels in non-differentiated human cardiac AC16 cells transfected with: (A) *lacZ*- or miR-146a-carrying plasmids, or (B) a human anti-miR-146a inhibitor or an anti-miR negative control (Anti-miR). The graphs represent the quantification of 18S-normalized mRNA levels, expressed as a percentage of control samples ±s.d. (C) Spearman rank correlation between *TNF-α* and miR-146a, miR-146a and *Fos*, and miR-146a and *MMP-9* gene expression in left ventricular tissue obtained from patients undergoing heart transplantation. The relative transcript levels of the target genes, in arbitrary units, were used to calculate the Spearman correlation coefficients (n.s., non-significant). (D) Determination by ELISA of MMP-9 secretion into the culture media in AC16 cells transfected with *lacZ*- or miR-146a-carrying plasmids. (E) Representative gel zymography and corresponding densitometric analysis of MMP-9 gelatinolytic activity in culture media of cells transfected with *lacZ*- or miR-146a-carrying plasmids. MW, molecular weight; rMMP-9, human recombinant MMP-9. (A,D,E) **P*<0.05, ***P*<0.01 and ****P*<0.001 vs *lacZ*; (B) **P*<0.05 and ****P*<0.001 vs Anti-miR–TNF-α; ‡*P*<0.05 vs Anti-miR+TNF-α.

modifications, selective dimerization, protein stability, and interactions with other regulatory proteins and transcription factors (Chinenov and Kerppola, 2001; Schonthaler et al., 2011).

Interstitial fibrosis is a characteristic pathological alteration of myocardial remodeling that occurs in several cardiomyopathies and is considered as a primary determinant of deteriorated performance of the heart. Fibrosis occurs as a result of excess deposition of extracellular matrix proteins in the myocardium (Pan et al., 2012). A complex interplay of transcription factors is implicated in the regulation of extracellular matrix protein homeostasis, including NF-κB and AP-1. In particular, the Fos–AP-1 pathway transcriptionally stimulates the synthesis of ET-1 and the deposition of collagen (type I, type IV collagens), fibronectin and TGF-β, thereby causing changes in the extracellular matrix that alter cardiac cell proliferation and function, ultimately leading to cardiomyocyte hypertrophy and heart failure (Pan et al., 2012; Wang et al., 2009; Avouac et al., 2012). Even so, miR-146a overexpression did not inhibit the expression of most cardiac-fibrosis-related genes examined in human cardiac cells, except for *MMP-9*. MMPs are under the transcriptional control of AP-1 (Takimoto and Kass, 2007) and NF-κB (Meiners et al., 2004), which are in turn induced by growth factors and inflammatory cytokines in cardiac cells, although MMP activity is also dependent on post-translational modifications. MMPs are the enzymes responsible for controlling extracellular matrix remodeling in the heart and, interestingly, inhibition of these enzymes is associated with reduced collagen deposition and lower cardiac fibrosis (Meiners et al., 2004). This astonishing paradox is due to the fact that total collagen amount in the heart depends on both the synthesis and degradation. The results reported here demonstrate that miR-146a can inhibit MMP-9 expression and activity in human cardiac cells. Infiltrating cells (i.e. neutrophils, macrophages and fibroblasts) together with cardiomyocytes are the major source of MMPs in the myocardium (Li et al., 2001). Macrophages are an important source of MMP-9 during acute myocardial infarction and, for instance, MMP-9-knockout mice show a reduced rupture rate and attenuated ventricular dilation during myocardial infarction (Fang et al., 2010). A recent study has also reported that miR-146a might be a potential inhibitor of MMP-9 secretion in macrophages, although regulation in these cells was achieved through attenuation of the inflammatory response by blocking the TRAF6-IRAK1 pathway (Yang et al., 2011). Likewise, cardiac fibroblasts express

Disease Models & Mechanisms (2015) 8, 1081-1091 doi:10.1242/dmm.020768

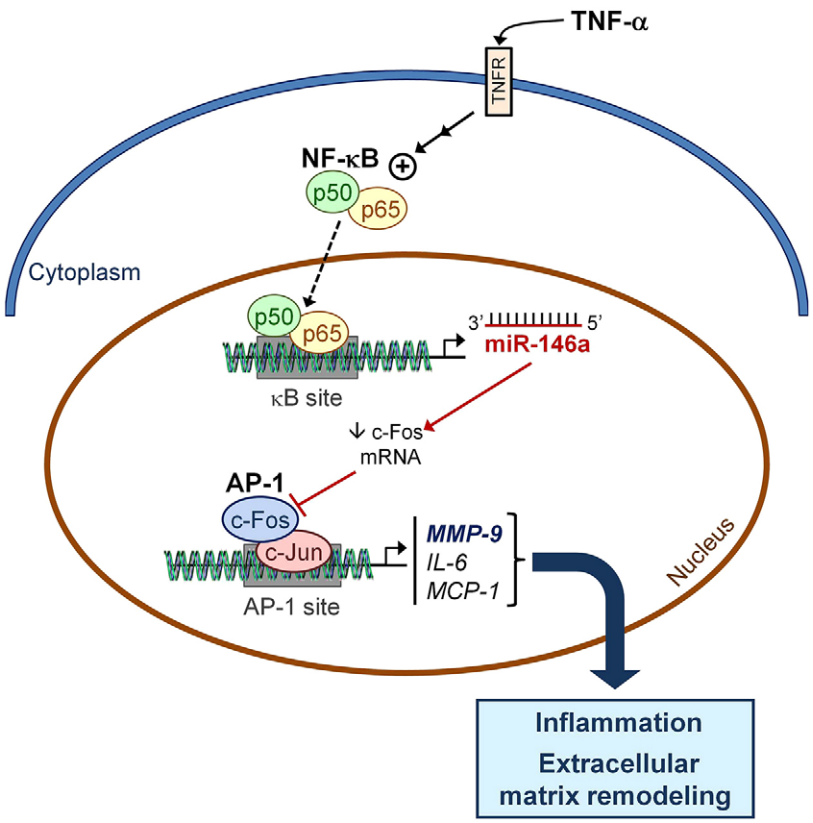

Fig. 6. Schematic model depicting the potential role of miR-146a in TNF-α-induced effects in the heart. Exposure of cardiac cells to TNF-α strongly induces miR-146a, probably in a process dependent on NF-κB transcriptional activity (dashed arrow). Enhanced miR-146a levels are directly responsible for *Fos* expression downregulation. The subsequent reduction in AP-1 DNA-binding activity results in the modulation of inflammation by attenuating *IL-6* and *MCP-1* expression, together with a reduction in MMP-9 expression and activity. AP-1, activator protein-1; Fos, FBJ murine osteosarcoma viral oncogene homolog; IL-6, interleukin 6; MCP-1, monocyte chemoattractant protein 1; MMP-9, matrix metalloproteinase 9; NF-κB, nuclear factor-κB; TNF-α, tumor necrosis factor α.

MMP-9 after treatment with TNF-α, a fact that is concomitant with a decrease in collagen synthesis (Brown et al., 2007). Therefore, all these results indicate that the miR-146a-mediated inhibition of MMP-9 might occur in both infiltrating cells and cardiomyocytes in the heart, by this means magnifying its beneficial effects.

A major drawback of this study is the origin of the AC16 cells, which were derived from the fusion of primary ventricular cells and SV-40-transformed fibroblasts. The heart consists of various cell types, including cardiomyocytes and cardiac fibroblasts, which play a pivotal role in cardiac development and function (Palomer et al., 2009). Both cell types are capable of secreting TNF-α and are responsive to the action of this cytokine (Turner et al., 2007) but, in diseased states, quiescent cardiac fibroblasts are transformed into myofibroblasts, becoming a major source of pro-inflammatory molecules (Brown et al., 2005), in addition to the main source of extracellular matrix production (Pan et al., 2012). As stated above, excess extracellular matrix production by activated cardiac fibroblasts during cardiac hypertrophy, heart failure and myocardial infarction promotes interstitial fibrosis. The consequent cardiac remodeling might eventually lead to functional decompensation and development of heart failure due to apoptosis of cardiac myofibroblasts (Camelliti et al., 2005).

Conclusions

In summary, the results reported here demonstrate that *Fos* is a direct target of miR-146a activity and that downregulation of the Fos–AP-1 pathway by miR-146a can inhibit MMP-9 activity (Fig. 6). Fos is one of the immediate early genes whose expression is boosted during ischemic injury, heart failure and cardiomyopathy. Likewise, it has been reported that *Fos* gene expression is stimulated as a result of insulin insufficiency in the diabetic myocardium (Wang et al., 1999) and also in the adipose tissue of streptozotocin-induced diabetic rats (Olson and Pessin, 1994). In fact, the transcriptional activity of AP-1 is among the most robustly enhanced of 54 transcription factors examined in the failing heart (Freire et al., 2007). In order to prevent the pathological effects caused by its dysfunction, regulation of AP-1 is complex and occurs at multiple interwoven transcriptional and post-transcriptional levels. This includes transcription of its subunits, mRNA translation and turnover, protein stability and activity, subcellular localization, and interaction with other transcription factors and cofactors (Schonthaler et al., 2011). Here, we demonstrate that miR-146a might post-transcriptionally regulate Fos levels and, consequently, AP-1 activity as well. Furthermore, the results presented here are very appealing because numerous studies have shown that upregulation of *MMP-2* and *MMP-9* expression correlates fairly well with heart failure, whereas their inhibition suppresses ventricular remodeling, myocardial dysfunction and development of heart failure (Meiners et al., 2004). In recent years, the development of antisense-oligonucleotide-mediated (anti-miR) knockdown and miRNA overexpression techniques has become a very attractive pharmacological target in the treatment of cardiovascular disease. In this respect, miR-146a emerges as a new and promising therapeutic tool for preventing cardiac disorders associated with inflammatory states in the heart.

MATERIALS AND METHODS

Cell culture and transfection

The human AC16 cell line, which develops many of the biochemical and morphological properties characteristic of cardiac muscle cells, even though it does not form completely differentiated cardiomyocytes, was grown as previously described (Davidson et al., 2005). Briefly, non-differentiated AC16 cells were maintained in medium composed of Dulbecco's modified Eagle's medium (DMEM):F12 (Life Technologies, Spain) supplemented with 12.5% fetal bovine serum (FBS), 1% penicillin-streptomycin and 1%

Fungizone (Life Technologies), and grown at 37°C in a humid atmosphere of 5% CO_2/95% air until they reached 70-80% confluence. For *in vitro* overexpression studies, AC16 cells were transfected with pcDNA3/pre-miR-146a (Addgene plasmid #15092) (Taganov et al., 2006) and the corresponding *lacZ*-carrying plasmid (Life Technologies) as a control. Cells were transfected for 48 h with Lipofectamine 2000 in OPTI-MEM reduced serum medium following the manufacturer's recommendations (Life Technologies). Transfection time and the DNA to Lipofectamine ratio were set after optimization with the corresponding *lacZ*-carrying plasmid and using a β-galactosidase reporter gene staining kit (Sigma-Aldrich Co. LLC., St Louis, MO, USA). Downregulation of miR-146a activity was carried out by transfecting AC16 cells with 50 nmol/l human anti-miR-146a inhibitor, using a random sequence anti-miR molecule as negative control (Life Technologies).

To obtain neonatal rat cardiomyocytes, 1- to 2-day-old Sprague-Dawley rats were decapitated and their hearts removed. Hearts were digested with a collagenase solution (Collagenase Type I, Life Technologies) followed by differential plating. Cells were plated at a density of 2.5×10^4 cells/well in six-well plates coated with 1% gelatin, and cultured overnight in plating medium [DMEM supplemented with 10% horse serum, 5% newborn calf serum, 50 mg/l gentamicin and 10 mM cytosine b-D-arabino furanoside (Ara C)]. Ara C was added to suppress the growth of the remaining fibroblasts. Sixteen hours after isolating cells, neonatal rat cardiomyocytes were incubated in serum-free medium consisting of DMEM and gentamicin (50 mg/l) as the sole substrate for 24 h. Thereafter, the medium was replaced with experimental medium consisting of serum-free medium enriched with 0.25 mM L-carnitine, 0.25 mU/ml insulin and 1% bovine serum albumin. All procedures were approved by the University of Barcelona Bioethics Committee, as stated in Law 5/21 July 1995 passed by the Generalitat de Catalunya.

After treatment, RNA and protein were extracted from cardiac cells as described below. Culture supernatants were collected, and secretion of MMP-9 was assessed by enzyme-linked immunosorbent assay (Life Technologies).

TNF-α transgenic mouse cardiac sample preparation

We used transgenic TNF1.6 male mice (8- to 12-weeks old) with cardiac-specific overexpression of TNF-α, which has been established as a suitable model of cytokine-induced cardiomyopathy and congestive heart failure (Kubota et al., 1997). These transgenic mice develop myocardial inflammation with premature death from heart failure in association with extracellular matrix remodeling (Kubota et al., 1997; Li et al., 2000). Left ventricular end-diastolic diameter and left ventricular end-diastolic pressure are significantly greater, and fractional shortening is significantly less in TNF1.6 than in wild-type mice (Matsusaka et al., 2005). Myocyte cross-sectional area and collagen volume fraction are also enhanced in the transgenic TNF1.6 mice compared with littermate controls (Matsusaka et al., 2005).

Mice were housed under standard light-dark cycle (12-h light/dark cycle) and temperature (21±1°C) conditions, and food and water were provided *ad libitum*. Ventricular sample tissues were obtained from mice euthanized using deep isoflurane (5%) anesthesia, rinsed in ice-cold phosphate buffer saline and snap-frozen in liquid nitrogen, as described previously (Álvarez-Guardia et al., 2010). The study was approved by the Institutional Animal Care and Use Committee of Thomas Jefferson University and conformed to the *Guide for the Care and Use of Laboratory Animals* published by the US National Institutes of Health (NIH Publication No. 85-23, revised 1996).

Tissue collection

Left ventricular tissue was obtained from patients undergoing heart transplantation at the Hospital de la Santa Creu i Sant Pau, Barcelona. All participants provided informed consent. Transmural tissue samples (near the apex) were collected from patients (eight male and five female) with both dilated (DCM; n=10) and ischemic (ICM; n=3) cardiomyopathy. Samples were quickly frozen in liquid nitrogen in the operating room and stored at −80°C until processing for gene expression analysis. All the procedures were approved by the Reviewer Institutional Committee on Human Research of the Hospital de la Santa Creu i Sant Pau and conformed to the Declaration of Helsinki.

RNA preparation and analysis

Total RNA was isolated using Ultraspec reagent (Biotecx, Houston, TX, USA). RNA samples were cleaned (NucleoSpin RNA II; Macherey-Nagel, Düren, Germany) and checked for integrity by agarose gel electrophoresis. The total RNA isolated by this method was undegraded and free of protein and DNA contamination. Relative levels of specific mRNAs were assessed by real-time reverse transcription-polymerase chain reaction (RT-PCR), as previously described (Palomer et al., 2014). Reverse transcription was performed from 0.5 µg total RNA using Oligo$(dT)_{23}$ and M-MLV Reverse Transcriptase (Life Technologies). The PCR reaction contained 10 ng of reverse-transcribed RNA, 2X IQ™ SYBRGreen Supermix (Bio-Rad, Barcelona, Spain) and 900 nM of each primer. PCR assays were performed on a MiniOpticon™ Real-Time PCR system (Bio-Rad). Thermal cycling conditions were as follows: activation of Taq DNA polymerase at 95°C for 10 min, followed by 40 cycles of amplification at 95°C for 15 s and at 60°C for 1 min. The sequences of the forward and reverse primers used for amplification are shown in supplementary material Table S1. Optimal primer amplification efficiency for each primer set was assessed and a dissociation protocol was carried out to ensure a single PCR product. The results for the expression of specific mRNAs are always presented relative to the expression of the control gene.

To quantify the abundance of selected mature miRNAs, total miRNAs were reverse-transcribed using the Megaplex Primer Pools (Human Pool A v2.1 and Rodent Pool A) and the Taqman MicroRNA Reverse Transcription according to the manufacturer's instructions (Life Technologies). The RT reaction product was combined with 1 µl Taqman miRNA assay and 10 µl Taqman Universal PCR Master Mix No AmpErase UNG (Life Technologies) to a final volume of 20 µl. The quantitative real-time RT-PCR reaction was carried out on a MiniOpticon™ Real-Time PCR system at 95°C for 10 min, followed by 40 cycles at 95°C for 15 s and 60°C for 1 min. All samples were run in duplicates. *U6sRNA* expression was used for normalization purposes.

Immunoblot analysis

To obtain total protein extracts, AC16 cardiac cells or frozen tissue slides were lysed in cold RIPA buffer with phosphatase and protease inhibitors (0.2 mmol/l phenylmethylsulfonyl fluoride, 1 mmol/l sodium orthovanadate, 5.4 µg/ml aprotinin). The homogenate was then centrifuged at 10,000 ***g*** for 30 min at 4°C, and the supernatant protein concentration was determined using the Bradford method (Bradford, 1976). Isolation of cytosolic and nuclear fractions was adapted from a previously described method (Ba et al., 2010). Briefly, AC16 cells were incubated on ice for 30 min in buffer A (10 mmol/l HEPES, pH 7.9, 10 mmol/l KCl, 0.2 mmol/l EDTA, 1 mmol/l dithiothreitol, plus phosphatase and protease inhibitors) containing 0.625% (v:v) Nonidet P-40. Cell lysates were centrifuged at 4°C, 10,000 ***g*** for 1 min, and supernatants were stored as cytosolic fraction. Pellets were suspended in buffer B (20 mmol/l HEPES, pH 7.9, 0.42 mol/l NaCl, 2 mmol/l EDTA and 1 mmol/l dithiothreitol, with phosphatase and protease inhibitors), centrifuged at 4°C, 13,000 ***g*** for 5 min, and the resultant supernatant (nuclear extract) stored at −80°C.

Proteins from whole-cell lysates and cytosolic/nuclear extracts were separated by sodium dodecyl sulfate-polyacrylamide gel electrophoresis (SDS-PAGE) on 10% separation gels and transferred to Immobilon polyvinylidene difluoride membranes (Millipore, Bedford, MA, USA). Proteins were detected using the Western Lightning® Plus-ECL chemiluminescence kit (PerkinElmer, Waltham, MA, USA) and their size was estimated using protein molecular mass standards (Life Technologies). All antibodies were purchased from Santa Cruz Biotechnology (Inc., Heidelberg, Germany), except Actin (Sigma-Aldrich Co. LLC.).

Electrophoretic mobility shift assay

The EMSA was performed using double-stranded oligonucleotides for the consensus binding sites of AP-1 and NF-κB (Santa Cruz Biotechnology).

Nuclear extracts (NEs) from AC16 cells were isolated as previously reported (Palomer et al., 2011). Oligonucleotides were labeled by incubating the following reaction at 37°C for 2 h:2 µl oligonucleotide (1.75 pmol/µl), 2 µl of 5× kinase buffer, 1 µl of T4 polynucleotide kinase (10 U/µl) and 2.5 µl [γ-^{32}P] ATP (3000 Ci/mmol at 10 mCi/ml, PerkinElmer, Waltham, MA, USA). The reaction was stopped by adding 90 µl of TE buffer (10 mmol/l Tris-HCl, pH 7.4, and 1 mmol/l EDTA). To separate the labeled probe from the unbound ATP, the reaction mixture was eluted in a Nick column (GE Healthcare Life Sciences, Barcelona, Spain) according to the manufacturer's instructions. Five micrograms of crude nuclear protein was incubated for 10 min on ice in binding buffer [10 mmol/l Tris-HCl, pH 8.0, 25 mmol/l KCl, 0.5 mmol/l dithiothreitol, 0.1 mmol/l EDTA, pH 8.0, 5% (v:v) glycerol, 5 mg/ml BSA and 50 µg/ml poly(dI-dC)] in a final volume of 15 µl. Then, specific competitor oligonucleotide or antibody for supershift assays were added and incubated for 15 min on ice. Subsequently, the labeled probe (100,000 cpm) was added and the reaction was incubated for an additional 15 min on ice. Finally, protein-DNA complexes were resolved by electrophoresis at 4°C on 5% (w:v) polyacrylamide gels in 0.5× Tris-borate-EDTA buffer and subjected to autoradiography.

Gelatinase activity assay

MMP-9 activity was examined by gelatin zymography as previously reported in AC16 cell cultures after protein concentration using 3000 MW Amicon Ultra centrifugal filters (Millipore) (Casals et al., 2013). 150 µg of protein per lane were subjected to 10% SDS-PAGE electrophoresis (125 V for 90 min) using 0.2% gelatin-containing gels. After electrophoresis, gels were washed and incubated for 30 min at room temperature in Renaturing Buffer (Novex, Life Technologies) to remove the SDS. After this, gels were incubated with gentle agitation for 30 min with Developing Buffer (Life Technologies), rinsed three times with deionized water and stained by adding SimplyBlue Safe Stain (Life Technologies) for 1 h. 50 pg recombinant human MMP-9 (Life Technologies) were also run in parallel as a positive control for enzymatic activity. Proteolytic bands of 92 kDa, which correspond to the active form of MMP-9, were scanned and the intensity of the bands analyzed.

Statistical analysis

Results are expressed as the mean±s.d. of three independent experiments for the *in vitro* studies, each consisting of three culture plates (n=9), and of five mice for the *in vivo* experiments. Significant differences were established by either the Student's t-test or one-way ANOVA, according to the number of groups compared, using GraphPad Prism software (GraphPad Software Inc. V4.03, San Diego, CA, USA). When significant variations were found by one-way ANOVA, the Tukey-Kramer multiple comparison post-test was performed. The non-parametric Spearman rank correlation coefficient was used to calculate the correlation between *Fos*, *miR-146a* and *TNF-α* expression. Differences were considered significant at P<0.05.

Acknowledgements

We thank Dr D. Baltimore (California Institute of Technology, Pasadena, CA, USA) for providing the pcDNA3/miR-146a plasmid. We thank the University of Barcelona's Language Advisory Service for their assistance.

Competing interests

The authors declare no competing or financial interests.

Author contributions

All authors contributed substantially to the work presented in this paper. X.P. and M.V.-C. designed the study. X.P., E.C.-B. and G.B. performed all *in vitro* and *in vivo* experiments. M.M.D. developed and provided the human cardiac cell line. C.R., J.M.-G. and F.V. collected and provided the left ventricular tissue from patients. T.O.C. and A.M.F. provided the heart samples from transgenic mice. E.B. analyzed the quantitative data and contributed to data interpretation. X.P. wrote the paper with input from all authors.

Funding

This study was supported by funds from the Ministerio de Economía y Competitividad of the Spanish Government [SAF2009-06939, SAF2012-30708 and SAF2012-40127]. CIBER de Diabetes y Enfermedades Metabólicas Asociadas (CIBERDEM) is an initiative of the Instituto de Salud Carlos III (ISCIII) - Ministerio de Economía y Competitividad.

Supplementary material

Supplementary material available online at
http://dmm.biologists.org/lookup/suppl/doi:10.1242/dmm.020768/-/DC1

References

Álvarez-Guardia, D., Palomer, X., Coll, T., Davidson, M. M., Chan, T. O., Feldman, A. M., Laguna, J. C. and Vazquez-Carrera, M. (2010). The p65 subunit of NF-kappaB binds to PGC-1alpha, linking inflammation and metabolic disturbances in cardiac cells. *Cardiovasc. Res.* **87**, 449-458.

Álvarez-Guardia, D., Palomer, X., Coll, T., Serrano, L., Rodriguez-Calvo, R., Davidson, M. M., Merlos, M., El Kochairi, I., Michalik, L., Wahli, W. et al. (2011). PPARbeta/delta activation blocks lipid-induced inflammatory pathways in mouse heart and human cardiac cells. *Biochim. Biophys. Acta* **1811**, 59-67.

Avouac, J., Palumbo, K., Tomcik, M., Zerr, P., Dees, C., Horn, A., Maurer, B., Akhmetshina, A., Beyer, C., Sadowski, A. et al. (2012). Inhibition of activator protein 1 signaling abrogates transforming growth factor beta-mediated activation of fibroblasts and prevents experimental fibrosis. *Arthritis Rheum.* **64**, 1642-1652.

Ba, X., Gupta, S., Davidson, M. and Garg, N. J. (2010). Trypanosoma cruzi induces the reactive oxygen species-PARP-1-RelA pathway for up-regulation of cytokine expression in cardiomyocytes. *J. Biol. Chem.* **285**, 11596-11606.

Bergman, M. R., Kao, R. H., McCune, S. A. and Holycross, B. J. (1999). Myocardial tumor necrosis factor-alpha secretion in hypertensive and heart failure-prone rats. *Am. J. Physiol.* **277**, H543-H550.

Bradford, M. M. (1976). A rapid and sensitive method for the quantitation of microgram quantities of protein utilizing the principle of protein-dye binding. *Anal. Biochem.* **72**, 248-254.

Brown, R. D., Ambler, S. K., Mitchell, M. D. and Long, C. S. (2005). The cardiac fibroblast: therapeutic target in myocardial remodeling and failure. *Annu. Rev. Pharmacol. Toxicol.* **45**, 657-687.

Brown, R. D., Jones, G. M., Laird, R. E., Hudson, P. and Long, C. S. (2007). Cytokines regulate matrix metalloproteinases and migration in cardiac fibroblasts. *Biochem. Biophys. Res. Commun.* **362**, 200-205.

Camelliti, P., Borg, T. K. and Kohl, P. (2005). Structural and functional characterisation of cardiac fibroblasts. *Cardiovasc. Res.* **65**, 40-51.

Casals, G., Fernández-Varo, G., Melgar-Lesmes, P., Marfà, S., Reichenbach, V., Morales-Ruiz, M. and Jiménez, W. (2013). Factors involved in extracellular matrix turnover in human derived cardiomyocytes. *Cell Physiol. Biochem.* **32**, 1125-1136.

Chinenov, Y. and Kerppola, T. K. (2001). Close encounters of many kinds: Fos-Jun interactions that mediate transcription regulatory specificity. *Oncogene* **20**, 2438-2452.

Davidson, M. M., Nesti, C., Palenzuela, L., Walker, W. F., Hernandez, E., Protas, L., Hirano, M. and Isaac, N. D. (2005). Novel cell lines derived from adult human ventricular cardiomyocytes. *J. Mol. Cell. Cardiol.* **39**, 133-147.

Durchdewald, M., Angel, P. and Hess, J. (2009). The transcription factor Fos: a Janus-type regulator in health and disease. *Histol. Histopathol.* **24**, 1451-1461.

Fang, L., Du, X.-J., Gao, X.-M. and Dart, A. M. (2010). Activation of peripheral blood mononuclear cells and extracellular matrix and inflammatory gene profile in acute myocardial infarction. *Clin. Sci.* **119**, 175-183.

Freire, G., Ocampo, C., Ilbawi, N., Griffin, A. J. and Gupta, M. (2007). Overt expression of AP-1 reduces alpha myosin heavy chain expression and contributes to heart failure from chronic volume overload. *J. Mol. Cell. Cardiol.* **43**, 465-478.

Gupta, S., Young, D., Maitra, R. K., Gupta, A., Popovic, Z. B., Yong, S. L., Mahajan, A., Wang, Q. and Sen, S. (2008). Prevention of cardiac hypertrophy and heart failure by silencing of NF-kappaB. *J. Mol. Biol.* **375**, 637-649.

Isic, A., Scharin Täng, M., Haugen, E. and Fu, M. (2008). TNFalpha-antagonist neither improve cardiac remodelling or cardiac function at early stage of heart failure in diabetic rats. *Autoimmunity* **41**, 473-477.

Kubota, T., McTiernan, C. F., Frye, C. S., Slawson, S. E., Lemster, B. H., Koretsky, A. P., Demetris, A. J. and Feldman, A. M. (1997). Dilated cardiomyopathy in transgenic mice with cardiac-specific overexpression of tumor necrosis factor-alpha. *Circ. Res.* **81**, 627-635.

Li, Y. Y., Feng, Y. Q., Kadokami, T., McTiernan, C. F., Draviam, R., Watkins, S. C. and Feldman, A. M. (2000). Myocardial extracellular matrix remodeling in transgenic mice overexpressing tumor necrosis factor alpha can be modulated by anti-tumor necrosis factor alpha therapy. *Proc. Natl. Acad. Sci. USA* **97**, 12746-12751.

Li, Y. Y., Feng, Y., McTiernan, C. F., Pei, W., Moravec, C. S., Wang, P., Rosenblum, W., Kormos, R. L. and Feldman, A. M. (2001). Downregulation of matrix metalloproteinases and reduction in collagen damage in the failing human heart after support with left ventricular assist devices. *Circulation* **104**, 1147-1152.

Li, N., Xu, X., Xiao, B., Zhu, E.-D., Li, B.-S., Liu, Z., Tang, B., Zou, Q.-M., Liang, H.-P. and Mao, X.-H. (2012). H. pylori related proinflammatory cytokines contribute to the induction of miR-146a in human gastric epithelial cells. *Mol. Biol. Rep.* **39**, 4655-4661.

Lu, X., Ma, L., Ruan, L., Kong, Y., Mou, H., Zhang, Z., Wang, Z., Wang, J. and Le, Y. (2010). Resveratrol differentially modulates inflammatory responses of microglia and astrocytes. *J. Neuroinflammation* **7**, 46.

Matsusaka, H., Ikeuchi, M., Matsushima, S., Ide, T., Kubota, T., Feldman, A. M., Takeshita, A., Sunagawa, K. and Tsutsui, H. (2005). Selective disruption of MMP-2 gene exacerbates myocardial inflammation and dysfunction in mice with cytokine-induced cardiomyopathy. *Am. J. Physiol. Heart Circ. Physiol.* **289**, H1858-H1864.

Meiners, S., Hocher, B., Weller, A., Laule, M., Stangl, V., Guenther, C., Godes, M., Mrozikiewicz, A., Baumann, G. and Stangl, K. (2004). Downregulation of matrix metalloproteinases and collagens and suppression of cardiac fibrosis by inhibition of the proteasome. *Hypertension* **44**, 471-477.

Olson, A. L. and Pessin, J. E. (1994). Regulation of c-fos expression in adipose and muscle tissue of diabetic rats. *Endocrinology* **134**, 271-276.

Palomer, X., Álvarez-Guardia, D., Rodriguez-Calvo, R., Coll, T., Laguna, J. C., Davidson, M. M., Chan, T. O., Feldman, A. M. and Vazquez-Carrera, M. (2009). TNF-alpha reduces PGC-1alpha expression through NF-kappaB and p38 MAPK leading to increased glucose oxidation in a human cardiac cell model. *Cardiovasc. Res.* **81**, 703-712.

Palomer, X., Álvarez-Guardia, D., Davidson, M. M., Chan, T. O., Feldman, A. M. and Vázquez-Carrera, M. (2011). The interplay between NF-kappaB and E2F1 coordinately regulates inflammation and metabolism in human cardiac cells. *PLoS ONE* **6**, e19724.

Palomer, X., Capdevila-Busquets, E., Álvarez-Guardia, D., Barroso, E., Pallàs, M., Camins, A., Davidson, M. M., Planavila, A., Villarroya, F. and Vázquez-Carrera, M. (2013a). Resveratrol induces nuclear factor-kappaB activity in human cardiac cells. *Int. J. Cardiol.* **167**, 2507-2516.

Palomer, X., Salvadó, L., Barroso, E. and Vazquez-Carrera, M. (2013b). An overview of the crosstalk between inflammatory processes and metabolic dysregulation during diabetic cardiomyopathy. *Int. J. Cardiol.* **168**, 3160-3172.

Palomer, X., Capdevila-Busquets, E., Botteri, G., Salvadó, L., Barroso, E., Davidson, M. M., Michalik, L., Wahli, W. and Vázquez-Carrera, M. (2014). PPARbeta/delta attenuates palmitate-induced endoplasmic reticulum stress and induces autophagic markers in human cardiac cells. *Int. J. Cardiol.* **174**, 110-118.

Pan, Z., Sun, X., Shan, H., Wang, N., Wang, J., Ren, J., Feng, S., Xie, L., Lu, C., Yuan, Y. et al. (2012). MicroRNA-101 inhibited postinfarct cardiac fibrosis and improved left ventricular compliance via the FBJ osteosarcoma oncogene/transforming growth factor-beta1 pathway. *Circulation* **126**, 840-850.

Perry, M. M., Moschos, S. A., Williams, A. E., Shepherd, N. J., Larner-Svensson, H. M. and Lindsay, M. A. (2008). Rapid changes in microRNA-146a expression negatively regulate the IL-1beta-induced inflammatory response in human lung alveolar epithelial cells. *J. Immunol.* **180**, 5689-5698.

Schonthaler, H. B., Guinea-Viniegra, J. and Wagner, E. F. (2011). Targeting inflammation by modulating the Jun/AP-1 pathway. *Ann. Rheum. Dis.* **70** Suppl. 1, i109-i112.

Schroen, B. and Heymans, S. (2012). Small but smart-microRNAs in the centre of inflammatory processes during cardiovascular diseases, the metabolic syndrome, and ageing. *Cardiovasc. Res.* **93**, 605-613.

Shieh, J. T. C., Huang, Y., Gilmore, J. and Srivastava, D. (2011). Elevated miR-499 levels blunt the cardiac stress response. *PLoS ONE* **6**, e19481.

Small, E. M., Frost, R. J. A. and Olson, E. N. (2010). MicroRNAs add a new dimension to cardiovascular disease. *Circulation* **121**, 1022-1032.

Stetson, S. J., Perez-Verdia, A., Mazur, W., Farmer, J. A., Koerner, M. M., Weilbaecher, D. G., Entman, M. L., Quinones, M. A., Noon, G. P. and Torre-Amione, G. (2001). Cardiac hypertrophy after transplantation is associated with persistent expression of tumor necrosis factor-alpha. *Circulation* **104**, 676-681.

Taganov, K. D., Boldin, M. P., Chang, K.-J. and Baltimore, D. (2006). NF-kappaB-dependent induction of microRNA miR-146, an inhibitor targeted to signaling proteins of innate immune responses. *Proc. Natl. Acad. Sci. USA* **103**, 12481-12486.

Takimoto, E. and Kass, D. A. (2007). Role of oxidative stress in cardiac hypertrophy and remodeling. *Hypertension* **49**, 241-248.

Tanic, M., Zajac, M., Gómez-López, G., Benítez, J. and Martínez-Delgado, B. (2012). Integration of BRCA1-mediated miRNA and mRNA profiles reveals microRNA regulation of TRAF2 and NFkappaB pathway. *Breast Cancer Res. Treat.* **134**, 41-51.

Turner, N. A., Mughal, R. S., Warburton, P., O'regan, D. J., Ball, S. G. and Porter, K. E. (2007). Mechanism of TNFalpha-induced IL-1alpha, IL-1beta and IL-6 expression in human cardiac fibroblasts: effects of statins and thiazolidinediones. *Cardiovasc. Res.* **76**, 81-90.

van de Vrie, M., Heymans, S. and Schroen, B. (2011). MicroRNA involvement in immune activation during heart failure. *Cardiovasc. Drugs Ther.* **25**, 161-170.

Wang, P. H., Almahfouz, A., Giorgino, F., McCowen, K. C. and Smith, R. J. (1999). In vivo insulin signaling in the myocardium of streptozotocin-diabetic rats: opposite effects of diabetes on insulin stimulation of glycogen synthase and c-Fos. *Endocrinology* **140**, 1141-1150.

Wang, M., Zhang, W.-B., Zhu, J.-H., Fu, G.-S. and Zhou, B.-Q. (2009). Breviscapine ameliorates hypertrophy of cardiomyocytes induced by high glucose in diabetic rats via the PKC signaling pathway. *Acta Pharmacol. Sin.* **30**, 1081-1091.

Wang, X., Ha, T., Liu, L., Zou, J., Zhang, X., Kalbfleisch, J., Gao, X., Williams, D. and Li, C. (2013). Increased expression of microRNA-146a decreases myocardial ischaemia/reperfusion injury. *Cardiovasc. Res.* **97**, 432-442.

Yang, K., He, Y. S., Wang, X. Q., Lu, L., Chen, Q. J., Liu, J., Sun, Z. and Shen, W. F. (2011). MiR-146a inhibits oxidized low-density lipoprotein-induced lipid accumulation and inflammatory response via targeting toll-like receptor 4. *FEBS Lett.* **585**, 854-860.

Biochimica et Biophysica Acta 1861 (2016) 1569–1578

Contents lists available at ScienceDirect

Biochimica et Biophysica Acta

journal homepage: www.elsevier.com/locate/bbalip

Review

PPARβ/δ and lipid metabolism in the heart☆

Xavier Palomer, Emma Barroso, Mohammad Zarei, Gaia Botteri, Manuel Vázquez-Carrera *

Pharmacology Unit, Department of Pharmacology and Therapeutic Chemistry, Institut de Biomedicina de la UB (IBUB), Faculty of Pharmacy, University of Barcelona, Barcelona, Spain
Institut de Recerca Pediàtrica, Hospital Sant Joan de Déu, Barcelona, Spain
CIBER de Diabetes y Enfermedades Metabólicas Asociadas (CIBERDEM), Instituto de Salud Carlos III, Barcelona, Spain

ARTICLE INFO

Article history:
Received 3 November 2015
Received in revised form 23 December 2015
Accepted 22 January 2016
Available online 26 January 2016

Keywords:
PPARβ/δ
Cardiomyocyte
Fatty acid
Inflammation
Lipid metabolism

ABSTRACT

Cardiac lipid metabolism is the focus of attention due to its involvement in the development of cardiac disorders. Both a reduction and an increase in fatty acid utilization make the heart more prone to the development of lipotoxic cardiac dysfunction. The ligand-activated transcription factor peroxisome proliferator-activated receptor (PPAR)β/δ modulates different aspects of cardiac fatty acid metabolism, and targeting this nuclear receptor can improve heart diseases caused by altered fatty acid metabolism. In addition, PPARβ/δ regulates glucose metabolism, the cardiac levels of endogenous antioxidants, mitochondrial biogenesis, cardiomyocyte apoptosis, the insulin signaling pathway and lipid-induced myocardial inflammatory responses. As a result, PPARβ/δ ligands can improve cardiac function and ameliorate the pathological progression of cardiac hypertrophy, heart failure, cardiac oxidative damage, ischemia–reperfusion injury, lipotoxic cardiac dysfunction and lipid-induced cardiac inflammation. Most of these findings have been observed in preclinical studies and it remains to be established to what extent these intriguing observations can be translated into clinical practice. This article is part of a Special Issue entitled: Heart Lipid Metabolism edited by G.D. Lopaschuk.

1. Introduction

Constant pump function of the heart requires a high-energy demand in the form of adenosine triphosphate (ATP), which is mainly satisfied by fatty acids (FAs) and glucose. Thus, in the adult heart, about 70% of cardiac energy metabolism relies on the oxidation of FAs, whereas glucose (20%), lactate and ketone bodies are additional fuel sources [1]. The heart, unlike other tissues such as the brain, adapts its metabolism to substrate availability for ATP generation [2]. Due to low oxygen pressure, the fetal heart mainly depends on anaerobic glucose and lactate for ATP generation. In contrast, the adult heart primarily relies on mitochondrial fatty acid oxidation (FAO) to ensure ATP generation, but conserves the metabolic flexibility to switch to other substrates, mainly glucose. This switch in substrate preference from FAO towards increased glucose utilization in the heart for ATP generation is observed in myocardial ischemia, cardiac hypertrophy and heart failure [1]. This metabolic shift has long been interpreted as an oxygen-sparing mechanism of the heart. Consequently, several animal studies have demonstrated that inhibition of FAO might be useful for protecting the heart from the consequences of ischemia and ischemia–reperfusion injury [1,3]. However, the reduction in FAO has a major impact on the availability of ATP [4], since long-chain FAO produces 3–4 times more ATP per molecule compared with glucose oxidation, and this decrease in ATP synthesis can limit energy supply, contributing to cardiac remodeling. Further, the reduction in FAO can promote an imbalance between FA uptake and its oxidation, leading to accumulation of FA derivatives, including triglycerides, but also more toxic lipids, such as diacylglycerol (DAG) and ceramide that can alter cellular structures and activate downstream pathways leading to inflammation and toxicity. On the other hand, excessive FAO is also harmful [5]. Thus, in hearts of obese and/or diabetic patients, myocardial insulin resistance and increased rates of systemic lipolysis force the heart to rely almost exclusively on FAO as an energy source, indicating the presence of a loss of substrate flexibility [5,6]. When sustained over long term, increased myocardial FA utilization makes the heart more prone to the development of lipotoxic cardiac dysfunction characterized by lipid accumulation, mitochondrial dysfunction and the generation of reactive oxygen species (ROS) [5,6].

Since the discovery of the first peroxisome proliferator-activated receptor (PPAR), the PPARα isoform, by Isseman and Green [7], the biological roles of these receptors in the heart have received widespread attention due to their key role in controlling cardiac lipid metabolism. The pioneering work by Cheng et al. [8] demonstrated that the nuclear receptor PPARβ/δ plays a major role in cardiac lipid metabolism, since mice with cardiac-specific deletion of this receptor developed myocardial lipid accumulation and cardiomyopathy. This review discusses

☆ This article is part of a Special Issue entitled: Heart Lipid Metabolism edited by G.D. Lopaschuk.

* Corresponding author at: Unitat de Farmacologia, Facultat de Farmàcia, Diagonal 643, E-08028 Barcelona, Spain.
E-mail address: mvazquezcarrera@ub.edu (M. Vázquez-Carrera).

http://dx.doi.org/10.1016/j.bbalip.2016.01.019
1388-1981/

new insights on the role of PPARβ/δ in cardiac lipid metabolism and how targeting this nuclear receptor can ameliorate cardiac disorders caused by altered FA metabolism.

2. Peroxisome proliferator-activated receptors (PPARs)

PPARs belong to a subfamily of the nuclear receptor superfamily that allows the cell to respond to extracellular stimuli by regulating transcriptional gene expression. The PPAR family comprises three isoforms; PPARα (NR1C1, according to the unified nomenclature system for the nuclear receptor superfamily), PPARβ/δ (NR1C2) and PPARγ (NR1C3) [9]. When PPARβ/δ was initially cloned in *Xenopus laevis* it was named PPARβ. However, when cloned in other species it was not clearly identified as being homologous to the *Xenopus* PPARβ and it was alternatively called NUC-1 in humans [10] and PPARδ in mice [11,12]. Currently, it is accepted that *Xenopus* PPARβ is homologous to murine PPARδ and this explains the terminology PPARβ/δ.

Like most members of the nuclear-receptor superfamily, PPARs have a common domain structure consisting of four major functional domains: the N-terminal ligand-independent transactivation domain (A/B domain) often known as activation function 1 (AF-1), the DNA binding domain (DBD or C domain), hinge region (D domain) and the carboxy-terminal E domain or AF-2, including the ligand-binding domain and the ligand-dependent transactivation domain [13] (Fig. 1A).

The physiological role of PPARs depends on tissue distribution, ligand binding and the recruitment of co-activators and co-repressors. PPARα is the molecular target of the fibrate hypolipidemic class of drugs and is expressed primarily in tissues with a high level of fatty acid catabolism such as liver, brown fat, kidney, heart and skeletal muscle [14]. The γ isoform is the molecular target for the anti-diabetic drugs thiazolidinediones or glitazones and is expressed as two splice variants, PPARγ1 and γ2. PPARγ1 is mainly expressed in white and brown adipose tissues, colon, retina, spleen and hematopoietic cells. PPARγ2 is exclusively expressed in white and brown adipose tissues [15] and differs from PPARγ1 in the presence of 28 (mouse) or 30 (human) additional amino acids at its N-terminal end. PPARβ/δ is almost ubiquitously expressed, although it is most abundant in metabolically active tissues such as skeletal and cardiac muscles [16]. The predominant isoforms in the heart are PPARα and PPARβ/δ, more specifically in cardiac muscle cells and fibroblasts [17,18], while the abundance of PPARγ is very low.

To be transcriptionally active, PPARs need to heterodimerize with the 9-cis retinoic acid receptor (RXR or NR2B). PPAR–RXR heterodimers bind to peroxisome proliferator response elements (PPREs) located in the promoter regions of their target genes, thereby increasing gene transcription in a ligand-dependent manner (transactivation) [16,19] (Fig. 1B). In the absence of ligand, high-affinity complexes are formed between PPAR–RXR heterodimers and nuclear co-repressor proteins, such as the nuclear receptor co-repressor (N-CoR) and the silencing mediator of retinoid and thyroid signaling (SMRT), which block transcriptional activation by sequestering the heterodimer from the promoter. Binding of the ligand to PPAR induces a conformational change resulting in dissociation of co-repressor proteins, so that the PPAR–RXR heterodimer can then bind to PPREs. Moreover, once activated by the ligand, the heterodimer recruits co-activator proteins that promote the initiation of transcription [20], such as PPARγ co-activator 1α (PGC-1α) or steroid receptor co-activator 1 (SRC-1) with intrinsic histone acetylase (HAT)

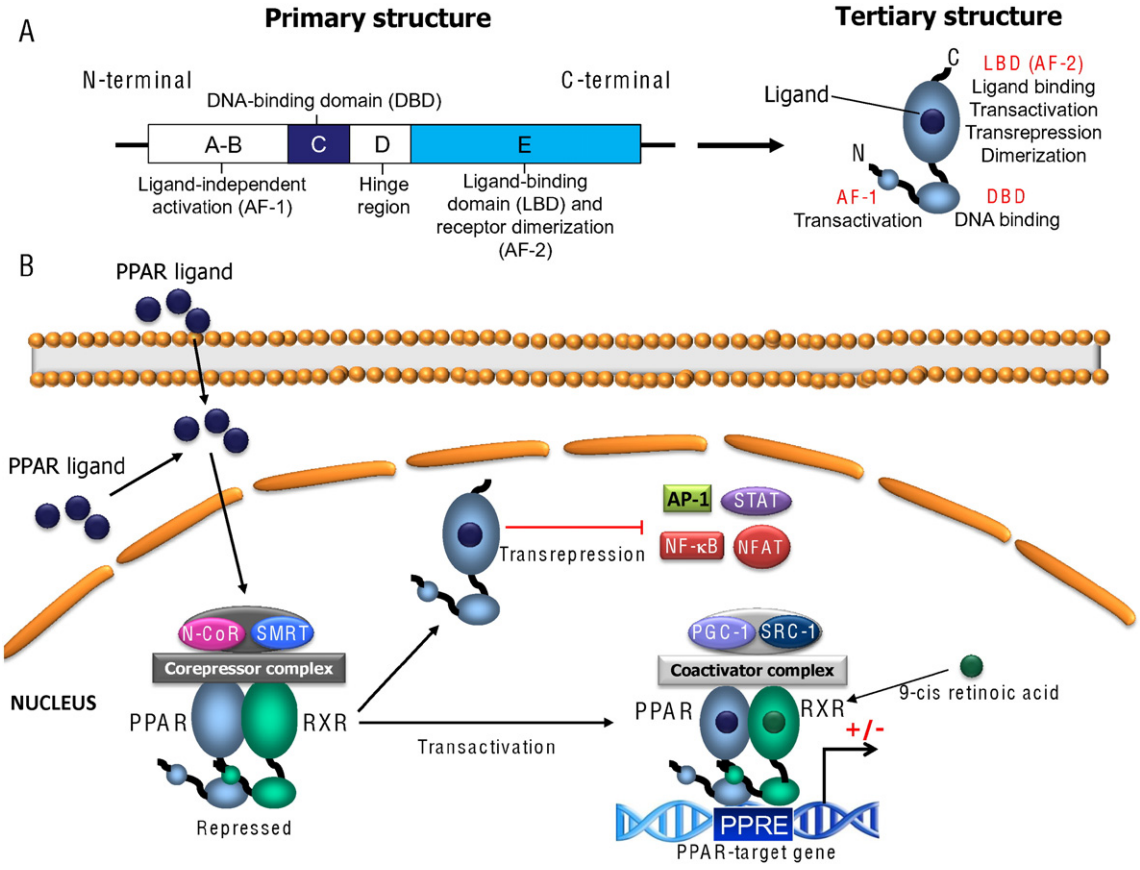

Fig. 1. Structure and transcriptional activation of PPARs. A, Primary and tertiary PPAR domain structures. N and C represent the amino and carboxyl termini, respectively. Activation function 1 (AF-1) is a variable amino-terminal transactivation domain. The ligand-binding domain (LBD) also mediates dimerization, transcriptional activation, and transcriptional repression functions. B, PPAR mechanisms of action. PPAR activation leads to heterodimerization with RXR. Binding of the ligand to PPAR results in a conformational change that allows its dissociation from a repressed binding protein complex which may contain the nuclear receptor co-repressor (N-CoR) and the silencing mediator of retinoid and thyroid signaling (SMRT) and the subsequent recruitment of a transcriptional complex that may contain the steroid receptor co-activator-1 (SRC-1) or the PPARγ co-activator 1α (PGC-1α), among others. DBD, DNA-binding domain. PPRE, Peroxisome proliferator response element.

activity, or recruit proteins with HAT activity to initiate transcription [21]. In a specific cellular context, the activity of PPARs in terms of regulating the transcription of their target genes depends on many factors (relative expression of the PPARs, the promoter context of the target gene, the presence of co-activator and co-repressor proteins, etc.).

The regulation of gene transcription by PPARs extends beyond their ability to transactivate specific target genes in an agonist-dependent manner. PPARs also regulate gene expression independently of binding to PPREs (Fig. 1B). They cross-talk with other types of transcription factors and influence their function without binding to DNA, through a mechanism termed receptor-dependent transrepression [22]. Most of the anti-inflammatory effects of PPARs are probably explained by this mechanism [23,24]. Thus, through this DNA-binding independent mechanism, PPARs suppress the activities of several transcription factors, including nuclear factor κB (NF-κB), activator protein 1 (AP-1), signal transducers and activators of transcription (STATs) and nuclear factor of activated T cells (NFAT). There are three main transrepression mechanisms by which ligand-activated PPAR–RXR complexes negatively regulate the activities of other transcription factors (Fig. 2). First, transrepression may result from competition for limiting amounts of shared co-activators. Under conditions in which the levels of specific co-activators are rate-limiting, activation of PPAR may suppress the activity of other transcription factors that use the same co-activators [25,26]. In the second mechanism, activated PPAR–RXR heterodimers are believed to act through physical interaction with other transcription factors (for example AP-1, NF-κB, NFAT or STATs). This association prevents the transcription factor from binding to its response element and thereby inhibits its ability to induce gene transcription [27]. The third transrepression mechanism relies on the ability of activated PPAR–RXR heterodimers to inhibit the phosphorylation and activation of certain members of the mitogen-activated protein kinase (MAPK) cascade [28], preventing activation of downstream transcription factors.

The crystal structure of the ligand-binding domain of the PPARβ/δ isoform revealed an exceptionally large pocket of approximately 1300 Å^3. This pocket is similar to that of PPARγ, but much larger than the pockets of other nuclear receptors [29,30], which may explain, at least in part, the great variety of natural and synthetic ligands that bind to and activate this nuclear receptor. Saturated (14 to 18 carbons) and polyunsaturated (20 carbons in length) fatty acids in the low micromolar range have affinity for PPARβ/δ, but also for the other PPAR isoforms [30–33], showing little affinity towards the different isoforms. In addition, all-trans-retinoic acid (vitamin A) [34] and fatty acids derived from VLDL [35] can activate PPARβ/δ. Finally, the availability of three synthetic ligands (GW501516, GW0742 and L-165041) that activate PPARβ/δ at very low concentrations both in vivo and in vitro with high selectivity over other PPAR isoforms [36] led to a huge increase in experimental studies on the role of PPARβ/δ in cellular processes. The EC_{50} for these compounds assessed with recombinant human PPARβ/δ was 1.0 nM for GW0742, 1.1 nM for GW501516 and 50 nM for L-165041 [37,38]. There are no clinically available drugs targeting PPARβ/δ, but two PPARβ/δ agonists are in clinical trials: MBX-8025 (Metabolex) [39] and KD-3010 (Kalypsys) [40]. PPARβ/δ antagonists have also been used to study the functions of this receptor, especially GSK0660 [38], although its poor bioavailability has reduced its use in in vivo studies. GSK3787 is another potent PPARβ/δ antagonist with good bioavailability that allows its use in animal studies [41,42].

In addition to pharmacological approaches, the development of genetically-modified mouse models has allowed the study of the biological functions of PPARβ/δ. For more detailed information on these animal models, the reader is referred to the excellent review by Giordano et al. [43].

3. PPARβ/δ effects in cardiac lipid metabolism

The heart obtains lipids from de novo synthesis or it acquires them from the exogenous supply provided by albumin-bound non-esterified or free fatty acids (FFA) or esterified FAs bound to triglyceride-rich lipoproteins [44]. Although it is thought that the heart has a limited capacity for de novo FA synthesis from glucose, this pathway seems to be important for maintaining cardiac function in aortic constriction and aging [45].

Lipoprotein-derived FAs are acquired by the heart following triglyceride hydrolysis by endothelial-bound lipoprotein-lipase (LpL). FAs can be imported into the cardiomyocytes through passive diffusion, but this is a very slow process, and the uptake is facilitated by the presence of several FA transporters, including fatty acid translocase (FAT)/CD36, FA transport protein (FATP), and plasma membrane FA-binding protein ($FABP_{pm}$) (Fig. 2). Of these FA transporters, CD36 is the best characterized due to its key role in FA translocation. Thus, studies using CD36-null mice have demonstrated that this transporter is responsible for up to 70% of FA uptake in contracting cardiomyocytes [46]. Once within the cytosol, approximately 75% of FAs are transferred into the mitochondria and oxidized for ATP generation, while the remainder is converted to triglycerides for storage. Long-chain FAs cannot freely enter

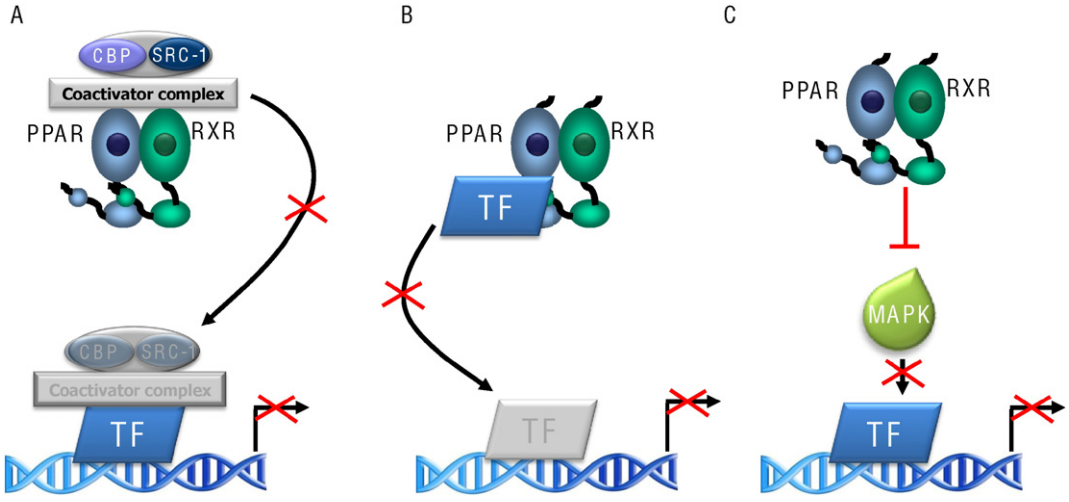

Fig. 2. PPAR-dependent transrepresssion mechanism. Most of the anti-inflammatory effects of PPARs are likely mediated through this DNA-independent mechanism. Three main transrepression mechanisms have been described for PPARs. A, PPARs compete for limiting amounts of co-activator proteins – such as cAMP response element binding (CREB)-binding protein (CBP) and steroid receptor co-activator (SRC1) – reducing the availability of these co-activators to other transcription factors (TF). B, PPARs associate physically with other TF, preventing the binding of this TF to its response elements and thereby inhibits its ability to induce gene transcription. C, PPARs inhibit the activation of a mitogen-activates protein kinase (MAPK), resulting in the attenuation of the activity of the MAPK for phosphorylating and activating TF.

the mitochondria and need to be esterified into fatty acyl-coenzyme A (CoA) by cytosolic fatty acyl-CoA synthetase (ACS). The acyl group of fatty acyl-CoA can be transferred to carnitine via carnitine palmitoyltransferase 1 (CPT-1) and the acylcarnitine is then shuttled into the mitochondria by carnitine translocase to undergo β-oxidation, producing acetyl-CoA, which can be used in the tricarboxylic acid (TCA) cycle to produce ATP. The rate of FA uptake by the heart is largely determined by plasma FFA levels, and patients with diabetes and metabolic syndrome have elevated circulating plasma FFA [47,48], promoting greater FFA uptake by the heart. If FA uptake exceeds the requirements for energy production, these FA accumulate as lipid metabolites leading to accumulation of triglycerides and other more harmful lipids, such as diacylglycerol (a toxic lipid intermediate generated in triglyceride synthesis) and ceramide (whose de novo synthesis is initiated by the action of serine palmitoyl transferase on the saturated fatty acid palmitate) (Fig. 3). For instance, cardiac-specific overexpression of human LpL promotes increased FA uptake and utilization from circulating VLDL, causing cardiac lipid accumulation and dilated cardiomyopathy [49].

3.1. PPARβ/δ effects in FA transport and oxidation

Proteins involved in FA transport and oxidation are under the transcriptional control of PPARβ/δ. In fact, specific *knockout* of PPARβ/δ in cardiomyocytes decreased the basal expression of genes involved in FAO, including mitochondrial FA uptake (CPT-1), malonyl-CoA metabolism (malonyl-CoA decarboxylase), mitochondrial FA β-oxidation (very-long-chain acyl-CoA dehydrogenase, long-chain acyl-CoA dehydrogenase), peroxisomal oxidation (acyl-CoA oxidase) and glucose oxidation (pyruvate dehydrogenase kinase 4) [8]. As a result of these changes, basal myocardial fatty acid oxidation was reduced and subsequent lipid accumulation was observed. In addition, these mice displayed cardiac dysfunction, cardiac hypertrophy and congestive heart failure with reduced survival. In another mouse model, short-term PPARβ/δ specific deletion in the adult heart confirmed the role of this nuclear receptor in transcriptional regulation of FAO as well as in glucose oxidation, showing a reduction in both cardiac fatty acid and glucose oxidation rates [50]. It is worth noting that this study also demonstrated that PPARβ/δ has an important role in regulating endogenous antioxidants (Cu/Zn superoxide dismutase and manganese superoxide dismutase) and that the attenuation in the expression of these genes leads to increased oxidative damage to the heart. Moreover, expression of PGC-1α, a transcriptional co-activator involved in FAO and a key mitochondrial biogenesis determinant, was decreased in the heart of these mice, concomitant with a reduction in mitochondrial DNA copy number. As a result of PPARβ/δ deficiency in the adult heart, depressed cardiac performance and cardiac hypertrophy were observed in this model. On the other hand, constitutive cardiomyocyte-specific expression of PPARβ/δ (driven by the myosin heavy chain promoter, MHC-PPARβ/δ mice) induced the expression of FAO-associated genes and did not lead to lipid accumulation and cardiac dysfunction, in contrast to that observed in MHC-PPARα mice [51]. Besides the role of elevated FAO in the prevention of fatty acid accumulation

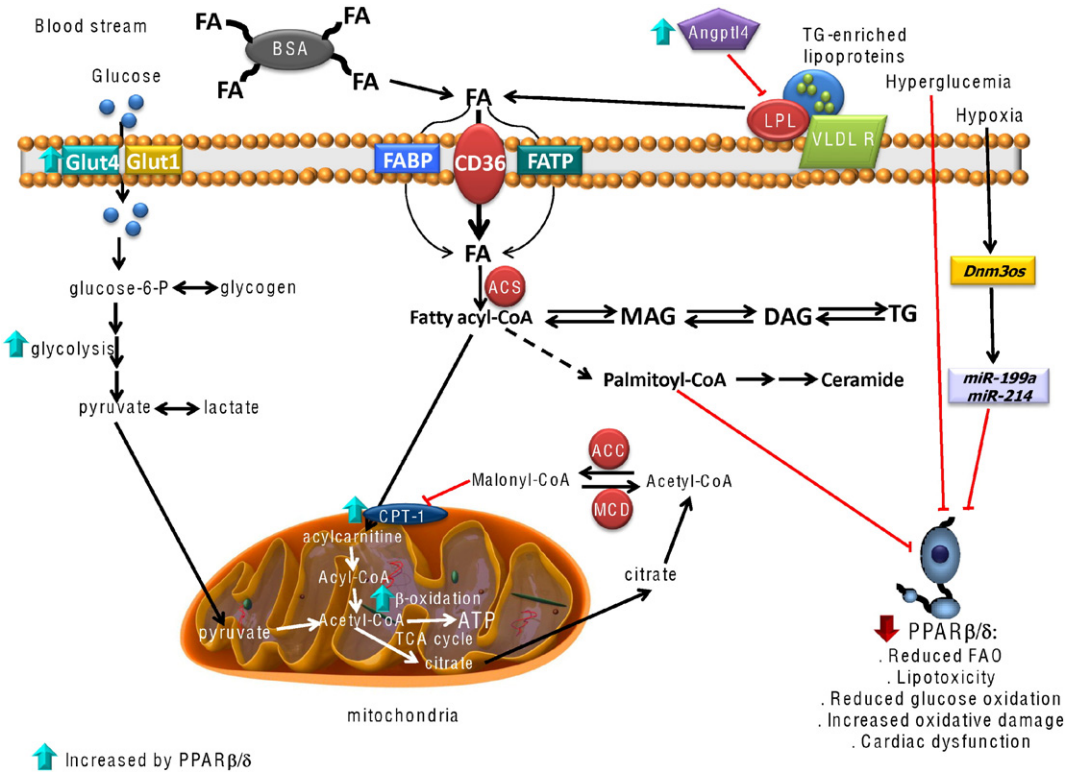

Fig. 3. Effects of PPARβ/δ activation on cardiac and glucose metabolic pathways. Fatty acids (FA) derived from triglyceride-rich lipoproteins, chylomycrons, and VLDL are hydrolyzed by lipoprotein lipase (LpL). This lipase is inhibited by angiopoietin-like 4 (Angptl4). Lipoprotein-derived FA or albumin-bound free FA are internalized by the cells via membrane receptors such as CD36 or other transporters (FA transport protein, FATP; FA-binding protein, FABP). Internalization of whole lipoproteins is also possible through the VLDL receptor (VLDL-R). Once inside the cardiomyocyte, FA are converted to fatty acyl-CoAs by acyl-CoA synthetase (ACS), which can either be stored as triglycerides or imported into mitochondria for β-oxidation. Triglyceride synthesis is achieved in several steps by incorporating them into a glycerol backbone forming mono- (monoacylglycerol, MAG), di- (diacylglycerol, DAG) and triacylglycerol or triglycerides (TG). The stored TG can be made available for oxidation by its hydrolysis into DAG and MAG, releasing fatty acyl-CoA that can be oxidized into the mitochondria. The de novo synthesis of ceramide is initiated by palmitoyl-CoA. Carnitine palmitoyltransferase 1 (CPT-1) converts acyl-CoA into acylcarnitine, which then crosses the outer mitochondrial membrane. This is the first step in mitochondrial fatty acid β-oxidation. CPT-1 activity is inhibited by malonyl-CoA, which is formed via carboxylation of acetyl-CoA by acetyl-CoA carboxylase (ACC). The effect of PPARβ/δ-mediated upregulation is shown by blue arrows. Palmitate, hyperglycemia, and hypoxia have been reported to reduce PPARβ/δ levels in cardiomyocytes, causing deleterious effects that can result in cardiac dysfunction. MCD: malonyl-CoA decarboxylase. TCA, tricarboxylic acid.

and heart dysfunction in the MHC-PPARβ/δ mouse, the increased expression of the LpL inhibitor angiopoietin-like 4 may also contribute by attenuating FA uptake [52] (Fig. 3). It is worth pointing out that the expression of genes involved in cellular FA transport (CD36 and FATP1) was activated in hearts of MHC-PPARα, but not in MHC-PPARβ/δ mice. In contrast, cardiac glucose transport and glycolytic genes were activated in MHC-PPARβ/δ mice, but repressed in MHC-PPARα mice. This increased capacity for myocardial glucose utilization in MHC-PPARβ/δ mice may explain the reduction in myocardial injury due to ischemia/reperfusion in these mice compared to the MHC-PPARα mice. More recently, PPARβ/δ activation in the adult heart by generating a transgenic mouse model expressing a constitutively active form of PPARβ/δ upon tamoxifen administration in a tissue-specific manner [53] resulted in enhanced expression of genes involved in FAO and endogenous antioxidants, increased mitochondrial DNA copy number and elevated cardiac performance. Moreover, PPARβ/δ activation improved cardiac function and attenuated progression to cardiac hypertrophy induced by pressure-overload stimuli. Consistent with genetic approaches, PPARβ/δ ligands (L-165,041, GW501516 and GW0742) increased the expression of genes involved in FAO and FA oxidation rates in both neonatal and adult cardiomyocytes as well as in embryonic rat heart-derived H9c2 cells [17,54].

Given the important role of PPARβ/δ in regulating FAO, the reduction of its expression or activity might lead to activation of pathological processes causing cardiac dysfunction. By regulating the stability and translation of messenger RNAs by base-pairing with the 3′ UTRs, small noncoding RNAs (~18–24 nucleotides), such as microRNAs (miRNAs, miRs), have emerged as important regulators of gene expression in cardiac disease [55]. Interestingly, PPARβ/δ levels are strongly repressed by the miRNA cluster *miR-199a~214*, embedded in chromosome 1 in a large noncoding RNA, *Dnm3os* [56] (Fig. 2). Moreover, myocardial hypoxia, a characteristic of heart failure, provokes activation of *Dnm3os* and the subsequent increase in the expression of the miRNA cluster *miR-199a~214* that decreases PPARβ/δ protein levels and mitochondrial FAO. These changes facilitate a metabolic shift from predominant reliance on FAO in the healthy myocardium towards increased reliance on glucose metabolism at the onset of heart failure. Likewise, exposure of neonatal cardiomyocytes to the saturated FA palmitate, but not the monounsaturated FA oleate, downregulates the protein levels of both CPT-1β and PPARβ/δ [57] (Fig. 2), suggesting that palmitate can exacerbate lipotoxicity by reducing FAO. Similarly, it has been reported that hyperglycemia reduces PPARβ/δ levels in cardiomyocytes through a mechanism that might involve ROS production or MAPK activation [58].

On the other hand, activation of PPARβ/δ can also improve some cardiac pathologies linked to reductions in FAO. Thus, cardiac hypertrophy is associated with an increase in glucose utilization and a decrease in FAO, which is characteristic of the fetal heart [59]. It is still a matter of controversy whether changes in intracellular substrate and metabolite levels in cardiomyocytes are a consequence or the reason for cardiac hypertrophy. However, several factors support a role for cardiac metabolism in the development of cardiac hypertrophy. Thus, defects in mitochondrial FAO enzymes cause childhood hypertrophic cardiomyopathy [60], and perturbation of FAO in animal models cause cardiac hypertrophy [61], demonstrating that substrate utilization is important in the pathogenesis of hypertrophy. We have reported that PPARβ/δ activation prevents hypertrophy in neonatal rat cardiomyocytes [62]. More recently it has been reported that PPARβ/δ activation in the adult heart improved cardiac performance and reduced fibrosis and mitochondrial abnormalities in mice subjected to pressure-overload cardiac hypertrophy [53]. Therefore, PPARβ/δ ligands might prevent cardiac hypertrophy, a process that although initially is compensatory for an increase in workload in the setting of several pathologies (hypertension, valvular heart disease, etc.), when prolonged frequently results in congestive heart failure, arrhythmia, and sudden death [63].

4. Signaling effects of lipids promoting cardiac dysfunction

Although lipids are important to meet the heart's demand for energy, allowing its function, an excess of lipids, both in amount or distribution, can also be detrimental and may lead to cardiac dysfunction, due to abnormal cardiac structure and function. This cardiac lipotoxicity can be the result of the activation of different pathological processes by several lipids (including FA, ceramide and diacylglycerol [64]), that can be regulated by PPARβ/δ.

4.1. PPARβ/δ effects in apoptosis pathways

Apoptosis, among other factors, is involved in the development of myocardial dysfunction [65]. Saturated FA can induce apoptosis by several mechanisms in isolated cardiomyocytes, including accumulation of the toxic lipid ceramide or by activating endoplasmic reticulum (ER) stress [66]. Recently it has been reported that palmitate-induced apoptosis in neonatal cardiomyocytes was prevented by PPARβ/δ ligands as well as by AMP-activated protein kinase (AMPK) activators through its ability to prevent an increase in IL-6 levels [57]. AMPK is a master regulator of mechanisms relevant to cardiac energy production by regulating glucose and fatty acid metabolism, but it also regulates mitochondrial function, ER stress, autophagy and apoptosis [67]. It is worth noting that activation of AMPK attenuates the apoptotic effect of palmitate on cardiomyocytes [68]. This effect has been attributed to the ability of AMPK to phosphorylate and inactivate acetyl-CoA carboxylase (ACC), decreasing the intracellular concentration of malonyl-CoA. Since malonyl-CoA is a negative regulator of CPT-1, AMPK promotes FAO by reducing the accumulation of toxic FA derivatives. Interestingly, we [69] and others [70] have previously reported that PPARβ/δ activates AMPK in skeletal muscle cells, but it remains to be determined whether PPARβ/δ ligands prevent palmitate-induced apoptosis in cardiac cells through a mechanism involving this kinase.

Chronic ER stress contributes to apoptotic cell death in the myocardium, thereby playing a critical role in the development of cardiomyopathy [71]. Activation of the unfolded protein response (UPR) initially aims to mitigate adverse effects of ER stress and thus enhance cell survival by halting general mRNA translation, facilitating protein degradation via the ER-associated degradation (ERAD) pathway and enhancing the production of molecular chaperones involved in protein folding. If ER stress is limited, the UPR will potentiate autophagy to protect the cells [72]. This pro-survival pathway has evolved as an alternative mechanism for saving nutrients, recycling intracellular components and eliminating abnormal protein aggregates and misfolded proteins formed during the ER stress that cannot be removed through the ERAD pathway. However, if ER stress is not mitigated within a certain time period or the disturbance is prolonged, then the UPR will turn on apoptosis to remove cells that threaten the integrity of the organism [73]. Cardiomyocytes rarely proliferate within the adult heart and, as a consequence, their loss due to apoptosis may play an essential pathogenic role during cardiovascular diseases [71].

It has been reported that exposure to a high-fat diet (HFD) induces cardiomyocyte apoptosis via the inhibition of autophagy and the promotion of ER stress [74]. Interestingly, we have reported that PPARβ/δ activation by GW501516 prevented palmitate-induced ER stress in human AC16 cardiac cells [75]. Although AMPK activation inhibits ER stress and autophagy [67], the effect of GW501516 on palmitate-induced ER stress occurred in an AMPK-independent manner. In addition, we also found that PPARβ/δ activation by GW501516 upregulated the protein levels of beclin 1 and LC3-II, two well-known markers of autophagy, in cardiac cells [75]. In accordance with this, PPARβ/δ knockout mice also displayed a reduction in autophagic markers, which indicates that this nuclear receptor plays a key role in the control of the autophagic process in cardiac cells.

Although it is believed that palmitate-induced apoptosis is not associated with increased ROS in neonatal rat cardiomyocytes [76], it has

been reported that the PPARβ/δ ligands prevent oxidative stress-induced apoptosis in cardiac cells by increasing the expression of the antioxidative enzyme catalase [77]. More recently, it has been suggested that the PPARβ/δ ligand GW0742 protects cardiac myocytes from oxidative stress-induced apoptosis through its ability to prevent the increase in the expression of the metalloproteinases 2 and 9, an effect that was blunted in the presence of the PPARβ/δ antagonist GSK0660 [78]. Since oxidative stress is an important contributing factor in the pathogenesis of ischemic heart disease and heart failure, it has been suggested that this nuclear receptor might represent a new target for oxidative stress-induced cardiac dysfunction.

Although it has been suggested that inhibition of FAO might be useful for protecting the heart from the consequences of ischemia and ischemia–reperfusion injury [1,3], in vivo activation of PPARβ/δ protects the heart from ischemia–reperfusion injury in Zucker fatty rats through several mechanisms, including attenuation of lipotoxicity (PPARβ/δ activation increased cardiac FAO and ameliorated the downregulation of CD36, CPT-1 and β-oxidation gene expression caused by ischemia–reperfusion injury) and upregulation of the prosurvival signaling (Akt signaling pathway and Bcl family genes) in the heart [79].

4.2. PPARβ/δ effects in lipid-induced defective insulin signaling

One of the earliest disturbances observed in the heart following exposure to a HFD is the development of insulin resistance [80], which leads to increased left-ventricle remodeling and dysfunction [81]. Lipid accumulation in the heart results in cardiomyocyte insulin resistance, which is characterized by increased FA uptake and decreased glucose uptake [82–86]. Therefore, defective insulin signaling might exacerbate lipotoxic cardiomyopathy. In human patients with type 2 diabetes mellitus and heart failure, a dramatic accumulation of lipids within the myocardium has also been observed [87]. The fact that lipid accumulation is also observed in the heart of diabetic patients with normal cardiac function suggests that metabolic disturbances precede the development of ventricular dysfunction [88]. In these patients and those with metabolic syndrome, circulating FA and triglyceride levels are significantly elevated [89]. This is the result of the consumption of high levels of FA as part of the Western diet and the presence of obesity. Under these conditions, the storage capacity of fat depots in the body is exceeded, increased lipolysis of fat releases FA to the blood, and this leads to enhanced secretion of triglyceride-enriched lipoproteins (VLDL) by the liver. In contrast to glucose, whose uptake is tightly regulated by the action of insulin, FA uptake in the heart is not hormonally regulated and depends on the availability of FA in the circulation [90]. Thus, the type 2 diabetic heart increases the rate of FA uptake, leading to reliance on FAs as the main energy source, but also provokes the accumulation of FA-derived complex lipids (mainly ceramide and diacylglycerol). In contrast to what it has been observed in cardiac hypertrophy, the accumulation of cardiac FA-derived complex lipids in the setting of diabetes is not the result of impaired mitochondrial FAO, quite the opposite, studies in animals [91,92] and humans [93,94] have shown that myocardial FAO is increased in diabetic states. Thus, in this pathology, oversupply of FA is responsible for the accumulation of lipid intermediates in the heart as the result of the incapacity of FA oxidation to compensate the high rates of FA uptake.

The mechanisms underlying the lipid-derived attenuation of the insulin signaling pathway have not been completely elucidated; however, several mechanisms have been suggested based on findings in cells other than cardiomyocytes. Thus, accumulation of FA-derivatives fatty acyl-CoA, diacylglycerol and ceramide attenuates insulin signaling through the activation of serine kinases such as protein kinase C (PKC), inhibitor κB kinase β (IKKβ), c-Jun N-terminal kinase (JNK) and mammalian target of rapamycin (mTOR) [95–99]. Binding of insulin to its receptor leads to the subsequent phosphorylation of its substrates including insulin receptor substrate 1 (IRS1) on tyrosine residues. These phosphorylated tyrosine residues provide specific docking sites for other signaling proteins, leading to the activation of downstream signaling molecules, including phosphoinositide-3-kinase (PI3K), that finally result in Akt phosphorylation and glucose uptake. However, phosphorylation of IRS-1 on serine residues by lipid-activated kinases interferes with the functional domains of IRS1 and, for instance, reduces the binding between IRS1 and PI3K, thereby negatively regulating insulin signaling.

Ceramide-mediated insulin resistance can also be mediated by its ability to activate protein phosphatase 2A, thereby leading to dephosphorylation of Akt [99]. In a heart model of cardiac lipotoxicity induced by heart specific expression of LpL, the inhibitor of de novo synthesis of ceramide myriocin or heterozygosity for one of the subunits of serine palmitoyltransferase, which is involved in ceramide synthesis, improved cardiac function and corrected cardiac hypertrophy [100].

Cardiac insulin resistance is mimicked by cardiac specific overexpression of PPARα in MHC-PPARα mice [51]. It has been proposed that despite the increased capacity of diabetic hearts and MHC-PPARα hearts to oxidize FA, FAO rates are insufficient to match the high rates of FA uptake and esterification, leading to accumulation of the toxic lipid derivatives diacylglycerol and ceramide. As mentioned above, MHC-PPARβ/δ did not develop myocyte lipid accumulation or cardiomyopathy, even when fed a HFD [51].

On the other hand, PPARβ/δ activation can prevent the deleterious effects of the accumulation of FA-derivatives by increasing FAO, thereby reducing the availability of FAs to be stored in the form of complex lipids. In fact, we have observed in C2C12 myotubes that PPARβ/δ activation reduced palmitate-induced diacylglycerol accumulation and insulin resistance [101].

Generation of ROS also plays a major role in the development of insulin resistance [102] and given that ROS generation can reduce PPARβ/δ levels in the heart [58], the ROS-mediated reduction of this nuclear receptor can exacerbate insulin resistance and FA accumulation.

4.3. PPARβ/δ effects in lipid-induced inflammation

Owing to its fat content, the classical Western diet has a range of adverse effects on the heart, including enhanced inflammation. Pro-inflammatory factors such as tumor necrosis factor α (TNF-α), monocyte chemoattractant protein-1 (MCP-1), and IL-6, can exert several autocrine pleiotropic effects in cardiac cells that may contribute to states that are associated with myocardial inflammation, including myocardial injury, heart failure, and dilated cardiomyopathy [103,104]. Pro-inflammatory cytokines are under the transcriptional control of the ubiquitous inducible nuclear factor-κB (NF-κB), which is activated in myocarditis, congestive heart failure, and cardiac hypertrophy [105].

As mentioned above, an increase in glucose utilization and a decrease in FAO are observed during cardiac hypertrophy and congestive heart failure [106]. Interestingly, the changes that cardiac hypertrophy causes in the expression of genes involved in fatty acid metabolism were not observed when NF-κB activity was inhibited [107–109]. These data pointed to the involvement of the pro-inflammatory transcription factor NF-κB in the downregulation of FAO during cardiac hypertrophy. The mechanism by which activation of NF-κB results in reduced expression of FAO genes seems to involve a dramatic reduction in the binding of PPARβ/δ to the PPRE. This reduction was partially reversed by co-incubation of the cells with NF-κB inhibitors. Therefore, the reduced DNA-binding activity of PPARβ/δ seems to be related to the activation of NF-κB in cardiac cells. NF-κB is present in the cytoplasm as an inactive heterodimer that consists mostly of the p50 and p65 subunits. However, after activation, this heterodimer translocates to the nucleus and regulates the expression of genes involved in inflammatory and immune processes. Our results indicated that once the p65 subunit of NF-κB reaches the nucleus it interacts with PPARβ/δ. This association prevents PPARβ/δ from binding to its response element, and thereby inhibits its ability to induce gene transcription (Fig. 4). It has also been

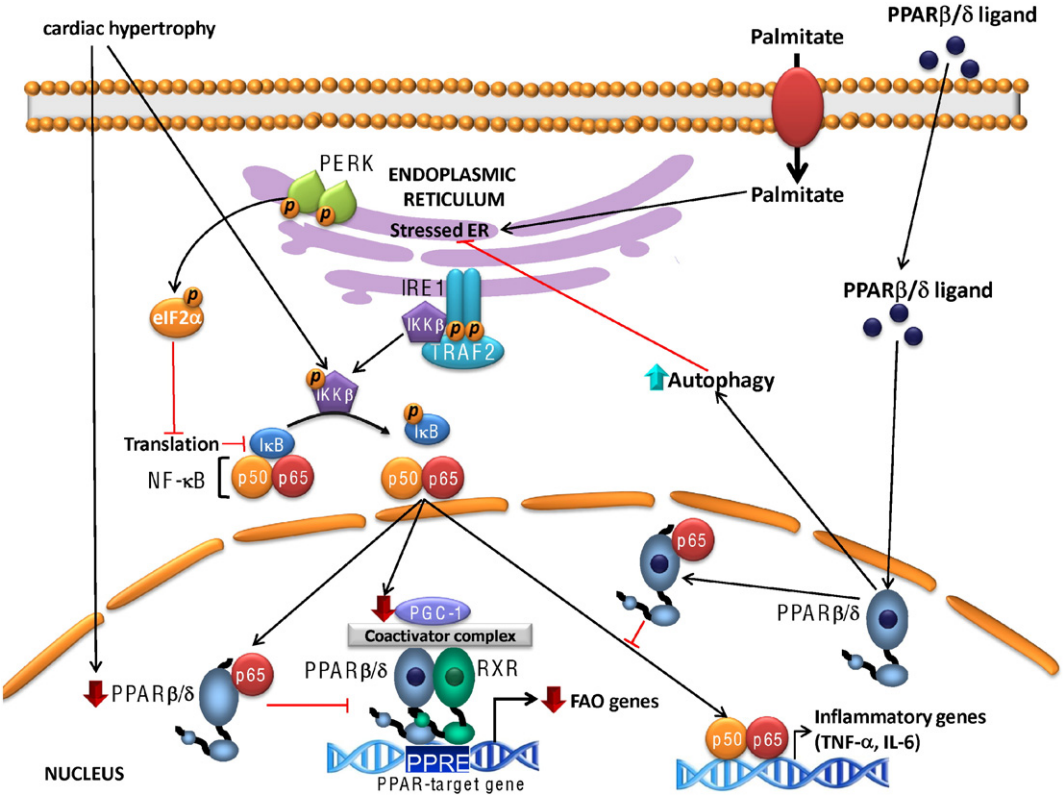

Fig. 4. Inflammation is involved in the reduction in FAO observed during cardiac hypertrophy and PPARβ/δ activation attenuates myocardial inflammatory responses. Cardiac hypertrophy activates the pro-inflammatory transcription factor NF-κB, which in turn interacts with PPARβ/δ and reduces its DNA-binding activity causing a decrease in the expression of the genes involved in FAO. Alternatively, pressure-overload cardiac hypertrophy reduces protein levels of PPARβ/δ. Inflammatory and hypertrophic stimuli, such as TNF-α, can reduce the expression of FAO genes by decreasing the levels of the transcriptional co-activator PGC-1α through NF-κB activation. FA overload results in the induction of ER stress and the subsequent activation of inflammatory pathways. Thus, during ER stress, protein kinase R (PKR)-like ER kinase (PERK)–eukaryotic initiation factor 2α (eIF2α) pathway activation and, thus, protein translation inhibition, together with the shorter half-life of IκBα compared with that of NF-κB, results in a reduction in the IκBα/NF-κB ratio, leading to nuclear NF-κB translocation and a consequent increase in the expression of pro-inflammatory genes. In addition, following activation of ER stress, the cytoplasmic domain of phosphorylated inositol-requiring enzyme 1 α (IRE-1α) recruits TNF-α receptor-associated factor 2 (TRAF2), forming a complex that interacts and activates IκB kinase (IKKβ), leading to NF-κB activation. PPARβ/δ activation prevents lipid-induced NF-kB activation by interacting with the p65 subunit of NF-κB, thereby reducing its availability to increase the expression of pro-inflammatory genes. It also prevents palmitate-induced ER stress and inflammation by increasing the expression of autophagic markers. PPRE, peroxisome proliferator response element.

reported that PPARβ/δ ligands and overexpression of this nuclear receptor suppressed myocardial inflammatory responses, such as the lipopolysaccharide-mediated production of TNFα. This had beneficial effects on animals that had undergone ischemia/reperfusion injury or cardiac hypertrophy [110].

The shift in glucose metabolism observed during cardiac hypertrophy induced by the TNF-α may also involve PPARβ/δ through the down-regulation of the transcriptional co-activator PGC-1α [111]. In the myocardium, PGC-1α may co-activate PPARα and PPARβ/δ subtypes, although it also interacts with and co-activates the estrogen-related receptor α (ERRα) [112]. We have reported that exposure of cardiac cells to TNF-α activates both p38 MAPK and NF-κB, causing PGC-1α down-regulation (Fig. 4). This results in an elevated glucose oxidation rate, which involves a reduction in pyruvate dehydrogenase kinase 4, an inhibitor of the key glycolytic enzyme pyruvate dehydrogenase, caused by the reduction of the DNA-binding activity of both PPARβ/δ and estrogen-related receptor α (ERRα).

We have also evaluated whether PPARβ/δ activation prevents the inflammatory processes induced in the heart of mice fed a HFD for 3 weeks [113]. This short period of exposure was selected to study the specific effects of lipid-induced inflammation on the heart, while avoiding other confounding factors such as obesity and established insulin resistance. The HFD induced the expression of TNF-α, MCP-1 and IL-6, and promoted the activity of NF-κB in the heart of mice. Interestingly, the PPARβ/δ agonist GW501516 abrogated this enhanced inflammatory profile. Moreover, since many inconsistencies have been observed when results obtained with murine models have been extrapolated to humans, we used AC16 cells, a cardiac cell line of human origin, and exposed them to palmitate. This is of interest, given that PPARs are known to be expressed at lower levels in human cells than in rodent cells [114], and gene expression is also differentially regulated by PPARs in human versus rodent cells [115]. When human cardiac AC16 cells were incubated with palmitate in the presence of GW501516, similar results were obtained to those reported in the heart of mice exposed to the HFD. Activation of PPARβ/δ in AC16 cells enhanced the physical interaction between PPARβ/δ and the p65 subunit of NF-κB, suggesting that this was the mechanism that interferes with NF-κB transactivation in the heart of mice exposed to a HFD.

Accumulation of FAs has been linked to the induction of ER stress and this process intersects with many different inflammatory signaling pathways, including the NF-κB pathway [116]. Thus, UPR activation results in a general repression of mRNA translation. Since inhibitor of κB (IκB), which inhibits NF-κB, has a shorter half-life than NF-κB, UPR activation shifts the IκB/NF-κB ratio, thereby releasing NF-κB, which translocates to the nucleus and increases the expression of its target genes, such as IL-6 and TNF-α [117]. In addition, in response to ER stress, the cytoplasmic domain of phosphorylated inositol-requiring enzyme 1 α (IRE-1α) can recruit TNF-α receptor-associated factor 2, forming a complex that interacts with and activates IκB kinase, leading to NF-κB activation [117,118]. In AC16 cells we have reported that the PPARβ/δ agonist GW501516 attenuated palmitate-induced ER stress [75]. Although we have recently reported that PPARβ/δ activation by GW501516 prevents palmitate-induced ER stress by activating AMPK in myotubes [69], in cardiac cells the effect of GW501516 seems to be

independent of AMPK. In addition, ER stress induced by an HFD in the heart of mice was exacerbated in PPARβ/δ-deficient mice. As mentioned above, PPARβ/δ activation by GW501516 upregulated markers of autophagy in cardiac cells and PPARβ/δ knockout mice also displayed a reduction in autophagic markers [75]. Based on these findings and considering our previous data showing that PPARβ/δ can limit myocardial inflammation by NF-κB inhibition [113], we hypothesized that GW501516 might prevent palmitate-induced ER stress and inflammation in human cardiac cells by inducing autophagy (Fig. 3). In fact, studies performed in mice fed an HFD reported that autophagy is downregulated in adipose tissue [119] and in the heart [120]. The former study also demonstrated that suppression of autophagy induces the inflammatory response via ER stress activation, while the opposite, that is activation of autophagy with rapamycin, decreases inflammatory gene expression [119]. These effects of PPARβ/δ on autophagy have important implications in cardiac disease since suppression of autophagy favors the development of heart failure during diabetes [121], whereas its induction may reduce myocardial ischemia/reperfusion-induced lethal injury [72].

5. Concluding remarks

Cardiac energy metabolism to assure constant pumping of the heart mainly relies on the oxidation of FAs. The reduction in cardiac FAO promotes the accumulation of FA derivatives that can alter cellular structures and activate downstream pathways leading to cardiac inflammation and toxicity. Moreover, despite its preference for FAs, the heart is also vulnerable to the pathological effects of FA overload. Therefore, dysregulation in cardiac FA metabolism leads to cardiac dysfunction.

PPARβ/δ is endowed with the dual capacity to modulate both FA metabolism and inflammation. A reduction in the activity of this nuclear receptor might be involved in the development of several cardiac disorders, whereas its activation by ligands may offer a therapeutic approach to attenuate both cardiac disorders caused by FAO inhibition and lipid-activated signaling pathways that promote cardiac dysfunction. Despite the abundance of preclinical data supporting the notion that treatment with PPARβ/δ ligands offers protection to the heart in several cardiac disorders, there is still a gap to bridge between preclinical data and clinical trials that needs filling in the future to clearly demonstrate the beneficial effects of these ligands in the clinical setting.

Transparency document

The Transparency document associated with this article can be found, in online version.

Acknowledgments

Funding support for the authors is from the Ministerio de Economía y Competitividad of the Spanish Government (SAF2012-30708) and CIBER de Diabetes y Enfermedades Metabólicas Asociadas (CIBERDEM) (ISCIII CB07/08/0003). CIBERDEM is an initiative of the Instituto de Salud Carlos III (ISCIII) — Ministerio de Economía y Competitividad. We thank the University of Barcelona's Language Advisory Service for editing the manuscript.

References

[1] G.D. Lopaschuk, J.R. Ussher, C.D. Folmes, J.S. Jaswal, W.C. Stanley, Myocardial fatty acid metabolism in health and disease, Physiol. Rev. 90 (2010) 207–258.
[2] P.M. Barger, D.P. Kelly, PPAR signaling in the control of cardiac energy metabolism, Trends Cardiovasc. Med. 10 (2000) 238–245.
[3] G.W. Goodwin, C.S. Taylor, H. Taegtmeyer, Regulation of energy metabolism of the heart during acute increase in heart work, J. Biol. Chem. 273 (1998) 29530–29539.
[4] F. Di Lisa, M. Canton, R. Menabò, N. Kaludercic, P. Bernardi, Mitochondria and cardioprotection, Heart Fail. Rev. 12 (2007) 249–260.
[5] H. Taegtmeyer, P. McNulty, M.E. Young, Adaptation and maladaptation of the heart in diabetes: part I: general concepts, Circulation 105 (2002) 1727–1733.
[6] M.E. Young, P. McNulty, H. Taegtmeyer, Adaptation and maladaptation of the heart in diabetes: part II: potential mechanisms, Circulation 105 (2002) 1861–1870.
[7] I. Issemann, S. Green, Activation of a member of the steroid hormone receptor superfamily by peroxisome proliferators, Nature 347 (1990) 645–650.
[8] L. Cheng, G. Ding, Q. Qin, Y. Huang, W. Lewis, et al., Cardiomyocyte-restricted peroxisome proliferator-activated receptor-delta deletion perturbs myocardial fatty acid oxidation and leads to cardiomyopathy, Nat. Med. 10 (2004) 1245–1250.
[9] Nuclear Receptors Nomenclature Committee, A unified nomenclature system for the nuclear receptor superfamily, Cell 97 (1999) 161–163.
[10] A. Schmidt, N. Endo, S.J. Rutledge, R. Vogel, D. Shinar, et al., Identification of a new member of the steroid hormone receptor superfamily that is activated by a peroxisome proliferator and fatty acids, Mol. Endocrinol. 6 (1992) 1634–1641.
[11] F. Chen, S.W. Law, B.W. O'Malley, Identification of two mPPAR related receptors and evidence for the existence of five subfamily members, Biochem. Biophys. Res. Commun. 196 (1993) 671–677.
[12] S.A. Kliewer, B.M. Forman, B. Blumberg, E.S. Ong, U. Borgmeyer, D.J. Mangelsdorf, et al., Differential expression and activation of a family of murine peroxisome proliferator-activated receptors, Proc. Natl. Acad. Sci. U. S. A. 91 (1994) 7355–7359.
[13] C.K. Glass, Going nuclear in metabolic and cardiovascular disease, J. Clin. Invest. 116 (2006) 556–560.
[14] O. Braissant, F. Foufelle, C. Scotto, M. Dauça, W. Wahli, Differential expression of peroxisome proliferator-activated receptors (PPARs): tissue distribution of PPAR-alpha, -beta, and -gamma in the adult rat, Endocrinology 137 (1996) 354–366.
[15] S. Kersten, J. Seydoux, J.M. Peters, F.J. Gonzalez, B. Desvergne, et al., Peroxisome proliferator-activated receptor alpha mediates the adaptive response to fasting, J. Clin. Invest. 103 (1999) 1489–1498.
[16] B. Desvergne, W. Wahli, Peroxisome proliferator-activated receptors: nuclear control of metabolism, Endocr. Rev. 20 (1999) 649–688.
[17] A.J. Gilde, K.A. van der Lee, P.H. Willemsen, G. Chinetti, F.R. van der Leij, G.J. van der Vusse, et al., Peroxisome proliferator-activated receptor (PPAR) alpha and PPARbeta/delta, but not PPARgamma, modulate the expression of genes involved in cardiac lipid metabolism, Circ. Res. 92 (2003) 518–524.
[18] B.E. Teunissen, P.J. Smeets, P.H. Willemsen, L.J. De Windt, G.J. Van der Vusse, et al., Activation of PPARdelta inhibits cardiac fibroblast proliferation and the transdifferentiation into myofibroblasts, Cardiovasc. Res. 75 (2007) 519–529.
[19] J.N. Feige, L. Gelman, L. Michalik, B. Desvergne, W. Wahli, From molecular action to physiological outputs: peroxisome proliferator-activated receptors are nuclear receptors at the crossroads of key cellular functions, Prog. Lipid Res. 45 (2006) 120–159.
[20] G. Chinetti, J.C. Fruchart, B. Staels, Peroxisome proliferator-activated receptors (PPARs): nuclear receptors at the crossroads between lipid metabolism and inflammation, Inflamm. Res. 49 (2000) 497–505.
[21] P. Puigserver, B.M. Spiegelman, Peroxisome proliferator-activated receptor-gamma coactivator 1 alpha (PGC-1 alpha): transcriptional coactivator and metabolic regulator, Endocr. Rev. 24 (2003) 78–90.
[22] R.A. Daynes, D.C. Jones, Emerging roles of PPARs in inflammation and immunity, Nat. Rev. Immunol. 2 (2002) 748–759.
[23] M. Li, G. Pascual, C.K. Glass, Peroxisome proliferator-activated receptor gamma-dependent repression of the inducible nitric oxide synthase gene, Mol. Cell. Biol. 20 (2000) 4699–4707.
[24] Y. Kamei, L. Xu, T. Heinzel, J. Torchia, R. Kurokawa, B. Gloss, et al., A CBP integrator complex mediates transcriptional activation and AP-1 inhibition by nuclear receptors, Cell 85 (1996) 403–414.
[25] P. Delerive, K. De Bosscher, S. Besnard, W. Vanden Berghe, J.M. Peters, F.J. Gonzalez, et al., Peroxisome proliferator-activated receptor alpha negatively regulates the vascular inflammatory gene response by negative cross-talk with transcription factors NF-kappaB and AP-1, J. Biol. Chem. 274 (1999) 32048–32054.
[26] P. Delerive, F. Martin-Nizard, G. Chinetti, F. Trottein, J.C. Fruchart, J. Najib, et al., Peroxisome proliferator-activated receptor activators inhibit thrombin-induced endothelin-1 production in human vascular endothelial cells by inhibiting the activator protein-1 signaling pathway, Circ. Res. 85 (1999) 394–402.
[27] P. Desreumaux, L. Dubuquoy, S. Nutten, M. Peuchmaur, W. Englaro, K. Schoonjans, et al., Attenuation of colon inflammation through activators of the retinoid X receptor (RXR)/peroxisome proliferator-activated receptor gamma (PPARgamma) heterodimer. A basis for new therapeutic strategies, J. Exp. Med. 193 (2001) 827–838.
[28] T.E. Johnson, M.K. Holloway, R. Vogel, S.J. Rutledge, J.J. Perkins, et al., Structural requirements and cell-type specificity for ligand activation of peroxisome proliferator-activated receptors, J. Steroid Biochem. Mol. Biol. 63 (1997) 1–8.
[29] I. Takada, R.T. Yu, H.E. Xu, M.H. Lambert, V.G. Montana, et al., Alteration of a single amino acid in peroxisome proliferator-activated receptor-alpha (PPAR alpha) generates a PPAR delta phenotype, Mol. Endocrinol. 14 (2000) 733–740.
[30] H.E. Xu, M.H. Lambert, V.G. Montana, D.J. Parks, S.G. Blanchard, et al., Molecular recognition of fatty acids by peroxisome proliferator-activated receptors, Mol. Cell 3 (1999) 397–403.
[31] B.M. Forman, B. Ruan, J. Chen, G.J. Schroepfer Jr., R.M. Evans, The orphan nuclear receptor LXRα is positively and negatively regulated by distinct products of mevalonate metabolism, Proc. Natl. Acad. Sci. U. S. A. 94 (1997) 10588–10593.
[32] K. Yu, W. Bayona, C.B. Kallen, H.P. Harding, C.P. Ravera, et al., Differential activation of peroxisome proliferator-activated receptors by eicosanoids, J. Biol. Chem. 270 (1995) 23975–23983.
[33] G. Krey, O. Braissant, F. L'Horset, E. Kalkhoven, M. Perroud, et al., Fatty acids, eicosanoids, and hypolipidemic agents identified as ligands of peroxisome proliferator-activated receptors by coactivator-dependent receptor ligand assay, Mol. Endocrinol. 11 (1997) 779–791.
[34] N. Shaw, M. Elholm, N. Noy, Retinoic acid is a high affinity selective ligand for the peroxisome proliferator-activated receptor β/δ, J. Biol. Chem. 278 (2003) 41589–41592.

[35] A. Chawla, C.-H. Lee, Y. Barak, W. He, J. Rosenfeld, et al., PPARδ is a very low-density lipoprotein sensor in macrophages, Proc. Natl. Acad. Sci. U. S. A. 100 (2003) (2003) 1268–1273.
[36] M.L. Sznaidman, C.D. Haffner, P.R. Maloney, A. Fivush, E. Chao, et al., Novel selective small molecule agonists for peroxisome proliferator-activated receptor δ (PPARδ)-synthesis and biological activity, Bioorg. Med. Chem. Lett. 13 (2003) 1517–1521.
[37] J. Berger, M.D. Leibowitz, T.W. Doebber, A. Elbrecht, B. Zhang, et al., Novel peroxisome proliferator-activated receptor (PPAR) γ and PPARδ ligands produce distinct biological effects, J. Biol. Chem. 274 (1999) 6718–6725.
[38] B.G. Shearer, D.J. Steger, J.M. Way, T.B. Stanley, D.C. Lobe, et al., Identification and characterization of a selective peroxisome proliferator-activated receptor β/δ (NR1C2) antagonist, Mol. Endocrinol. 22 (2008) 523–529.
[39] A.N. Billin, PPAR-beta/delta agonists for Type 2 diabetes and dyslipidemia: an adopted orphan still looking for a home, Expert Opin. Investig. Drugs 17 (2008) 1465–1471.
[40] K. Iwaisako, M. Haimerl, Y.H. Paik, K. Taura, Y. Kodama, et al., Protection from liver fibrosis by a peroxisome proliferator-activated receptor δ agonist, Proc. Natl. Acad. Sci. U. S. A. 109 (2012) E1369–E1376.
[41] B.G. Shearer, R.W. Wiethe, A. Ashe, A.N. Billin, J.M. Way, et al., Identification and characterization of 4-chloro-N-(2-{[5-trifluoromethyl)-2-pyridyl]sulfonyl}ethyl)benzamide (GSK3787), a selective and irreversible peroxisome proliferator-activated receptor delta (PPARdelta) antagonist, J. Med. Chem. 53 (2010) 1857–1861.
[42] P.S. Palkar, M.G. Borland, S. Naruhn, C.H. Ferry, C. Lee, et al., Cellular and pharmacological selectivity of the peroxisome proliferator-activated receptor-beta/delta antagonist GSK3787, Mol. Pharmacol. 78 (2010) 419–430.
[43] G.M.P. Giordiano Attianese, B. Desvergne, Integrative and systemic approaches for evaluating PPARβ/δ (PPARD) function, Nucl. Recept. Signal. 13 (2015), e001.
[44] G.J. van der Vusse, M. van Bilsen, J.F. Glatz, Cardiac fatty acid uptake and transport in health and disease, Cardiovasc. Res. 45 (2000) 279–293.
[45] B. Razani, H. Zhang, P.C. Schulze, J.D. Schilling, J. Verbsky, et al., Fatty acid synthase modulates homeostatic responses to myocardial stress, J. Biol. Chem. 286 (2011) 30949–30961.
[46] D.D. Habets, W.A. Coumans, P.J. Voshol, M.A. den Boer, M. Febbraio, et al., AMPK-mediated increase in myocardial long-chain fatty acid uptake critically depends on sarcolemmal CD36, Biochem. Biophys. Res. Commun. 355 (2007) 204–210.
[47] G.D. Lopaschuk, D.D. Belke, J. Gamble, T. Itoi, B.O. Schönekess, Regulation of fatty acid oxidation in the mammalian heart in health and disease, Biochim. Biophys. Acta 1213 (1994) 263–276.
[48] V.A. Kurien, M.F. Oliver, Free fatty acids during acute myocardial infarction, Prog. Cardiovasc. Dis. 13 (1971) 361–373.
[49] H. Yagyu, G. Chen, M. Yokoyama, K. Hirata, A. Augustus, et al., Lipoprotein lipase (LpL) on the surface of cardiomyocytes increases lipid uptake and produces a cardiomyopathy, J. Clin. Invest. 111 (2003) 419–426.
[50] P. Wang, J. Liu, Y. Li, S. Wu, J. Luo, et al., Peroxisome proliferator-activated receptor δ is an essential transcriptional regulator for mitochondrial protection and biogenesis in adult heart, Circ. Res. 106 (2010) 911–919.
[51] E.M. Burkart, N. Sambandam, X. Han, R.W. Gross, M. Courtois, et al., Nuclear receptors PPARbeta/delta and PPARalpha direct distinct metabolic regulatory programs in the mouse heart, J. Clin. Invest. 117 (2007) 3930–3939.
[52] A. Georgiadi, L. Lichtenstein, T. Degenhardt, M.V. Boekschoten, M. van Bilsen, et al., Induction of cardiac Angptl4 by dietary fatty acids is mediated by peroxisome proliferator-activated receptor beta/delta and protects against fatty acid-induced oxidative stress, Circ. Res. 106 (2010) 1712–1721.
[53] J. Liu, P. Wang, J. Luo, Y. Huang, et al., Peroxisome proliferator-activated receptor β/δ activation in adult hearts facilitates mitochondrial function and cardiac performance under pressure-overload condition, Hypertension 57 (2011) 223–230.
[54] L. Cheng, G. Ding, Q. Qin, Y. Xiao, D. Woods, et al., Peroxisome proliferator-activated receptor delta activates fatty acid oxidation in cultured neonatal and adult cardiomyocytes, Biochem. Biophys. Res. Commun. 313 (2004) 277–286.
[55] H.E. Azzouzi, S. Leptidis, P.A. Doevendans, L.J. De Windt, HypoxamiRs: regulators of cardiac hypoxia and energy metabolism, Trends Endocrinol. Metab. 26 (2015) 502–508.
[56] H. el Azzouzi, S. Leptidis, E. Dirkx, J. Hoeks, B. van Bree, et al., The hypoxia-inducible microRNA cluster miR-199a~214 targets myocardial PPARδ and impairs mitochondrial fatty acid oxidation, Cell Metab. 18 (2013) 341–354.
[57] T. Haffar, F.A. Bérubé-Simard, N. Bousette, Cardiomyocyte lipotoxicity is mediated by Il-6 and causes down-regulation of PPARs, Biochem. Biophys. Res. Commun. 459 (2015) 54–59.
[58] B.C. Yu, C.K. Chang, H.Y. Ou, K.C. Cheng, J.T. Cheng, Decrease of peroxisome proliferator-activated receptor delta expression in cardiomyopathy of streptozotocin-induced diabetic rats, Cardiovasc. Res. 80 (2008) 78–87.
[59] M.N. Sack, T.A. Rader, S. Park, J. Bastin, S.A. McCune, et al., Fatty acid oxidation enzyme gene expression is downregulated in the failing heart, Circulation 94 (1996) 2837–2842.
[60] D.P. Kelly, A.W. Strauss, Inherited cardiomyopathies, N. Engl. J. Med. 330 (1994) 913–919.
[61] H.C. Chiu, A. Kovacs, D.A. Ford, F.F. Hsu, R. Garcia, et al., A novel mouse model of lipotoxic cardiomyopathy, J. Clin. Invest. 107 (2001) 813–822.
[62] A. Planavila, R. Rodríguez-Calvo, M. Jové, L. Michalik, W. Wahli, et al., Peroxisome proliferator-activated receptor beta/delta activation inhibits hypertrophy in neonatal rat cardiomyocytes, Cardiovasc. Res. 65 (2005) 832–841.
[63] B.H. Lorell, B.A. Carabello, Left ventricular hypertrophy: pathogenesis, detection, and prognosis, Circulation 102 (2000) 470–479.
[64] K. Drosatos, P.C. Schulze, Cardiac lipotoxicity: molecular pathways and therapeutic implications, Curr. Heart Fail. Rep. 10 (2013) 109–121.
[65] K. Konstantinidis, R.S. Whelan, R.N. Kitsis, Mechanisms of cell death in heart disease, Arterioscler. Thromb. Vasc. Biol. 32 (2012) 1552–1562.
[66] M. Park, A. Sabetski, Y. Kwan Chan, S. Turdi, G. Sweeney, Palmitate induces ER stress and autophagy in H9c2 cells: implications for apoptosis and adiponectin resistance, J. Cell. Physiol. 230 (2015) 630–639.
[67] D. Qi, L.H. Young, AMPK: energy sensor and survival mechanism in the ischemic heart, Trends Endocrinol. Metab. 26 (2015) 422–429.
[68] D.L. Hickson-Bick, L.M. Buja, J.B. McMillin, Palmitate-mediated alterations in the fatty acid metabolism of rat neonatal cardiac myocytes, J. Mol. Cell. Cardiol. 32 (2000) 511–519.
[69] L. Salvadó, E. Barroso, A.M. Gómez-Foix, X. Palomer, L. Michalik, et al., PPARβ/δ prevents endoplasmic reticulum stress-associated inflammation and insulin resistance in skeletal muscle cells through an AMPK-dependent mechanism, Diabetologia 57 (2014) 2126–2135.
[70] D.K. Krämer, L. Al-Khalili, B. Guigas, Y. Leng, P.M. Garcia-Roves, et al., Role of AMP kinase and PPARdelta in the regulation of lipid and glucose metabolism in human skeletal muscle, J. Biol. Chem. 282 (2007) 19313–19320.
[71] T. Minamino, I. Komuro, M. Kitakaze, Endoplasmic reticulum stress as a therapeutic target in cardiovascular disease, Circ. Res. 107 (2010) 1071–1082.
[72] G. Petrovski, S. Das, B. Juhasz, A. Kertesz, A. Tosaki, et al., Cardioprotection by endoplasmic reticulum stress-induced autophagy, Antioxid. Redox Signal. 14 (2011) 2191–2200.
[73] H. Zhao, Y. Liao, T. Minamino, Y. Asano, M. Asakura, et al., Inhibition of cardiac remodeling by pravastatin is associated with amelioration of endoplasmic reticulum stress, Hypertens. Res. 31 (2008) 1977–1987.
[74] H.C. Hsu, C.Y. Chen, B.C. Lee, M.F. Chen, High-fat diet induces cardiomyocyte apoptosis via the inhibition of autophagy, Eur. J. Nutr. (Sep 10 2015).
[75] X. Palomer, E. Capdevila-Busquets, G. Botteri, L. Salvadó, E. Barroso, et al., PPARβ/δ attenuates palmitate-induced endoplasmic reticulum stress and induces autophagic markers in human cardiac cells, Int. J. Cardiol. 174 (2014) 110–118.
[76] D.L. Hickson-Bick, G.C. Sparagna, L.M. Buja, J.B. McMillin, Palmitate-induced apoptosis in neonatal cardiomyocytes is not dependent on the generation of ROS, Am. J. Physiol. Heart Circ. Physiol. 282 (2002) H656–H664.
[77] M. Pesant, S. Sueur, P. Dutartre, M. Tallandier, P.A. Grimaldi, et al., Peroxisome proliferator-activated receptor delta (PPARdelta) activation protects H9c2 cardiomyoblasts from oxidative stress-induced apoptosis, Cardiovasc. Res. 69 (2006) 440–449.
[78] E. Barlaka, A. Görbe, R. Gáspár, J. Pálóczi, P. Ferdinandy, et al., Activation of PPARβ/δ protects cardiac myocytes from oxidative stress-induced apoptosis by suppressing generation of reactive oxygen/nitrogen species and expression of matrix metalloproteinases, Pharmacol. Res. 95–96 (2015) 102–110.
[79] T.L. Yue, S.S. Nerurkar, W. Bao, B.M. Jucker, L. Sarov-Blat, et al., In vivo activation of peroxisome proliferator-activated receptor-delta protects the heart from ischemia/reperfusion injury in Zucker fatty rats, J. Pharmacol. Exp. Ther. 325 (2008) 466–474.
[80] S.Y. Park, Y.R. Cho, H.J. Kim, T. Higashimori, C. Danton, et al., Unraveling the temporal pattern of diet-induced insulin resistance in individual organs and cardiac dysfunction in C57BL/6 mice, Diabetes 54 (2005) 3530–3540.
[81] M.J. Raher, H.B. Thibault, E.S. Buys, D. Kuruppu, N. Shimizu, et al., A short duration of high-fat diet induces insulin resistance and predisposes to adverse left ventricular remodeling after pressure overload, Am. J. Physiol. Heart Circ. Physiol. 295 (2008) H2495–H2502.
[82] P. Iozzo, P. Chareonthaitawee, D. Dutka, D.J. Betteridge, E. Ferrannini, et al., Independent association of type 2 diabetes and coronary artery disease with myocardial insulin resistance, Diabetes 51 (2002) 3020–3024.
[83] P.K. Mazumder, B.T. O'Neill, M.W. Roberts, J. Buchanan, U.J. Yun, et al., Impaired cardiac efficiency and increased fatty acid oxidation in insulin-resistant ob/ob mouse hearts, Diabetes 53 (2004) 2366–2374.
[84] M.E. Young, P.H. Guthrie, P. Razeghi, B. Leighton, S. Abbasi, et al., Impaired long-chain fatty acid oxidation and contractile dysfunction in the obese Zucker rat heart, Diabetes 51 (2002) 2587–2595.
[85] O.J. How, E. Aasum, D.L. Severson, W.Y. Chan, M.F. Essop, et al., Increased myocardial oxygen consumption reduces cardiac efficiency in diabetic mice, Diabetes 55 (2006) 466–473.
[86] D.D. Belke, S. Betuing, M.J. Tuttle, C. Graveleau, M.E. Young, et al., Insulin signaling coordinately regulates cardiac size, metabolism, and contractile protein isoform expression, J. Clin. Invest. 109 (2002) 629–639.
[87] S. Sharma, J.V. Adrogue, L. Golfman, I. Uray, J. Lemm, et al., Intramyocardial lipid accumulation in the failing human heart resembles the lipotoxic rat heart, FASEB J. 18 (2004) 1692–1700.
[88] H.E. Lebovitz, B. Ludvik, I. Yaniv, W. Haddad, T. Schwartz, et al., Fasting plasma triglycerides predict the glycaemic response to treatment of type 2 diabetes by gastric electrical stimulation. A novel lipotoxicity paradigm, Diabet. Med. 30 (2013) 687–693.
[89] R.M. Krauss, Lipids and lipoproteins in patients with type 2 diabetes, Diabetes Care 27 (2004) 1496–1504.
[90] D. An, B. Rodrigues, Role of changes in cardiac metabolism in development of diabetic cardiomyopathy, Am. J. Physiol. Heart Circ. Physiol. 291 (2006) H1489–H1506.
[91] A. Onay-Besikci, S. Guner, E. Arioglu, I. Ozakca, A.T. Ozcelikay, et al., The effects of chronic trimetazidine treatment on mechanical function and fatty acid oxidation in diabetic rat hearts, Can. J. Physiol. Pharmacol. 85 (2007) 527–535.
[92] V. Sharma, P. Dhillon, R. Wambolt, H. Parsons, R. Brownsey, et al., Metoprolol improves cardiac function and modulates cardiac metabolism in the streptozotocin-diabetic rat, Am. J. Physiol. Heart Circ. Physiol. 294 (2008) H1609–H1620.
[93] L.R. Peterson, P. Herrero, K.B. Schechtman, S.B. Racette, A.D. Waggoner, et al., Effect of obesity and insulin resistance on myocardial substrate metabolism and efficiency in young women, Circulation 109 (2004) 2191–2196.

[94] L.J. Rijzewijk, R.W. van der Meer, H.J. Lamb, H.W. de Jong, M. Lubberink, et al., Altered myocardial substrate metabolism and decreased diastolic function in nonischemic human diabetic cardiomyopathy: studies with cardiac positron emission tomography and magnetic resonance imaging, J. Am. Coll. Cardiol. 54 (2009) 1524–1532.
[95] G.P. Sykiotis, A.G. Papavassiliou, Serine phosphorylation of insulin receptor substrate-1: a novel target for the reversal of insulin resistance, Mol. Endocrinol. 15 (2001) 1864–1869.
[96] J.F. Tanti, J. Jager, Cellular mechanisms of insulin resistance: role of stress-regulated serine kinases and insulin receptor substrates (IRS) serine phosphorylation, Curr. Opin. Pharmacol. 9 (2009) 753–762.
[97] J.K. Kim, J.J. Fillmore, M.J. Sunshine, B. Albrecht, et al., PKC-theta knockout mice are protected from fat-induced insulin resistance, J. Clin. Invest. 114 (2004) 823–827.
[98] M. Yuan, N. Konstantopoulos, J. Lee, L. Hansen, et al., Reversal of obesity- and diet-induced insulin resistance with salicylates or targeted disruption of Ikkbeta, Science 293 (2001) 1673–1677.
[99] B. Chaurasia, S.A. Summers, Ceramides — lipotoxic inducers of metabolic disorders, Trends Endocrinol. Metab. 26 (2015) 538–550.
[100] T.S. Park, Y. Hu, H.L. Noh, K. Drosatos, K. Okajima, et al., Ceramide is a cardiotoxin in lipotoxic cardiomyopathy, J. Lipid Res. 49 (2008) 2101–2112.
[101] T. Coll, D. Alvarez-Guardia, E. Barroso, A.M. Gómez-Foix, X. Palomer, et al., Activation of peroxisome proliferator-activated receptor-{delta} by GW501516 prevents fatty acid-induced nuclear factor-{kappa}B activation and insulin resistance in skeletal muscle cells, Endocrinology 151 (2010) 1560–1569.
[102] N. Houstis, E.D. Rosen, E.S. Lander, Reactive oxygen species have a causal role in multiple forms of insulin resistance, Nature 440 (2006) 944–948.
[103] F.J. Neumann, I. Ott, M. Gawaz, G. Richardt, H. Holzapfel, et al., Cardiac release of cytokines and inflammatory responses in acute myocardial infarction, Circulation 92 (1995) 748–755.
[104] A. Matsumori, T. Yamada, H. Suzuki, Y. Matoba, S. Sasayama, Increased circulating cytokines in patients with myocarditis and cardiomyopathy, Br. Heart J. 72 (1994) 561–566.
[105] W.K. Jones, M. Brown, X. Ren, S. He, M. McGuinness, NF-kappaB as an integrator of diverse signaling pathways: the heart of myocardial signaling? Cardiovasc. Toxicol. 3 (2003) 229–254.
[106] Y. Kagaya, Y. Kanno, D. Takeyama, N. Ishide, Y. Maruyama, et al., Effects of long-term pressure overload on regional myocardial glucose and free fatty acid uptake in rats. A quantitative autoradiographic study, Circulation 81 (1990) 1353–1361.
[107] A. Planavila, J.C. Laguna, M. Vázquez-Carrera, Nuclear factor-kappaB activation leads to down-regulation of fatty acid oxidation during cardiac hypertrophy, J. Biol. Chem. 280 (2005) 17464–17471.
[108] A. Planavila, J.C. Laguna, M. Vázquez-Carrera, Atorvastatin improves peroxisome proliferator-activated receptor signaling in cardiac hypertrophy by preventing nuclear factor-kappa B activation, Biochim. Biophys. Acta 1687 (2005) 76–83.
[109] P.J. Smeets, B.E. Teunissen, A. Planavila, H. de Vogel-van den Bosch, P.H. Willemsen, et al., Inflammatory pathways are activated during cardiomyocyte hypertrophy and attenuated by peroxisome proliferator-activated receptors PPARalpha and PPARdelta, J. Biol. Chem. 283 (2008) 29109–29118.
[110] G. Ding, L. Cheng, Q. Qin, S. Frontin, Q. Yang, et al., PPARdelta modulates lipopolysaccharide-induced TNFalpha inflammation signaling in cultured cardiomyocytes, J. Mol. Cell. Cardiol. 40 (2006) 821–828.
[111] X. Palomer, D. Alvarez-Guardia, R. Rodríguez-Calvo, T. Coll, J.C. Laguna, et al., TNF-alpha reduces PGC-1alpha expression through NF-kappaB and p38 MAPK leading to increased glucose oxidation in a human cardiac cell model, Cardiovasc. Res. 81 (2009) 703–712.
[112] B.N. Finck, D.P. Kelly, Peroxisome proliferator-activated receptor gamma coactivator-1 (PGC-1) regulatory cascade in cardiac physiology and disease, Circulation 115 (2007) 2540–2548.
[113] D. Alvarez-Guardia, X. Palomer, T. Coll, L. Serrano, R. Rodríguez-Calvo, et al., PPARβ/δ activation blocks lipid-induced inflammatory pathways in mouse heart and human cardiac cells, Biochim. Biophys. Acta 1811 (2011) 59–67.
[114] C.N. Palmer, M.H. Hsu, K.J. Griffin, J.L. Raucy, E.F. Johnson, Peroxisome proliferator activated receptor-alpha expression in human liver, Mol. Pharmacol. 53 (1998) 14–22.
[115] J.W. Lawrence, Y. Li, S. Chen, J.G. DeLuca, J.P. Berger, et al., Differential gene regulation in human versus rodent hepatocytes by peroxisome proliferator-activated receptor (PPAR) alpha. PPAR alpha fails to induce peroxisome proliferation-associated genes in human cells independently of the level of receptor expression, J. Biol. Chem. 276 (2001) 31521–31527.
[116] G.S. Hotamisligil, Endoplasmic reticulum stress and the inflammatory basis of metabolic disease, Cell 140 (2010) 900–917.
[117] K. Zhang, R.J. Kaufman, From endoplasmic-reticulum stress to the inflammatory response, Nature 454 (2008) 455–462.
[118] L. Salvadó, X. Palomer, E. Barroso, M. Vázquez-Carrera, Targeting endoplasmic reticulum stress in insulin resistance, Trends Endocrinol. Metab. 26 (2015) 438–448.
[119] T. Yoshizaki, C. Kusunoki, M. Kondo, M. Yasuda, S. Kume, et al., Autophagy regulates inflammation in adipocytes, Biochem. Biophys. Res. Commun. 417 (2012) 352–357.
[120] R. Guo, Y. Zhang, S. Turdi, J. Ren, Adiponectin knockout accentuates high fat diet-induced obesity and cardiac dysfunction: role of autophagy, Biochim. Biophys. Acta 1382 (2013) 1136–1148.
[121] C. He, H. Zhu, H. Li, M.H. Zou, Z. Xie, Dissociation of Bcl-2–Beclin1 complex by activated AMPK enhances cardiac autophagy and protects against cardiomyocyte apoptosis in diabetes, Diabetes 62 (2013) 1270–1281.

Acknowledgments

This work couldn't exist without Xevi. Actually, I would have never started a PhD if I hadn't met him, and at this point of my career I am not really sure if I have to thank him or blame him (I say it with love and humor). I have always thought that words between us are not necessary and, anyway, words are not enough to express how much I owe him and how much he means to me. He has taught me everything I know as scientist, and, most important, he has taught me to always question things and to pursuit the truth without giving up when facing difficulties. He has always been there for me, willing to help, to teach and to share. He has always understood me without asking questions, and he has mentored me with intelligence, irony and rigor. He has passed down to me all his love and enthusiasm for science. He has guided me and let me become the person I am now, and for this, and for many other reasons, he will always have the greatest place in my heart.

I am deeply thankful to Manel, for giving me the opportunity to carry out this experience in his group. None of this would have been possible without him. He has been the best guide and mentor I could have ever desired. He has tutored me and helped me when I needed most. He has always been there supporting me and managing any issue. I have learned so much from him and I will never forget these four years of my life under his trail. He has all my gratitude and my admiration.

I thank all my colleagues and friends at lab, particularly people from my group. They have been much more than colleagues to me. They really were my family at lab, and a million thanks would not be enough to express how grateful I am.

Thanks Emma, for helping me every time I needed. Thank you for helping me when I was asking, and also when I was not. Thank you for your smile, your kindness and your positivism.

Thank you Marta, for encouraging me and cheering me up when I was down. It meant a lot to me. Thank you for your precious help at lab.

Thanks Mohammed for always being there, willing to help. Thank you for being exactly the way you are. You got me angry, and you got me laugh and I will always have the best memories of my PhD in your company.

Thanks to Mei, the first friend I made at lab. You accepted me from the very beginning, you helped me to arrange my new life in Barcelona and supported me in any moment. I owe you many things, and I know that the first year at work wouldn't have been so funny without you!

Thanks to Silvi, one of the best person I have ever met. I admire your intelligence and your big heart. Thanks for sharing with me so many unforgettable moments.

My most heart-felt and sincere thanks to Javi. My staying at the lab wouldn't have been the same without you! Thank you for helping me in any situation, professionally and, above all, personally. Thank you for always being there for me, thank you for letting me see things from another point of view. You are a wonderful person and I admire you so much. I admire your positivism, your willingness and your professionalism, but most of all I admire your ability not to judge anyone. You are an example to me and I want to learn more from you. During these years, you have been a precious shelter, and a real friend, and you will always have a very important place in my heart!

Thanks to Luci. You are the best person, colleague and friend I have ever met. Thank you for being always there for me, always helping, always have a comforting word. I am grateful that our pathways had crossed and I really do hope that we can continue being so close and sharing many other experiences.

Thanks to David, for your company, your humor, your help. Thanks for listening to me and putting up with me, which I know it is hard sometimes.

Thanks to Dan, for his humor, his kindness and for sharing with me a large, hot and boring working-august at lab. You made it much easier and funnier!

Thanks to Patty, the loyalest and craziest friend I have ever had. Thank you for always being there when I needed most. Now I really do miss you!

Thanks to Mario, for always having the right word in the right moment, for making me laugh and showing me the bright side when I was only seeing the dark one. Thanks for our talks, our beers, our trips.

A big thank to Miren, for many and many things. For being a friend, for giving me advices that I have never followed (now I know that I should have). For our coffees on the stairs, for our laughs, and for sharing with me this tough, large and emotional adventure. I admire the way you are and you will always have a very important place in my heart!

Thanks to Raul for being there in one of the darkest moment of our lives. I will never forget it. I admire your strength and your big heart.

Thanks to Dolors, the clearest and brightest soul I have ever met. Thank for your smile, for your sweetness, for you concern. It has been a great support to me.

Thanks to Vane, for sharing with me so many moments and many philosophic talks, for helping me to open up myself, for making me laugh, and for supporting me not only as a colleague, but also as a friend.

Thanks to Miguel, for his smile and his optimism. Thank you for introducing me to people at lab (you were the very first person that invited me to have lunch with you all). Thank

you for helping me with the classes. I would have never made it without you! Thanks for making the day funnier at lab with your football disquisitions.

Thanks to Sonia for her support and her many advices, thanks to Gemma for her kindness and her willingness.

Thanks to Leti, for being a friend, always willing to help. Thank you for always having a kind word when I was stressed or sad. Thank you for all the moments we have shared!

Thanks to Vero for always helping me, not only at lab and with the thesis, but also in my life. Thank you for your words, your advices and your sensibility. You have been an example to me!

The biggest thanks to Edu, for being an amazing person and an incredible friend. Thank you for always being there for me (even when I was harsh), without asking anything in return. Thank you for making me laugh, for helping me have the trust in people, for helping me open up myself, for always having a word, a story, a smile. Thanks for being the only person from Barcelona that understood my jokes and laughed at them!! You made me feel like home and you mean a lot to me.

Thanks to David Porquet, for teaching me about neuronal cells and mice, and for his humor.
Thanks to Laia, for helping me at the beginning of this phase, and for handing down her precious inheritance to me.

Thanks to Maria Calderón for helping me with the fatty acid oxidation assay.
Thanks to Anna Orozco for providing me the human cell cultures.
Thanks to Joan Carles Escòla-Gil and Lidia for supplying me the VLDL fractions.

Thanks to all the other people that have passed through the lab and have shared with me a piece of this long journey: Christian, Oriol, Julia, Fotini, Sergi, Alexia, Timi, Dimitri, Andrés, Nacho, Luisa, and many others, whom mentioning here would be too long (unless I start writing a second thesis).

I sincerely thank Professor Laura Herrero for her kindness and her willingness in any moment, and for mentoring me and encouraging me when I was uncertain.

I thank Professor Anna Gumà for helping me with the organ bath assay and for her precious advices.

I am deeply thankful to Professor Jordi Camarasa, Professor Juan Carlos Laguna and Professor Elena Escubedo, for assure me all their resources, for being a reference and for helping me when I needed.

I thank Professor Toni Camins for encouraging me during these years. I thank Professor Annamaria Canuda for her kindness and our nice talks about Italy. I thank Professor Mercé Pallas for her willingness and for helping me with my fellowship at the beginning of my PhD. I thank Professor Roser Vila and Professor Salvador Cañigueral for their courteousness and their support.
I thank Professors Rosa Maria Sanchez, Andrés Gimenez, David Pubill and Nuria Roglans for helping me with the classes.

Thanks to Professors Maria Luisa Garcia and Montserrat Mitjans for tutoring me and supporting me in the last phase of my PhD.
Thanks to all the members of the PhD Committee, Professors Marta Espina, Juan Llobet and Elisabet González, for counseling me during these four years. Your precious advices helped me to improve my work, and made me a more self-confident and determined person.

A big thanks to Mar Morales and Silvia Soriano for their precious help. I am sure that without their patience and their efficiency my PhD would have last much longer than 4 years. Thank you for always being there, thank you for your every-morning smile, thank you for managing any issue with kindness and professionalism.

Many thanks to Stanis who so generously helped me fixing my laptop and found a solution to all my informatics troubles.

Thanks to Mariangeles Barceló Vidal for helping me with the paper work.
Thanks to all the members of the cartaker's office for finding me a classroom for my numerous oral presentations.

Finally, I would like to thank the city of Barcelona, my second home. I wouldn't have been able to get to the end of my PhD if I hadn't lived here. Barcelona means a lot to me because it represents a place of connection between people, a place where you can share so many variegated experiences. Living in Barcelona has enriched me as a person and has allowed me to find myself. Here I met people that became essential in my life: Sara, Riccardo, Valentino and Valeria. You are family to me and my life wouldn't be the same without you. Thank you for always being there, in the good moments and in the bad ones. Thank you for making me feel loved, and for making these years a wonderful, unforgettable journey.

I thank all my friends from Barcelona (Guille, Albert, Victor, Enri, Peppe, Ursula, Diana, Sus, Estefi, Elen, Eli) for always supporting me when I was sad and when I was about to quit. Your example and your encouraging words gave me the strength to carry on in the hardest moments. Thank you for sharing with me so many amazing experiences.

I thank my family, for everything. They are the reason of my life.